ResearchOnline@JCU

This file is part of the following reference:

Dight, Ian John (1991) ***Numerical simulation of larval dispersal and recruitment within the Great Barrier Reef and its application to the Acanthaster phenomenon and coral reef resource management.*** **PhD thesis, James Cook University of North Queensland.**

Access to this file is available from:

http://researchonline.jcu.edu.au/33766/

If you believe that this work constitutes a copyright infringement, please contact ResearchOnline@jcu.edu.au and quote **http://researchonline.jcu.edu.au/33766/**

JAMES COOK UNIVERSITY AUSTRALIA

NUMERICAL SIMULATION OF LARVAL DISPERSAL AND RECRUITMENT WITHIN THE GREAT BARRIER REEF AND ITS APPLICATION TO THE *ACANTHASTER* PHENOMENON AND CORAL REEF RESOURCE MANAGEMENT

Thesis submitted by
Ian John Dight BSc (Hons)
in December 1991.

for the degree of Doctor of Philosophy in
the Departments of Civil and Systems Engineering
and Zoology
at James Cook University of North Queensland

STATEMENT OF ACCESS

I, the undersigned, the author of this thesis, understand that James Cook University will make it available for use within the University library and, by microfilm or other photographic means, allow access to users in other approved libraries. All users consulting this thesis will have to sign the following statement:

> "In consulting this thesis I agree not to copy or closely paraphrase it in whole or in part without the written consent of the author; and to make proper written acknowledgement for any assistance which I have obtained from it."

Beyond this, I do not wish to place any restriction on access to this thesis.

.....	20/12/91 .....
Ian J. Dight	Date

DECLARATION

I declare that this thesis is my own work and has not been submitted in any form for another degree or diploma at any university or other institution of tertiary education. Information derived from the published or unpublished work of others has been acknowledged in text and a list of references is given.

.....
Ian J. Dight

20/12/91
.....
Date

ACKNOWLEDGEMENTS

The research documented in this thesis represents a multi-disciplinary approach to the study of marine science. As such, it has required input from individuals with expertise in research areas of which I had only limited exposure before this project commenced. In particular, I refer to numerical modelling techniques and physical oceanography. This expertise was provided primarily by Drs Maurice James and Lance Bode respectively, to whom I am very appreciative for their time and patience. Setting-up and running the hydrodynamic model SURGE (including the implementation of reef, island and coastal barriers, bathymetry, and boundary conditions), modelling and calibrating the different forcings (tides, wind and EAC), and the design and development of the computer programmes TRACK and INSECT were entirely my own responsibility.

The research was supervised by Dr Maurice James (Systems Engineering) and Professor Rhondda Jones (Zoology). I am grateful for their advice and direction. Maurice James, in particular, played a very supportive role as supervisor, and in the development of the research programme. Rhondda Jones took on the role of mentor with finesse at critical times. The late Professor Kevin Stark was also very supportive up until his unfortunate death.

Mr Luciano Mason provided assistance with the setting-up and running of SURGE, and a great deal of helpful interpretation of hydrodynamic model outputs. Chris Gossett and Lauchlan Stewart provided assistance with computer programming, while James Scandol provided advice and assistance with statistical analysis.

I am thankful to Dr Kerry Black, of Victorian Institute of Marine Sciences, for use of his models and computer facilities. These provided the basis for fine-scale simulations around the schematized reefs. Design of the schematized reefs and particle release patterns, and the parameterization of results into the large-scale dispersal model were entirely my own work.

This thesis has benefited through publications and the critical comment that was provided by Maurice James and Lance Bode, as well as several anonymous reviewers. The final draft was critically reviewed by Maurice James and Rhondda Jones, and greatly improved as a result. James Scandol, Moya Tomlinson and Lea Scherl proofread several chapters.

Last, but not least, I thank Lea Scherl for her moral support, patience and generosity over many years.

This research was supported by grants from the Australian Research Council (ARC), the Crown-Of-Thorns Starfish Advisory Review Committee (COTSARC), and the Crown-Of-Thorns Starfish Research Committee (COTSREC).

Page

TABLE OF CONTENTS

ACKNOWLEDGEMENTS iv
LIST OF TABLES xiii
LIST OF FIGURES xiv
ABSTRACT xxv

CHAPTER ONE

INTRODUCTION 1

1.1 PHYSICAL OCEANOGRAPHY OF THE GREAT BARRIER REEF 2
1.1.1 The Cairns Section 2
1.1.2 The Central Section 4
1.1.3 An Overview of the Dynamics and Processes 4

1.2 LARVAL DISPERSAL, RECRUITMENT AND SPECIES DISTRIBUTIONS 6
1.2.1 Pelagic Larval Development 7
1.2.2 Recruitment 11
1.2.3 Cross-shelf and Regional Variation in Community Structure within the Great Barrier Reef 13

1.3 THE *ACANTHASTER* PHENOMENON 15
1.3.1 *Acanthaster planci* 15
1.3.1.1 Observations of a synchronous spawning of starfish 16
1.3.2 Patterns of Population Spread 17
1.3.3 Origin of Outbreaks 20
1.3.4 Cause of Outbreaks 21

1.4 RESEARCH OBJECTIVES 22

Page

CHAPTER TWO

MODELLING PROCEDURES 24

2.1 THE HYDRODYNAMIC MODEL 'SURGE' 24
2.1.1 Tides 27
2.1.2 Wind 31
2.1.3 East Australian Current 32

2.2 PARTICLE TRACKING 33
2.2.1 Advection of Particles 34
2.2.2 Particles as Larvae 35

2.3 FINE-SCALE CIRCULATION AND THE ENTRAINMENT OF LARVAE ONTO REEFS 36
2.3.1 Fine-scale Circulation Modelling 37
2.3.1.1 Implementation and forcings 37
2.3.2 Fine-scale Dispersal Modelling 39
2.3.3 Schematized Reefs 39
2.3.3.1 Reef shapes and sizes 40
2.3.3.2 Reef bathymetry and habitat 40
2.3.4 Simulating Larval Transport onto Reefs 41

2.4 METHODOLOGICAL APPROACH 41
2.4.1 The Northern Region 42
2.4.2 The Central Region 43
2.4.3 The Southern Region 45

Page

CHAPTER THREE

RESULTS 48

3.1 LARGE-SCALE HYDRODYNAMICS 48
3.1.1 Tides 48
3.1.1.1 Model validation 48
3.1.2 Wind 61
3.1.2.1 Patterns of wind-driven currents and model validation 61
3.1.2.2 Dynamics of wind-driven currents 68
3.1.3 East Australian Current 68
3.1.4 Summary and Conclusions 71

3.2 FINE-SCALE HYDRODYNAMICS 72
3.2.1 Flow Dynamics 72
3.2.2 Eddy Circulation 76
3.2.3 Applicability of Results 77

3.3 THE ENTRAINMENT OF LARVAE ONTO REEFS 78
3.3.1 Recruitment Variation within a Reef 78
3.3.2 Recruitment Variation between Reefs 81
3.3.3 Interpretation 83

3.4 ANALYSIS OF PARTICLE TRAJECTORIES AND REEF CONNECTIVITY 92
3.4.1 Distributing Probabilities - INSECT 92
3.4.2 Parameterization of Fine-scale Circulation and the Entrainment of Larvae onto Reefs 93

		Page
3.5	LARVAL DISTRIBUTIONS AND REEF CONNECTIVITY	94
3.5.1	The Northern Region	94
3.5.1.1	Cross-shelf connectivity	94
3.5.1.2	Long-shelf connectivity	101
3.5.1.3	Relative strength of connectivity	101
3.5.2	The Central Region	119
3.5.2.1	Cross-shelf connectivity	119
3.5.2.2	Long-shelf connectivity	123
3.5.2.3	Relative strength of connectivity	128
3.5.3	The Southern Region	145
3.5.3.1	Cross-shelf connectivity	145
3.5.3.2	Long-shelf connectivity	147
3.5.3.3	Relative strength of connectivity	154
3.5.4	An overview of the patterns of reef connectivity	155
3.6	SHORT PRE-COMPETENT PERIOD OF LARVAL DEVELOPMENT	171
3.6.1	The Northern Region	171
3.6.1.1	Cross-shelf connectivity	171
3.6.1.2	Long-shelf connectivity	171
3.6.1.3	Relative strength of connectivity	171
3.6.2	The Southern Region	172
3.6.2.1	Cross-shelf connectivity	172
3.6.2.2	Long-shelf connectivity	173
3.6.2.3	Relative strength of connectivity	174

Page

CHAPTER FOUR

SENSITIVITY TESTING 176

4.1 FINE-SCALE HYDRODYNAMICS AND LARVAL TRANSPORT 176
4.1.1 Fine-scale Hydrodynamics 177
4.1.1.1 Long-shelf currents 178
4.1.1.2 Cross-shelf tidal currents 178
4.1.2 Entrainment of Larvae onto Reefs 178
4.1.2.1 Long-shelf currents 179
4.1.2.2 Cross-shelf tidal currents 180
4.1.2.3 Distribution of habitat 180
4.1.2.4 Diffusion coefficients 182

4.2 LARGE-SCALE HYDRODYNAMICS AND LARVAL TRANSPORT 183
4.2.1 Reproducibility of Results 183
4.2.2 Time-varying Wind 185
4.2.2.1 Interpolated wind field 185
4.2.2.2 Response time of the hydrodynamic system 187
4.2.3 Larval Cloud Simulation 190
4.2.4 Number of Particles 191
4.2.5 Mortality on Reefs 200
4.2.6 Summary and Conclusions 201

4.3 THE APPROXIMATION OF PHYSICAL PROCESSES 203
4.3.1 Grid Scale 204
4.3.2 East Australian Current 204
4.3.3 Non-linear Interactions between the Hydrodynamic Forcing Components 205
4.3.4 Diffusion/dispersion 206

4.4 MODEL VALIDATION AND TESTING 207

Page

CHAPTER FIVE

DISCUSSION 274

5.1 PHYSICAL PROCESSES AND LARVAL DISPERSAL 277
5.1.1 Regional Scale Phenomena 277
5.1.1.1 Hydrodynamics 277
5.1.1.2 Larval distributions 278
5.1.2 Shelf Scale Phenomena 279
5.1.2.1 Hydrodynamcis 279
5.1.2.2 Larval distributions 279
5.1.3 Inter-reef Scale Phenomena 280
5.1.3.1 Hydrodynamics 280
5.1.3.2 Larval distributions 282
5.1.4 Recruitment 282

5.2 THE *ACANTHASTER* PHENOMENON 284
5.2.1 Source of Outbreaks 288
5.2.2 Pattern of Outbreaks 289
5.2.3 Path of Outbreaks 293
5.2.4 Cause of Outbreaks 296

5.3 CROSS-SHELF AND REGIONAL VARIATION IN COMMUNITY STRUCTURE 299
5.3.1 Cross-shelf Variation 300
5.3.2 Regional variation 303

5.4 LARVAL DISPERSAL AND LIFE-HISTORY THEORY 304
5.4.1 Environmental Predictability and Sources of Mortality 305
5.4.2 Duration of Larval Life 306

Page

5.5 THE APPLICATION OF HYDRODYNAMIC AND DISPERSAL MODELS TO THE MANAGEMENT OF MARINE RESOURCES 307
5.5.1 The *Acanthaster* Phenomenon 307
5.5.2 Zoning of the Great Barrier Reef Marine Park 308
5.5.3 Environmental Impact Assessment 310

5.6 SUMMARY AND CONCLUSIONS 312

REFERENCES 315

APPENDIX A 327

APPENDIX B 347

APPENDIX C 377

APPENDIX D 404

APPENDIX E 425

Page

LIST OF TABLES

CHAPTER TWO

Table 2.1 Listing of the 15 northern region source reefs from which dispersal events were simulated. 44

Table 2.2 Listing of the 15 central region source reefs from which dispersal events were simulated. 44

Table 2.3 Listing of the 12 southern region source reefs from which dispersal events were simulated. 47

CHAPTER FOUR

Table 4.1 Results of Wilcoxon Matched Pairs Test comparing base data with the simulation of a further 40 dispersal events (replicate) and the analysis of all 80 dispersal events combined. 184

Table 4.2 Results of Wilcoxon Matched Pairs Test comparing base data with the simulation of 40 dispersal events using an interpolated wind field and incorporation of the response time of the hydrodynamic system. 189

Table 4.3 Results of Wilcoxon Matched Pairs Test comparing base data with the simulation of 40 dispersal events represented by a small larval cloud and a large larval cloud. 191

Page

LIST OF FIGURES

CHAPTER ONE

Figure 1.1 Map of the Great Barrier Reef Marine Park indicating the Cairns and Central Sections. 3

CHAPTER TWO

Figure 2.1 Diagramatic representation of the simulation model of larval dispersal. 25

Figure 2.2 Model grid of the Cairns Section of the Great Barrier Reef Marine Park. 28

Figure 2.3 Model grid of the Central Section of the Great Barrier Reef Marine Park. 29

Figure 2.4 Arrangement of schematized reef shapes and sizes and their relationship to the hydrodynamic forcings. 38

Figure 2.5 Model representation of the particle release locations and the distribution of habitat. 41

Figure 2.6 Map showing the location of the 15 northern region source reefs from which dispersal events were simulated. 43

Figure 2.7 Map showing the location of the 15 central region source reefs from which dispersal events were simulated. 45

Figure 2.8 Map showing the location of the 12 southern region source reefs from which dispersal events were simulated. 46

CHAPTER THREE

Figure 3.1a Comparison of observed and predicted values of tidal elevation amplitude for the M2 lunar constituent within the Cairns Section of the GBR Marine Park. 49

Figure 3.1b Comparison of observed and predicted values of tidal elevation phase for the M2 lunar constituent within the Cairns Section of the GBR Marine Park. 50

Figure 3.2a Comparison of observed and predicted values of tidal elevation amplitude for the K1 diurnal constituent within the Cairns Section of the GBR Marine Park. 51

Figure 3.2b Comparison of observed and predicted values of tidal elevation phase for the K1 diurnal constituent within the Cairns Section of the GBR Marine Park. 52

Page

Figure 3.3a Comparison of observed and predicted values of tidal elevation amplitude for the M2 lunar constituent within the Central Section of the GBR Marine Park. 53

Figure 3.3b Comparison of observed and predicted values of tidal elevation phase for the M2 lunar constituent within the Central Section of the GBR Marine Park. 54

Figure 3.4a Comparison of observed and predicted values of tidal elevation amplitude for the K1 diurnal constituent within the Central Section of the GBR Marine Park. 55

Figure 3.4b Comparison of observed and predicted values of tidal elevation phase for the K1 diurnal constituent within the Central Section of the GBR Marine Park. 56

Figure 3.5 Tidal current ellipse showing the semi-major and the semi-minor axes. 58

Figure 3.6 Current ellipse axes predicted for the major semi-diurnal constituent M2 within the Cairns Section of the GBR Marine Park. 59

Figure 3.7 Current ellipse axes predicted for the major semi-diurnal constituent M2 within the Central Section of the GBR Marine Park. 60

Figure 3.8 Current vectors within the Cairns Section of the GBR Marine Park corresponding to steady-state 15 knot winds from the north. 62

Figure 3.9 Current vectors within the Cairns Section of the GBR Marine Park corresponding to steady-state 15 knot winds from the north-east. 63

Figure 3.10 Current vectors within the Cairns Section of the GBR Marine Park corresponding to steady-state 15 knot winds from the south-east. 64

Figure 3.11 Current vectors within the Cairns Section of the GBR Marine Park corresponding to steady-state 15 knot winds from the south-west. 65

Figure 3.12 Current vectors within the Central Section of the GBR Marine Park corresponding to steady-state 15 knot winds from the north. 66

Figure 3.13 Current vectors within the Central Section of the GBR Marine Park corresponding to steady-state 15 knot winds from the south-east. 67

Figure 3.14 Current vectors within the Cairns Section of the GBR Marine Park corresponding to flow associated with the East Australian Current. 69

Page

Figure 3.15 Current vectors within the Central Section of the GBR Marine Park corresponding to flow associated with the East Australian Current. 70

Figure 3.16 Representative plots of current vectors over a tidal cycle for reef type L2. 74

Figure 3.17 Current vectors representing the residual circulation around reef type L2. 77

Figure 3.18 Potential recruitment for all upstream particle releases from reef types P3 and L1. 79

Figure 3.19 Potential recruitment for all particle releases from reef types P4, L2, EL and NP. 79

Figure 3.20 Potential recruitment for all upstream particle releases from reef types L3, ML and P5. 80

Figure 3.21 Potential recruitment for all upstream particle releases from reef types R1 and R2. 80

Figure 3.22 Potential recruitment for all upstream particle releases from reef types P1 to P5. 82

Figure 3.23 Regression analysis of potential recruitment, averaged over all upstream particle releases from each of the schematized reefs, verses reef size. 83

Figure 3.24 Particle numbers per cell expressed as a percentage of the total number of particles released; 10 hours (a), 20 hours (b), and 30 hours (c) after release. 84

Figure 3.25 Particle numbers per cell expressed as a percentage of the total number of particles released; 10 hours (a), 20 hours (b), and 30 hours (c) after release. 85

Figure 3.26 Particle numbers per cell expressed as a percentage of the total number of particles released; 10 hours (a), and 20 hours (b) after release. 86

Figure 3.27 Particle numbers per cell expressed as a percentage of the total number of particles released; 10 hours (a), and 20 hours (b) after release. 88

Figure 3.28 Particle numbers per cell expressed as a percentage of the total number of particles released; 20 hours (a), and 30 hours (b) after release. 89

Figure 3.29 Particle numbers per cell expressed as a percentage of the total number of particles released; 10 hours (a), 20 hours (b), and 30 hours (c) after release. 90

Figure 3.30 Particle numbers per cell expressed as a percentage of the total number of particles released; 10 hours after release on the ebb tide (a), and the flood tide (b). 91

Page

Figure 3.31 Particle trajectories representing a single dispersal event originating from Opal Reef. 95

Figure 3.32 Particle trajectories representing a single dispersal event originating from Opal Reef. 96

Figure 3.33 Level of reef connectivity with respect to the cross-shelf transport of larvae within the northern_region for all source reefs. 97

Figure 3.34 Level of reef connectivity with respect to the cross-shelf transport of larvae within the northern region for each of the five outer matrix source reefs. 98

Figure 3.35 Level of reef connectivity with respect to the cross-shelf transport of larvae within the northern region for each of the five central matrix source reefs. 98

Figure 3.36 Level of reef connectivity with respect to the cross-shelf transport of larvae within the northern region for each of the five inner matrix source reefs. 99

Figure 3.37 Particle trajectories representing twenty dispersal events from Ribbon Reef No.2. 100

Figure 3.38 Level of reef connectivity with respect to the long-shelf transport of larvae within the northern region for all source reefs. 102

Figure 3.39 Level of reef connectivity with respect to the long-shelf transport of larvae within the northern region for each of the five outer matrix source reefs. 102

Figure 3.40 Level of reef connectivity with respect to the long-shelf transport of larvae within the northern region for each of the five central matrix source reefs. 103

Figure 3.41 Level of reef connectivity with respect to the long-shelf transport of larvae within the northern region for each of the five inner matrix source reefs. 103

Figure 3.42 Strength of connectivity with respect to Ribbon Reef No.9. 104

Figure 3.43 Strength of connectivity with respect to Ribbon Reef No.7. 105

Figure 3.44 Strength of connectivity with respect to Ribbon Reef No.5. 106

Figure 3.45 Strength of connectivity with respect to Ribbon Reef No.2. 107

Figure 3.46 Strength of connectivity with respect to Escape Reef. 108

Page

Figure 3.47 Strength of connectivity with respect to Mackay Reef. 109

Figure 3.48 Strength of connectivity with respect to Lark Reef. 110

Figure 3.49 Strength of connectivity with respect to reef No.15-047. 111

Figure 3.50 Strength of connectivity with respect to Emily Reef. 112

Figure 3.51 Strength of connectivity with respect to Evening Reef. 113

Figure 3.52 Strength of connectivity with respect to Forrester Reef. 114

Figure 3.53 Strength of connectivity with respect to Egret Reef. 115

Figure 3.54 Strength of connectivity with respect to Hope Island. 116

Figure 3.55 Strength of connectivity with respect to Pickersgill Reef. 117

Figure 3.56 Strength of connectivity with respect to Undine Reef. 118

Figure 3.57 Level of reef connectivity with respect to the cross-shelf transport of larvae within the central region for all source reefs. 121

Figure 3.58 Level of reef connectivity with respect to the cross-shelf transport of larvae within the central region for each of the five outer matrix source reefs. 122

Figure 3.59 Level of reef connectivity with respect to the cross-shelf transport of larvae within the central region for each of the five central matrix source reefs. 122

Figure 3.60 Level of reef connectivity with respect to the cross-shelf transport of larvae within the central region for each of the five inner matrix source reefs. 123

Figure 3.61 Particle trajectories representing twenty dispersal events from Channel Reef. 124

Figure 3.62 Particle trajectories representing twenty dispersal events from Green Island. 125

Figure 3.63 Level of reef connectivity with respect to the long-shelf transport of larvae within the central region for all source reefs. 126

Page

Figure 3.64 Level of reef connectivity with respect to the long-shelf transport of larvae within the central region for each of the five outer matrix source reefs. 126

Figure 3.65 Level of reef connectivity with respect to the long-shelf transport of larvae within the central region for each of the five central matrix source reefs. 127

Figure 3.66 Level of reef connectivity with respect to the long-shelf transport of larvae within the central region for each of the five inner matrix source reefs. 127

Figure 3.67 Particle trajectories representing twenty dispersal events from Batt Reef. 129

Figure 3.68 Strength of connectivity with respect to Opal Reef. 130

Figure 3.69 Strength of connectivity with respect to Norman Reef. 131

Figure 3.70 Strength of connectivity with respect to Flynn Reef. 132

Figure 3.71 Strength of connectivity with respect to Channel Reef. 133

Figure 3.72 Strength of connectivity with respect to Noggin Reef. 134

Figure 3.73 Strength of connectivity with respect to Tongue Reef. 135

Figure 3.74 Strength of connectivity with respect to Michaelmas Reef. 136

Figure 3.75 Strength of connectivity with respect to Thetford Reef. 137

Figure 3.76 Strength of connectivity with respect to Maori Reef. 138

Figure 3.77 Strength of connectivity with respect to Cayley Reef. 139

Figure 3.78 Strength of connectivity with respect to Batt Reef. 140

Figure 3.79 Strength of connectivity with respect to Upolu Reef. 141

Figure 3.80 Strength of connectivity with respect to Green Island. 142

Figure 3.81 Strength of connectivity with respect to Scott Reef. 143

Page

Figure 3.82 Strength of connectivity with respect to Howie Reef. 144

Figure 3.83 Level of reef connectivity with respect to the cross-shelf transport of larvae within the southern region for all source reefs. 147

Figure 3.84 Level of reef connectivity with respect to the cross-shelf transport of larvae within the southern region for each of the three outer matrix source reefs. 148

Figure 3.85 Level of reef connectivity with respect to the cross-shelf transport of larvae within the southern region for each of the three central matrix source reefs. 148

Figure 3.86 Level of reef connectivity with respect to the cross-shelf transport of larvae within the southern region for each of the three inner matrix source reefs. 149

Figure 3.87 Level of reef connectivity with respect to the cross-shelf transport of larvae within the southern region for each of the three nearshore source reefs. 149

Figure 3.88 Particle trajectories representing twenty dispersal events from Bramble Reef. 150

Figure 3.89 Particle trajectories representing twenty dispersal events from Pelorus Island. 151

Figure 3.90 Level of reef connectivity with respect to the long-shelf transport of larvae within the southern region for all source reefs. 152

Figure 3.91 Level of reef connectivity with respect to the long-shelf transport of larvae within the southern region for each of the three outer matrix source reefs. 152

Figure 3.92 Level of reef connectivity with respect to the long-shelf transport of larvae within the southern region for each of the three central matrix source reefs. 153

Figure 3.93 Level of reef connectivity with respect to the long-shelf transport of larvae within the southern region for each of the three inner matrix source reefs. 153

Figure 3.94 Level of reef connectivity with respect to the long-shelf transport of larvae within the southern region for each of the three nearshore source reefs. 154

Figure 3.95 Strength of connectivity with respect to Pith Reef. 156

Figure 3.96 Strength of connectivity with respect to Needle Reef. 157

Page

Figure 3.97 Strength of connectivity with respect to Bowl Reef. 158

Figure 3.98 Strength of connectivity with respect to Trunk Reef. 159

Figure 3.99 Strength of connectivity with respect to Arab Reef. 160

Figure 3.100 Strength of connectivity with respect to Grub Reef. 161

Figure 3.101 Strength of connectivity with respect to Otter Reef. 162

Figure 3.102 Strength of connectivity with respect to Bramble Reef. 163

Figure 3.103 Strength of connectivity with respect to John Brewer Reef. 164

Figure 3.104 Strength of connectivity with respect to Pelorus Island. 165

Figure 3.105 Strength of connectivity with respect to Pandora Reef. 166

Figure 3.106 Strength of connectivity with respect to Acheron Island. 167

Figure 3.107 Patterns of larval transport from December to March within the Cairns Section of the Great Barrier Reef Marine Park. 169

Figure 3.108 Patterns of larval transport from December to March within the Central Section of the Great Barrier Reef Marine Park. 170

Figure 3.109 Level of reef connectivity with respect to the cross-shelf transport of short pre-competent period larvae within the northern region for all source reefs. 172

Figure 3.110 Level of reef connectivity with respect to the long-shelf transport of short pre-competent period larvae within the northern region for all source reefs. 173

Figure 3.111 Level of reef connectivity with respect to the cross-shelf transport of short pre-competent period larvae within the southern region for all source reefs. 174

Figure 3.112 Level of reef connectivity with respect to the long-shelf transport of short pre-competent period larvae within the southern region for all source reefs. 175

Page

CHAPTER FOUR

Figure 4.1 Potential recruitment, averaged over all upstream particle releases, with respect to long-shelf current strength for reef type L2. 179

Figure 4.2 Potential recruitment, averaged over all upstream particle releases, with respect to the maximum cross-shelf tidal current speed for reef type L2. 181

Figure 4.3 Potential recruitment, averaged over all upstream particle releases, with respect to the distribution of habitat for reef type L2. 181

Figure 4.4 Potential recruitment, averaged over all upstream particle releases, with respect to different diffusion coefficients for reef type L2. 182

Figure 4.5 Level of reef connectivity with respect to the cross-shelf and long-shelf transport of larvae from Ribbon Reef No.5 for seven sensitivity analyses. 192

Figure 4.6 Level of reef connectivity with respect to the cross-shelf and long-shelf transport of larvae from Ribbon Reef No.2 for five sensitivity analyses. 193

Figure 4.7 Level of reef connectivity with respect to the cross-shelf and long-shelf transport of larvae from Evening Reef for seven sensitivity analyses. 194

Figure 4.8 Level of reef connectivity with respect to the cross-shelf and long-shelf transport of larvae from Pickersgill Reef for five sensitivity analyses. 195

Figure 4.9 Level of reef connectivity with respect to the cross-shelf and long-shelf transport of larvae from Opal Reef for seven sensitivity analyses. 196

Figure 4.10 Level of reef connectivity with respect to the cross-shelf and long-shelf transport of larvae from Norman Reef for six sensitivity analyses. 197

Figure 4.11 Level of reef connectivity with respect to the cross-shelf and long-shelf transport of larvae from Michaelmas Reef for six sensitivity analyses. 198

Figure 4.12 Level of reef connectivity with respect to the cross-shelf and long-shelf transport of larvae from Green Island for seven sensitivity analyses. 199

Figures 4.13a to **g** Strength of connectivity with respect to Ribbon Reef No.5 for the base data and six sensitivity analyses. 209

Page

Figures 4.14a to **e** Strength of connectivity with respect to Ribbon Reef No.2 for the base data and four sensitivity analyses. 216

Figures 4.15a to **g** Strength of connectivity with respect to Evening Reef for the base data and six sensitivity analyses. 221

Figures 4.16a to **e** Strength of connectivity with respect to Pickersgill Reef for the base data and four sensitivity analyses. 228

Figures 4.17a to **g** Strength of connectivity with respect to Opal Reef for the base data and six sensitivity analyses. 233

Figures 4.18a to **f** Strength of connectivity with respect to Norman Reef for the base data and five sensitivity analyses. 240

Figures 4.19a to **f** Strength of connectivity with respect to Michaelmas Reef for the base data and five sensitivity analyses. 246

Figures 4.20a to **g** Strength of connectivity with respect to Green Island for the base data and six sensitivity analyses. 252

Figure 4.21 Comparison of a base data particle trajectory with one simulated using an interpolated wind field . 259

Figure 4.22 Comparison of a base data particle trajectory with one simulated using an interpolated wind field. 260

Figure 4.23 The trajectories of all 40 dispersal events representing the base data analysis. 261

Figure 4.24 The trajectories of all 40 dispersal events representing the response time analysis. 262

Figure 4.25 Level of reef connectivity with respect to the cross-shelf and long-shelf transport of larvae from Opal Reef for larval clouds represented by 7, 13 and 25 particles. 263

Figure 4.26a to **c** Strength of connectivity with respect to Opal Reef larval clouds represented by 7, 13 and 25 particles. 264

Figure 4.27 The trajectories of 7 particles representing a single dispersal event from Opal Reef. 267

Figure 4.28 The trajectories of 13 particles representing a single dispersal event from Opal Reef. 268

Figure 4.29 The trajectories of 25 particles representing a single dispersal event from Opal Reef. 269

Page

Figure 4.30 Level of reef connectivity with respect to the cross-shelf and long-shelf transport of larvae from Opal Reef for three analyses (base data, 50% mortality and 100% mortality factors). 270

Figure 4.31 Level of reef connectivity with respect to the cross-shelf and long-shelf transport of larvae from Norman Reef for three analyses (base data, 50% mortality and 100% mortality factors). 171

Figure 4.32 Level of reef connectivity with respect to the cross-shelf and long-shelf transport of larvae from Michaelmas Reef for three analyses (base data, 50% mortality and 100% mortality factors). 272

Figure 4.33 Level of reef connectivity with respect to the cross-shelf and long-shelf transport of larvae from Green Island for three analyses (base data, 50% mortality and 100% mortality factors). 273

CHAPTER FIVE

Figure 5.1 Particle trajectories representing thirty dispersal events from Opal and Tongue Reefs. 281

Figure 5.2 Particle trajectories, representing a single dispersal event originating from Green Island. 285

Figure 5.3 Reef connectivity representing a single dispersal event originating from Green Island. 286

Figure 5.4 Reef connectivity representing a single dispersal event originating from Green Island. 287

Figure 5.5 Strength of connectivity with respect to St. Crispin Reef. 295

ABSTRACT

This research was motivated by debate surrounding the causes of population fluctuations of the crown-of-thorns starfish *Acanthaster planci* within the Great Barrier Reef (GBR), Australia. The patterns of *Acanthaster* population spread have led to the widespread belief that the propagation of populations is by means of larval dispersal, and that population fluctuations are strongly influenced by larval recruitment. The spatial and temporal scales over which larvae disperse, and of the *Acanthaster* phenomenon itself, pointed to the need for a more complete picture of the large-scale dynamics of water motion and larval dispersal. The research aimed to investigate the relationship between reefs (reef connectivity) which results from pelagic larval dispersal. Modelling has provided the only feasible approach to this problem.

An understanding of the observed patterns of *Acanthaster* population spread throughout the GBR has necessitated the development of numerical models which are capable of simulating the hydrodynamics associated with large assemblages of reefs over the time scale of larval dispersal. The model is modular in design and has incorporated the principal processes forcing water circulation within the GBR. Its development has required a new modelling approach which pays attention to the geometric representation of reef structure and the large-scale dynamics of water motion, while incorporating the fine-scale features of water circulation over and around individual reefs. The particle tracking component of the model uses a Lagrangian 'marker and cell' technique which runs under time-dependent tidal flow and a randomly varying wind field based upon an historical record. The entrainment of larvae from the mainstream water circulation into the near-field circulation of reefs is incorporated into the dispersal model through a parameterization scheme based on schematized reefs. Attention has been paid to the accurate representation of the dynamics of water motion.

This study identifies hydrodynamic processes which result in distinctive patterns of larval dispersal and recruitment at three

spatial scales: (1) regional scale (100s kilometres); (2) shelf scale (10s kilometres); and (3) inter-reef scale (kilometres). Regional scale variation may result in differences in the level and pattern of recruitment and, therefore, in population density and age-structure. Shelf scale variation can result in passive mechanisms which both concentrate and separate larval pools, which in turn can account for some of the cross-shelf variation in species abundance and community structure that has been documented. Inter-reef scale variation results in differences in potential recruitment of larvae to coral reefs as a consequence of a combination of both stochastic and deterministic factors, including reef size and shape, the location of trajectory intercept with respect to the reef edge, and the state of the tide.

Model simulations of the large-scale patterns of larval dispersal and reef connectivity are compared with the distribution of adults and the observed pattern of *Acanthaster* population spread throughout the central GBR. Results provide a physical explanation for many of the observed features of *Acanthaster* population spread throughout the region. These include: (1) identification of a source region from which *Acanthaster* populations are proposed to have spread; (2) the apparent southward spread of populations from this region; (3) the high incidence of outbreaks on mid-shelf reefs south from Green Island; (4) the susceptibility of particular reefs to repeated recruitment, notably Green Island and many others which border the main lagoon; and (5) the cessation of outbreaks causing high coral mortality throughout the mid-shelf reefs within the Central Section of the Marine Park. The high incidence of outbreaks on inner matrix reefs south from Green Island can be explained as a purely physical phenomenon, without the need to invoke human interference in the ecology of these more accessible reefs.

Model results are also applied to other issues, including cross-shelf and regional variation in community structure, life-history theory and the management of tropical marine resources. Variation in larval transport and reef connectivity is believed to be reflected in regional and cross-shelf differences in community structure and population abundance of many species of invertebrate and fish within the central

GBR. Larval dispersal and recruitment to coral reefs is shown to be a highly unpredictable and variable process. Inappropriate scales of dispersal and predation by reef-associated species are identified as potentially significant sources of larval mortality during the dispersal phase of many tropical marine species. There appears to be a decided disadvantage to extending the pre-competent period of larval development beyond a relatively short period of 4 days if predation within the pelagic environment or from reef-associated species is intense. Consideration of how physical oceanographic processes might interact with life-history characteristics, and thereby influence species distributions and dynamics, is identified as a potentially rewarding area for future research.

Larval dispersal models are well suited to management issues and applications. Most coral reef invertebrates and fish have a pelagic larval phase to their life-cycle, during which they have the potential to disperse quite widely. Recruitment from this larval pool is likely to structure communities and influence the population abundance of many species. On this basis, models which are capable of predicting reef connectivity can provide a stronger, and more rational, biological basis for the management of tropical marine resources.

CHAPTER ONE

INTRODUCTION

Understanding of many biological phenomena requires the integration of material from diverse disciplines, and of processes which are manifest at widely varying spatial and temporal scales. A modelling approach to understanding such phenomena is frequently both cost efficient and effective. Modelling provides the opportunity to investigate processes and provide understanding in a way which is frequently not logistically or economically feasible by the collection of field data alone. An understanding of larval dispersal is one example. The development and application of models of larval dispersal to the *Acanthaster* phenomenon has provided the motivation for the research which is documented here.

The crown-of-thorns starfish *Acanthaster planci* (Linnaeus, 1758) has risen to notoriety over the past three decades as a result of the extensive damage inflicted by large aggregated populations on coral reefs. Adults of *A. planci* feed primarily on the polyps of corals, and through the complex interactions and interdependence of coral reef communities have influenced the distribution and abundance of other organisms (Moran, 1986).

Debate surrounding the causes of population fluctuations of *A. planci* that have been observed within the Great Barrier Reef (GBR) region since the early 1960s has largely been centred around the issue of whether they are natural or human-influenced phenomena. The importance of resolving these alternatives is embodied within Australian Government legislation, through the Great Barrier Reef Marine Park Act and obligations of the Government to protect the National Estate and World Heritage values of the GBR. The patterns of *Acanthaster* population spread, both within the GBR and through the Ryukyu Islands to Japan, have led to a widespread belief that the propagation of populations is by means of larval dispersal (e.g., Kenchington, 1977; Williams et al., 1984; Moran, 1986; Yamaguchi, 1986; Birkeland & Lucas, 1990). The temporal and

spatial scales over which larvae disperse (weeks and many kilometres), and of the *Acanthaster* phenomenon itself (years and hundreds of kilometres), point to the need for a more complete picture of the dynamics of water motion and dispersal processes at the relevant scales.

This chapter will review the physical oceanographic processes which transport larvae, the biological implications of larval dispersal and the *Acanthaster* phenomenon.

1.1 PHYSICAL OCEANOGRAPHY OF THE GREAT BARRIER REEF

Acanthaster activity within the GBR region has been largely restricted to the Cairns and Central Sections of the GBR Marine Park (see Fig. 1.1). This region is the focus of the models and research that are presented here.

1.1.1 The Cairns Section

The Cairns Section is of particular interest as it is within this region that, during the two recorded episodes of *Acanthaster* activity, large populations were first observed. More importantly, the central area to the north of Green Island, which lies off Cairns, has been implicated as the source of primary outbreaks from which secondary outbreaks have developed farther to the south (Kenchington, 1977).

The physical organization of the Cairns Section is both distinct with respect to surrounding regions and diverse in reef structure. Its northern portion is characterized by an almost continuous chain of narrow ribbon reefs along the outer edge of the continental shelf which is estimated to have a linear density of around 80% (G. Pickard, pers. comm.). Water depth increases rapidly beyond the shelf edge. The relatively dense reef matrix behind the ribbon reefs extends across almost the entire shelf width, leaving only a narrow lagoon separating it from the mainland. The southern area, in contrast, has a linear density of shelf edge reefs estimated to be upwards of 10% (Pickard et al., 1977; G. Pickard, pers. comm.) and a

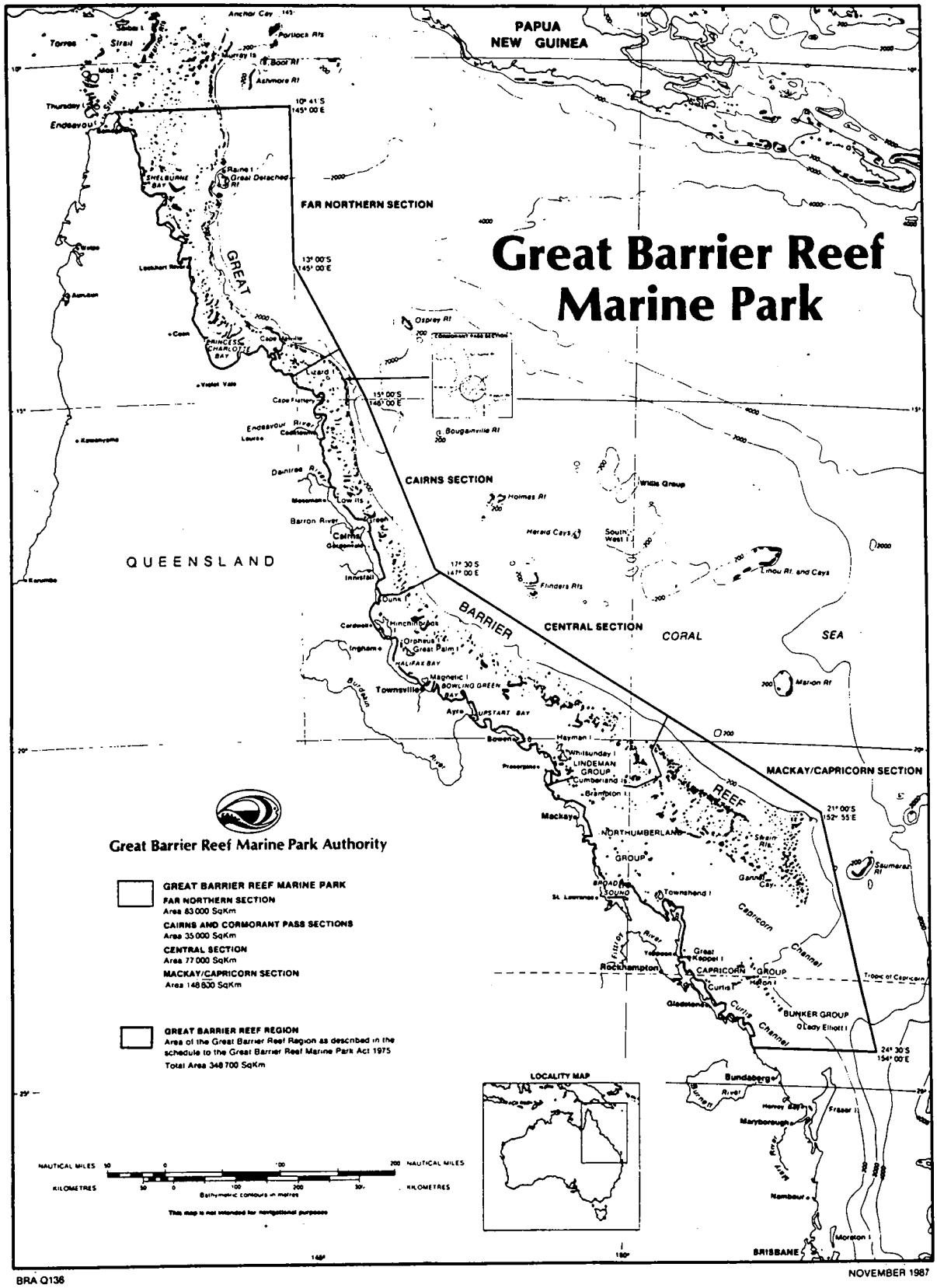


Figure 1.1 Map of the Great Barrier Reef Marine Park indicating the Cairns and Central Sections.

well developed lagoon between the reef matrix and coastline. In this southern portion the shelf broadens and the water depth increases, while beyond the shelf edge the continental slope is more gradual.

1.1.2 The Central Section

The physical organization of the Central Section is, in many respects, similar to that of the southern portion of the Cairns Section. It has a linear density of shelf edge reefs estimated to be upwards of 10% (Pickard et al., 1977) and a well developed lagoon between the reef matrix and coastline. However, in the Central Section, both the main lagoon and the shelf broaden still further, water depth continues to increase across the shelf, and beyond the shelf edge the continental slope is still more gradual. The reef matrix within the Central Section is, in general, less dense. Towards the southern end of the Central Section there is a further change in shelf topography; reefs in this region are more massive, with those along the shelf edge estimated to have a linear density of around 90% (Pickard et al., 1977).

It is precisely these characteristics (bathymetry, reef density and shelf width) which have been identified as the major determinants of circulation patterns on continental shelves (Allen, 1980; Wolanski et al., 1986; Middleton, 1987; Andrews & Bode, 1988). Regional differences in circulation, as a consequence of such variation in these physical characteristics, could result in significant differences in the movement of larvae (Frith et al., 1986).

1.1.3 An Overview of the Dynamics and Processes

While Pickard et al. (1977) in their review of the physical oceanography of the GBR noted a paucity of good information on water currents, subsequent physical oceanographic studies have provided more insight into the dynamics and identification of the major processes forcing water circulation within the region. Recent research includes Andrews and Gentien (1982), Andrews (1983), Wolanski and Bennett (1983), Wolanski and Pickard (1985), Andrews and Furnas (1986) and Church (1987). However, while many of these field studies have been based on long time series, currents are

recorded only at discrete points within a topographically complex system. In spite of these studies, there has been little attempt within the physical oceanographic literature to place in perspective the relative importance of the distinct processes or to understand the impact that the dynamics of water motion will have on larval dispersal and other biological processes.

Current meter recordings from within the central GBR region have determined the spectrum of water motions which have the most prominent roles in the dispersal process. These are identified as: (1) low frequency, essentially barotropic, flow associated with the East Australian Current (EAC); (2) shorter period, although still essentially low frequency, wind-forced currents; and (3) considerably higher frequency tidal flow (Wolanski & Pickard, 1985; Andrews & Bode, 1988).

The large-scale picture of water motion derived from field studies is one of diversity and complexity. The longer period circulation dominates within the main passages over the continental shelf and is predominantly longshore, parallel to the isobaths. The direction (poleward or equatorward) fluctuates with periods of several days to months and is strongly correlated with the longshore wind component. Observations both within the main lagoon and near the shelf edge suggest that there is considerable modulation of currents by the wind and that this general picture is coherent from site to site (Wolanski & Pickard, 1985). In contrast, currents within the relatively dense reef matrix are directed topographically and do not correlate with the wind (Wolanski & Pickard, 1983). Tidal currents are predominantly cross-isobath (Andrews & Bode, 1988).

To date the best estimates of larval advection within the region have been limited to progressive vector plots (e.g., Andrews, 1983; Williams et al., 1984; Frith et al., 1986). While such estimates may be based on data from a number of moorings, they cannot account for the spatial variation in the current field due to changing bathymetry and reef geometry, nor the longer term temporal variability within the system. Low frequency forcing of water motion, including current modulation and reversals as a result of synoptic-scale meteorological

forcing, results in variability over several temporal scales. The neglect of such spatial and temporal variation leads to an over-simplified view of dispersal processes. In such physically complex environments as the GBR, progressive vector plots must be interpreted with caution. More recently, Parslow and Gabric (1989) have modelled the advection and dispersion of larvae through an idealized representation of the central GBR. Their emphasis was on the relative dispersion of larvae within a patch, rather than a realistic representation of advection. Numerical hydrodynamic models provide the only feasible approach to understanding the dynamics of dispersal processes and their impact upon recruitment at the same spatial and temporal scales as the biological phenomena under investigation. Yet, models capable of simulating the dispersal of larvae over large spatial and temporal scales have not previously been developed.

The models presented here are an attempt to overcome the limitations in our understanding of the impact of meso-scale processes on larval dispersal within a physically complex reef system. The models provide both a qualitative and quantitative description of large-scale patterns of water circulation and larval transport within the Cairns and Central Sections of the GBR Marine Park.

1.2 LARVAL DISPERSAL, RECRUITMENT AND SPECIES DISTRIBUTIONS

Over recent years, interest in larval dispersal and recruitment processes within coral reef systems has greatly increased. This has resulted in an awareness that these same processes may be largely responsible for the maintenance of species distributions and community structure that have been documented within the GBR (Done 1982; Williams & Hatcher 1983; Sale et al. 1984). *A. planci*, like most coral reef invertebrates and fish, has the potential to disperse quite widely as pelagic larvae. Recent advances in our understanding of the population structure of many coral reef fish and invertebrates suggest a relationship between the physical

oceanographic processes which transport larvae, recruitment pulses and population abundance (Doherty & Williams, 1988a).

1.2.1 Pelagic Larval Development

Various classifications of larval developmental types have been proposed, however, four general categories are commonly recognized in marine benthic organisms (Thorson, 1950; Jablonski & Lutz, 1983; Day & McEdward, 1984). These are: pelagic development; demersal development; direct development; and viviparity. In the former category, pelagic, all growth and development occurs in the plankton. Demersal development larvae, in addition to their period of growth and development in some attached form of egg mass, may also undergo additional growth and development in the plankton. Pelagic larval development has been further sub-divided into various types by a number of authors (e.g., Thorson, 1950; Jablonski & Lutz, 1983; Scheltema & Williams, 1983). Thorson (1950) identified pelagic larval development as the most common type in Recent seas, estimating that it was characteristic of 80% to 85% of all tropical species. More recent research within the GBR has identified more than 133 species of scleractinian coral (Babcock et al., 1986; Willis & Oliver, 1988) and 43 species of reef fish (Brothers et al., 1983) with pelagic larval development. The duration of larval life for these species varies between 4 days and 12 weeks. There are, without doubt, many more species with pelagic larval development as Leis and Goldman (1987) collected pelagic larval fishes representing 96 families from the GBR near Lizard Island. Pelagic larval development is clearly characteristic of most coral reef fishes and scleractinian corals.

There is considerable debate over the adaptive significance of pelagic larval development. Thorson (1950) argued that dispersal and the opportunity to find a suitable habitat (i.e., increased gene flow and geographic range) were of primary importance, followed by feeding on the plankton. Other authors have since proposed that the ability to exploit spatial and temporal patchiness in the adult environment (Vance, 1973; Strathmann, 1974), and predation avoidance (Johannes, 1978) are the most significant selection pressures which

provide a short term advantage to dispersal. Johannes (1978) argues that the reproductive behaviour of many reef fish favours the transport of eggs and larvae away from their source reef, at least initially. He proposes that the adaptive advantage of this is reduced predation pressure in the pelagic environment away from coral reefs, and that this is more important than the availability of food in influencing such behaviour. Barlow (1981) rejects both feeding on the plankton and predation avoidance as the most significant selection pressures and favours selection based on adult survival due to life in a patchy and unpredictable environment. This emphasis on adult survival has been questioned by Doherty et al. (1985) who argue that the selection advantage could lie with patchy and unpredictable survival in the pelagic environment, mediated principally by food availability. Iteroparity in spawning behaviour (a series of separate spawnings over a single season) may also be an adaptation to unpredictable survival in the pelagic environment (Murphy, 1968; Stearns, 1976).

A simple comparison between fecundity and recruitment for almost any reef species illustrates that larval mortality must be very high (Sale, 1980). Thorson (1950) estimated that 99% or more of larvae die prior to settlement. He identified predation while in the plankton and starvation as the major sources of mortality. Other sources of mortality have been identified as physical environmental factors (e.g., temperature and salinity) and inappropriate scales of dispersal (Day & McEdward, 1984). Daily mortality rates due to predation have been estimated to range between 10% and 57% (Jones & Hall, 1974; Fortier & Leggett, 1985). Predation pressure over reefs by suspension feeding invertebrates and planktivorous fish may be still more intense (Glynn, 1973; Hamner et al., 1988; Westneat & Resing, 1988). A number of authors have rejected starvation as a significant source of larval mortality (e.g., Vance, 1973; Christensen & Fenchel, 1979; Sale, 1980; Olson, 1987; Olson & Olson, 1989) while others have considered it to be a major cause of larval mortality (e.g., Birkeland 1982; Lucas, 1982; Leiby, 1984).

Thorson (1950) considered fertilization success to be a relatively minor source of mortality in eggs. Yet, it may not always be

insignificant. Pennington (1985) has shown that, for the echinoid *Strongylocentrotus droebachiensis*, fertilization success may be as low as 15% when conditions aid dilution or as high as 95%, both at relatively dense sperm concentrations. At low sperm concentrations or adult densities, fertilization success may be extremely low or negligible (Lucas, 1986). Oliver and Willis (1987) report that over 99% of coral eggs and embryos within coral-spawn slicks were dead, although such high mortality was not observed in later studies where 90% of eggs and larvae were found to be alive (Willis & Oliver, 1988).

Two stages to pelagic larval development are recognized: a pre-competent period - a time for growth and development; and a competent period - a time to delay settlement and metamorphosis while in search of a habitat. The duration of both pre-competent and competent periods varies markedly between species. The factors controlling the delay capability of larvae and subsequent success at settlement and metamorphosis are not well understood (Day & McEdward, 1984) and few generalizations are evident.

There is an assumption within most discussions of the adaptive significance of pelagic larval dispersal that most, if not all, larvae are dispersed away from their parents' habitat. However, dispersal away from the source reef has not been taken for granted by coral reef ecologists (e.g., Williams et al., 1984; Wolanski et al., 1989). There has been much speculation about the role of oceanographic features, such as eddies, gyres and seasonal current reversals, in retaining or returning larvae to their source (e.g., Watson & Leis, 1974; Johannes, 1978; Leis, 1986). Johannes argued that the elaborate spawning behaviour of many coral reef fishes maximizes the opportunity for return of the larvae to their point of origin. However, within coral reef systems such as the GBR these physical oceanographic features are unpredictable and of short duration (Williams et al., 1984).

Oceanographic field studies and hydrodynamic modelling have identified physical mechanisms for larval retention around reefs or groups of reefs (e.g., Black, 1988; Wolanski et al., 1989), but little consideration has been given to increased mortality as a consequence of exposure, for extended periods of time, to predation by reef

invertebrates and fish. Sammarco and Andrews (1988) concluded, on the basis of a correlation between coral recruitment and low residual circulation patterns, that coral reefs appeared to be self-seeding. However, their argument is weak as such patterns could equally result from larvae approaching from the far-field. Their results do suggest the possibility that fine-scale features of water circulation around reefs might influence spatial patterns of coral recruitment. The influence of hydrodynamics on the location of initial recruitment is also proposed by Black and Moran (pers. comm.) for *A. planci*. Several studies have, nevertheless, provided strong support for the dominant role of inter-reef dispersal of corals (e.g., Wallace, 1985a; Willis & Oliver, 1988; Harriott & Fisk, 1988). Willis and Oliver (1988) point out that coral larvae, which have a pre-competent period of only four days, may be retained around the source reef in relatively low numbers under light wind conditions.

While the relative importance of larval retention versus influx from other reefs has not been clearly determined, available data suggest that most pelagic eggs and larvae will be advected off their natal reef (Williams et al., 1984; Bull, 1986; Harriott and Fisk, 1988; Willis & Oliver, 1988; Wolanski et al., 1989) and transported by mainstream water circulation.

Larvae of most coral reef invertebrates and many fish are thought to be dispersed as passive particles, since the speed at which they can swim is far lower than that of the water currents by which they are transported. Also, it seems unlikely that most larvae could detect the presence of a reef until they were very close (Sale, 1980). While this may be a reasonable generalization, larval behaviour, such as vertical migration, can significantly affect the distance and direction of transport (Phillips, 1981; Rothlisberg et al., 1983). Controlled diurnal vertical migration has not been documented for any species of reef fish (Goldman et al., 1983), although Leis (1986) reports that many prefer deeper water during the day and move upward at night. Larval distributions of some fish within the GBR nevertheless display patterns which are not consistent with totally passive dispersal (Leis et al., 1987), particularly for more specialized or older larvae (Leis & Goldman, 1987) which may be able to cue on physical oceanographic

features to maintain position.

In summary, pelagic larvae are generally considered to be the most important dispersive stage in the life-cycle of most benthic invertebrates and fish and their dispersal patterns are important determinants of patterns of recruitment and species distribution (Sale, 1980; Day & McEdward, 1984). On this point, Williams et al. (1986) postulate that the cross-shelf distribution of many species of coral reef fish within the central GBR is largely determined during the larval dispersal phase of their life-cycle.

1.2.2 Recruitment

The degree to which the size and structure of benthic populations are determined by recruitment limitation and/or density-dependent factors involving the established population continues to be discussed and debated (Doherty & Williams, 1988b; Keough, 1988; Warner & Hughes, 1988). Doherty and Williams (1988a,b) argue that recruitment limitation and density-independent mortality are most consistent with the available database for coral reef fish populations. However, Warner and Hughes (1988) argue that density-dependence may also act to control the population abundance of some species and that the focus should be on the relative importance of recruitment limitation, density-independent mortality and density dependence. Population dynamics models which aim to distinguish between recruitment limitation and density-dependence show sensitivity to both variable recruitment and density-independent post-settlement mortality. Warner and Hughes (1988) highlight the importance of research which investigates the causes of variable recruitment and density-independent post-settlement mortality.

Patterns of recruitment of coral reef organisms have been best documented for fish and scleractinian corals. Recruitment of coral reef fish has been recently and thoroughly reviewed by Doherty and Williams (1988a). They identify patterns of recruitment for a variety of reef fish, mostly pomacentrids, over a range of spatial and temporal scales. These patterns include: (1) pulses of recruitment, often lasting several days; (2) a degree of coherence in these pulses to adjacent

reefs, particularly in the long-shore direction; (3) consistently higher or lower recruitment densities to particular reefs, while others show extreme variation both spatially and temporally; and (4) regional and cross-shelf scale differences in the density of recruitment.

Only two studies within the GBR have documented between-reef variation in coral recruitment for species with pelagic larvae. Sammarco (1983) compared recruitment densities, based on two depths at a single site, for three reefs lying across the continental shelf within the Central Section of the GBR Marine Park. Overall, he found that coral settlement was greatest and most consistent on the mid-shelf reef. Fïlk & Harriott (1990) compared recruitment densities, based on a single depth at four sites, for three adjacent mid-shelf reefs over two summers. They found order of magnitude differences in recruitment between reefs, with Green Island having consistently higher levels of recruitment over both years. The low coral abundance on Green Island, which had the highest level of recruitment, provided strong evidence for the dominant role of inter-reef dispersal of corals.

Wallace (1985a,b), in contrast, documents within-reef and inter-annual variation in coral recruitment to Big Broadhurst Reef. She notes significant inter-annual variation in the overall level of recruitment, but a quite consistent pattern in the relative levels of recruitment between depths at a single site. Other studies of coral recruitment have concentrated on within-reef differences between sites over a single season (e.g., Harriott, 1985; Babcock, 1988; Sammarco & Andrews, 1988). The between and within-reef variation in recruitment densities are reported to be roughly equal, and therefore illustrate that caution must be exercised in comparing single sites between reefs. Observed differences may simply reflect the choice of sites, and not recruitment densities overall.

Recruitment patterns in most benthic invertebrates are characterized by extreme spatial and temporal variability (Keough, 1988), and echinoderms are no exception (Ebert, 1983; Bak, 1985). Recruitment of *A. planci* has been documented by Zann et al. (1987,1990) from Fiji and Doherty and Davidson (1988) from the GBR, both of which

showed considerable variablity. Both studies also report massive recruitment of a single year-class which continued to dominate the population structure despite high mortality.

The most parsimonious explanation for the spatial and temporal variation in recruitment that has been documented is that it results from the passage of occasional dense patches of larvae over and around reefs (Victor, 1986; Doherty & Williams, 1988a). Although there is substantial agreement that physical oceanographic processes will influence recruitment through larval transport, the degree to which they do so is unclear. While considerable progress has been made in documentation of the spatial and temporal patterns in recruitment and our understanding of the processes, models of larval dispersal have been inadequate for a more critical assessment of the role of hydrodynamics.

1.2.3 Cross-shelf and Regional Variation in Community Structure within the Great Barrier Reef

Large-scale surveys within the Central Section of the GBR Marine Park have established that there are major changes in the composition of communities across the continental shelf from the nearshore to outer shelf (Done, 1982; Williams, 1982; Birtles & Arnold, 1983; Dinesen, 1983; Williams & Hatcher, 1983; Sammarco & Crenshaw, 1984; Hammond et al., 1985; Wilkinson, 1986). Species density and diversity are reported to be greatest on mid-shelf reefs for corals (Done, 1982; Dinesen, 1983), fish (Williams & Hatcher, 1983; Williams et al., 1986) and holothurians (Hammond et al., 1985). The trophic structure of fish communities is also reported to vary across the shelf, with planktivorous fish being most abundant on mid-shelf reefs, while still relatively plentiful on inner-shelf or nearshore reefs (Williams & Hatcher, 1983). Wilkinson and Cheshire (1988) summarize much of the literature on cross-shelf distributions within the central GBR.

This cross-shelf change in the biotic communities is accompanied by a major gradient in the physical and chemical environment (e.g., salinity, turbidity, wave energy, nutrients). It is reasonable to

assume that such variation in the physical and chemical environment could determine or, at least, influence cross-shelf zonation, either directly through survivorship of juveniles or adults, or indirectly through competitive interactions. Williams and Hatcher (1983) observe that the proximate causes of the observed distributions could act at various stages of the life cycle, and that the patterns could result from: (a) differential availability of larvae across the shelf; (b) patterns of settlement and habitat selection by postlarvae; or (c) differential survivorship after settlement.

It has been argued that, while mainstream currents are predominantly along-shore, there exist within the central region of the GBR physical mechanisms which should aid the wide dispersal of pelagic larvae (Williams et al., 1986). Yet, recruitment of juveniles to both coral (Sammarco, 1983) and fish (Williams et al., 1986) communities across the continental shelf within the Central Section strongly mirrors the distribution of adult populations. Furthermore, the distribution of mature fish larvae from nearshore and mid-shelf communities similarly reflects the distribution of adults (Williams et al., 1986). On this basis, Williams et al. (1986) conclude that adult distributions are largely determined during the larval dispersal phase of the life cycle. The uneven distribution might therefore result either from limited cross-shelf dispersal, differential larval survivorship or habitat selection by larvae. Williams et al. (1986) favour either differential larval survivorship or habitat selection by larvae on the basis that physical oceanographic processes should promote the widespread dispersal of larvae.

Regional variation in community structure along the GBR has also been reported for corals (Done, 1983) and fish (Williams, 1983; Williams et al., 1986). Done (1983) notes similarities in the community structure of scleractinian corals from mid and outer-shelf reefs in the Central Section to that of inner reefs from the Pompey complex further to the south. Similarities are also noted between the outer Pompey reefs and inner and outer Swain reefs within the Capricorn Section of the GBR Marine Park. Somewhat similar patterns are also evident for fish (Williams, 1983). Insufficient physical and biological data are presently available to permit

plausible hypotheses to be formulated regarding the proximate causes of variation in the observed long-shelf distributions and the possible role of hydrodynamic processes.

1.3 THE *ACANTHASTER* PHENOMENON

The *Acanthaster* phenomenon has been reviewed by Potts (1981), Moran (1986) and, most recently, by Birkeland and Lucas (1990). Only relevant or more recent references are included in this synopsis.

1.3.1 *Acanthaster planci*

The reproductive characteristics of *A. planci* are, in general, well understood. Moran (1986) notes that *A. planci* is gonochoristic and reproduces sexually by spawning eggs and sperm into the water column where fertilization takes place externally. Spawning within the GBR is believed to occur during December and January (Moran, 1986) on repeated occasions (Birkeland & Lucas, 1990; see also Section 1.3.1.1 below) and may involve large aggregations of starfish (pers. obs.). Birkeland and Lucas (1990) observe that there does not appear to be any tidal, lunar or diel periodicity in spawning. The fecundity of *A. planci* increases rapidly with size, and may be as high as 60 million eggs in individuals a little over 40 cm in diameter (Kettle & Lucas, 1987). Kettle and Lucas (1987) note, as a consequence, that the total fecundity of a population will vary markedly not only with the number of females, but also their size distribution.

Laboratory and field studies have established that the pelagic larvae of *A. planci* pass through an initial pre-competent period of development lasting approximately two weeks (Lucas, 1973; Olson, 1985,1987), and may spend up to a month being dispersed by water currents (Yamaguchi, 1973). Larvae may be able to settle after as few as 10 days under certain conditions, such as favourable water temperatures, food availability and substrate for settlement (Olson, 1987; Moran & Johnson, 1990). The eggs and larvae of *A. planci* are close to neutrally buoyant, at least until just prior to settlement when they may become negatively buoyant (Olson, 1985). Moran and

Johnson (1990) report that the specific gravity of larvae varies between 1.02 and 1.03.

Larvae are reported to settle preferentially on coralline algae, particularly *Lithothamnium pseudosorum* (Moran & Johnson, 1990), which are generally widespread around the perimeter of coral reefs. Juvenile *A. planci* initially feed on coralline algae before switching to scleractinian corals after approximately 6 months (Moran, 1986), although the algal feeding stage may be prolonged to over a year (Zann et al., 1987). Sexual maturity is attained towards the end of their second year (Moran, 1986; Zann et al., 1987). While *A. planci* have survived for up to 8 years in the laboratory (Lucas, 1984), their life-expectancy in the field it is not known, but may be substantially lower (Moran et al., 1985) and quite variable.

1.3.1.1 Observations of a synchronous spawning of starfish

A mass spawning of starfish was observed by the author at approximately 4pm on the afternoon of 5th January, 1987 at Wheeler Reef off Townsville. Fifteen individuals were observed to spawn over a period of forty minutes, within an area of approximately 400 m^2. The eggs appeared to be neutrally buoyant and were transported quickly downstream by a 0.5 knot current. The spawning starfish were generally dispersed, rather than densely aggregated, and many more *A. planci* than those observed were likely to have been involved in the mass-spawning. Moran and Johnson (1990) report that the spawning involved approximately 100 starfish over a total area of 2,000 m^2, while Hartwick and McCauley (in Birkeland & Lucas, 1990) estimated that the same spawning event involved approximately 200 starfish. Not all individuals within the aggregation were observed to spawn. The gonads of some individuals were already spent, indicating that they had spawned earlier, possibly as part of the same episode. Some female starfish appeared to spawn eggs from only part of their body cavity. Spawning females commonly took up a hunched position to spawn, while males appeared to move around or display no particular behavioural traits while spawning. A single spawning female was observed in the same area later that same night at 9.30 pm. This spawning lasted between 15 and 20 minutes and eggs were observed

to be released from one half of the body cavity only. Dissection of the starfish after spawning had terminated showed that the remaining portion of the body cavity from which no eggs had been released did, in fact, contain large numbers of apparently ripe eggs.

Field observations during the following days involving the dissection of crown-of-thorns starfish indicated that aggregations on a single reef which were separated by relatively short distances (tens of metres) could have distinctly different reproductive states. The gonads of starfish within neighbouring aggregations sometimes varied from being totally spent to gravid, with their entire body cavity full of ripe eggs. Less dramatic variation between adjacent aggregations was, however, more common with only subtle differences in the volume of gonad within the body cavity. These observations suggest that: (1) aggregations of starfish are likely to spawn independently; and (2) individuals have some degree of control over the proportion of eggs (and possibly sperm) released and, therefore, are likely to release eggs repeatedly over a spawning season. Birkeland and Lucas (1990) report similar observations of partially spawned gonads from animals in the field, and repeated spawnings from aquarium-held starfish.

1.3.2 Patterns of Population Spread

Two major episodes of *Acanthaster* population outbreaks have been observed to take place within the GBR (Moran, 1986; Reichelt, Bradbury & Moran, 1990a). In both instances, large populations of *A. planci* were first recorded on Green Island, off Cairns (Barnes & Endean, 1964; Kenchington & Pearson, 1982). Subsequent surveys indicated that large populations were also present on other reefs in the region at about the same time (Barnes, 1966; Nash & Zell, 1982). Later surveys revealed large populations of *A. planci* farther to the south where previously none had been noted (Pearson & Endean, 1969; Endean & Stablum, 1973; Endean, 1974). At the same time, population numbers decreased on reefs in the vicinity of Green Island (Pearson, 1972; Endean & Stablum, 1973; Endean, 1974) followed by the reefs off Innisfail (Kenchington & Morton, 1976; Barnett et al., 1985; Brunckhorst & Young, 1985a; Great Barrier Reef Marine Park Authority database, unpublished). Surveys covering the entire length

of the GBR during 1985-1986 confirmed that, at the time, outbreaks associated with the most recent period of *Acanthaster* activity had been mainly confined to reefs between Lizard Island and Townsville (Moran et al., 1988). The large active outbreaks were then on many of the reefs off Townsville, whereas populations had virtually disappeared from reefs to the north. By 1987-1988 outbreaks had declined on the reefs off Townsville and were appearing on reefs further to the south (Johnson et al., 1988). The surveys during both episodes of *Acanthaster* outbreaks suggest that populations progressively became established to the south in a step-wise manner.

On the basis of size-frequency data and the apparent southward pattern in the spread of *A. planci* populations over time, Kenchington (1977) proposed that the populations south of Green Island resulted from successive waves of larval recruitment. The source of the populations was hypothesized to have been to the north of Green Island. A thorough review of the patterns and extent of outbreaks can be found in Moran (1986), who notes a number of apparent inconsistencies in Kenchington's model, including an absence of direct evidence that primary outbreaks were present on reefs to the north of Green Island prior to the initial observations and an inconsistent southward trend in the pattern of outbreaks. With respect to the second point, Moran notes that certain reefs experienced large populations years before the majority of reefs in the area were reported to have had outbreaks. There is, however, strong support for the idea that the propagation of populations is through larval dispersal and juvenile recruitment (Williams et al., 1984; Yamaguchi, 1986).

Survey results indicate that, within the region of Cairns and farther south, the distribution of outbreaks and subsequent coral mortality did not affect all reefs equally. Barnes (1966) notes that reefs contiguous with Green Island - Arlington, Michaelmas and Upolu - were affected at about the same time. Similarly, at the beginning of the second episode of *Acanthaster* activity, Nash and Zell (1982) observed populations on contiguous reefs - Arlington and Oyster. An extensive survey over a period of three years from 1966 by Pearson

and Endean (1969) noted large numbers of *A. planci* on eight reefs between Cairns and Innisfail - Green, Fitzroy and Frankland Islands, Scott, Flora, Gibson, Howie and Feather Reefs. The enormous concentrations of starfish on these reefs led Pearson and Endean to observe that the inner matrix reefs bordering the lagoon carried higher populations than the central matrix reefs, and much higher populations than the reefs of the outer matrix. Pearson (1972) noted that coral mortality attributable to *A. planci* was negligible on almost all outer matrix reefs. Many of the same reefs which were noted by Pearson and Endean (1969) to have carried large populations in the 1960s also carried large populations and suffered extensive coral mortality during the 1980s, notably Green Island, Arlington, Gibson, Howie, Peart and Feather Reefs (Cameron & Endean, 1982; Barnett et al., 1985; Brunckhorst & Young, 1985a; Great Barrier Reef Marine Park Authority database, unpublished). More recently, Moran et al. (1988) note that more mid-shelf reefs off Cairns, Innisfail and Townsville were experiencing or had recently experienced outbreaks than outer-shelf reefs. In contrast, this situation is reversed for the Cooktown-Lizard Island region where more outer-shelf reefs appear to have experienced outbreaks. During the first episode of *Acanthaster* activity, the southward spread of outbreaks which caused severe coral mortality throughout the mid-shelf reefs appeared to terminate towards the southern end of the Central Section of the Marine Park (Moran, 1986; Moran et al., 1988). A similar pattern is now apparent for the second episode (Reichelt, Bradbury & Moran, 1990a).

These features of the *Acanthaster* phenomenon, including the high incidence of outbreaks on mid-shelf (i.e., inner and central matrix) reefs, the susceptibility of some reefs in particular, notably Green Island and Feather, and the cessation of outbreaks within the Central Section of the Marine Park are important features of the pattern of *Acanthaster* population spread which require, but presently lack, a full understanding (Moran, 1986).

1.3.3 Origin of Outbreaks

A distinction between primary and secondary outbreaks of *A. planci* has been widely acknowledged (e.g., Potts, 1981; Moran, 1986;

Birkeland & Lucas, 1990). This distinction, by Endean (1973), equated the initial appearance of high density populations of adults *de novo* (sensu Potts, 1981) with primary outbreaks and their subsequent spread by means of larval dispersal or the migration of adults with secondary outbreaks.

The origin of primary outbreaks is speculative. Moran (1986) notes that their existence has been demonstrated by implication rather than by any direct evidence. During the two recorded episodes of *Acanthaster* activity within the GBR, large populations were first recorded on Green Island off Cairns (Barnes & Endean, 1964; Kenchington & Pearson, 1982). Endean (1973,1974) hypothesized that the initial appearance of large populations of *A. planci* occurred on many reefs within the Cairns Section of the GBR Marine Park which were readily accessible to humans. However, models based on size frequency data (Kenchington, 1977) and progressive vector plots (Williams et al., 1984) have since predicted that the origin of populations on Green Island, and subsequently on reefs further to the south, was to the north of this region.

Williams et al. (1984) argue that in light of field data which suggest that the net transport of larvae during the summer months will be to the south within the central GBR, the region is unlikely to behave as a closed or self-recruiting system. Rather, populations of *A. planci* within the region must originate from, and be maintained by, larval recruitment from source populations farther to the north. Surveys subsequent to the initial appearance of large populations of *A. planci* on Green Island in 1963 and 1979, indicated that populations were also present on other reefs within the region at the same time (Barnes 1966; Nash & Zell, 1982). Pearson and Endean (1969) conducted the first systematic surveys several years after the initial appearance of *A. planci* on Green Island reef. From their records, we know that in 1966 there were also large numbers of *A. planci* on reefs as far north as Lizard Island. Surveys by Nash and Zell (1982) were conducted shortly after the initial appearance of *A. planci* at Green Island during the second episode of *Acanthaster* activity. These results indicate that not only reefs contiguous with Green Island, but many as far north as Lizard Island again carried populations of *A. planci* in 1980.

Available records suggest then, that there were probably large populations of *A. planci* throughout the northern region of the Cairns Section at the same time or prior to the appearance of outbreaks on Green Island.

1.3.4 Cause of Outbreaks

Moran (1986) reviews the various hypotheses, and their permutations, concerned with the cause, or causes, of population outbreaks of *A. planci*. He notes that they fall into two categories: "those based on the premise that outbreaks of *A. planci* are natural phenomena and those that assume them to be unnatural" (p. 457). Within the former category, those based on larval recruitment, either resulting from adult aggregation (Dana et al., 1972) or increased larval survivorship (Lucas, 1982), possibly mediated by terrestrial run-off (Birkeland, 1982), are best supported by available data. Potts (1981) criticized the larval recruitment hypotheses on the basis that no outbreak originating from juveniles had been recorded. However, such outbreaks have since been documented (Zann et al., 1987,1990; Doherty & Davidson, 1988). Hypotheses falling into the 'unnatural' category link human activities with outbreaks. Of these, the predator removal hypothesis, originally proposed by Endean (1977,1982), has some theoretical support (McCallum, 1987; Reichelt, Greve et al., 1990). This hypothesis proposes that *A. planci* abundance is normally low as a result of regulation by predators, which have recently been reduced in number as a consequence of human activities. The empirical database for this belief has been based largely on early observations by Pearson and Endean (1969) that outbreaks were more common on reefs adjacent to the coast and near centres of human population. On the basis of more recent theoretical models, Bradbury and co-workers (Bradbury, Done et al., 1985; Bradbury, Hammond et al., 1985a,b; Moran et al., 1985) have proposed that the system may be cyclic, and driven either internally by the starfish-coral interaction, by some as yet undetermined exogenous forcing, or by a combination of both. They suggest the possibility that outbreaks may occur independently in many parts of the system (Bradbury, Done et al., 1985), although their more recent research does not support this (Reichelt, Bradbury & Moran, 1990b).

Each of these hypotheses has some empirical support, albeit limited in some cases. Each could lead to circumstances which result in increased larval survivorship and recruitment, and in turn, outbreaks of *A. planci*. Only the larval survivorship and recruitment hypotheses fit all the observed patterns of outbreaks worldwide (Birkeland & Lucas, 1990). The emphasis on single cause hypotheses, therefore, should be reconsidered in light of the possibility that the cause of outbreaks may lie in some combination of all (Moran, 1986). However, the data do not exclude the possibility that what has been observed are two repeated episodes of a naturally occurring phenomenon which is endogenously driven.

1.4 RESEARCH OBJECTIVES

The research documented in this thesis aims to investigate the relationships between reefs (or reef connectivity) which results from pelagic larval dispersal. The approach taken is one which postulates the hydrodynamic null hypothesis (sensu Butman, 1987): that hydrodynamic processes may provide a more parsimonious explanation for patterns of larval dispersal, juvenile recruitment, and population distribution and dynamics than do more complex explanations. The objective is to compare and contrast larval distributions and patterns of reef connectivity resulting from numerical simulation of passive particle transport with the distribution of adult populations. Model results will be discussed in light of their significance to further understanding of the *Acanthaster* phenomenon.

More specifically, four research objectives are identified. These are as follows:

(1) to investigate the physical processes which drive water circulation and govern the dispersal of larvae;

(2) to develop numerical models capable of simulating the hydrodynamics and dispersal of larvae within large assemblages of reefs;

(3) to compare the patterns which emerge when the results of many simulations are integrated with the distribution of adults and the observed pattern of *Acanthaster* population spread; and

(4) to interpret the documented patterns of recruitment and species distribution within the central GBR in light of model results.

The research reported here will be of interest to physical oceanographers by providing an overview of the components controlling the advection of larvae over disparate spatial scales; from kilometres to hundreds of kilometres. However, the research is directed primarily at biologists interested in an understanding of the physical processes which govern the dispersal of larvae at these scales, and how these processes have influenced the pattern and distribution of *A. planci* outbreaks within the GBR. The aim is to provide a clearer understanding of what can be expected as a result of the interaction between physical and biological systems.

CHAPTER TWO

MODELLING PROCEDURES

The simulation model of larval dispersal is designed in a modular format and is depicted diagramatically in Figure 2.1. The hydrodynamic component is based largely on the numerical hydrodynamic model, SURGE, of Sobey et al. (1977). Outputs from SURGE represent the major components forcing water circulation and the dispersal of larvae within the central GBR: the astronomical tides, wind-driven flows and the East Australian Current (EAC). These provide the database by which the advection and dispersion of larvae as passive particles are simulated. Fine-scale water circulation and the entrainment of larvae from the mainstream circulation onto and around individual reefs is incorporated into the dispersal model through a parameterization scheme based on schematized reefs. The final outputs of the dispersal model are interpreted as probabilities which describe the relationship between a source reef and all its sink reefs in terms of larval connectivity.

2.1 THE HYDRODYNAMIC MODEL 'SURGE'

SURGE was originally developed to predict tropical cyclone induced storm surge along the coast of Queensland, Australia. SURGE has since been further developed and extensively modified to make it more relevant to the study of tidal and wind-driven flows within the GBR (Bode et al., 1981,1991). The incorporation of reefs in regional scale circulation models poses particular problems with respect to their resolution and the accurate reproduction of long wave dynamics. These problems have, however, been largely overcome by the sub-grid scale representation of reefs. This version of SURGE has been tested and validated within the GBR, and can reproduce both the magnitude and direction of tidal and wind-driven currents (Bode et al. 1981; Frith & Mason, 1986; Griffin et al., 1987; Andrews & Bode, 1988; Middleton & Bode, unpublished manuscript).

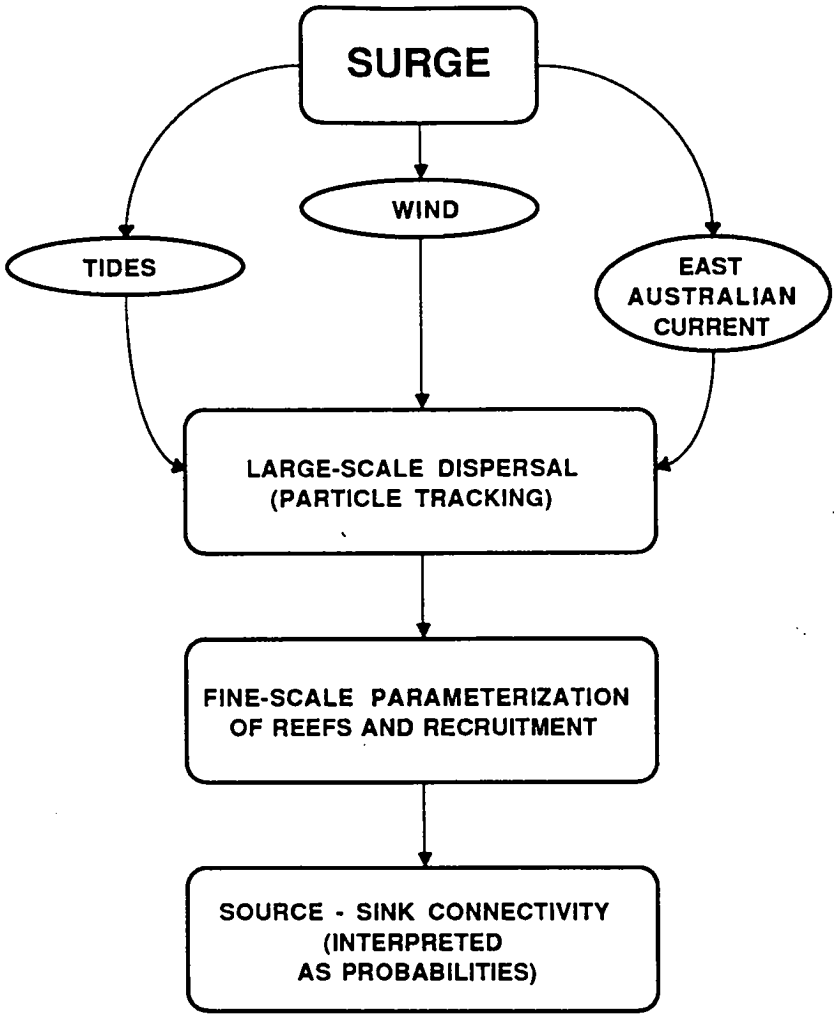


Figure 2.1 Diagramatic representation of the simulation model of larval dispersal.

The numerical hydrodynamic model is based on the principles of mass and momentum conservation in the form of the Navier-Stokes equations for a homogeneous, incompressible fluid. The three-dimensional equations are reduced to two spatial dimensions by integrating throughout the water depth. These equations are solved for the two components of depth-integrated horizontal velocity and sea surface elevation. The equations of motion are as follows:

$$\frac{\partial U}{\partial t} + \frac{\partial}{\partial x}\left(\frac{U^2}{H}\right) + \frac{\partial}{\partial y}\left(\frac{UV}{H}\right) - fV = -H\frac{\partial}{\partial x}\left(g\eta + \frac{p_s}{\rho_w}\right) + \frac{1}{\rho_w}(\tau_{sx} - \tau_{bx}) \qquad (1)$$

$$\frac{\partial V}{\partial t} + \frac{\partial}{\partial x}\left(\frac{UV}{H}\right) + \frac{\partial}{\partial y}\left(\frac{V^2}{H}\right) + fU = -H\frac{\partial}{\partial y}\left(g\eta + \frac{p_s}{\partial\rho_w}\right) + \frac{1}{\rho_w}(\tau_{sy} - \tau_{by}) \qquad (2)$$

$$\frac{\partial \eta}{\partial t} + \frac{\partial U}{\partial x} + \frac{\partial V}{\partial y} = 0 \qquad (3)$$

Here, t = time; (x,y) = local horizontal cartesian coordinates; η = $\eta\ (x, y, t)$ = sea-surface elevation, referred to Mean Sea Level (M.S.L.) datum; $h = h\ (x, y)$ = undisturbed water depth referred to M.S.L. datum; $H = h + \eta$ = total water depth; f = Coriolis parameter, assumed constant; g = gravitational acceleration; p_s = surface atmospheric pressure; ρ_w = water density, assumed constant; (τ_{sx}, τ_{sy}) = components of surface stress τ_s due to wind forcing; (τ_{bx}, τ_{by}) = components of frictional bottom stress τ_b ; (U, V) components of depth-integrated horizontal velocity or transport per unit of cross section, defined by $U = \int_{-h}^{\eta} u dz = H\bar{u}$, where $u(x, y, z, t)$ and $\bar{u}\ (x, y, t)$ are the *x*-directed components of the velocity and depth-averaged mean velocity, respectively - a similar definition holds for V (and $\bar{v}$).

The equations were linearized by omitting the normally small advective acceleration terms and are solved by an explicit finite-difference technique on a uniform grid which is staggered both spatially and temporally. This brought about significant savings in computational time. See Bode et al. (1991) for more detailed discussion.

SURGE is designed to be neither site nor resolution specific and accounts for the physical characteristics of the continental shelf including bathymetry, coastal details such as headlands, bays and offshore islands, and reefs. By use of a system of codes, barriers to flow are represented either as complete, as in the case of the coastline and continental islands, or as partial barriers where the crest may lie below water level. This latter form of barrier is used to characterize coral reefs whereby flow over the reef top will depend upon the state of the tide and water build-up or draw-down due to wind and pressure gradients. The reef crest elevation is set at 1.4 m below mean sea level.

It is necessary in areas of extensive reef coverage that the organization of reefs be represented accurately, both geometrically and dynamically, yet without being resolved explicitly. The explicit resolution of reefs requires that the grid scale be reduced to such an extent that little more than the hydrodynamics associated with a single reef can be determined with the computer resources which are presently available. To overcome this problem, reefs are resolved by parameterizing both reef length and width at the sub-grid scale. In such cases, the two horizontal momentum equations are solved with separate equations for flow through the reef gaps and across the reef flats. The grid scale chosen, 5 nautical miles, represents a compromise between that required to adequately resolve the physical features of the continental shelf and limitations imposed by the computational time-step and computer speed and storage. At this scale, both the reefs and the gaps between reefs are resolved down to 0.5 nautical miles. The maximum time-step (approximately 90 seconds) was determined by the standard CFL criterion (Sobey et al., 1977), which considers the grid scale and maximum water depth. A maximum cut-off water depth of 500 m was applied. The model grids are presented in Figures 2.2 and 2.3. The Cairns Section grid extends from Lizard Island in the north to Hinchinbrook Island in the south, 4 degrees of latitude (Fig. 2.2). The Central Section grid extends from Hinchinbrook Island in the north to the Whitsunday Islands in the south, 3.5 degrees of latitude (Fig. 2.3). The Coral Sea forms a deep water open boundary to the east of both grids.

2.1.1 Tides

Tidal flow is time-dependent and therefore requires a more complex description than does flow resulting from wind stress or the effect of the East Australian Current, both of which are treated as steady-state. Tidal oscillations can be resolved and expressed mathematically by harmonic analysis into 'constituent' components corresponding to the principal tide-producing forces of the moon and the sun. The amplitudes and phase lags of each tidal constituent at any location are derived from observations. The uniform rate of change in the tidal phase for each constituent depends upon its

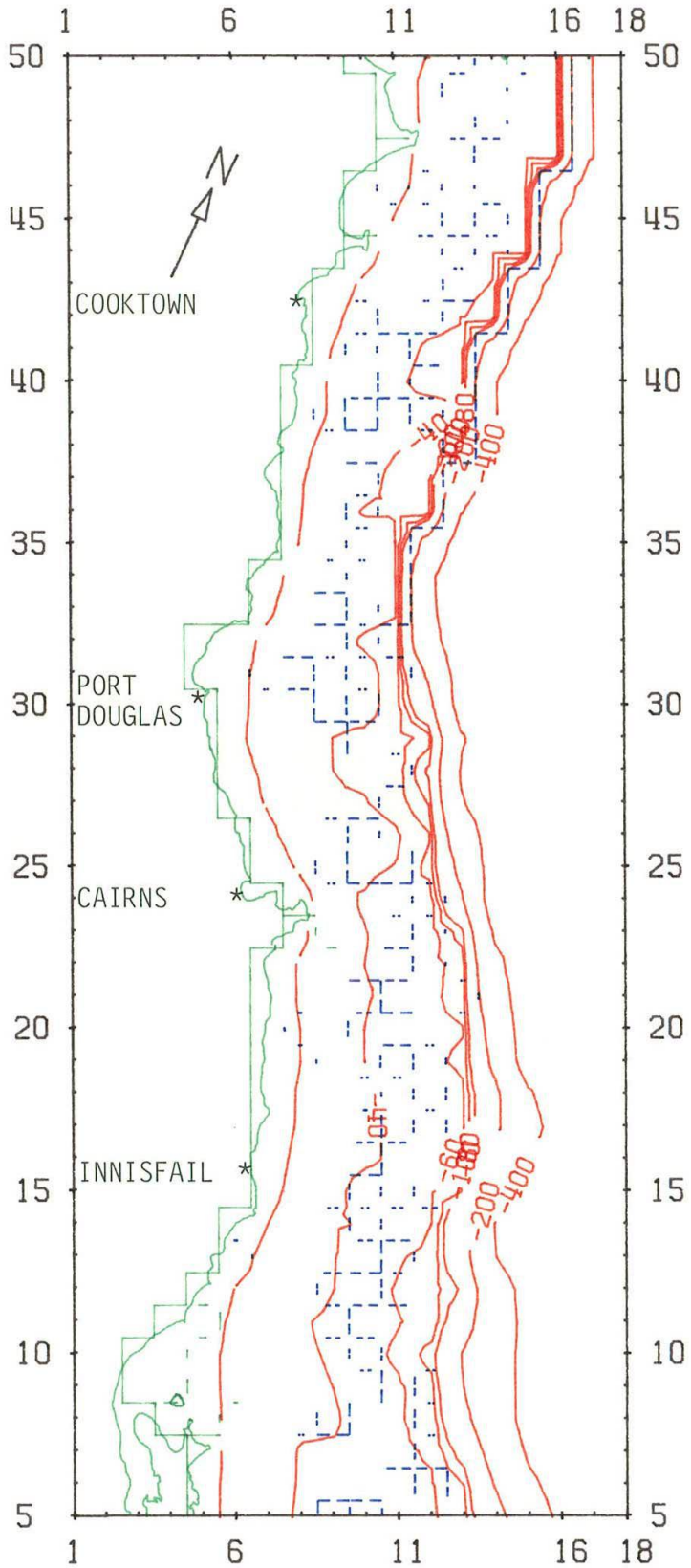


Figure 2.2 Model grid of the Cairns Section of the Great Barrier Reef Marine Park. The solid rectilinear coastal boundary is superimposed upon the actual coastline, while reef and continental island barriers are displayed as dashed lines. The grid spacing (5 nautical miles) is indicated around the boundary. Bathymetry contours are in metres below M.S.L.

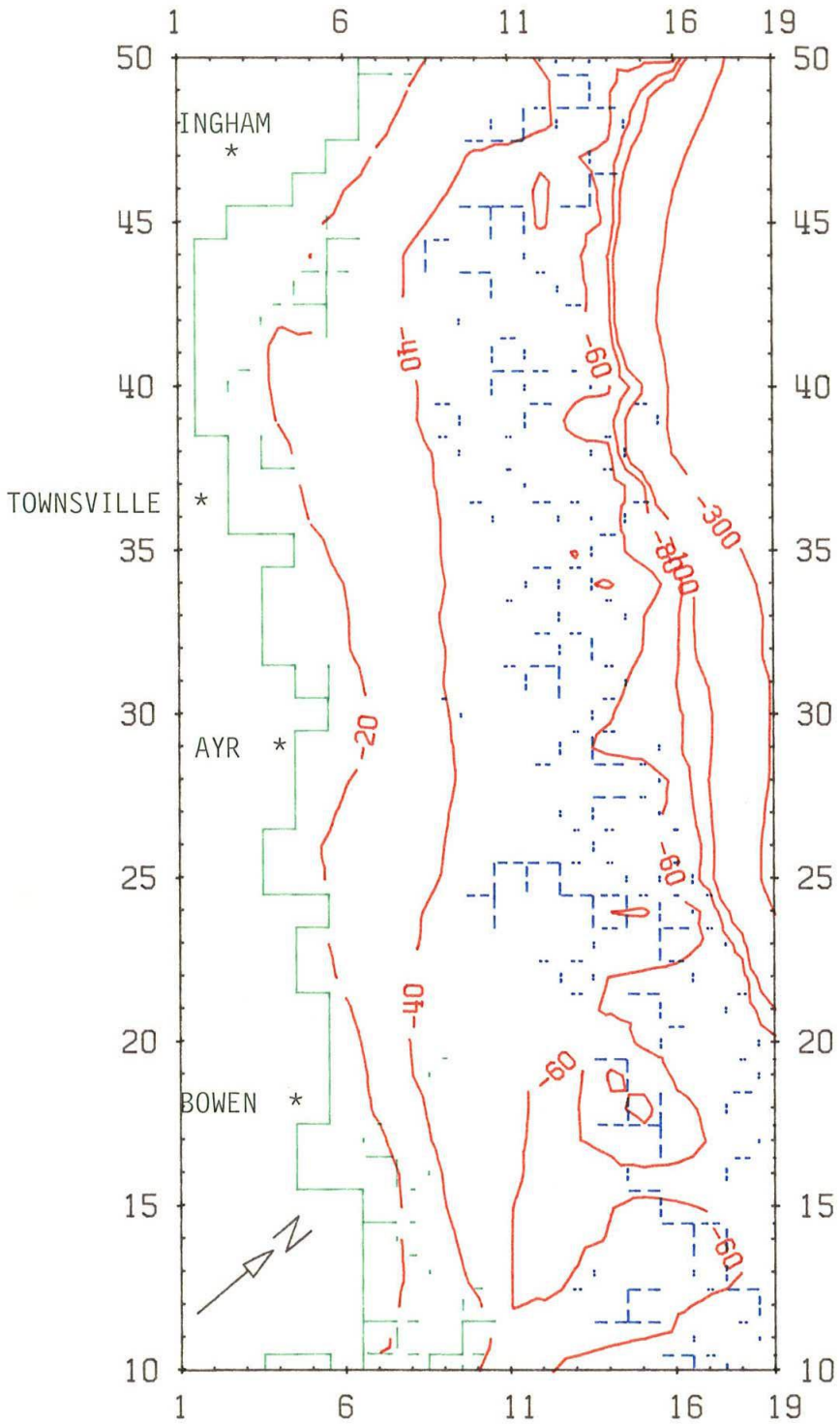


Figure 2.3 Model grid of the Central Section of the Great Barrier Reef Marine Park. The grid spacing (5 nautical miles) is indicated around the boundary. Bathymetry contours are in metres below M.S.L. See caption, Figure 2.2, for further details.

period, semi-diurnal constituents having periods of approximately 12 to 12.5 hours and the diurnal constituents of 24 to 26 hours.

The four major semi-diurnal (M2,S2,N2 and K2) and three major diurnal (01,P1 and K1) tidal constituents were analysed separately. The water elevation histories were specified along the open-water boundaries and built up gradually over 6.21 hours to minimise initial transients (Bode & Sobey, 1984). Model outputs are data-sets of tidal amplitude and phase over the entire computational field. Together, this subset of seven constituents has been demonstrated to reproduce accurately both the vertical amplitudes and tidally induced water currents in both the reef matrix and lagoonal zone of the Central Section of the GBR Marine Park (Andrews & Bode, 1988) and to account for 97% of tidal amplitude at Townsville (Hamon, 1984). A more detailed description of the numerical procedures is provided by Andrews and Bode (1988).

The ability of models to reproduce accurately the physical phenomena of specific interest is of primary concern. The process of calibration and validation by which the accuracy of a model is established is therefore crucial. The calibration process was initiated by estimating values of tidal amplitude and phase at each grid point along the open-water boundaries of the model region from harmonic records derived from the field studies of Hammon (1984), J.C. Andrews (pers. comm.) and J.H. Middleton (pers. comm.). These were then used as boundary conditions to force the tidal model. Model outputs were then compared with published data from a range of other locations within the model grid. This process was repeated for each of the seven constituents separately and small adjustments were made iteratively to the boundary values until model results showed close agreement with observations. The restricted amount of data from offshore stations along the edge of the continental shelf in this area poses a limitation to the ultimate accuracy of numerical tidal models.

2.1.2 Wind

Surface wind forcing, represented by a stress vector in equations (1) and (2), is related to the wind velocity at 10 m above mean sea level (see Wu, 1980; Frith & Mason, 1986). As in the case of the tides and East Australian Current, bottom friction is implemented through a quadratic stress coefficient which is weakly depth dependent. A Bathystrophic Storm Tide (BST), or 'radiation', condition was applied to the cross-shelf open boundaries. Under the BST approximation sea-surface elevations are initially set to zero, but are allowed to rise and fall in response to local meteorological forces. In theory, the BST boundary condition permits one-dimensional, non-dispersive hydrostatic surface gravity waves to pass freely through the open boundary without suffering internal reflections which degrade the solution. In practise, it provides more realistic water levels and flow patterns in close proximity to the open boundaries. Coriolis accelerations were similarly applied along either one or both of the cross-shelf open boundaries, in addition, of course, to all internal computations. Further details and discussion of the open boundary conditions can be found in Sobey et al. (1977,1980), Bode and Sobey (1984) and Frith and Mason (1986).

Wind forcing was built up gradually over 6.2 hours and was simulated initially for a period of 100 hours with time-histories of the u and v components of velocity and sea-surface elevation being output at a number of fixed locations. Steady-state conditions were achieved within sixty hours. This time-period thus provided a suitable limit to simulation.

Steady-state surface wind shear forcing was then applied to the model grid over an entire spectrum of directions, 16 in all, at 22.5 degree intervals. These directions correspond to Bureau of Meteorology records. While steady-state forcing is only an approximation to reality, Frith et al. (1986) note that currents near Lizard Island responded very rapidly to the wind. A non-linear relationship between surface wind velocity and shear stress necessitated a similar procedure for the range of wind speeds, at 5 knot intervals, that would be experienced by dispersing larvae. Wind

records from the Low Isles weather station were analysed to provide the relevant range of speeds for each direction. Data-sets of the two horizontal components of mass transport and sea-surface elevation over the entire computational field were output from the model after a steady-state was achieved (60 hours simulation). In all, outputs corresponding to 88 different combinations of wind direction and speed were produced. A similar technique using only 8 wind directions and monthly mean velocities was implemented by Prandle (1978) to simulate the response to wind forcing in the southern North Sea.

2.1.3 East Australian Current

Various methods were investigated to force flow in a long-shelf direction polewards off the edge of the continental shelf. These included, in one combination or other, defining the sea-surface elevations along the open boundaries, stipulating the direction and size of mass transports and the positioning of barriers to direct flow.

Initially, sea-surface elevations were defined along the open boundaries. However, this technique provided few means of controlling the direction of flow. Transport was mostly directed from regions of high water level to those of low water level via the most direct route and the resulting patterns of water motion displayed no resemblance to observation.

The second method to be investigated was the application of mass transports to the deep water grid points in a poleward direction along the northern cross-shelf open boundary. This technique also proved largely unsuccessful. The most serious shortcoming was that the magnitude of currents over the shelf became too great relative to those in deeper water off the shelf edge. It was clear that a considerable mass of water was being lost along the deep water open boundary.

The positioning of barriers to direct and constrain flow within a relatively narrow envelope along the shelf edge appeared to offer a possible solution. Complete barriers to flow were placed at a constant

distance (four grid spaces or twenty nautical miles) from the continental shelf edge. Mass transports were then applied to the deep water grid points within the envelope in a similar manner to the previous method. The magnitude of the transports were adjusted to produce current velocities along the shelf edge that were consistent with observations. This technique provided a good representation of the EAC within the southern half of the Cairns Section grid but was inconsistent with observations of a bifurcation of the current between latitude 14°S and 16°S which results in an equatorward flow offshore from the northern ribbon reefs.

The method of forcing the EAC within the Cairns Section which provided the most acceptable results was by the application of mass transports in an onshore direction across the deep water open boundary in the region where bifurcation of the current is reported. Along the remainder of the deep water open boundary cross-shelf transports were maintained at or close to zero. This technique forced flow along the shelf to the north and south of the bifurcation. The resulting flows were then calibrated to match published data on current velocity from Church and Boland (1983) and Church (1987). Mass transports along the southern boundary of the Cairns Section grid provided input to the Central Section grid where barriers were positioned to direct and constrain flow within a relatively narrow envelope along the shelf edge. Water motion associated with the EAC is assumed to be steady-state.

2.2 PARTICLE TRACKING

A computer program, TRACK, has been developed to simulate the dispersal of larvae as passive particles. While essentially deterministic, given a specific set of forcing parameters, TRACK runs under time-dependent tidal flow and a randomly varying wind field based upon an historical record. The net water transport at any point within the computational field is found by linear superposition of the three transport components (tide, wind and EAC) which are output from SURGE. While non-linearities are particularly important to the dynamics in regions of shallow water, particularly on and around reefs, scaling arguments can be used to show that linear dynamics

provide a reasonably accurate description of the flow in deeper regions where the transport of most larvae occurs. This issue is dealt with in more detail in Section 4.3.3. The present methodology provides the only feasible means which are currently available of representing these multifarious events, in the geometrically complex setting of the GBR, over many years of simulation time.

2.2.1 Advection of Particles

The advection of larvae is effected by using a Lagrangian 'marker and cell' technique. Particle velocity is calculated by linear interpolation between data points which define the surrounding velocity field. The choice of a suitable time-step for particle tracking was made by comparing the final positions of particles after 100 hours simulation under tidal forcing alone. The range of time-steps investigated was between three seconds and ten hours. The magnitude and direction of tidal currents is time dependent, with the rate of change being continuous. In contrast, forcing by both the East Australian Current and wind-driven currents is essentially steady-state; hence the reasoning for investigation of the time-step under tidal forcing alone. Variation in net particle displacement over 100 hours was small for time-steps up to one hour (26 metres); beyond this however, variation increased considerably (156 metres at five hours and 419 metres at ten hours). The time-step chosen, one hour, therefore represents a compromise between adequate resolution of the time-varying tidal currents and limitations imposed by computer speed and storage.

Nineteen years of twice-daily surface wind records from the Low Isles weather station drive the simulation. The wind record from the Low Isles was selected because it came from within the region of interest; it was less affected by the land-sea breeze phenomenon than the other stations that were available; and it was long enough to capture most of the variability in wind-driven current patterns. The wind is assumed to be constant for 12 hour intervals between records. The state of the tide over a 28 day cycle and the wind record at which to begin particle tracking are randomly selected to represent the initiation of each dispersal event. The ensuing sequence of wind speeds and directions determines the variation in wind-driven

current patterns for the duration of larval transport. Since *A. planci* is of chief interest, only segments of the wind record corresponding to the spawning season of the starfish (December and January) are used to initiate particle tracking. In all, three months of records (December to March) for each of the nineteen years of data that are available determine the spectrum of wind-driven currents likely to be encountered by the dispersing larvae of *A. planci.*

2.2.2 Particles as Larvae

In the absence of any knowledge of the behaviour of *Acanthaster* larvae in the field, they are assumed to behave as passive, neutrally buoyant particles. This assumption appears justified as a first approximation on the basis of our limited knowledge of other echinoderm larvae. Larvae of the irregular echinoid *Dendraster excentricus*, for example, are reported to behave as passively dispersed particles except in the advanced larval stages (Emlet, 1986). Furthermore, Olson (1985) reports that the eggs and larvae of *A. planci* are close to neutrally buoyant, but may become negatively buoyant just prior to settlement.

The movement of larvae following a spawning event is simulated for a period of 28 days. The larval cloud is represented by seven particles, the movements of which are tracked and intersections with reefs recorded. The initial arrangement of the seven particles is in the form of a hexagon (one particle corresponding to each vertex and one for the centroid) with a long axis of half a nautical mile. The hexagon approximates the initial spread of larvae soon after a mass-spawning. Two release locations were selected for each reef; one at each extremity of the reef in a cross-shelf direction. This corresponds closely to the distribution of larvae from fine-scale model results and observations of the transport of coral larvae off reefs (K.P. Black, pers. comm.; Oliver & Willis, 1987; pers. obs). Relative dispersion of the seven particles representing the larval cloud occurs as a result of spatial variation in the velocity field. This approximation of diffusion/dispersion processes is discussed in more detail in Section 4.3.4. During the initial two weeks of development, larvae of *A. planci* are assumed to be pre-competent and unable to settle. Only

intersections with reefs following the two week pre-competent period are therefore considered.

2.3 FINE-SCALE CIRCULATION AND THE ENTRAINMENT OF LARVAE ONTO REEFS

Once advected off their natal or source reef, larvae will be transported by mainstream circulation towards other reefs. However, the fine-scale features of water circulation around individual reefs, or groups of reefs, will strongly influence recruitment by determining the proportion of the available larval pool which is able to settle onto a reef under particular conditions (Dight et al., 1988). Hamner and Wolanski (1988) point out that a shelf current approaching a reef will diverge around the reef with only a fraction of the water mass coming into direct contact with the reef itself. That is, a significant proportion of an approaching larval cloud may not be provided with the opportunity to settle onto the reef but will be transported farther afield.

There was a clear need within the context of this research to consider fine-scale circulation around reefs and to distribute larval connectivity between sink reefs (i.e. to ensure that all larvae will not necessarily settle on the first reef encountered). In doing so, the following questions were posed: Do different fine-scale hydrodynamic conditions influence the entrainment of larvae onto reefs?; are there differences between reefs in their capacity to entrain larvae?; and if so, what aspects of reef morphology play the most prominent roles in determining these differences? Research to date has concentrated primarily on larval retention by reefs and the initial aggregation and transport of coral larvae off reefs (e.g., Black, 1988; Oliver & Willis, 1987; Sammarco & Andrews, 1988; Willis & Oliver, 1988; Wolanski et al., 1989). There have been no systematic studies which have investigated the entrainment of larvae onto reefs from the mainstream circulation.

2.3.1 Fine-scale Circulation Modelling

Modelling of the fine-scale circulation around individual reefs was undertaken using the numerical hydrodynamic model 2DD (Black, 1983,1988; Black & Gay, 1987a,b) in collaboration with Dr K.P. Black at the Victorian Institute of Marine Sciences. This model solves the two dimensional depth-integrated momentum and continuity equations using an explicit finite difference solution in a similar manner to the numerical hydrodynamic model SURGE (see Section 2.1). Like SURGE, features such as wetting and drying of inter-tidal areas are included. Non-linear advective acceleration terms are also included. The bed friction is derived from measurements of velocity profiles and waves over a coral reef, and by direct model calibration.

Black and Gay (1987b) note that flows can be strongly interactive around reefs where there is high bottom friction or strong tidal currents. The model therefore incorporates the non-linear interactions between tidal and long-period currents. Black's model 2DD has been calibrated against field measurements and verified using drogues at John Brewer Reef (Black & Gay, 1987b). It has been shown to provide a good representation of currents both over and around coral reefs.

2.3.1.1 Implementation and forcings

The grid scale was set at 500 m. This scale, while relatively coarse, was considered sufficient to resolve the major features of reef morphology, as high resolution bathymetry was not to be incorporated into the models. Simulations were carried out on a 50 by 61 cell grid.

Analysis of a low frequency current record, provided by J.C. Andrews and K.P. Black, of 136 days duration from near John Brewer Reef in the Central Section of the GBR Marine Park established a mean current speed of 12.7 cm s^{-1} over the period. The current speed varied widely during the 136 days, however, ranging between 2 and 38 cm s^{-1}. On this basis, the 'standard' forcing for the long-shelf current was established at 12 cm s^{-1}.

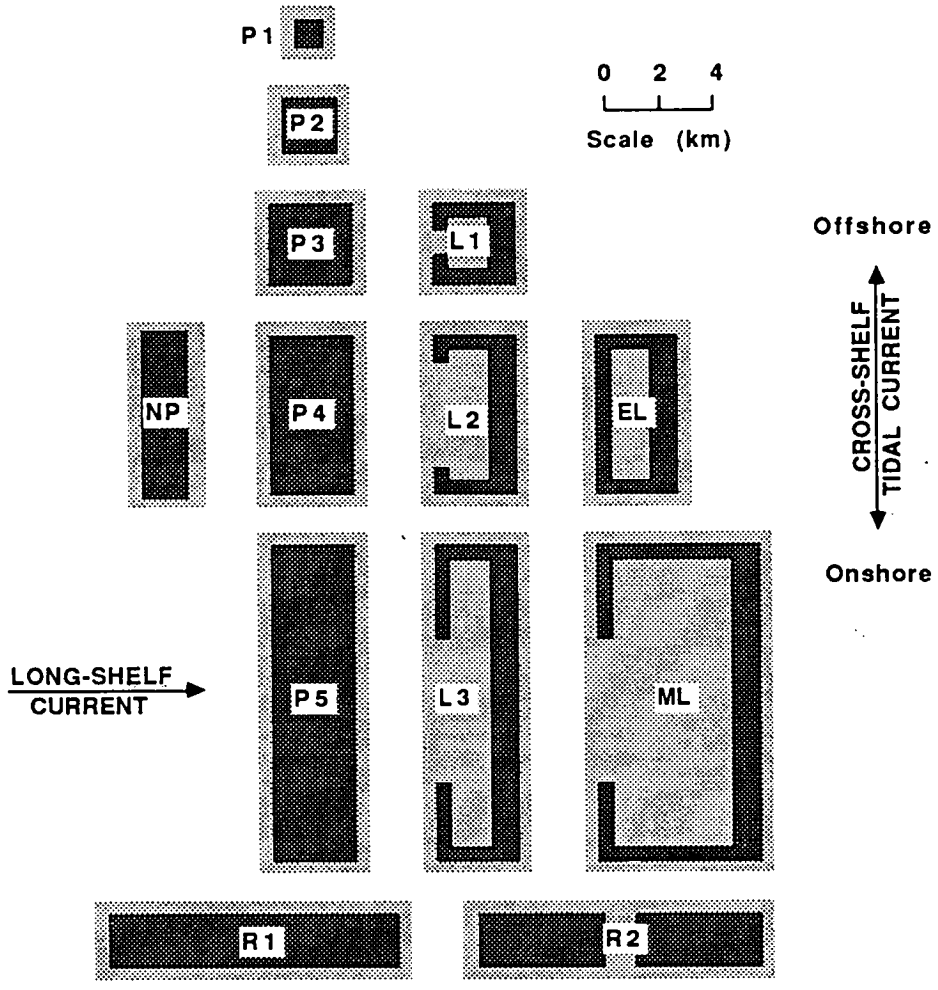


Figure 2.4 Arrangement of schematized reef shapes and sizes and their relationship to the hydrodynamic forcings.

Tidal currents are implemented in 2DD by specifying the orientation, amplitude and period of the tidal wave. The orientation of the major axis of the tidal ellipse was perpendicular to the direction of the long-shelf current (see Fig. 2.4), thus providing a reasonable representation of their relative relationship within the Cairns and Central Sections of the GBR Marine Park. The tidal amplitude was set to generate a peak current speed along the major axis of the tidal current ellipse of 20 cm s^{-1}. This value is representative of peak mid to spring tidal current speeds over most of the Cairns and Central Sections of the GBR Marine Park. The period was assigned to the M2 tidal constituent (12.42 hours).

2.3.2 Fine-scale Dispersal Modelling

Multiple fine-scale dispersal simulations were undertaken using the 2 dimensional Lagrangian particle model 2AD (Black, 1988). In this model, particles can be released instantaneously or over time from any one or number of cells within the model grid. Particles are evenly distributed within each cell. The horizontal diffusion of particles following their release is modelled as a random walk using separate longitudinal and lateral diffusion coefficients, and superimposed on an advective current taken from the hydrodynamic model. This methodology simulates advection and the processes of vertical shear and random diffusion (Black et al., 1990).

One hundred (100) particles were released from within each of the selected grid cells at half hour intervals over the first tidal cycle (12 hours). In total, 2500 particles were released from each grid cell for each simulation. Releases were, therefore, time averaged over a single tidal cycle. Following each release, particles were advected freely under the influence of a steady-state long-shelf current and an oscillating cross-shelf tidal current.

2.3.3 Schematized Reefs

Reefs within the GBR vary greatly in their shape and size. Hopley (1982) provides a classification of eight reef types based on their evolutionary development. The geographical distribution of these types varies markedly throughout the GBR (Hopley et al., 1989). In the absence of any systematic investigations of the effects of reef morphology on circulation patterns and the entrainment of larvae onto reefs, an exploratory approach was required. The classification by Hopley provided the basis for the design of a series of schematized reefs which would include the principal morphological features of coral reefs within the GBR. These include: (1) the presence or absence of a partially and fully enclosed lagoon, the long axis of which is essentially perpendicular to the long-shelf currents, and (2) planar reef types which are aligned with their long axis parallel to the long-shelf currents. This latter form corresponds to Hopley's ribbon reef type.

2.3.3.1 Reef shapes and sizes

Thirteen combinations of reef shape and size were designed. These are presented in Figure 2.4. For each of the two major types, planar (P) and lagoonal/cresentic (L), the cross-shelf extent of the reef was varied systematically (P1 to P5 and L1 to L3). The planar reef types varied systematically from 1 km x 1 km to 3 km x 12 km, while the lagoonal/cresentic types varied from 3 km x 3 km to 3 km x 12 km. Three variants of these two designs are also represented: a narrow planar reef type (NP - 1.5 km x 6 km), one characterized by having a fully enclosed lagoon (EL - 3 km x 6 km) and a large massive lagoonal/crescentic reef type (ML - 6 km x 12 km). A further two reef types characterized the ribbon reefs: one representing an isolated ribbon reef (R1 - 10 km x 1.5 km) and the other representing the more common situation of two ribbon reefs in close proximity (R2 - each 4.5 km x 1.5 km). The variation in reef shape and size was intended to be schematically representative of the broad range of reefs within the Cairns and Central Sections of the GBR Marine Park. They would provide for the controlled examination of the effects of varying reef shape and size on the entrainment of larvae onto reefs.

2.3.3.2 Reef bathymetry and habitat

Only the gross features of shelf and reef bathymetry are incorporated into the schematized models. Reef flats were set to datum (0 m), typically about 0.3 m below low tide level (Black & Gay, 1987b). Where lagoons were incorporated into the schematized reef shapes, the lagoon floor was established at 10 m below datum. Beyond the reef in deep water, the sea bed was established at 40 m below datum. While actual bathymetries vary markedly throughout the GBR, these values approximate those for mid-shelf reefs within the Cairns and Central Sections of the GBR Marine Park.

Habitat, i.e. areas where larvae may settle, was defined to cover the entire reef flat and lagoon (where incorporated) and to extend one grid cell (500 m) beyond the reef margin (see Fig. 2.5).

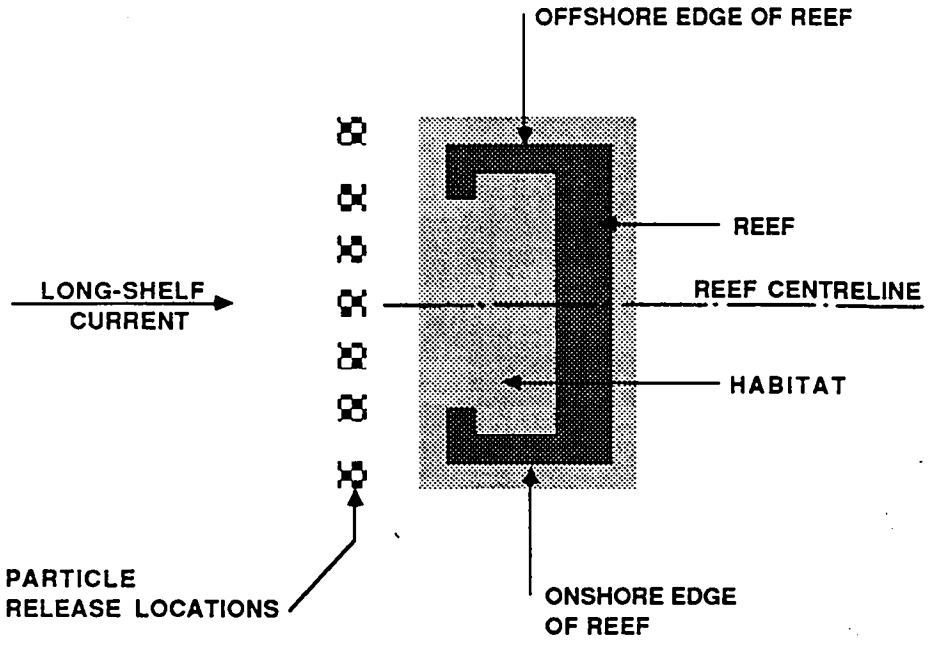


Figure 2.5 Model representation of the particle release locations and the distribution of habitat.

2.3.4 Simulating Larval Transport onto Reefs

Multiple simulations were conducted for each reef type. Two thousand five hundred (2,500) particles were released from a single grid cell for each simulation. Particles were distributed evenly within each cell. Releases were simulated at one kilometer intervals, perpendicular to the long-shelf current and reef centreline, over the cross-shelf extent of the reef. The number of releases therefore varied with reef size. All releases were from cells lying upstream and outside of the sphere of influence of all but the largest reefs. The number of particles from each release that were transported over the area defined as habitat was recorded. The general arrangement of release locations, habitat and reef are presented in Figure 2.5.

2.4 METHODOLOGICAL APPROACH

On the basis of variation in the physical organization of the Cairns and Central Sections of the GBR Marine Park, and knowledge of the pattern of *A. planci* outbreaks, three distinct regions were identified. These regions are contiguous and correspond to the northern half of

the Cairns Section adjacent to the ribbon reefs, the southern half of the Cairns Section and the northern half of the Central Section of the GBR Marine Park. They are here referred to as the northern, central and southern regions respectively.

Reefs were chosen within each of these three regions from which to simulate spawning events and the subsequent transport of larvae. The locations of all reefs are identified in Figures 2.6 to 2.8 for the northern, central and southern regions respectively. All reefs have some record of *Acanthaster* activity (Great Barrier Reef Marine Park Authority database, unpublished). Fifteen reefs were selected from within each of the northern and central regions. Five reefs were from each of three cross-shelf geographical zones: (i) the outer edge of the reef matrix along the continental shelf edge, (ii) central within the reef matrix and (iii) the inner edge of the reef matrix bordering the main lagoon. Within the southern region, twelve reefs were selected. Here, three reefs were from each of four cross-shelf geographical zones: the three above plus (iv) nearshore lying on the western side of the main lagoon. From each of the reefs within all regions, forty dispersal events were simulated using randomly selected tide and wind histories. Each dispersal event and subsequent larval track over a period of 28 days ran under a different current regime. The reefs with which particles intersected were recorded and similarly classified with respect to the four cross-shelf geographical zones identified above, as well as their long-shelf location (north or south) with respect to the source reef. The method of analysis of particle trajectories and distribution of larval connectivity is detailed in Section 3.4.

2.4.1 The Northern Region

Fifteen reefs were chosen within the northern region from which to simulate spawning events and the subsequent movement of larvae (see Fig. 2.6). The fifteen source reefs are listed in Table 2.1. In all, 600 dispersal events were simulated and the trajectories of 4200 particles were analysed from this northern region (see Section 3.4 for further details of the analysis of particle trajectories).

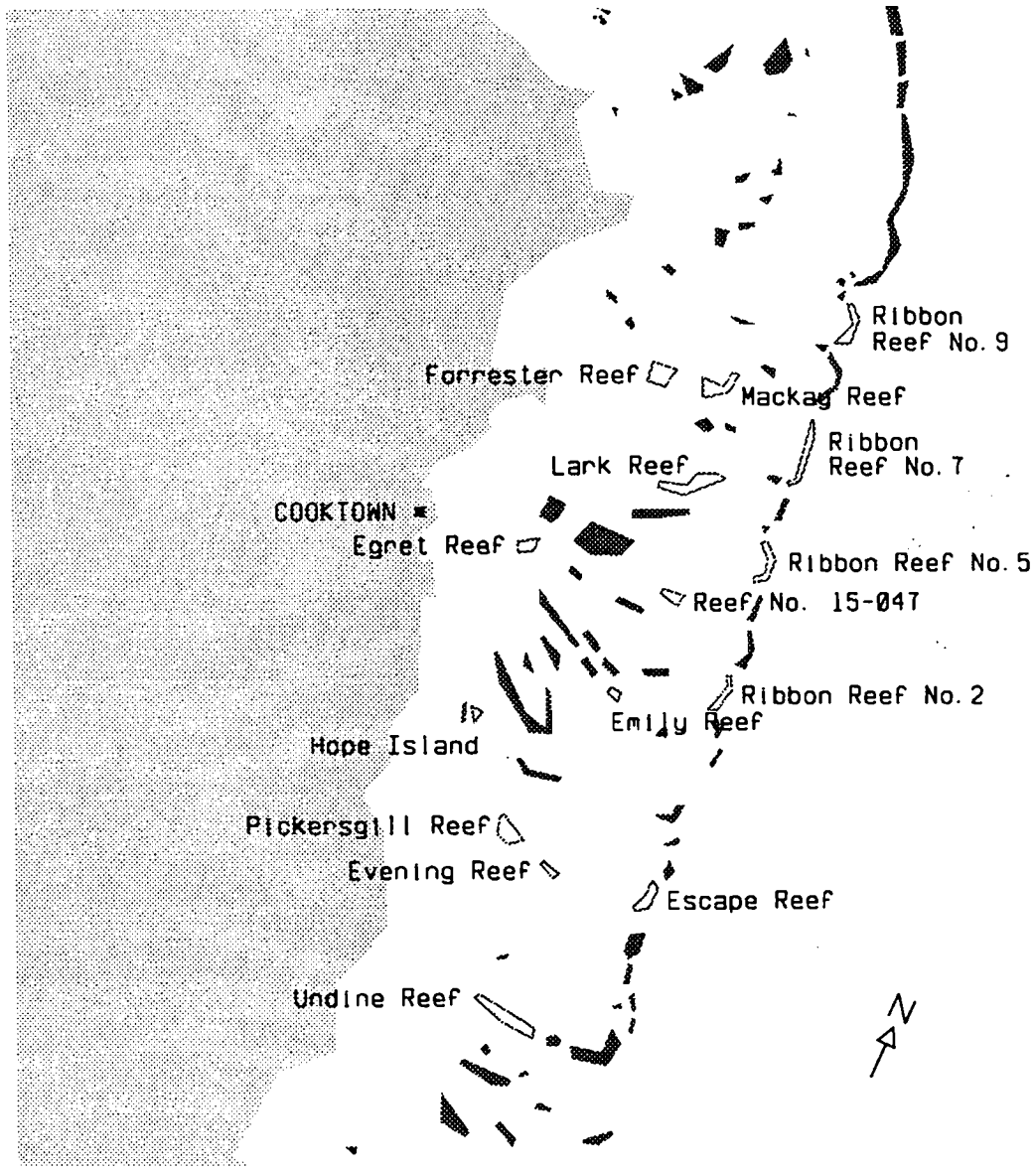


Figure 2.6 Map showing the location of the 15 northern region source reefs from which dispersal events were simulated. The source reefs all lie within the northern portion of the Cairns Section of the GBR Marine Park and are indicated without fill.

2.4.2 The Central Region

Fifteen reefs were also chosen within the central region from which to simulate spawning events and the subsequent movement of larvae (see Fig. 2.7). The fifteen source reefs are listed in Table 2.2. In all, 600 dispersal events were simulated and the trajectories of 4200 particles were analysed from this central region (see Section 3.4 for further details of the analysis of particle trajectories).

Reef Name	Reef Number	Cross-shelf Location	Latitude	Longitude
Ribbon No.9	14-154	Outer matrix	14° 59'	145° 43'
Ribbon No.7	15-026	Outer matrix	15° 11'	145° 44'
Ribbon No.5	15-038	Outer matrix	15° 22'	145° 44'
Ribbon No.2	15-075	Outer matrix	15° 33'	145° 44'
Escape	15-094	Outer matrix	15° 53'	145° 47'
Mackay	15-024	Central matrix	15° 08'	145° 34'
Lark	15-033	Central matrix	15° 17'	145° 35'
	15-047	Central matrix	15° 28'	145° 38'
Emily	15-082	Central matrix	15° 37'	145° 37'
Evening	15-095	Central matrix	15° 54'	145° 38'
Forrester	15-009	Inner matrix	15° 10'	145° 29'
Egret	15-013	Inner matrix	15° 29'	145° 25'
Hope Is.	15-065	Inner matrix	15° 44'	145° 27'
Pickersgill	15-093	Inner matrix	15° 52'	145° 34'
Undine	16-020	Inner matrix	16° 07'	145° 43'

Table 2.1 Listing of the 15 northern region source reefs from which dispersal events were simulated.

Reef Name	Reef Number	Cross-shelf Location	Latitude	Longitude
Opal	16-025	Outer matrix	16° 13'	145° 53'
Norman	16-030	Outer matrix	16° 26'	145° 59'
Flynn	16-065	Outer matrix	16° 44'	146° 16'
Channel	16-075	Outer matrix	16° 56'	146° 26'
Noggin	17-008	Outer matrix	17° 08'	146° 28'
Tongue	16-026	Central matrix	16° 23'	145° 53'
Michaelmas	16-060	Central matrix	16° 35'	146° 01'
Thetford	16-068	Central matrix	16° 49'	146° 11'
Maori	17-006	Central matrix	17° 07'	146° 20'
Cayley	17-023	Central matrix	17° 29'	146° 28'
Batt	16-029	Inner matrix	16° 25'	145° 46'
Upolu	16-046	Inner matrix	16° 40'	145° 56'
Green Is.	16-049	Inner matrix	16° 46'	145° 58'
Scott	17-004	Inner matrix	17° 05'	146° 11'
Howie	17-018	Inner matrix	17° 24'	146° 24'

Table 2.2 Listing of the 15 central region source reefs from which dispersal events were simulated.

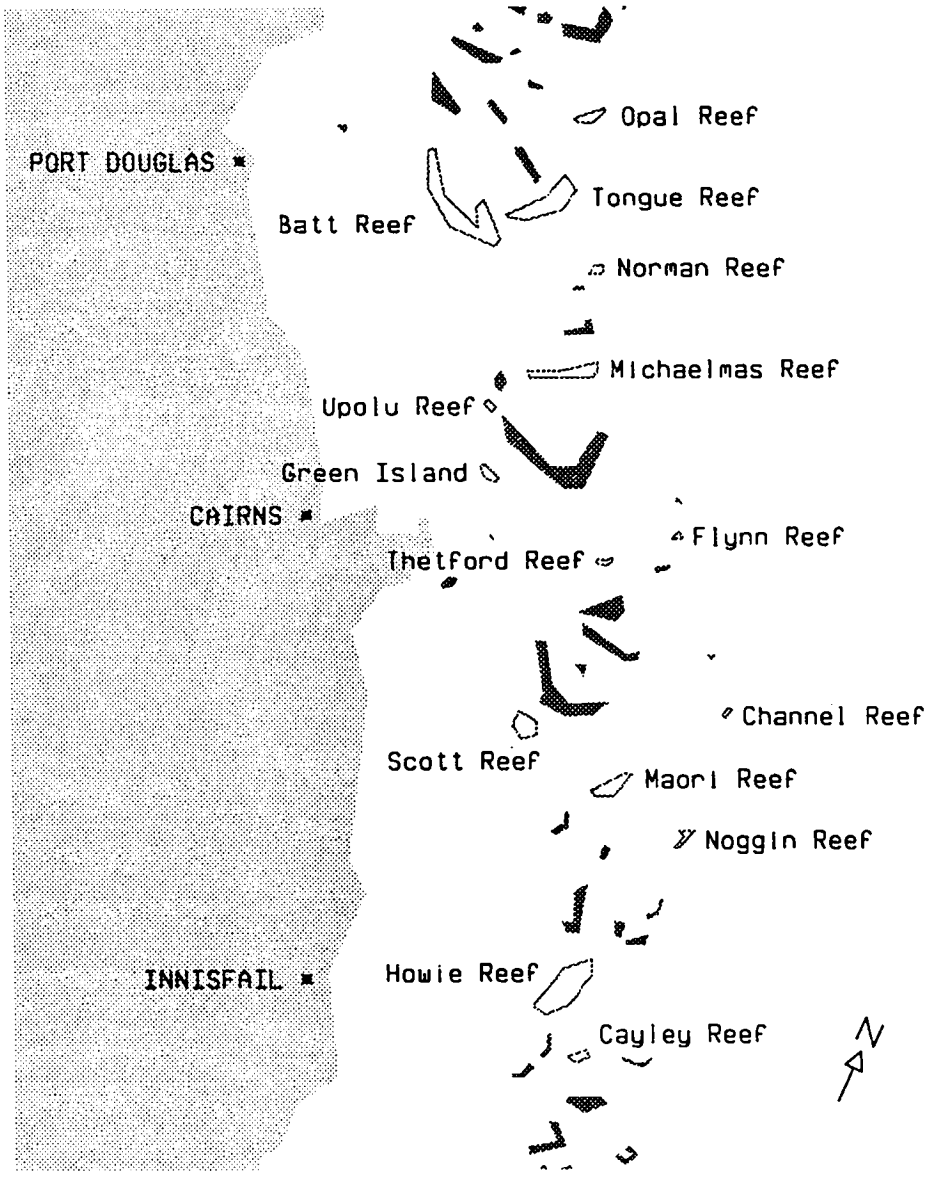


Figure 2.7 Map showing the location of the 15 central region source reefs from which dispersal events were simulated. The source reefs all lie within the southern portion of the Cairns Section of the GBR Marine Park and are indicated without fill.

2.4.3 The Southern Region

Twelve reefs were chosen within the southern region from which to simulate spawning events and the subsequent movement of larvae (see Fig. 2.8). The twelve source reefs are listed in Table 2.3. In all, 480 dispersal events were simulated and the trajectories of 3360 particles were analysed from this southern region (see Section 3.4 for further details of the analysis of particle trajectories).

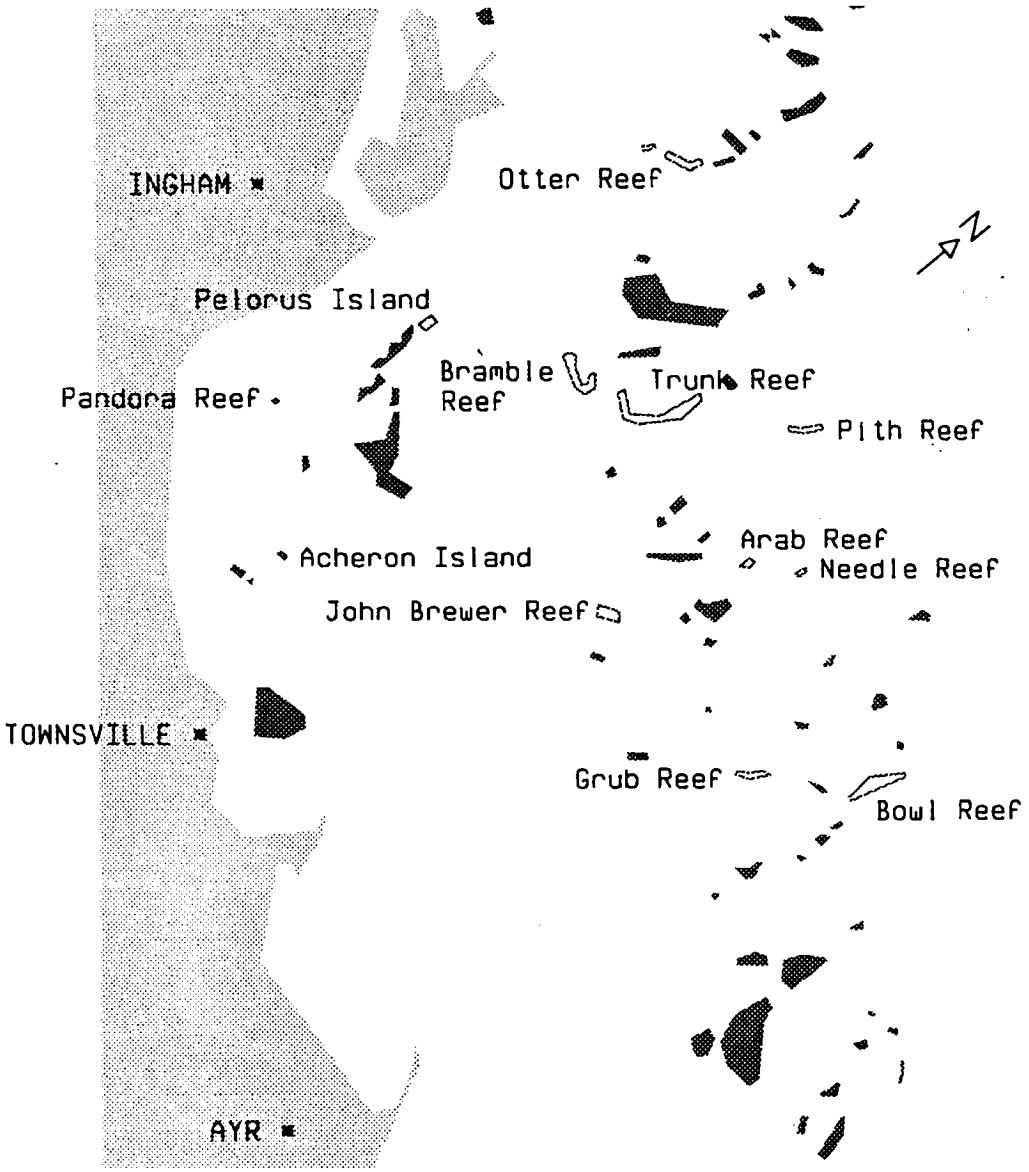


Figure 2.8 Map showing the location of the 12 southern region source reefs from which dispersal events were simulated. The source reefs all lie within the northern portion of the Central Section of the GBR Marine Park and are indicated without fill.

Reef Name	Reef Number	Cross-shelf Location	Latitude	Longitude
Pith	18-033	Outer matrix	18^0 13'	147^0 02'
Needle	18-037	Outer matrix	18^0 22'	147^0 12'
Bowl	18-080	Outer matrix	18^0 29'	147^0 33'
Trunk	18-027	Central matrix	18^0 22'	146^0 50'
Arab	18-040	Central matrix	18^0 25'	147^0 08'
Grub	18-077	Central matrix	18^0 38'	147^0 25'
Otter	18-018	Inner matrix	18^0 04'	146^0 34'
Bramble	18-029	Inner matrix	18^0 25'	146^0 44'
John Brewer	18-075	Inner matrix	18^0 38'	147^0 03'
Pelorus Is.	18-048	Nearshore	18^0 33'	146^0 29'
Pandora	18-051	Nearshore	18^0 48'	146^0 25'
Acheron Is.	18-066	Nearshore	18^0 58'	146^0 38'

Table 2.3 Listing of the 12 southern region source reefs from which dispersal events were simulated.

CHAPTER THREE

RESULTS

3.1 LARGE-SCALE HYDRODYNAMICS

The hydrodynamics of the Cairns and Central Sections of the GBR Marine Park are presented together in this section.

3.1.1 Tides

Griffin et al. (1987) note that a GBR tidal model is often more appropriately assessed by its predictions of tidal elevations rather than by currents, as the former are less affected by local topography. The practical limitations on the location of current meters may provide some difficulty with the interpretation of current recordings due to the possibility of steering by reefs (Griffin et al., 1987; Andrews & Bode, 1988).

Observed and predicted values of tidal amplitude and phase for the M2 semi-diurnal principal lunar constituent and K1 declinational diurnal constituent are presented for both the Cairns and Central Sections in Figures 3.1 to 3.4. Observed and predicted values of tidal amplitude and phase for the S2, N2 and K2 semi-diurnal and O1 and P1 diurnal constituents are presented for both the Cairns and Central Sections in Appendix A.

3.1.1.1 Model validation

Comparison of observed and predicted values of tidal amplitude and phase over the entire grids correspond closely (Figs. 3.1 to 3.4). Overall, the model agrees well with published data of amplitude and phase for all seven tidal constituents (see also Appendix A). Deviations between observed and predicted values of amplitude and phase may result from the location of recording instruments with respect to reefs (see Wolanski and Pickard, 1983a) as well as the quality and duration of records. This variation is evident in the range

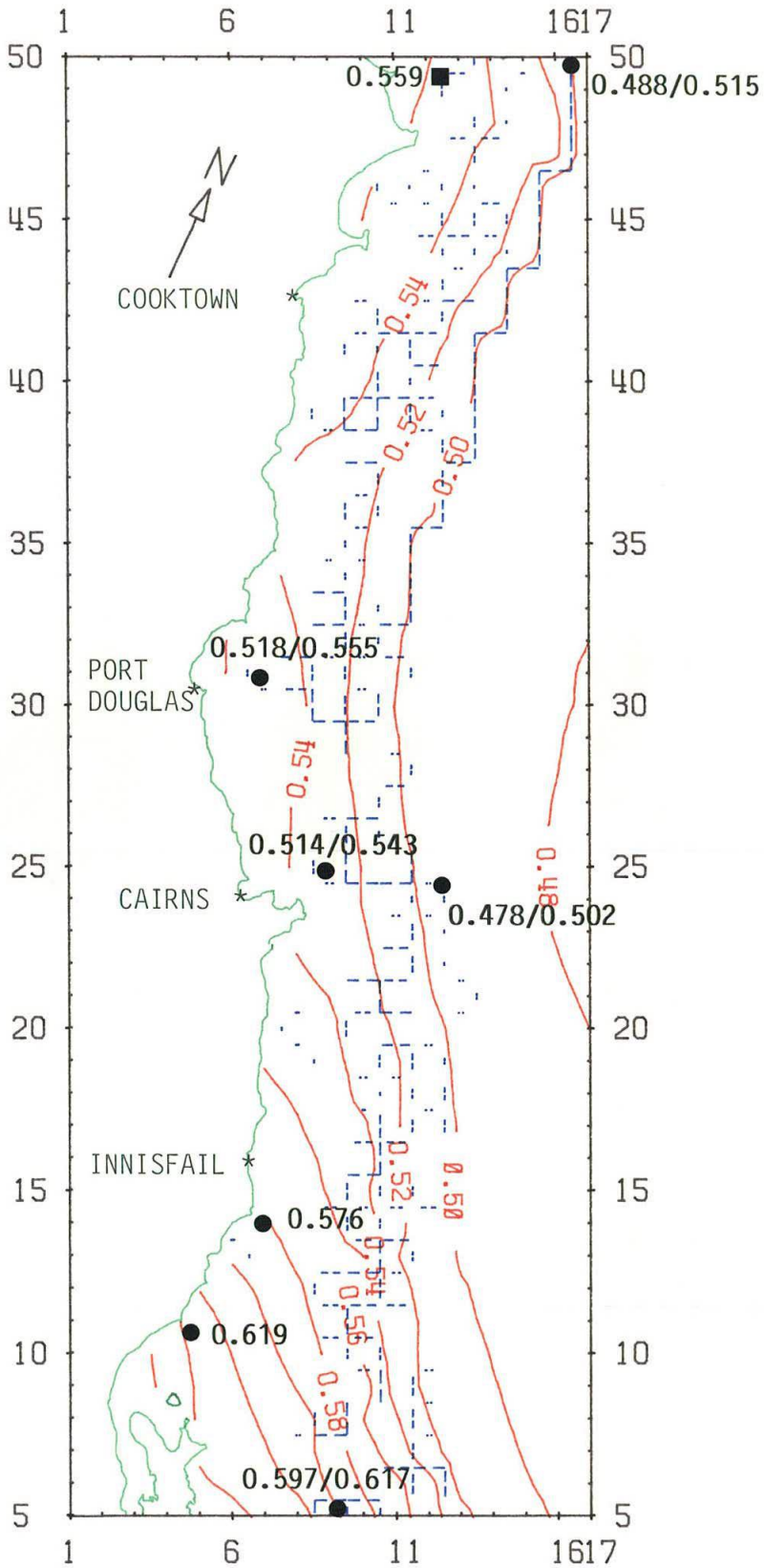


Figure 3.1a Comparison of observed and predicted values of tidal elevation amplitude for the M2 semi-diurnal principal lunar constituent within the Cairns Section of the GBR Marine Park. Published data are from Hamon (1984) (denoted ●) and from J.H. Middleton (pers. comm.) (denoted ■). Where two values are noted, these represent the range of published observations. Tidal amplitudes are in metres.

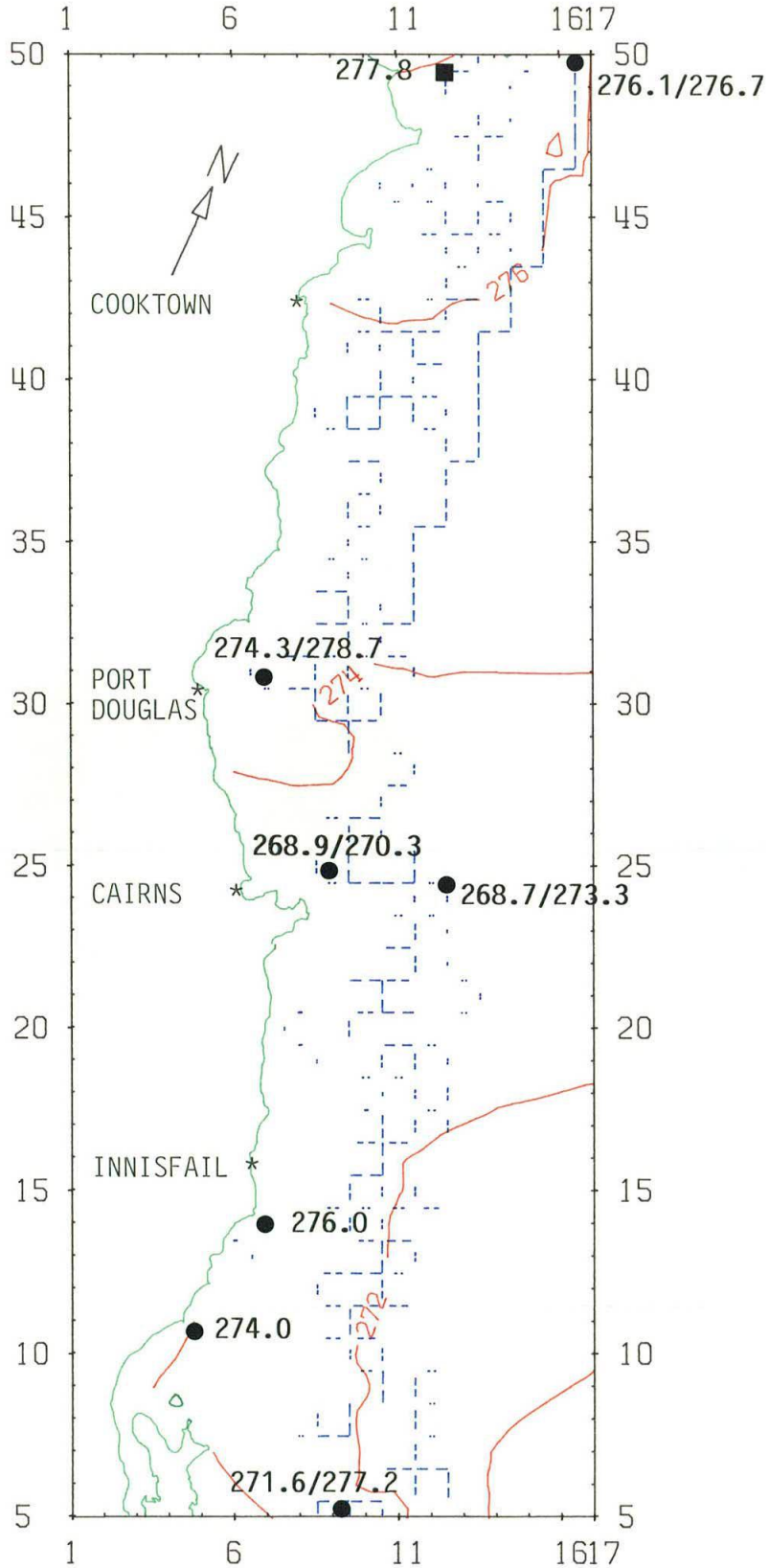


Figure 3.1b Comparison of observed and predicted values of tidal elevation phase for the M2 semi-diurnal principal lunar constituent within the Cairns Section of the GBR Marine Park. Published data are from Hamon (1984) (denoted ●) and from JH Middleton (pers. comm.) (denoted ■). Where two values are noted, these represent the range of published observations. Greenwich phase lags are for GMT-10.

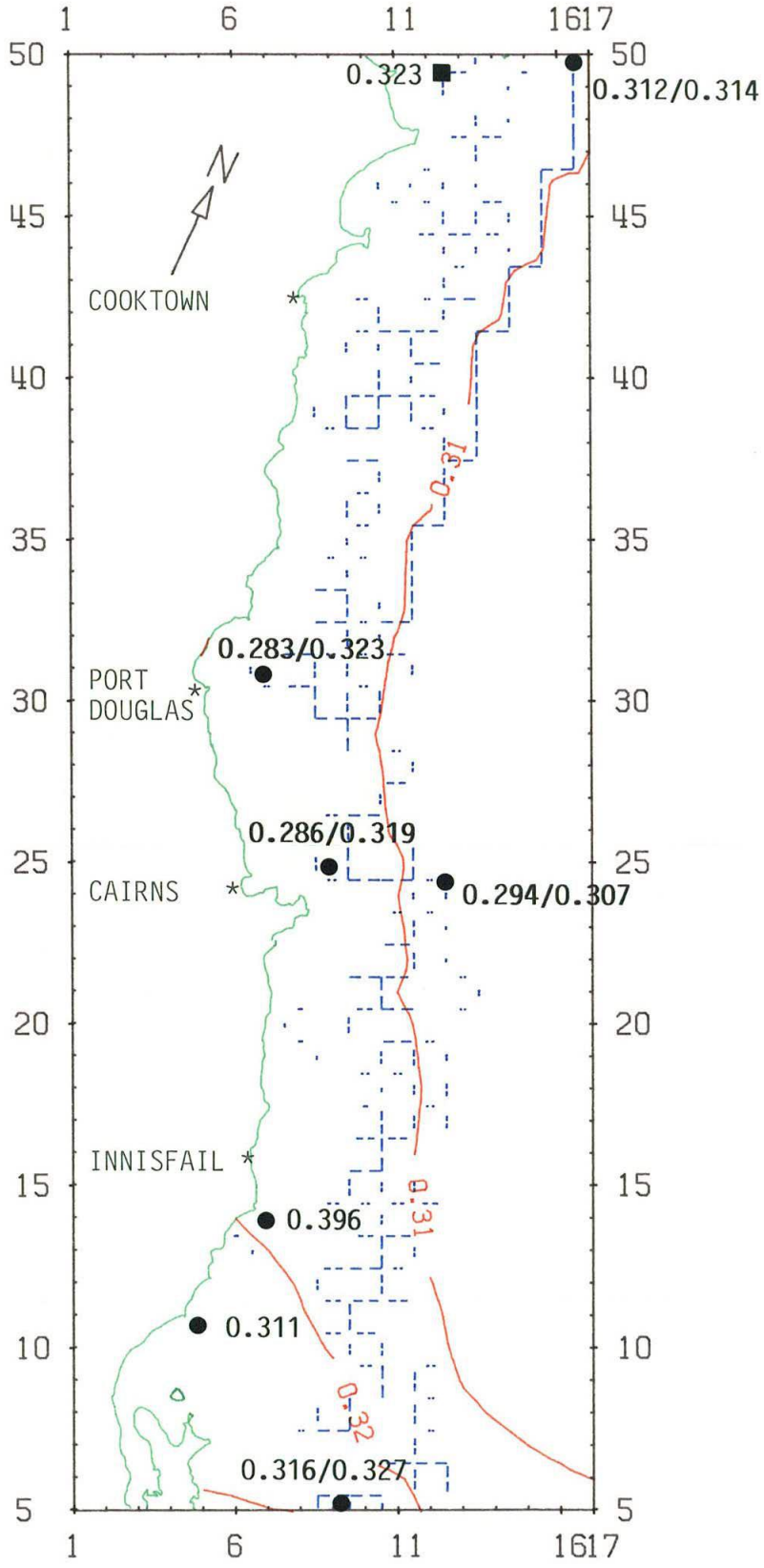


Figure 3.2a Comparison of observed and predicted values of tidal elevation amplitude for the K1 declinational diurnal constituent within the Cairns Section of the GBR Marine Park. See caption, Figure 3.1a, for further details.

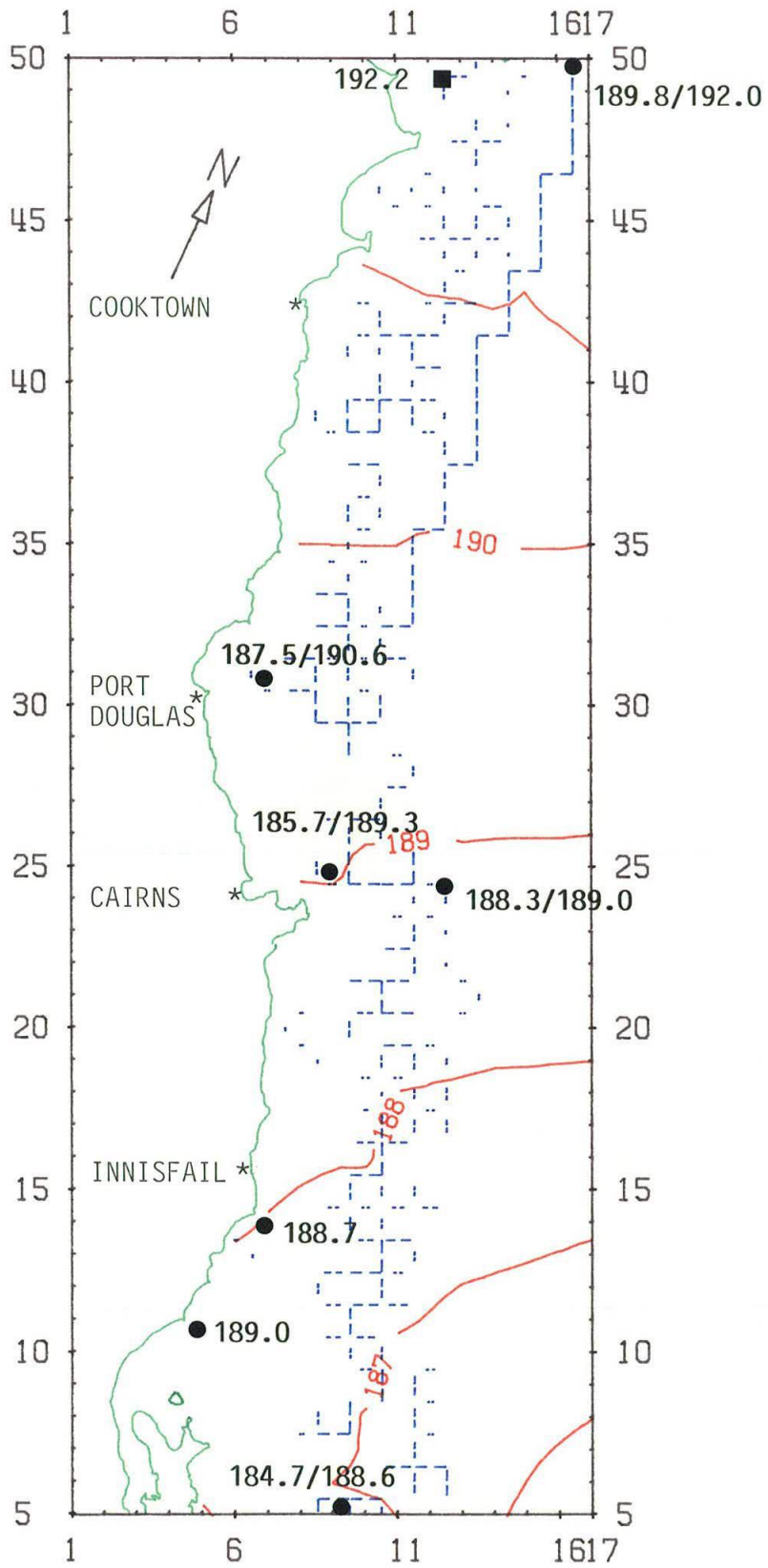


Figure 3.2b Comparison of observed and predicted values of tidal elevation phase for the K1 declinational diurnal constituent within the Cairns Section of the GBR Marine Park. See caption, Figure 3.1b, for further details.

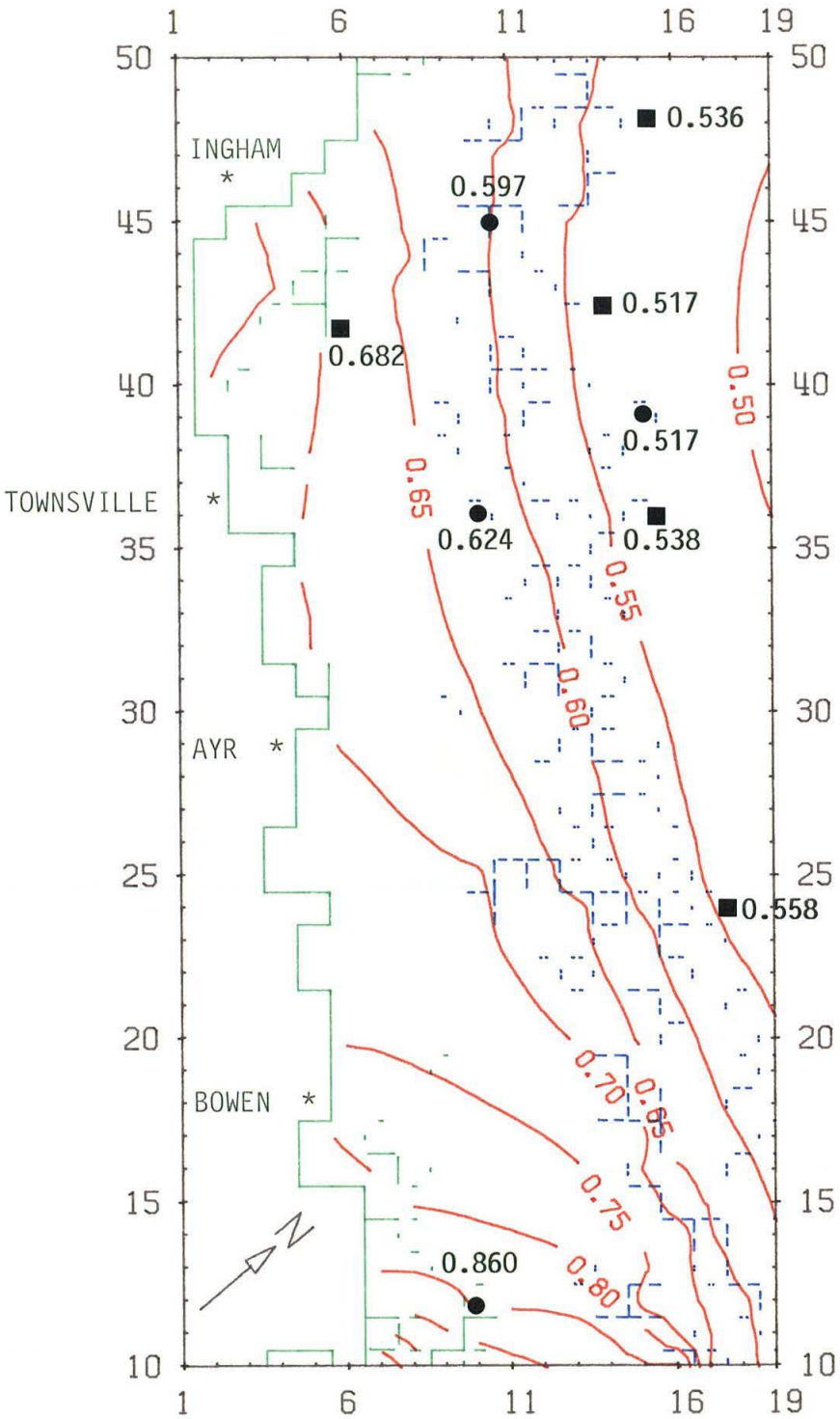


Figure 3.3a Comparison of observed and predicted values of tidal elevation amplitude for the M2 semi-diurnal principal lunar constituent within the Central Section of the GBR Marine Park. Published data are from Hamon (1984) (denoted ●) and Andrews and Bode (1988) (denoted ■). Tidal amplitudes are in metres.

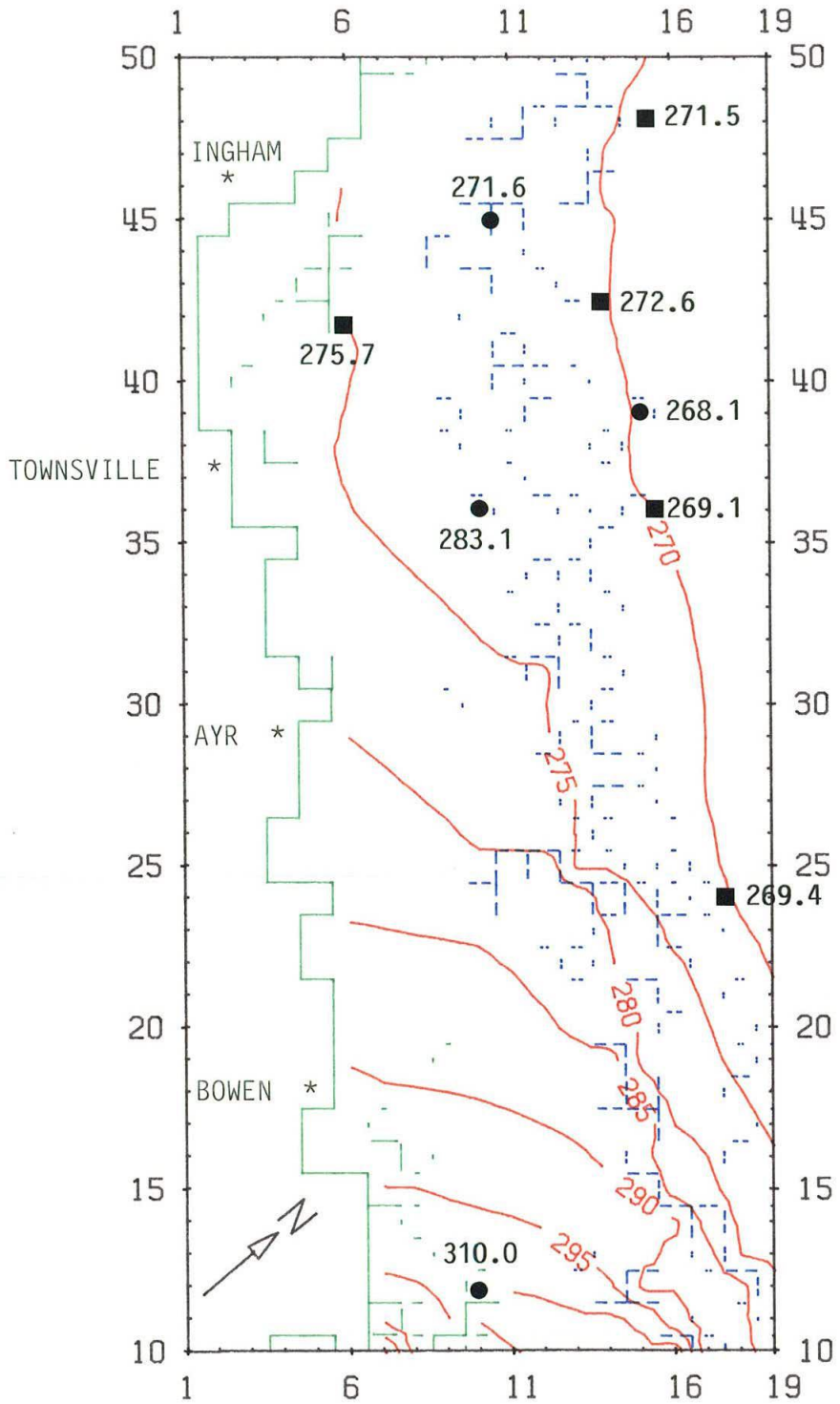


Figure 3.3b Comparison of observed and predicted values of tidal elevation phase for the M2 semi-diurnal principal lunar constituent within the Central Section of the GBR Marine Park. Published data are from Hamon (1984) (denoted ●) and Andrews and Bode (1988) (denoted ■). Greenwich phase lags are for GMT-10.

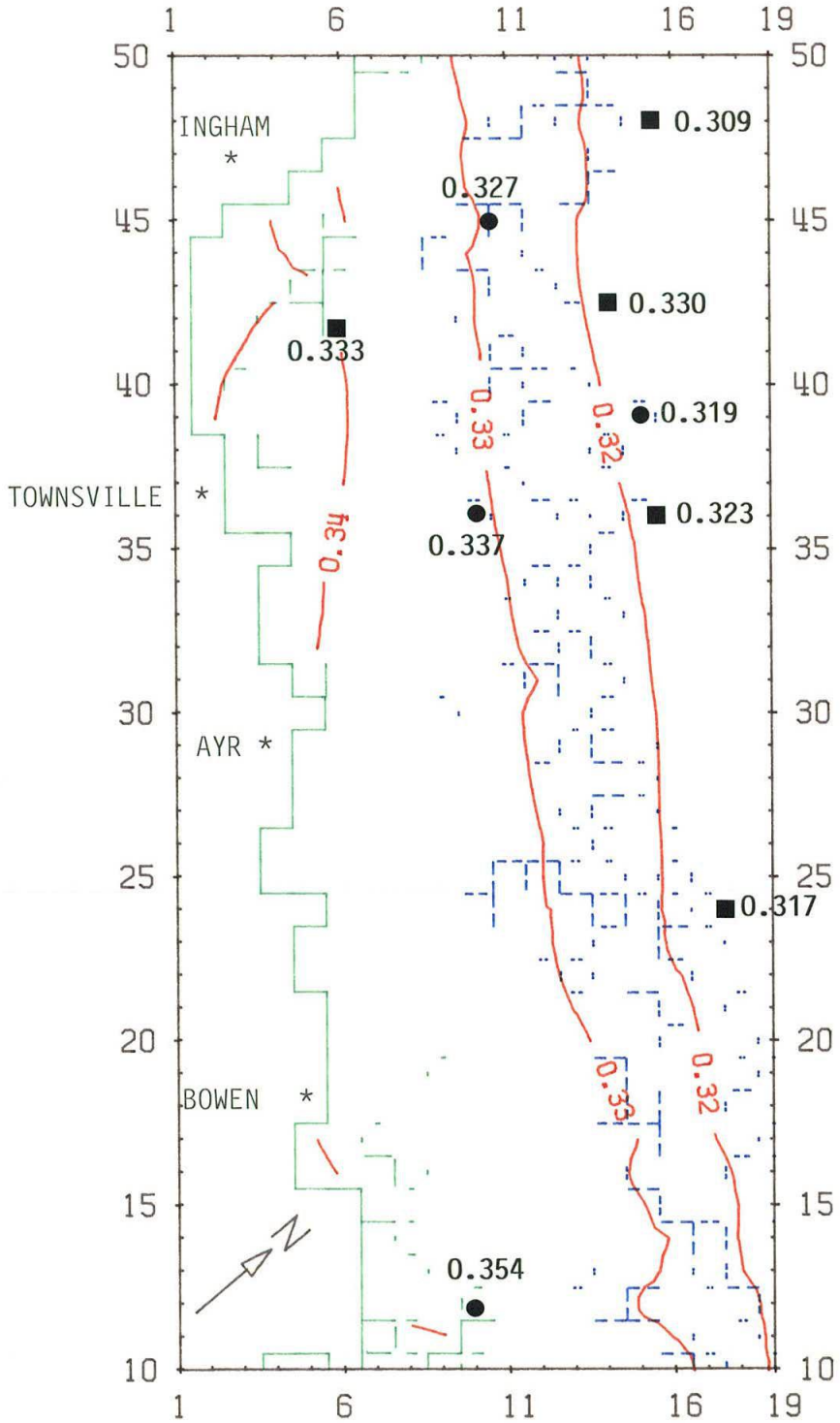


Figure 3.4a Comparison of observed and predicted values of tidal elevation amplitude for the K1 declinational diurnal constituent within the Central Section of the GBR Marine Park. See caption, Figure 3.3a, for further details.

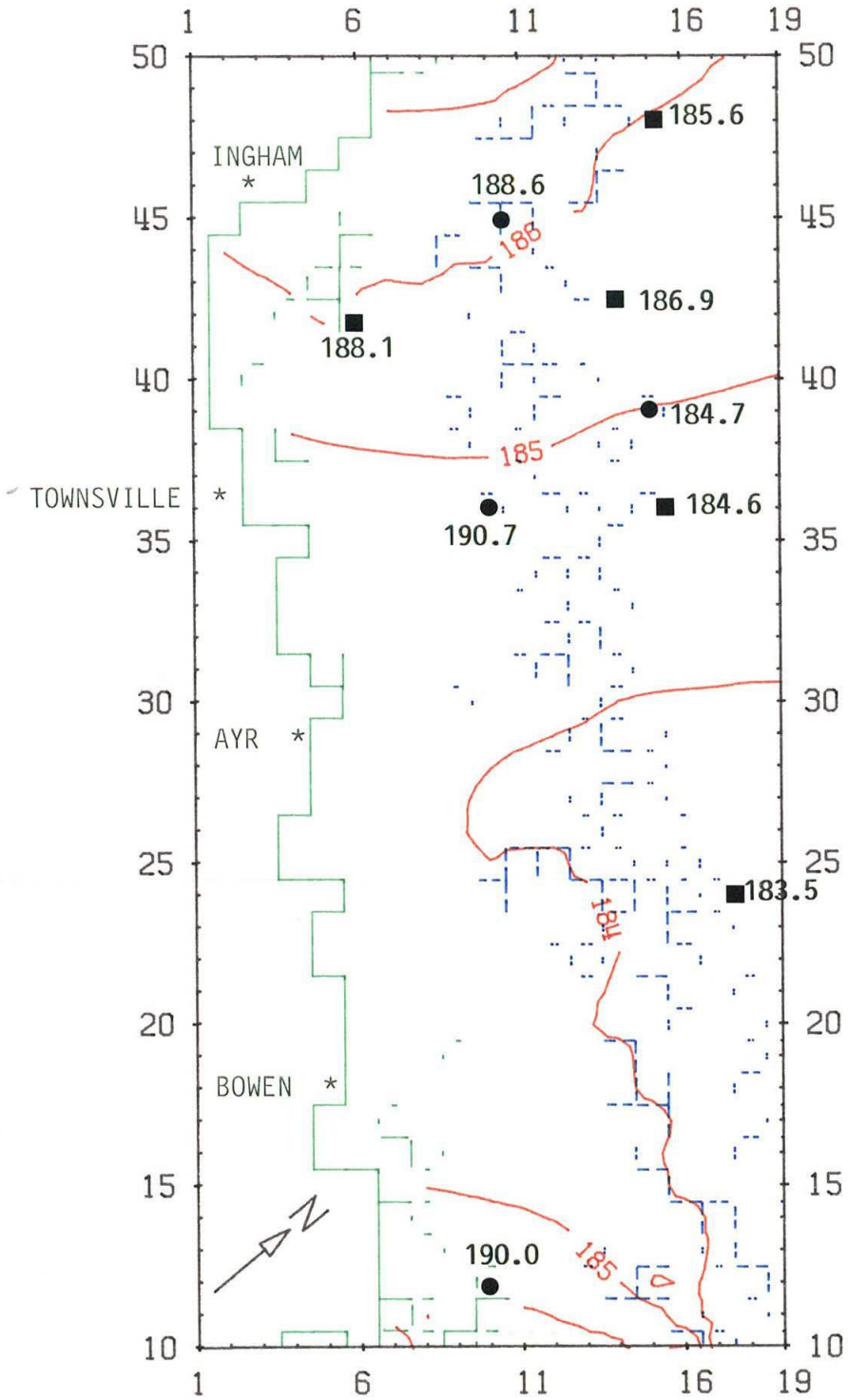


Figure 3.4b Comparison of observed and predicted values of tidal elevation phase for the K1 declinational diurnal constituent within the Central Section of the GBR Marine Park. See caption, Figure 3.3b, for further details.

of observed values from some locations (Figs. 3.1 and 3.2). Notable features predicted by the model are the increased amplification of the tides and a high degree of phase retardation resulting from the blocking effect of the reefs in the south of the Central Section (Figs. 3.3 and 3.4). These results are consistent with those of Middleton et al. (1984). Decrease in water depth as the tidal wave progresses across the shelf results in a general, and expected, increase in tidal amplitude shorewards.

Current ellipses (see Fig. 3.5) corresponding to the tidal constituents provide an effective way of summarizing complex time-dependent tidal flows over large spatial scales. For each constituent, the current vector is resolved into two perpendicular components, each oscillating at the same frequency. The resultant path traced out by the current vector over a tidal period is an ellipse. The maximum tidal current speed for any given constituent is provided by the magnitude of the semi-major axis; the minimum tidal current is given by the length of the semi-minor axis. Where the length of the semi-minor axis is insignificant, the current can be considered as rectilinear rather than rotary. The phase lag associated with the ellipse determines the time of maximum current, by convention on the flood tide. Tidal currents can be provided either by the analysis of field measurements or as the output of a numerical model.

An almost complete absence of published data on tidal currents within the Cairns Section precludes a direct comparison between observed and predicted current ellipse axes over the entire grid. Slightly more data are available for the Central Section. Predicted current ellipse axes for the major semi-diurnal constituent M2 are presented for both the Cairns and Central Sections in Figures 3.6 and 3.7 respectively. Comparison is possible with observed current ellipse axes for the M2 and K1 constituents from stations C1, C2 and C3 of Andrews and Bode (1988) at the southern end of the Cairns Section grid, and for their stations C5 to C8, C10, C11, C13, C14 and C16 within the Central Section grid. Agreement is very good, both with respect to current velocity and the orientation of ellipse axes.

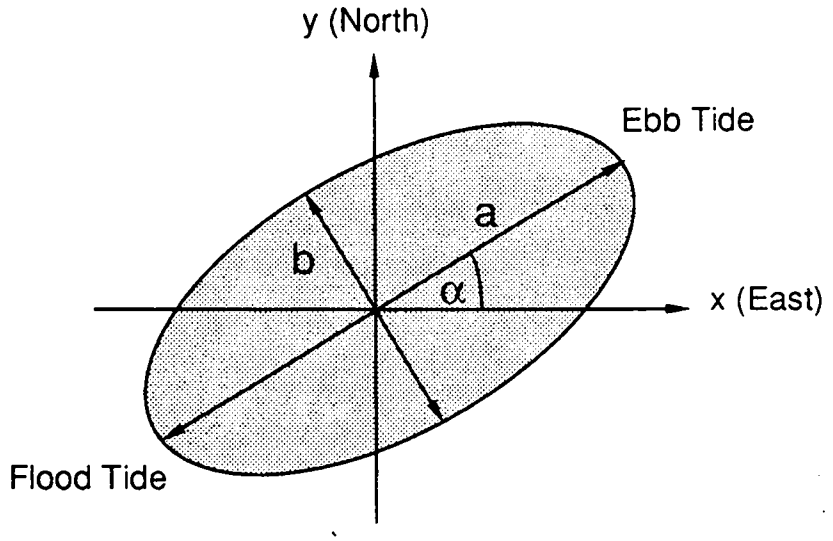


Figure 3.5 Tidal current ellipse showing the semi-major axis *a* and the semi-minor axis *b*, with the major axis inclined at angle α to the x-axis. During the course of a tidal cycle, the tip of the velocity vector traces out an ellipse, the axes of which are alligned to the new coordinate system.

The characteristics of tidal flow are exemplified by the current ellipses predicted for the M2 constituent (Figs. 3.6 and 3.7). The M2 constituent accounts for approximately half of the observed tidal signal. Significant tidal currents are restricted to the relatively shallow waters over the continental shelf, where flow is essentially onshore-offshore throughout the Cairns Section and the northern half of the Central Section. Tidal ebb and flood directions are offshore and onshore respectively. Exceptions to this cross-shelf flow occur close inshore along the coast south of Innisfail (Fig. 3.6) and within the southern half of the Central Section (Fig. 3.7) where currents are longshore. Tidal ebb and flood directions for these areas are towards the north and south respectively. These model predictions, with respect to the longshore orientation of tidal flow, are in agreement with observations by Andrews and Bode (1988) for their stations C1 and C16. Middleton et al. (1984) have shown that it is the inhibitory effect of the dense offshore reefs to tidal flow which results in the tides flooding towards Broad Sound from the north in the southern portion of the Central Section. Beyond the continental shelf edge, tidal currents are greatly reduced, particularly in the northern portion of the Cairns Section where water depth increases rapidly (Fig. 3.6).

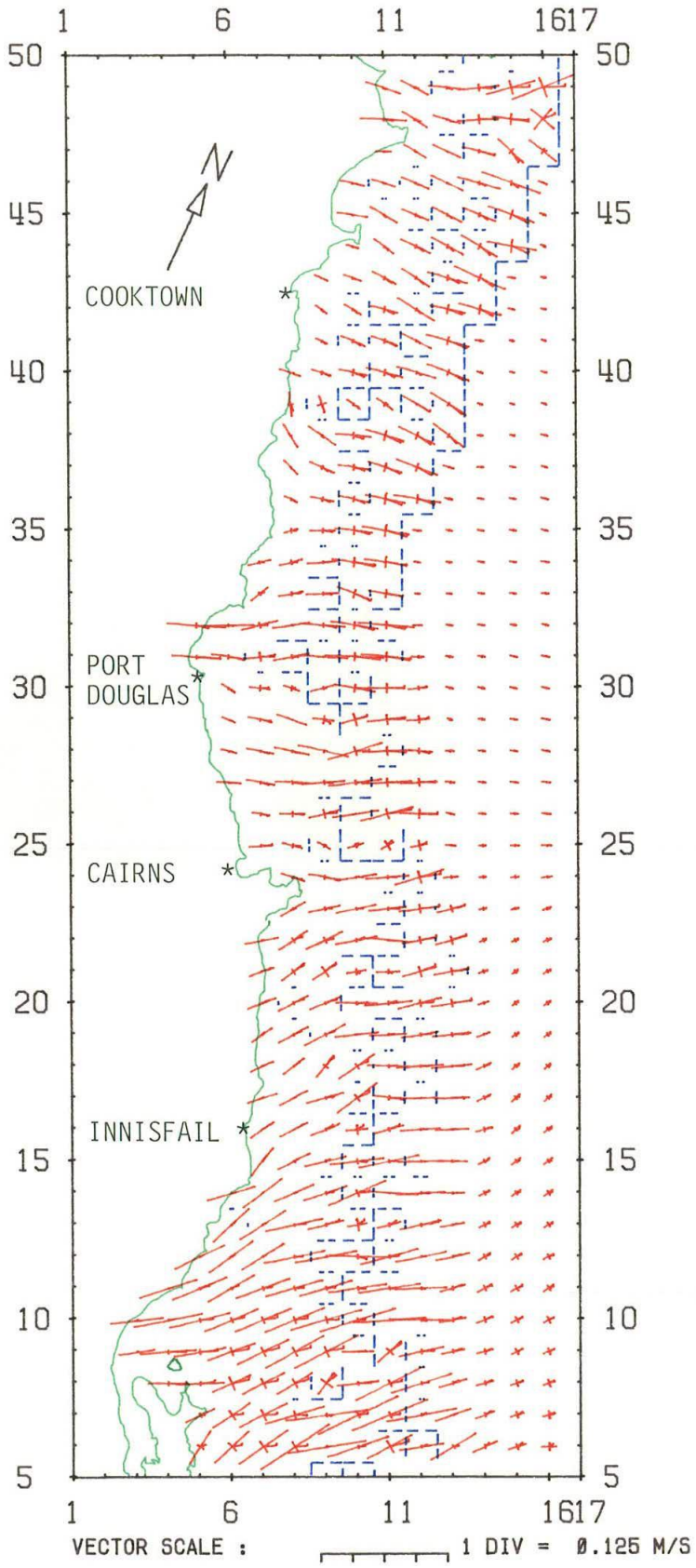


Figure 3.6 Current ellipse axes predicted for the major semi-diurnal constituent M2 (period=12.42 hrs.) within the Cairns Section of the GBR Marine Park. The ellipse axes represent components of vectors originating from their intersection.

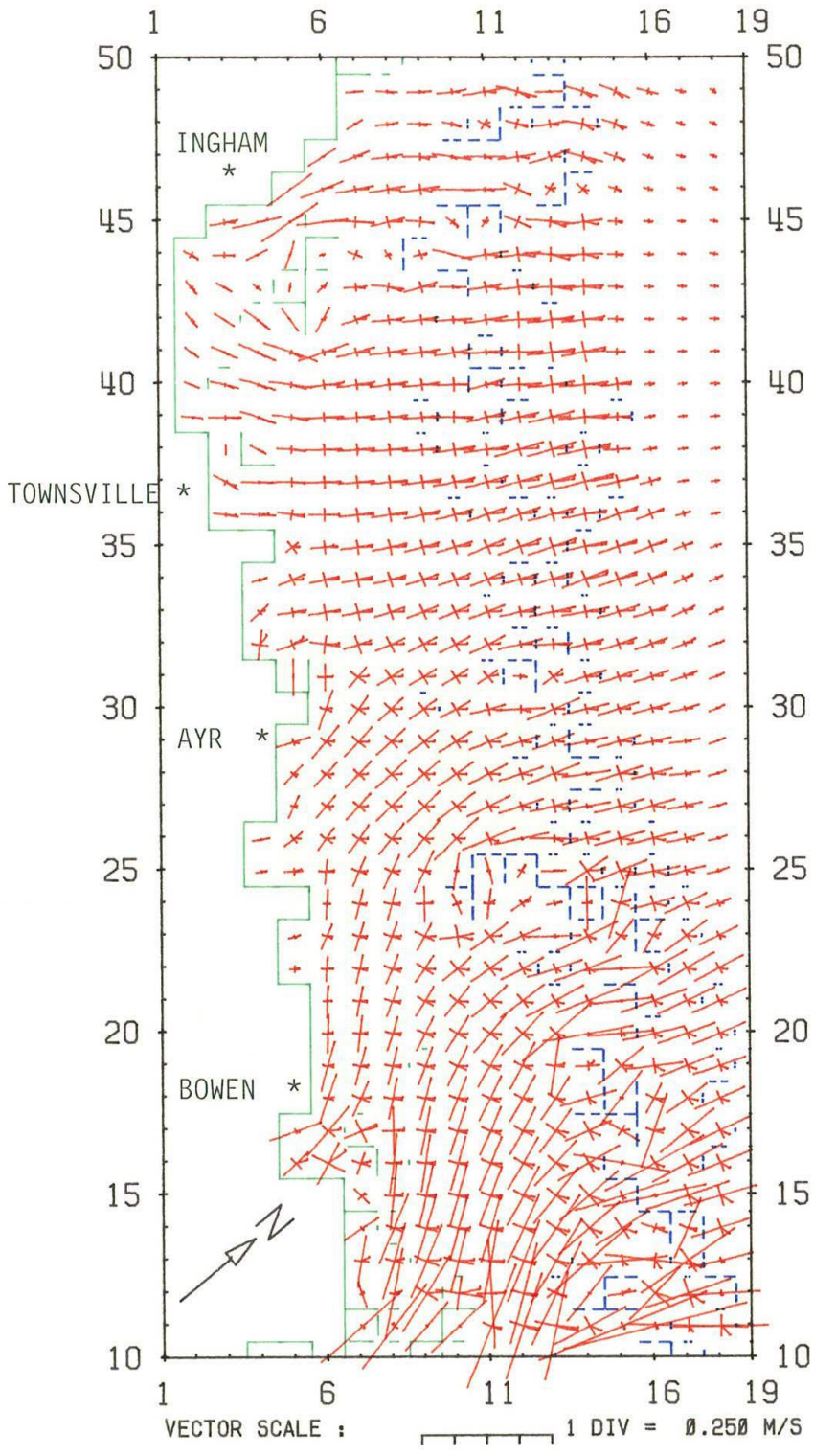


Figure 3.7 Current ellipse axes predicted for the major semi-diurnal constituent M2 (period=12.42 hrs.) within the Central Section of the GBR Marine Park. The ellipse axes represent components of vectors originating from their intersection.

3.1.2 Wind

Representative plots of current vectors are presented for four wind directions (north, north-east, south-east and south-west) over the Cairns Section grid (Figs. 3.8 to 3.11) and for two wind directions (north and south-east) over the Central Section grid (Figs. 3.12 and 3.13).

3.1.2.1 Patterns of wind-driven currents and model validation

The development of appreciable water currents due to wind stress is depth dependent and therefore, like tidal currents, largely restricted to the relatively shallow waters over the continental shelf (Figs. 3.8 to 3.13). Current speeds are greatly reduced off the shelf edge, particularly in the northern portion of the Cairns Section. The combination of Coriolis forces and shelf topography results in flow being channelled essentially along-shore and into the natural passages of this coastal/reef complex. This is particularly evident in the main lagoon which lies between the reef matrix and coastline, and in passages behind the ribbon reefs where currents are longshore and barotropic, but may also be observed in the larger passages connecting the main lagoon and Coral Sea. This pattern has been observed in field studies within the central GBR (Cresswell & Greig, 1978; Wolanski & Pickard, 1985; Frith et al., 1986). In contrast to the southern portion of the Cairns Section and the Central Section, where the water circulation is dominated by relatively large transports within the main lagoon, flow within the northern portion of the Cairns Section is concentrated in two narrow passages. In the north of the Cairns Section, the dense reef matrix extends across most of the shelf leaving one passage against the coast as a continuation of the lagoon and a second directly behind the ribbon reefs. Within the reef matrix wind driven current vectors exhibit no apparent pattern, and current speeds are greatly reduced as a result of the blocking effect of reefs to the development of long-shelf currents. Andrews and Gentien (1982) note the absence of longshore low frequency currents within the matrix of the relatively less dense Central Section of the GBR, while Wolanski and Pickard (1983a) observed a predominantly westward flow at Britomart Reef

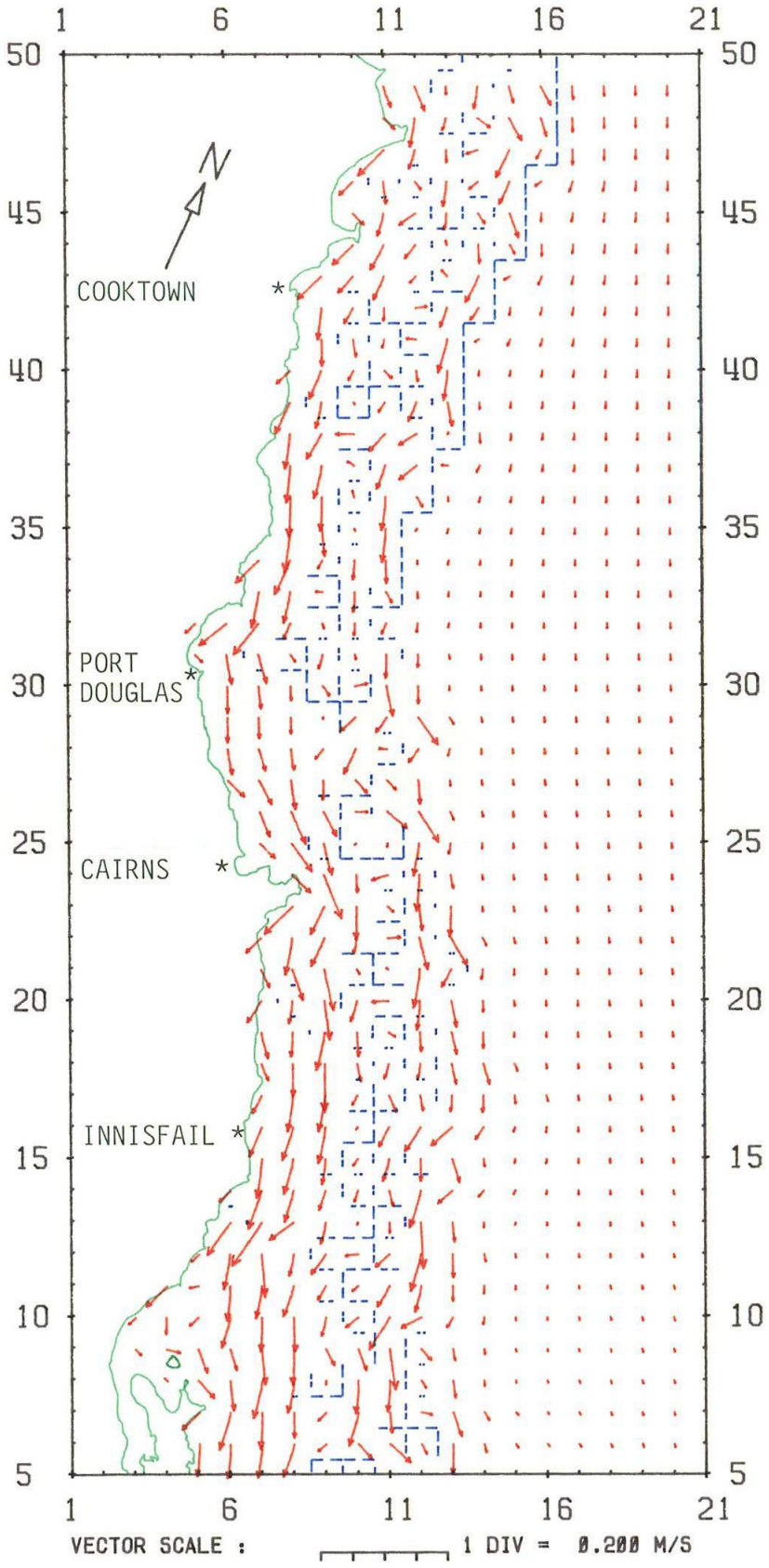


Figure 3.8 Current vectors within the Cairns Section of the GBR Marine Park corresponding to steady-state 15 knot winds from the north.

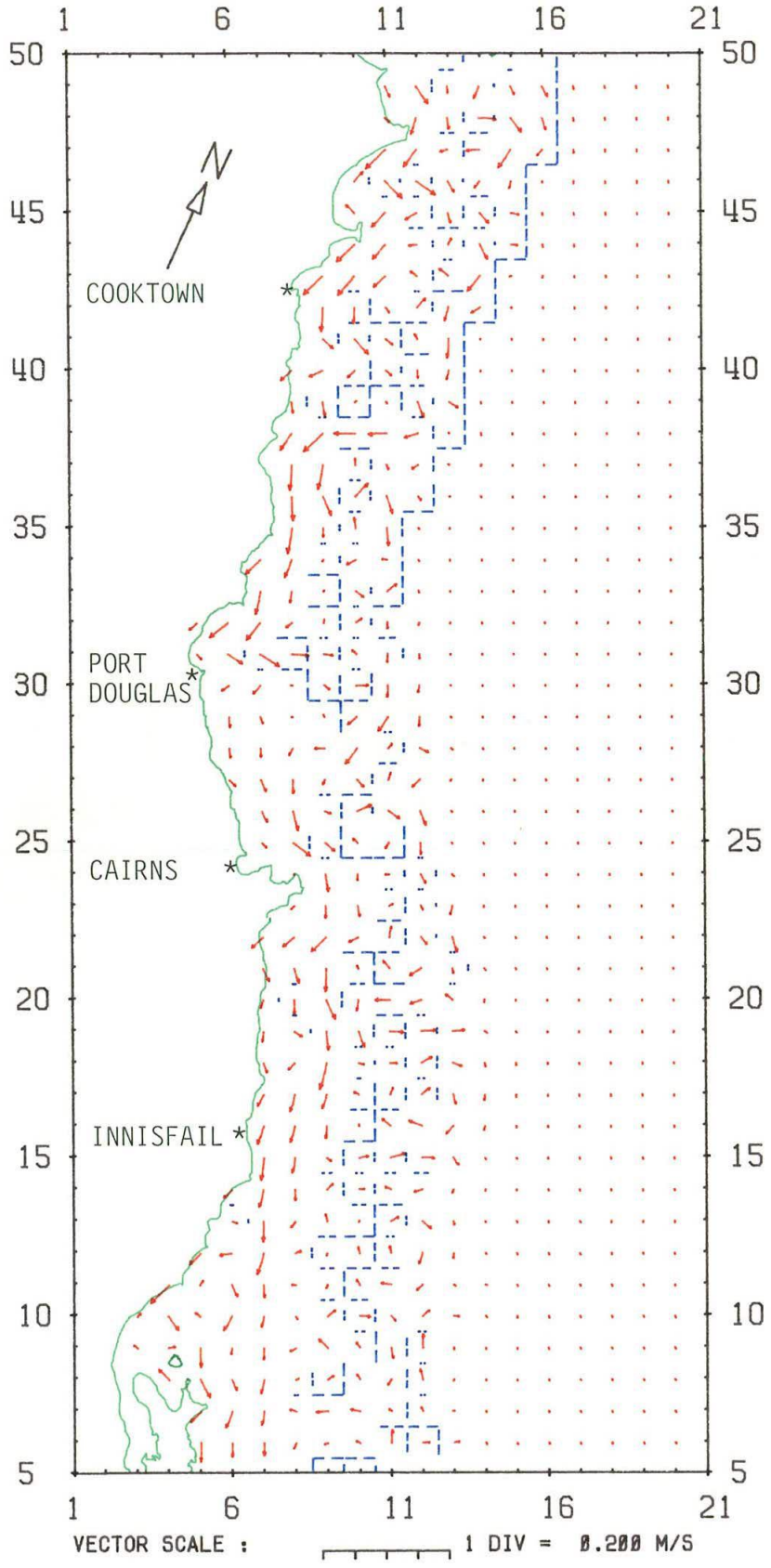


Figure 3.9 Current vectors within the Cairns Section of the GBR Marine Park corresponding to steady-state 15 knot winds from the north-east.

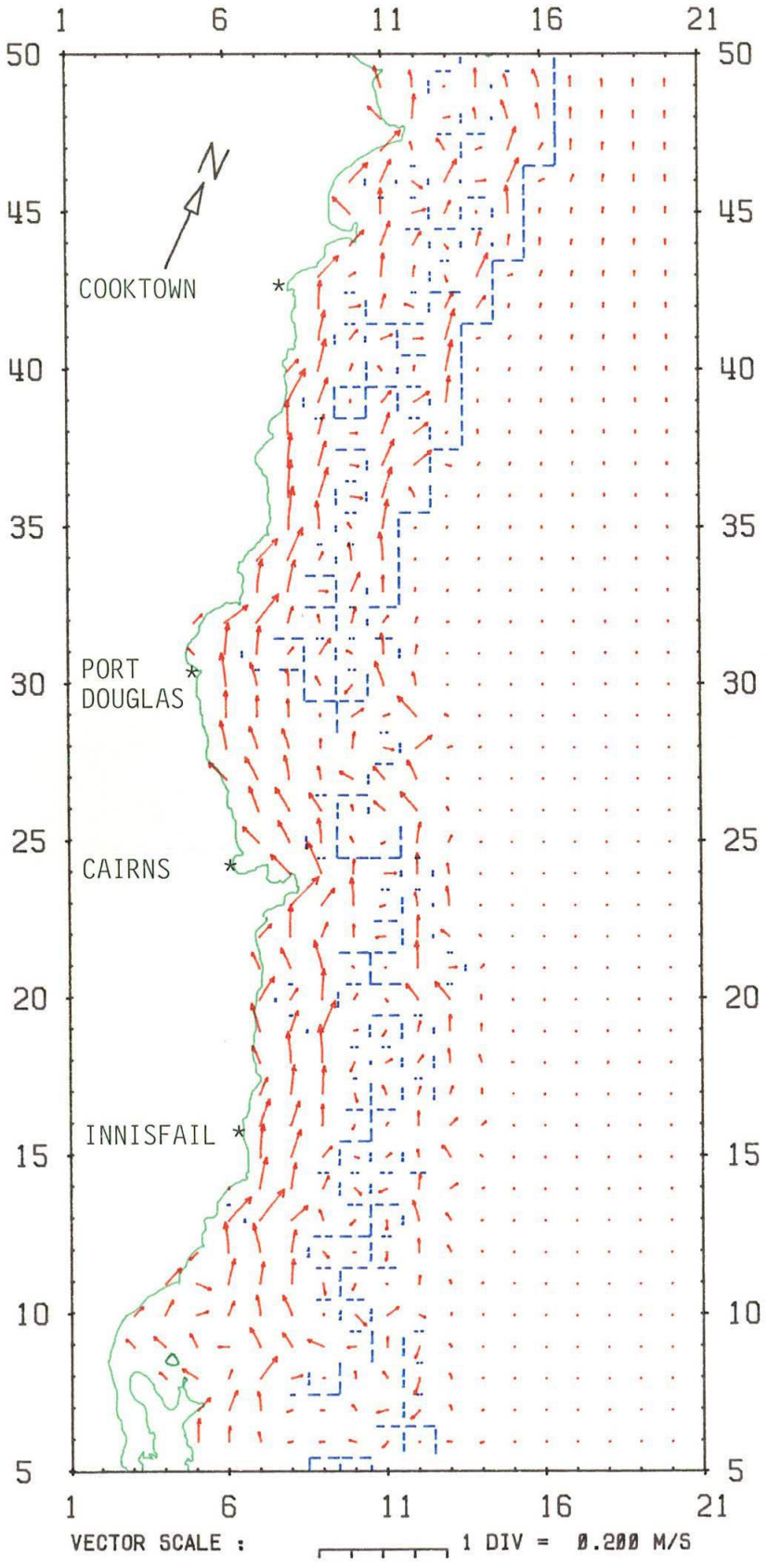


Figure 3.10 Current vectors within the Cairns Section of the GBR Marine Park corresponding to steady-state 15 knot winds from the south-east.

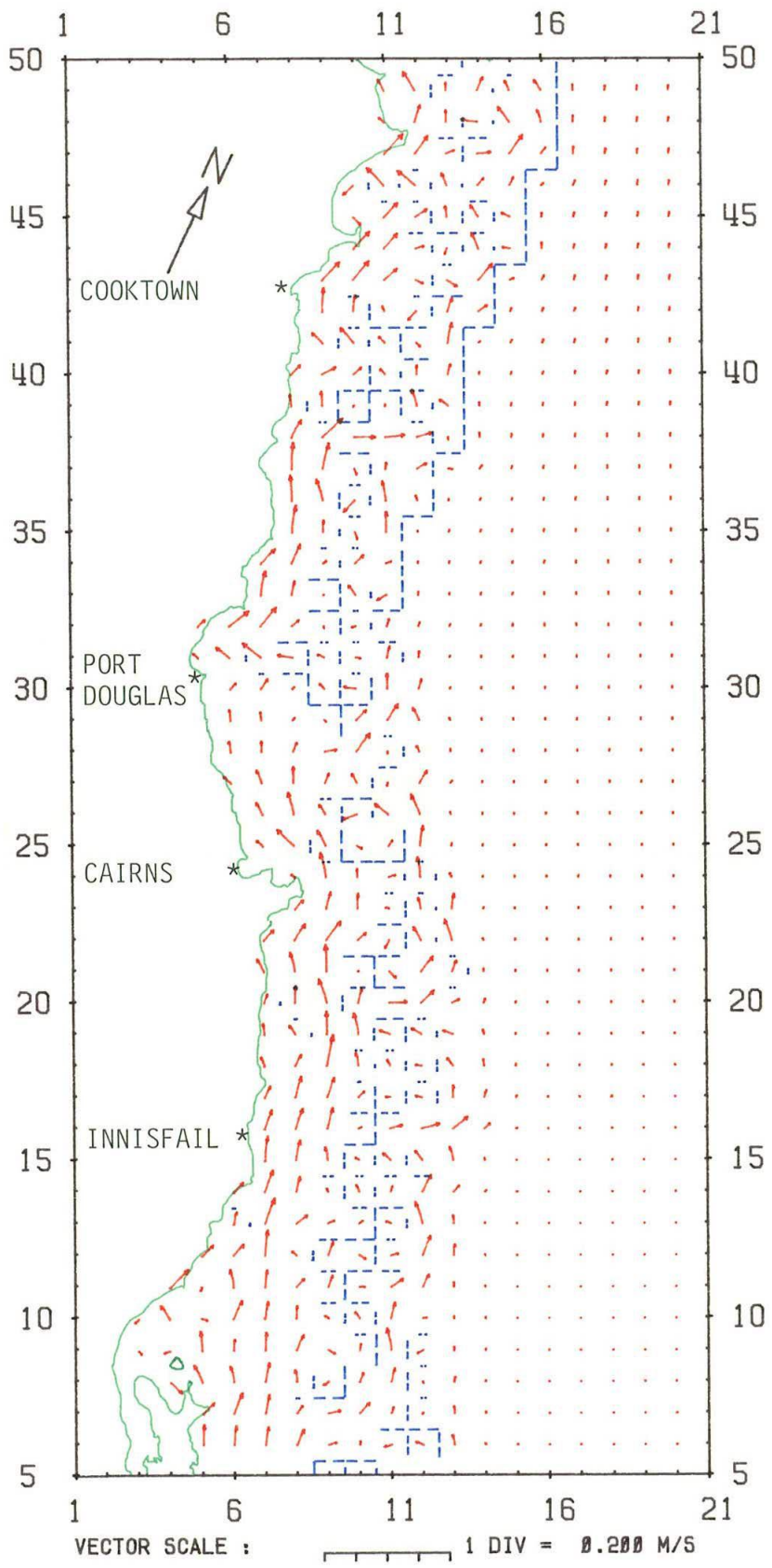


Figure 3.11 Current vectors within the Cairns Section of the GBR Marine Park corresponding to steady-state 15 knot winds from the south-west.

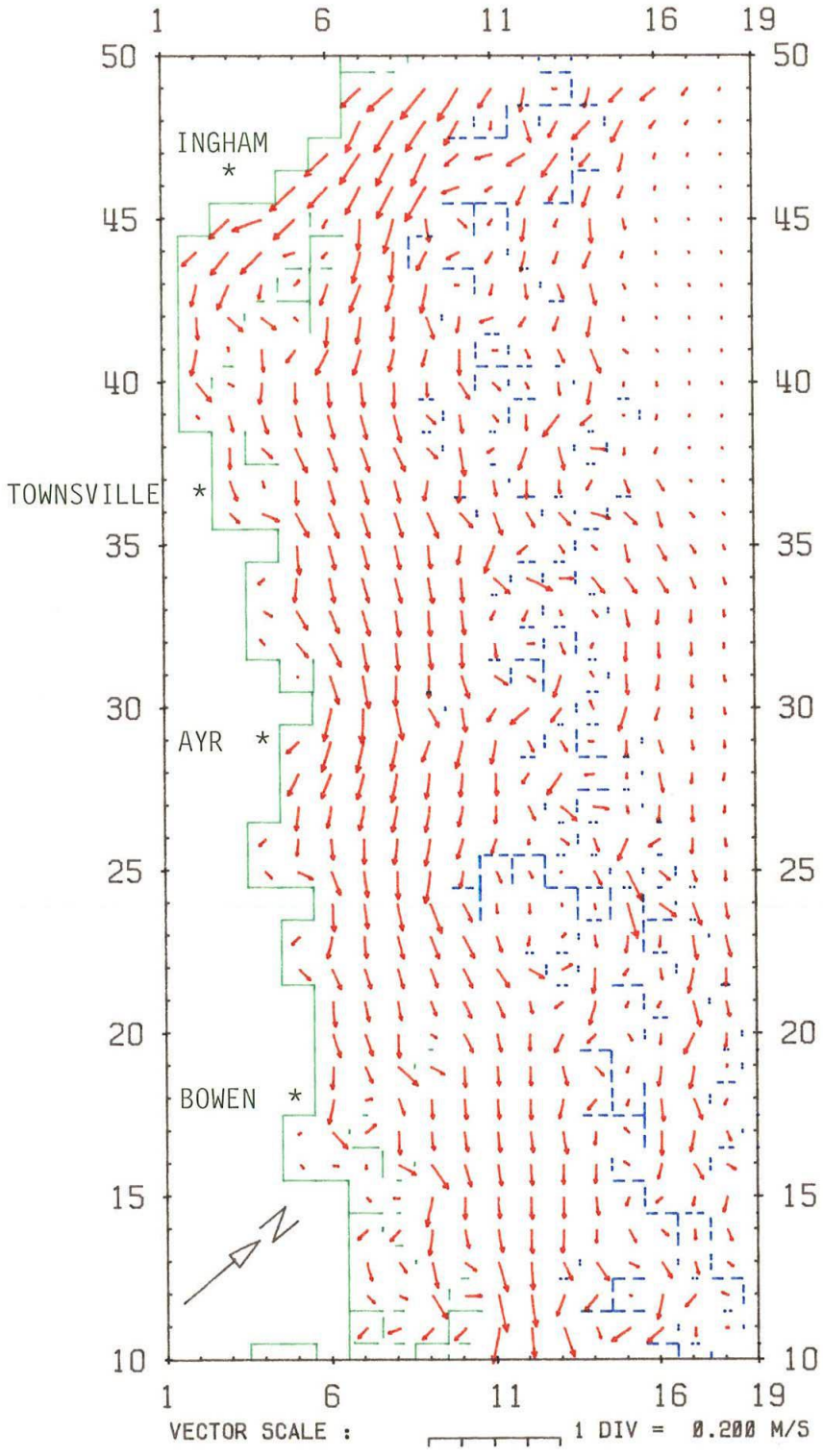


Figure 3.12 Current vectors within the Central Section of the GBR Marine Park corresponding to steady-state 15 knot winds from the north.

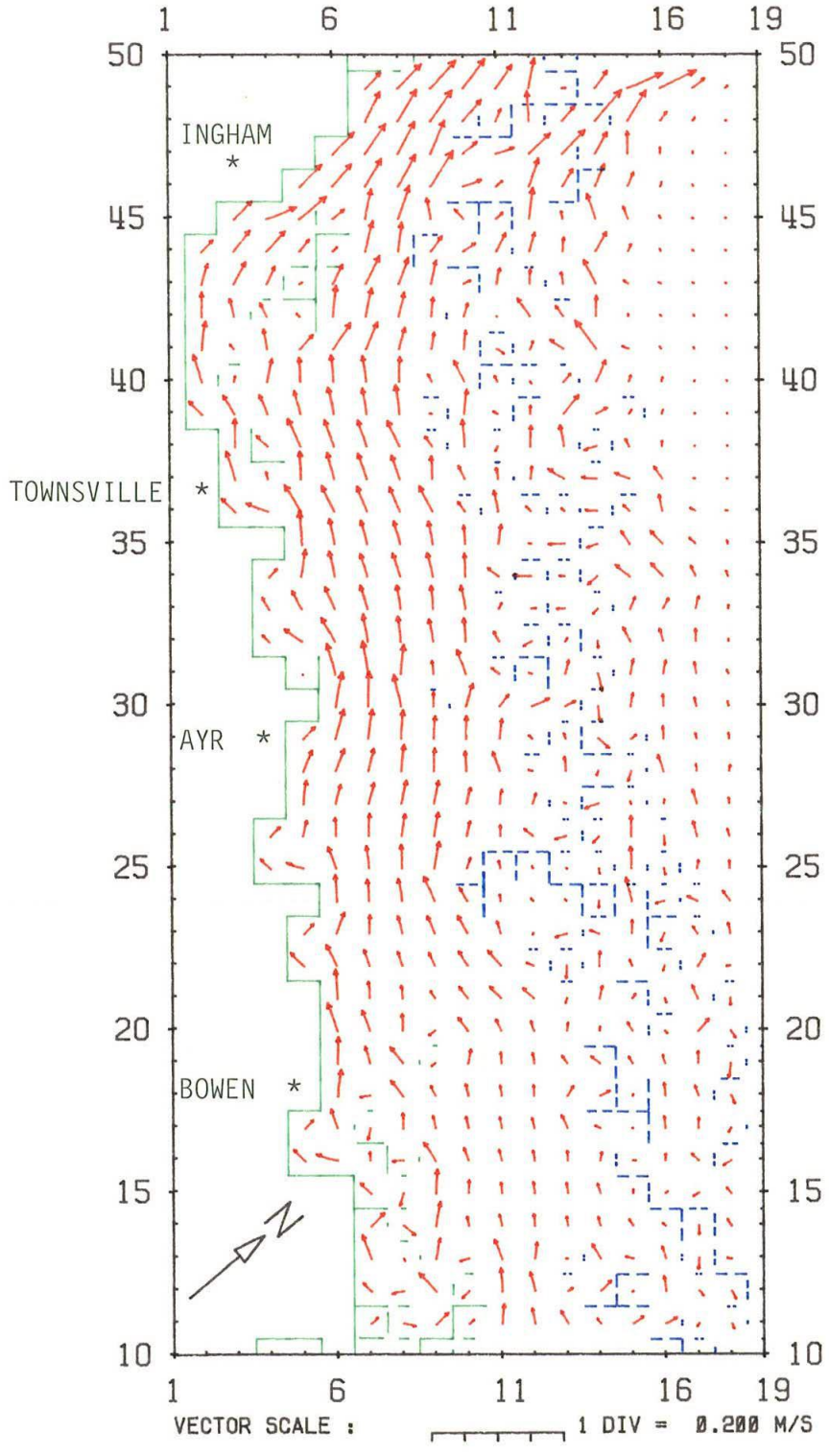


Figure 3.13 Current vectors within the Central Section of the GBR Marine Park corresponding to steady-state 15 knot winds from the south-east.

which was not correlated significantly with the longshore wind component. Within the reef matrix, flow will be directed by the complex and relatively dense arrangement of coral reefs and is expected to follow the natural passages. The absence of any apparent pattern in the current vectors within the matrix is a reflection of the relatively coarse grid scale and not an inadequacy of the model *per se*. Flow patterns around individual reefs could be resolved simply by using a finer grid scale. The current vectors within the matrix are a reasonable representation of the gross flow patterns within this physically complex region.

3.1.2.2 Dynamics of wind-driven currents

The general pattern described above is characteristic of all wind directions and speeds. Variation in wind direction results in flow being directed either poleward or equatorward roughly parallel to the isobaths within the main lagoon, passages behind the ribbon reefs and along the shelf edge south of the ribbon reefs. Apart from the long-shelf direction of flow, only the magnitude of the long-shelf currents varies significantly with wind direction and speed. Winds from the northerly and southerly quarters generally forced stronger currents than those from the east and west. Current velocities in the main lagoon south of Cairns and into the Central Section should exceed 50 cm s^{-1} during periods of strong winds. However, wind driven current velocities under more normal conditions may reach 20 to 30 cm s^{-1} (Figs. 3.8 to 3.13). Predicted current velocities in the vicinity of Low Isles, Green Island and Euston Reef correspond well with observations of wind strength and current speed (see Cresswell & Greig, 1978; Wolanski & Bennett, 1983; Wolanski & Pickard, 1985).

3.1.3 East Australian Current

Model results as current vectors are presented for the Cairns and Central Sections in Figures 3.14 and 3.15 respectively. In principle, output agrees with our limited knowledge of the East Australian Current. In the north of the Cairns Section (Fig. 3.14), currents off the shelf edge are generally weak, but farther to the south away from

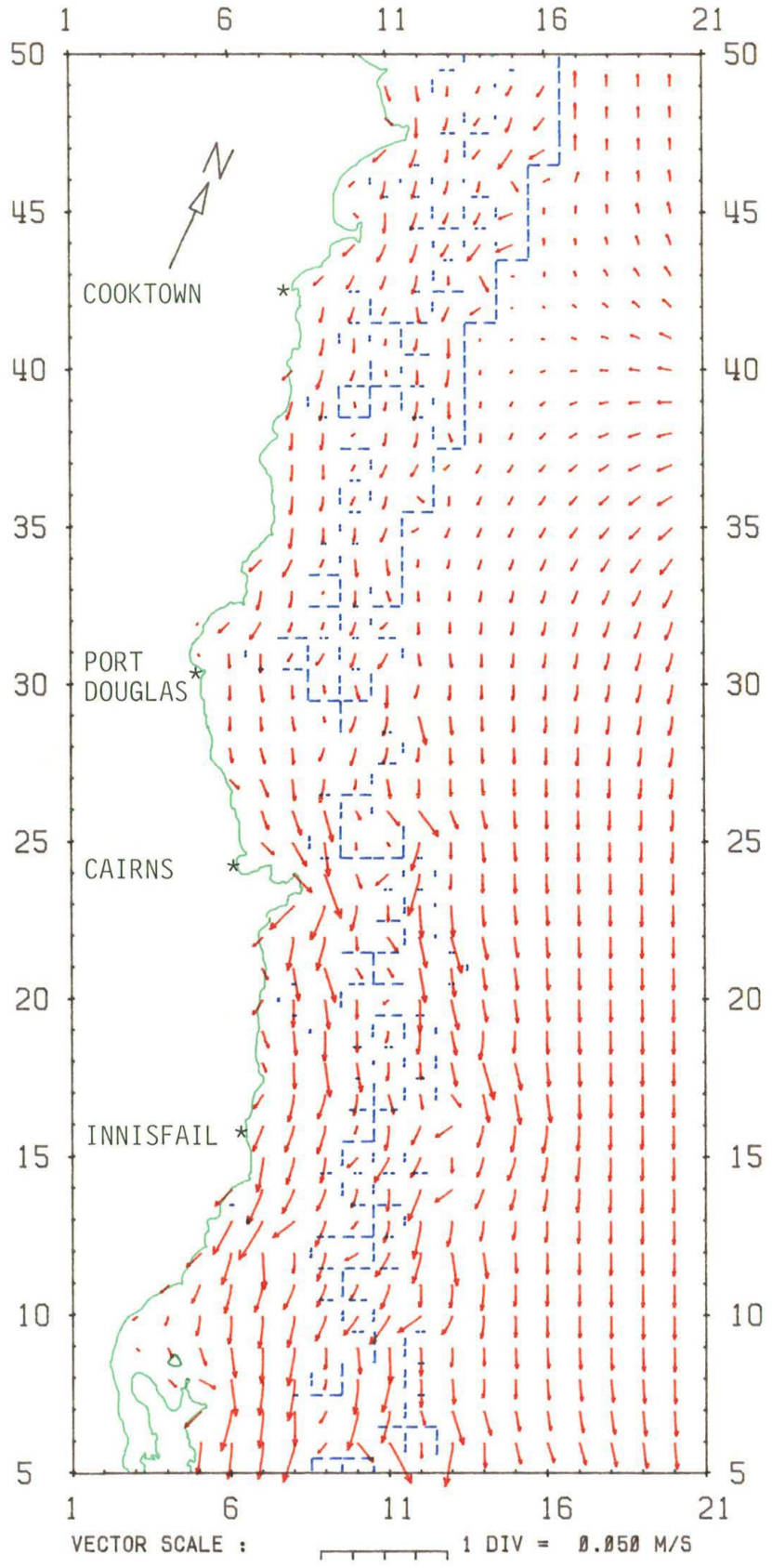


Figure 3.14 Current vectors within the Cairns Section of the GBR Marine Park corresponding to flow associated with the East Australian Current. Velocities are calibrated to match published observations.

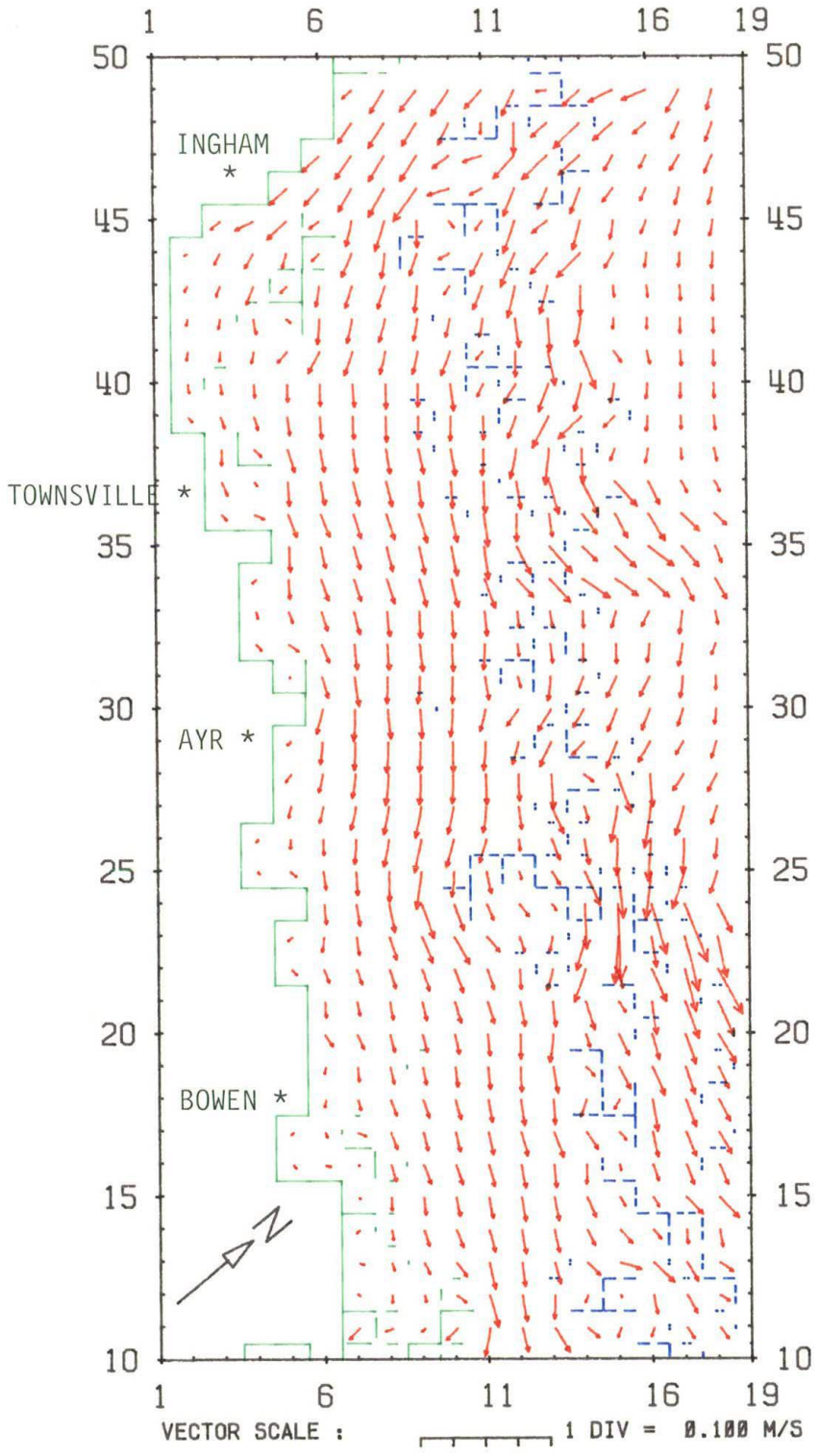


Figure 3.15 Current vectors within the Central Section of the GBR Marine Park corresponding to flow associated with the East Australian Current. Velocities are calibrated to match published observations.

the EAC bifurcation, they intensify and flow polewards. Church (1988) identifies the region of bifurcation with weak westward flowing currents to lie between 14 and 16 degrees latitude over the summer period. The exact location of the bifurcation point, however, varies seasonally as it shifts along the shelf. The strength of surface currents off the edge of the continental shelf are reported to vary up to a maximum of about 8 cm s^{-1} (Church, 1988). Seasonal and inter-annual variations in current velocity have been identified by Wolanski and Pickard (1985). A longshore pressure gradient associated with the EAC results in flow penetrating across the continental shelf (Middleton, 1987). In contrast to both tidal and wind driven flows, currents associated with the EAC are predicted to be of roughly equal intensity both on and off the continental shelf. This is consistent with the findings of Andrews (1983) who recorded currents of 7 cm s^{-1} off John Brewer Reef during summer which are attributable to the EAC. There appears to be some substantiation for the accelerating flow patterns observed in Figures 3.14 and 3.15. The calibrated current velocities have values of up to approximately 8 cm s^{-1}, with 5 cm s^{-1} being more typical. The almost continuous chain of outer ribbon reefs in the north of the Cairns Section appear to act as a semi-permeable barrier, greatly reducing the effect of the current on the continental shelf in this area. Frith et al. (1986) were unable to detect any flow which could be directly attributed to the EAC in the passage between the ribbon reefs and Lizard Island. While the EAC results in a net southerly drift along the shelf, it may be as much as an order of magnitude less than the currents associated with wind driven circulation.

3.1.4 Summary and Conclusions

Currents of tidal period may for short intervals be greater than 20 cm s^{-1} and of a similar magnitude to those of wind driven currents. Calculated particle displacements along the major axes of the tidal ellipses, usually in a cross-shelf direction, show strong spatial variation. Behind the ribbon reefs the maximum tidal excursion predicted is 5.2 km, corresponding closely to that observed by Frith et al. (1986). Within the main lagoon, however, the maximum calculated tidal excursion does not greatly exceed 3 km within the

Cairns and northern portion of the Central Sections. A cross-shelf displacement of this magnitude resulting from tidal currents will generally be superimposed upon longer-period currents parallel to the isobaths. The relative magnitudes of these two components of circulation indicate that the cross-isobath flow resulting from tidal currents will not obscure the currents resulting from wind stress. Tidal currents within the lagoon are rarely likely to reverse the direction of longer-period flow but act primarily to modulate the low-frequency longshore currents (Wolanski & Bennett, 1983). In summary, residual displacements associated with the tides are normally small, except possibly over and close to reefs, and are therefore unlikely to contribute significantly to the net advection of larvae or to cross-shelf exchange within this lagoonal region once larvae have left their natal reef.

Overall, the model results correspond well to our understanding of the large-scale features and dynamics of water circulation on the continental shelf within the Cairns and Central Sections of the GBR Marine Park. The results also indicate a markedly different hydrodynamic regime in the northern portion of the Cairns Section behind the ribbon reefs compared to that further south within the southern portion of the Cairns Section and the Central Section.

3.2 FINE-SCALE HYDRODYNAMICS

The results of fine-scale hydrodynamic modelling are consistent with research previously published by Black and Gay (Black, 1983,1988; Black and Gay, 1987a,b). Representative plots of current vectors over a tidal cycle (12 hours) and residual circulation are presented for reef type L2 in Figures 3.16 and 3.17. Representative plots of current vectors over a tidal cycle and residual circulation for all other reef types are presented in Appendix B.

3.2.1 Flow Dynamics

The sequence of flow patterns over a tidal cycle (Fig. 3.16) illustrate the dynamics of water motion around and over reefs. Initially (plot 1,

at 69 hours), the tide has just passed low water, tidal currents are relatively weak and flow roughly opposite in direction to the long-shelf current. Progressively over the next three hours tidal currents reach their maximum flood velocity (plot 4), perpendicular to the long-shelf current and in an on-shore direction. Subsequently, tidal currents weaken and approximately three hours later the tide is high, tidal currents are again relatively weak and now flow in the same direction as the long-shelf current (plot 7). A further three hours later (plot 10), tidal currents reach their maximum ebb velocity and again flow perpendicular to the long-shelf current, this time in an off-shore direction. Two hours later (plot 12) the tide is still ebbing, but is approaching low water.

The residual circulation (Fig. 3.17), attained by summing all current vectors at each grid location over a tidal cycle, indicates that there is a stronger net flow of water in an anti-clockwise direction around the reef. These results are consistent for all schematized reefs (see Apendix B). The net anti-clockwise circulation has important implications for larvae approaching the reef from the far field (see Section 3.3). Black and Gay (1987b) propose that the anti-clockwise residual circulation around reefs within the GBR results from negative Coriolis forcing in the southern hemisphere. Such strong residual circulation may not be representative of reefs which are in close proximity to others, as circulation is strongly influenced by neighbouring reefs (Black & Gay, 1987). The anti-clockwise circulation is consistent with simulations of the hydrodynamics around Bowden, Davies and Wheeler Reefs (Black & Gay, 1987) and with field observations from Stanley Reef (Wolanski et al., 1989).

These dynamics and patterns are generally representative of all the schematized reefs (see Appendix B). Variation in reef shape (e.g., between P4 and L2, see Fig. 2.4) has no major effect on water circulation around the reefs. Some small differences are observed over the reef due to the presence or absence of a lagoon and extended area of reef flat. Variation in reef size has a far more noticeable effect on mainstream circulation patterns. Small reefs, such as type P1, have only a relatively minor influence on the mainstream circulation. In contrast, large reefs, such as types P5, L3 and ML, strongly

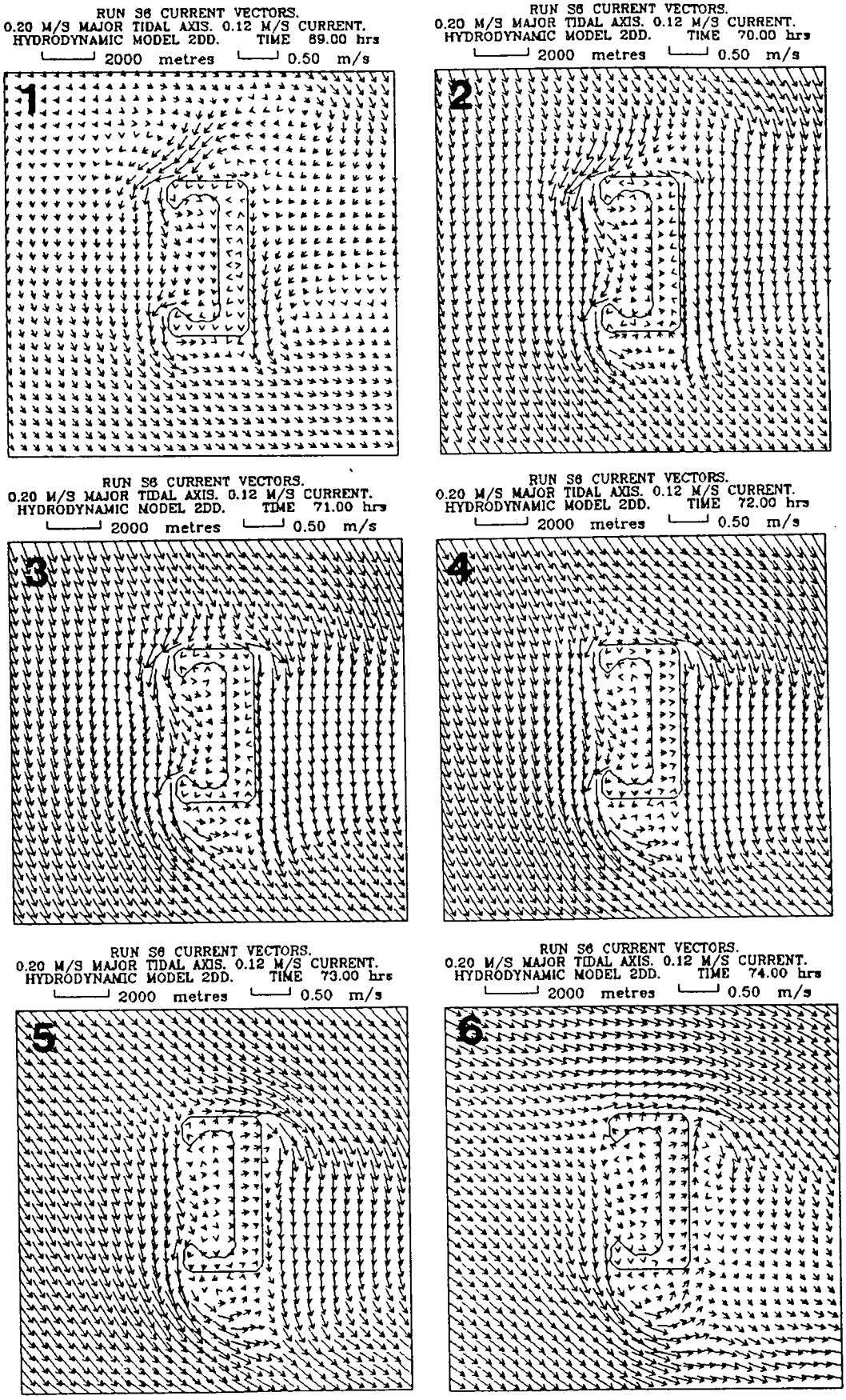


Figure 3.16a Representative plots of current vectors over a tidal cycle for reef type L2. Plots (labelled 1 to 6) represent currents at one hour intervals from when the tide begins to flood.

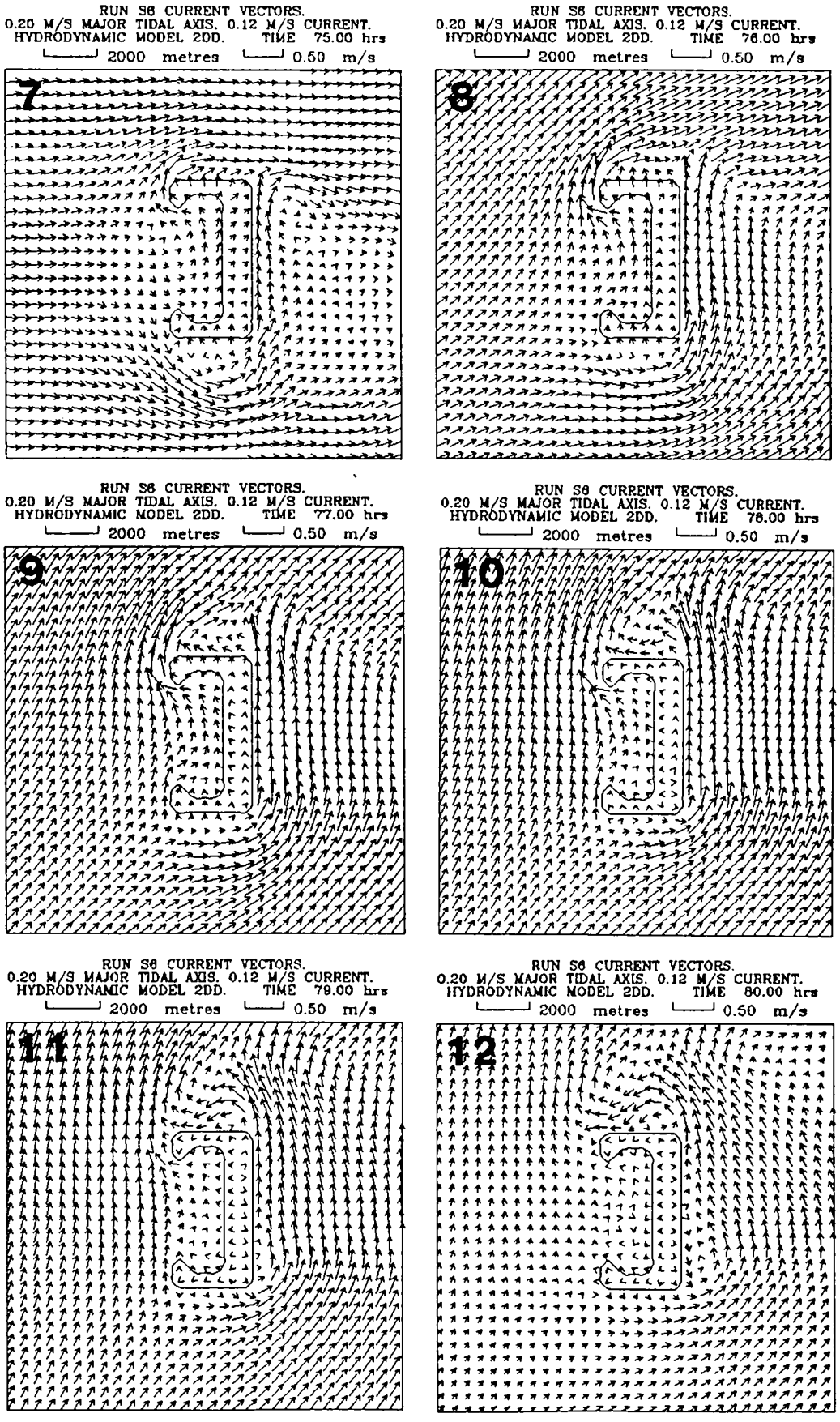


Figure 3.16b Representative plots of current vectors over a tidal cycle for reef type L2. Plots (labelled 7 to 12) represent currents at one hour intervals from when the tide begins to ebb.

influence the mainstream circulation by deflecting it around and along the reef face. Strongest currents and the general flow of water are largely restricted to the deeper water off the reefs, rather than over the reefs (Appendix B).

3.2.2 Eddy Circulation

Eddy circulation is evident to varying degrees throughout the tidal cycle (Fig. 3.16). The location and intensity of the eddy circulation, however, vary over time. Black and Gay (1987) describe this as phase eddy circulation. They argue that this is the dominant form of eddy in shallow-water continental shelf environments, such as the GBR, and that the physical process which is responsible for their formation is the unsteadyness of flow at the M2-S2 tidal frequencies (approximately 12 hours). Phase eddies develop during periods of flow deceleration due to variation in the phase of tidal currents on and around the reef. Figure 3.16 shows that the duration of phase eddies is quite short, of the order of a few hours. Such eddies cannot, therefore, be expected to retain larvae for long periods of time. They do, however, create regions of high shear which increase advective mixing and act to disperse a patch of larvae.

Phase eddies are also evident adjacent to the ribbon reef type R2 (Appendix B). These model results are consistent with observations (Wolanski et al., 1988). The details of phase eddy formation depend on the orientation and effective width of the reef relative to the major axis of tidal flow (Black, 1988). An elongate reef (such as type R1) which lies perpendicular to the dominant direction of tidal flow causes the formation of two counter-rotating eddies in the lee of the reef (Appendix B, see also Wolanski et al., 1986). These results suggest that mixing processes around these reefs will be significant.

Areas of weak residual circulation are apparent in Figure 3.17. Black and Moran (pers. comm.) propose that such features, which reflect areas of high larval retention, influence the location of initial recruitment. However, the significance of weak residual circulation to the physical conditions which facilitate larval recruitment is not clear. For example, low residual circulation vectors provide no

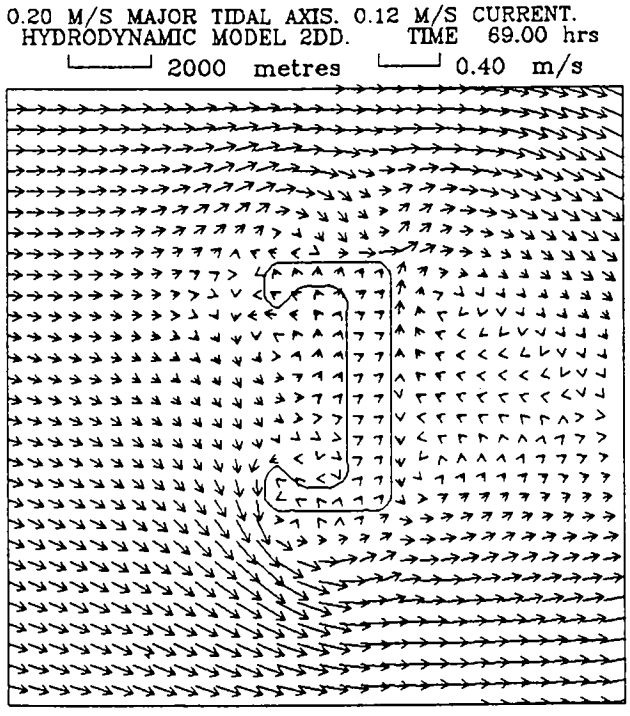


Figure 3.17 Current vectors representing the residual circulation around reef type L2.

indication of the intensity of currents within the region, only that the net intensity over a tidal cycle is close to zero.

3.2.3 Applicability of Results

The results of the present study, together with the more extensive simulations on schematized and real reefs within the central GBR by Black and Gay (1987b), show that the dominant features of circulation patterns on and around coral reefs within the central GBR are robust. The diverse selection of morphological features of coral reefs that have been investigated indicate that while the flow patterns are complex, they are probably representative of the majority of reefs within the Cairns and Central Sections of the GBR Marine Park. While there is no doubt that the complex bathymetry, three-dimensional flows and interactions with neighbouring reefs will affect the detail of water circulation, these simulations based on schematized reefs provide a strong physical basis upon which to investigate the entrainment of larvae onto reefs.

3.3 THE ENTRAINMENT OF LARVAE ONTO REEFS

Conceptually, each release containing the 2500 particles is most appropriately viewed as a patch of larvae in its own right. The particles within each larval patch that are transported over the area which is defined as habitat are viewed as having the potential to recruit to that reef type. These particles are referred to as 'potential recruitment', and the number is expressed as a percentage of the total number of particles released from each cell. Results are presented for all individual upstream releases (or cells) for each of the 13 schematized reefs, and for the mean of all upstream releases (or cells) from each of the schematized reefs. The latter set of results provides a spatial average of potential recruitment over the entire reef. The results of all individual upstream releases have been incorporated into the large-scale dispersal model through a parameterization scheme based on the analysis of particle trajectories and reef connectivity. Marked differences in the proportion of an approaching larval patch which is transported over habitat, and therefore recruitment, are evident between release locations both within and between reefs.

3.3.1 Recruitment Variation within a Reef

Results for all releases for each of the schematized reefs are presented in Figures 3.18 to 3.22. All reefs display a similar pattern: highest potential recruitment is for larval patches approaching on the offshore side of the reef centreline. Further offshore towards the reef edge, potential recruitment is slightly reduced. Potential recruitment for larval patches approaching on the onshore side of the reef centreline decreases towards the reef edge where it is reduced to very low levels. Only one exception to this pattern is evident, for reef type R2 (Fig. 3.21), which displayed no marked differences between the release locations. The labels 'onshore' and 'offshore' with respect to the relative magnitude of potential recruitment relate to circumstances when the long-shore current is from the north. While this is the most frequent situation during the period from December to March when the crown of thorns starfish spawns, current reversals resulting in flow from the south do occur frequently. Based on a

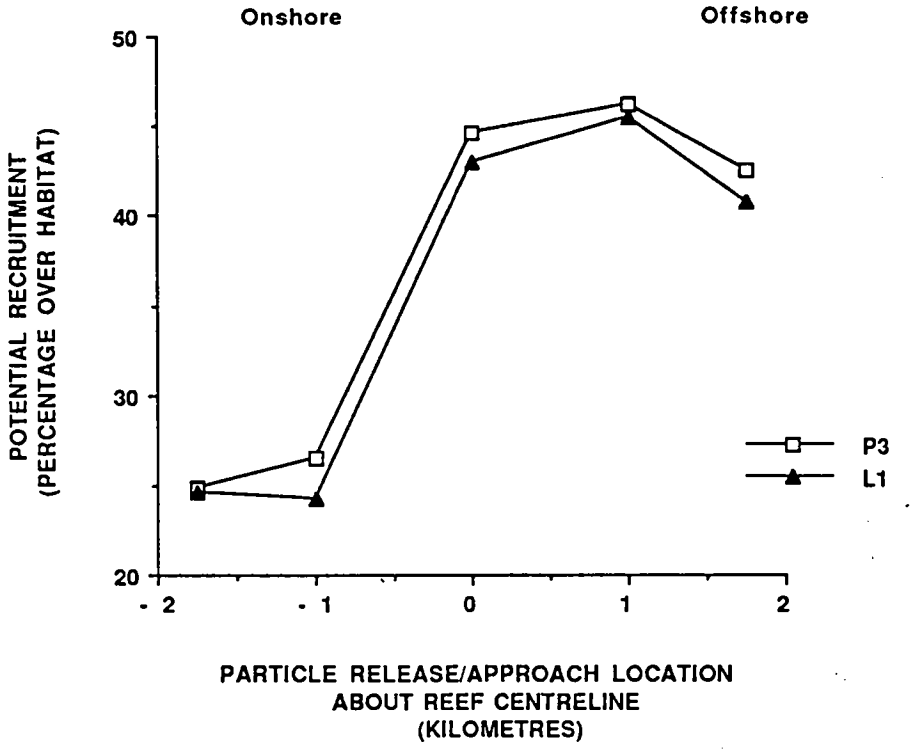


Figure 3.18 Potential recruitment for all upstream particle releases for reef types P3 and L1. The locations of particle releases/approaches are identified with respect to the reef centreline which lies parallel to the longshelf current direction and divides the reef into an offshore and onshore side.

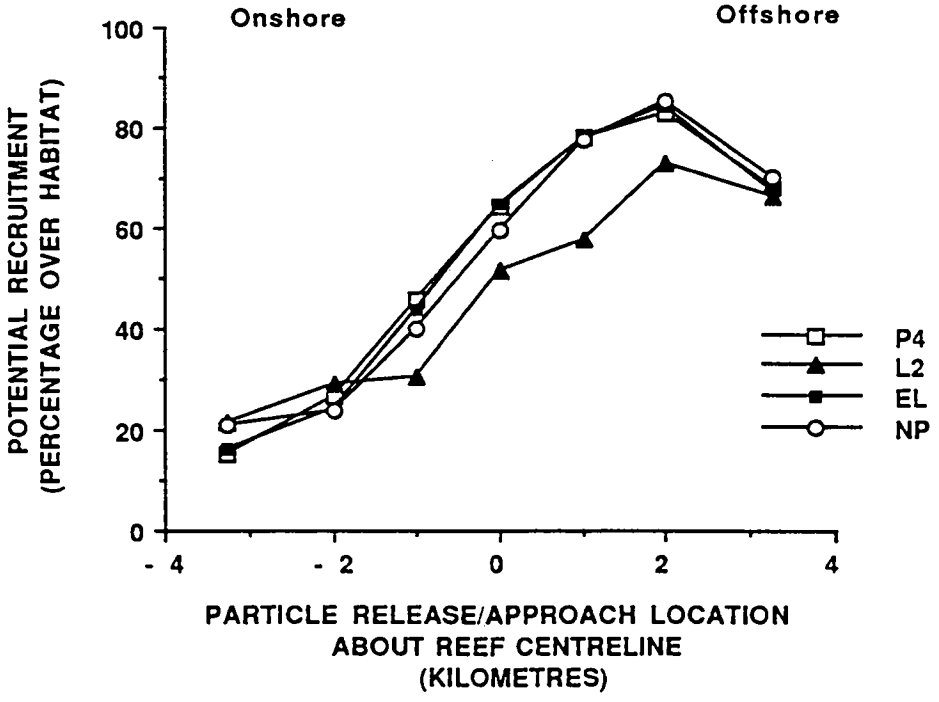


Figure 3.19 Potential recruitment for all particle releases for reef types P4, L2, EL and NP. The locations of particle releases/approaches are identified with respect to the reef centreline which lies parallel to the longshelf current direction and divides the reef into an offshore and onshore side.

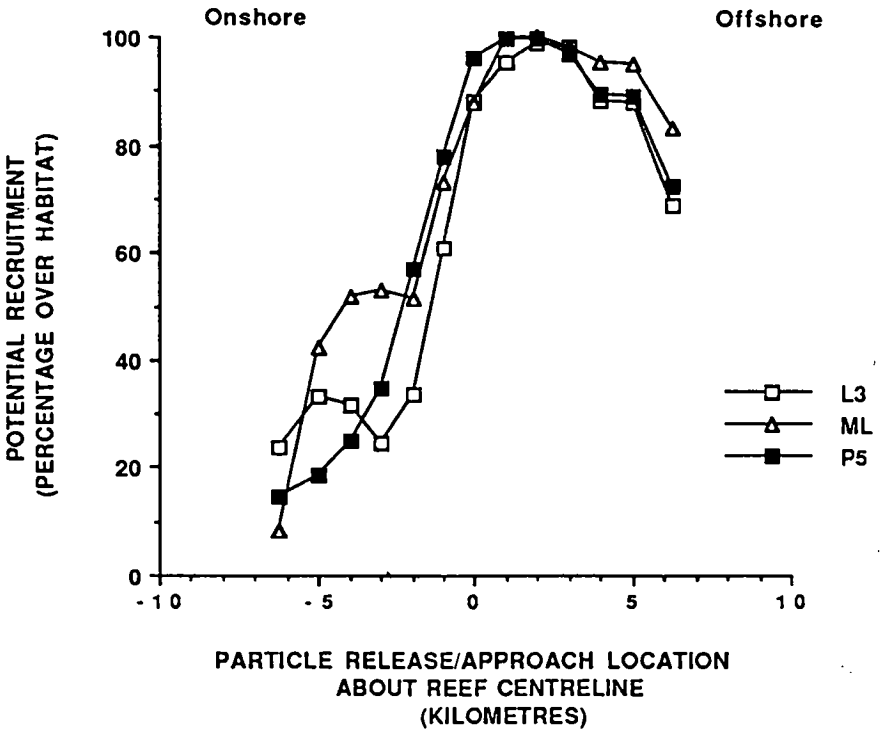


Figure 3.20 Potential recruitment for all upstream particle releases for reef types L3, ML and P5. The locations of particle releases/approaches are identified with respect to the reef centreline which lies parallel to the longshelf current direction and divides the reef into an offshore and onshore side.

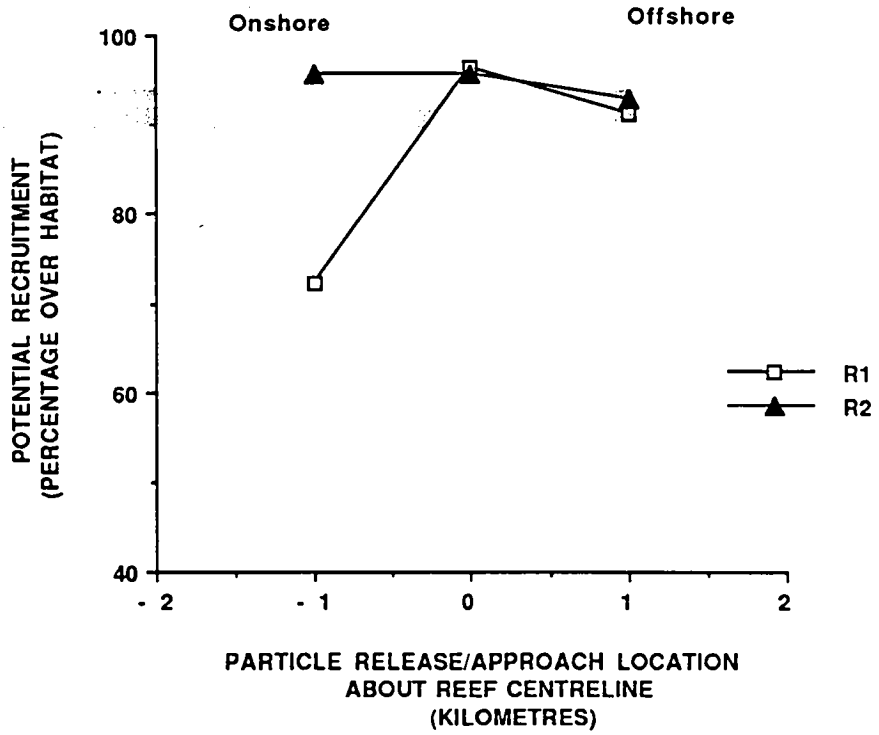


Figure 3.21 Potential recruitment for all upstream particle releases for reef types R1 and R2. The locations of particle releases/approaches are identified with respect to the reef centreline which lies parallel to the longshelf current direction and divides the reef into an offshore and onshore side.

symmetry argument, highest potential recruitment is expected to be for larval patches approaching on the onshore side of the reef under such circumstances.

3.3.2 Recruitment Variation between Reefs

Comparison of reef types P3 and L1, which differ only in the presence of a semi-enclosed lagoon within the latter, establishes only minor differences in potential recruitment between equivalent release/approach locations (Fig. 3.18). Potential recruitment is marginally less for the lagoonal reef, but these differences are not as great as those observed between release/approach locations within a reef. Comparison of reef types P4, NP, L2 and EL, which again do not differ in their cross-shelf dimension, but rather, in other morphological features, also display only relatively minor differences (Fig. 3.19). However, for these larger reefs, the lagoonal type L2 exhibits somewhat lower potential recruitment for most release/approach locations. This is probably related to the higher retention rates for lagoonal reef types (K.P. Black. pers. comm.), which indicate a corresponding weak exchange of water between this reef type and the offshore watermass. Comparison of the largest reef types, P5, L3 and ML, similarly, demonstrates relatively minor differences in potential recruitment between equivalent release/approach locations (Fig. 3.20). Results for the ribbon reef types, R1 and R2, are presented in Figure 3.21. There is no apparent difference in potential recruitment between these two reef types for larval patches approaching along the centreline or offshore side of the reef. The only marked difference is that the asymmetry which was identified above for all other reef types is absent from reef type R2.

These results demonstrate that morphological features such as the presence or absence of a semi-enclosed or enclosed lagoon, or the reef depth (distance along the reef centreline), when the ribbon reef types are excluded, result in only relatively minor variation in levels of potential recruitment. Much larger effects arise from differences between release/approach locations within a reef, and from the reef size measured perpendicular to the reef centreline along the cross-shelf axis. The effect of reef size is most clearly shown by comparing

the five planar reef types, P1 to P5, which differ primarily in their cross-shelf dimension (Fig. 3.22). With the exception of the two smallest reefs, whose relative positions are reversed, larger reefs receive more recruits.

Potential recruitment, when averaged over all upstream releases from each of the schematized reefs, was strongly correlated (R^2=0.901) with reef size (measured along the major or cross-shelf axis which lies perpendicular to the long-shelf current direction) when types R1 and R2 were excluded (Fig. 3.23). Reefs which extend many kilometres across the shelf clearly have the potential to entrain more larvae per unit width than small reefs. Ribbon reef types R1 and R2 have anomalously high potential recruitment for their size, apparently because of their extent in the direction of the long-shelf current and the high level of mixing associated with these reef types (see also Section 3.3.3).

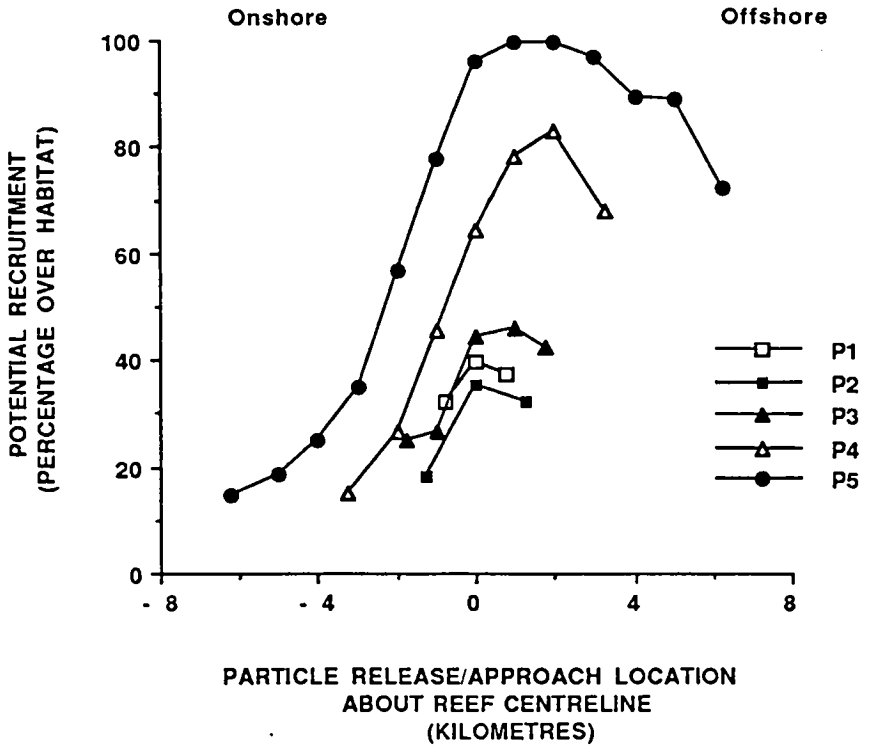


Figure 3.22 Potential recruitment for all upstream particle releases for reef types P1 to P5. The locations of particle releases/approaches are identified with respect to the reef centreline which lies parallel to the longshelf current direction and divides the reef into an offshore and onshore side.

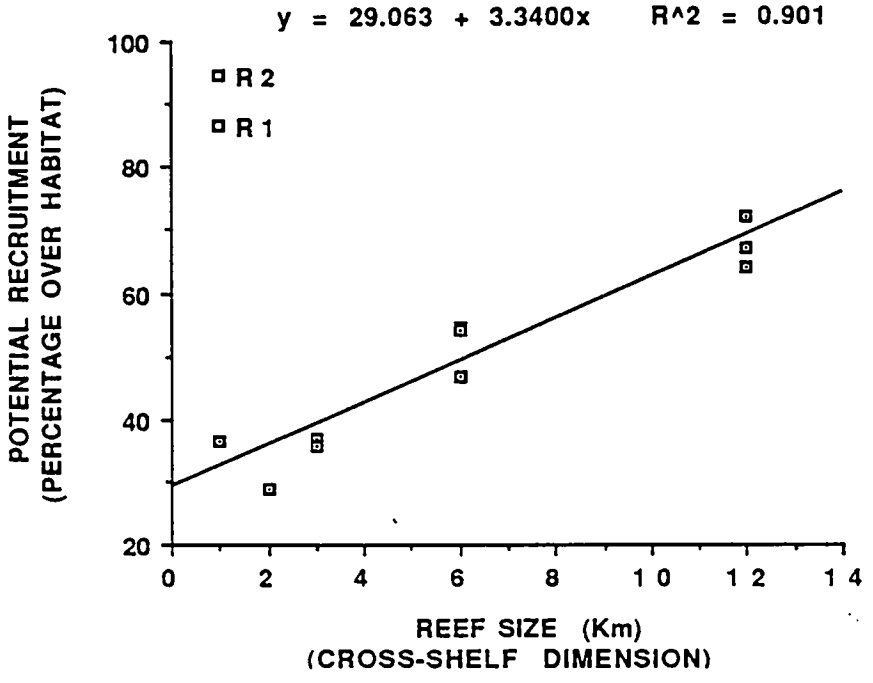


Figure 3.23 Regression analysis of potential recruitment, averaged over all upstream particle releases from each of the schematized reefs, versus reef size. Reef types R1 and R2 are excluded from the analysis.

3.3.3 Interpretation

The asymmetry in potential recruitment that is observed for all schematized reefs, except type R2, probably results from the anti-clockwise residual circulation around reefs due to negative Coriolis forcing (Black & Gay, 1987b) (see Section 3.2.1). Larval patches approaching along the centreline of reef type L2 (see Fig. 3.24) are spread, initially, in highest concentrations along the reef edge facing the long-shelf current (Fig. 3.24a). Subsequently, highest concentrations of particles are transported in an anti-clockwise direction around the onshore edge of the reef and then downstream (Fig. 3.24b and c). Larval patches approaching along the offshore edge of reef type L2 are spread around the reef on both the onshore and offshore edges (Fig. 3.25). In both cases, only relatively few larvae enter the lagoon. Most larvae are transported within the circulation around the reef. Larval patches approaching along the onshore edge of reef type L2 are rapidly transported around the reef edge and then downstream (Fig. 3.26), with few particles being transported over habitat.

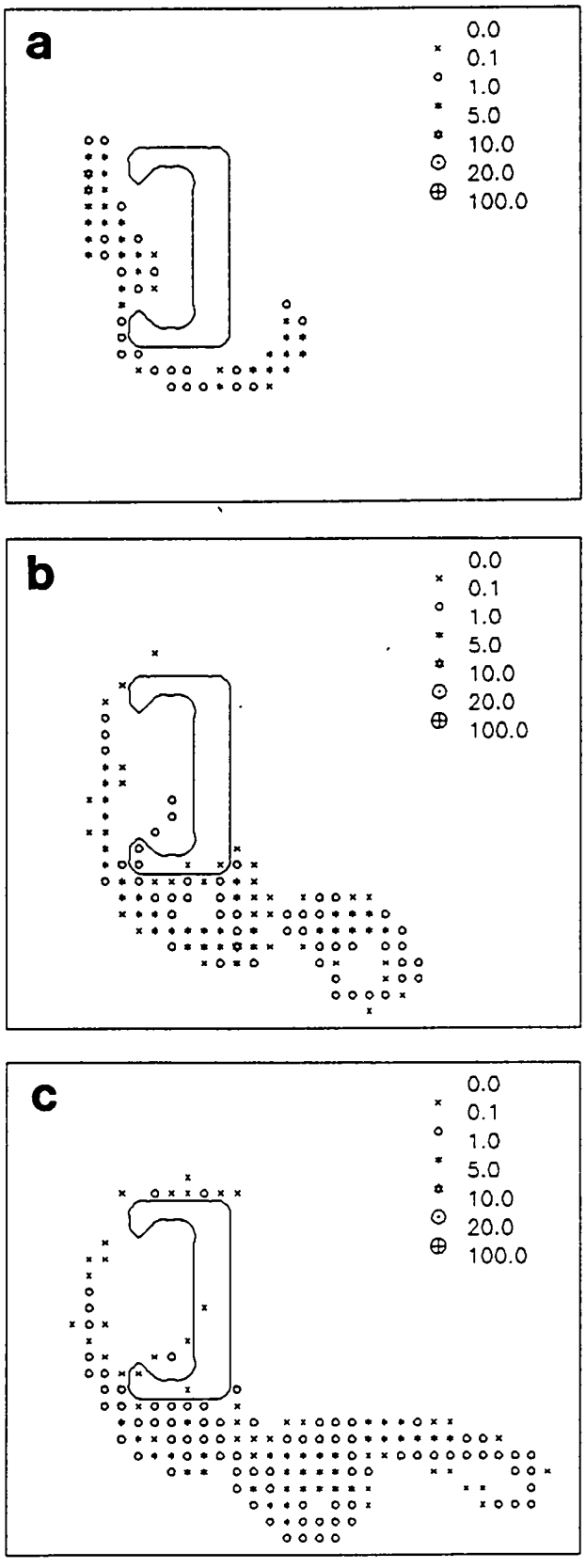


Figure 3.24 Particle numbers per cell expressed as a percentage of the total number of particles released; 10 hours (a), 20 hours (b), and 30 hours (c) after release. Particles were released upstream along the centreline of reef type L2.

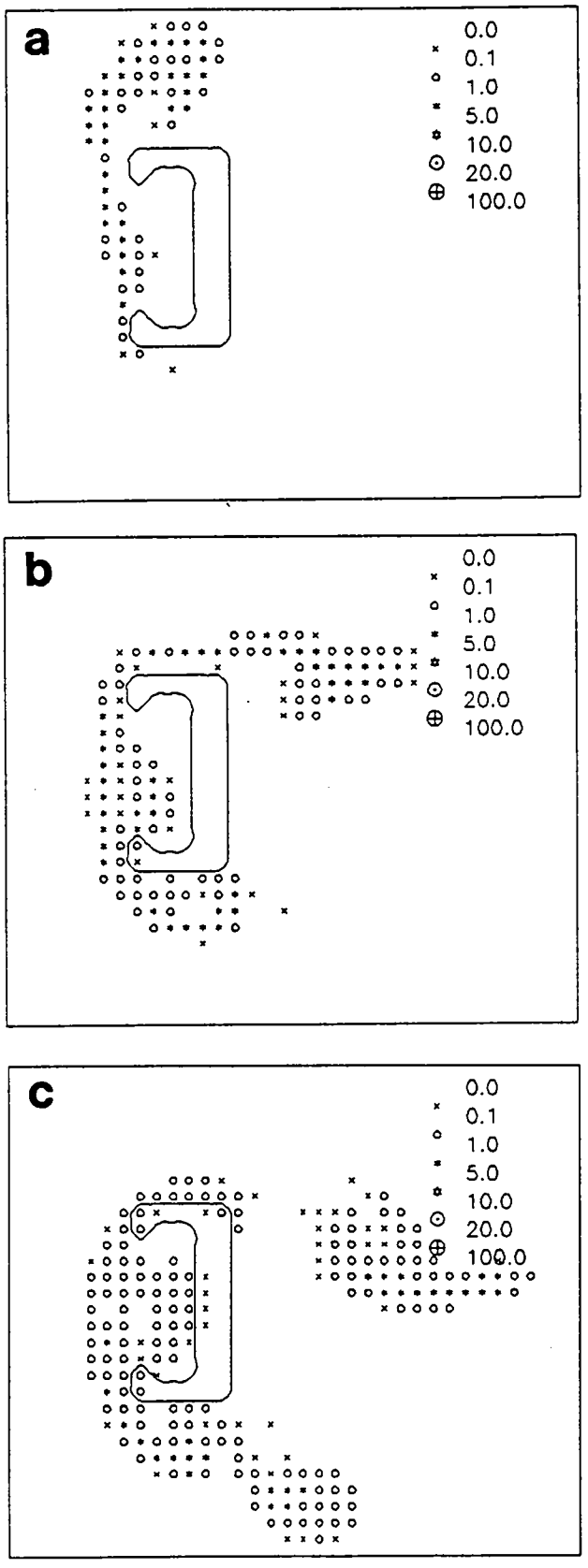


Figure 3.25 Particle numbers per cell expressed as a percentage of the total number of particles released; 10 hours (a), 20 hours (b), and 30 hours (c) after release. Particles were released upstream along the offshore edge of reef type L2.

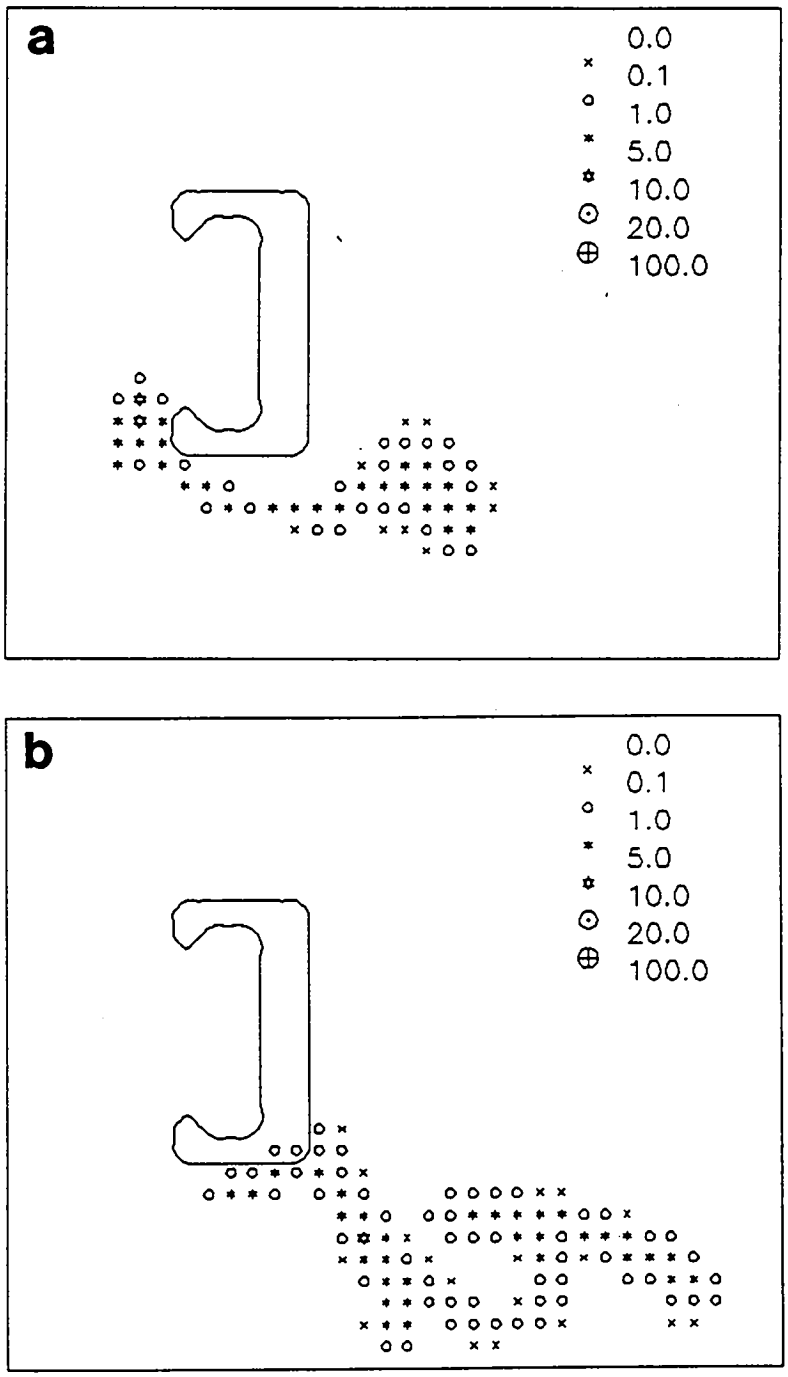


Figure 3.26 Particle numbers per cell expressed as a percentage of the total number of particles released; 10 hours (a), and 20 hours (b) after release. Particles were released upstream along the onshore edge of reef type L2.

In contrast to the intermediate sized reefs (e.g. type L2), particles approaching along the centreline of reef type P1 are quickly deflected around and past (Fig. 3.27). This results in relatively low potential recruitment. Towards the other end of the spectrum of reef sizes, particles approaching on the offshore side of the large reef type L3 remain on and around the reef in significant numbers long after they have been advected far downstream of the smaller reefs (Fig. 3.28).

Strong mixing processes associated with the narrow passage between reefs in type R2 result in particles being transported through the passage and generally dispersed around the reef (Fig. 3.29). It is this mixing process, apparently, which results in the lack of asymmetry with respect to potential recruitment.

Overall, the presence of cross-shelf tidal currents plays a major role in determining the patterns and levels of potential recruitment that are evident. A patch of larvae approaching a reef which is small relative to the tidal excursion may be transported around and past the reef over a tidal cycle, with few larvae coming into direct contact with habitat. In contrast, a patch of larvae approaching a reef which is large relative to the tidal excursion may not be transported clear of the reef before being returned with the tide. In the case of the ribbon reef types R1 and R2, their high levels of potential recruitment probably result from the tides returning particles into the strong mixing processes associated with these reef types before they clear the reefs entirely.

Similarly, the timing of the approach of a small larval patch with respect to the tidal cycle can have an important influence on the level of potential recruitment. This is illustrated by instantaneous releases of particles, each covering an area of 500 m x 500 m, from the same location at different stages in the tidal cycle. A patch of larvae may completely miss the reef (Fig. 3.30a) or some proportion of it will be transported over habitat (Fig. 3.30b) at a different stage in the tidal cycle, separated by three hours. In the former, the tide is ebbing while in the latter it is beginning to flood.

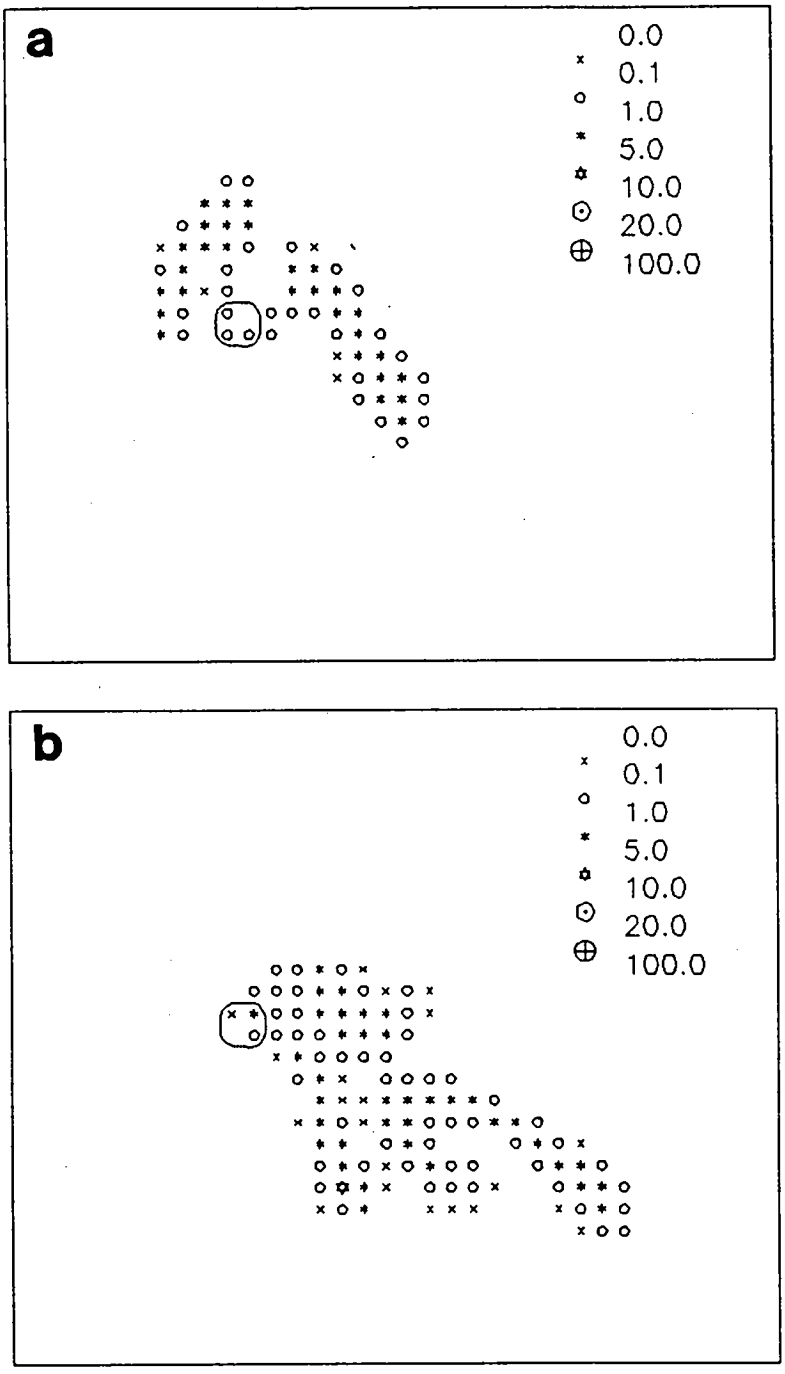


Figure 3.27 Particle numbers per cell expressed as a percentage of the total number of particles released; 10 hours (a), and 20 hours (b) after release. Particles were released upstream along the centreline of reef type P1. Larvae approaching this small planar reef are quickly deflected around it.

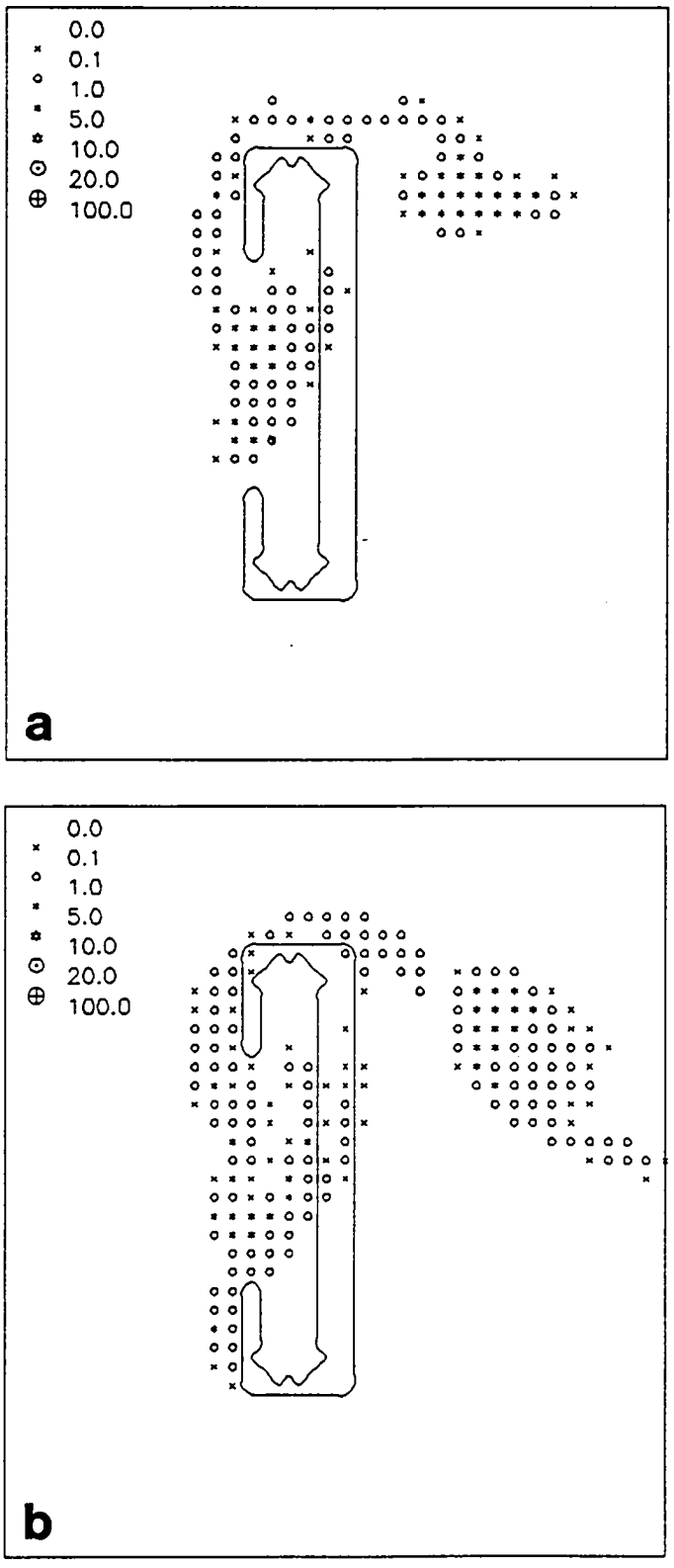


Figure 3.28 Particle numbers per cell expressed as a percentage of the total number of particles released; 20 hours (a), and 30 hours (b) after release. Particles were released upstream along the offshore side of reef type L3. Larvae approaching this large reef remain on and around the reef in significant numbers long after they have been advected far downstream of the smaller reefs.

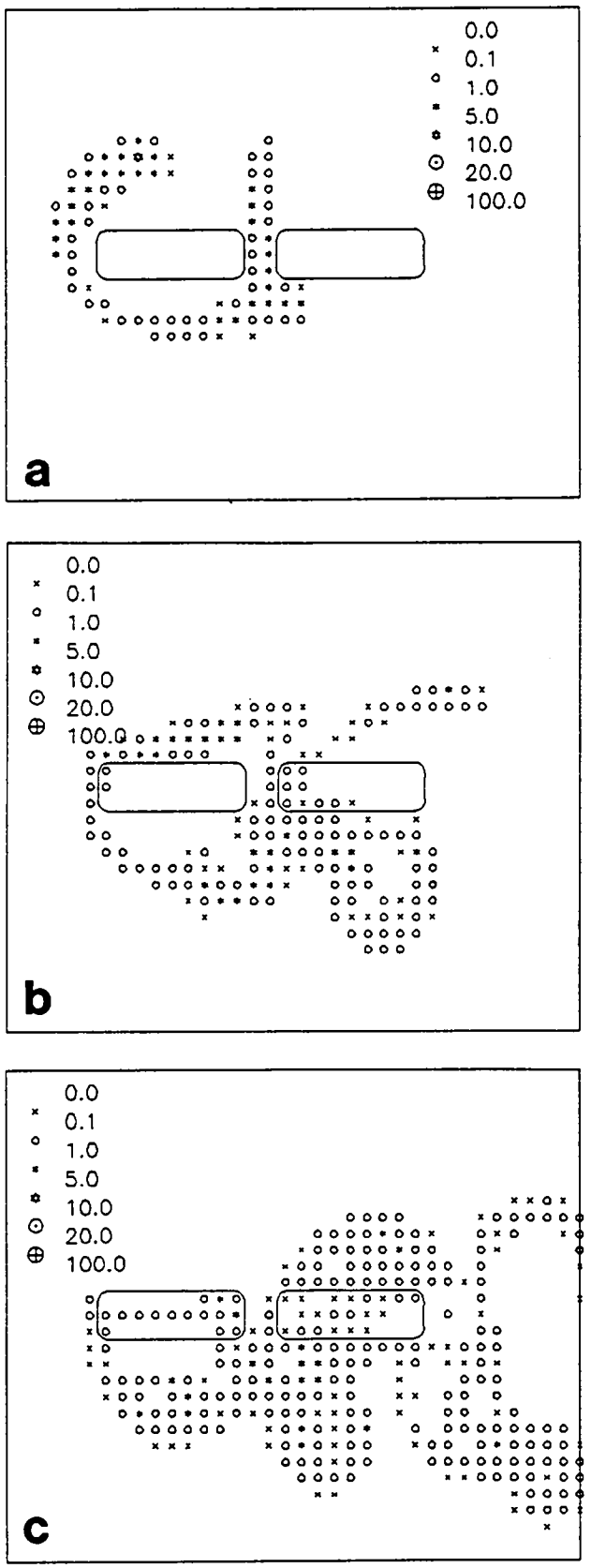


Figure 3.29 Particle numbers per cell expressed as a percentage of the total number of particles released; 10 hours (a), 20 hours (b), and 30 hours (c) after release. Particles were released upstream along the offshore side of reef type R2.

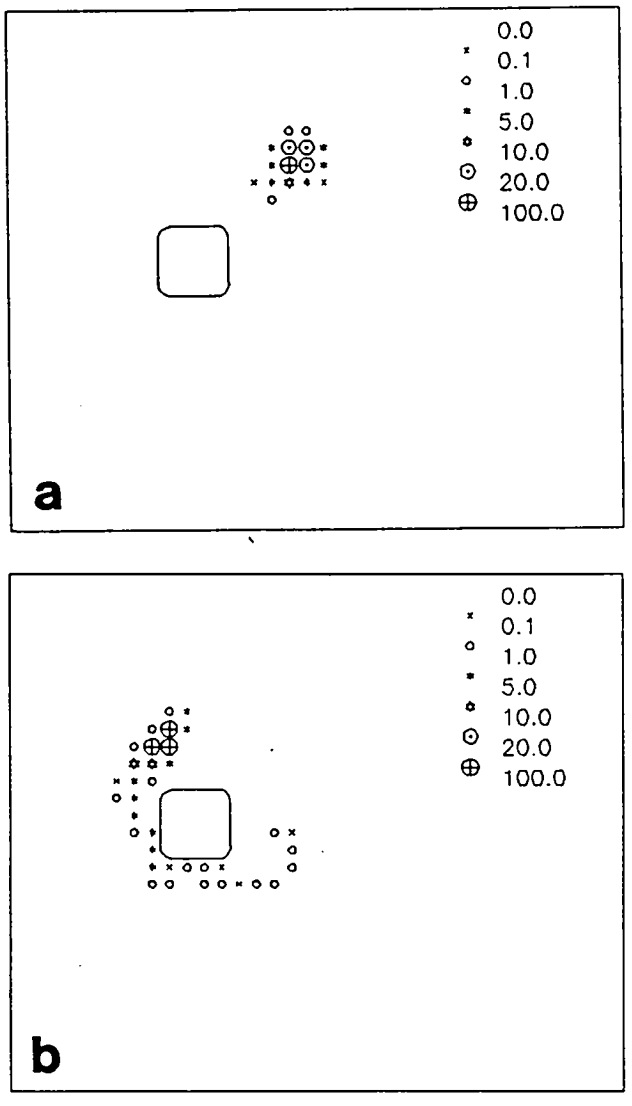


Figure 3.30 Particle numbers per cell expressed as a percentage of the total number of particles released; 10 hours after release on the ebb tide (a), and the flood tide (b). Particles were released upstream along the offshore side of reef type P2.

Note that for the other results that have been presented within this Chapter, particle releases were over an entire tidal cycle, thus averaging such differences. This approach is possibly more representative of elongate patches of larvae which approach a reef over an extended period of time.

3.4 ANALYSIS OF PARTICLE TRAJECTORIES AND REEF CONNECTIVITY

The particle trajectories are best viewed conceptually as the movement of patches of larvae, corresponding to centres of mass within each larval cloud. At the large scale, the distributions of larvae about their centres of mass are not defined. However, on intersection with a reef each particle is assumed to represent a distribution corresponding to that of the fine-scale particle releases described in Section 2.4. Depending upon where the particle intercepts a reef and its long-shelf direction of transport, some proportion of the larval patch is assumed to become entrained within the near-reef circulation as potential recruitment and is attributed to that reef as connectivity. The entrainment of larvae onto reefs is implemented through a parameterization scheme (see Section 3.4.2 below) based on the results of the fine-scale modelling (see Section 3.3 above).

3.4.1 Distributing Probabilities - INSECT

The computer programme INSECT was developed to analyse particle trajectories for intersections with reefs. All reefs are represented as polygons. The number of polygon sides or segments varies between reefs depending on their complexity. The reef polygons represent the extent of each reef including outlying bommie fields, and therefore reflect the distribution of reef habitat for larvae of *A. planci*.

During the initial two weeks of development, larvae of *A. planci* were assumed to be pre-competent and unable to settle. Only intersections with reefs following the two week pre-competent period were considered. Larvae were, therefore, provided with a window of two weeks (14 days) during which they could potentially encounter one or more sink reefs: their competent period. Following the first intersection during the competent period at which some proportion of the larval patch is attributed to that reef as connectivity, the remaining proportion of the larval patch is then available to other reefs it encounters.

Analyses of reef connectivity for short pre-competent period larvae are as detailed above and below, except that intersections with reefs are considered after four (4) days. Larvae were still provided with a window of two weeks during which they could potentially encounter one or more sink reefs.

3.4.2 Parameterization of Fine-scale Circulation and the Entrainment of Larvae onto Reefs

The results presented in Section 3.3 have been used to parameterize the fine-scale patterns of circulation and the entrainment of larvae onto reefs. The computer program INSECT determines whether or not there are intersections between particle trajectories, which are represented as straight line segments output from TRACK, and reef edges which are defined as polygon boundaries. All reef polygons have been classified with respect to reef shape and correspond to one of the reef types considered in Section 2.3 (i.e. planar, lagoonal, massive lagoonal, ribbon, etc.). For each intersection that is identified, the point of intercept is located with respect to the cross-shelf dimension of the reef polygon and both are normalized to the appropriate schematized reef size corresponding to its designated shape classification. The corresponding value, representing potential recruitment (i.e. the proportion of the larval patch which is transported over habitat), taken from the results presented in Section 3.3, is then assigned to that reef. Where the trajectory direction is opposite that for which the fine-scale simulations were performed, then the value representing potential recruitment is taken to be equal to that at an equivalent location on the opposite side of the reef. The proportion of the larval patch remaining after an intersection is then available to other reefs if further intersections occur. Following the analysis of all seven particles (patches) for each dispersal event from the designated source reef, connectivity is summed and normalized to the total number of particle trajectories analysed and assigned a value between zero and one. Results correspond to connectivity associated with each individual sink reef and their sum, which represents the total connectivity for the particular source reef.

3.5 LARVAL DISTRIBUTIONS AND REEF CONNECTIVITY

In general, the seven particles representing the larval cloud remained reasonably coherent over the 28 day simulation period. At times, however, the particles could be dispersed over a considerable area as a result of cross-shelf tidal flow, but more often, the initial hexagons became elongate and appeared as streaks, often many kilometres long. Representative particle trajectories are presented in Figures 3.31 and 3.32.

Reef connectivity is defined as a property of the source reef and is described in terms of level and strength. Level of connectivity relates to the likelihood of encountering a sink reef. That is, a high level of connectivity corresponds to a relationship whereby most dispersal events result in the transport of larvae to other reefs. Strength of connectivity relates to the relative magnitude of the relationship between a source reef and each of its identified sink reefs. Strong connectivity corresponds to a relationship whereby many dispersal events are directed to specific sink reefs. The relative strengths can be interpreted as the probability that larvae associated with any randomly dispersal event will encounter habitat at a particular sink reef. The relative strengths (S) are classified into 3 classes: weak, moderate and strong, where weak $S < 0.005$; moderate $0.005 <= S < 0.05$; and strong $S => 0.05$.

3.5.1 The Northern Region

3.5.1.1 Cross-shelf connectivity

Reef connectivity within the northern region, expressed as source-sink relationships with respect to the cross-shelf movement of larvae, is presented in Figures 3.33 to 3.36. Considering all five reefs in each zone collectively (Fig. 3.33), it is evident that:

(1) connectivity of outer matrix source reefs was almost exclusively with other ribbon reefs lying along the outer edge of the continental shelf (45.4%). Only relatively rare events resulted in the transport of larvae onshore to central matrix reefs (3.0%). Connectivity with inner matrix reefs was virtually absent (0.1%).

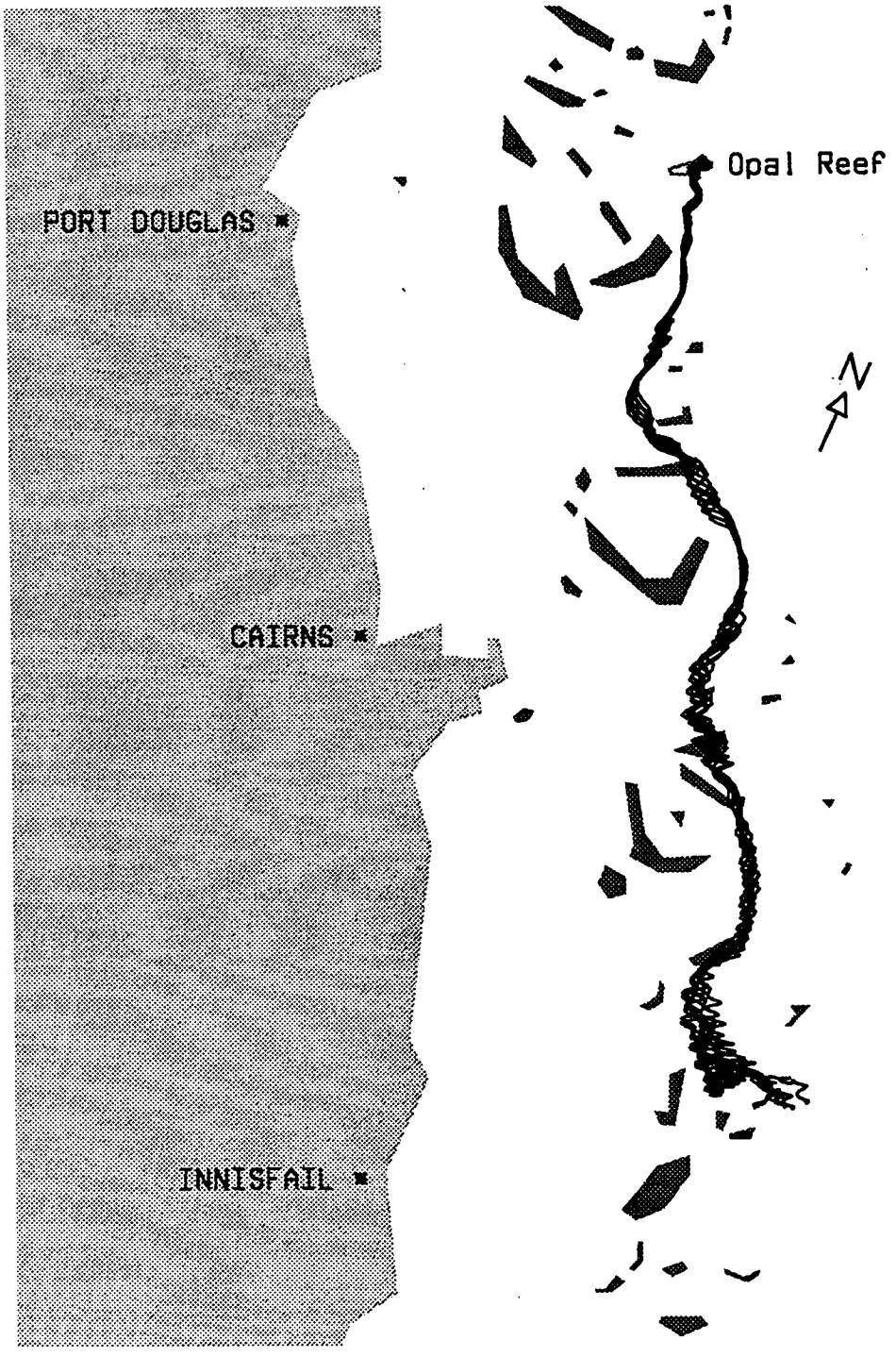


Figure 3.31 Particle trajectories representing a single dispersal event originating from Opal Reef. Particles representing a cloud of larvae generally remained reasonably coherent, becoming elongate and appearing as streaks, often many kilometres long. Scale: 1cm = 5 nautical miles.

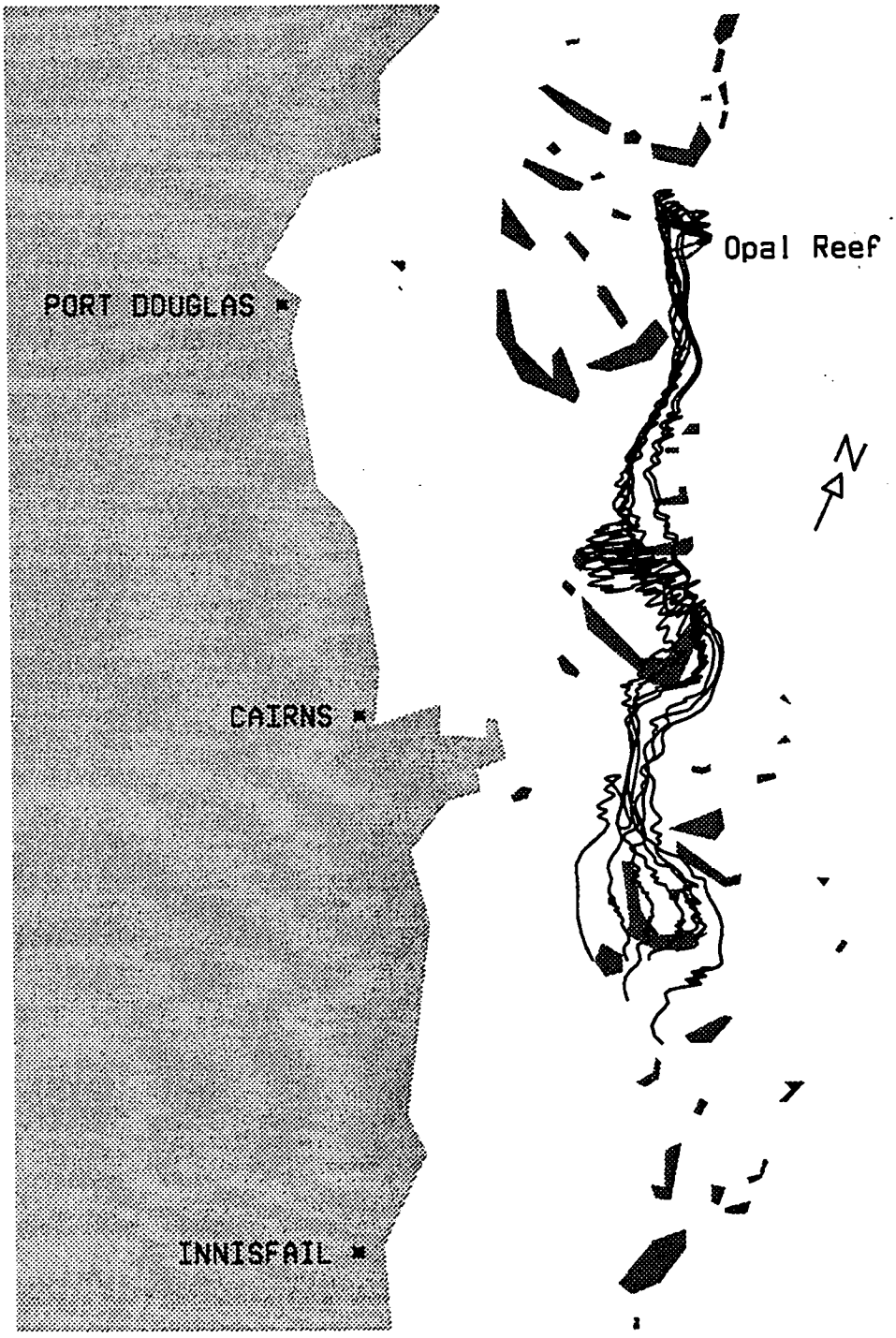


Figure 3.32 Particle trajectories representing a single dispersal event originating from Opal Reef. Particles representing a cloud of larvae can become dispersed over a considerable area due to cross-shelf tidal flow. Scale: 1cm = 5 nautical miles.

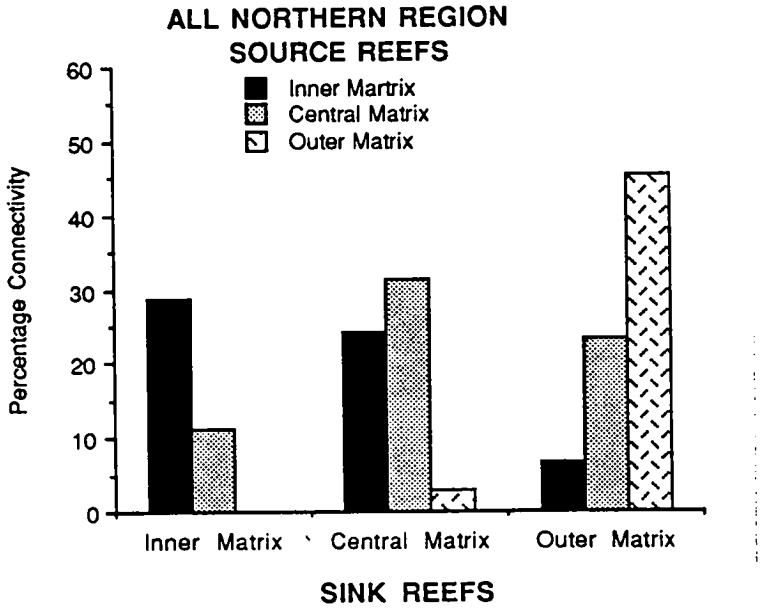


Figure 3.33 Level of reef connectivity with respect to the cross-shelf transport of larvae within the northern region. Data represent the number of particles from five source reefs within each of three cross-shelf geographical zones that intersect with sink reefs, expressed as a percentage of the total number of particle trajectories simulated from each zone. Cross-shelf zones correspond to reefs which lie along the outer edge of the reef matrix and continental shelf (outer matrix), reefs central within the reef matrix (central matrix) and reefs which lie along the inner edge of the reef matrix bordering the main lagoon (inner matrix).

Many dispersal events originating from outer matrix source reefs failed to transport larvae to other reefs within the time constraints of larval life that were imposed (51.5%);

(2) connectivity of central matrix source reefs was primarily with other reefs lying within the same cross-shelf zone (31.4%), but with a substantial proportion of dispersal events resulting in the transport of larvae offshore to outer matrix ribbon reefs (23.2%). The transport of larvae onshore to inner matrix reefs was also relatively frequent (11.1%). The proportion of dispersal events originating from central matrix source reefs which did not result in the transport of larvae to other reefs was substantially lower than from outer matrix source reefs (34.3%);

(3) connectivity of inner matrix source reefs was also primarily with other reefs lying within the same cross-shelf zone (28.8%), but not substantially more than to central matrix reefs (24.1%). The transport of larvae offshore to outer matrix reefs was less frequent (6.7%). Many dispersal events originating from inner matrix source reefs did not transport larvae to other reefs (40.4%).

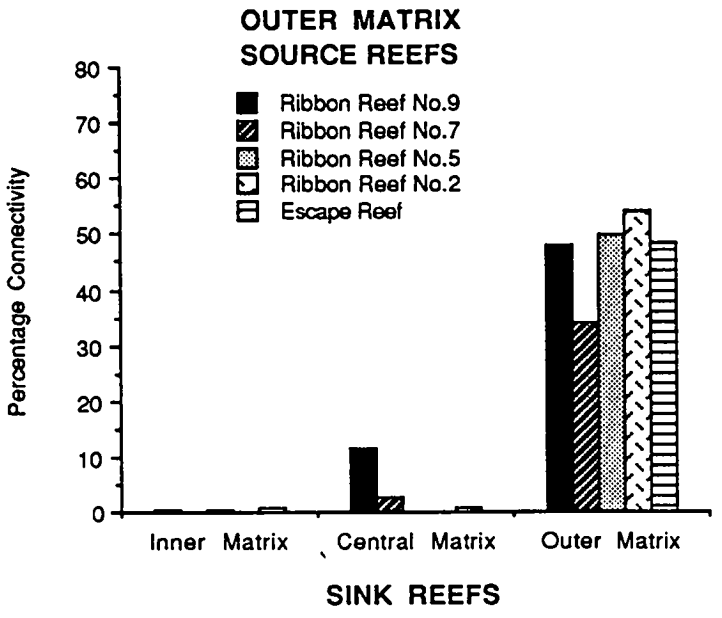


Figure 3.34 Level of reef connectivity with respect to the cross-shelf transport of larvae within the northern region for each of the five **outer** matrix source reefs. See caption, Figure 3.33, for further details.

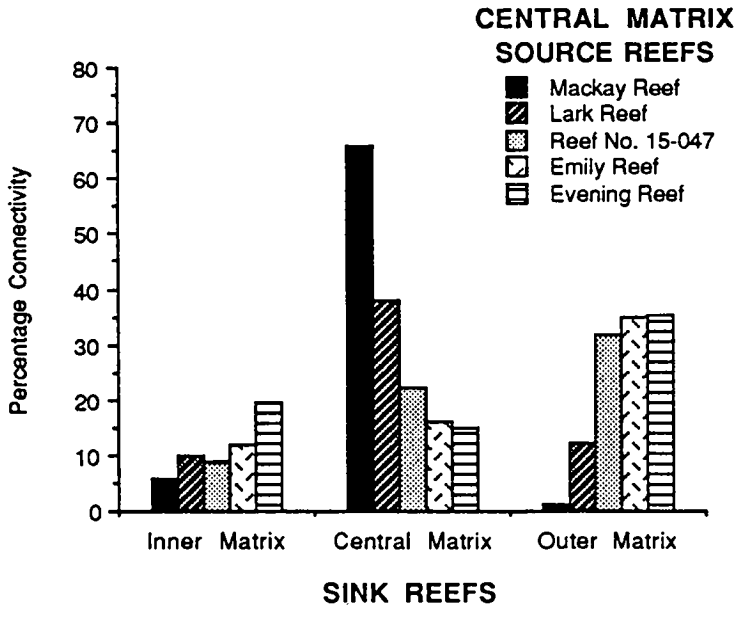


Figure 3.35 Level of reef connectivity with respect to the cross-shelf transport of larvae within the northern region for each of the five **central** matrix source reefs. See caption, Figure 3.33, for further details.

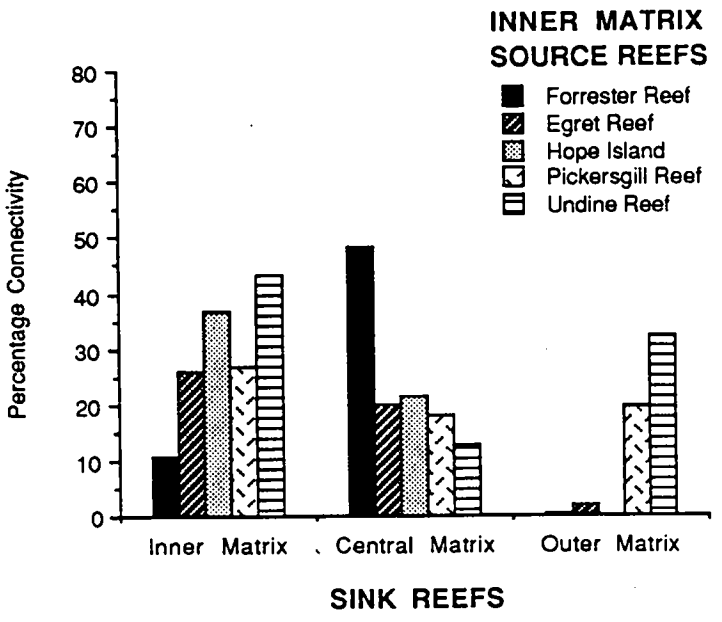


Figure 3.36 Level of reef connectivity with respect to the cross-shelf transport of larvae within the northern region for each of the five **inner** matrix source reefs. See caption, Figure 3.33, for further details.

In summary, connectivity of source reefs in each of the cross-shelf geographical zones was primarily with sink reefs lying within the same cross-shelf zone. However, substantial mixing of larvae between reefs in different zones is evident for larvae originating from inner and central matrix reefs. In contrast, the onshore transport of larvae originating from outer matrix ribbon reefs is relatively infrequent. The level of connectivity from outer matrix ribbon reefs was much lower, with only 48.5% of larvae being transported to other reefs. Frequently, larvae from outer matrix reefs were transported offshore where they became entrained within the East Australian Current and, oftentimes, were not transported back onshore (see Fig. 3.37).

Examination of results from individual reefs (Figs. 3.34 to 3.36) indicate a more complex picture, one of diversity in patterns of reef connectivity. Most consistent was the connectivity of individual outer matrix source reefs (Fig. 3.34). Only Ribbon Reef No.9, the most northern of the outer matrix reefs, displayed substantial connectivity with central matrix sink reefs (11.4%). The overall levels of connectivity did not differ greatly between the individual outer matrix source reefs, with only one exception; Ribbon Reef No.7, which was lower. Connectivity of individual central and inner matrix source reefs

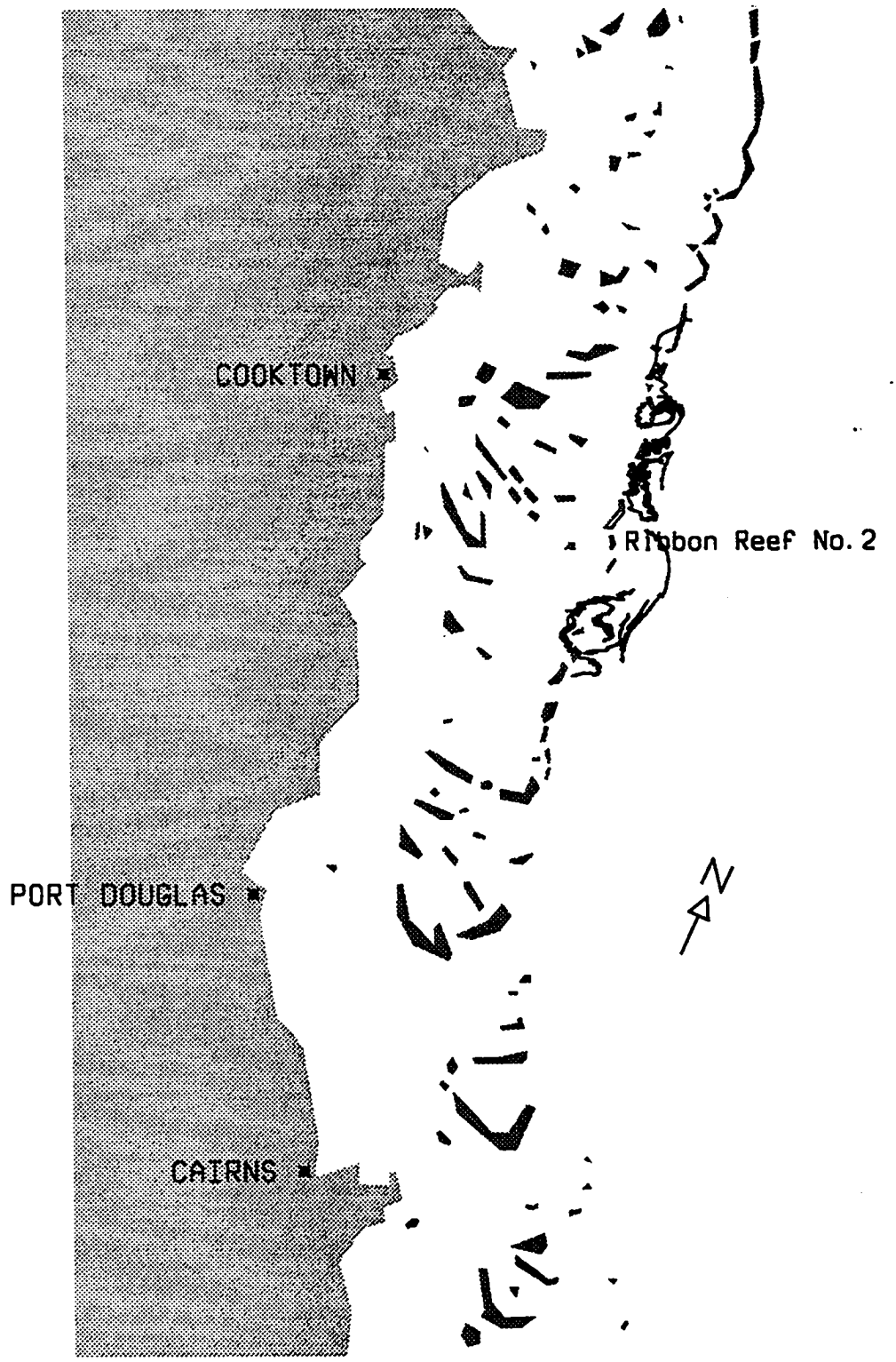


Figure 3.37 Particle trajectories representing twenty dispersal events from Ribbon Reef No.2 (source reef indicated without fill). Each trajectory corresponds to the centroid of the larval cloud during the second two weeks of dispersal when the larvae of *A. planci* are assumed to be competent to settle. Frequently, larvae from outer matrix ribbon reefs are predicted to be transported offshore where they become entrained within the East Australian Current and, oftentimes, will not be transported back onshore. Scale: 1cm = 7.5 nautical miles.

displayed considerably more diversity in patterns (Figs. 3.35 and 3.36 respectively). Connectivity of three of the central matrix source reefs was highest with outer matrix sink reefs. These were the three most southerly reefs. The overall distribution of connectivity from the five source reefs to all cross-shelf zones was variable. Connectivity of only one inner matrix source reef was directed primarily to central matrix sink reefs, but the overall distribution of connectivity from the five reefs to all cross-shelf zones was extremely variable.

3.5.1.2 Long-shelf connectivity

Reef connectivity, with respect to the long-shelf movement of larvae, is presented in Figures 3.38 to 3.41. Considering all five source reefs in each cross-shelf zone collectively (Fig. 3.38), it is evident that connectivity was with sink reefs lying both to the north and south. Overall, 42.8% of larvae which intersected with reefs were transported to the north, 50.5% were transported to the south, while 6.7% were transported back onto the source reef as a result of current reversals.

Individual source reefs within all cross-shelf zones varied in the relative proportions of larvae that were transported to sink reefs lying to the north and south (Figs. 3.39 to 3.41). The more northerly reefs may have slightly higher connectivity with reefs to the south, while the more southerly reefs have slightly higher connectivity with reefs to the north. Interestingly, these same reefs also displayed contrasting patterns in cross-shelf connectivity (Figs. 3.34 to 3.36).

3.5.1.3 Relative strength of connectivity

The relative strengths of connectivity between each northern region source reef and all its sink reefs are presented in Figures 3.42 to 3.56.

All the outer matrix source reefs displayed strongest connectivity with neighbouring ribbon reefs lying along the outer edge of the continental shelf (Figs. 3.42 to 3.46). In all cases these reefs lie to both the north and south of the source reef. The relatively high

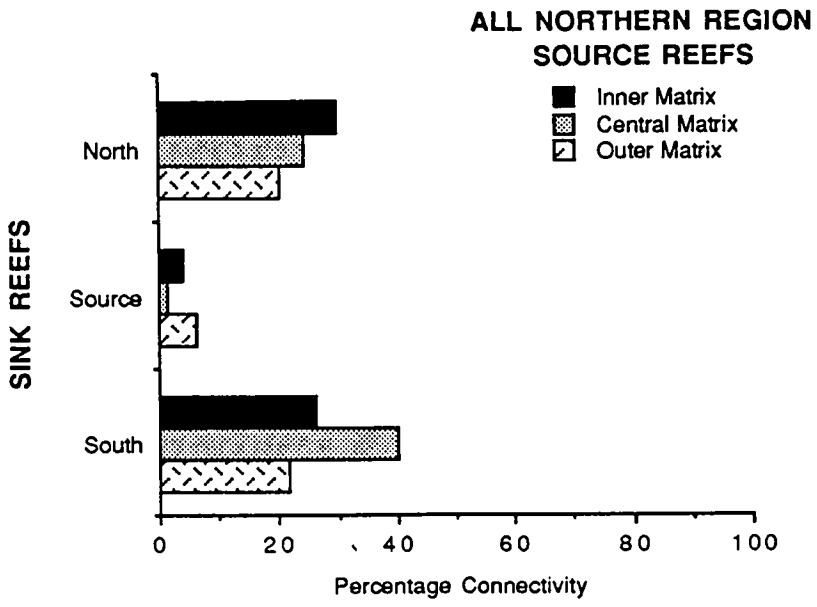


Figure 3.38 Level of reef connectivity with respect to the long-shelf transport of larvae within the northern region. Data represent the number of particles from all five source reefs within each of three cross-shelf geographical zones that intersect with sink reefs, expressed as a percentage of the total number of particle trajectories simulated from each zone. Cross-shelf zones correspond to reefs which lie along the outer edge of the reef matrix and continental shelf (outer matrix), reefs central within the reef matrix (central matrix) and reefs which lie along the inner edge of the reef matrix bordering the main lagoon (inner matrix). Sink reefs are classified as lying to the north or south with respect to the source reef, or recruitment back onto the parent reef (source).

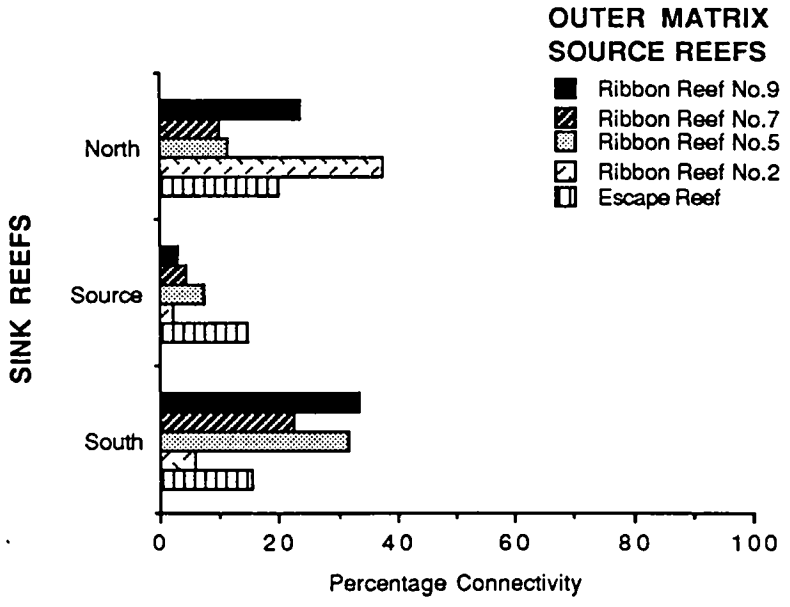


Figure 3.39 Level of reef connectivity with respect to the long-shelf transport of larvae within the northern region for each of the five **outer** matrix source reefs. See caption, Figure 3.38, for further details.

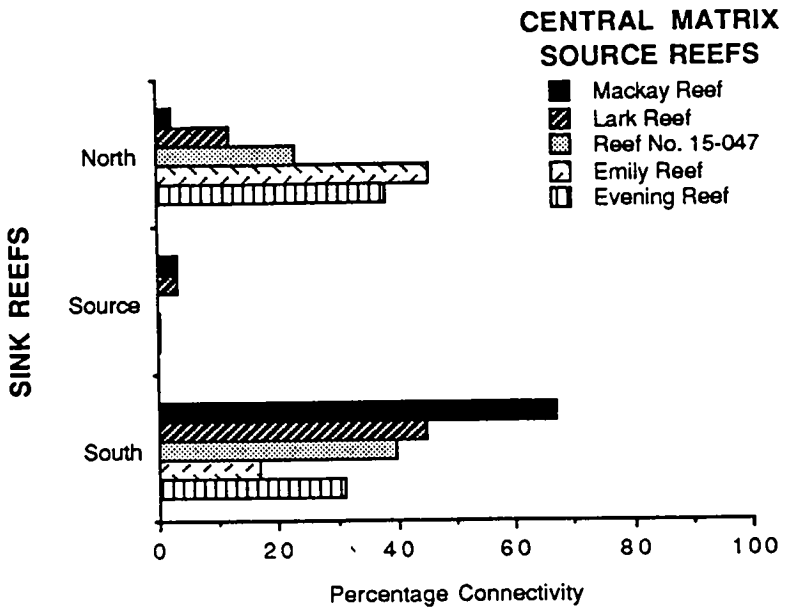


Figure 3.40 Level of reef connectivity with respect to the long-shelf transport of larvae within the northern region for each of the five **central** matrix source reefs. See caption, Figure 3.38, for further details.

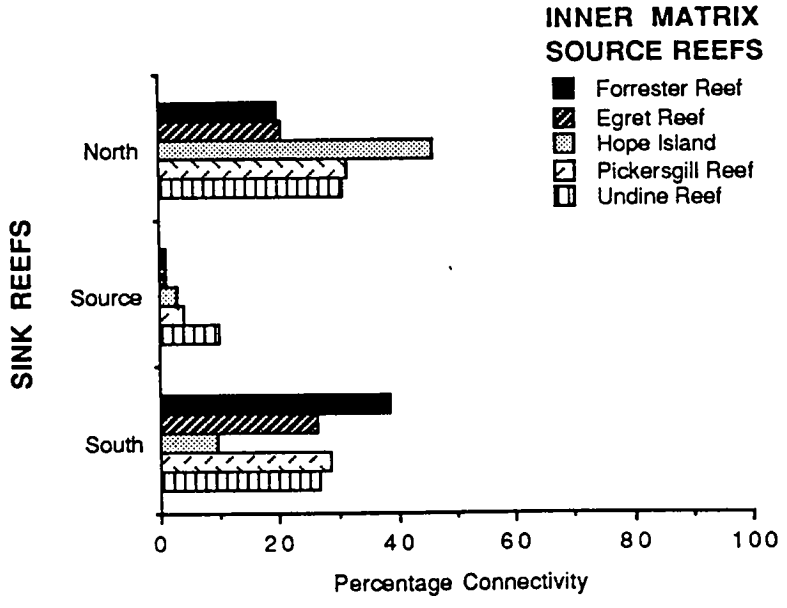


Figure 3.41 Level of reef connectivity with respect to the long-shelf transport of larvae within the northern region for each of the five **inner** matrix source reefs. See caption, Figure 3.38, for further details.

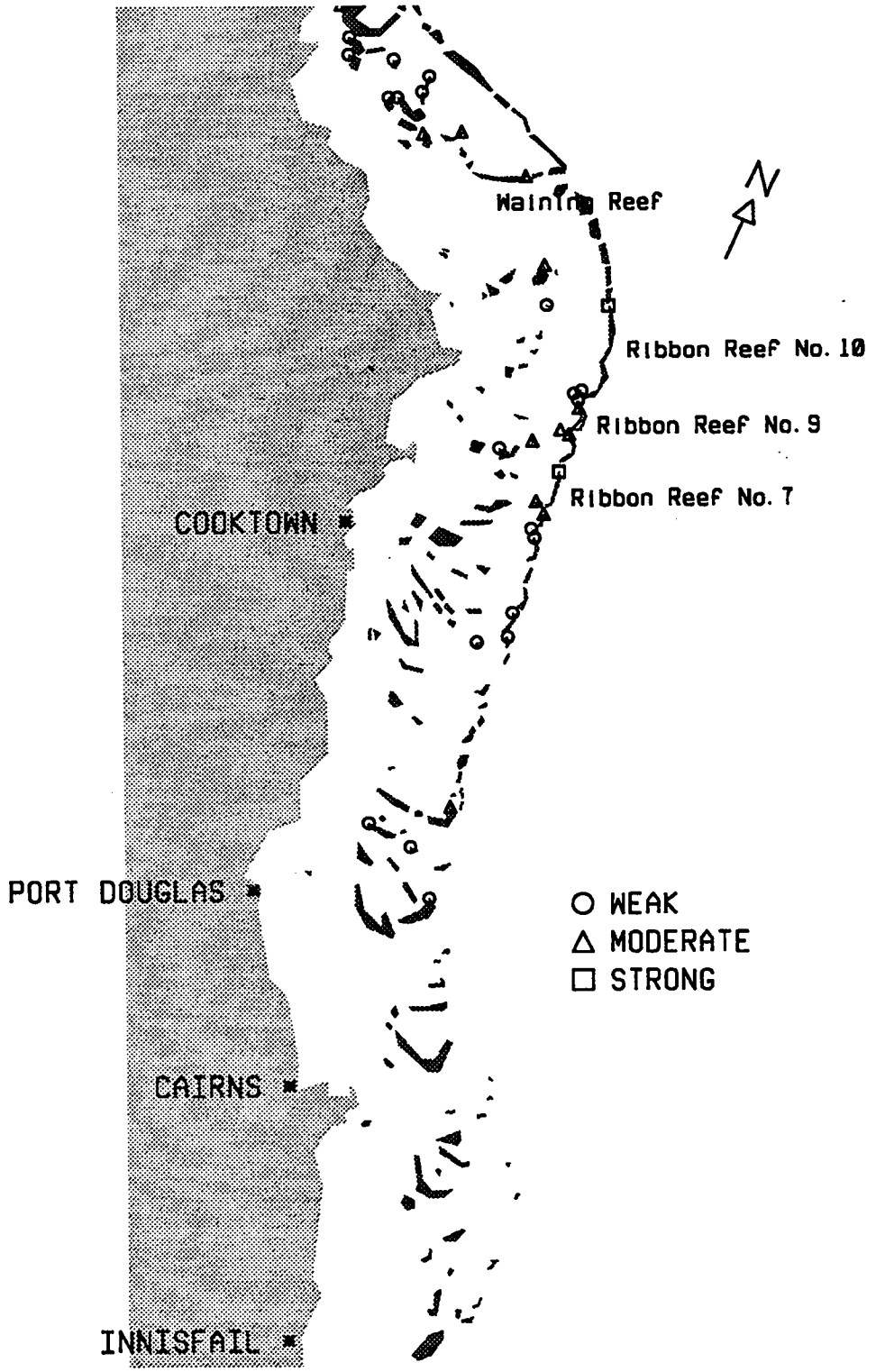


Figure 3.42 Strength of connectivity with respect to Ribbon Reef No.9 (source reef indicated without fill). The relative strength classes (weak, moderate and strong) represent probabilities separated by an order of magnitude. Strongest connectivity is with Ribbon Reef Nos. 7 and 10. Scale: 1cm = 12 nautical miles.

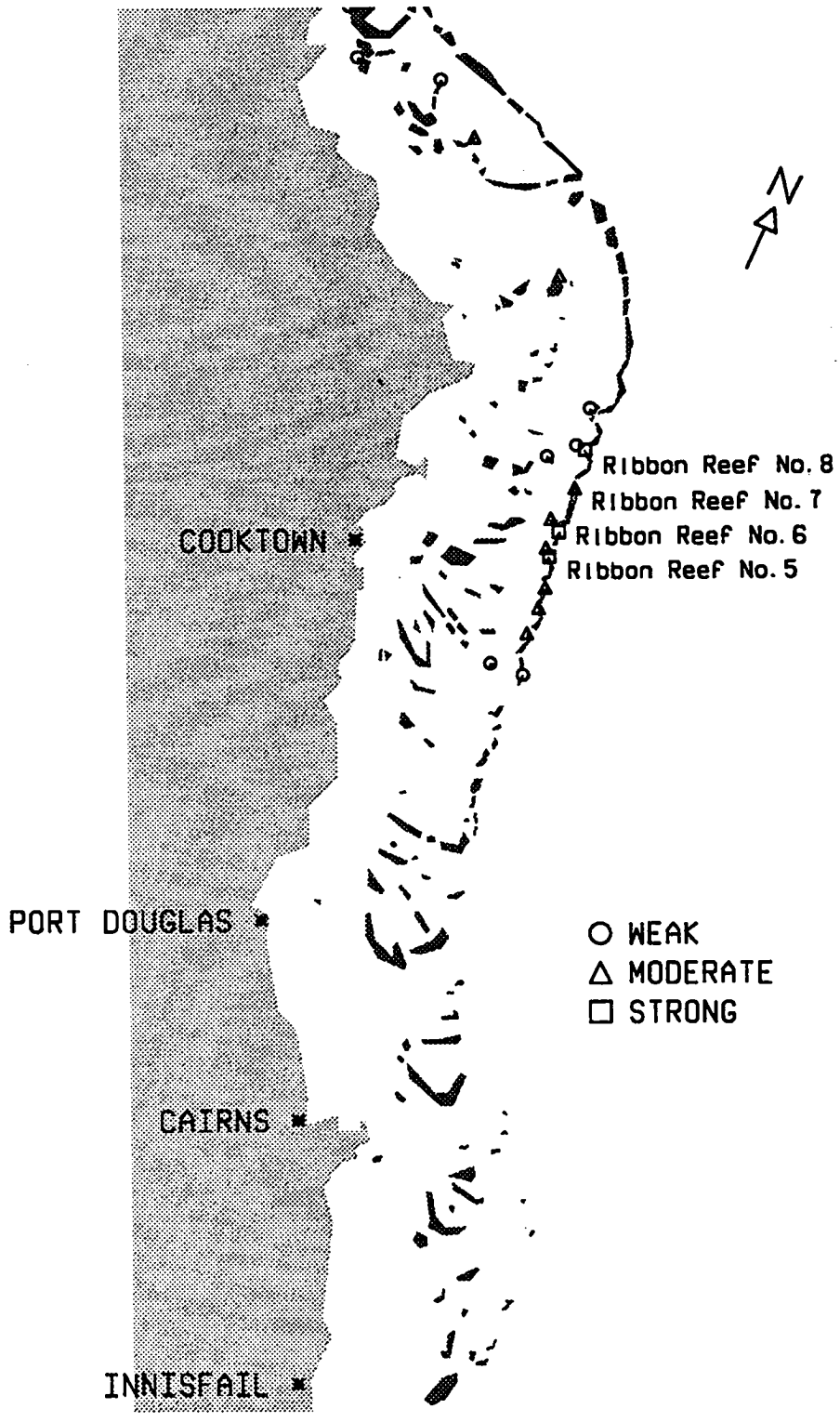


Figure 3.43 Strength of connectivity with respect to Ribbon Reef No.7 (source reef indicated without fill). The relative strength classes (weak, moderate and strong) represent probabilities separated by an order of magnitude. Strongest connectivity is with Ribbon Reef Nos. 5, 6 and 8. Scale: 1cm = 12 nautical miles.

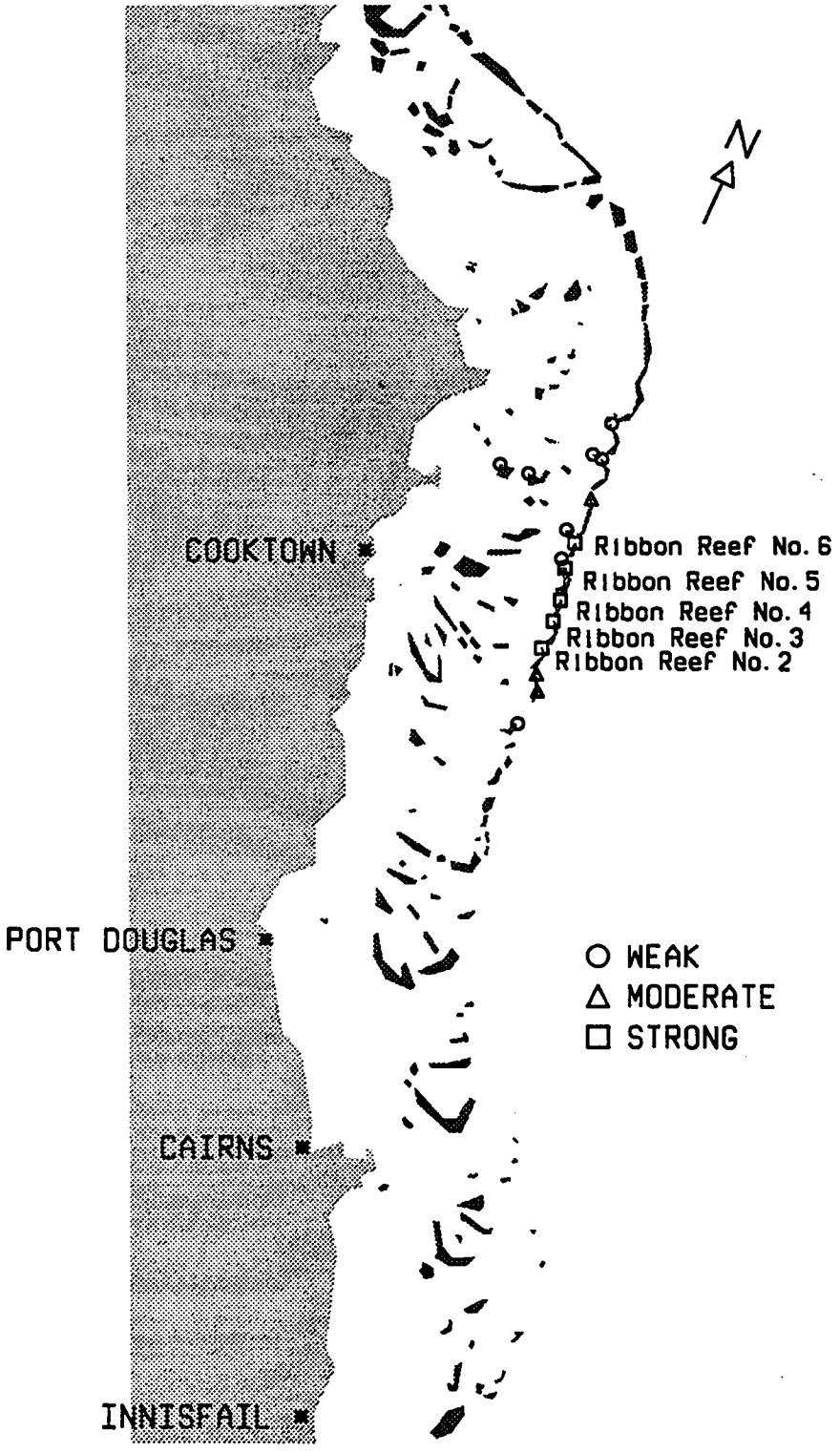


Figure 3.44 Strength of connectivity with respect to Ribbon Reef No.5 (source reef indicated without fill). The relative strength classes (weak, moderate and strong) represent probabilities separated by an order of magnitude. Strongest connectivity is with Ribbon Reef Nos. 2, 3, 4, 5 and 6. Scale: 1cm = 12 nautical miles.

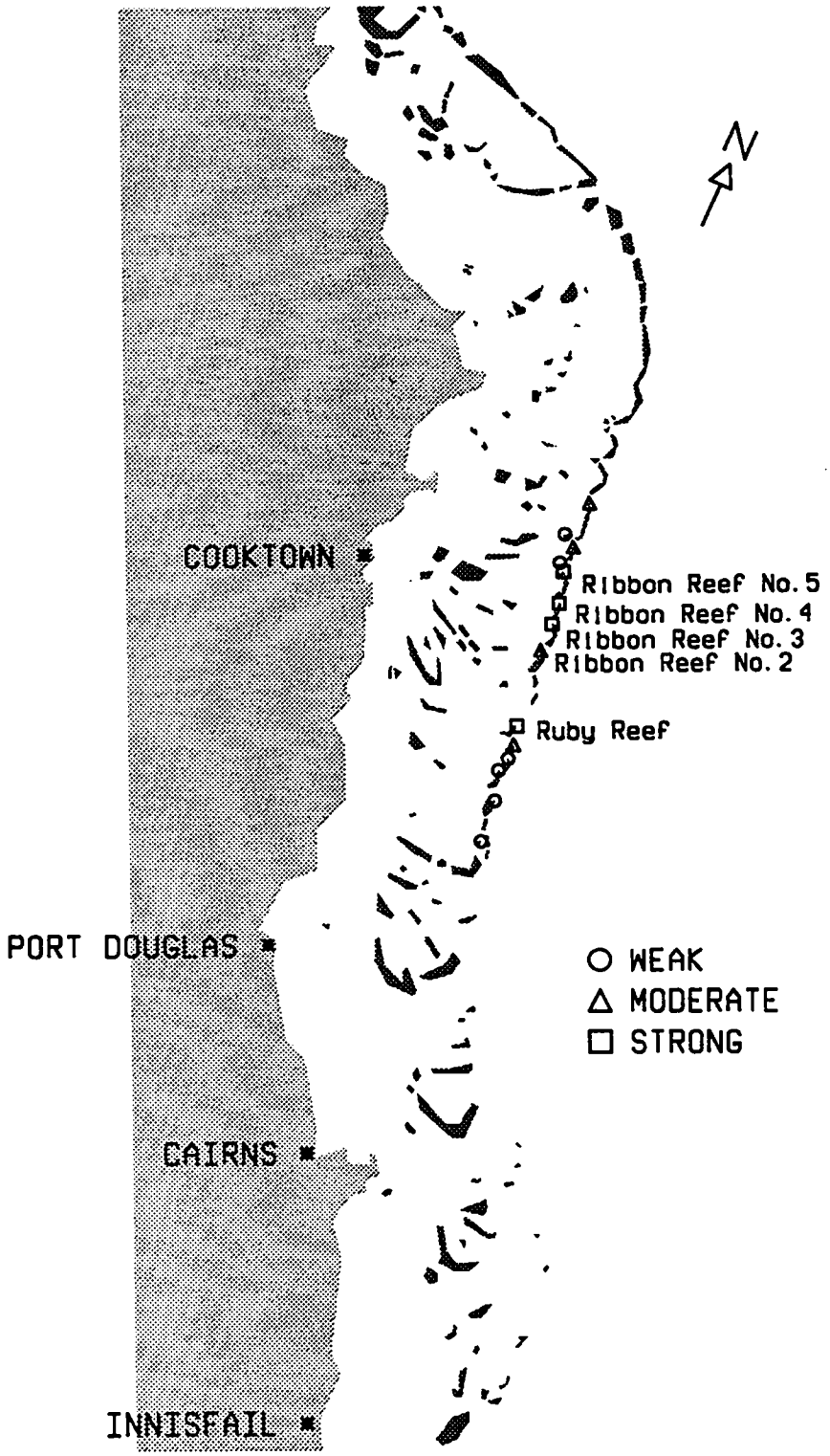


Figure 3.45 Strength of connectivity with respect to Ribbon Reef No.2 (source reef indicated without fill). The relative strength classes (weak, moderate and strong) represent probabilities separated by an order of magnitude. Strongest connectivity is with Ruby Reef and Ribbon Reef Nos. 3, 4 and 5. Scale: 1cm = 12 nautical miles.

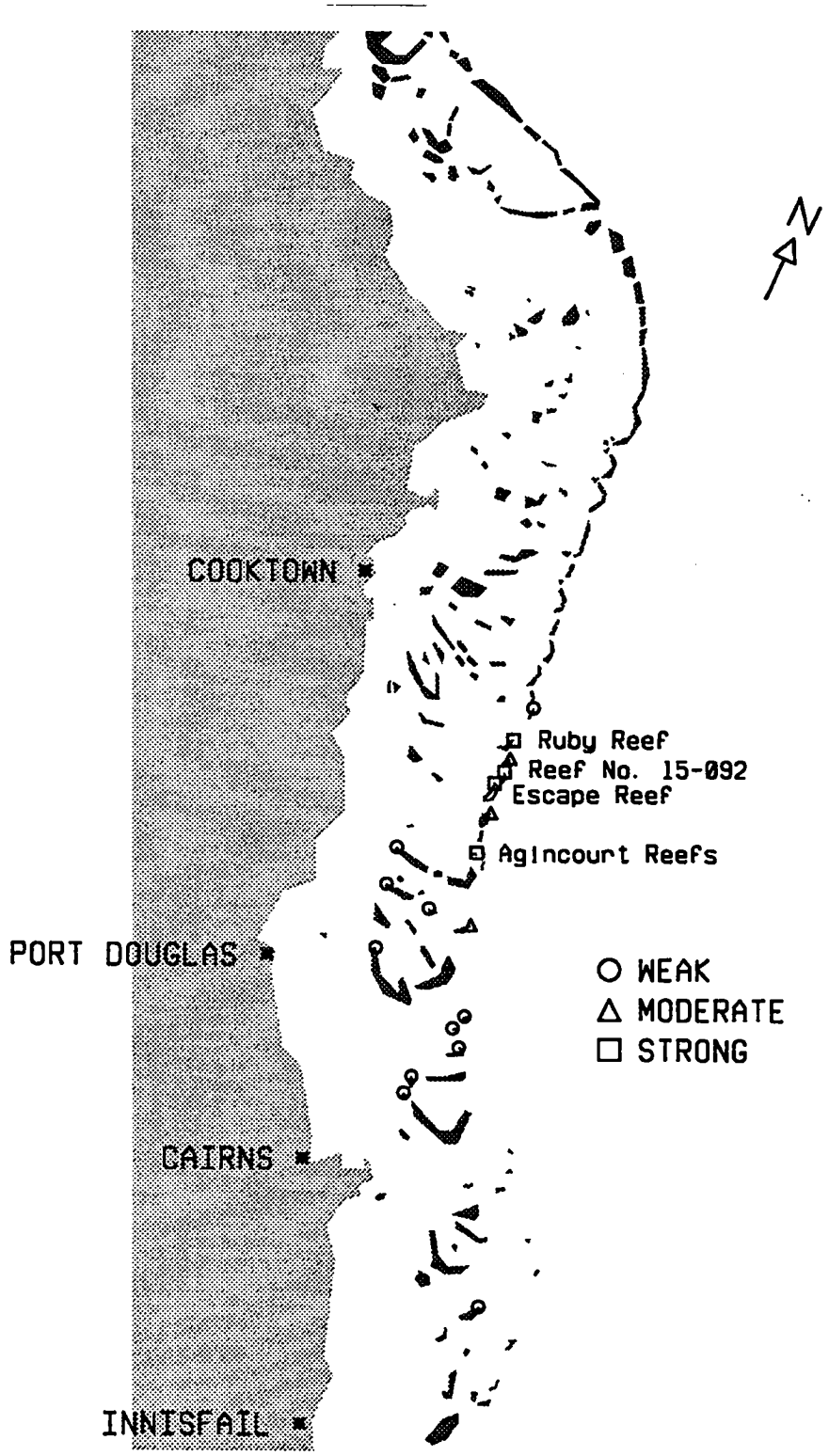


Figure 3.46 Strength of connectivity with respect to Escape Reef (source reef indicated without fill). The relative strength classes (weak, moderate and strong) represent probabilities separated by an order of magnitude. Strongest connectivity is with Agincourt, Escape, 15-092 and Ruby Reefs. Scale: 1cm = 12 nautical miles.

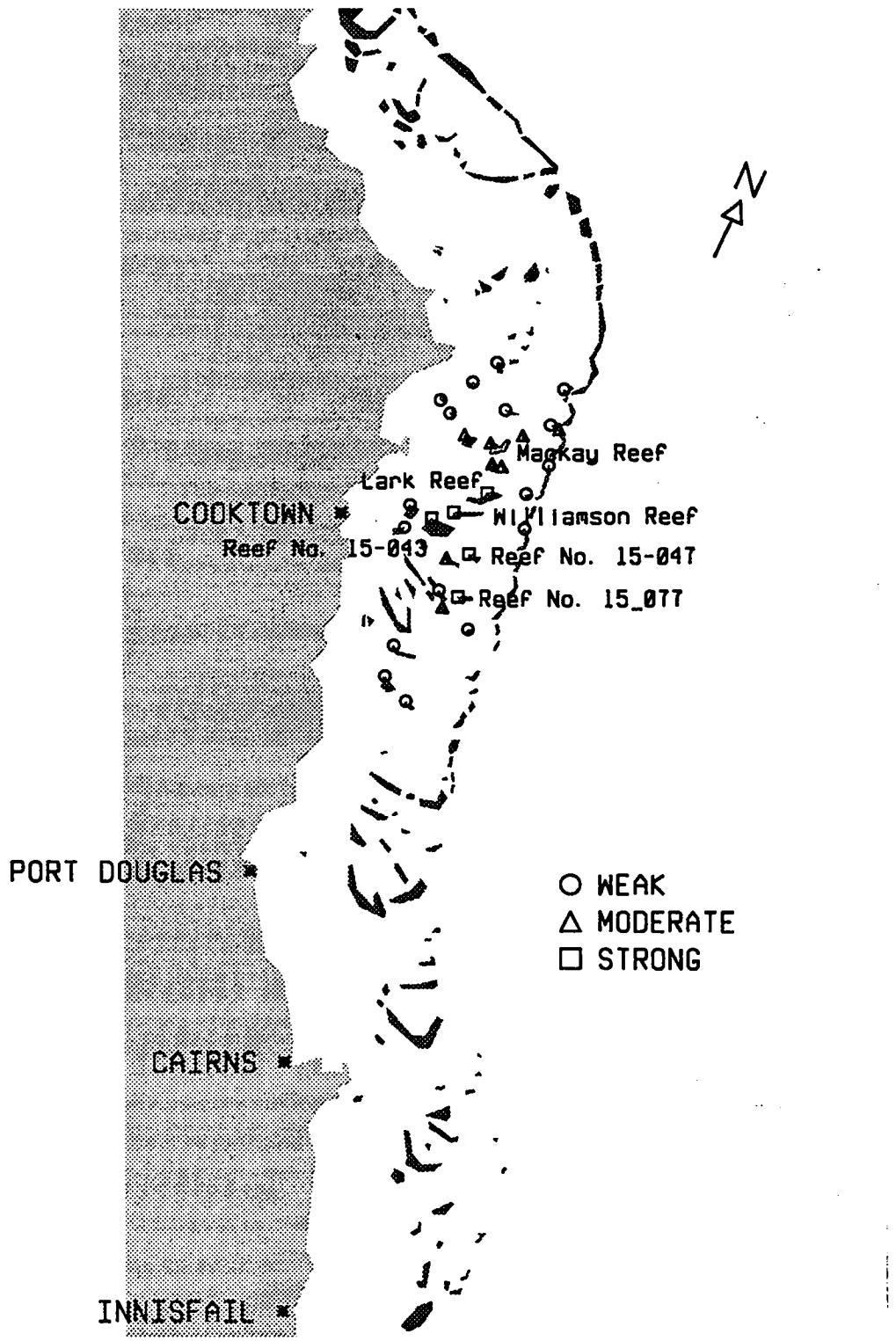


Figure 3.47 Strength of connectivity with respect to Mackay Reef (source reef indicated without fill). The relative strength classes (weak, moderate and strong) represent probabilities separated by an order of magnitude. Strongest connectivity is with Lark, Williamson, 15-043, 15-047 and 15-077 Reefs. Scale: 1cm = 12 nautical miles.

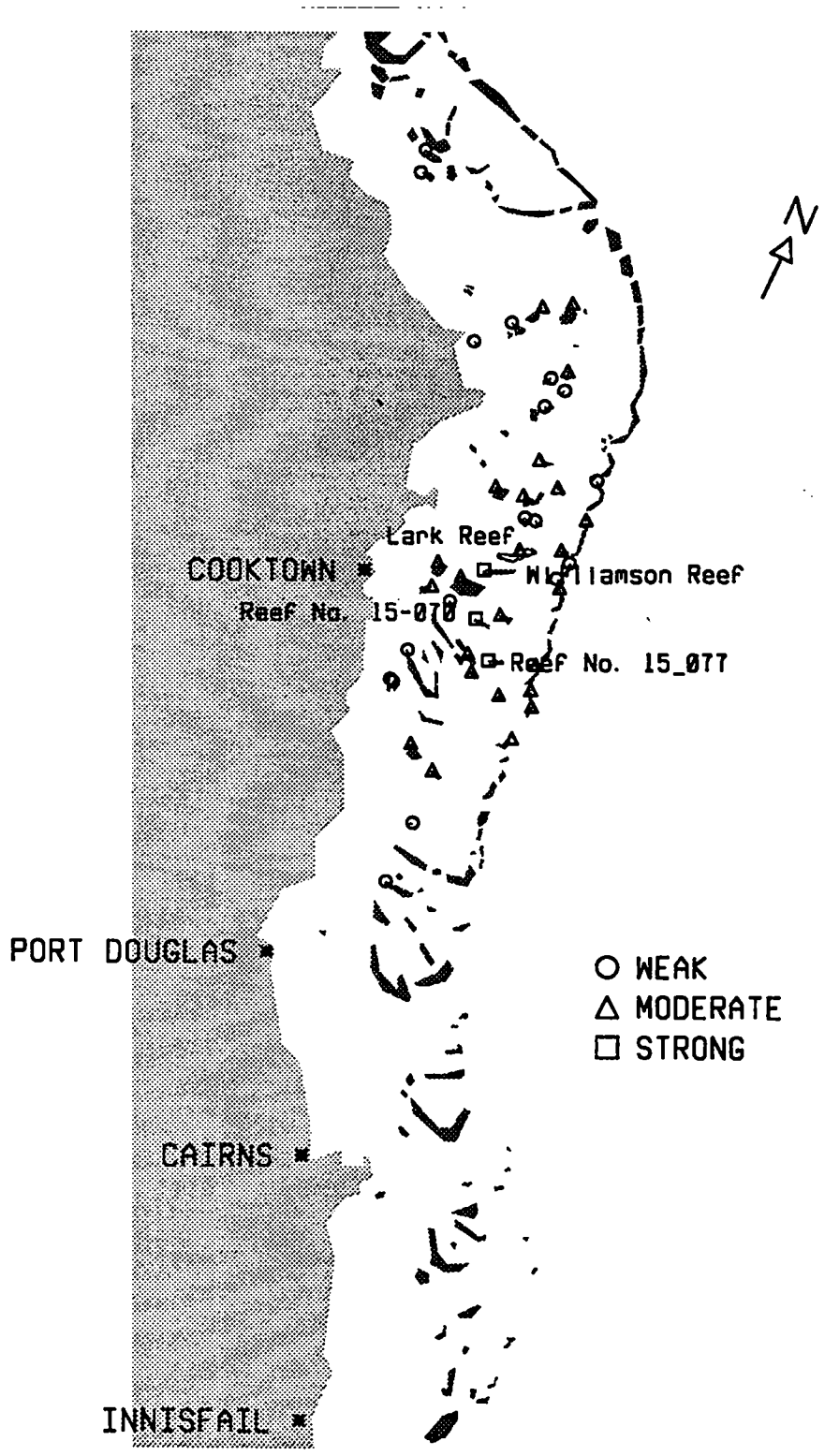


Figure 3.48 Strength of connectivity with respect to Lark Reef (source reef indicated without fill). The relative strength classes (weak, moderate and strong) represent probabilities separated by an order of magnitude. Strongest connectivity is with Williamson, 15-070 and 15-077 Reefs. Scale: 1cm = 12 nautical miles.

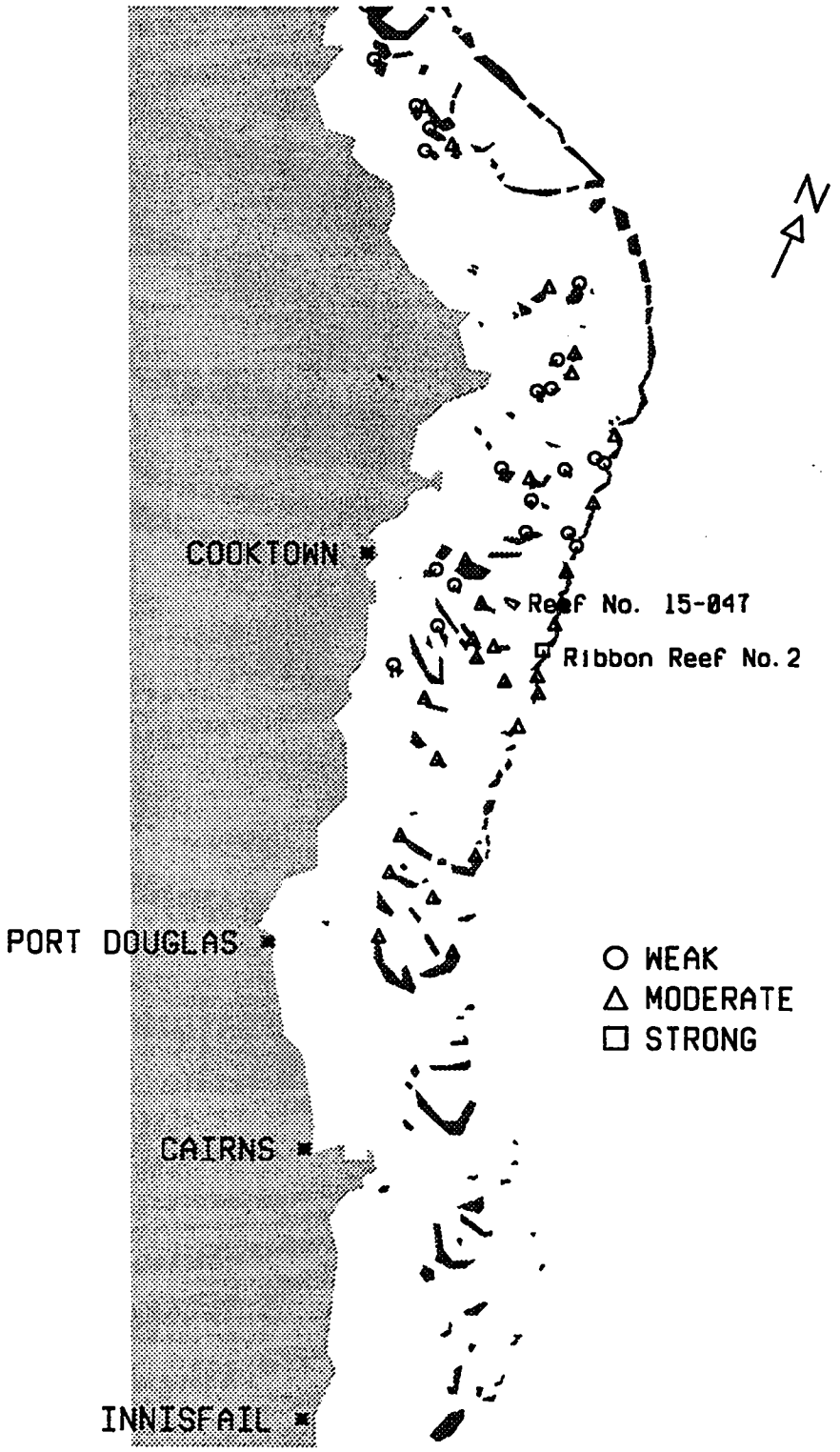


Figure 3.49 Strength of connectivity with respect to reef No.15-047 (source reef indicated without fill). The relative strength classes (weak, moderate and strong) represent probabilities separated by an order of magnitude. Strongest connectivity is with Ribbon Reef No.2. Scale: 1cm = 12 nautical miles.

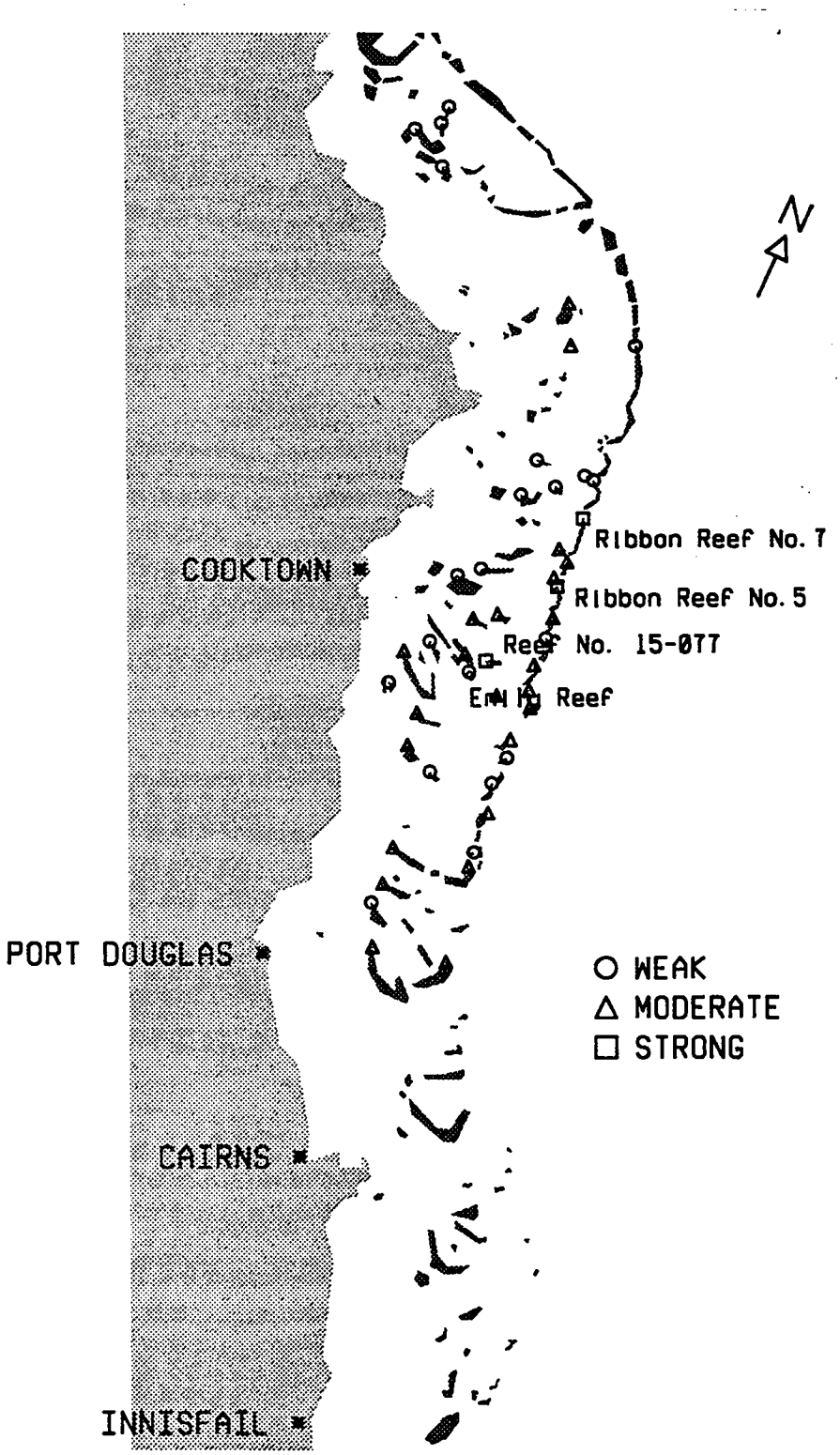


Figure 3.50 Strength of connectivity with respect to Emily Reef. The relative strength classes (weak, moderate and strong) represent probabilities separated by an order of magnitude. Strongest connectivity is with 15-077 and Ribbon Reef Nos. 5 and 7. Scale: 1cm = 12 nautical miles.

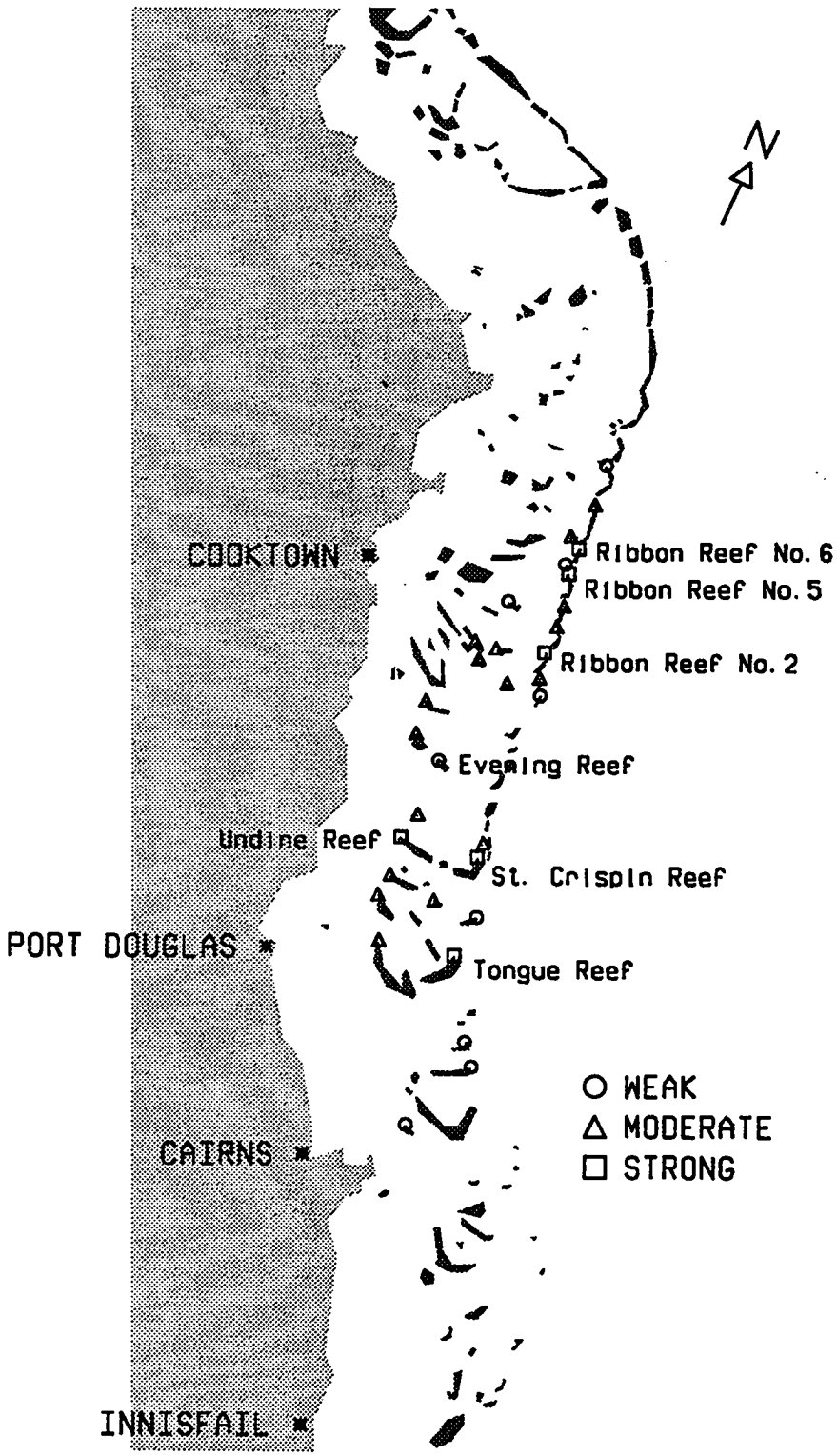


Figure 3.51 Strength of connectivity with respect to Evening Reef. The relative strength classes (weak, moderate and strong) represent probabilities separated by an order of magnitude. Strongest connectivity is with Tongue, St. Crispin, Undine, and Ribbon Reef Nos. 2, 5 and 6. Scale: 1cm = 12 nautical miles.

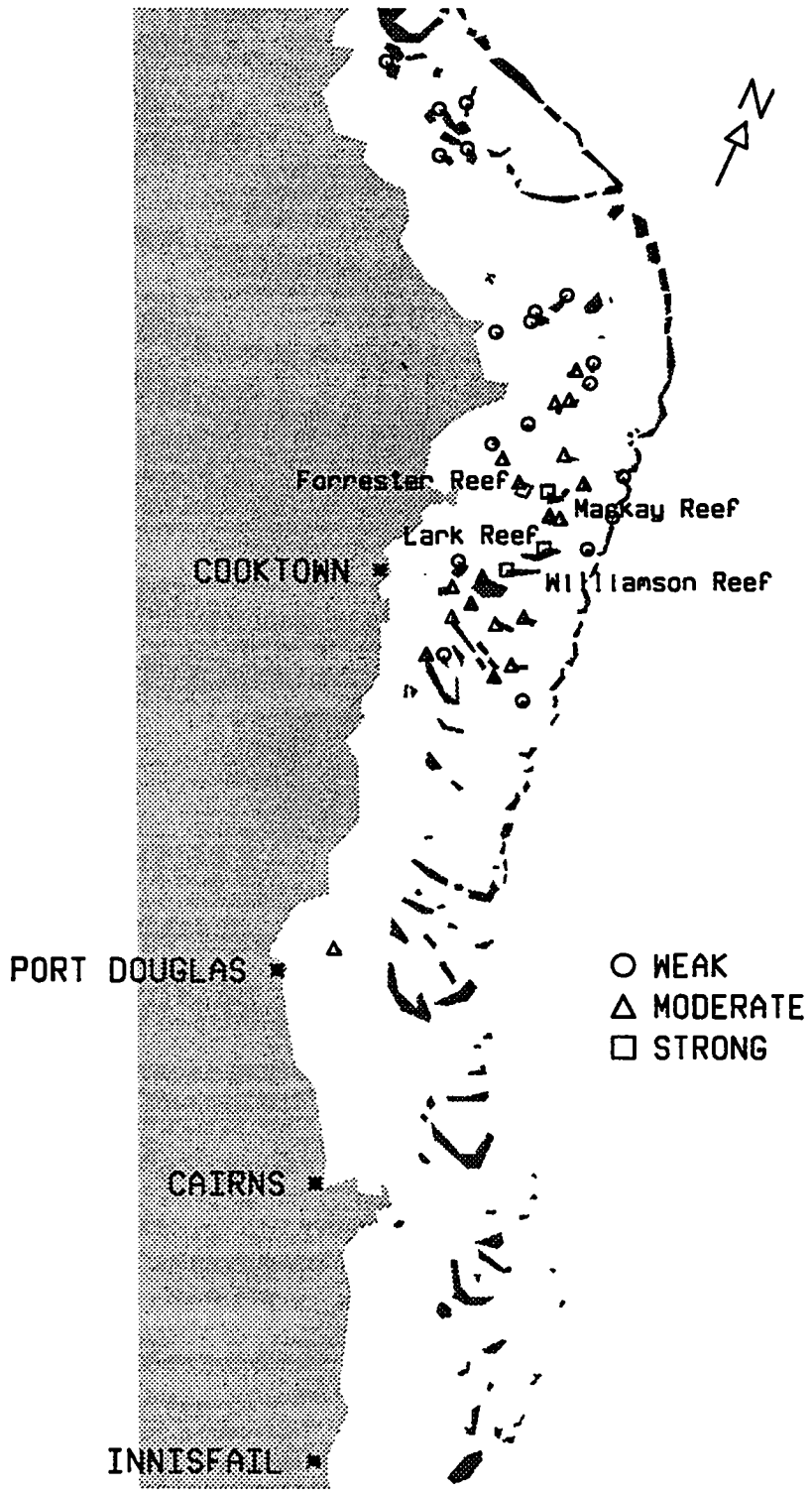


Figure 3.52 Strength of connectivity with respect to Forrester Reef (source reef indicated without fill). The relative strength classes (weak, moderate and strong) represent probabilities separated by an order of magnitude. Strongest connectivity is with Mackay, Lark and Williamson Reefs. Scale: 1cm = 12 nautical miles.

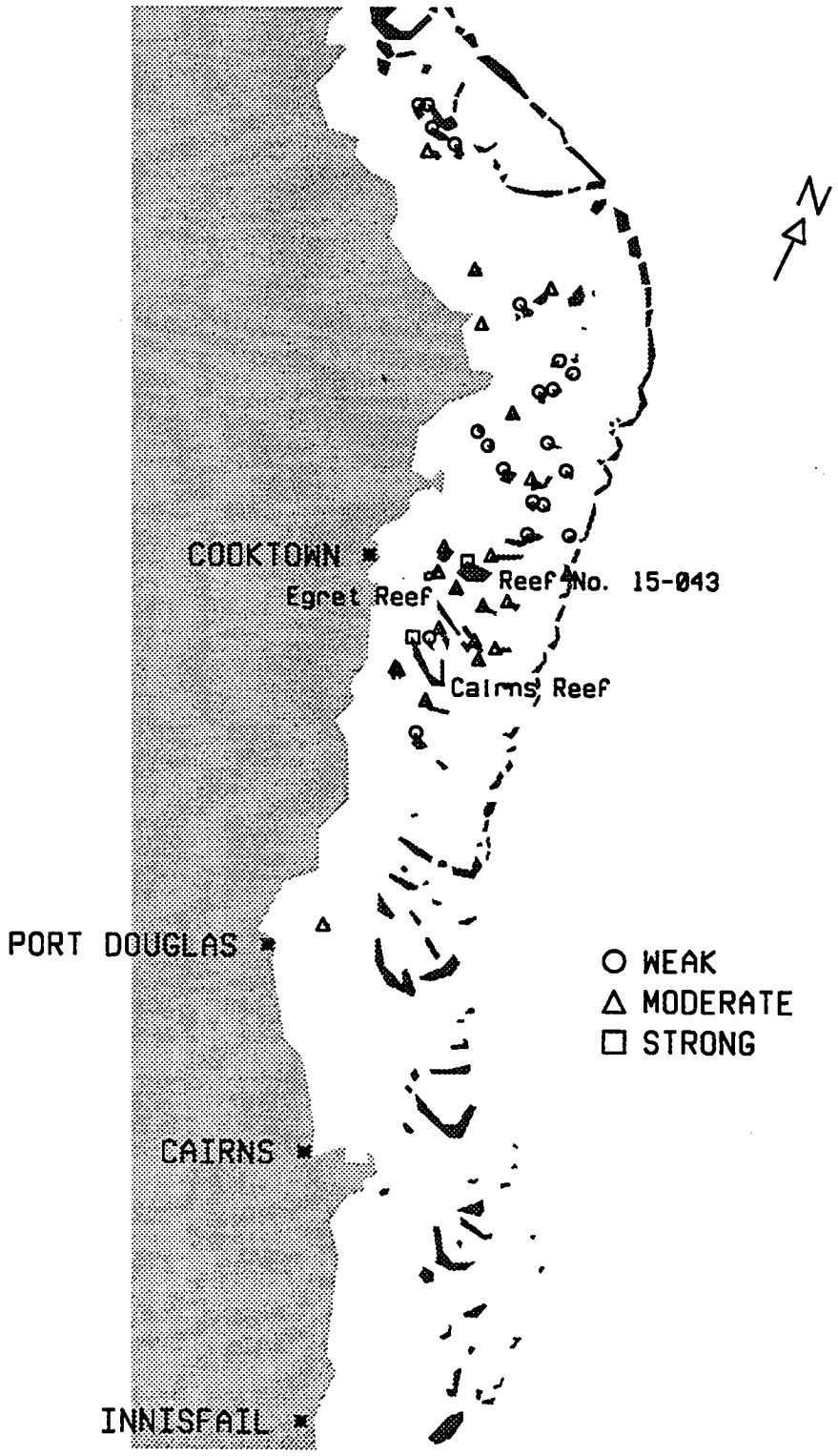


Figure 3.53 Strength of connectivity with respect to Egret Reef (source reef indicated without fill). The relative strength classes (weak, moderate and strong) represent probabilities separated by an order of magnitude. Strongest connectivity is with 15-043 and Cairns Reefs. Scale: 1cm = 12 nautical miles.

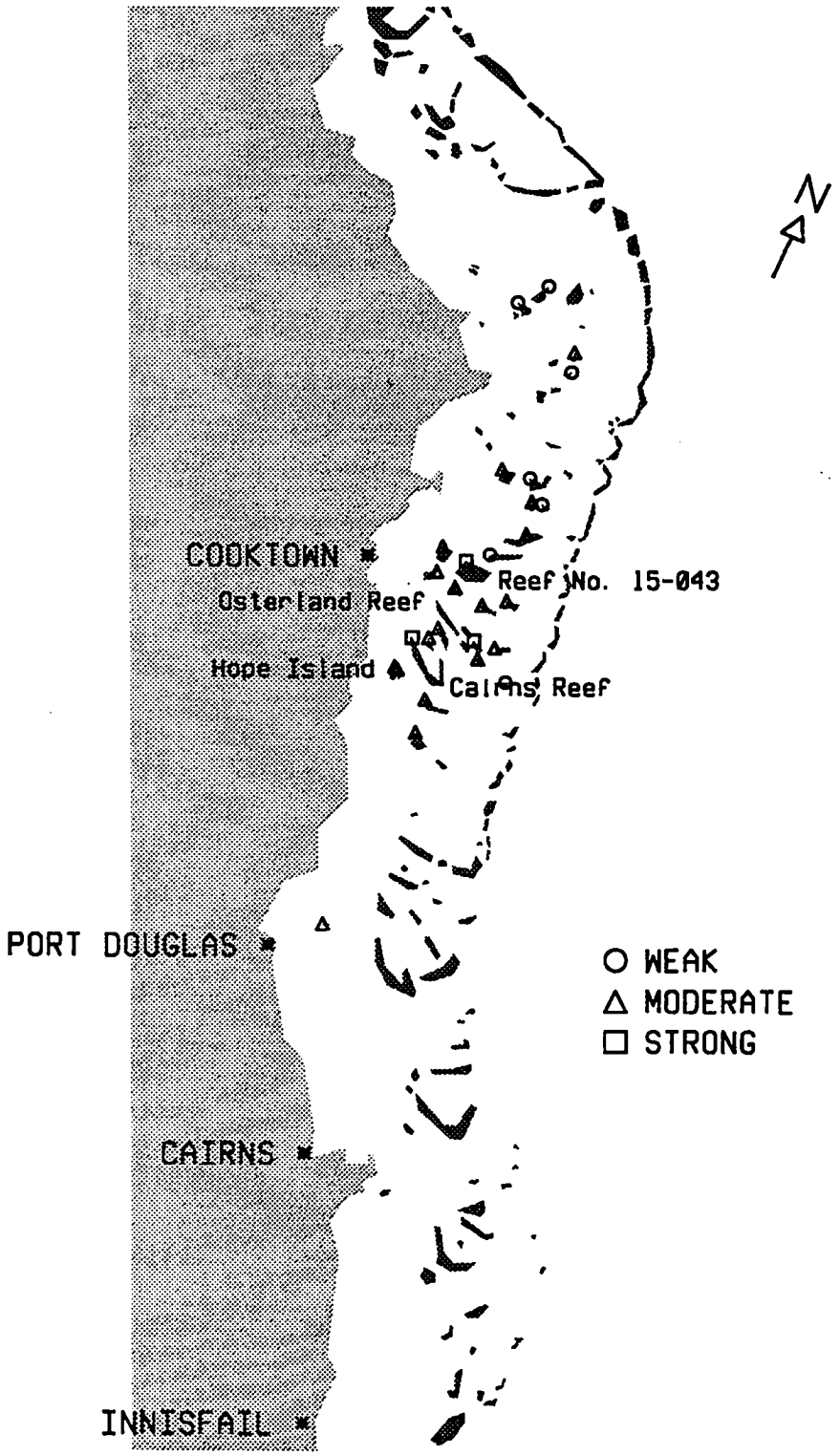


Figure 3.54 Strength of connectivity with respect to Hope Island. The relative strength classes (weak, moderate and strong) represent probabilities separated by an order of magnitude. Strongest connectivity is with 15-043, Osterland and Cairns Reefs. Scale: 1cm = 12 nautical miles.

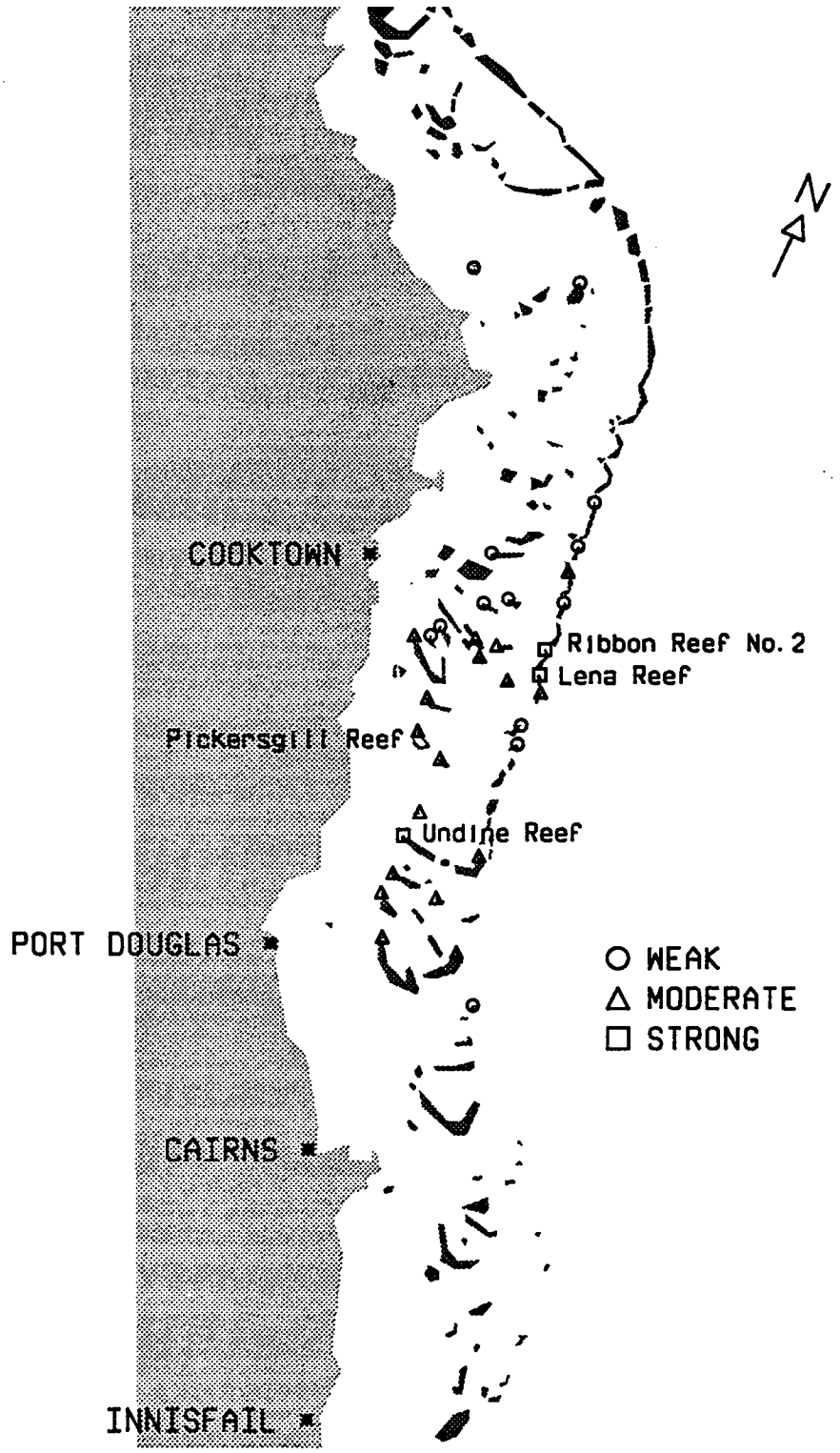


Figure 3.55 Strength of connectivity with respect to Pickersgill Reef (source reef indicated without fill). The relative strength classes (weak, moderate and strong) represent probabilities separated by an order of magnitude. Strongest connectivity is with Undine, Lena and Ribbon Reef No. 2. Scale: 1cm = 12 nautical miles.

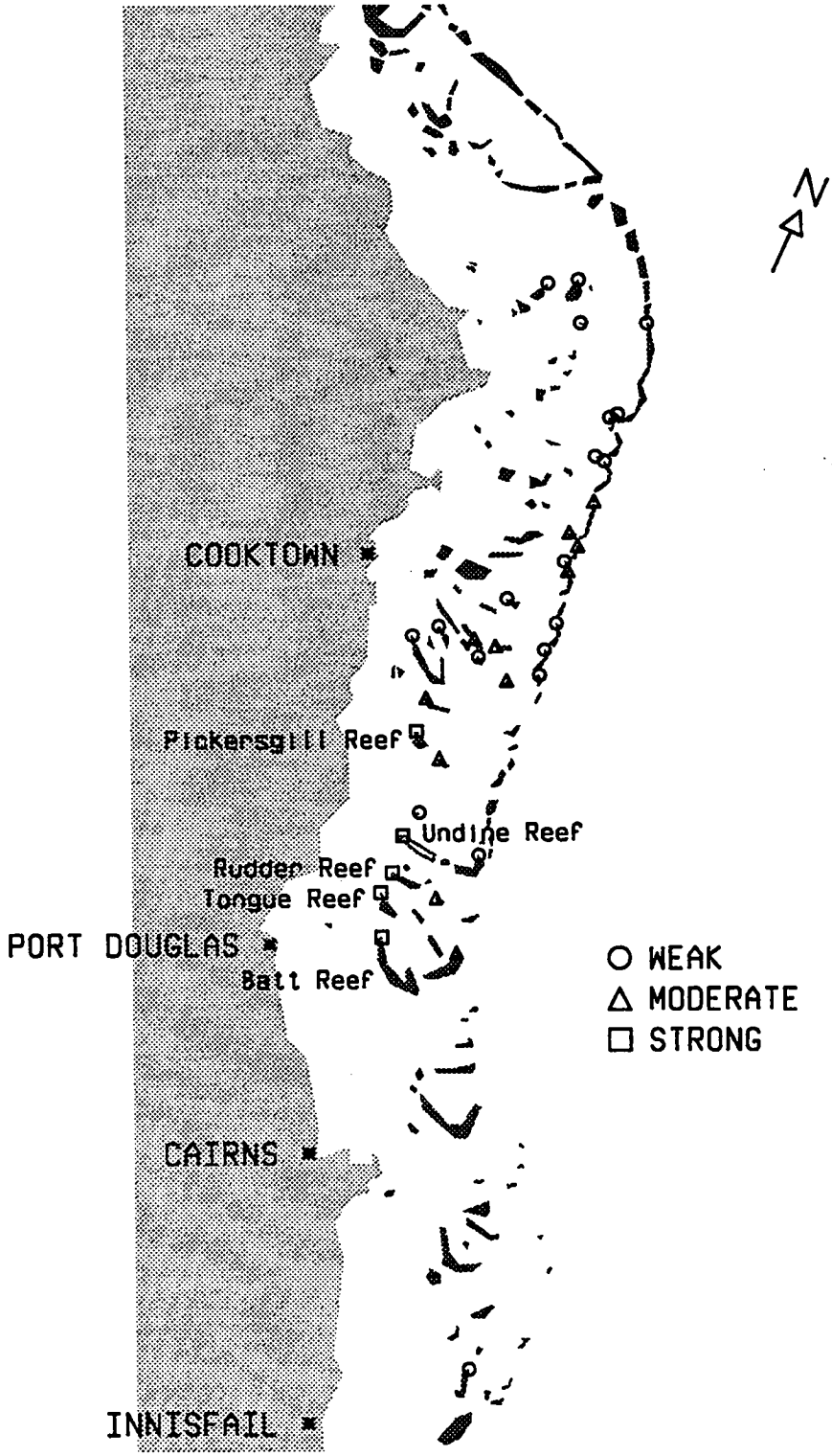


Figure 3.56 Strength of connectivity with respect to Undine Reef (source reef indicated without fill). The relative strength classes (weak, moderate and strong) represent probabilities separated by an order of magnitude. Strongest connectivity is with Pickersgill, Undine, Rudder, Tongue and Batt Reefs. Scale: 1cm = 12 nautical miles.

connectivity of Ribbon Reef No.9 (see Section 3.5.1.1 above) with central matrix sink reefs to the north of Waining Reef is evident in Figure 3.42. The hydrodynamics in this area deflect larvae around Waining Reef in an onshore direction when the currents are flowing to the north.

Significant differences in the pattern of connectivity are evident for central and inner matrix source reefs (Figs. 3.47 to 3.56). Connectivity is spread over many more reefs, which lie over the entire shelf. The most northern reefs, Mackay, Lark, Forrester and 15-047, show strongest connectivity with reefs lying to the south while the remainder show strongest connectivity with reefs lying both to the north and south, or to the north alone.

Three northern region source reefs, Ribbon No.5, Escape and Undine, displayed strong connectivity with themselves. Dispersal events from these reefs frequently transported larvae back to the source reef as a result of current reversals. Most other source reefs displayed moderate levels of connectivity with themselves. Within the northern region, therefore, there appears to be considerable self-seeding of reefs. This is not, though, as a consequence of larval retention by reefs. The distances over which larvae are transported to reefs with strongest connectivity are very short for outer matrix source reefs, generally less than 10 nautical miles. These distances for central and inner matrix source reefs are substantially greater, but rarely more than about 20 nautical miles. However, there is weak to moderate connectivity with reefs up to 60 nautical miles away.

3.5.2 The Central Region

3.5.2.1 Cross-shelf connectivity

Reef connectivity within the central region, expressed as source-sink relationships with respect to the cross-shelf movement of larvae, is presented in Figures 3.57 to 3.60. Considering all five source reefs in each zone collectively (Fig. 3.57), it is evident that:

- (1) connectivity of outer matrix source reefs was primarily with central matrix sink reefs (36.6%). A substantial proportion of larvae

ended up in the vicinity of both inner matrix reefs (11.9%) and other outer matrix reefs (11.2%). Many dispersal events originating from outer matrix source reefs did not transport larvae to the near vicinity of other reefs within the time constraints of larval life that were imposed (40.3%);

(2) connectivity of central matrix source reefs was fairly evenly distributed between both central (23.5%) and inner matrix sink reefs (29.5%). Only relatively rare events resulted in larvae being transported offshore to the outer matrix reefs (2.0%). Again, many dispersal events failed to transport larvae to the near vicinity of other reefs (45.0%);

(3) connectivity of inner matrix source reefs was almost exclusively with other reefs bordering or within the lagoon (35.3%). Again, only relatively rare events resulted in larvae being transported offshore (6.1%). A very high proportion of dispersal events from inner matrix reefs failed to transport larvae to the near vicinity of other reefs (57.8%), a substantially higher proportion than from the central and outer matrix source reefs.

In summary, connectivity of outer and central matrix source reefs was primarily with sink reefs lying in adjacent cross-shelf zones in an onshore direction. Connectivity of inner matrix source reefs was almost exclusively with other inner matrix reefs bordering the main lagoon. Only relatively rare events resulted in the transport of particles offshore from inner and central matrix source reefs. Overall, levels of connectivity from source reefs within the central region (59.7, 55.0 and 42.8% for outer, central and inner matrix source reefs respectively) appear to be slightly lower than those for source reefs within the northern region (65.7, 59.6 and 48.8% for central, inner and outer matrix source reefs respectively). A very high proportion of particles originating from inner matrix source reefs became entrained within the main lagoon and were transported longshore without encountering another reef.

Examination of results from individual reefs (Figs. 3.58 to 3.60) once again indicate a more complex picture, but one in which the patterns of reef connectivity are more consistent than in the northern region. Connectivity of all individual outer matrix source reefs was with reefs

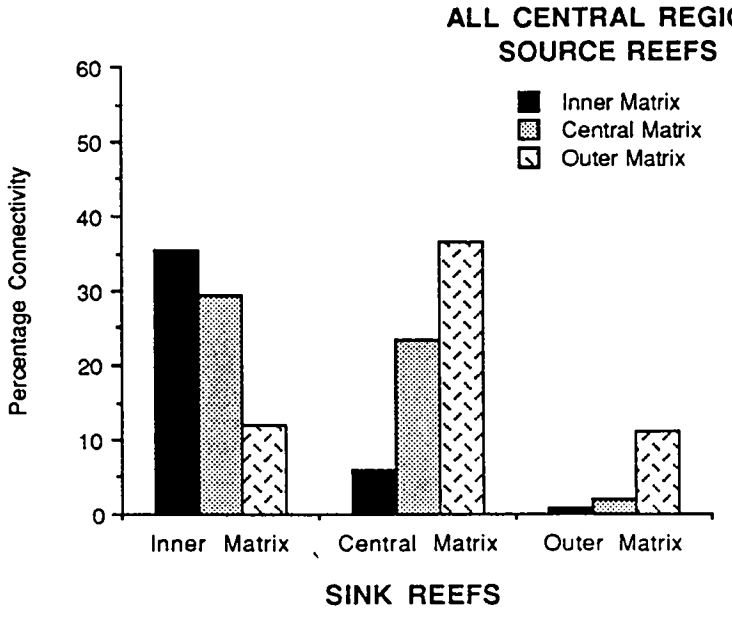


Figure 3.57 Level of reef connectivity with respect to the cross-shelf transport of larvae within the central region. Data represent the number of particles from five source reefs within each of three cross-shelf geographical zones that intersect with sink reefs, expressed as a percentage of the total number of particle trajectories simulated from each zone. Cross-shelf zones correspond to reefs which lie along the outer edge of the reef matrix and continental shelf (outer matrix), reefs central within the reef matrix (central matrix) and reefs which lie along the inner edge of the reef matrix bordering the main lagoon (inner matrix).

lying central within the matrix (Fig. 3.58). However, while most source reefs displayed quite high levels of connectivity overall, the level of connectivity from Channel Reef was relatively low (43.4%). This reef lies very much on the edge of the continental shelf and many larvae were transported offshore by tides and wind-driven currents where they became entrained within the EAC and, oftentimes, were not transported back onshore (see Fig. 3.61). Connectivity of individual central matrix source reefs was far more inconsistent, both with respect to the levels of connectivity overall and the cross-shelf location of sink reefs (Fig. 3.59). While Thetford, Michaelmas and Maori Reefs displayed high levels of connectivity (78.9, 67.9 and 67.6% respectively), Tongue and Cayley Reefs, the latter in particular, displayed low levels of connectivity (46.2 and 14.6% respectively). Larvae from these two reefs were moved onshore through large passages in the reef matrix and became entrained within the main lagoon where they were transported longshore. Maori Reef displayed higher connectivity with other central matrix reefs while Tongue Reef displayed higher connectivity with inner matrix reefs. Connectivity of individual inner matrix source reefs, while

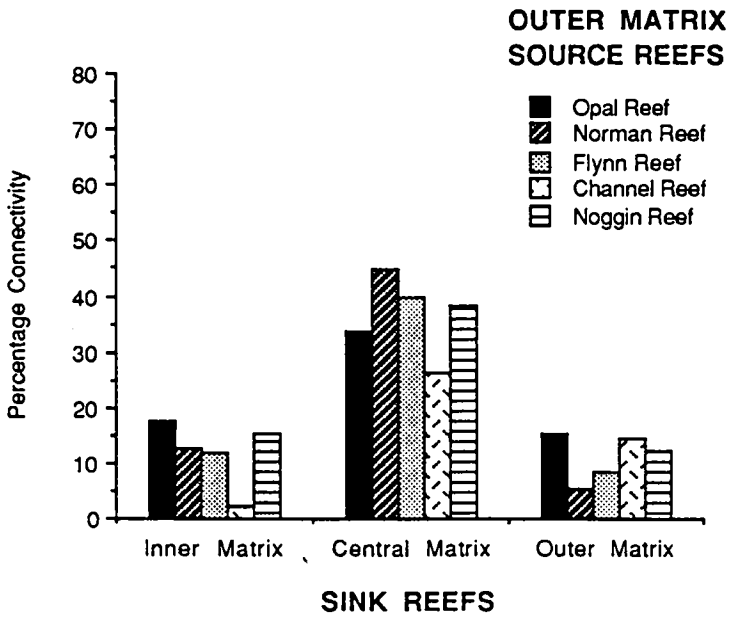


Figure 3.58 Level of reef connectivity with respect to the cross-shelf transport of larvae within the central region for each of the five **outer** matrix source reefs. See caption, Figure 3.57, for further details.

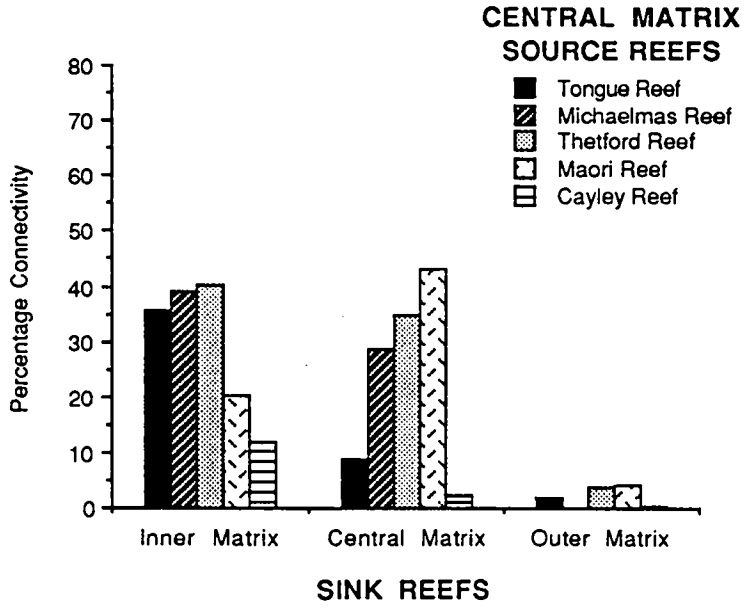


Figure 3.59 Level of reef connectivity with respect to the cross-shelf transport of larvae within the central region for each of the five **central** matrix source reefs. See caption, Figure 3.57, for further details.

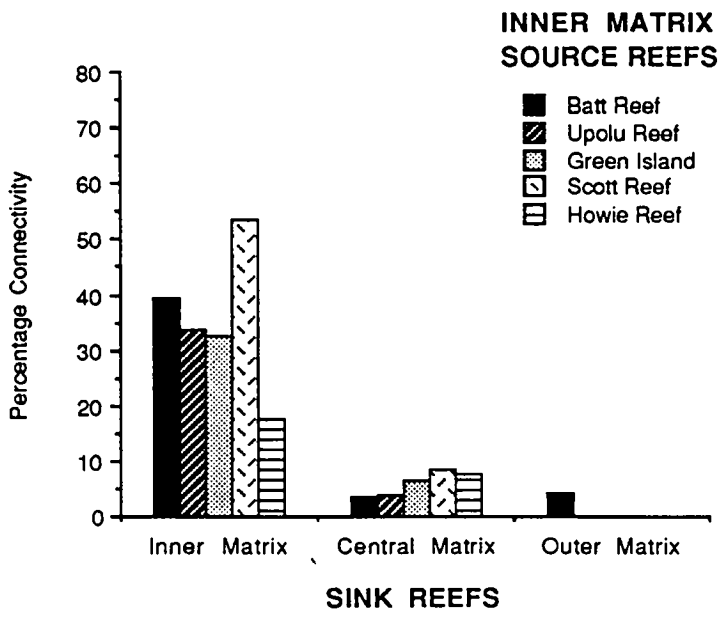


Figure 3.60 Level of reef connectivity with respect to the cross-shelf transport of larvae within the central region for each of the five **inner** matrix source reefs. See caption, Figure 3.57, for further details.

generally consistent with respect to the cross-shelf location of sink reefs, was inconsistent with respect to the levels of connectivity overall (Fig. 3.60). Scott Reef, on the one hand, displayed quite high connectivity (61.8%) while Howie Reef displayed very low connectivity (25.1%). Larvae from inner matrix source reefs frequently remained entrained within the main lagoon and were transported alongshore (see Fig. 3.62).

3.5.2.2 Long-shelf connectivity

Reef connectivity, with respect to the long-shelf movement of larvae, is presented in Figures 3.63 to 3.66. Considering all five source reefs in each cross-shelf zone collectively (Fig. 3.63), it is evident that connectivity was directed strongly southwards. Overall, 80.9% of particles which intersected with reefs were transported to the south, while only 16.8% were transported to the north. Only very limited potential for recruitment back onto the source reef as a result of current reversals is evident (2.3%). The northward transportation of larvae appears to become more frequent along a gradient from the outer to inner matrix reefs. The pattern of strong southward directed connectivity was consistent for reefs in all cross-shelf zones (Figs.

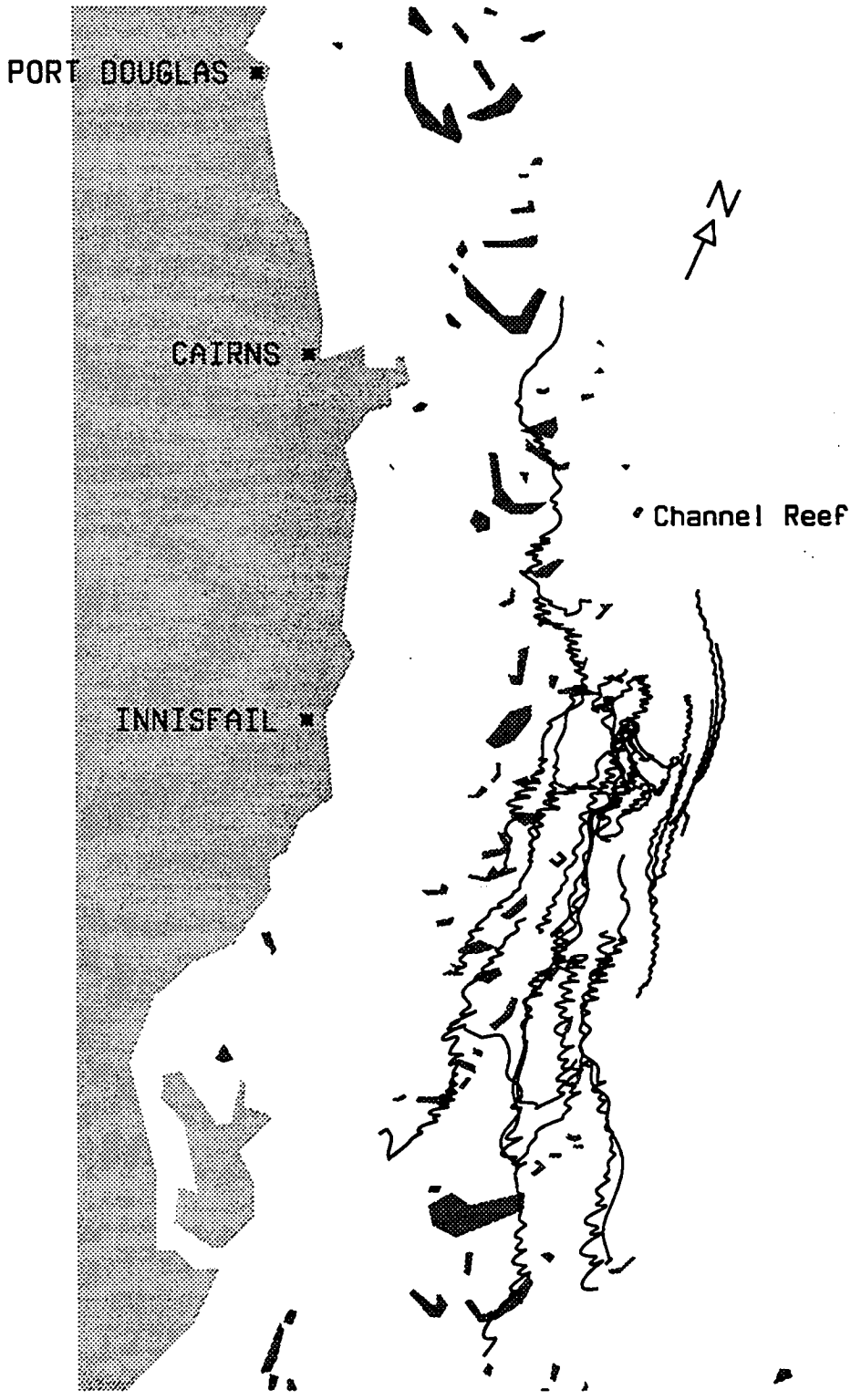


Figure 3.61 Particle trajectories representing twenty dispersal events from Channel Reef. Each trajectory corresponds to the centroid of the larval cloud during the second two weeks of dispersal when the larvae of *A. planci* are assumed to be competent to settle. Larvae originating from Channel Reef are frequently predicted to be transported offshore by tides and wind-driven currents where they become entrained within the EAC and, oftentimes, will not be transported back onshore. Scale: 1cm = 8 nautical miles.

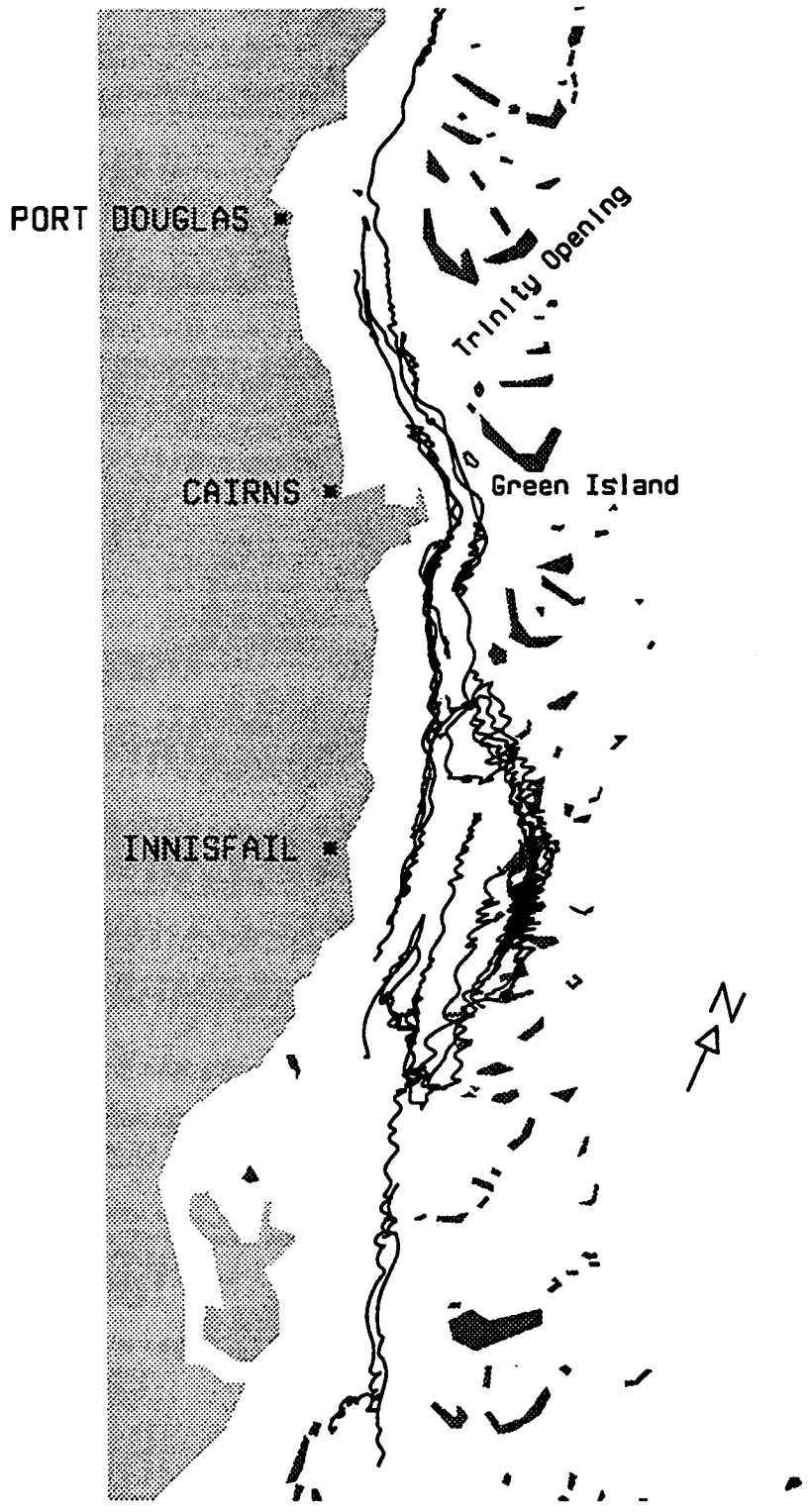


Figure 3.62 Particle trajectories representing twenty dispersal events from Green Island (source reef indicated without fill). Each trajectory corresponds to the centroid of the larval cloud during the second two weeks of dispersal when the larvae of *A. planci* are assumed to be competent to settle. The different trajectories represent within and between year variation in the transport of larvae based on the random selection of tide and wind records. Larvae from inner matrix source reefs frequently remained entrained within the main lagoon and are transported alongshore. Scale: 1cm = 9 nautical miles.

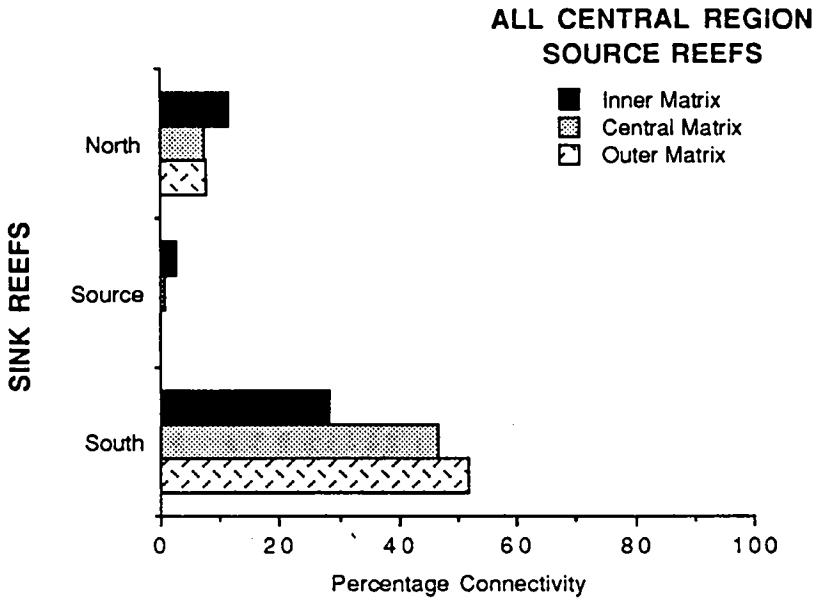


Figure 3.63 Level of reef connectivity with respect to the long-shelf transport of larvae within the central region. Data represent the number of particles from all five source reefs within each of three cross-shelf geographical zones that intersect with sink reefs, expressed as a percentage of the total number of particle trajectories simulated from each zone. Cross-shelf zones correspond to reefs which lie along the outer edge of the reef matrix and continental shelf (outer matrix), reefs central within the reef matrix (central matrix) and reefs which lie along the inner edge of the reef matrix bordering the main lagoon (inner matrix). Sink reefs are classified as lying to the north or south with respect to the source reef, or recruitment back onto the parent reef (source).

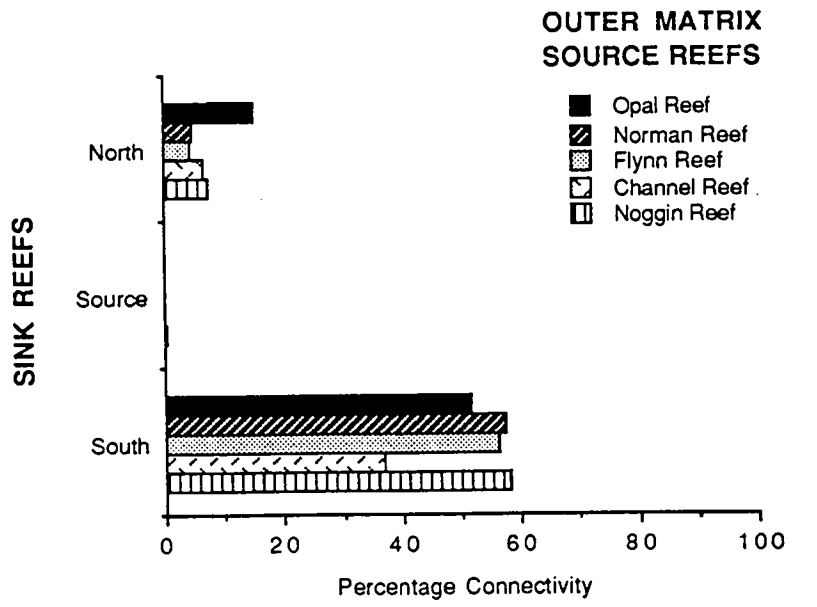


Figure 3.64 Level of reef connectivity with respect to the long-shelf transport of larvae within the central region for each of the five **outer** matrix source reefs. See caption, Figure 3.63, for further details.

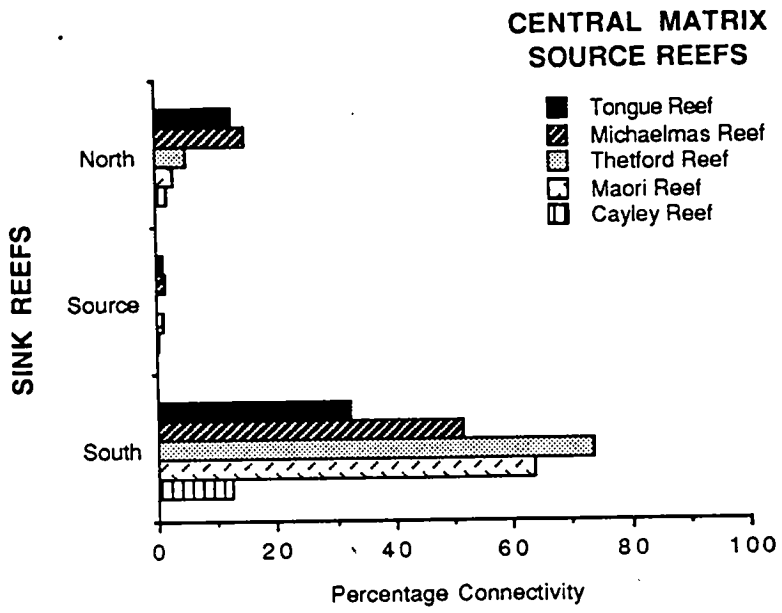


Figure 3.65 Level of reef connectivity with respect to the long-shelf transport of larvae within the central region for each of the five **central** matrix source reefs. See caption, Figure 3.63, for further details.

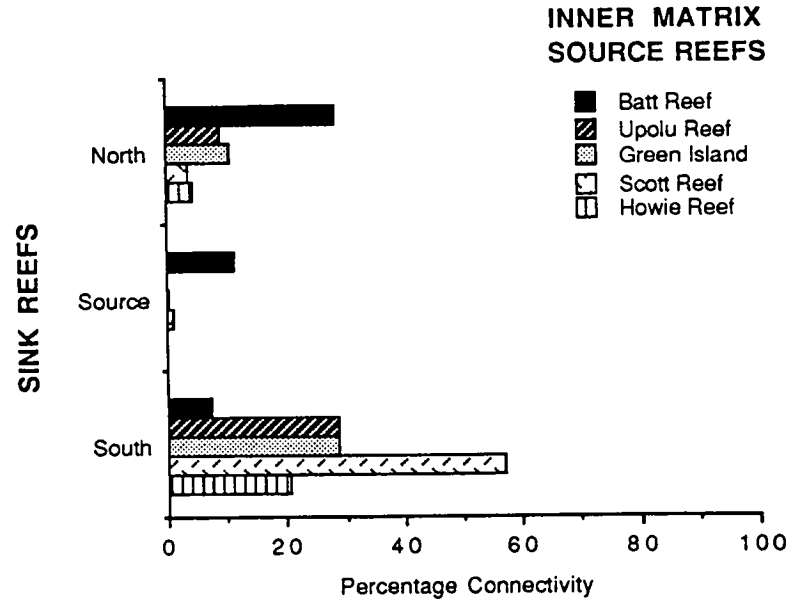


Figure 3.66 Level of reef connectivity with respect to the long-shelf transport of larvae within the central region for each of the five **inner** matrix source reefs. See caption, Figure 3.63, for further details.

3.64 to 3.66) with only one exception: Batt Reef, which is the northern most inner matrix source reef (Fig. 3.66). This reef displayed quite low connectivity overall (47.1%). Most dispersal events that transported larvae to the south did not result in connectivity. In

contrast, those dispersal events which transported larvae to the north resulted in high rates of connectivity (see Fig. 3.67).

3.5.2.3 Relative strength of connectivity

The relative strengths of connectivity between each central region source reef and all their sink reefs are presented in Figures 3.68 to 3.82.

Outer matrix source reefs consistently displayed strongest connectivity with central and inner matrix sink reefs lying to the south of the source (Figs. 3.68 to 3.72). Opal Reef, the most northerly of these (Fig. 3.68), showed low to moderate connectivity with many ribbon reefs to the north. The northern most central matrix source reefs, Tongue and Michaelmas (Figs. 3.73 and 3.74 respectively), displayed strongest connectivity with central and inner matrix sink reefs lying both to the north and south of the source. The most northerly of the inner matrix source reefs, Batt (Fig. 3.78), showed strong connectivity with itself and other inner matrix reefs lying to the north only. All remaining source reefs had strongest connectivity with sink reefs lying to the south of the source. Many reefs displayed strong to moderate connectivity with Arlington Reef, suggesting that this reef is likely to be an efficient sink for larvae. All of the central region source reefs lying to the north of Innisfail (12 in all) displayed at least moderate connectivity with the inner matrix reefs off Innisfail; Gibson, Howie, Peart and Feather (e.g., see Fig. 3.81). Many of these source reefs (Tongue, Thetford, Upolu, Green and Scott) had strong connectivity with this group of reefs. Only Howie Reef did not have strong connectivity with any sink reef at all (Fig. 3.82). A number of reefs (Cayley, Green, Scott and Howie) displayed low to moderate connectivity with Pelorus and Orpheus Island reefs which lie nearshore on the western side of the main lagoon (e.g., see Fig. 3.77). The frequency of events which transport larvae to these reefs from the mid-shelf is relatively low.

Only Batt Reef displayed strong connectivity with itself, resulting from the transport of larvae back to the source reef as a result of current reversals. The remainder of source reefs had relative

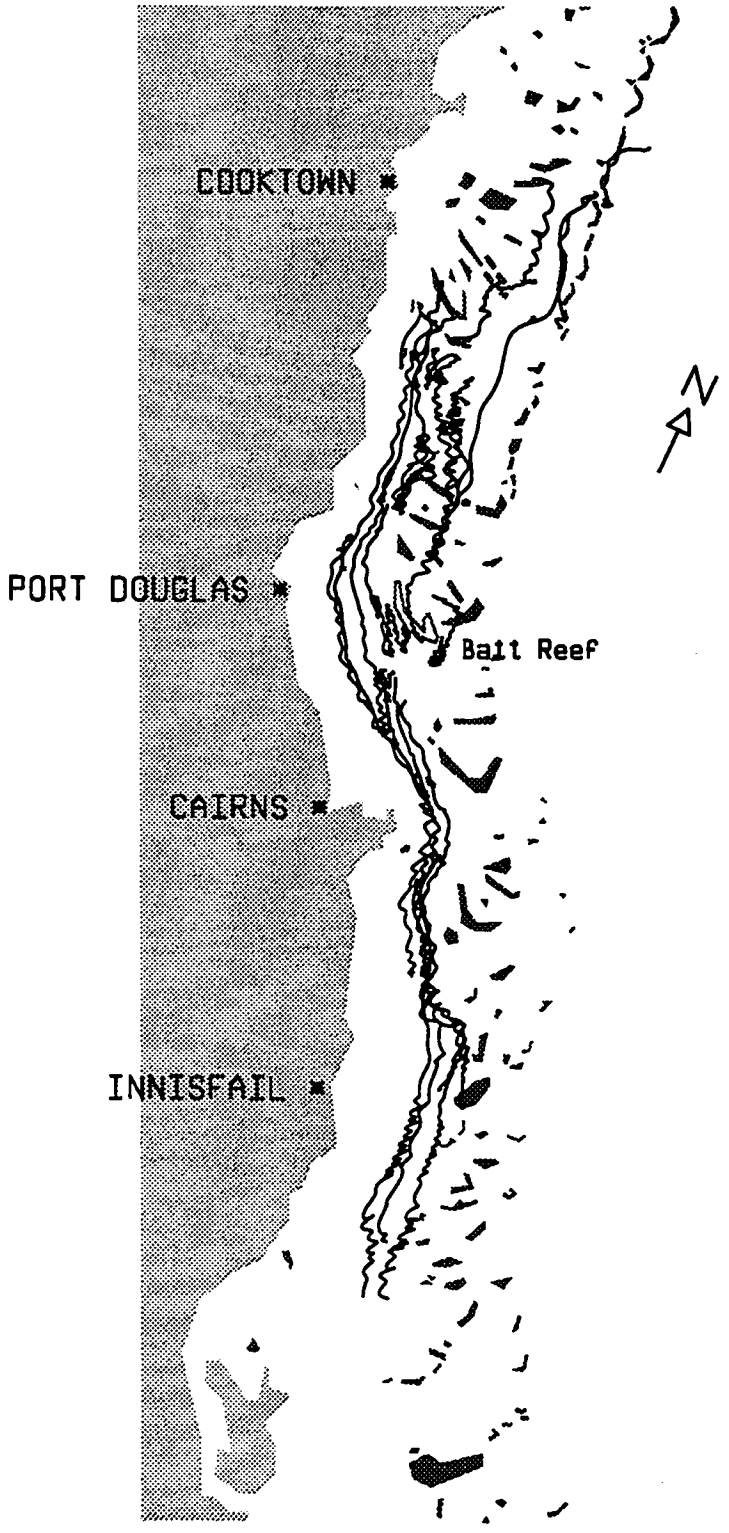


Figure 3.67 Particle trajectories representing twenty dispersal events from Batt Reef (source reef indicated without fill). Each trajectory corresponds to the centroid of the larval cloud during the second two weeks of dispersal when the larvae of *A. planci* are assumed to be competent to settle. Most dispersal events from Batt Reef that transport larvae to the south are not predicted to result in connectivity. In contrast, dispersal events which transport larvae to the north are predicted to result in relatively high rates of connectivity. Scale: 1cm = 11 nautical miles.

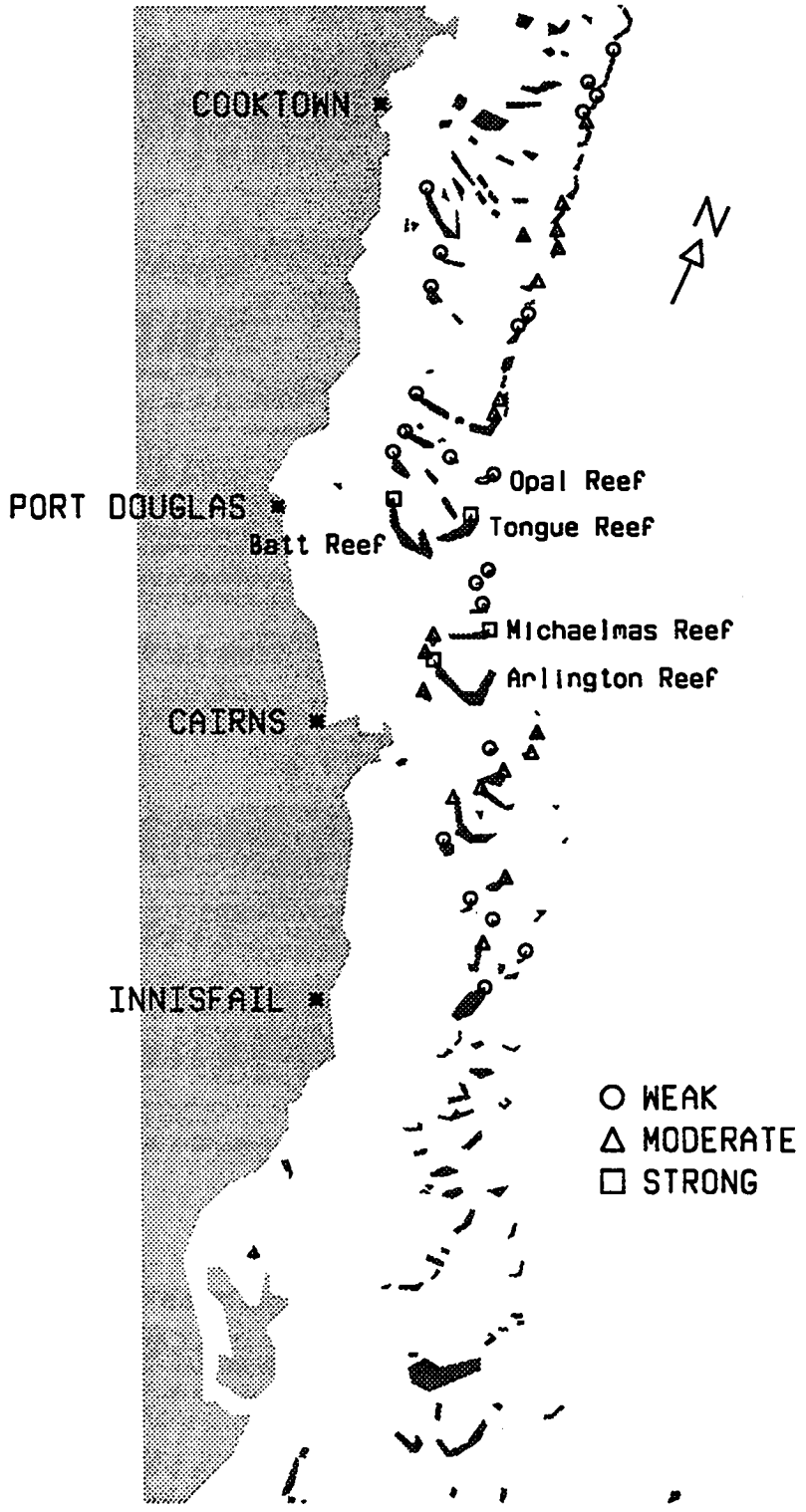


Figure 3.68 Strength of connectivity with respect to Opal Reef (source reef indicated without fill). The relative strength classes (weak, moderate and strong) represent probabilities separated by an order of magnitude. Strongest connectivity is with Tongue, Batt, Michaelmas and Arlington Reefs. All are inner and central matrix reefs which lie to the south of the source. Scale: 1cm = 12 nautical miles.

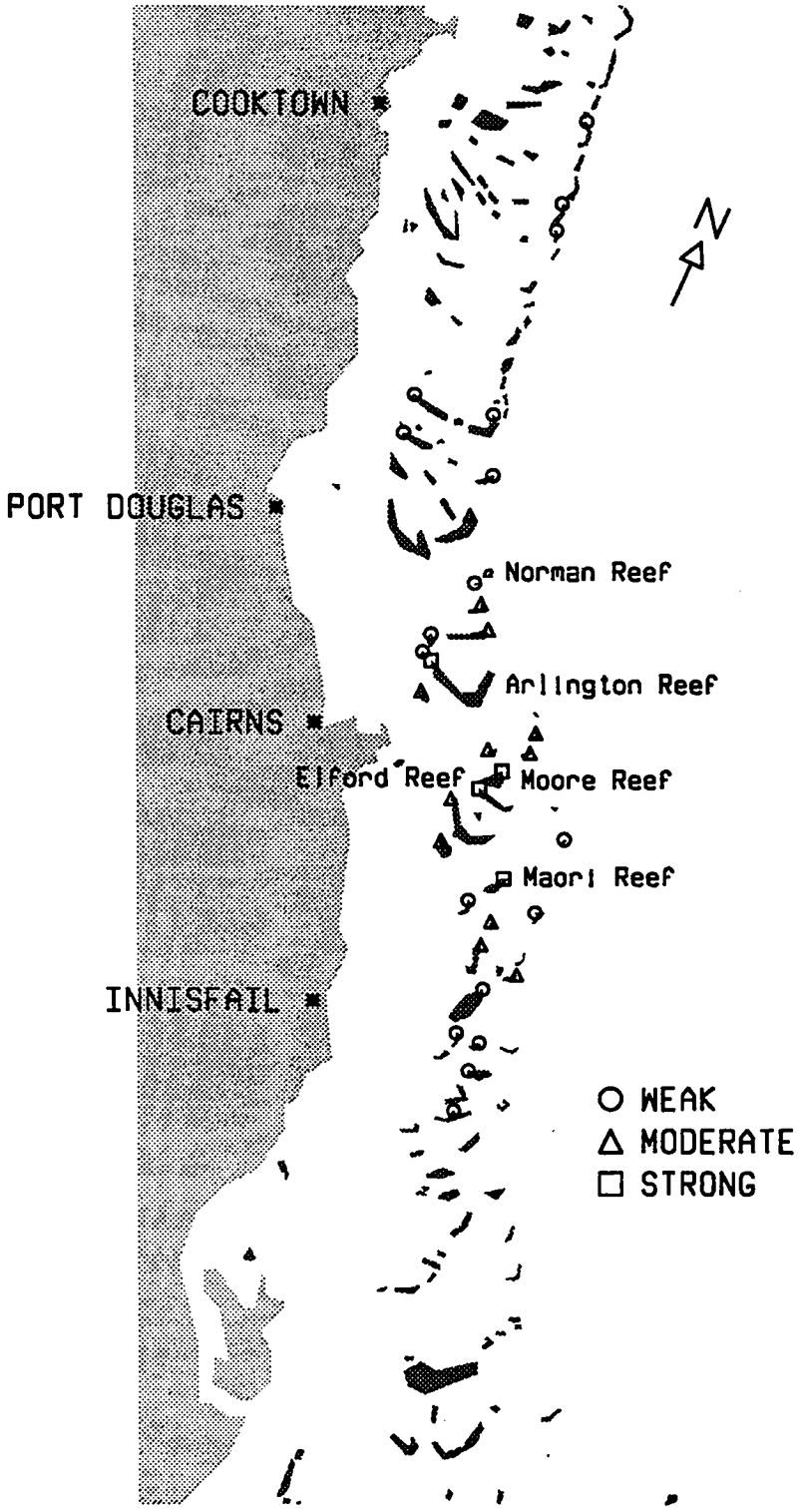


Figure 3.69 Strength of connectivity with respect to Norman Reef (source reef indicated without fill). The relative strength classes (weak, moderate and strong) represent probabilities separated by an order of magnitude. Strongest connectivity is with Arlington, Moore, Maori and Elford Reefs. All are central matrix reefs which lie to the south of the source. Scale: 1cm = 12 nautical miles.

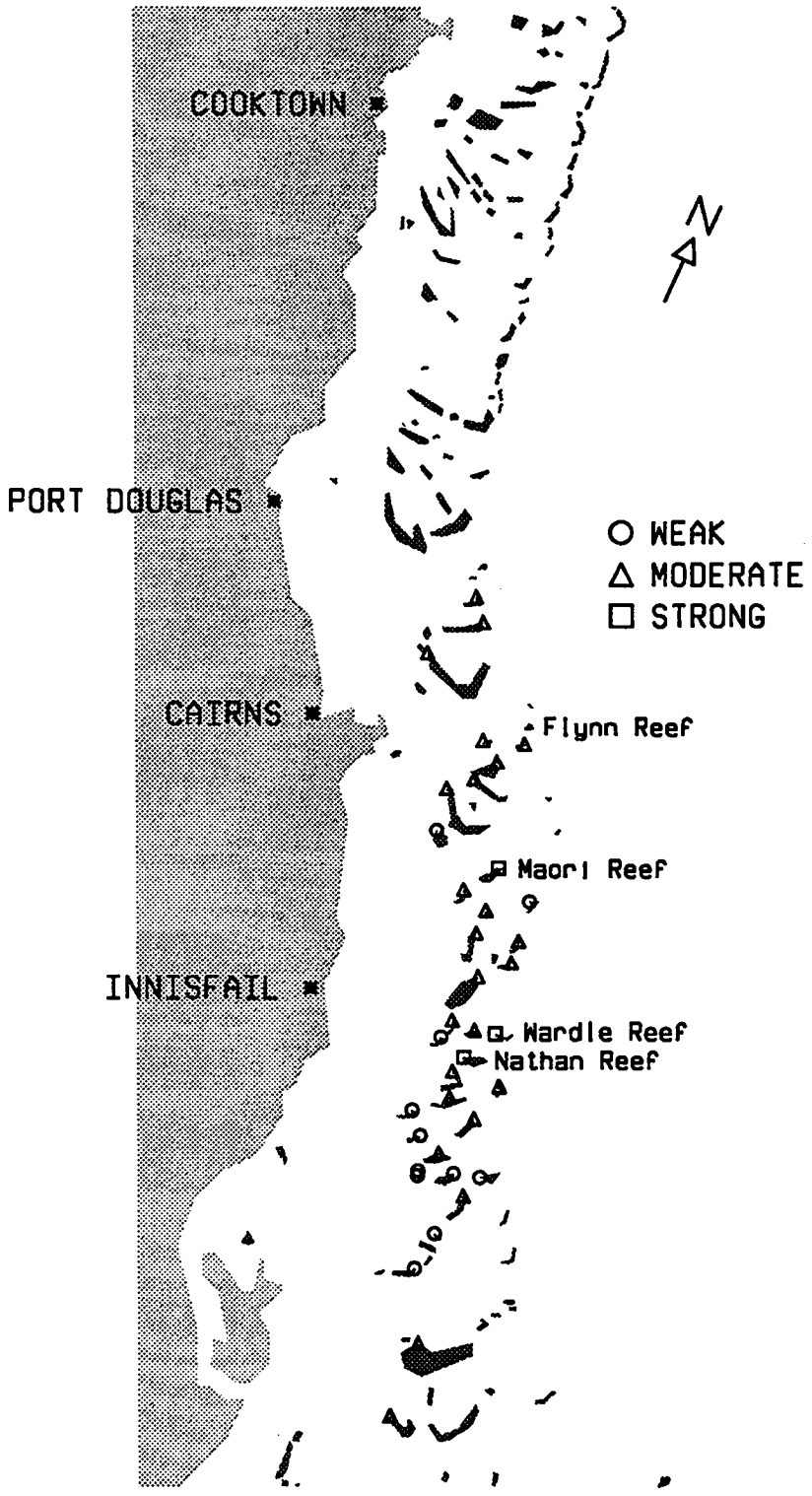


Figure 3.70 Strength of connectivity with respect to Flynn Reef. The relative strength classes (weak, moderate and strong) represent probabilities separated by an order of magnitude. Strongest connectivity is with Maori, Wardle and Nathan Reefs. All are central and outer matrix reefs which lie to the south of the source. Scale: 1cm = 12 nautical miles.

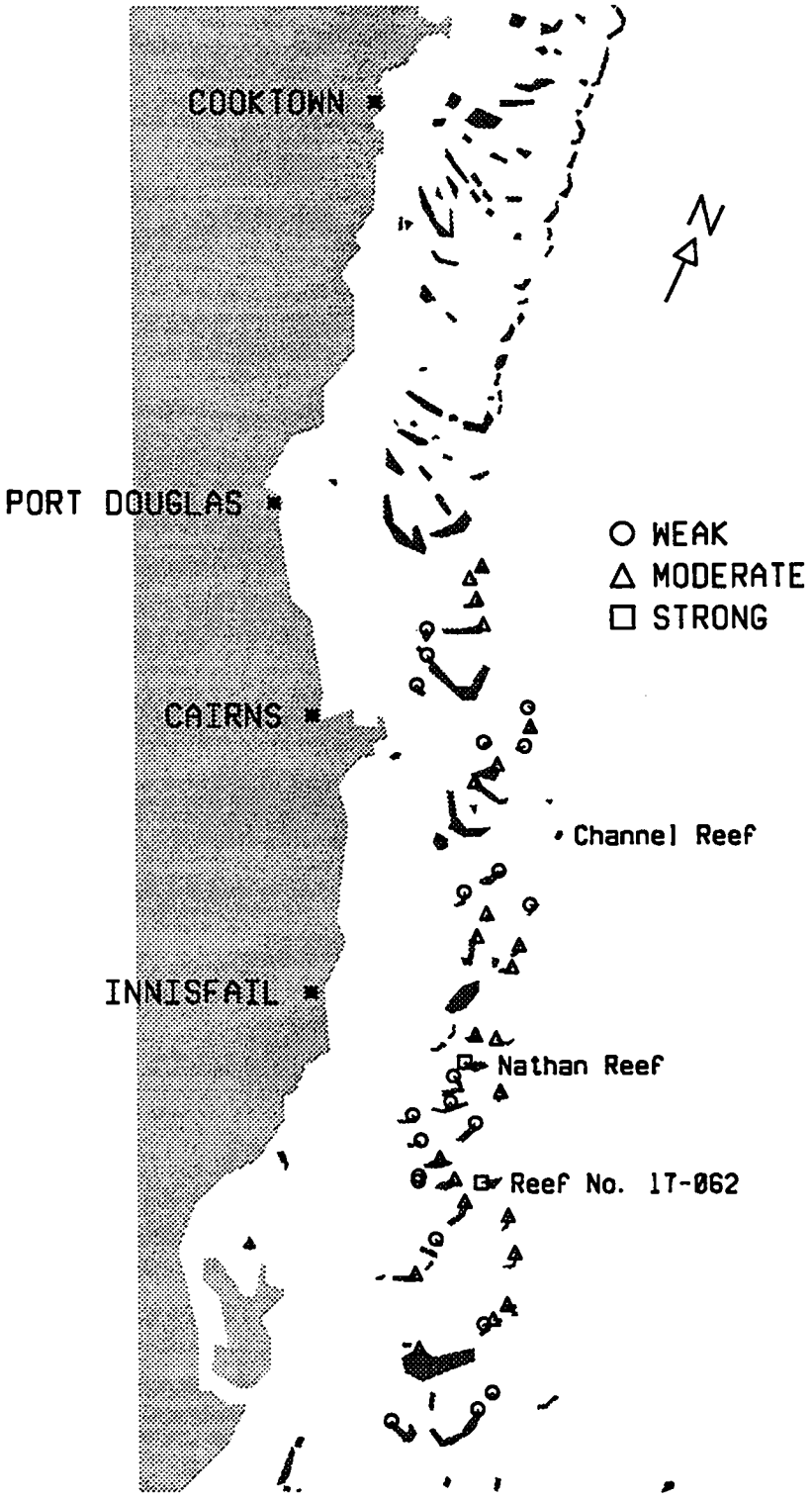


Figure 3.71 Strength of connectivity with respect to Channel Reef. The relative strength classes (weak, moderate and strong) represent probabilities separated by an order of magnitude. Strongest connectivity is with 17-062 and Nathan Reefs. Both are central matrix reefs which lie to the south of the source. Scale: 1cm = 12 nautical miles.

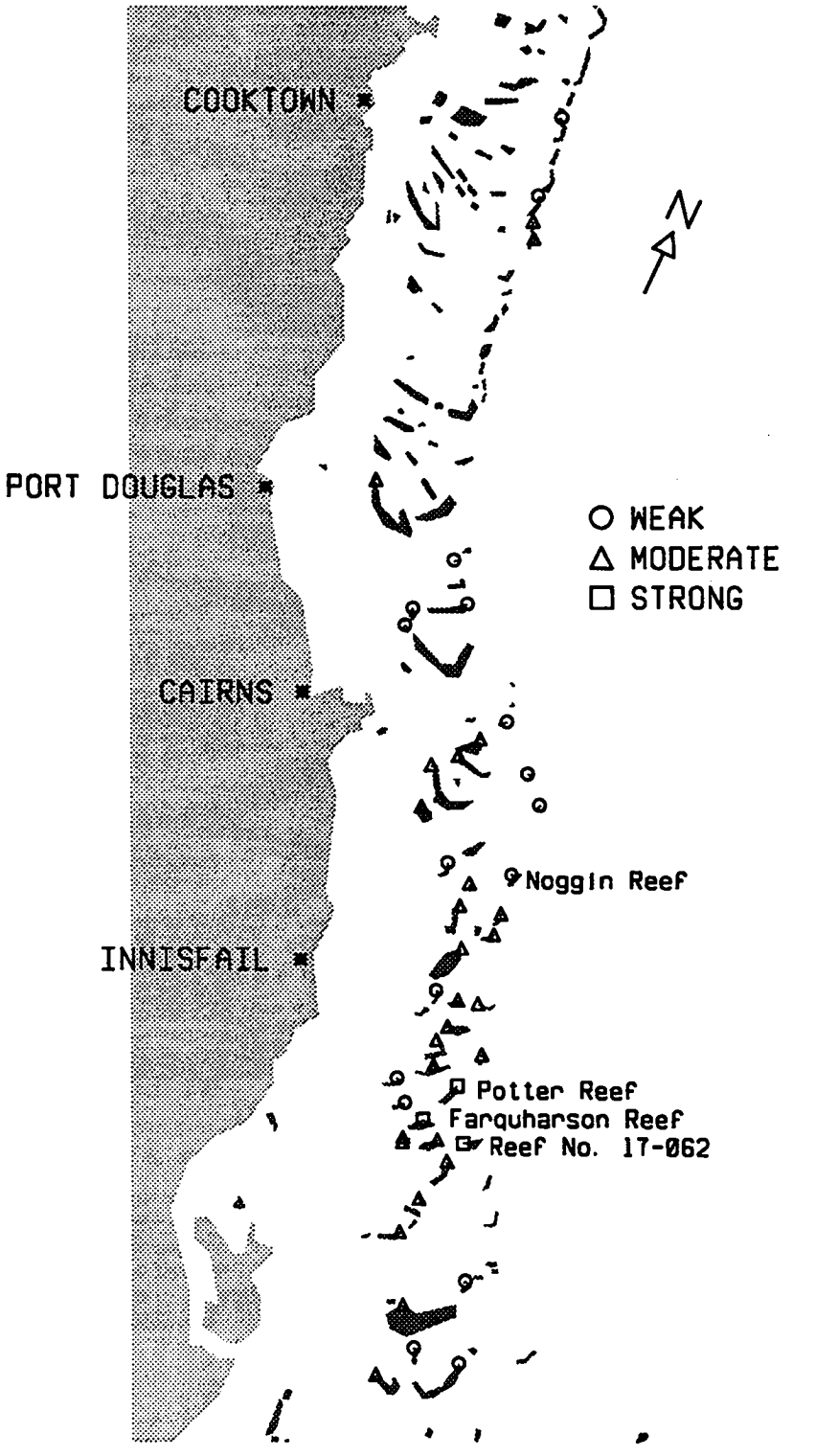


Figure 3.72 Strength of connectivity with respect to Noggin Reef. The relative strength classes (weak, moderate and strong) represent probabilities separated by an order of magnitude. Strongest connectivity is with 17-062, Farquharson and Potter Reefs. All are central matrix reefs which which lie to the south of the source. Scale: 1cm = 12 nautical miles.

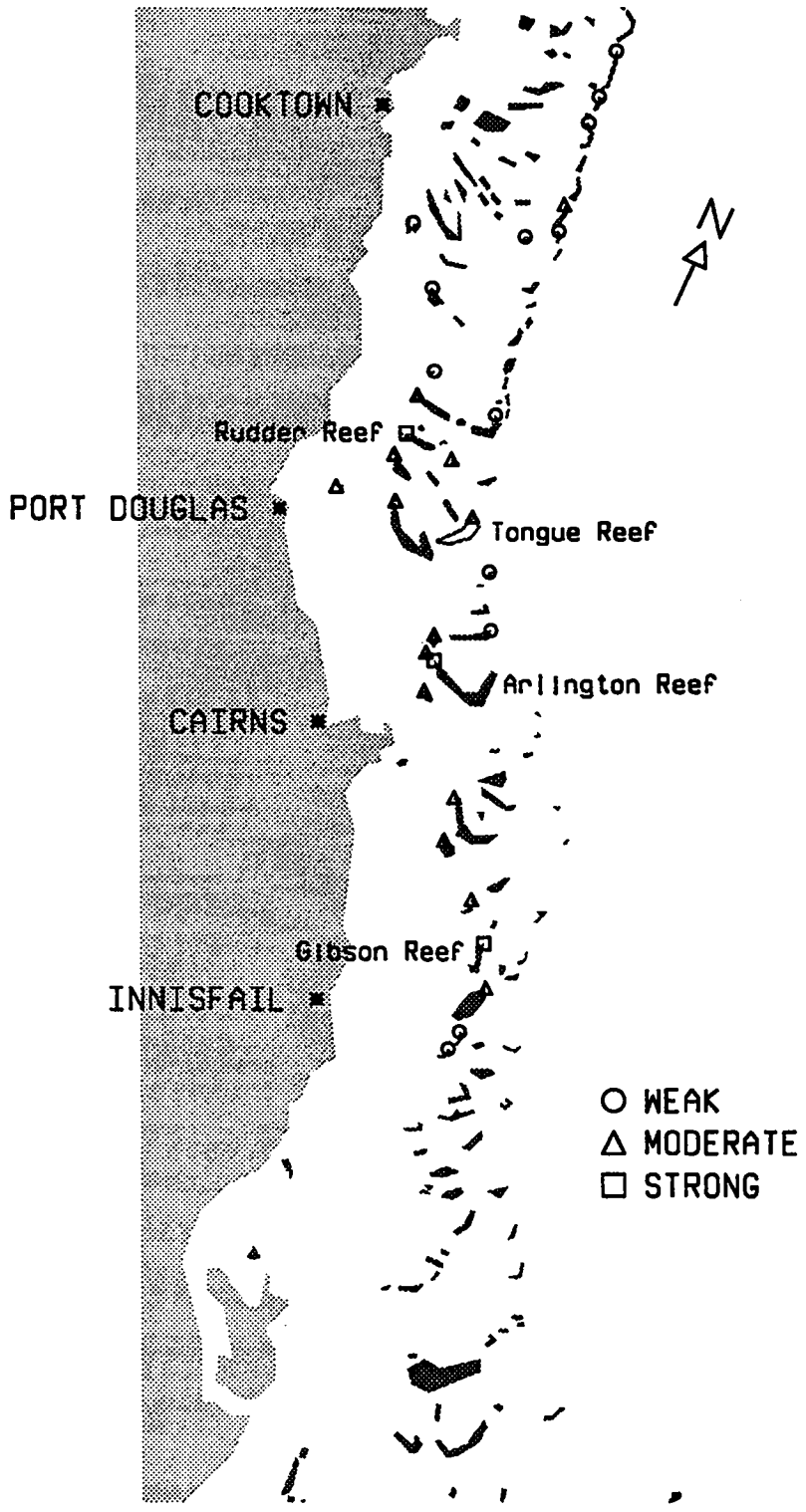


Figure 3.73 Strength of connectivity with respect to Tongue Reef (source reef indicated without fill). The relative strength classes (weak, moderate and strong) represent probabilities separated by an order of magnitude. Strongest connectivity is with Rudder, Arlington and Gibson Reefs. All are inner matrix reefs and only Rudder lies to the north of the source. Scale: 1cm = 12 nautical miles.

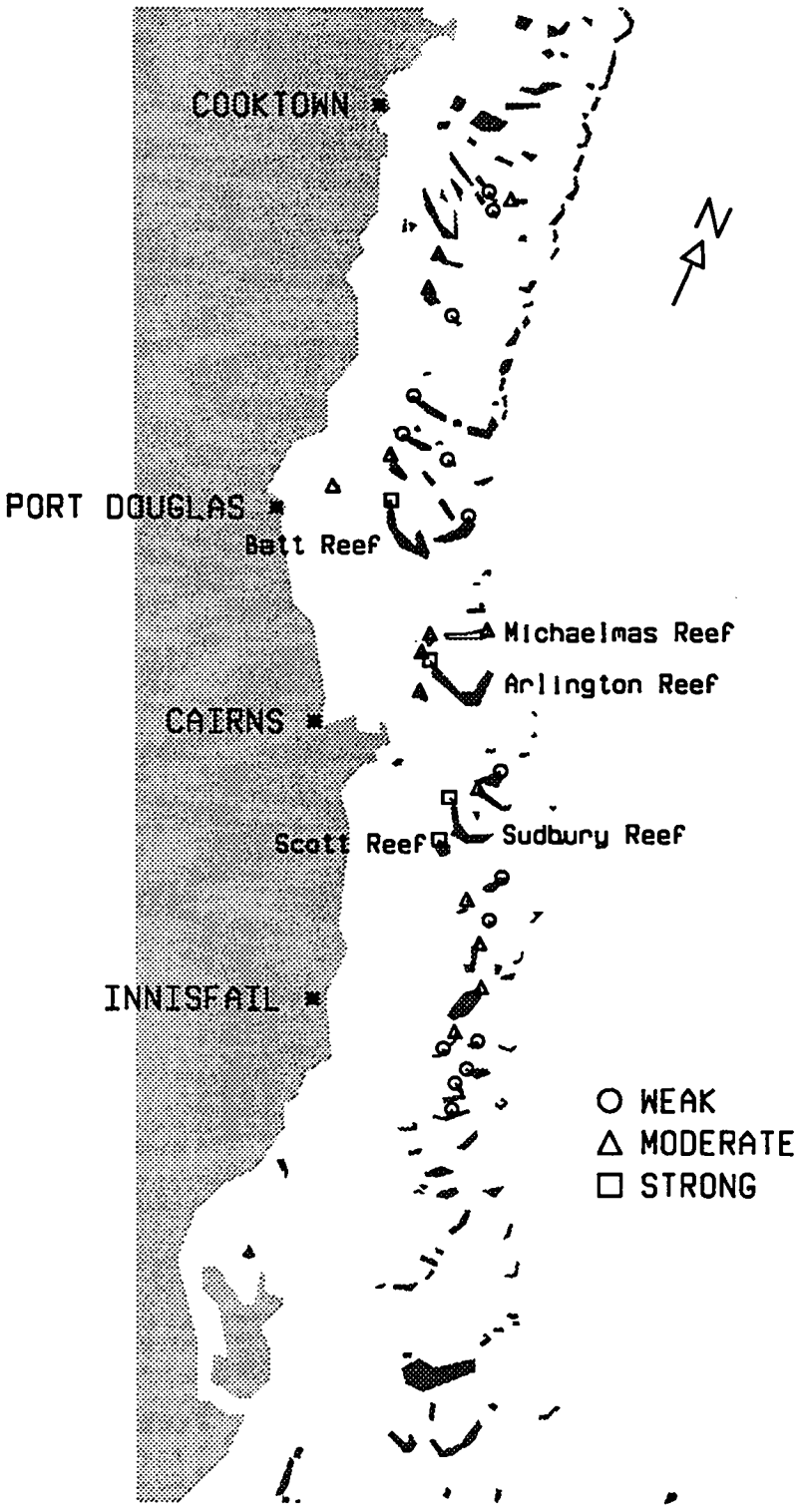


Figure 3.74 Strength of connectivity with respect to Michaelmas Reef (source reef indicated without fill). The relative strength classes (weak, moderate and strong) represent probabilities separated by an order of magnitude. Strongest connectivity is with Batt, Arlington, Sudbury and Scott Reefs. All are inner matrix reefs and only Batt lies to the north of the source. Scale: 1cm = 12 nautical miles.

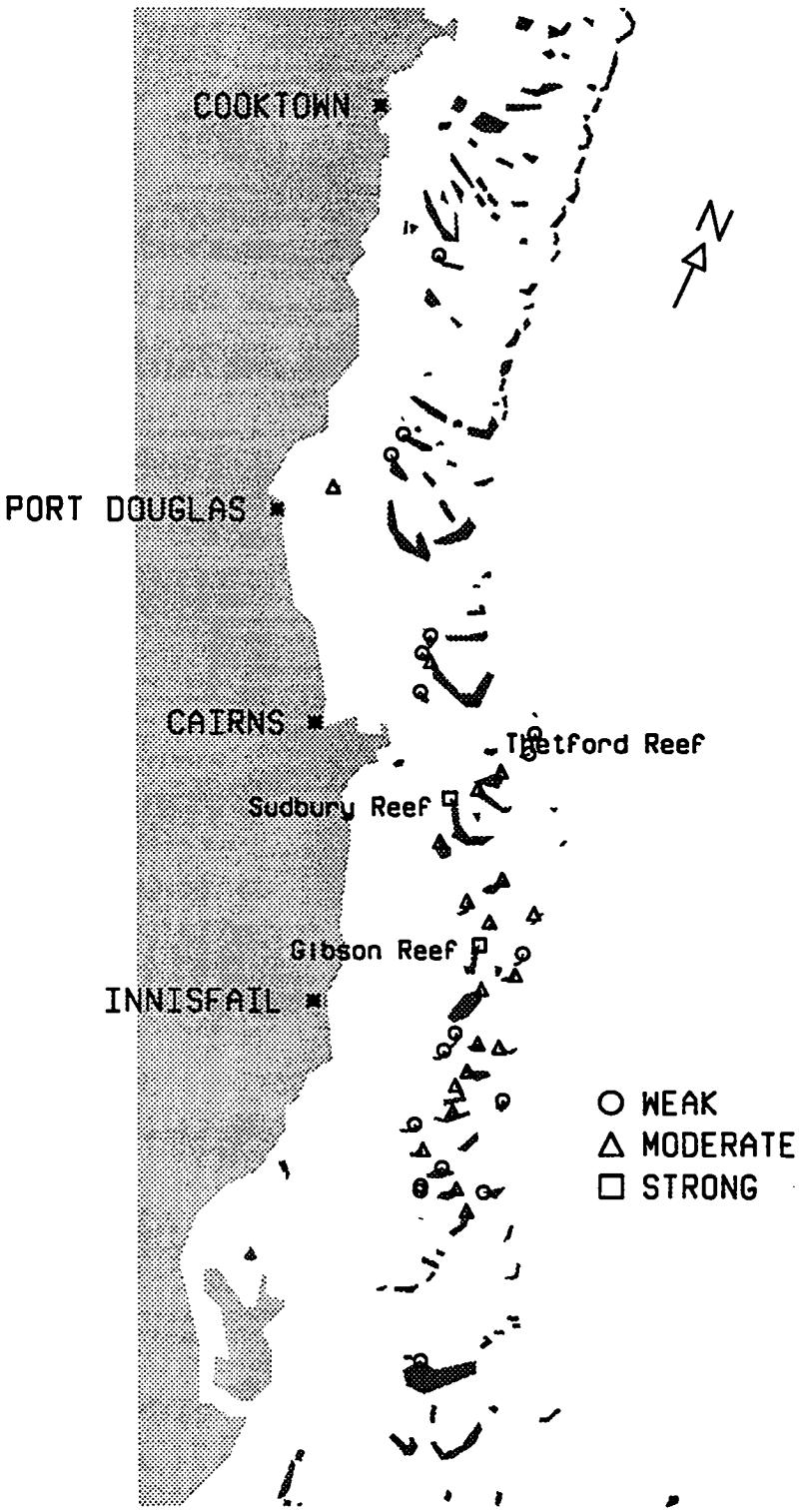


Figure 3.75 Strength of connectivity with respect to Thetford Reef. The relative strength classes (weak, moderate and strong) represent probabilities separated by an order of magnitude. Strongest connectivity is with Sudbury and Gibson Reefs. Both are inner matrix reefs which lie to the south of the source. Scale: 1cm = 12 nautical miles.

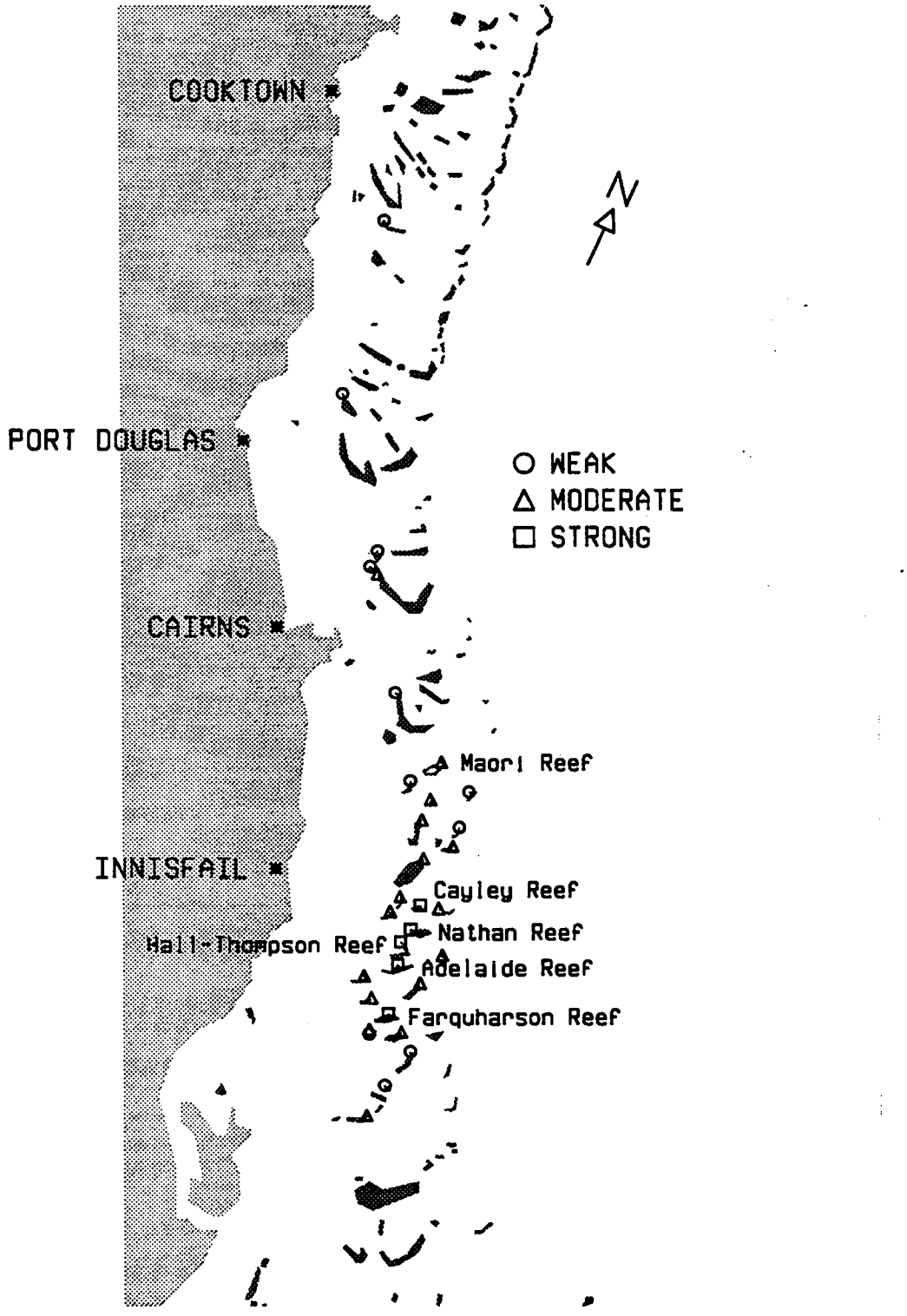


Figure 3.76 Strength of connectivity with respect to Maori Reef (source reef indicated without fill). The relative strength classes (weak, moderate and strong) represent probabilities separated by an order of magnitude. Strongest connectivity is with Cayley, Nathan, Hall-Thompson, Adelaide and Farquharson Reefs. All are central matrix reefs which which lie to the south of the source. Scale: 1cm = 12 nautical miles.

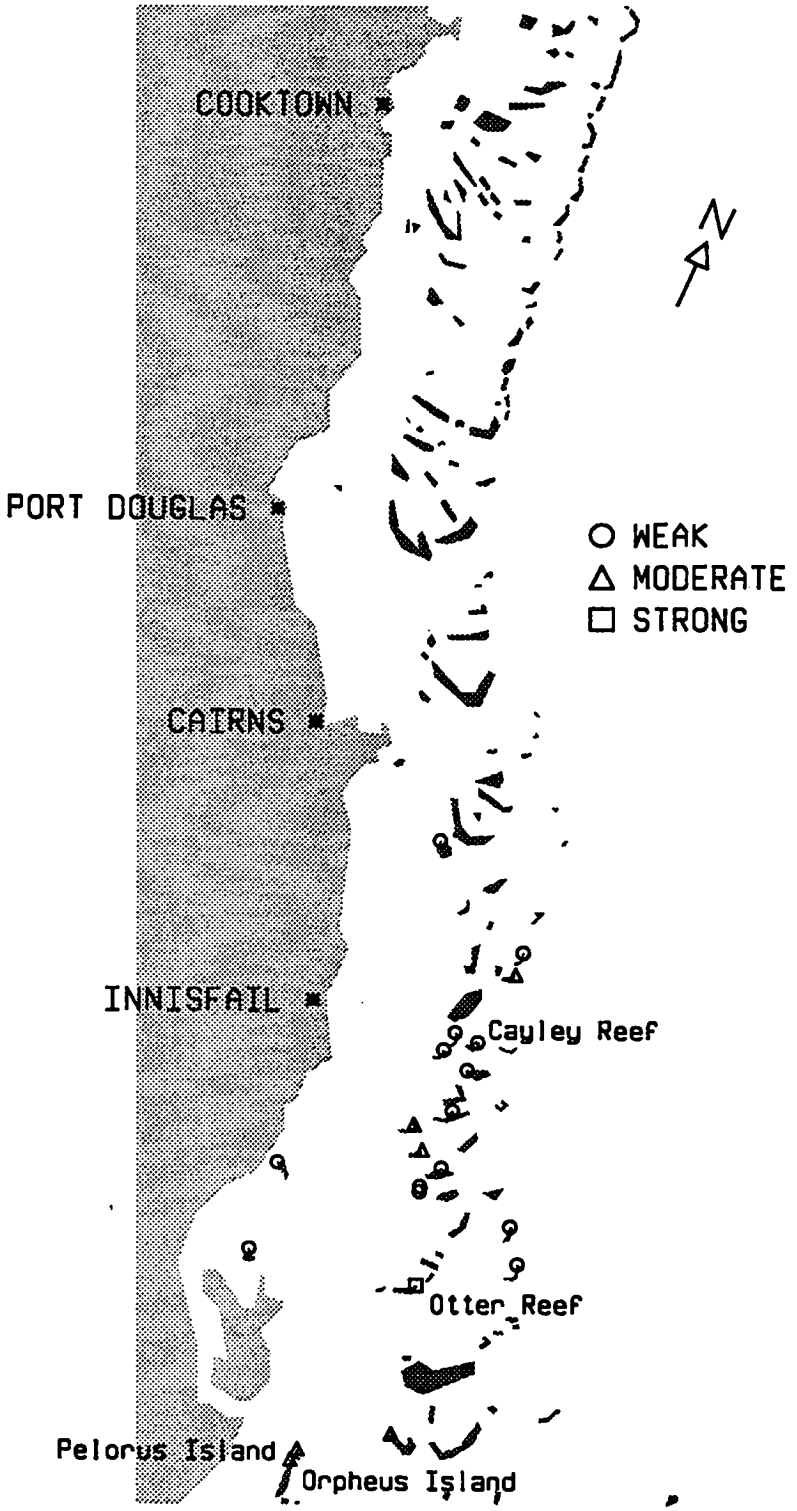


Figure 3.77 Strength of connectivity with respect to Cayley Reef. The relative strength classes (weak, moderate and strong) represent probabilities separated by an order of magnitude. Strongest connectivity is with Otter Reef which lies along the inner edge of the reef matrix to the south of the source. Scale: 1cm = 12 nautical miles.

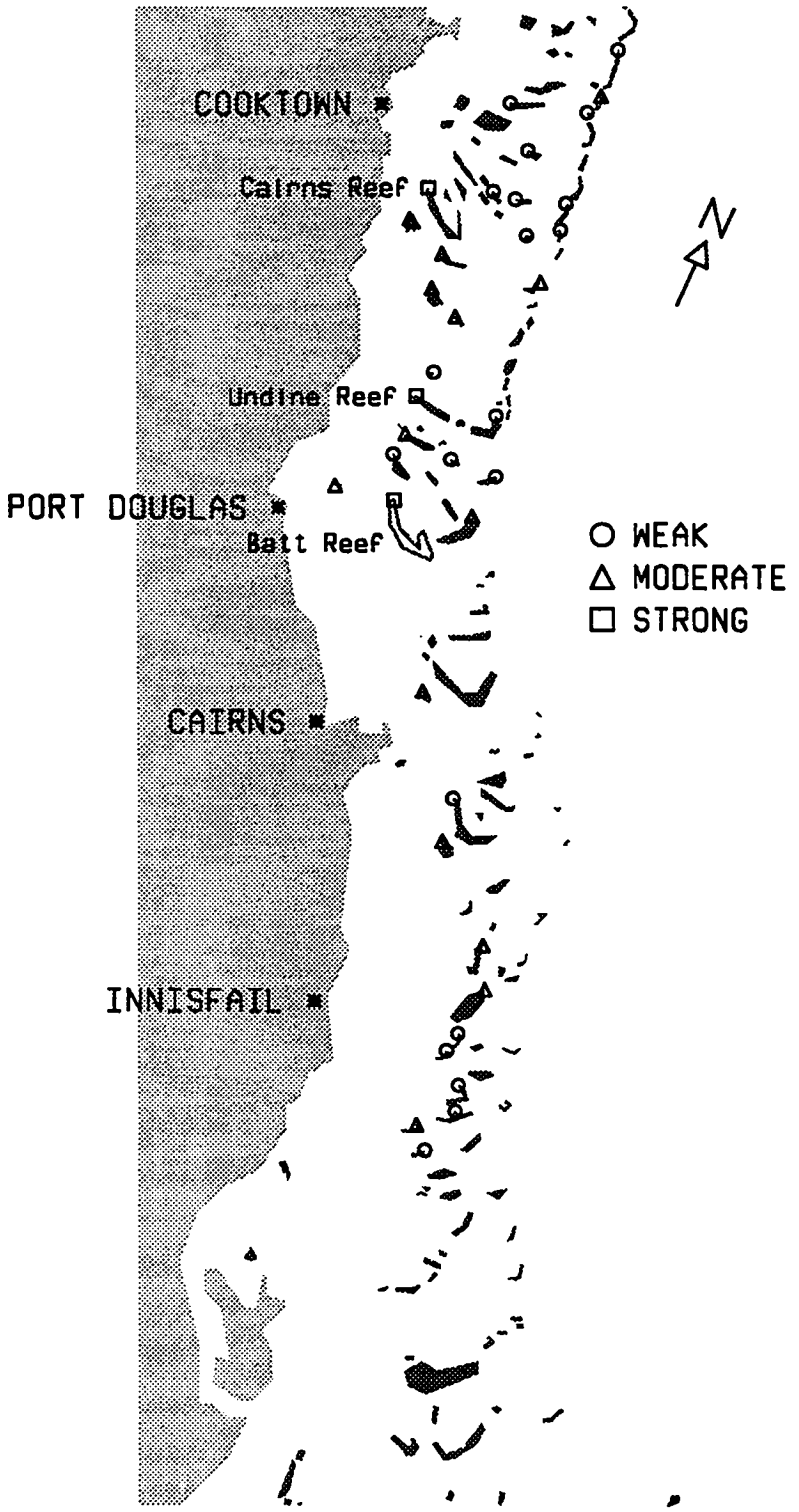


Figure 3.78 Strength of connectivity with respect to Batt Reef (source reef indicated without fill). The relative strength classes (weak, moderate and strong) represent probabilities separated by an order of magnitude. Strongest connectivity is with Cairns and Undine Reefs. Both these reefs lie to the north of the source. Scale: 1cm = 12 nautical miles.

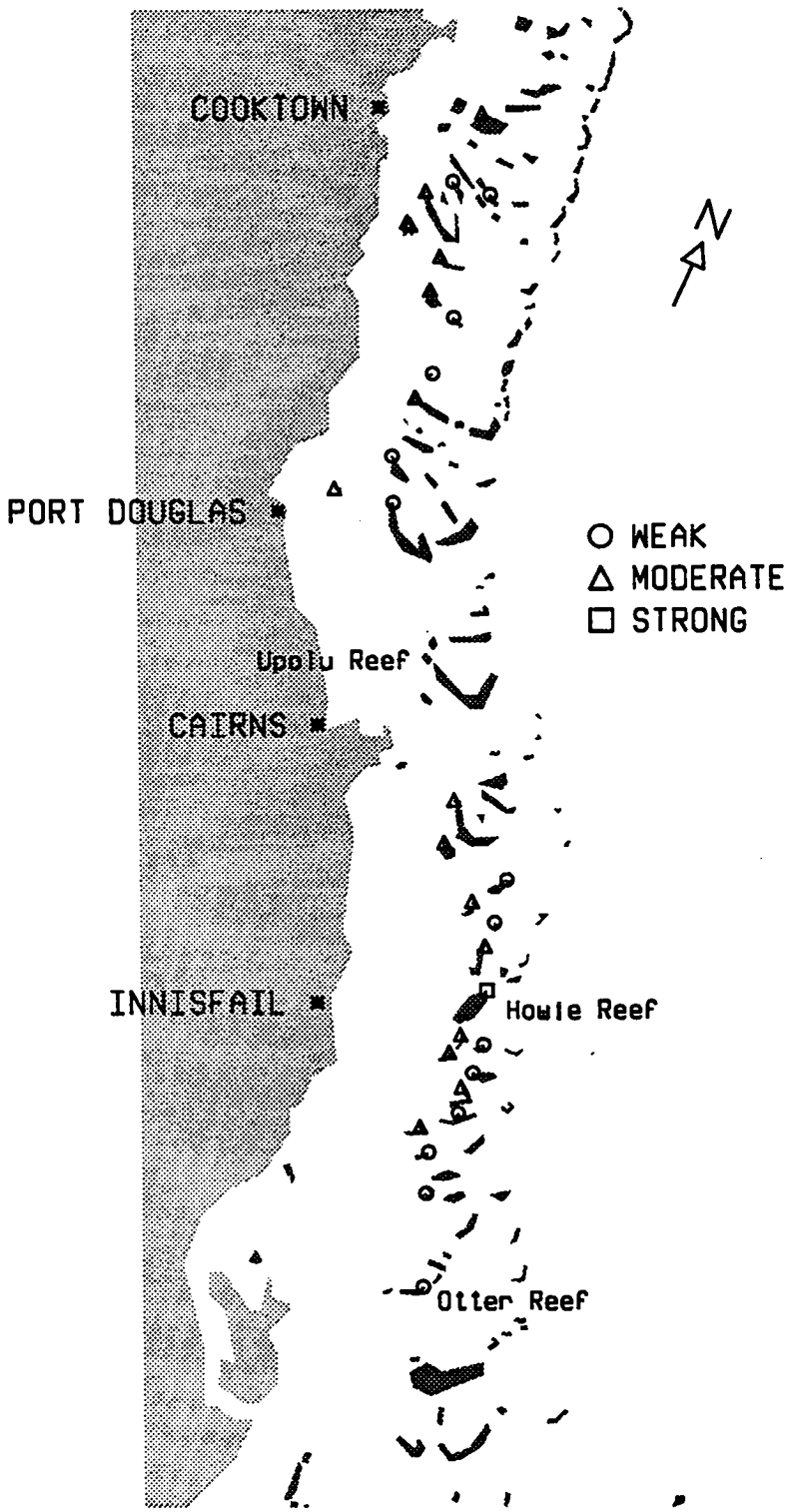


Figure 3.79 Strength of connectivity with respect to Upolu Reef. The relative strength classes (weak, moderate and strong) represent probabilities separated by an order of magnitude. Strongest connectivity is with Howie Reef which lies along the inner edge of the reef matrix to the south of the source. Scale: 1cm = 12 nautical miles.

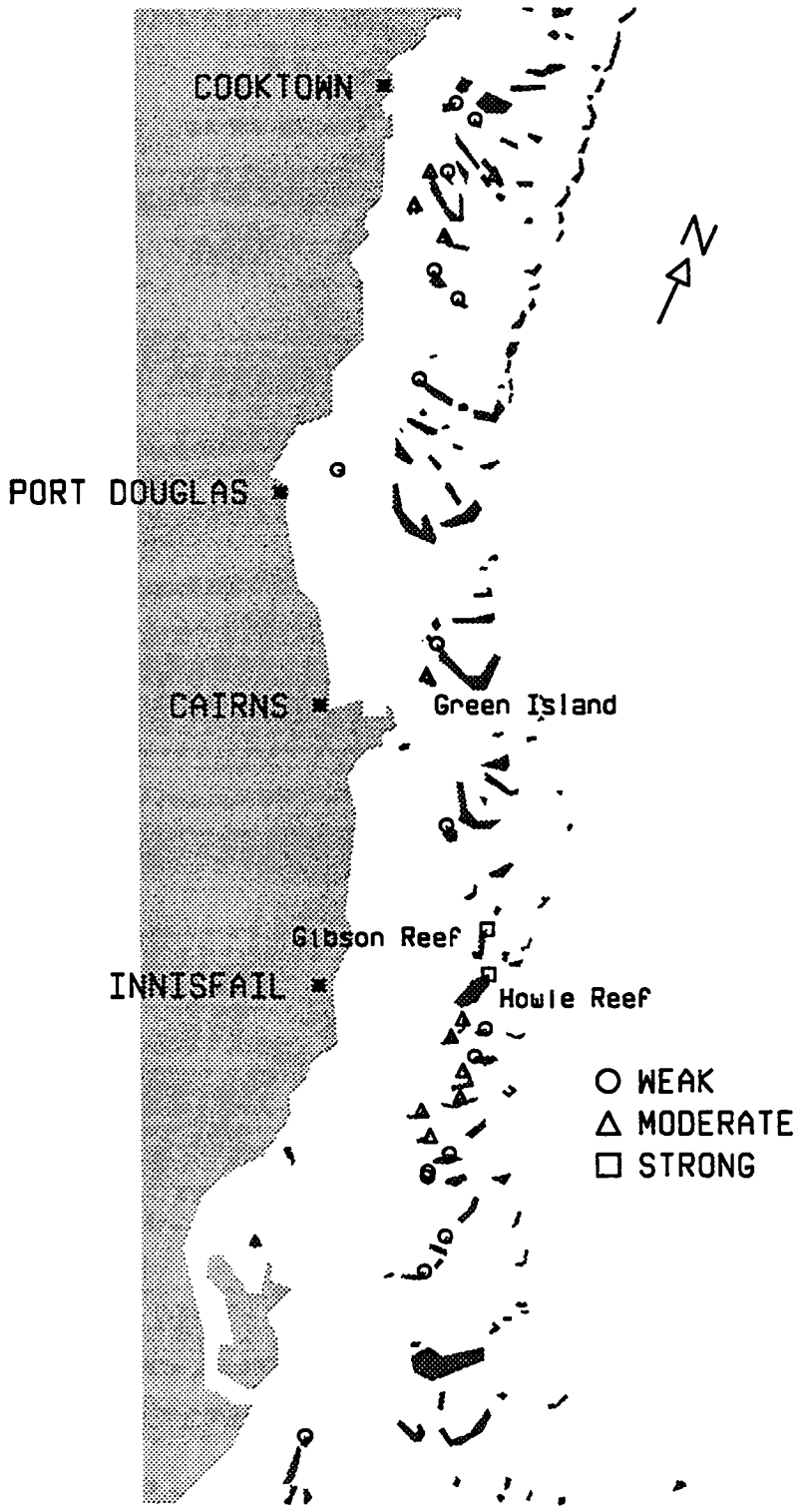


Figure 3.80 Strength of connectivity with respect to Green Island. The relative strength classes (weak, moderate and strong) represent probabilities separated by an order of magnitude. Strongest connectivity is with Gibson and Howie Reefs. Both are inner matrix reefs which lie to the south of the source. Scale: 1cm = 12 nautical miles.

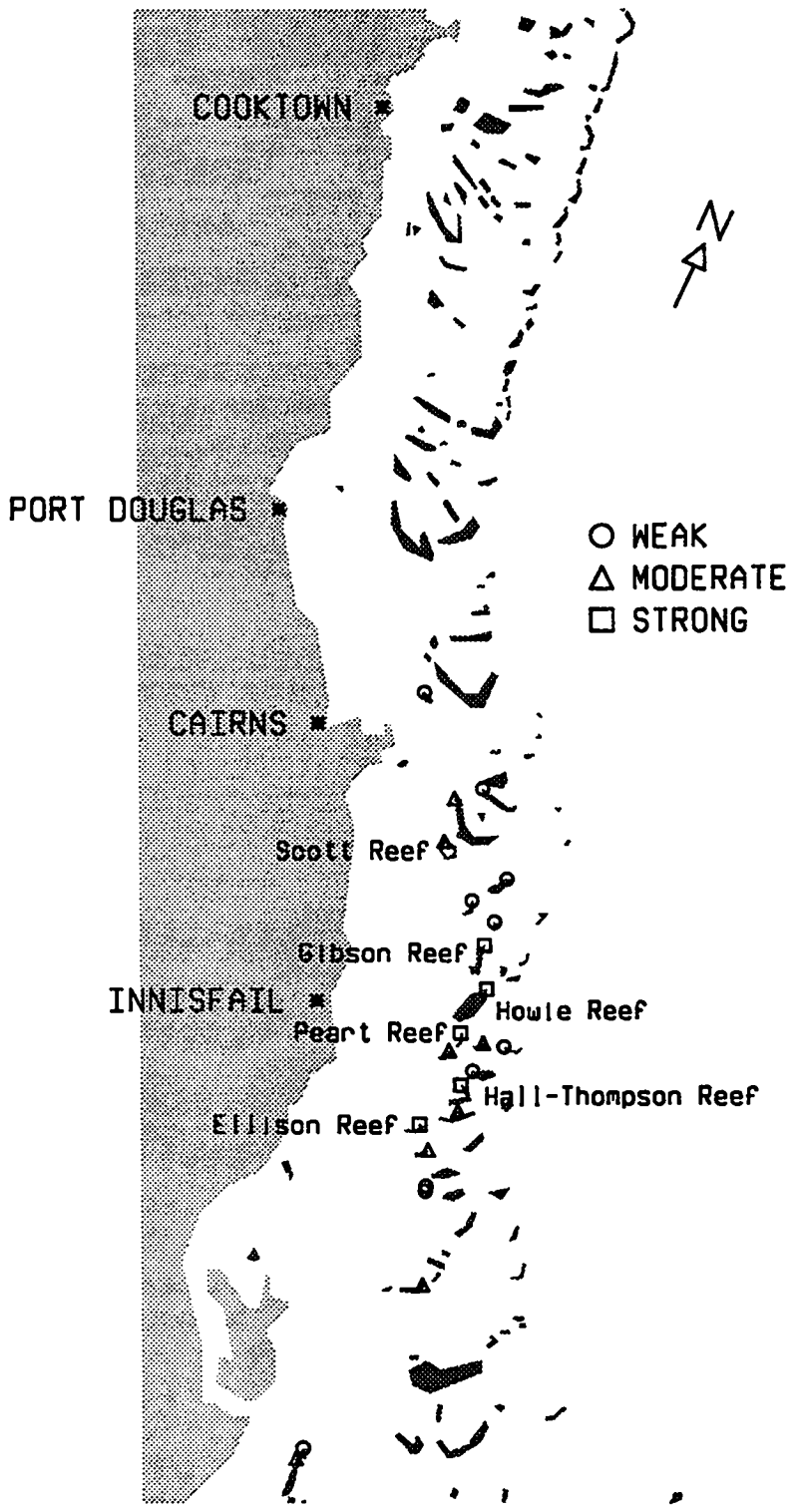


Figure 3.81 Strength of connectivity with respect to Scott Reef (source reef indicated without fill). The relative strength classes (weak, moderate and strong) represent probabilities separated by an order of magnitude. Strongest connectivity is with Gibson, Howie, Peart, Hall-Thompson and Ellison Reefs. All lie to the south of the source and, but for Hall-Thompson, are inner matrix reefs. Scale: 1cm = 12 nautical miles.

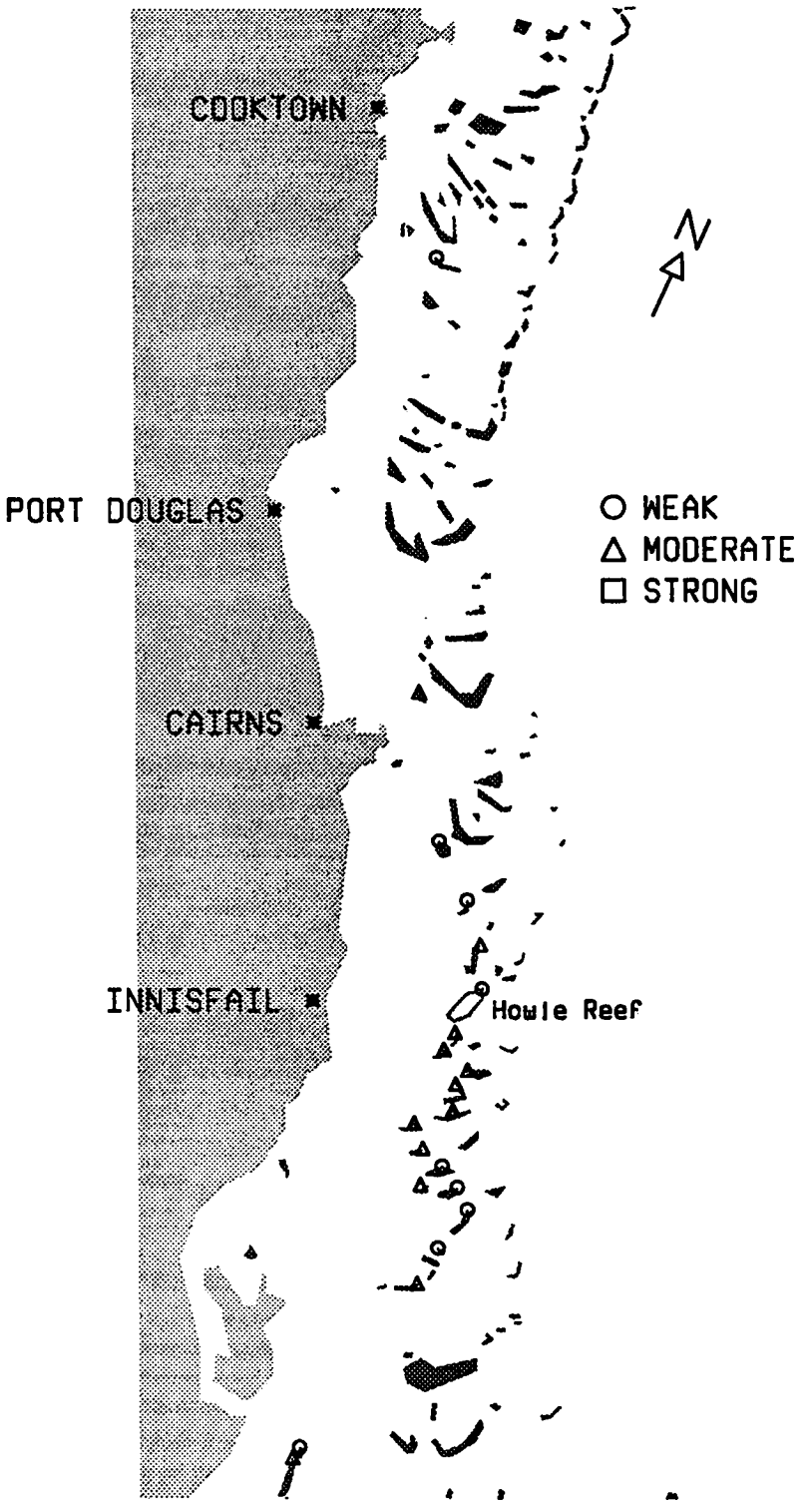


Figure 3.82 Strength of connectivity with respect to Howie Reef (source reef indicated without fill). The relative strength classes (weak, moderate and strong) represent probabilities separated by an order of magnitude. The overall level of connectivity with respect to Howie Reef appears to be quite low and no sink reefs with strong connectivity were identified. Scale: 1cm = 12 nautical miles.

probabilities of self-seeding ranging from moderate to none at all. The degree of self-seeding within the central region was not as great as within the northern region.

The distances over which larvae are transported to reefs with strongest connectivity varied markedly between source reefs in the central region. Opal reef showed strongest connectivity with Tongue, Batt, Michaelmas and Arlington Reefs (Fig. 3.68) which lie approximately 10, 15, 20 and 30 nautical miles away respectively. Another outer matrix reef, Flynn, showed strongest connectivity with Maori, Wardle and Nathan Reefs (Fig. 3.70) which lie approximately 20, 45 and 50 nautical miles away respectively. Similarly, Upolu Reef showed strongest connectivity with Howie Reef (Fig. 3.79) which lies approximately 50 nautical miles to the south. All source reefs display weak to moderate connectivity with sink reefs which are far more distant, up to 110 nautical miles away. In general, the distances over which larvae disperse within the central region are considerably greater than in the northern region.

3.5.3 The Southern Region

3.5.3.1 Cross-shelf connectivity

Reef connectivity within the southern region, expressed as source-sink relationships with respect to the cross-shelf movement of larvae, is presented in Figures 3.83 to 3.87. Considering all three source reefs in each zone collectively (Fig. 3.83), it is evident that:

(1) connectivity of outer matrix source reefs was primarily with central matrix sink reefs (58.7%), yet a substantial proportion of particles were transported to inner matrix reefs (21.4%). Connectivity with other outer matrix reefs was minimal (2.3%). Overall, connectivity was very high and few dispersal events failed to transport larvae to other reefs (17.6%);

(2) connectivity of central matrix source reefs was primarily with inner matrix sink reefs (32.8%), yet with a substantial proportion of dispersal events resulting in the transport of larvae to other central matrix reefs (18.4%). Offshore transportation of larvae to outer matrix reefs was virtually absent (0.1%). Many dispersal events originating

from central matrix source reefs did not transport larvae to other reefs (48.7%);

(3) connectivity of inner matrix source reefs was almost exclusively with other reefs lying along the inner edge of the reef matrix bordering the lagoon (6.8%). Larvae were seldom transported offshore to central matrix reefs (0.7%), and no transportation onshore across the main lagoon to nearshore reefs was recorded. The overall level of connectivity was exceptionally low. The vast majority of dispersal events originating from inner matrix source reefs failed to transport larvae to other reefs (92.5%);

(4) connectivity of nearshore source reefs was exclusively with other reefs lying along the western side of the main lagoon (23.6%). There was no transportation offshore across the main lagoon to inner matrix reefs. Once again, most dispersal events originating from inner matrix source reefs did not transport larvae to other reefs (76.4%).

In summary, connectivity of outer and central matrix source reefs was primarily with sink reefs lying in adjacent cross-shelf zones in an onshore direction. Connectivity of inner matrix source reefs was almost exclusively with other inner matrix reefs bordering the main lagoon, while connectivity of nearshore source reefs was exclusively with other reefs lying on the western side of the main lagoon. There was no transportation of larvae either onshore or offshore between inner matrix and nearshore reefs. The level of connectivity from outer matrix source reefs was particularly high (82.4%) and became progressively lower along a gradient from the outer to inner matrix reefs. Connectivity of central matrix source reefs was comparable with levels within the central and northern regions (51.3%). The level of connectivity from nearshore and, in particular, the inner matrix reefs was very low (23.6 and 7.5% respectively). Most particles became entrained within the main lagoon and were not transported to other reefs (see Figs. 3.88 and 3.89).

Examination of results from individual reefs (Figs. 3.84 to 3.87) again indicate a more complex picture, but one in which the patterns of reef connectivity are more consistent than in the northern and central regions. Connectivity of all outer matrix source reefs was primarily

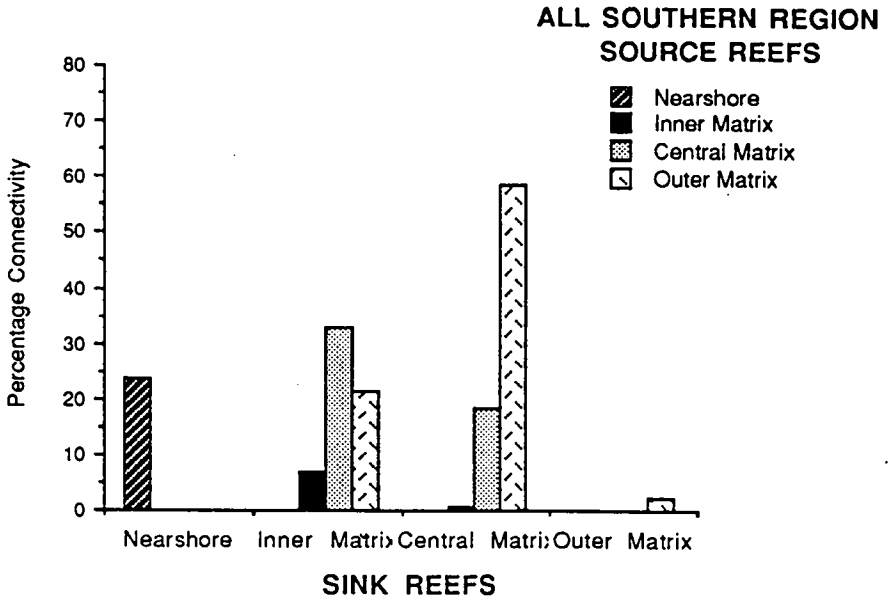


Figure 3.83 Level of reef connectivity with respect to the cross-shelf transport of larvae within the southern region. Data represent the number of particles from three source reefs within each of four cross-shelf geographical zones that intersect with sink reefs, expressed as a percentage of the total number of particle trajectories simulated from each zone. Cross-shelf zones correspond to reefs which lie along the outer edge of the reef matrix and continental shelf (outer matrix), reefs central within the reef matrix (central matrix,) reefs which lie along the inner edge of the reef matrix bordering the main lagoon (inner matrix) and reefs lying nearshore on the western side of the main lagoon (nearshore).

with reefs lying central within the matrix (Fig. 3.84). All displayed low connectivity with other outer matrix reefs, but high levels of connectivity overall. Connectivity of all central matrix source reefs was primarily with reefs lying along the inner edge of the reef matrix (Fig. 3.85), but all displayed good connectivity with other central matrix reefs. Connectivity of all inner matrix and nearshore source reefs is consistently low (Figs. 3.86 and 3.87 respectively).

3.5.3.2 Long-shelf connectivity

Reef connectivity, with respect to the long-shelf movement of larvae, is presented in Figures 3.90 to 3.94. Considering all five source reefs in each cross-shelf zone collectively (Fig. 3.90), it is evident that connectivity within the southern region was still more strongly directed towards the south. Overall, 88.4% of particles which intersected with reefs were transported to the south, while only 8.6% were transported to the north. Only very limited potential for recruitment back onto the source reef as a result of current reversals

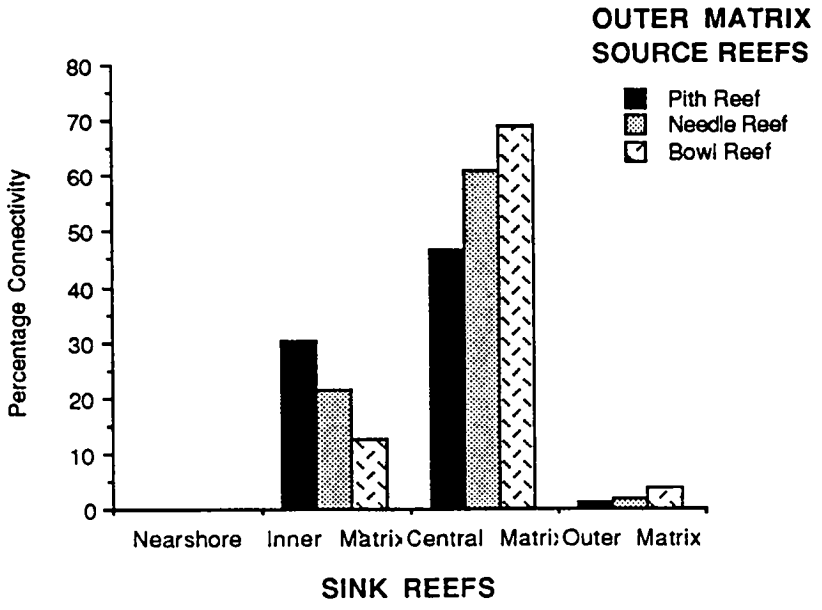


Figure 3.84 Level of reef connectivity with respect to the cross-shelf transport of larvae within the southern region for each of the three **outer** matrix source reefs. See caption, Figure 3.83, for further details.

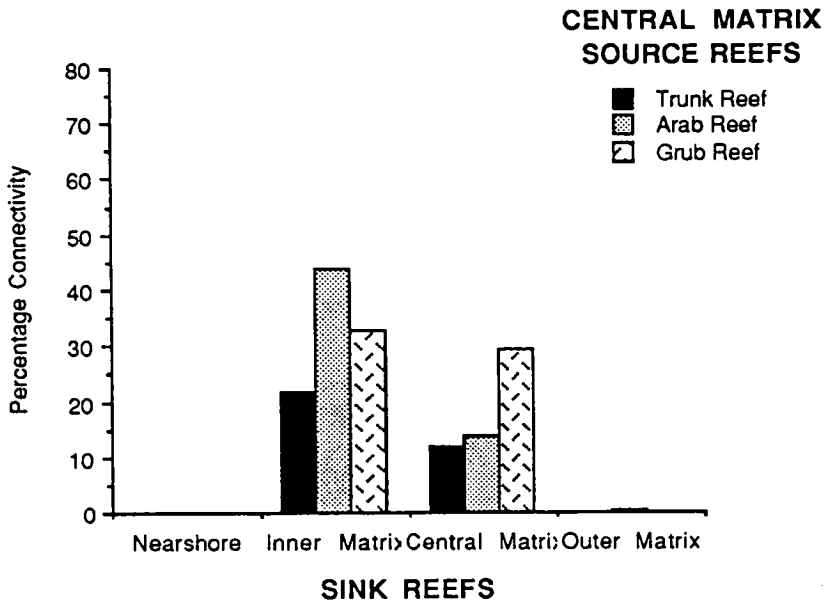


Figure 3.85 Level of reef connectivity with respect to the cross-shelf transport of larvae within the southern region for each of the three **central** matrix source reefs. See caption, Figure 3.83, for further details.

is evident (3.0%). The pattern of strong southward directed connectivity was generally consistent for all outer and central matrix reefs (Figs. 3.91 and 3.92). The inner matrix source reefs (Fig. 3.93), however, displayed similar characteristics to those described for Batt

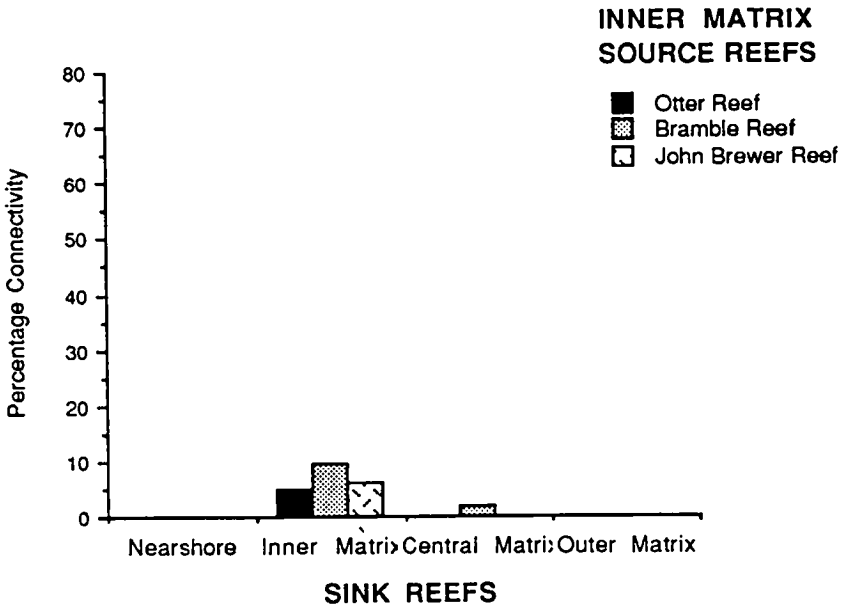


Figure 3.86 Level of reef connectivity with respect to the cross-shelf transport of larvae within the southern region for each of the three **inner** matrix source reefs. See caption, Figure 3.83, for further details.

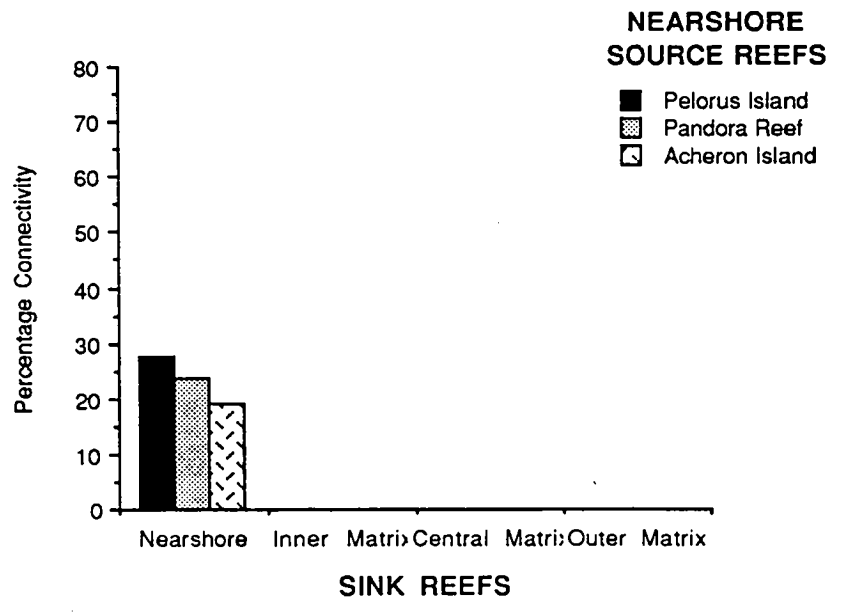


Figure 3.87 Level of reef connectivity with respect to the cross-shelf transport of larvae within the southern region for each of the three **nearshore** source reefs. See caption, Figure 3.83, for further details.

Reef within the central region. That is, most dispersal events that transported larvae to the south did not result in connectivity. In contrast, those dispersal events which transported larvae to the north resulted in relatively high rates of connectivity (see Fig. 3.88).

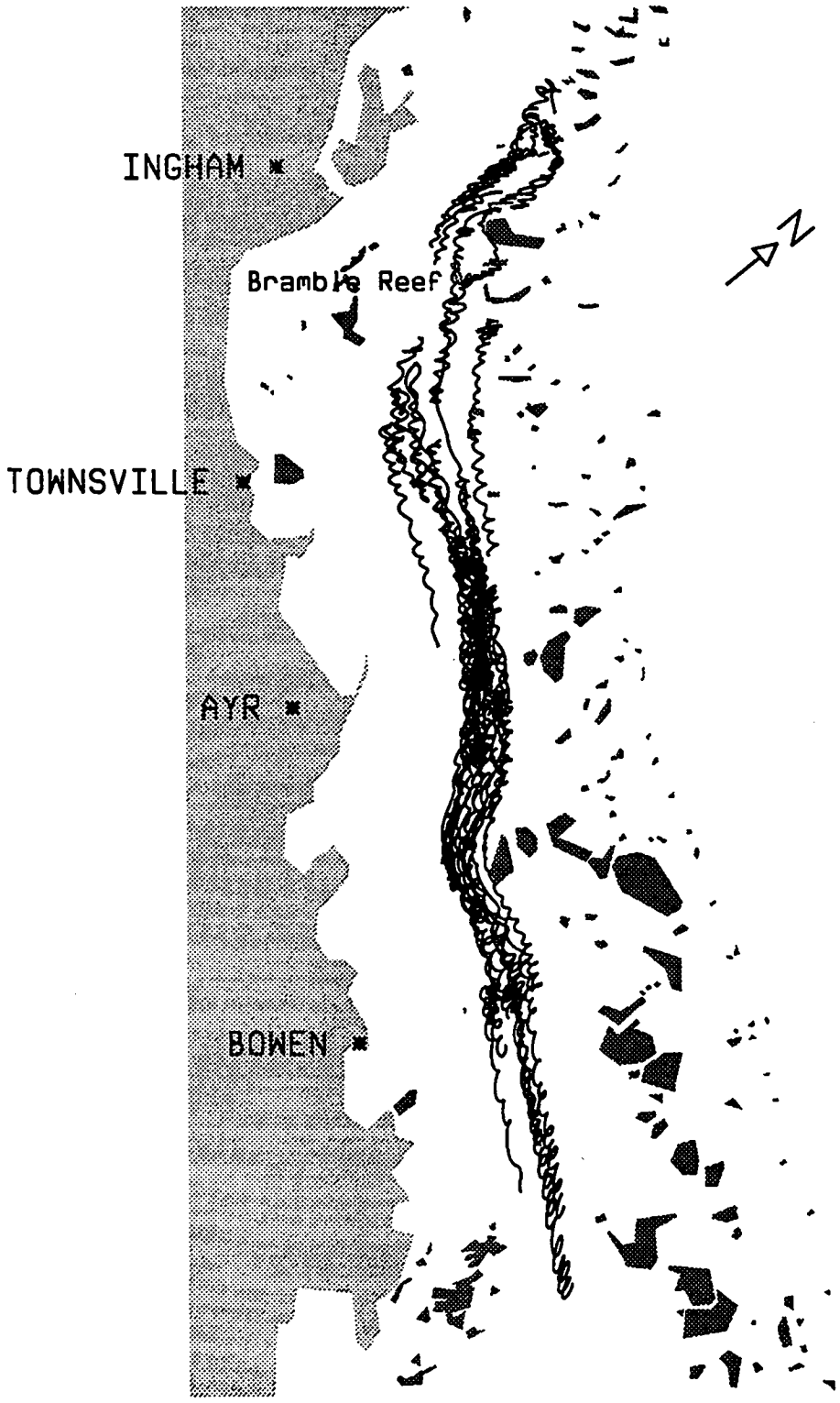


Figure 3.88 Particle trajectories representing twenty dispersal events from Bramble Reef (source reef indicated without fill). Each trajectory corresponds to the centroid of the larval cloud during the second two weeks of dispersal when the larvae of *A. planci* are assumed to be competent to settle. The level of connectivity from inner matrix reefs, such as Bramble Reef, is particularly low. Larvae originating from these reefs frequently become entrained within the main lagoon and are not transported to other reefs. Scale: 1cm = 11.5 nautical miles.

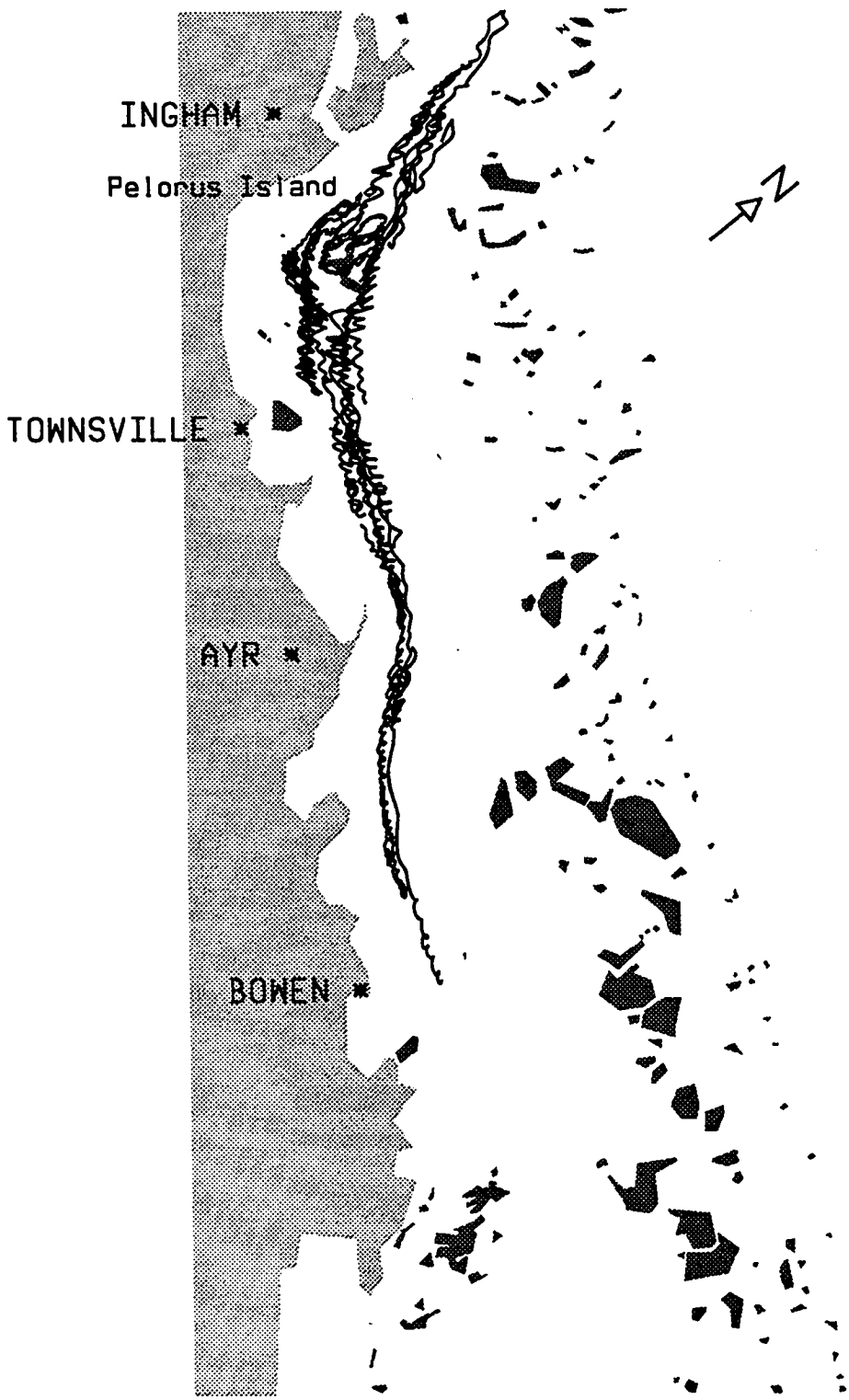


Figure 3.89 Particle trajectories representing twenty dispersal events from Pelorus Island (source reef indicated without fill). Each trajectory corresponds to the centroid of the larval cloud during the second two weeks of dispersal when the larvae of *A. planci* are assumed to be competent to settle. Larvae from nearshore source reefs frequently become entrained within the main lagoon and are transported alongshore without encountering another reef. Scale: 1cm = 11.5 nautical miles.

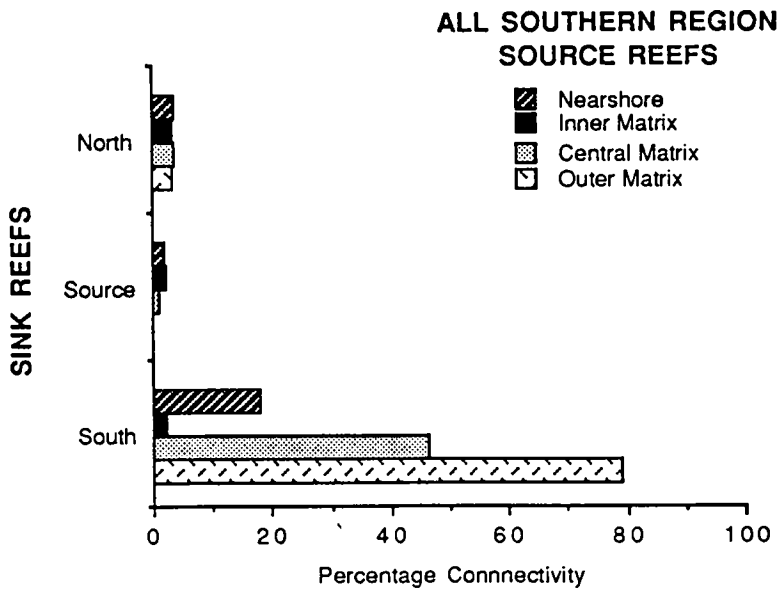


Figure 3.90 Level of reef connectivity with respect to the long-shelf transport of larvae within the southern region. Data represent the number of particles from all three source reefs within each of four cross-shelf geographical zones that intersect with sink reefs, expressed as a percentage of the total number of particle trajectories simulated from each zone. Cross-shelf zones correspond to reefs which lie along the outer edge of the reef matrix and continental shelf (outer matrix), reefs central within the reef matrix (central matrix), reefs which lie along the inner edge of the reef matrix bordering the main lagoon (inner matrix) and reefs which lie nearshore on the western side of the main lagoon (nearshore). Sink reefs are classified as lying to the north or south with respect to the source reef, or recruitment back onto the parent reef (source).

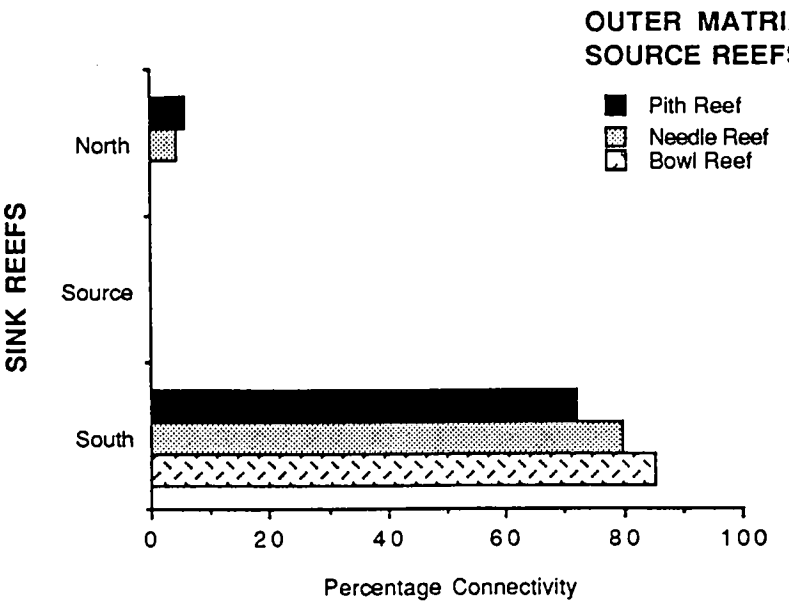


Figure 3.91 Level of reef connectivity with respect to the long-shelf transport of larvae within the southern region for each of the three **outer** matrix source reefs. See caption, Figure 3.90, for further details.

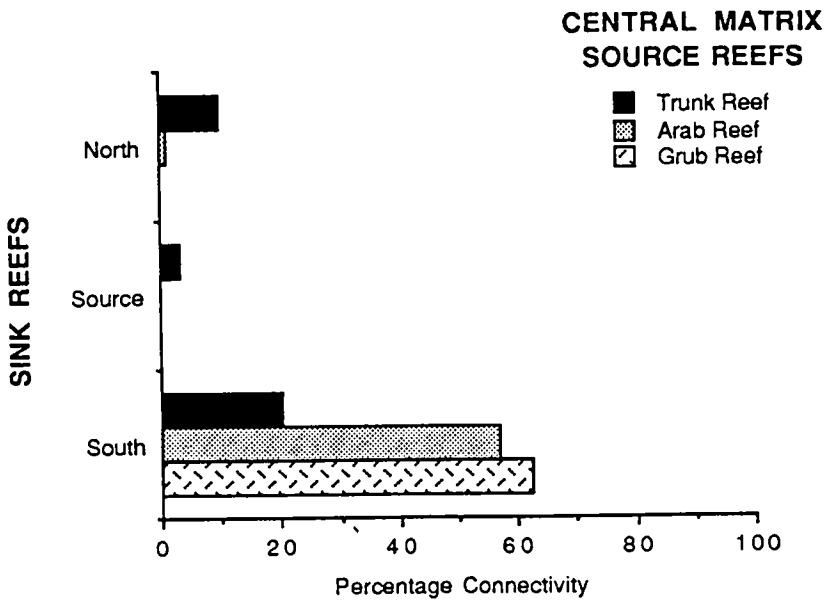


Figure 3.92 Level of reef connectivity with respect to the long-shelf transport of larvae within the southern region for each of the three **central** matrix source reefs. See caption, Figure 3.90, for further details.

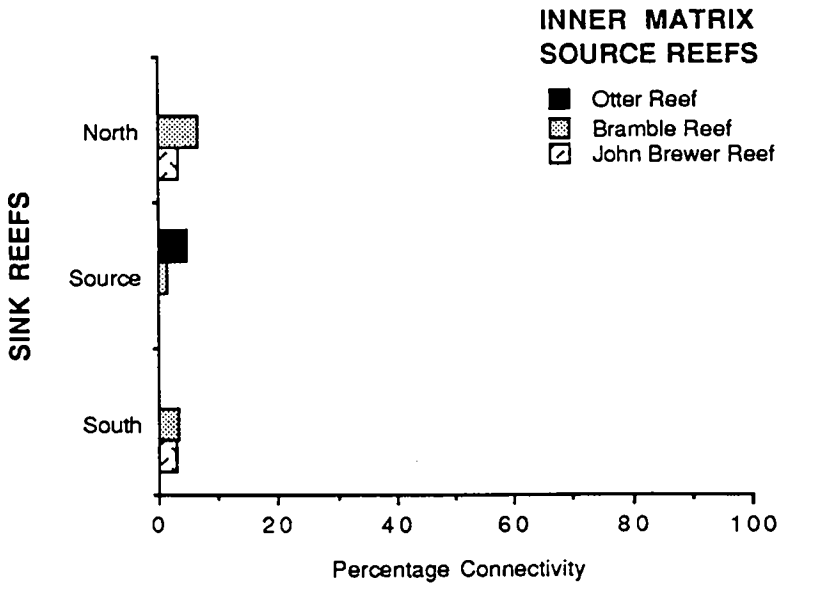


Figure 3.93 Level of reef connectivity with respect to the long-shelf transport of larvae within the southern region for each of the three **inner** matrix source reefs. See caption, Figure 3.90, for further details.

Although less frequent, they resulted in most of the connectivity. Although the southward directed pattern of connectivity was less strong for nearshore source reefs, it was fairly consistent between reefs (Fig. 3.94).

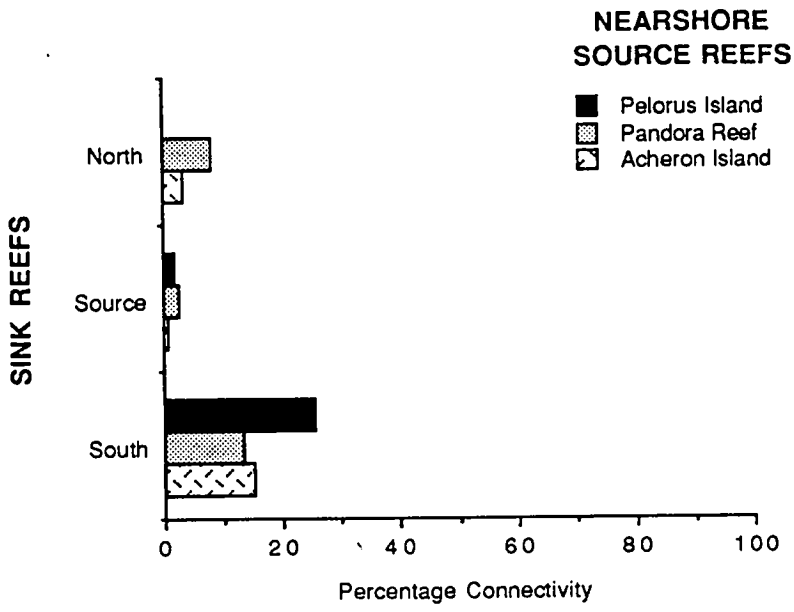


Figure 3.94 Level of reef connectivity with respect to the long-shelf transport of larvae within the southern region for each of the three **nearshore** source reefs. See caption, Figure 3.90, for further details.

3.5.3.3 Relative strength of connectivity

The relative strengths of connectivity between each southern region source reef and all their sink reefs are presented in Figures 3.95 to 3.106.

All outer and central matrix source reefs consistently displayed strongest connectivity with central and inner matrix sink reefs lying to the south of the source (Figs. 3.95 to 3.100). Only Trunk Reef also had strong connectivity with one reef lying immediately to the north (Fig. 3.98). None of the inner matrix source reefs had strong connectivity with any sink reefs (Figs. 3.101 to 3.103). Two nearshore source reefs, Pelorus and Acheron, displayed strongest connectivity with other nearshore sink reefs lying to the south of the source (Figs. 3.104 and 3.106 respectively). The third nearshore source reef, Pandora, did not have strong connectivity with any sink reef (Fig. 3.105). The nearshore reefs within Halifax Bay, including Magnetic Island (see Fig. 3.106), generally displayed a great deal of connectivity amongst themselves. Their relative isolation from other nearshore reefs therefore suggests that they probably rely heavily on each other as sources of larvae.

No outer or central matrix source reefs displayed strong connectivity with themselves, resulting from the transport of larvae back to the source reef as a result of current reversals. Of these, Trunk Reef had moderate connectivity with itself while the remainder had no connectivity at all. Two of the inner matrix source reefs, Otter and Bramble (Figs. 3.101 and 3.102), displayed moderate levels of self-seeding while the third, John Brewer, had no connectivity with itself at all (Fig. 3.103). Two of the nearshore source reefs, Pelorus and Acheron (Figs. 3.104 and 3.106), also displayed moderate levels of self-seeding while the third, Pandora, had no connectivity with itself at all (Fig. 3.105). The degree of self-seeding within the southern region appears to be still weaker than within the central region.

The distances over which larvae are transported to reefs with strongest connectivity once again varied markedly between source reefs. In general, the nearshore reefs displayed relatively short distances over which larvae were transported to sink reefs. Pelorus Island reef had strongest connectivity with Great Palm Island which lies only 10 nautical miles to the south, while Acheron Island reef had strongest connectivity with Magnetic Island which lies 15 nautical miles to the south (Figs. 3.104 and 3.106). The distances over which larvae were transported from the offshore reefs was far greater. Most outer and central matrix source reefs displayed strongest connectivity with sink reefs 50 to 100 nautical miles away (Figs. 3.95 to 3.100). All outer and central matrix source reefs display weak to moderate connectivity with sink reefs which are far more distant, up to 145 nautical miles away. The extremely low levels of connectivity from inner matrix source reefs resulted in relatively few sink reefs, most of which were much closer than those of central and outer matrix source reefs.

3.5.4 An Overview of the Patterns of Reef Connectivity

The overall patterns of larval transport within the Cairns and Central Sections of the GBR Marine Park are summarized in Figures 3.107 and 3.108 respectively.

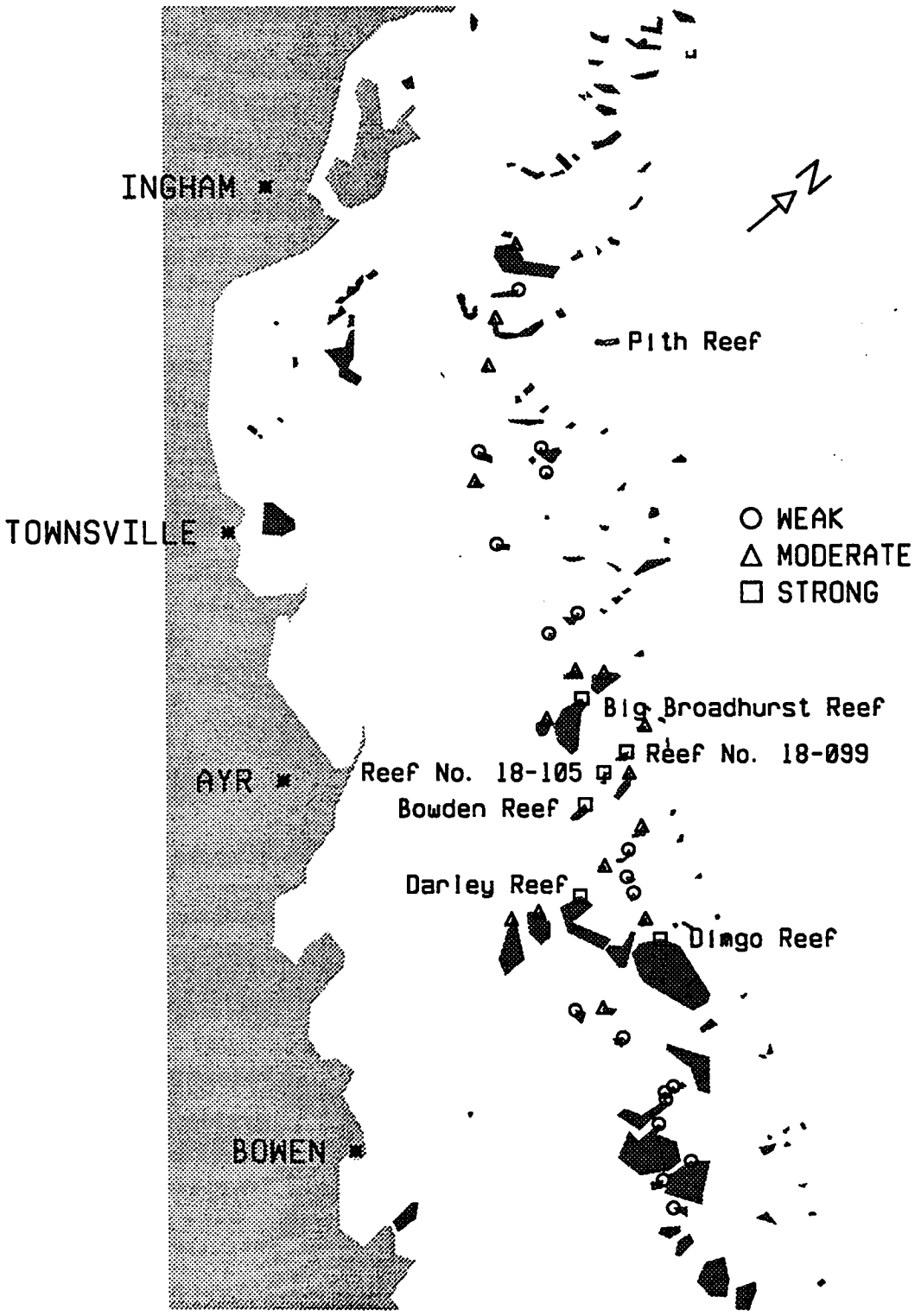


Figure 3.95 Strength of connectivity with respect to Pith Reef (source reef indicated without fill). The relative strength classes (weak, moderate and strong) represent probabilities separated by an order of magnitude. Strongest connectivity is with Big Broadhurst, 18-099, 18-105, Bowden, Darley and Dingo Reefs. All are inner and central matrix reefs which lie 60 to 100 nautical miles to the south of the source. Scale: 1cm = 10 nautical miles.

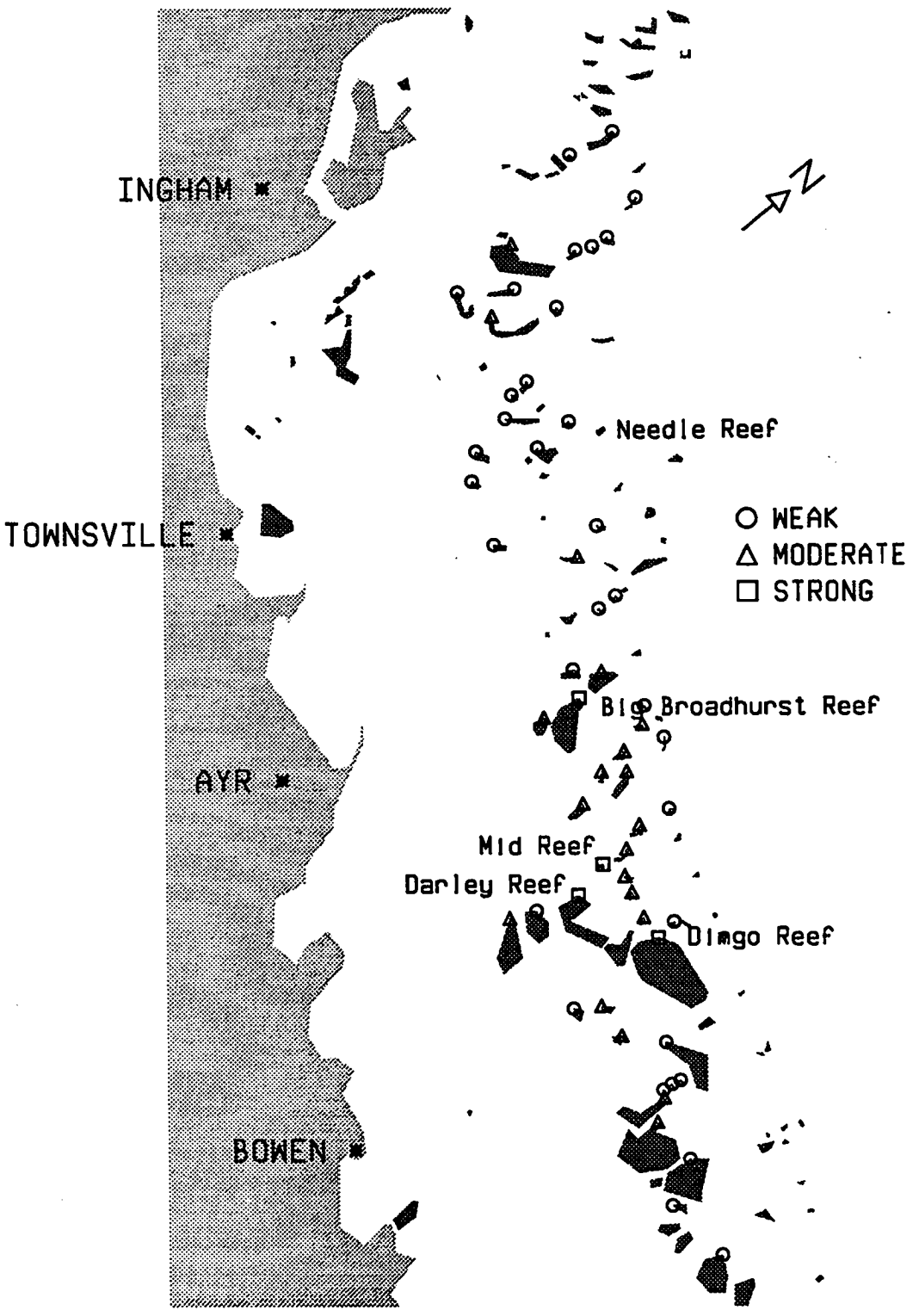


Figure 3.96 Strength of connectivity with respect to Needle Reef. The relative strength classes (weak, moderate and strong) represent probabilities separated by an order of magnitude. Strongest connectivity is with Big Broadhurst, Mid, Darley and Dingo Reefs. All are inner and central matrix reefs which lie 45 to 90 nautical miles to the south of the source. Scale: 1cm = 10 nautical miles.

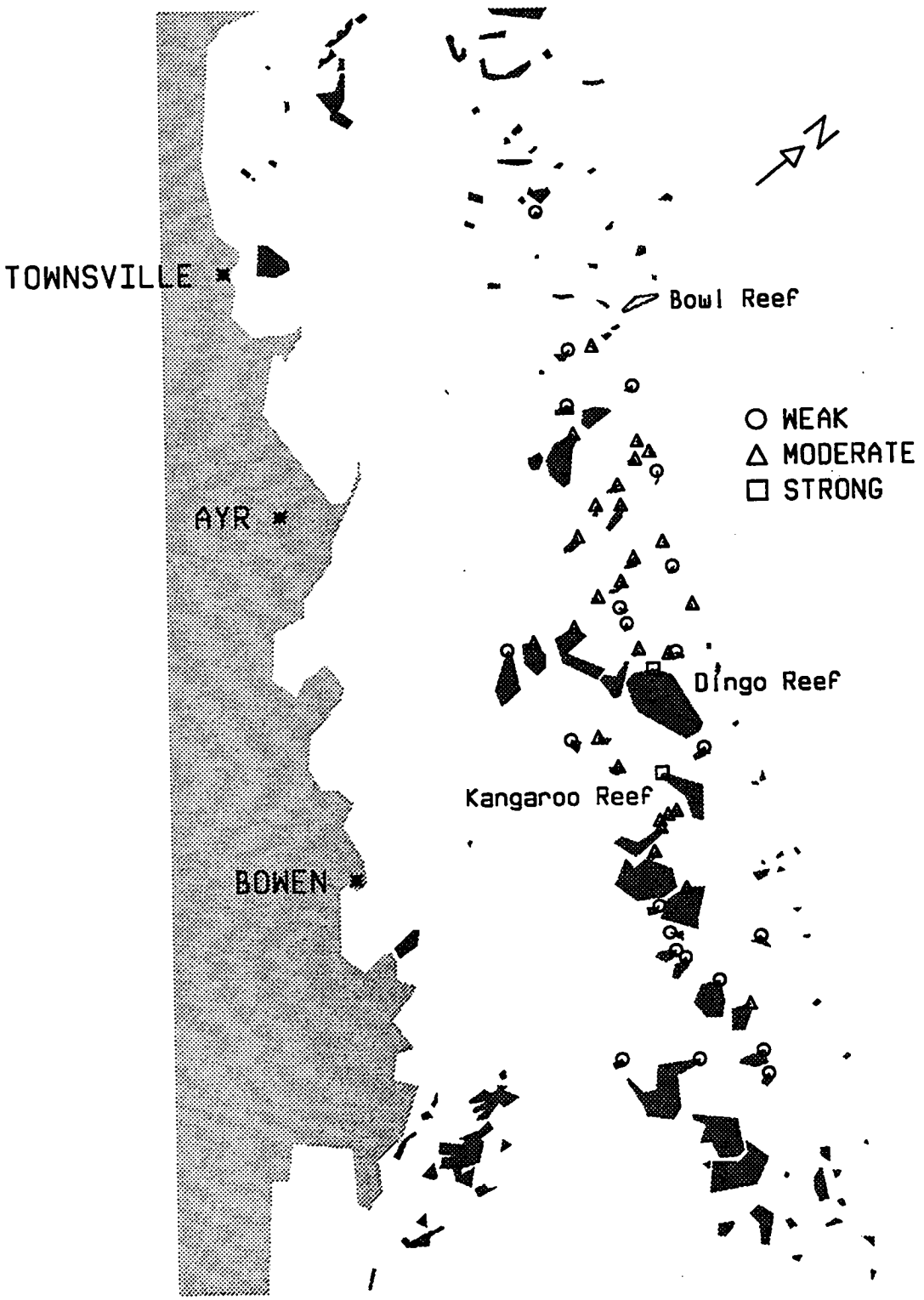


Figure 3.97 Strength of connectivity with respect to Bowl Reef (source reef indicated without fill). The relative strength classes (weak, moderate and strong) represent probabilities separated by an order of magnitude. Strongest connectivity is with Dingo and Kangaroo Reefs. Both are central matrix reefs which lie 60 to 80 nautical miles to the south of the source. Scale: 1cm = 10 nautical miles.

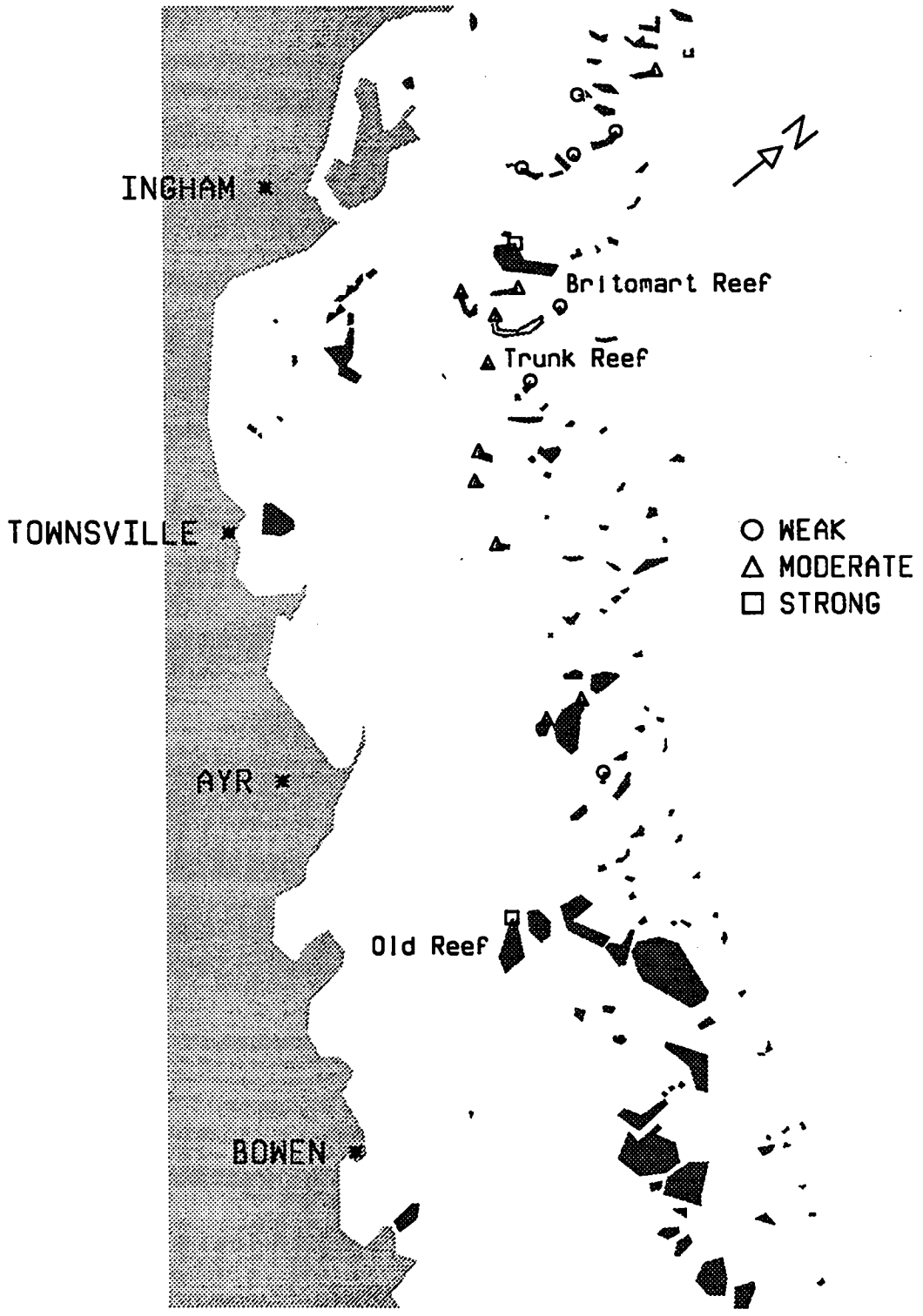


Figure 3.98 Strength of connectivity with respect to Trunk Reef (source reef indicated without fill). The relative strength classes (weak, moderate and strong) represent probabilities separated by an order of magnitude. Strongest connectivity is with Britomart and Old Reefs. Old Reef lies 100 nautical miles to the south of the source. Scale: 1cm = 10 nautical miles.

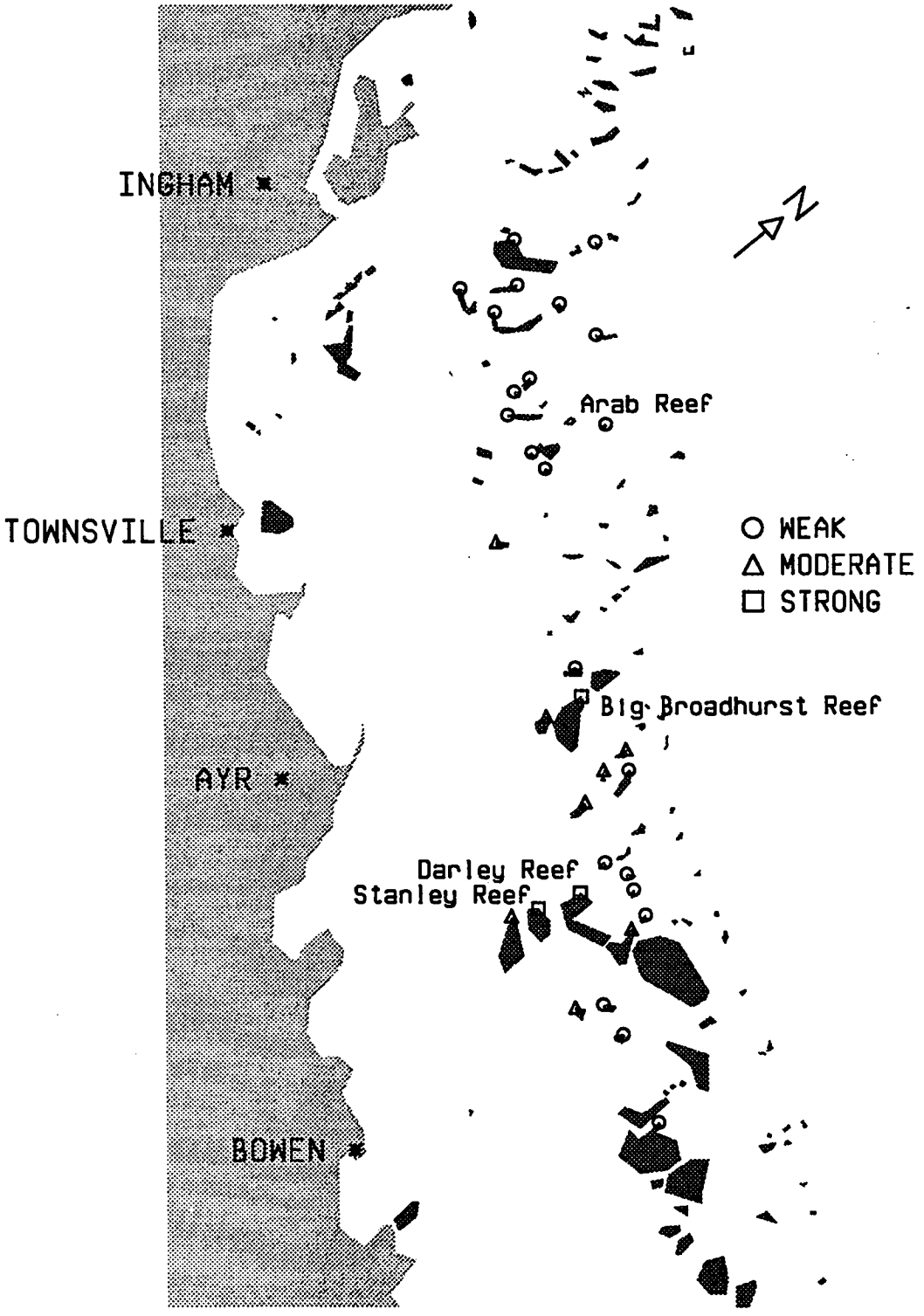


Figure 3.99 Strength of connectivity with respect to Arab Reef (source reef indicated without fill). The relative strength classes (weak, moderate and strong) represent probabilities separated by an order of magnitude. Strongest connectivity is with Big Broadhurst, Darnley and Stanley Reefs. All are inner and central matrix reefs which lie 45 to 80 nautical miles to the south of the source. Scale: 1cm = 10 nautical miles.

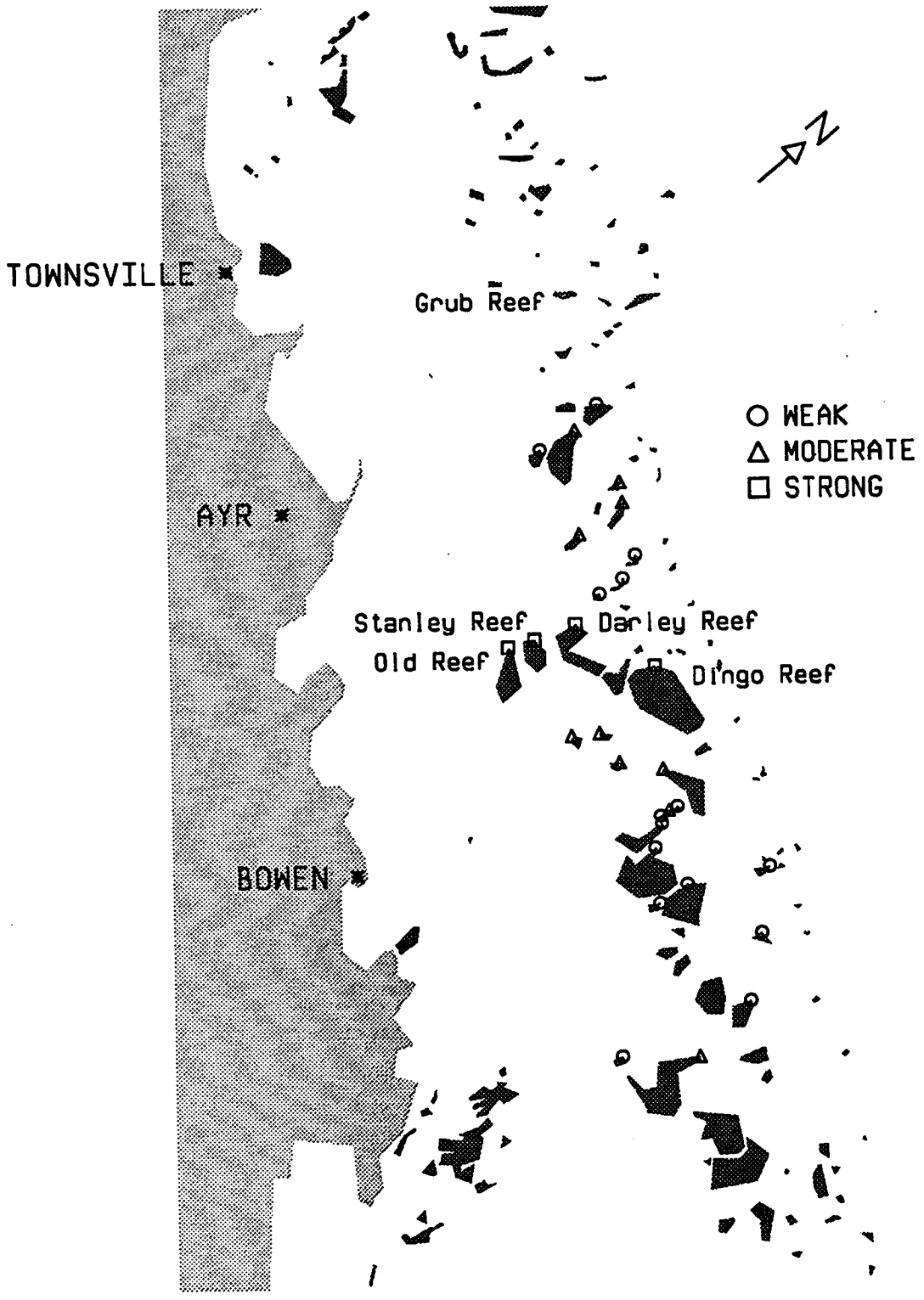


Figure 3.100 Strength of connectivity with respect to Grub Reef (source reef indicated without fill). The relative strength classes (weak, moderate and strong) represent probabilities separated by an order of magnitude. Strongest connectivity is with Darnley, Stanley, Old and Dingo Reefs. All are inner and central matrix reefs which lie 55 to 65 nautical miles to the south of the source. Scale: 1cm = 10 nautical miles.

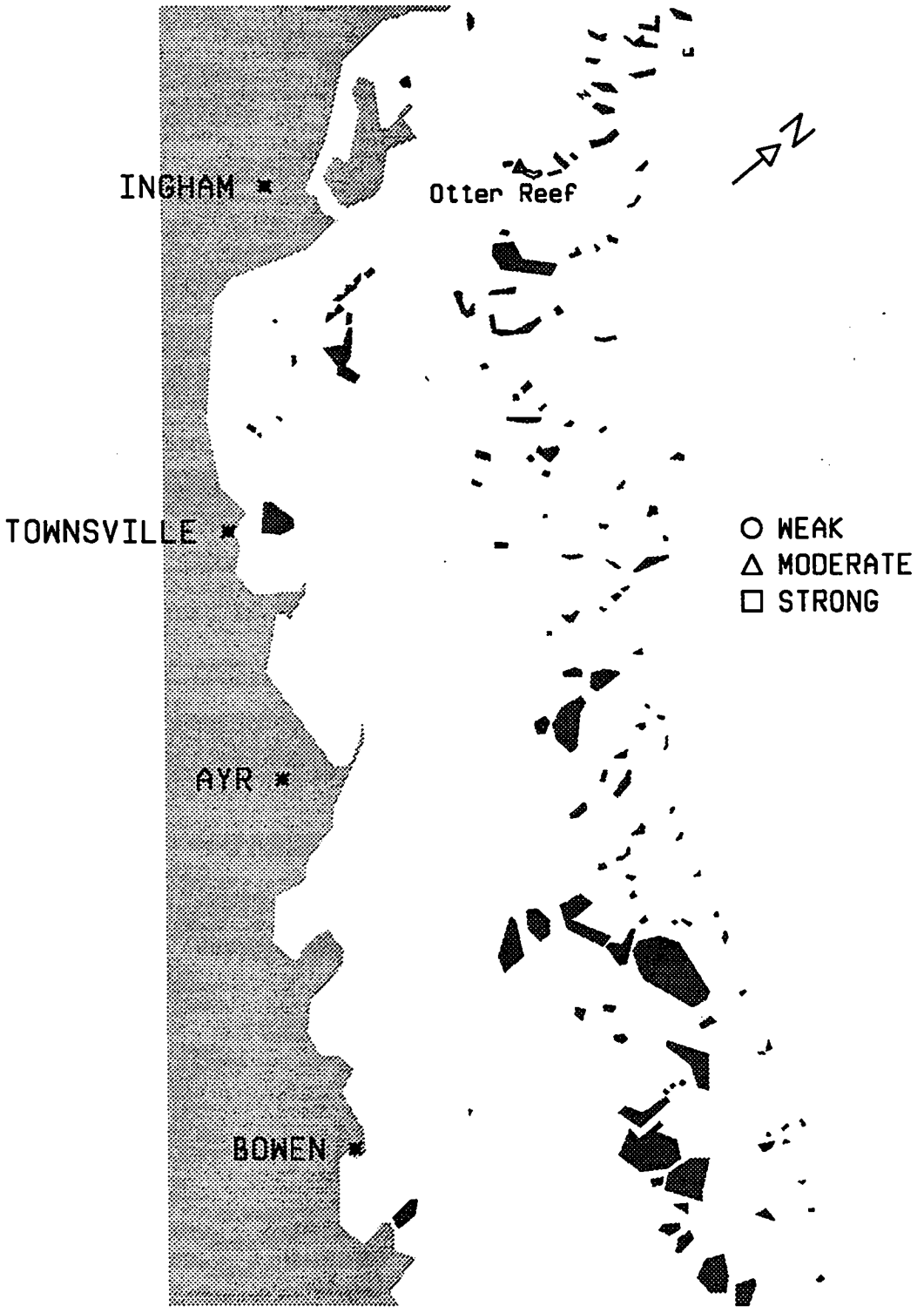


Figure 3.101 Strength of connectivity with respect to Otter Reef (source reef indicated without fill). The relative strength classes (weak, moderate and strong) represent probabilities separated by an order of magnitude. The overall level of connectivity with respect to Otter Reef was particularly low and no sink reefs other than itself were identified. Scale: 1cm = 10 nautical miles.

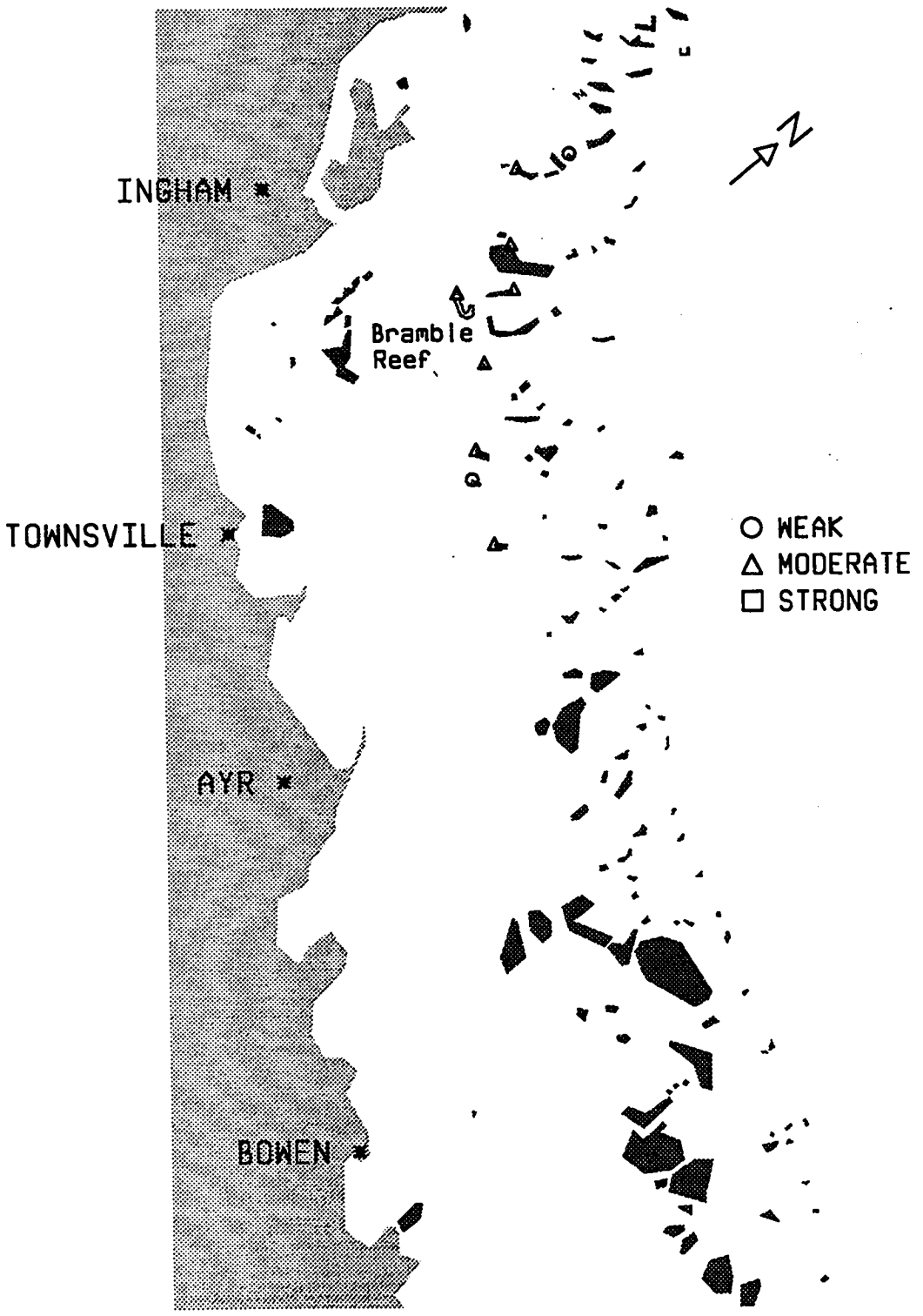


Figure 3.102 Strength of connectivity with respect to Bramble Reef (source reef indicated without fill). The relative strength classes (weak, moderate and strong) represent probabilities separated by an order of magnitude. The overall level of connectivity with respect to Bramble Reef appears to be quite low and no sink reefs with strong connectivity were identified. Scale: 1cm = 10 nautical miles.

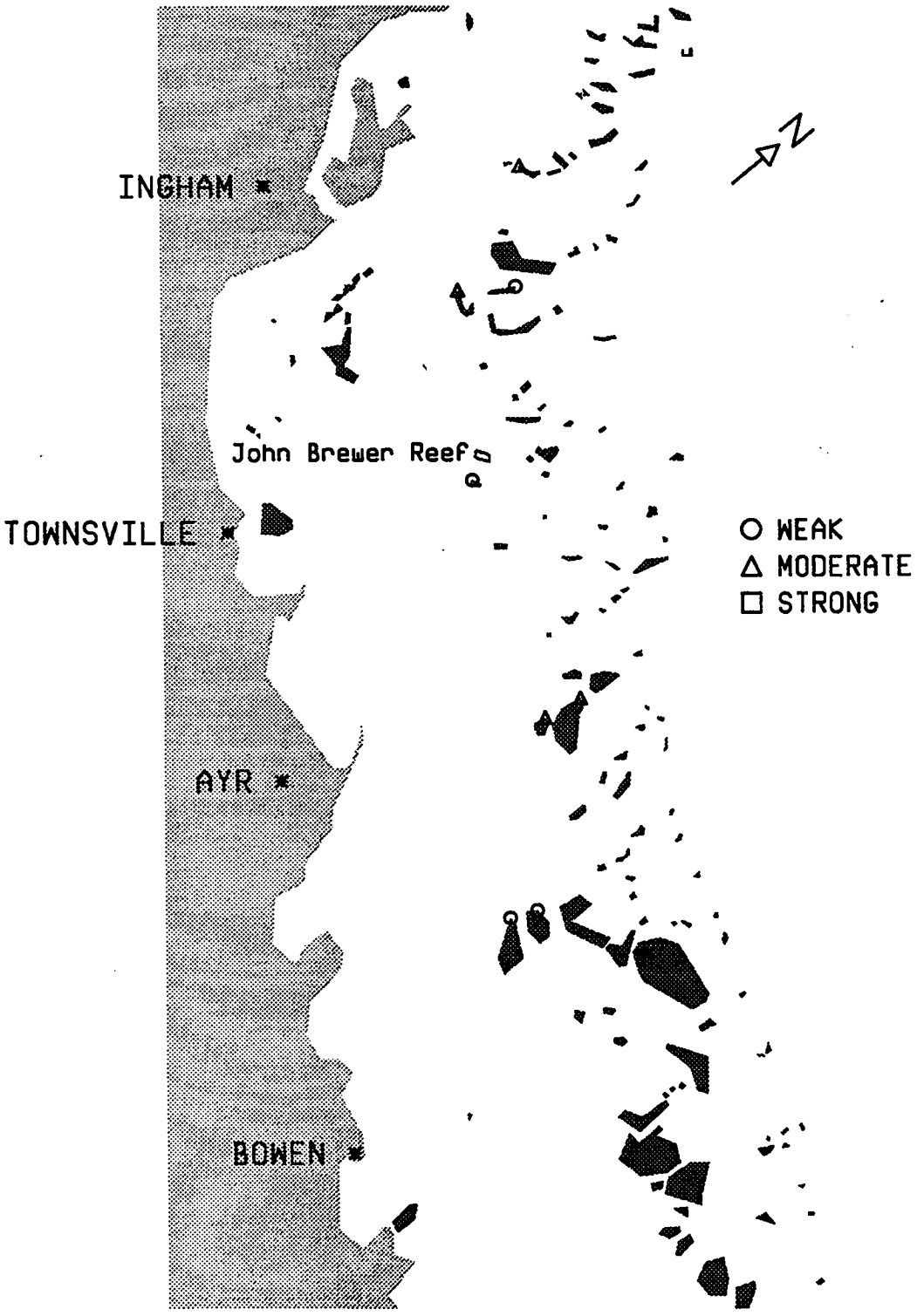


Figure 3.103 Strength of connectivity with respect to John Brewer Reef (source reef indicated without fill). The relative strength classes (weak, moderate and strong) represent probabilities separated by an order of magnitude. The overall level of connectivity with respect to John Brewer Reef appears to be quite low and no sink reefs with strong connectivity were identified. Scale: 1cm = 10 nautical miles.

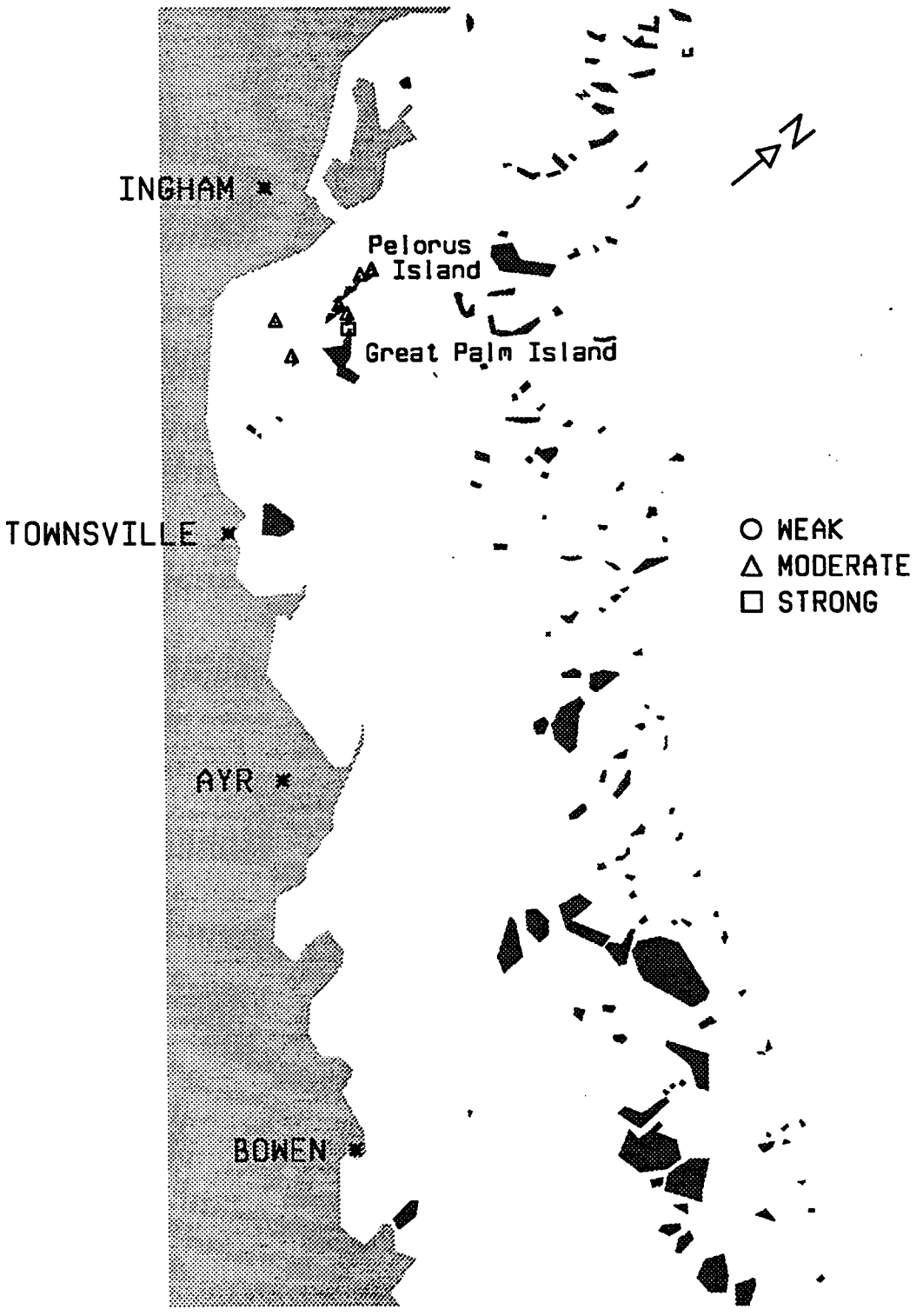


Figure 3.104 Strength of connectivity with respect to Pelorus Island. The relative strength classes (weak, moderate and strong) represent probabilities separated by an order of magnitude. Strongest connectivity is with Great Palm Island which lies 15 nautical miles to the south of the source. Scale: 1cm = 10 nautical miles.

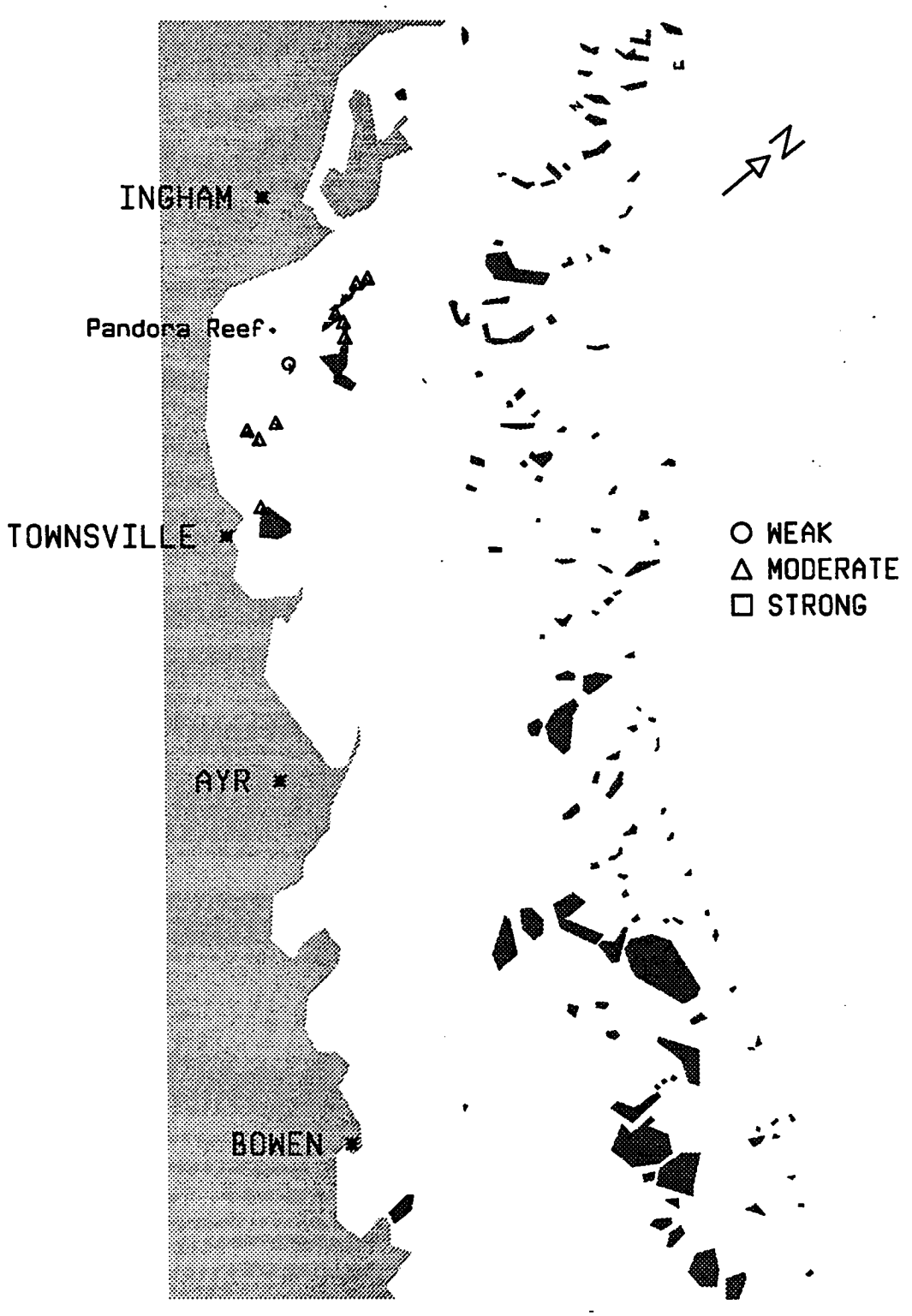


Figure 3.105 Strength of connectivity with respect to Pandora Reef. The relative strength classes (weak, moderate and strong) represent probabilities separated by an order of magnitude. No sink reefs with strong connectivity were identified, but many surrounding reefs displayed moderate connectivity. Scale: 1cm = 10 nautical miles.

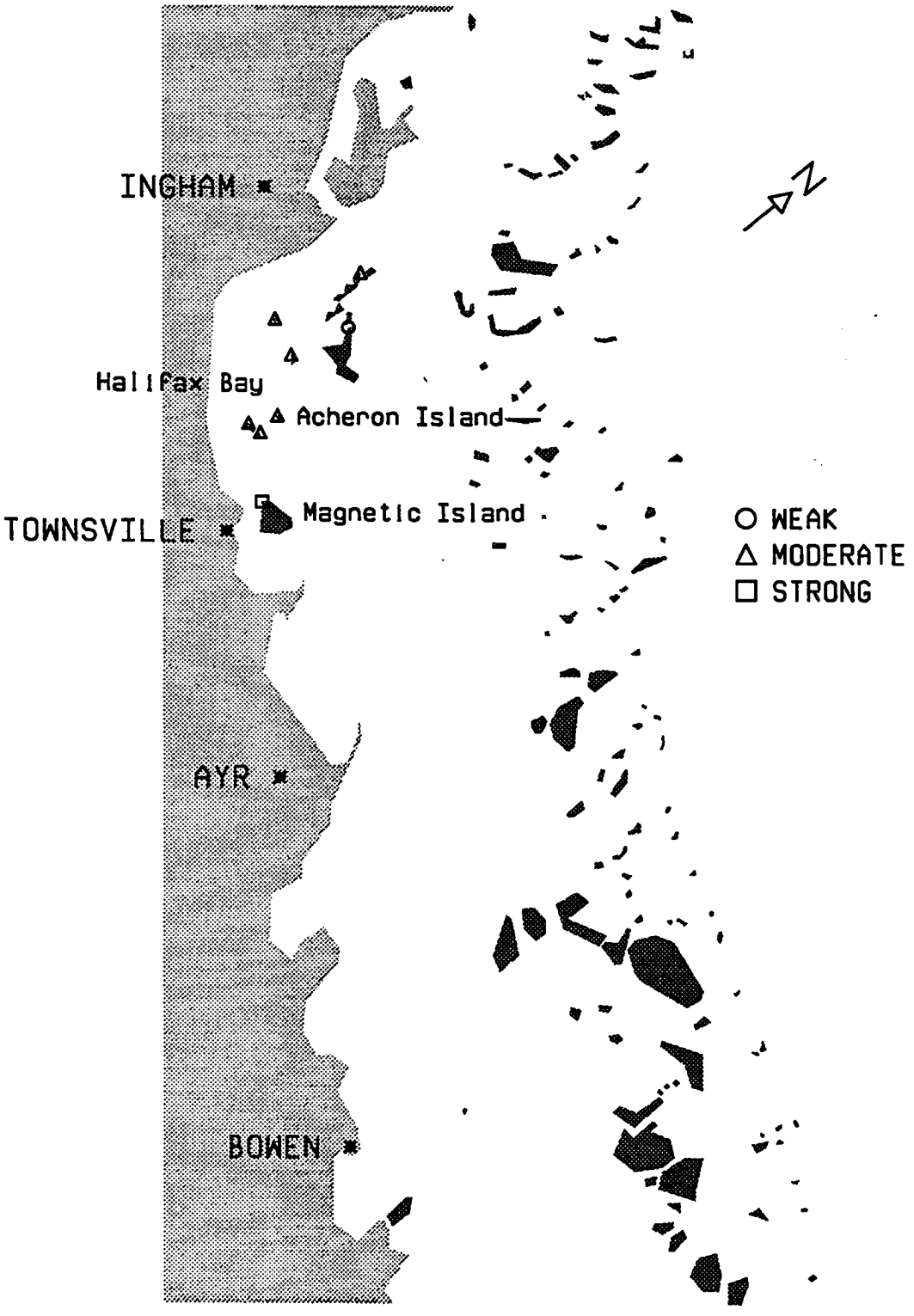


Figure 3.106 Strength of connectivity with respect to Acheron Island. The relative strength classes (weak, moderate and strong) represent probabilities separated by an order of magnitude. Strongest connectivity is with Magnetic Island which lies 15 nautical miles to the south of the source. Scale: 1cm = 10 nautical miles.

Model results from the northern region (Fig. 3.107) indicate that there should be substantial mixing of *A. planci* larvae between reefs, both across and along the shelf. This is particularly so for larvae originating from inner matrix reefs, which should frequently be transported offshore to central and outer matrix sink reefs, and from central matrix source reefs, which should be transported both offshore and onshore. Larval connectivity from the outer matrix ribbon reefs is directed primarily alongshore, with only limited onshore transport. The level of connectivity averaged over all fifteen reefs within the northern region is 59.9%. Long-shelf connectivity within the northern region was directed to reefs lying both north and south of the source (43.1% and 49.8% respectively, for larvae which intersected with reefs).

Model results from the central and southern regions (Figs. 3.107 and 3.108) identify a very different pattern. A general movement of larvae onshore, through the reef matrix, towards the lagoon is predicted within these regions. Once within the main lagoon, larvae are transported alongshore. Only relatively rare events resulted in larvae being transported offshore from inner and central matrix reefs. No connectivity is predicted between nearshore and mid-shelf reefs within the southern region. However, there is limited connectivity between central region mid-shelf reefs and nearshore reefs within the southern region. The level of connectivity averaged over all reefs within the central and southern regions is 52.3% and 41.3% respectively. Long-shelf connectivity within the central and southern regions was directed strongly to reefs lying to the south of the source (79.4% and 70.7% respectively, for larvae which intersected with reefs). The relative proportion of larvae which were transported onshore across the shelf and to the south became progressively greater towards the southern region.

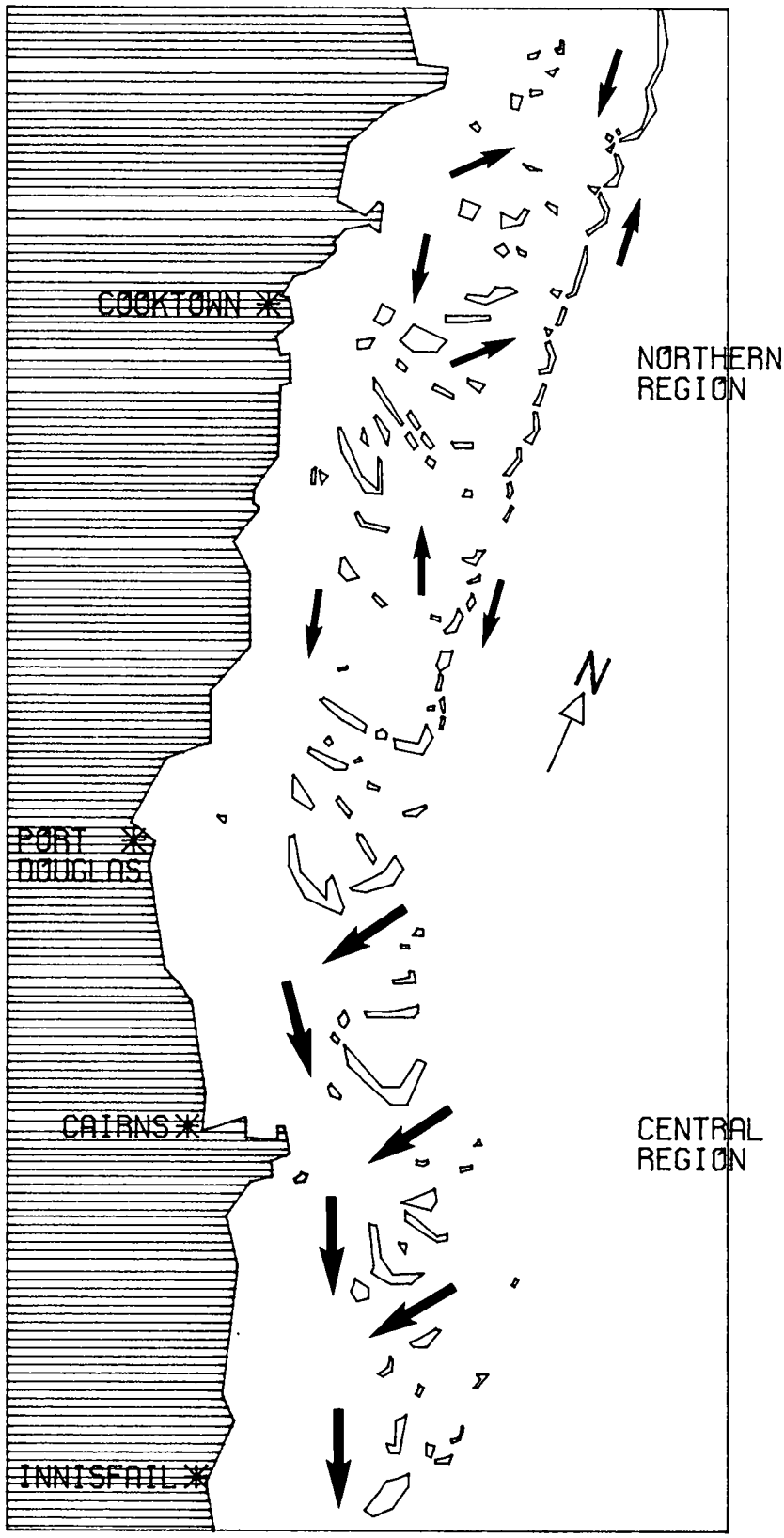


Figure 3.107 Patterns of larval transport from December to March within the Cairns Section of the Great Barrier Reef Marine Park. Contrasting patterns are evident between the northern and central regions.

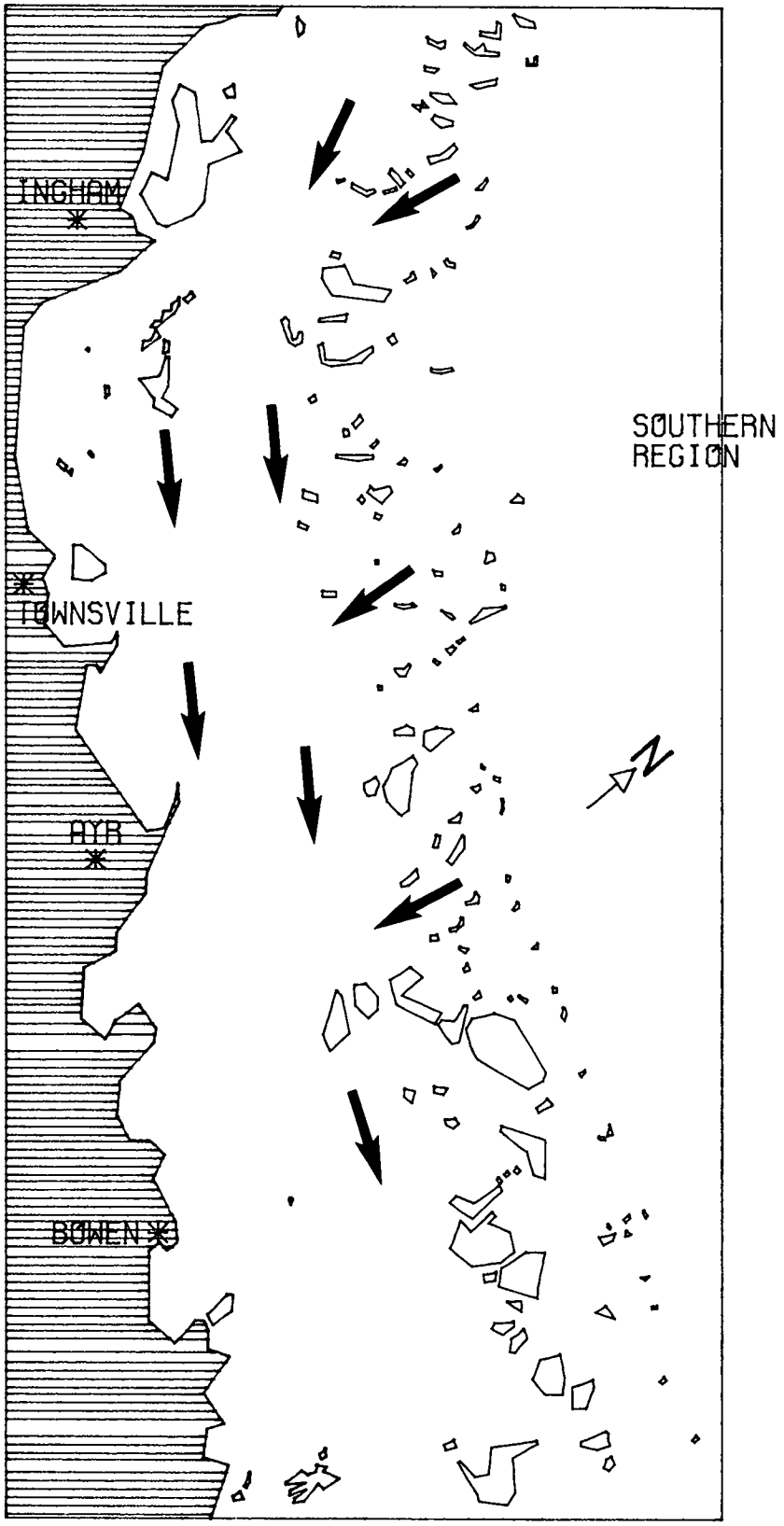


Figure 3.108 Patterns of larval transport from December to March within the Central Section of the Great Barrier Reef Marine Park. There is general movement of larvae onshore, through the reef matrix, towards the lagoon within the central and southern regions. Once within the main lagoon, larvae are transported alongshore.

3.6 SHORT PRE-COMPETENT PERIOD OF LARVAL DEVELOPMENT

Analysis of reef connectivity for short pre-competent period larvae are presented for the northern and southern regions only.

3.6.1 The Northern Region

3.6.1.1 Cross-shelf connectivity

Reef connectivity within the northern region, expressed as source-sink relationships with respect to the cross-shelf movement of short pre-competent period larvae, is presented in Figure 3.109. The broad patterns of connectivity for all reefs in each of the three cross-shelf geographical zones remain essentially the same as for long pre-competent period larvae (compare Figs. 3.33 and 3.109). Overall, the level of connectivity is slightly higher for short pre-competent period larvae, particularly for the outer matrix source reefs (69.8% compared to 48.5%). This pattern was consistent for all five individual outer matrix source reefs.

3.6.1.2 Long-shelf connectivity

Reef connectivity, with respect to the long-shelf movement of larvae, is summarized in Figure 3.110. Again, the broad patterns of connectivity for all reefs in each of the three cross-shelf geographical zones remain essentially the same as for long pre-competent period larvae (compare Figs. 3.38 and 3.110). That is, the relative proportion of larvae which are transported to the north and south remains the same. However, the slightly higher level of connectivity overall for short pre-competent period larvae which was identified above is evident in the increased connectivity back onto the source reef as a result of current reversals, particularly for the outer matrix source reefs (23.4% compared to 6.3%).

3.6.1.3 Relative strength of connectivity

The relative strengths of connectivity between each northern region source reef and all its sink reefs are presented in Appendix C. Very

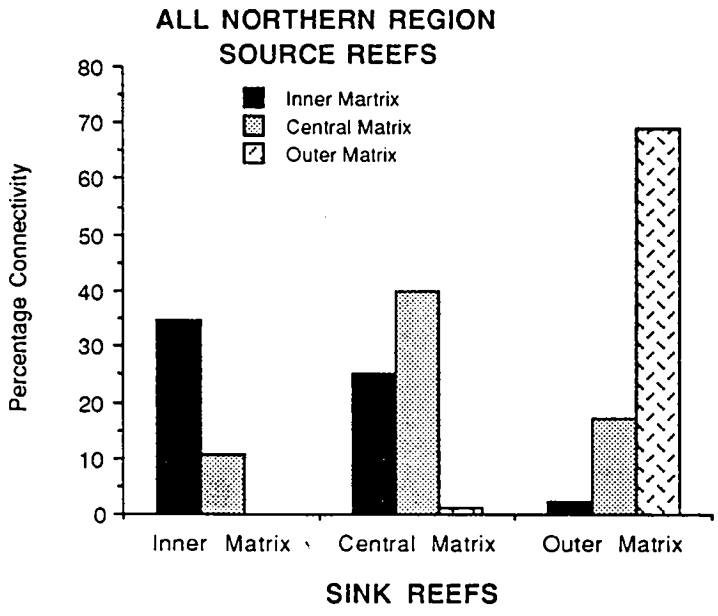


Figure 3.109 Level of reef connectivity with respect to the cross-shelf transport of short pre-competent period larvae within the northern region. Data represent the number of particles from five source reefs within each of three cross-shelf geographical zones that intersect with sink reefs, expressed as a percentage of the total number of particle trajectories simulated from each zone. Cross-shelf zones correspond to reefs which lie along the outer edge of the reef matrix and continental shelf (outer matrix), reefs central within the reef matrix (central matrix) and reefs which lie along the inner edge of the reef matrix bordering the main lagoon (inner matrix).

few differences are observed in the identities of sink reefs with moderate to strong connectivity when compared with long pre-competent period larvae. In general, short pre-competent period larvae are transported shorter distances than long pre-competent period larvae and, as a consequence, have connectivity with fewer sink reefs. However, it is the more distant sink reefs with weak connectivity for long pre-competent period larvae which are absent for short pre-competent period larvae.

3.6.2 The Southern Region

3.6.2.1 Cross-shelf connectivity

Reef connectivity within the southern region, expressed as source-sink relationships with respect to the cross-shelf movement of short pre-competent period larvae, is presented in Figure 3.111. The broad patterns of connectivity for all reefs in each of the four cross-shelf geographical zones remain essentially the same as for long pre-

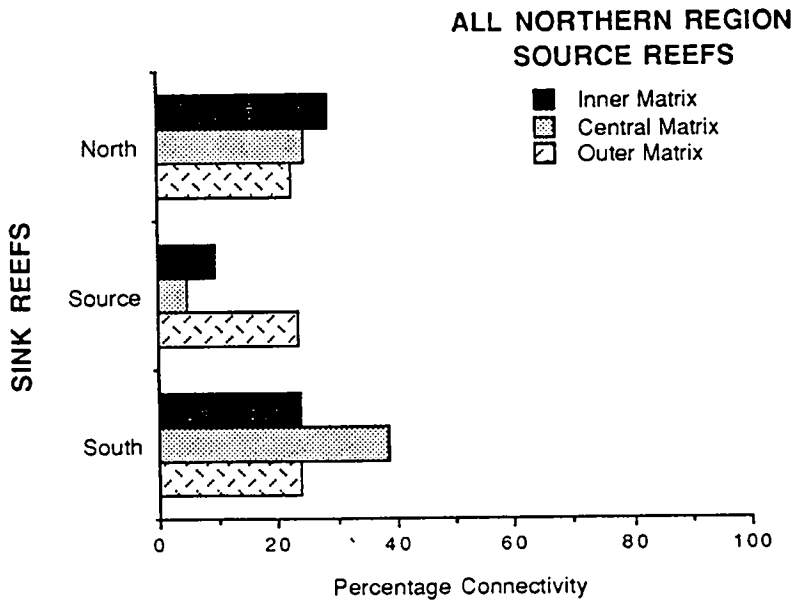


Figure 3.110 Level of reef connectivity with respect to the long-shelf transport of short pre-competent period larvae within the northern region. Data represent the number of particles from all five source reefs within each of three cross-shelf geographical zones that intersect with sink reefs, expressed as a percentage of the total number of particle trajectories simulated from each zone. Cross-shelf zones correspond to reefs which lie along the outer edge of the reef matrix and continental shelf (outer matrix), reefs central within the reef matrix (central matrix) and reefs which lie along the inner edge of the reef matrix bordering the main lagoon (inner matrix). Sink reefs are classified as lying to the north or south with respect to the source reef, or recruitment back onto the parent reef (source).

competent period larvae (compare Figs. 3.83 and 3.111). In general though, source reefs in each of the cross-shelf geographical zones displayed slightly higher connectivity with sink reefs in the same cross-shelf zone. That is, the cross-shelf movement of larvae onshore from central and outer matrix source reefs is weaker. Overall, the level of connectivity is again slightly higher for short pre-competent period larvae. In this case, particularly for the central matrix source reefs (72.4% compared to 51.3%). This pattern was consistent for all three individual central matrix source reefs.

3.6.2.2 Long-shelf connectivity

Reef connectivity, with respect to the long-shelf movement of larvae, is summarized in Figure 3.112. Again, the broad patterns of connectivity for all reefs in each of the three cross-shelf geographical zones remain essentially the same as for long pre-competent period larvae (compare Figs. 3.90 and 3.112). In this southern region, the

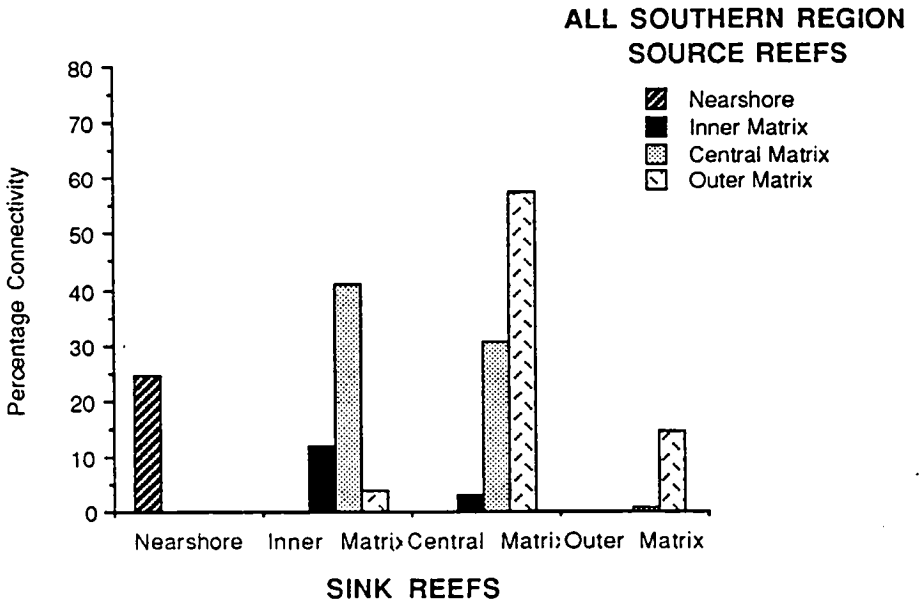


Figure 3.111 Level of reef connectivity with respect to the cross-shelf transport of short pre-competent period larvae within the southern region. Data represent the number of particles from three source reefs within each of four cross-shelf geographical zones that intersect with sink reefs, expressed as a percentage of the total number of particle trajectories simulated from each zone. Cross-shelf zones correspond to reefs which lie along the outer edge of the reef matrix and continental shelf (outer matrix), reefs central within the reef matrix (central matrix,) reefs which lie along the inner edge of the reef matrix bordering the main lagoon (inner matrix) and reefs lying nearshore on the western side of the main lagoon (nearshore).

strong southward transport of larvae lessens the possibility of connectivity back onto the source reef for short pre-competent period larvae as a result of current reversals.

3.6.2.3 Relative strength of connectivity

The relative strengths of connectivity between each southern region source reef and all its sink reefs are presented in Appendix C. In contrast to the northern region, many differences are observed in the identities of sink reefs with moderate to strong connectivity when compared with long pre-competent period larvae. This appears to be related to the greater distances over which larvae are transported within the southern region when compared to the northern region. Short pre-competent period larvae are, once again, transported shorter distances than long pre-competent period larvae and, as a consequence, have connectivity with fewer sink reefs.

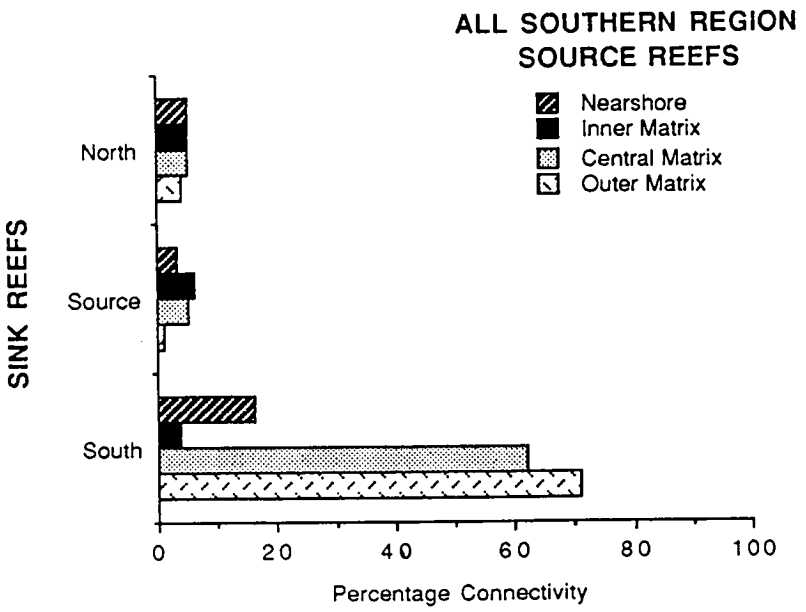


Figure 3.112 Level of reef connectivity with respect to the long-shelf transport of short pre-competent period larvae within the southern region. Data represent the number of particles from all three source reefs within each of four cross-shelf geographical zones that intersect with sink reefs, expressed as a percentage of the total number of particle trajectories simulated from each zone. Cross-shelf zones correspond to reefs which lie along the outer edge of the reef matrix and continental shelf (outer matrix), reefs central within the reef matrix (central matrix), reefs which lie along the inner edge of the reef matrix bordering the main lagoon (inner matrix) and reefs which lie nearshore on the western side of the main lagoon (nearshore). Sink reefs are classified as lying to the north or south with respect to the source reef, or recruitment back onto the parent reef (source).

CHAPTER FOUR

SENSITIVITY TESTING

This section of the thesis covers the results of sensitivity analyses of the chief assumptions and approximations made within the model.

4.1 FINE-SCALE HYDRODYNAMICS AND LARVAL TRANSPORT

The sensitivity of model results to the magnitude of long-shelf and cross-shelf tidal currents, distribution of habitat and diffusion coefficients has been investigated.

An understanding of the sensitivity of results to the magnitude of the long-shelf current is particularly important as current strength can vary greatly over a range of spatial and temporal scales. Steady-state forcing must only be considered as an approximation of the real system. In addition to the 'standard' current speed of 12 cm s^{-1}, larval entrainment onto reef type L2 (Fig. 2.4) was also simulated for current speeds of 6, 18, 30 and 45 cm s^{-1}. Particles were released from grid cells at one kilometre intervals upstream and outside the reef's influence in the manner described in Section 2.3.4. The number of particles from each release that were transported over the area defined as habitat was recorded for each of the current speeds.

The magnitude of cross-shelf tidal currents can also vary considerably from region to region. Within the Cairns and Central Sections, however, there is relatively little variation over the shelf, except towards the southern part of the Central Section where tidal currents become stronger and the major axes of the tidal ellipses are oriented along-shelf (see Fig. 3.7). In addition to the 'standard' peak current speed of 20 cm s^{-1}, larval entrainment onto reef type L2 (Fig. 2.4) was also measured for peak current speeds along the major axis of the tidal ellipse of 10 and 40 cm s^{-1}. This effectively provided a range in tidal excursions. The magnitude of the long-shelf current was maintained at 12 cm s^{-1}. Particle releases were as described in Section 2.3.4. The number of particles from each release that were

transported over the area defined as habitat was recorded for each of the peak tidal current speeds.

Two alternatives to the 'standard' distribution of habitat, which extended one grid cell beyond the reef margin, were investigated for reef type P3. In the first, habitat was restricted to the reef flat area and within the lagoon, while in the second, habitat was extended two grid cells (1 km) beyond the reef margin. Long-shelf and cross-shelf currents were maintained at 12 and 20 cm s^{-1} respectively. Particle releases were as described in Section 2.3.4. The number of particles from each release that were transported over the area defined as habitat was recorded.

The 'standard' lateral and longitudinal diffusion coefficients, 0.1 and 0.4 respectively, were derived by comparison between multiple simulations in 2-dimensions and 3-dimensional simulations of particle transport (K.P. Black, pers. comm.). The effect of vertical shear is simulated by a four-fold increase in the longitudinal diffusion coefficient. Two alternatives to the 'standard' diffusion coefficients were investigated for reef type L2. In the first, the lateral and longitudinal diffusion coefficients were set to 0.0 and 0.2 respectively, while in the second, they were set to 0.2 and 0.8. Long-shelf and cross-shelf currents were maintained at 12 and 20 cm s^{-1} respectively. Particle releases were as described in Section 2.3.4. The number of particles from each release that were transported over the area defined as habitat was recorded.

4.1.1 Fine-scale Hydrodynamics

The magnitudes of the long-shelf and cross-shelf tidal currents were varied systematically for reef type L2. A qualitative description of the effects of these variations on the patterns and dynamics of the hydrodynamic regime is presented below. A quantitative description of the effects of these variations on the entrainment of larvae onto reefs is presented in Section 4.1.2.

4.1.1.1 Long-shelf currents

Variation in the hydrodynamics associated with long-shelf currents of 6, 12, 18, 30 and 45 cm s^{-1} (0.06, 0.12, 0.18, 0.30 and 0.45 m s^{-1}) are presented in Appendix D as one hourly plots of current vectors over a tidal cycle. The magnitude of the peak current speed along the major axis of the tidal ellipse was maintained at 0.20 m s^{-1}.

The patterns and dynamics of water motion around the reef remained essentially unchanged, except that the eddy circulation became much stronger with increasing current strength. At higher current speeds, particularly 0.45 m s^{-1}, long-shelf currents dominate and a major eddy on the offshore and downstream side of the reef is seen to be shed (Fig. D5). Residual eddy circulation is more complex at low long-shelf current speeds when water motion is dominated by tidal flow (Fig. D6).

4.1.1.2 Cross-shelf tidal currents

Variation in the hydrodynamics associated with cross-shelf tidal currents having a maximum speed of 1, 2 and 4 cm s^{-1} (0.1, 0.2 and 0.4 m s^{-1}) along the major axis of the tidal ellipse is also presented in Appendix D as one hourly plots of current vectors over a tidal cycle. The magnitude of the long-shelf current was maintained at 12 cm s^{-1}. Again, the patterns and dynamics of water motion around the reef remained essentially unchanged over this range of current speeds, except that the eddy circulation became stronger with increasing current strength. At higher current speeds, eddies extend further from the reef.

4.1.2 Entrainment of Larvae onto Reefs

The sensitivity of results related to the entrainment of larvae onto and around reefs, discussed as potential recruitment, resulting from variation in the magnitudes of the long-shelf and cross-shelf tidal currents, the distribution of habitat and diffusion coefficients are detailed below for reef type L2.

4.1.2.1 Long-shelf currents

No marked differences in the patterns of potential recruitment within a reef was evident for the different current strengths. These patterns remain the same as described in Section 3.3.1. Larval patches approaching on the offshore side of the reef centreline display highest potential recruitment, while progressively declining towards the onshore edge of the reef. Potential recruitment, when averaged over all upstream releases for each current speed, is presented in Figure 4.1. Results indicate that at higher current speeds there is also increased potential recruitment. Overall, however, the differences are not nearly as great as between release locations within a reef or between reefs of different sizes. It is not clear why potential recruitment should be lower at a current speed of 12 cm s^{-1} than 6 cm s^{-1} (Fig. 4.1). It may result from some aspect of the hydrodynamics associated with this unique combination of reef size and current strength.

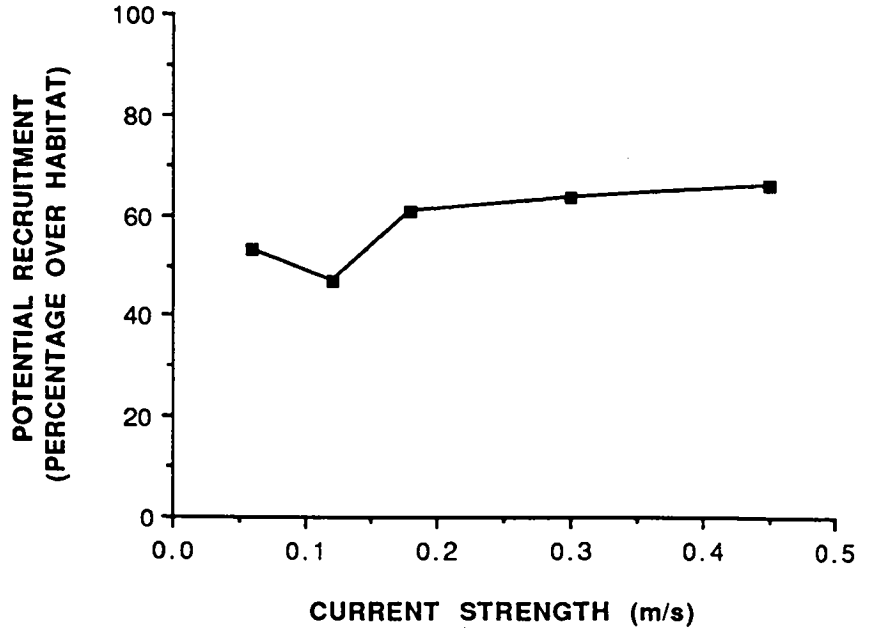


Figure 4.1 Potential recruitment, averaged over all upstream particle releases, with respect to long-shelf current strength for reef type L2.

4.1.2.2 Cross-shelf tidal currents

No marked differences in the within reef patterns of potential recruitment were evident for the different current strengths. Once again, these patterns remain essentially the same as described in Section 3.3.1. Larval patches approaching on the offshore side of the reef centreline display highest potential recruitment, while progressively declining towards the onshore edge of the reef. Potential recruitment, when averaged over all upstream releases for each maximum tidal current speed, is presented in Figure 4.2. Results show some sensitivity to the magnitude of cross-shelf tidal currents. As the maximum current speed along the major axis of the tidal ellipse is increased, so also is the tidal excursion correspondingly increased. Highest potential recruitment is associated with the smallest tidal excursion, and is consistent with the interpretation of results presented in Section 3.3.3. It is not clear why the intermediate tidal excursion should be associated with the lowest potential recruitment. Presumably, this also is related to the relatively low potential recruitment which is identified above (in Section 4.1.2.1) for this combination of reef size and current strength. Once a critical ratio between the tidal excursion and the cross-shelf extent of a reef is reached, then any further increase in the tidal excursion relative to the reef size may not result in further reduction in potential recruitment.

4.1.2.3 Distribution of habitat

Potential recruitment, when averaged over all upstream releases for each habitat distribution, is presented in Figure 4.3. Results are particularly sensitive to the distribution of habitat, and illustrate the importance of a realistic representation of habitat within the model. By extending the distribution of habitat an extra grid cell beyond the reef, the area of habitat was effectively increased by 43% for reef type L2. For smaller reefs the effective increase would be proportionally greater still and, therefore, a more marked increase in potential recruitment might be expected. On the other hand, the effective increase in area of habitat for the larger reefs would be relatively lower and, therefore, a less marked increase in potential recruitment

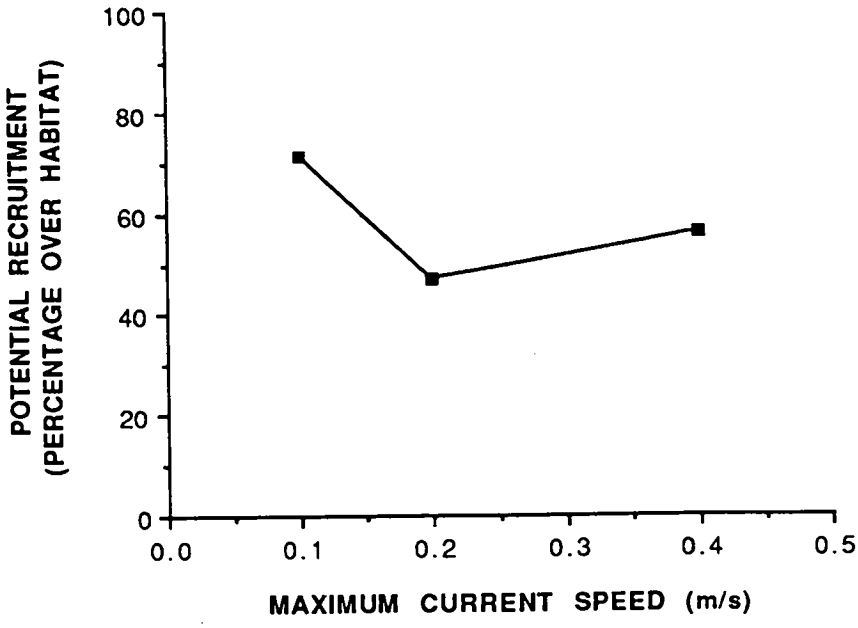


Figure 4.2 Potential recruitment, averaged over all upstream particle releases, with respect to the maximum cross-shelf tidal current speed for reef type L2.

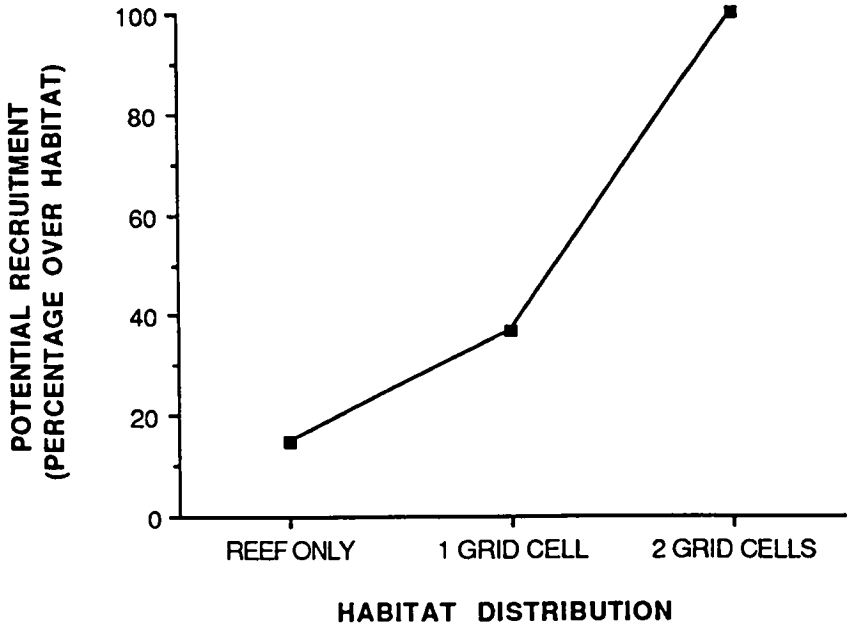


Figure 4.3 Potential recruitment, averaged over all upstream particle releases, with respect to the distribution of habitat for reef type L2.

might be expected.

Habitat was defined to extend one grid cell, 500 metres, beyond the reef edge in the present study. This is consistent with the known

distribution of crustose coralline algae, but may be greater than the distribution of habitat around some reefs. Moran (1986) reports that outbreaks often appear to have begun from recruitment off the reef edge in deep water. The recruitment of species to habitats which are restricted to the reef edge or reef flat may be greatly reduced unless they are able to actively swim towards such areas. This is probably the case for most, if not all, fish.

4.1.2.4 Diffusion coefficients

No marked differences in the within reef patterns of potential recruitment was evident for the different diffusion coefficients. Once again, these patterns remain essentially the same as described in Section 3.3.1. Potential recruitment, when averaged over all upstream releases for each diffusion coefficient, is presented in Figure 4.4. Clearly, the results are not sensitive to variation in the diffusion coefficients over the range that was investigated.

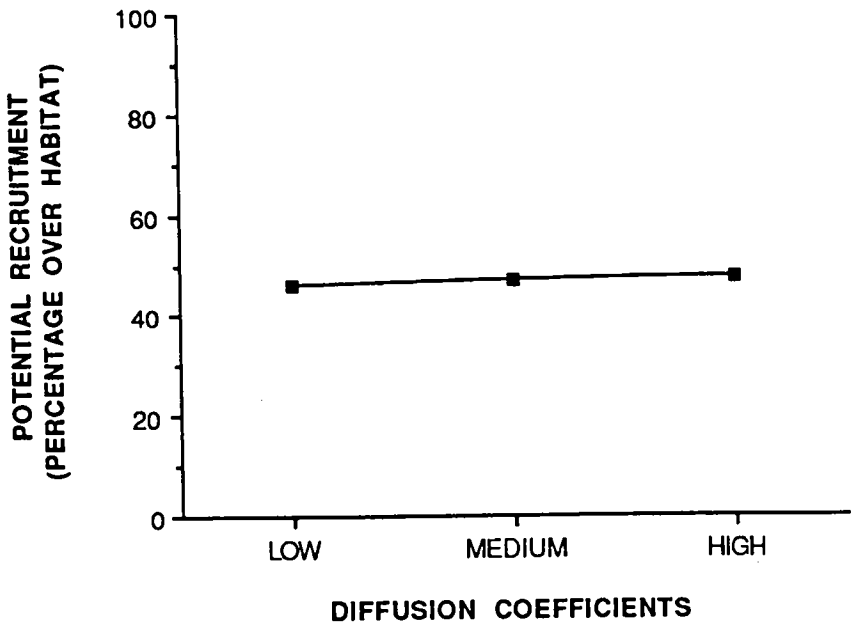


Figure 4.4 Potential recruitment, averaged over all upstream particle releases, with respect to different diffusion coefficients for reef type L2.

4.2 LARGE-SCALE HYDRODYNAMICS AND LARVAL TRANSPORT

Sensitivity analysis of large-scale hydrodynamics and larval transport have been carried out in relation to: (1) the reproducibility of results; (2) time-varying wind; (3) the larval cloud simulation; (4) the number of particles; and (5) the effects of larval mortality on and around reefs.

4.2.1 Reproducibility of Results

The patterns of connectivity which are presented in Section 3.5 were generated by simulating 40 dispersal events, based on the random selection of tide and wind records, from each selected source reef (base data). The robustness of the connectivity patterns was investigated by comparing these results for a sub-selection of eight source reefs, four from within each of the northern and central regions, with: (a) the simulation of a further 40 dispersal events from each of these reefs (replicate); and (b) analysis of all 80 dispersal events combined. The eight reefs are: Ribbon No.5, Ribbon No.2, Evening and Pickersgill Reefs in the northern region, and Opal, Norman, Michaelmas and Green Island Reefs in the central region. These particular reefs were chosen because they came from within regions and cross-shelf zones which displayed different patterns of connectivity in the previous simulations.

Results are presented for all eight reefs in Figures 4.5 to 4.12 (together with other results detailed below in this Section) and Figures 4.13 to 4.20. Results indicate that the cross-shelf and long-shelf patterns of connectivity that are identified in Section 3.5 are robust and well-founded. The patterns are adequately reproduced by any 40 randomly selected dispersal events and any increase in the sampling density does not produce a qualitatively different pattern (Figs. 4.5 to 4.12). Only for Ribbon Reef No.2 did the simulation of an additional 40 dispersal events result in a significant quantitative difference in the level of connectivity, but not to the overall patterns (Fig. 4.6).

Similarly, the relative strength of connectivity between a source reef and each of its identified sink reefs is not substantially changed

(compare 'a', 'b' and 'c' of Figs. 4.13 to 4.20) by either a different random selection of current conditions or the simulation of additional dispersal events. Only Ribbon No.2 and Pickersgill Reefs (Figs. 4.14 and 4.16 respectively) displayed some change in the relative strengths of connectivity with their sink reefs. However, differences between the actual values are not as great as suggested by the shifts in strength between the categories. As the categories are discrete, relatively small changes in the strength of connectivity can result in a reef shifting to a different strength category. This is in fact the case for both of these source reefs. As expected, the generation of additional dispersal events produces connectivity with an increased number of reefs. A statistical comparison of the base data connectivity values for each source reef with results from the simulation of all 80 dispersal events combined, using the nonparametric Wilcoxon Matched Pairs Test (Zar, 1974), showed that the differences are not significant (see Table 4.1). Only Ribbon Reef No.2 showed a marked quantitative difference in the magnitude of its connectivity with sink reefs.

Source Reef	Variables	Number of Pairs	p-level
Ribbon No.5	Base data & 80 dispersal events	30	0.876
Ribbon No.2	Base data & 80 dispersal events	21	0.079
Evening	Base data & 80 dispersal events	44	0.846
Pickersgill	Base data & 80 dispersal events	45	0.434
Opal	Base data & 80 dispersal events	53	0.254
Norman	Base data & 80 dispersal events	54	0.521
Michaelmas	Base data & 80 dispersal events	48	0.230
Green	Base data & 80 dispersal events	41	0.396

Table 4.1 Results of Wilcoxon Matched Pairs Test comparing **base data** with the analysis of **80 dispersal events.**

4.2.2 Time-varying Wind

Simulation of the current regime generated by time-varying wind is achieved through the use of a database of steady-state hydrodynamic information corresponding to a set of 88 different combinations of wind speed and direction. A twice-daily wind record is used and, in the interval between changes in the wind vector, the steady-state current field corresponding to the most recent wind reading is applied.

This method has been found to be computationally feasible for performing the large number of replicate simulations, based on different combinations of wind record and tidal phase, that are necessary to generate the base data which define the probabilistic patterns of connectivity. However, the method produces large abrupt changes in the wind forcing between records and ignores the finite time required for the hydrodynamic system to respond to a significant change in wind speed and/or direction. Alternative, but computationally expensive, approaches to this problem have been developed to assess the sensitivity of model results to changes in the modelling techniques. These are detailed below, together with simulation results.

4.2.2.1 Interpolated wind field

An initial approach to provide a more smoothly varying wind forcing was to interpolate between readings of the historical record. The simulation model was modified to examine the effect of using hourly wind speed and direction inputs rather than twelve hourly inputs. Hourly inputs were obtained by linear interpolation between the twelve hourly wind speed and direction records. Unfortunately, the interpolated wind record produced combinations of categories for which wind forcing files had not originally been produced. In view of the need to maintain the same database, it was decided to use a different approach, in which interpolation was performed between the existing current vectors on individual particles directly.

This alternative approach is computationally far more expensive. It

involved obtaining the wind forcings as current vectors on each particle at the appropriate point (p1) in the twice daily wind record, then obtaining the wind forcings on the same particles at the next point (p2) in the wind record and interpolating between these two sets of forcings. The particle movement process is then continued, using the appropriate interpolated forcing.

The robustness of the connectivity patterns (base data), which are presented in Section 3.5, was investigated by comparing these results with the simulation of 40 dispersal events using an interpolated wind field based on the same random selection of tide and wind records. Four source reefs were selected: Ribbon No.5 and Evening Reefs in the northern region, and Opal and Green Island Reefs in the central region.

Results are presented in Figures 4.5, 4.7, 4.9 and 4.12 (together with other results detailed above and below in this Section) and 'd' of Figures 4.13, 4.15, 4.17 and 4.20 for Ribbon No.5, Evening, Opal and Green Island Reefs respectively. Again, results indicate that the cross-shelf and long-shelf patterns of connectivity that were identified in Section 3.5 are robust. Similarly, the relative strength of connectivity between a source reef and each of its identified sink reefs remains substantially unchanged (compare 'a' and 'd' of Figs. 4.13, 4.15, 4.17 and 4.20). Only minor differences in the identity of sink reefs and the relative magnitude of connectivity are observed. A statistical comparison of the base data connectivity values for each source reef with results from the simulation of a further 40 dispersal events incorporating an interpolated wind field, using the Wilcoxon Matched Pairs Test, showed that the differences are not significant (see Table 4.2).

Comparison of individual particle trajectories is presented in Figures 4.21 and 4.22. While there may often be little or negligible difference between a base data trajectory and one simulated using an interpolated wind field (Fig. 4.21), trajectories indicate that in some cases there can be a substantial difference (Fig. 4.22). These results confirm the need to incorporate an historical wind record with more frequent sampling, particularly where accurate simulation of the

spawning and dispersal of specific populations in a given season is required.

4.2.2.2 Response time of the hydrodynamic system

Simulation of the current regime, which is generated by time-varying wind, is achieved through the use of a database of steady-state hydrodynamic information. This method ignores the finite time required for the hydrodynamic system to respond to a significant change in wind speed and/or direction. Estimation of the response time of the hydrodynamics - the time required for the wind-driven currents to respond to abrupt changes in the wind speed and direction - has been used to develop a 'weighted moving average' of the current at any point in time. In this way, the current will reflect the recent wind history, rather than the instantaneous wind.

An empirical study of the time dependent nature of water velocities generated by a varying wind field (L. Bode, pers. comm.) has shown, under certain simplifying assumptions, that the water velocity at a point is determined by:

$$S(t) = S_o-(S_o-S_i)e^{-t/T}$$

where S(t) = water velocity at time t; S_o = steady state velocity of water, i.e. water velocity induced by a constant wind velocity after large t; S_i = current velocity at t = 0; and T = e-folding period, i.e. response time for water velocity to reach 0.632 of steady state velocity.

The incorporation of time dependent water velocities into the model has required an estimation of T for all grid points, as the response time will be a function of depth. Estimation of T was available through the SURGE programme (Sobey et al., 1977) and achieved by monitoring the time taken for currents to reach steady state at a range of water depths over the model grid. A typical value for T is approximately 14 hours in 30 metres of water.

The resulting simulation of larval dispersal is based on the interpolated wind field database. Differences in connectivity when compared with the base data result from a combination of both sources of variation.

The effect of incorporating the response time of the hydrodynamic system was investigated by simulating 40 dispersal events for the same four reefs used in testing the interpolated wind field under the same sequence of current conditions: Ribbon No.5 and Evening Reefs in the northern region, and Opal and Green Island Reefs in the central region. Subsequently, simulations were performed for an additional two reefs, Norman and Michaelmas, for which no interpolated wind field analysis has been performed.

Results are presented in Figures 4.5, 4.7, and 4.9 to 4.12 (together with other results detailed above and below) for Ribbon No.5, Evening, Opal, Norman, Michaelmas and Green Island Reefs respectively. Results indicate that the incorporation of time dependent water velocities into the model can substantially alter the cross-shelf and long-shelf patterns of connectivity. This is evident for Ribbon Reef No.5 (Fig. 4.5b) and, to a lesser extent, Norman Reef (Fig. 4.10b) in the long-shelf patterns of connectivity, and Opal Reef (Fig. 4.9a) in the cross-shelf patterns of connectivity. Ribbon Reef No.5 displays a marked increase in connectivity with itself and a corresponding decrease in connectivity with sink reefs lying to both the north and south, while Norman Reef displays a marked increase in connectivity with sink reefs lying to the north when compared with the base data. Opal Reef displays a marked increase in connectivity with inner matrix sink reefs and a corresponding decrease in connectivity with central matrix sink reefs when compared to the base data. The patterns of connectivity otherwise remain essentially unchanged. These differences do not in any way invalidate the patterns of connectivity identified in Section 3.5. Rather, they suggest that the cross-shelf asymmetry within the central portion of the Cairns Section and the role of large passages such as Trinity Opening and Grafton passage in transporting larvae onshore across the shelf may be greater than previously thought. Clearly though, the effect of

incorporating the inertia of the water mass requires further investigation.

The relative strengths of connectivity between a source reef and each of its identified sink reefs are presented in 'e' of Figures 4.13, 4.15, 4.17 and 4.20 for Ribbon No.5, Evening, Opal and Green Island Reefs respectively, and 'd' of Figures 4.18 and 4.19 for Norman and Michaelmas Reefs respectively. All source reefs display some variation in the identity and strength of connectivity with sink reefs when compared with the base data. The variation in long-shelf connectivity that is identified in Figure 4.5b for Ribbon Reef No.5 is also evident in Figure 4.13e. However, in most cases the reefs with strongest connectivity remain the same. A statistical comparison of the base data connectivity values for each source reef with results from the simulation of a further 40 dispersal events incorporating the response time of the hydrodynamic system, using the Wilcoxon Matched Pairs Test, showed that the differences are not significant (see Table 4.2).

The domain of influence for all source reefs also remains largely unchanged, except for some of the more distant sink reefs with weak connectivity that are absent. This is also illustrated by comparison of Figures 4.23 and 4.24 for Opal Reef in which the trajectories of all dispersal events are presented for the base and response time data respectively.

Source Reef	Variables	Number of Pairs	p-level
Ribbon No.5	Base data & interpolated	30	0.983
Ribbon No.5	Base data & response time	30	0.126
Evening	Base data & interpolated	44	0.662
Evening	Base data & response time	44	0.756
Opal	Base data & interpolated	53	0.854
Opal	Base data & response time	53	0.473
Norman	Base data & response time	54	0.933
Michaelmas	Base data & response time	48	0.572
Green	Base data & interpolated	41	0.713
Green	Base data & response time	41	0.174

Table 4.2 Results of Wilcoxon Matched Pairs Test comparing **base data** with the simulation of 40 dispersal events using an **interpolated** wind field and incorporation of the **response time** of the hydrodynamic system.

4.2.3 Larval Cloud Simulation

The simulation of each dispersal event is represented as a larval cloud consisting of seven particles. The larval cloud is assumed initially to be hexagonal, with a major axis of 0.5 nautical miles. The robustness of the patterns of connectivity which are presented in Section 3.5 was investigated by comparing these results for the same sub-selection of eight source reefs (Ribbon No.5, Ribbon No.2, Evening, Pickersgill, Opal, Norman, Michaelmas and Green Island) with the simulation of 40 dispersal events using two alternative sized larval clouds: (a) a small larval cloud with a major axis of 0.25 nautical miles; and (b) a large larval cloud with a major axis of 0.75 nautical miles. Both larval clouds retained the same hexagonal arrangement of particles and the dispersal events were simulated using the same sequence of current conditions.

Results are presented in Figures 4.5 to 4.12 (together with other results detailed above in this Section), 'd' and 'e' of Figures 4.14 and 4.16, 'e' and 'f' of Figures 4.18 and 4.19, and 'f' and 'g' of Figures 4.13, 4.15, 4.17 and 4.20. These results indicate that the cross-shelf and long-shelf patterns of connectivity are robust and that variation in the initial size of the larval cloud will not provide a qualitatively different pattern (Figs. 4.5 to 4.12). Similarly, the relative strength of connectivity between a source reef and each of its identified sink reefs remains substantially unchanged (compare with 'a' for Figs. 4.13 to 4.20). Some variation between relative strength categories is evident. However, once again, differences between the actual values are not as great as suggested by the shifts in strength between the categories. A statistical comparison of the base data connectivity values for each source reef with results from the simulation of a further 40 dispersal events represented by a small and large larval cloud, using the Wilcoxon Matched Pairs Test, showed that the differences are not significant (see Table 4.3).

Source Reef	Variables	Number of Pairs	p-level
Ribbon No.5	Base data & small larval cloud	30	0.687
Ribbon No.5	Base data & large larval cloud	30	0.717
Ribbon No.2	Base data & small larval cloud	21	0.861
Ribbon No.2	Base data & large larval cloud	21	0.715
Evening	Base data & small larval cloud	44	0.623
Evening	Base data & large larval cloud	44	0.127
Pickersgill	Base data & small larval cloud	45	0.675
Pickersgill	Base data & large larval cloud	45	0.900
Opal	Base data & small larval cloud	53	0.491
Opal	Base data & large larval cloud	53	0.481
Norman	Base data & small larval cloud	54	0.264
Norman	Base data & large larval cloud	54	0.361
Michaelmas	Base data & small larval cloud	48	0.781
Michaelmas	Base data & large larval cloud	48	0.985
Green	Base data & small larval cloud	41	0.329
Green	Base data & large larval cloud	41	0.796

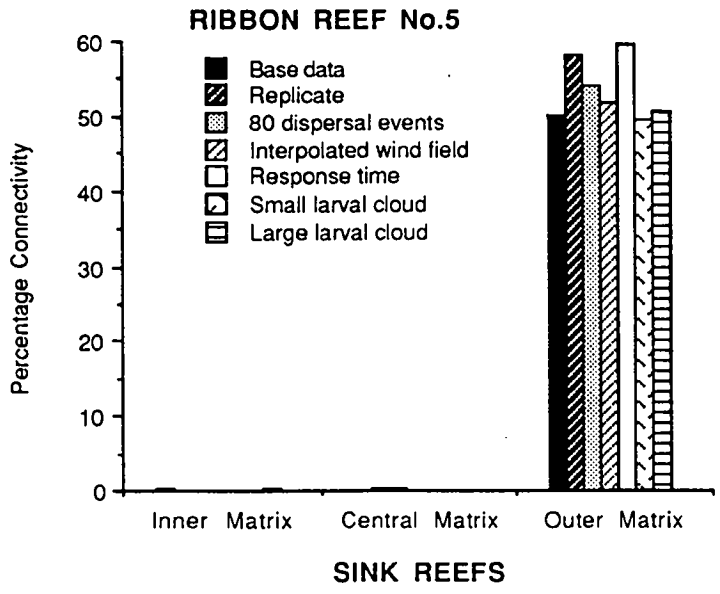
Table 4.3 Results of Wilcoxon Matched Pairs Test comparing **base data** with the simulation of 40 dispersal events represented by a **small larval cloud** and a **large larval cloud**.

4.2.4 Number of particles

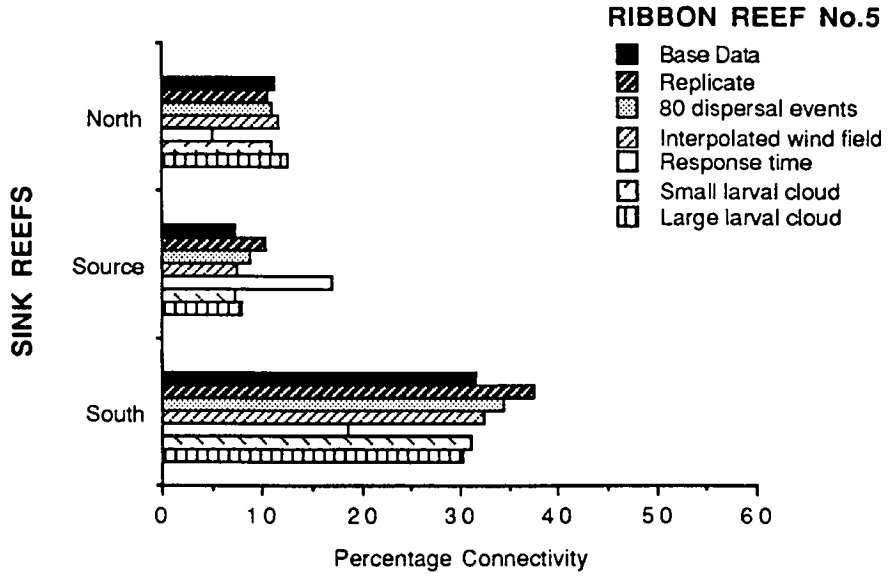
The larval cloud is represented by seven particles, the movements of which are tracked and intersections with reefs recorded. The sensitivity of model results to the number of particles representing the larval cloud was investigated by simulating twenty randomly selected dispersal events from Opal Reef using seven, thirteen and twenty five particles under the same sequence of current conditions. Only twenty dispersal events were simulated because of limitations in computer speed and storage.

Results are presented in Figures 4.25 and 4.26. They show no marked or consistent differences in the patterns of cross-shelf and long-shelf connectivity as a result of increasing the number of particles which represent the larval cloud (Fig. 4.25). Similarly, the relative strength of connectivity between the source reef and each of its identified sink reefs remains substantially unchanged (Fig. 4.26). Only very minor variation in relative strength categories is evident.

The trajectories of 7, 13 and 25 particles representing a single dispersal event from Opal Reef are presented in Figures 4.27 to 4.29

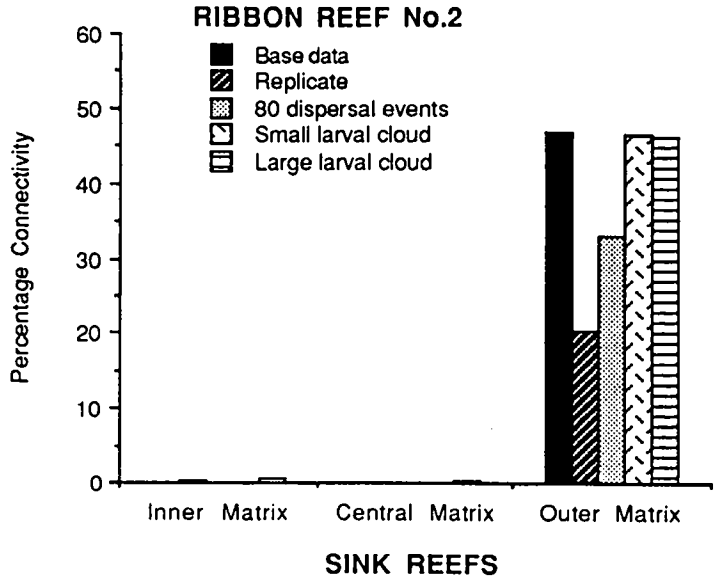


(a) Level of reef connectivity with respect to the cross-shelf transport of larvae from Ribbon Reef No.5. Sink reefs are classified as lying along the outer edge of the reef matrix and continental shelf (outer matrix), central within the reef matrix (central matrix) and along the inner edge of the reef matrix bordering the main lagoon (inner matrix).

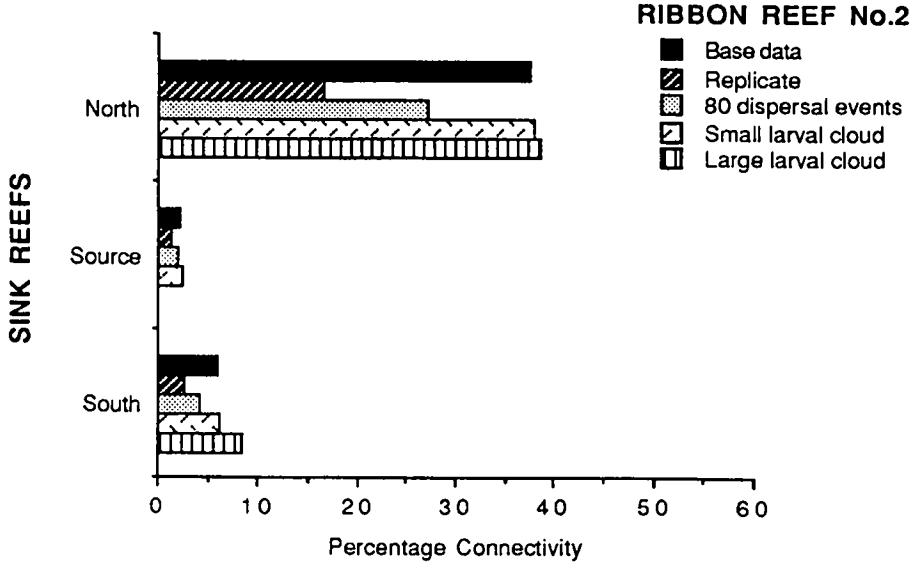


(b) Level of reef connectivity with respect to the long-shelf transport of larvae from Ribbon Reef No.5. Sink reefs are classified as lying to the north or south with respect to the source reef, or recruitment back onto the parent reef (source).

Figure 4.5 Data are presented for seven analyses and represent the number of particles that intersect with sink reefs, expressed as a percentage of the total number of particle trajectories simulated. The seven analyses correspond to: (1) **base data** derived from 40 randomly selected dispersal events with which the other analyses are compared; (2) a **replicate** random selection of 40 dispersal events; (3) the **80 dispersal events** combined; (4) use of an **interpolated wind field**; (5) incorporation of the **response time** of the hydrodynamic regime; (6) initiating the 40 dispersal events with a **small larval cloud**; and (7) initiating the 40 dispersal events with a **large larval cloud**.

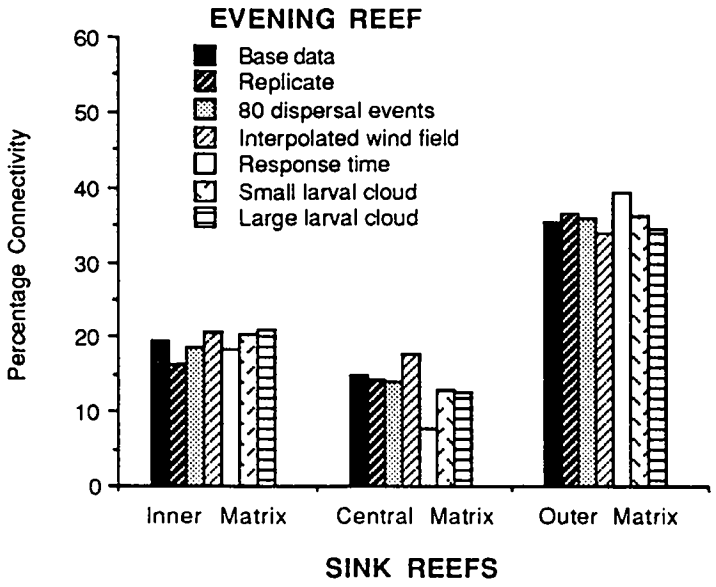


(a) Level of reef connectivity with respect to the cross-shelf transport of larvae from Ribbon Reef No.2. Sink reefs are classified as lying along the outer edge of the reef matrix and continental shelf (outer matrix), central within the reef matrix (central matrix) and along the inner edge of the reef matrix bordering the main lagoon (inner matrix).

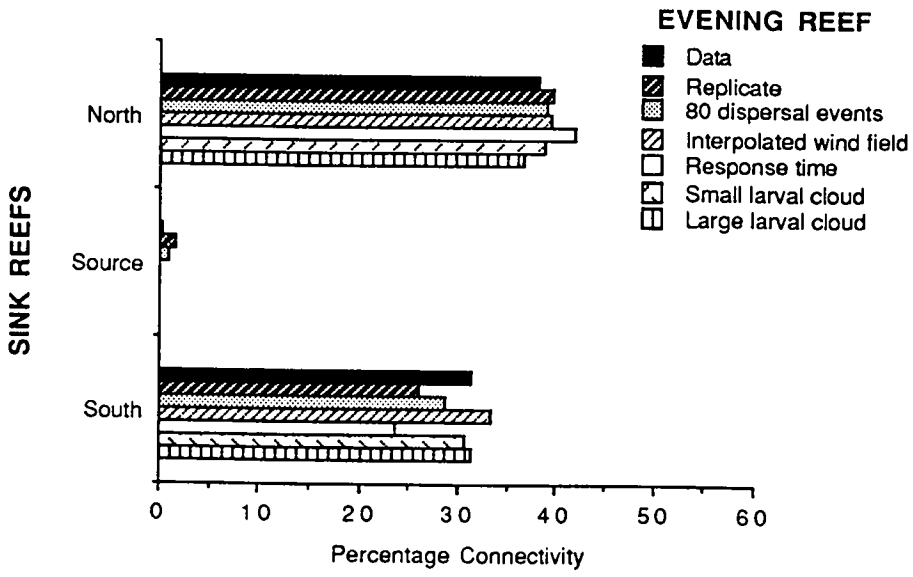


(b) Level of reef connectivity with respect to the long-shelf transport of larvae from Ribbon Reef No.2. Sink reefs are classified as lying to the north or south with respect to the source reef, or recruitment back onto the parent reef (source).

Figure 4.6 Data are presented for five analyses and represent the number of particles that intersect with sink reefs, expressed as a percentage of the total number of particle trajectories simulated. The five analyses correspond to: (1) **base data** derived from 40 randomly selected dispersal events with which the other analyses are compared; (2) a **replicate** random selection of 40 dispersal events; (3) the **80 dispersal events** combined; (4) initiating the 40 dispersal events with a **small larval cloud**; and (5) initiating the 40 dispersal events with a **large larval cloud**.

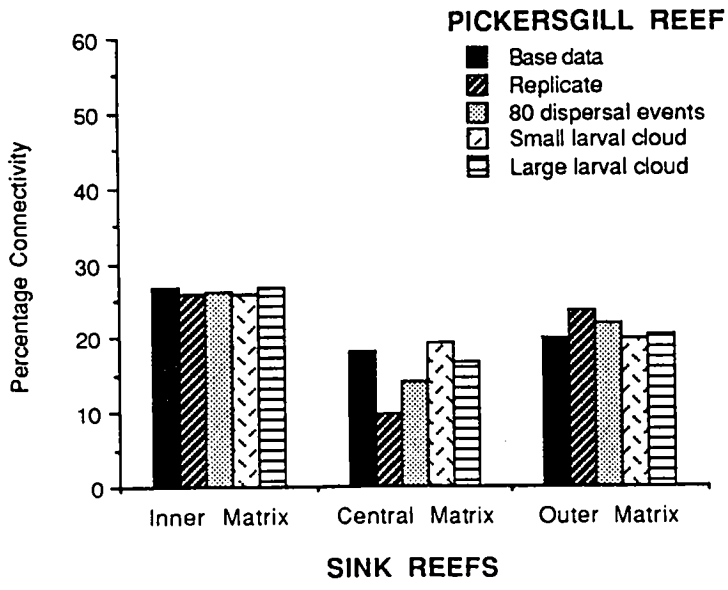


(a) Level of reef connectivity with respect to the cross-shelf transport of larvae from Evening Reef. Sink reefs are classified as lying along the outer edge of the reef matrix and continental shelf (outer matrix), central within the reef matrix (central matrix) and along the inner edge of the reef matrix bordering the main lagoon (inner matrix).

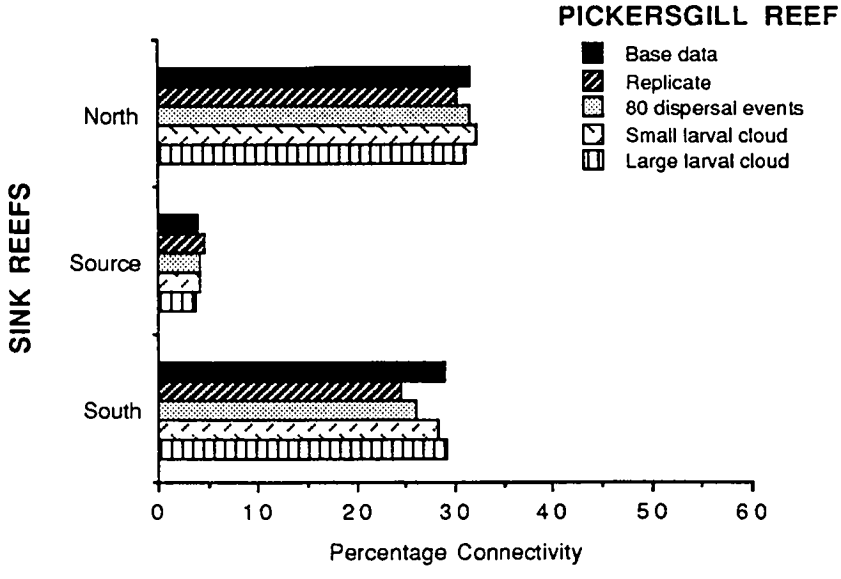


(b) Level of reef connectivity with respect to the long-shelf transport of larvae from Evening Reef. Sink reefs are classified as lying to the north or south with respect to the source reef, or recruitment back onto the parent reef (source).

Figure 4.7 Data are presented for seven analyses and represent the number of particles that intersect with sink reefs, expressed as a percentage of the total number of particle trajectories simulated. The seven analyses correspond to: (1) **base data** derived from 40 randomly selected dispersal events with which the other analyses are compared; (2) a **replicate** random selection of 40 dispersal events; (3) the **80 dispersal events** combined; (4) use of an **interpolated wind field**; (5) incorporation of the **response time** of the hydrodynamic regime; (6) initiating the 40 dispersal events with a **small larval cloud**; and (7) initiating the 40 dispersal events with a **large larval cloud**.

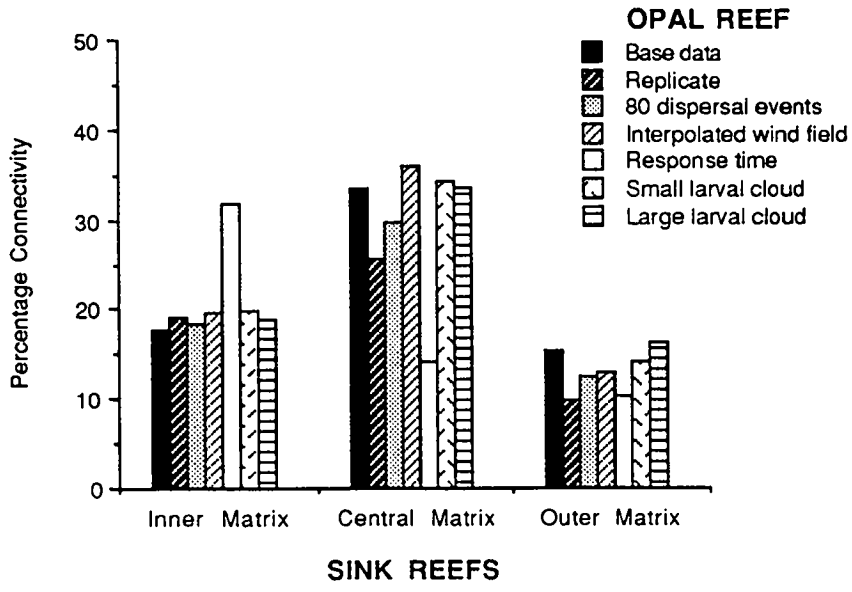


(a) Level of reef connectivity with respect to the cross-shelf transport of larvae from Pickersgill Reef. Sink reefs are classified as lying along the outer edge of the reef matrix and continental shelf (outer matrix), central within the reef matrix (central matrix) and along the inner edge of the reef matrix bordering the main lagoon (inner matrix).

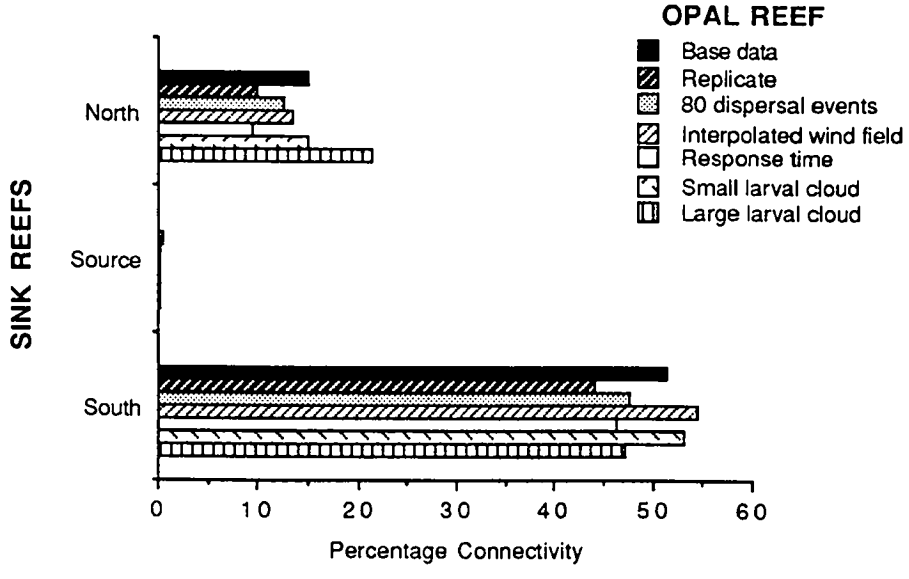


(b) Level of reef connectivity with respect to the long-shelf transport of larvae from Pickersgill Reef. Sink reefs are classified as lying to the north or south with respect to the source reef, or recruitment back onto the parent reef (source).

Figure 4.8 Data are presented for five analyses and represent the number of particles that intersect with sink reefs, expressed as a percentage of the total number of particle trajectories simulated. The five analyses correspond to: (1) **base data** derived from 40 randomly selected dispersal events with which the other analyses are compared; (2) a **replicate** random selection of 40 dispersal events; (3) the **80 dispersal events** combined; (4) initiating the 40 dispersal events with a **small larval cloud**; and (5) initiating the 40 dispersal events with a **large larval cloud**.

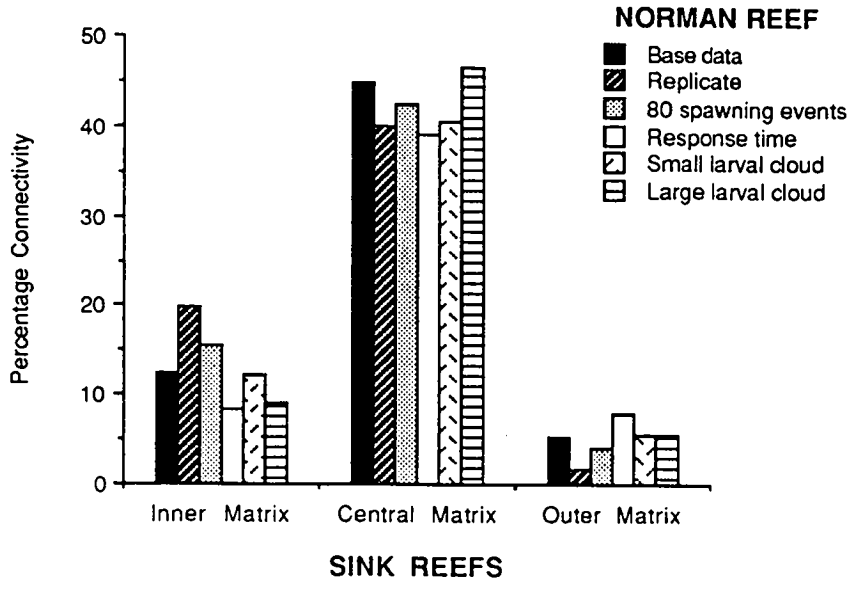


(a) Level of reef connectivity with respect to the cross-shelf transport of larvae from Opal Reef. Sink reefs are classified as lying along the outer edge of the reef matrix and continental shelf (outer matrix), central within the reef matrix (central matrix) and along the inner edge of the reef matrix bordering the main lagoon (inner matrix).

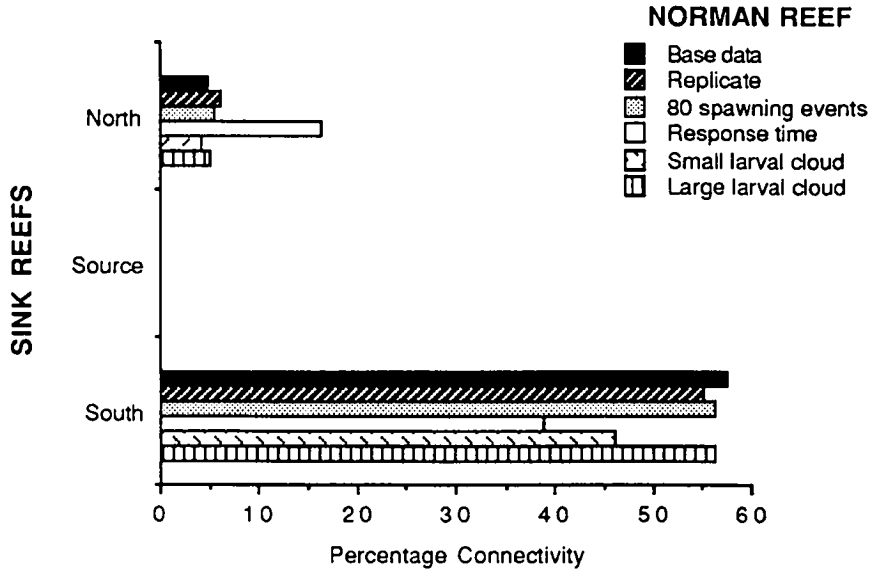


(b) Level of reef connectivity with respect to the long-shelf transport of larvae from Opal Reef. Sink reefs are classified as lying to the north or south with respect to the source reef, or recruitment back onto the parent reef (source).

Figure 4.9 Data are presented for seven analyses and represent the number of particles that intersect with sink reefs, expressed as a percentage of the total number of particle trajectories simulated. The seven analyses correspond to: (1) **base data** derived from 40 randomly selected dispersal events with which the other analyses are compared; (2) a **replicate** random selection of 40 dispersal events; (3) the **80 dispersal events** combined; (4) use of an **interpolated wind field**; (5) incorporation of the **response time** of the hydrodynamic regime; (6) initiating the 40 dispersal events with a **small larval cloud**; and (7) initiating the 40 dispersal events with a **large larval cloud**.

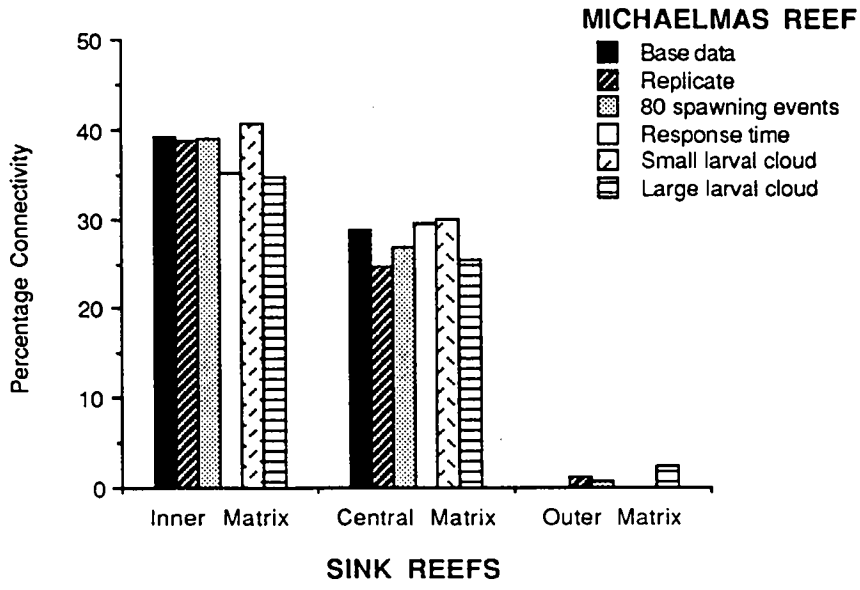


(a) Level of reef connectivity with respect to the cross-shelf transport of larvae from Norman Reef. Sink reefs are classified as lying along the outer edge of the reef matrix and continental shelf (outer matrix), central within the reef matrix (central matrix) and along the inner edge of the reef matrix bordering the main lagoon (inner matrix).

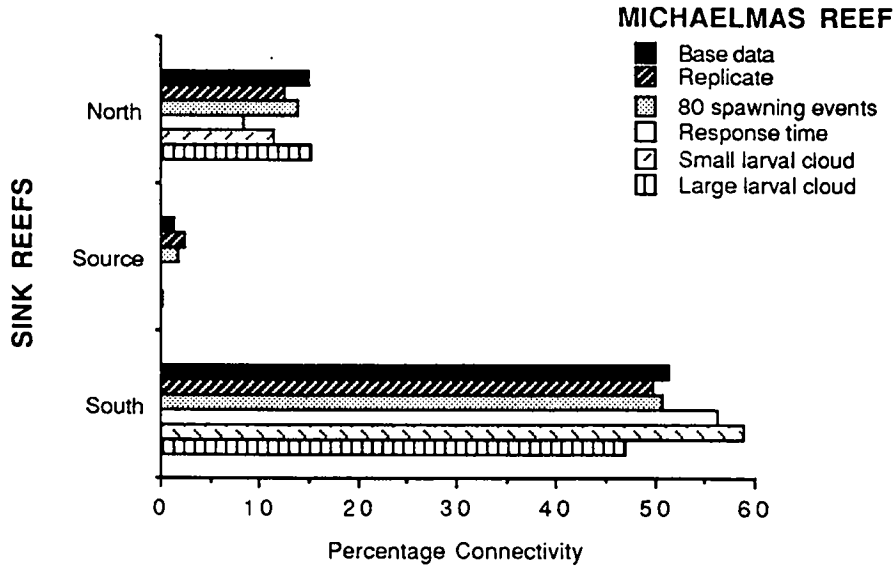


(b) Level of reef connectivity with respect to the long-shelf transport of larvae from Norman Reef. Sink reefs are classified as lying to the north or south with respect to the source reef, or recruitment back onto the parent reef (source).

Figure 4.10 Data are presented for six analyses and represent the number of particles that intersect with sink reefs, expressed as a percentage of the total number of particle trajectories simulated. The six analyses correspond to: (1) **base data** derived from 40 randomly selected dispersal events with which the other analyses are compared; (2) a **replicate** random selection of 40 dispersal events; (3) the **80 dispersal events** combined; (4) incorporation of the **response time** of the hydrodynamic regime; (5) initiating the 40 dispersal events with a **small larval cloud**; and (6) initiating the 40 dispersal events with a **large larval cloud**.

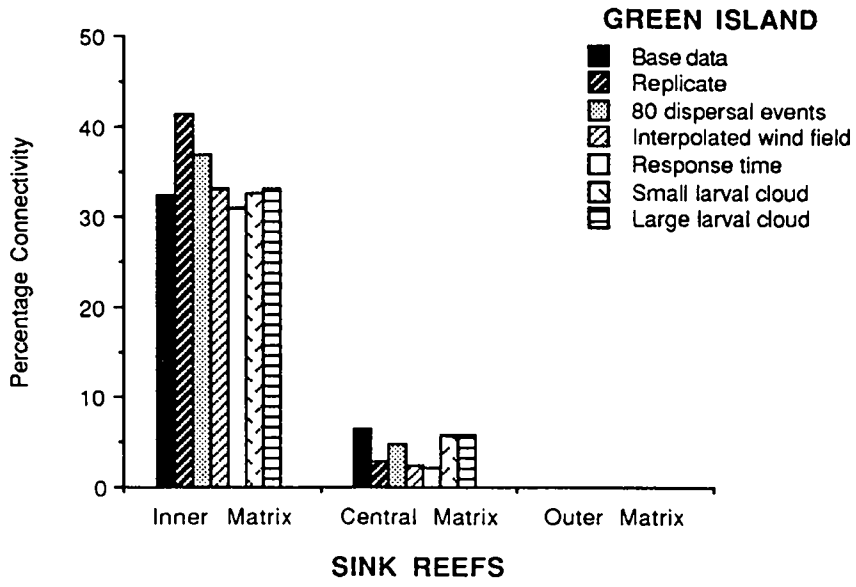


(a) Level of reef connectivity with respect to the cross-shelf transport of larvae from Michaelmas Reef. Sink reefs are classified as lying along the outer edge of the reef matrix and continental shelf (outer matrix), central within the reef matrix (central matrix) and along the inner edge of the reef matrix bordering the main lagoon (inner matrix).

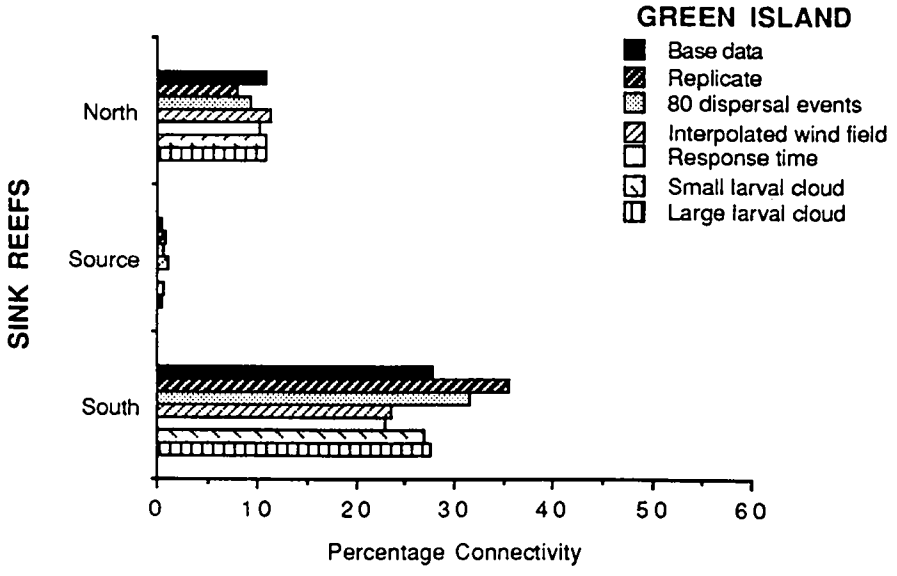


(b) Level of reef connectivity with respect to the long-shelf transport of larvae from Michaelmas Reef. Sink reefs are classified as lying to the north or south with respect to the source reef, or recruitment back onto the parent reef (source).

Figure 4.11 Data are presented for six analyses and represent the number of particles that intersect with sink reefs, expressed as a percentage of the total number of particle trajectories simulated. The six analyses correspond to: (1) **base data** derived from 40 randomly selected dispersal events with which the other analyses are compared; (2) a **replicate** random selection of 40 dispersal events; (3) the **80 dispersal events** combined; (4) incorporation of the **response time** of the hydrodynamic regime; (5) initiating the 40 dispersal events with a **small larval cloud**; and (6) initiating the 40 dispersal events with a **large larval cloud**.



(a) Level of reef connectivity with respect to the cross-shelf transport of larvae from Green Island. Sink reefs are classified as lying along the outer edge of the reef matrix and continental shelf (outer matrix), central within the reef matrix (central matrix) and along the inner edge of the reef matrix bordering the main lagoon (inner matrix).



(b) Level of reef connectivity with respect to the long-shelf transport of larvae from Green Island. Sink reefs are classified as lying to the north or south with respect to the source reef, or recruitment back onto the parent reef (source).

Figure 4.12 Data are presented for seven analyses and represent the number of particles that intersect with sink reefs, expressed as a percentage of the total number of particle trajectories simulated. The seven analyses correspond to: (1) **base data** derived from 40 randomly selected dispersal events with which the other analyses are compared; (2) a **replicate** random selection of 40 dispersal events; (3) the **80 dispersal events** combined; (4) use of an **interpolated wind field**; (5) incorporation of the **response time** of the hydrodynamic regime; (6) initiating the 40 dispersal events with a **small larval cloud**; and (7) initiating the 40 dispersal events with a **large larval cloud**.

respectively. An increase in particle density is evident without any change to the trajectory of the larval cloud as a whole. Results indicate, therefore, that the cross-shelf and long-shelf patterns of connectivity that were identified in Section 3.5 are unlikely to be significantly altered by increasing the number of particles which represent the larval cloud.

4.2.5 Mortality on Reefs

Johannes (1978) has argued that larval dispersal in coral reef fishes is an evolutionary response to intense predation pressure in their adult habitat. More recently, research by Hamner et al. (1988) indicates that predation by diurnally active reef-associated planktivorous fish is indeed intense. They estimate that approximately 500 individual planktivorous fish remove zooplankton from each cubic meter of water flowing over the reef crest. In addition, mortality due to predation by suspension feeding invertebrates, such as corals, could increase this rate substantially. The entrainment of larvae within the near-reef circulation during their pre-competent period of development, and consequent mortality from predation by reef-associated species, would affect the overall level of connectivity and could alter the patterns of connectivity.

Two scenarios were therefore investigated: that 50% and 100% of larvae encountering a reef during their pre-competent period suffered mortality from predation. Forty dispersal events were simulated from four selected reefs from within the central region and compared with the results from these same reefs which are presented in Section 3.5 (base data) using the same random selection of tide and wind records. The four reefs are: Opal, Norman, Michaelmas and Green Island.

Results are presented with respect to the cross-shelf and long-shelf patterns of connectivity in Figures 4.30 to 4.33 for Opal, Norman, Michaelmas and Green Island Reefs respectively. Results indicate that the cross-shelf and long-shelf patterns of connectivity that were identified in Section 3.5 are robust. However, the level of connectivity is substantially modified by both the 50% and 100% mortality

scenarios. This is particularly true for Opal, Norman and Michaelmas Reefs (Figs. 4.30 to 4.33) where the levels of connectivity are reduced by approximately 50% and 75% for the two scenarios respectively. Larvae originating from these reefs are predicted to be transported through the reef matrix and to frequently encounter other reefs during their pre-competent period of development. The level of connectivity with respect to Green island (Fig. 4.33) shows less modification by this source of mortality. Green Island, in contrast to the other reefs, lies adjacent to the main lagoon and it is probable that larvae originating from this reef will be less likely to encounter another reef during their pre-competent period of development as they are commonly transported alongshore within the main lagoon (see Fig. 3.63).

The relative strengths of connectivity between a source reef and each of its identified sink reefs remains substantially unchanged (see Appendix E). However, minor differences in the identity of sink reefs and the relative magnitude of connectivity are observed. In general, with increasing mortality from this source there appears to be a corresponding reduction in the relative strengths of connectivity and the number of sink reefs. Results (not presented) show that the potential recruitment from individual dispersal events may be more dramaticaly influenced by mortality during the pre-competent period than is apparent from the summary results which integrate many dispersal events. Under certain circumstances, a larval cloud may become almost entirely depleted prior to reaching competence to settle as a consequence of mortality from this cause.

4.2.6 Summary and Conclusions

Results indicate that the cross-shelf and long-shelf patterns of connectivity that were identified in Section 3.5 are, in general, robust. The patterns are adequately reproduced by any 40 randomly selected dispersal events and an increase in the sampling density will not produce a qualitatively different pattern. Similarly, an increase in the number of particles representing the larval cloud or the incorporation of mortality from predation by reef-associated species is unlikely to significantly alter the patterns of connectivity.

While alternative approaches to simulating the dynamics of water motion and the initial size of the larval cloud do not significantly alter the patterns of connectivity, they provide important insights into the future direction of research if models capable of predicting the fate of larvae under specific sets of conditions are to be developed. The most important of these is the use of a time-interpolated wind record and the incorporation of the inertia of the water mass into the model. Clearly, results based on models which use steady-state forcings entirely may not be appropriate for some applications. The dynamics of water motion appear to have a particularly important influence on the dispersal of larvae and reef connectivity.

Differences in particle trajectories and reef connectivity when time-varying wind conditions are taken more fully into account may result from a number of causes. At times when there is a large abrupt change in both wind speed and direction of relatively short duration, and when there are relatively small shifts in wind direction resulting from a land-sea breeze effect, the present model may generate current reversals which are not present under real conditions. It is possible, therefore, that the model generates more current reversals than would be evident from a current record. This is in spite of the fact that the wind record that was chosen, from the Low Isles, was considered to be less affected by the land-sea breeze phenomenon than other wind records that were available. Recently, Serate (1988) has shown, by vector correlation analysis of wind data from seventeen weather stations off the North Queensland coast, that wind records from Willis Island and, in particular, Flinders Reef are more representative of the Cairns and Central Sections of the Marine Park as a whole than records from the Low Isles. Wind records from these off-shore locations would not be affected by the land-sea breeze phenomenon. A wind record with more frequent sampling (3 hourly), probably from Willis Island, will be incorporated into the dispersal model for future applications.

Also, relatively small cross-shelf differences in the location of a patch of larvae due to differences in the time-dependent water velocities can, at a critical time and location, result in very different trajectories

for the larval cloud. This is illustrated in Figure 4.22 where the larval trajectory is directed to one side or the other of a reef complex. It appears also that the maximum distances over which larvae are transported are reduced under the more stringent time-varying wind conditions, but that this affects only the more distant sink reefs with the weakest connectivity.

It is evident from the results of larval cloud simulations that the development of dispersal models which are able to predict the fate of larvae under a specific set of conditions will also need to resolve the fine-scale circulation around the source reef. This will provide a more realistic distribution of larvae as they are advected away from their source reef and thus result in a better description of reef connectivity.

Mortality on reefs caused by predation by reef-associated invertebrates and fish could have significant implications for the effectiveness of particular reefs as sources of larvae, and therefore the population dynamics of reef species. Reefs which are located such that most of their larvae are not subjected to predation by reef associated planktivores during the pre-competent period may make a major contribution to large recruitment events. In contrast, reefs which are located such that their larvae are more likely to encounter and become entrained within the near-reef circulation of other reefs during their pre-competent period may contribute significantly fewer recruits to reef communities as a whole. Mortality on reefs caused by predation by reef-associated invertebrates and fish is likely to add a further source of variability to recruitment patterns and population abundance.

4.3 THE APPROXIMATION OF PHYSICAL PROCESSES

The following areas are identified where approximations, which could potentially result in differences in larval transport, have been made within the models, yet no sensitivity analysis has been conducted. The sensitivity of model results to these areas was considered to be beyond the scope of this thesis. It is intended, however, to pursue

these areas of research in the future. Some are analyses are currently underway by other graduate students.

4.3.1 Grid Scale

The simulation of larval dispersal over large spatial and temporal scales that was required for this project necessitated considerable computational speed and storage. Limitations did not permit resolution of the large-scale hydrodynamics at a finer grid scale than 5 nautical miles. Recognizing the limitations of such a coarse resolution of the hydrodynamics within a particularly complex region, the fine-scale patterns of circulation and the entrainment of larvae onto reefs were parameterized (see Section 3.4). Particle trajectories in the coarse-scale model can be seen to respond to mainstream circulation and the divergence of the water body around reefs (e.g. see Fig. 4.22). At a finer scale of resolution, there would probably be greater divergence between particles within a larval cloud. This could possibly result in connectivity being distributed over more reefs. At this stage, however, there is no reason to consider that the large-scale patterns of larval dispersal and reef connectivity would be substantially altered. The sensitivity of particle trajectories to the grid scale is presently being investigated with funding from COTSREC.

4.3.2 East Australian Current

The East Australian Current (EAC) has been incorporated into the model as steady-state forcing. Bifurcation of the westward flowing component from the Coral Sea is positioned near latitude 15^{o}S, slightly to the south of Cooktown (see Fig.3.14). Church (1987) notes, though, that the point of bifurcation is not fixed but moves along the coast during the year between approximately latitude 18^{o}S and 14^{o}S. His data show that during the period when the larvae of *A. planci* disperse (December to March) the point of bifurcation may lie between latitudes 15^{o}S and 14^{o}S. By May, the bifurcation may extend as far south as latitude 18^{o}S. Wolanski and Pickard (1985) note, also, that the magnitude of the current over the continental shelf which they attribute to the EAC may vary both seasonally and from year to year. Neither variation in the point of bifurcation nor

current strength is likely to have a significant influence on the patterns of connectivity that have been identified. Inter-annual variability could, however, alter the distances over which larvae are transported.

4.3.4 Non-linear Interactions between the Hydrodynamic Forcing Components

The net water transport within the large-scale dispersal model is found by linear superposition of the three transport components, tides, wind and EAC, which are output from SURGE. Bode and Mason (unpublished report, 1988) have shown that, even in relatively deep water (30 m), non-linear interactions between the tidal and wind-driven components can be significant. They found that there was a general tendency for the non-linear interactions to suppress net wind-driven currents within the Capricorn Passage. Wolanski et al. (1988) similarly identified a strong non-linear interaction between tidal and low-frequency currents within the Torres Strait. In both cases, however, tidal and wind-driven currents were directed along the same axis, thus increasing the magnitude of the interaction. This situation is not representative of the Cairns Section and most of the Central Section of the GBR Marine Park. Non-linear interactions within these areas are unlikely to be as significant, except in the relatively shallow water around reefs where model results have incorporated such interactions. Only within the main lagoon of the southern portion of the Central Section are tidal and wind-driven currents directed along the same axis. Failure to incorporate non-linear interactions at the large-scale may signify that the maximum distances over which larvae are predicted to be transported are overestimated, particularly in the southern portion of the Central Section. However, this need not alter the patterns and levels of connectivity or the identity of sink reefs to any significant degree. The results of Bode and Mason do, nevertheless, indicate the importance of including such effects into future models of larval dispersal.

4.3.5 Diffusion/dispersion.

The relative dispersion of model particles within a larval cloud occurs as a result of spatial variation in the horizontal velocity field alone, except near reefs where vertical shear and eddy diffusion have been incorporated into the fine-scale models. At the large-scale, shear dispersion will also result from variation in the vertical velocity profile. Vertical shear is recognized to be significantly greater than eddy diffusion, and will be greatest for particles distributed throughout the water column.

At the fine-scale, the complex circulation around reefs appears to cause material within its influence to be well mixed horizontally. Analytical and numerical models of particle retention around reefs indicate that the mixing results in an exponential decay of the number of larvae remaining on a reef after release (Black et al., 1990). The consequences of this to a patch of larvae entering the reef's domain of influence may be to alter the average long-shelf velocity of those larvae. In addition, the relative dispersion of larvae within a patch will be increased, both across the shelf due to tidal currents and along the shelf due to retention of a proportion of the larval patch. This process is evident in Figures 3.24 to 3.29.

Parslow and Gabric (1989) observe that the relative diffusion/ dispersion of larvae within a patch will affect the mean and variance of larval density and variability in recruitment within and between reefs. While the importance of incorporating a more realistic representation of diffusion/dispersion processes is considered to be a high priority, it was beyond the scope of this project and worthy of a research programme in its own right. The objective of the dispersal models was directed primarily towards the displacement of the centre of mass of the patch as a whole. As such, while a more realistic representation of diffusion/ dispersion processes may result in a slightly different relative distribution of larvae between reefs from a single patch, it is unlikely to result in patterns of connectivity which are substantially different from those presented in Section 3.5.

4.4 MODEL VALIDATION AND TESTING

The dispersal model which has been developed in the context of this research programme is probabilistic in its interpretation of larval dispersal and reef connectivity. The patterns of reef connectivity result from the integration of dispersal events over many years. As such, the model results that have been presented cannot be tested directly or experimentally by the collection of field data from only few reefs over a short time period. Nor are many conventional statistical analyses applicable. The most appropriate method of validation and testing of model results is by hypothesis formulation.

The hydrodynamic models SURGE and 2DD have both been calibrated and their outputs verified against field measurements. These models are based on well understood physical principals. Within the context of this research, outputs from SURGE which drive the dispersal model have been validated against field observations (see Section 3.1). Limitations and approximations are discussed above in this chapter.

Validation of the dispersal model is less simple. Various hypotheses are presented in the following chapter which can be tested by appropriately designed sampling programmes. These include: (1) identification of the source of outbreak populations of *A. planci* which have been observed south from Green Island during both episodes of activity within the GBR; (2) relatively higher densities of larvae within the main lagoon south of Cairns than further offshore; (3) relatively higher levels of recruitment of species with pelagic larvae to reefs bordering the main lagoon when compared to reefs lying further offshore; and (4) the southward spread of *A. planci* populations south of Green Island. These hypotheses require certain caveats, and are discussed in more detail in the following chapter.

Data already exist which provide support for all four hypotheses. Their significance, however, lies in the fact that they provide a physical explanation for many observations which have been documented in the literature. The testing of more specific predictions could be achieved by modification of the existing model to simulate

dispersal and recruitment over single seasons and individual dispersal events. Research with these goals is currently in progress. The *Acanthaster* phenomenon lends itself to such testing as populations within the Cairns Section of the GBR Marine Park are presently in low densities and, therefore, future population increases can be monitored by an appropriately designed programme and the paths of outbreaks determined and compared with model predictions.

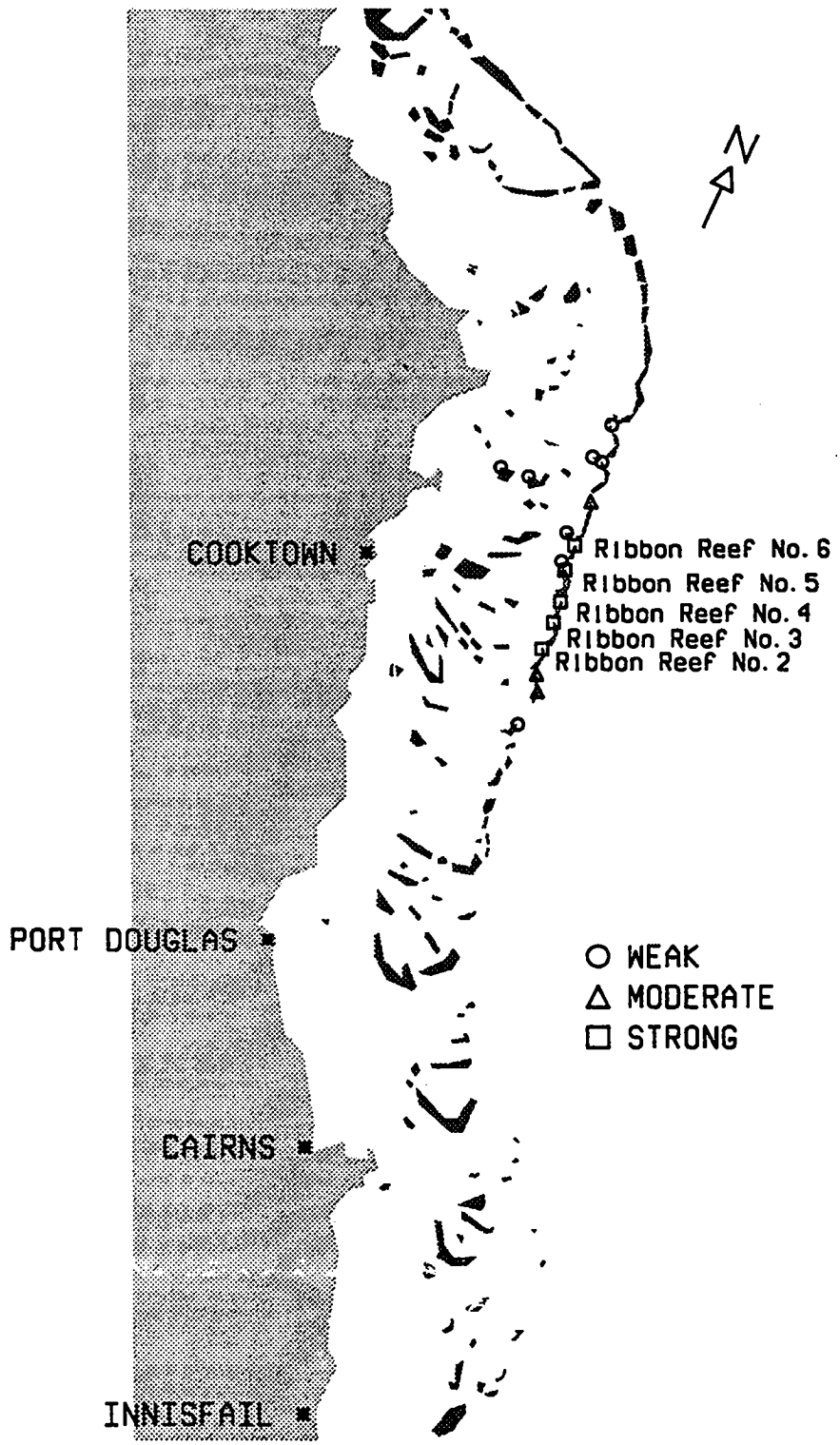


Figure 4.13a Strength of connectivity with respect to Ribbon Reef No.5. The relative strengths (weak, moderate and strong) are discrete classes separated by an order of magnitude and correspond to the base data. Scale: 1cm = 12 nautical miles.

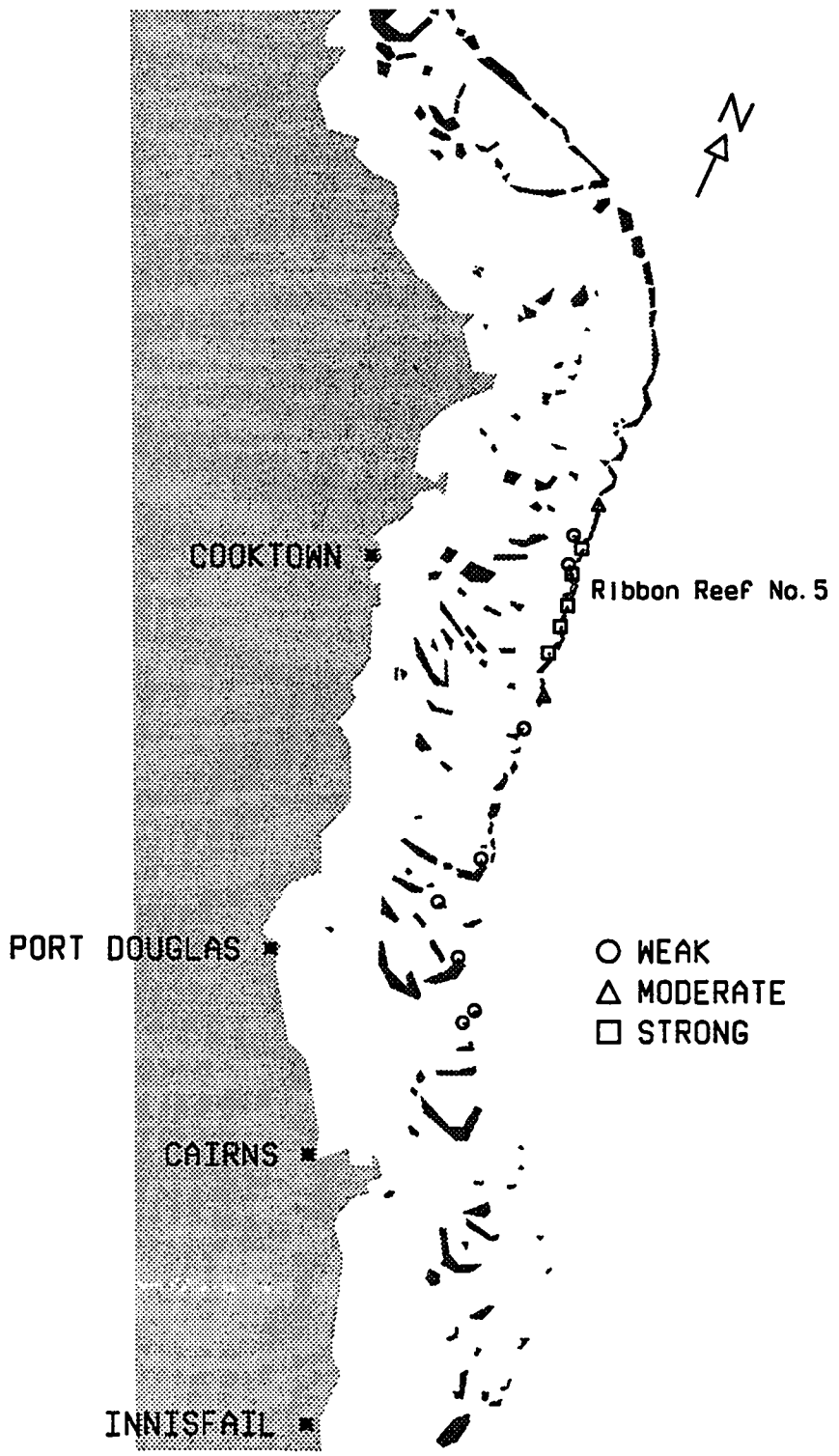


Figure 4.13b Strength of connectivity with respect to Ribbon Reef No.5. The relative strengths (weak, moderate and strong) are discrete classes separated by an order of magnitude and correspond to the replicate 40 dispersal events. Scale: 1cm = 12 nautical miles.

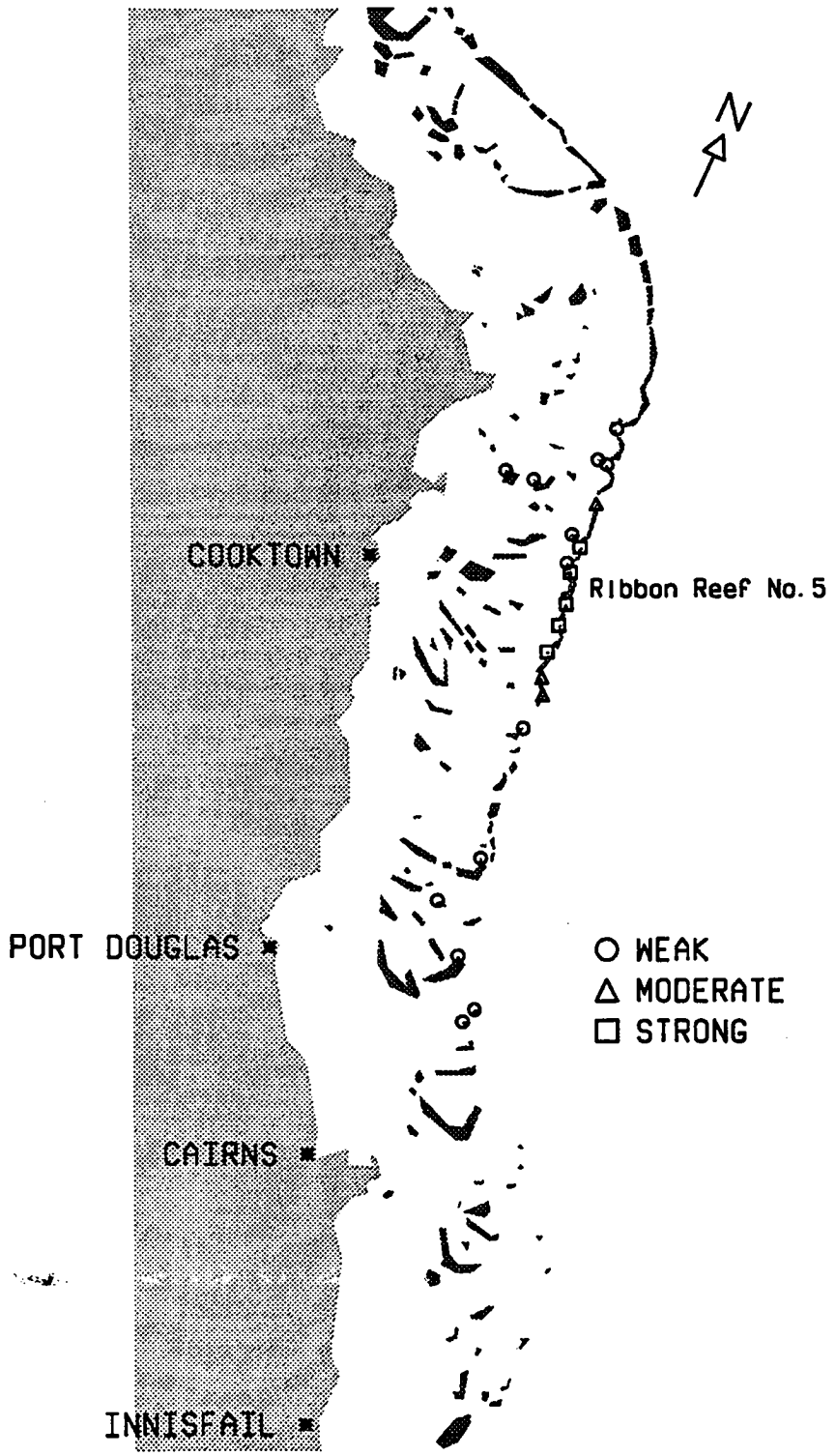


Figure 4.13c Strength of connectivity with respect to Ribbon Reef No.5. The relative strengths (weak, moderate and strong) are discrete classes separated by an order of magnitude and correspond to the combined **80 dispersal events**. Scale: 1cm = 12 nautical miles.

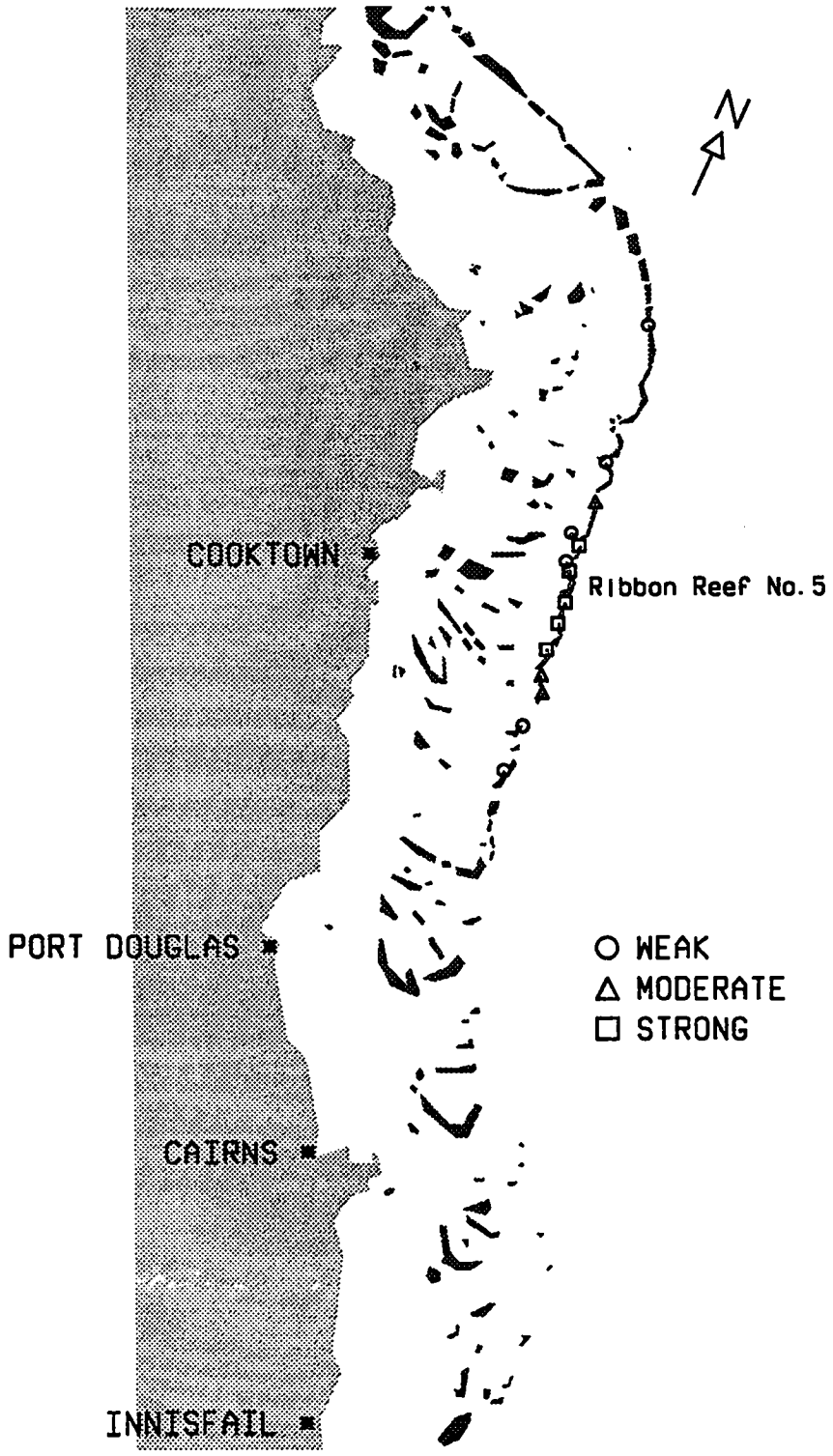


Figure 4.13d Strength of connectivity with respect to Ribbon Reef No.5. The relative strengths (weak, moderate and strong) are discrete classes separated by an order of magnitude and correspond to the **interpolated wind field** analysis. Scale: 1cm = 12 nautical miles.

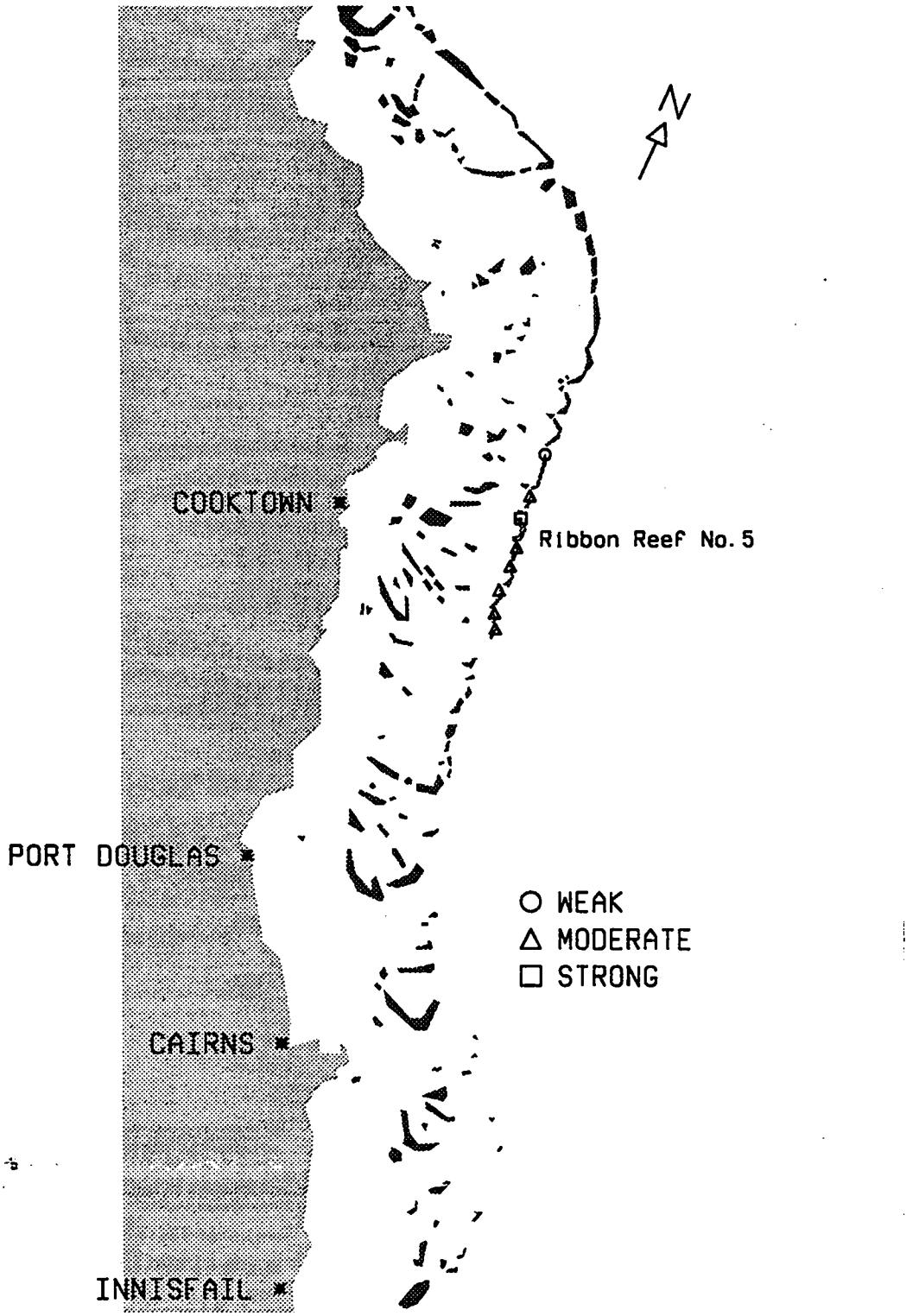


Figure 4.13e Strength of connectivity with respect to Ribbon Reef No.5. The relative strengths (weak, moderate and strong) are discrete classes separated by an order of magnitude and correspond to the **response time** analysis. Scale: 1cm = 12 nautical miles.

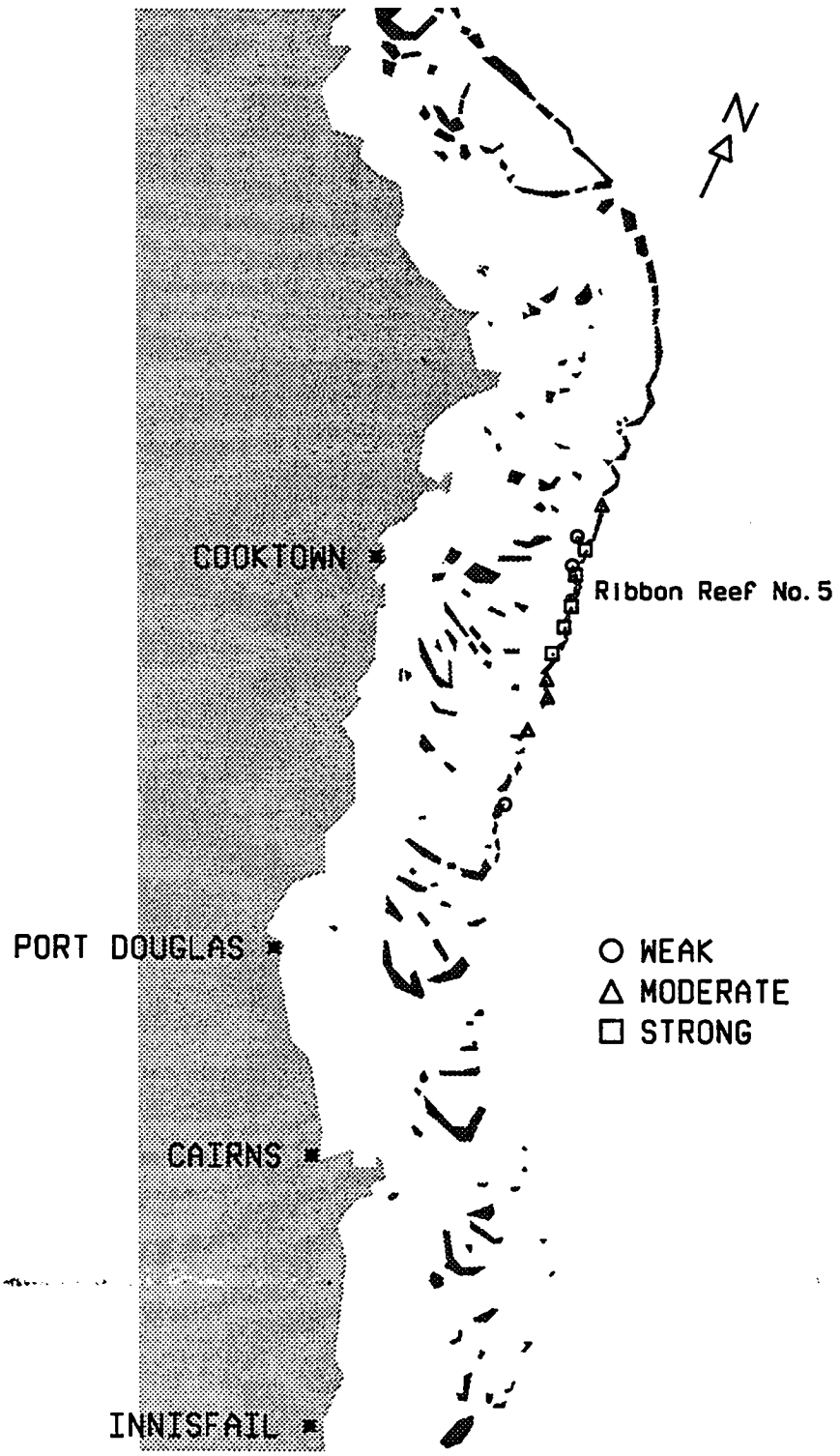


Figure 4.13f Strength of connectivity with respect to Ribbon Reef No.5. The relative strengths (weak, moderate and strong) are discrete classes separated by an order of magnitude and correspond to the **small larval cloud** analysis. Scale: 1cm = 12 nautical miles.

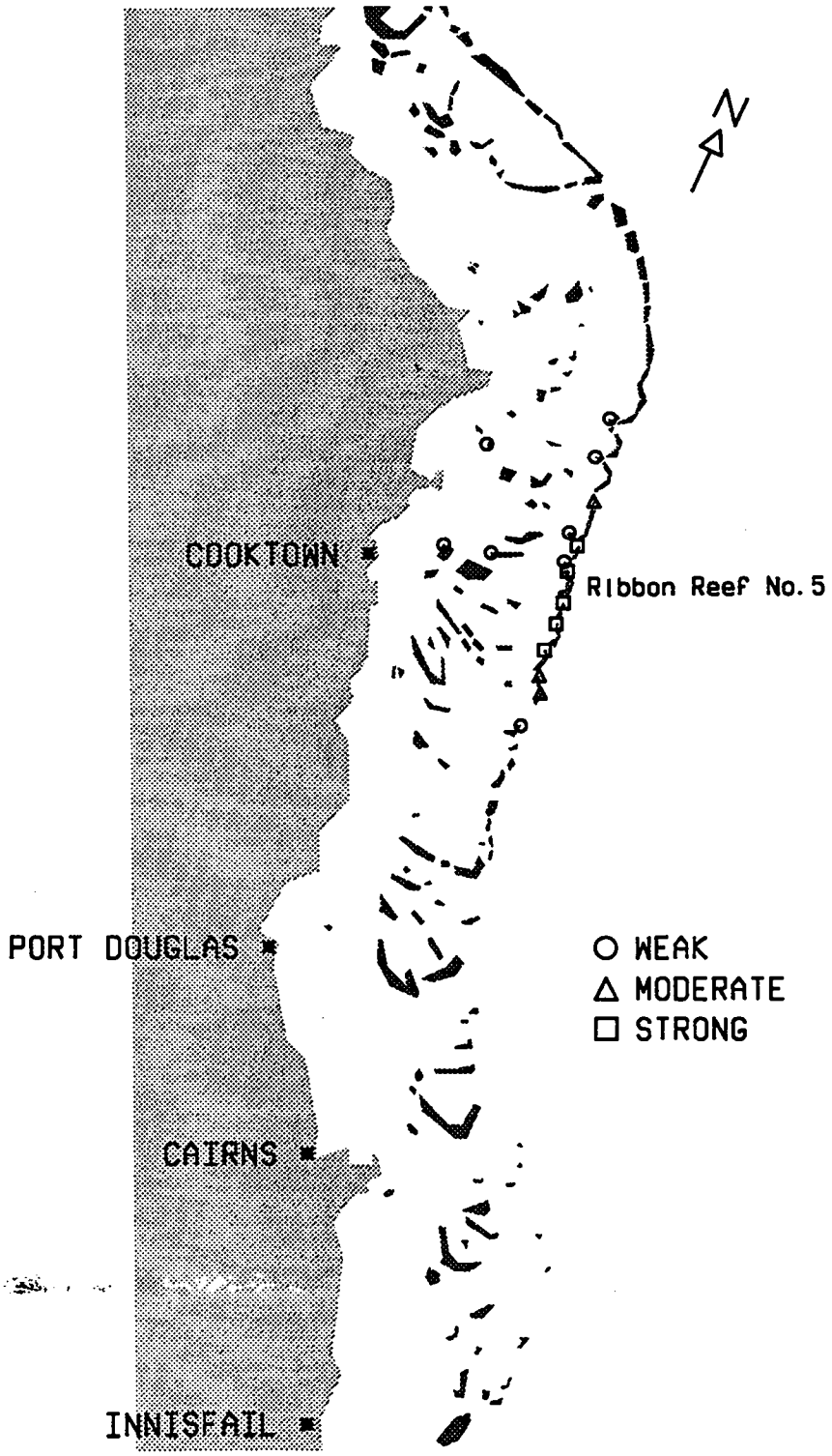


Figure 4.13g Strength of connectivity with respect to Ribbon Reef No.5. The relative strengths (weak, moderate and strong) are discrete classes separated by an order of magnitude and correspond to the **large larval cloud** analysis. Scale: 1cm = 12 nautical miles.

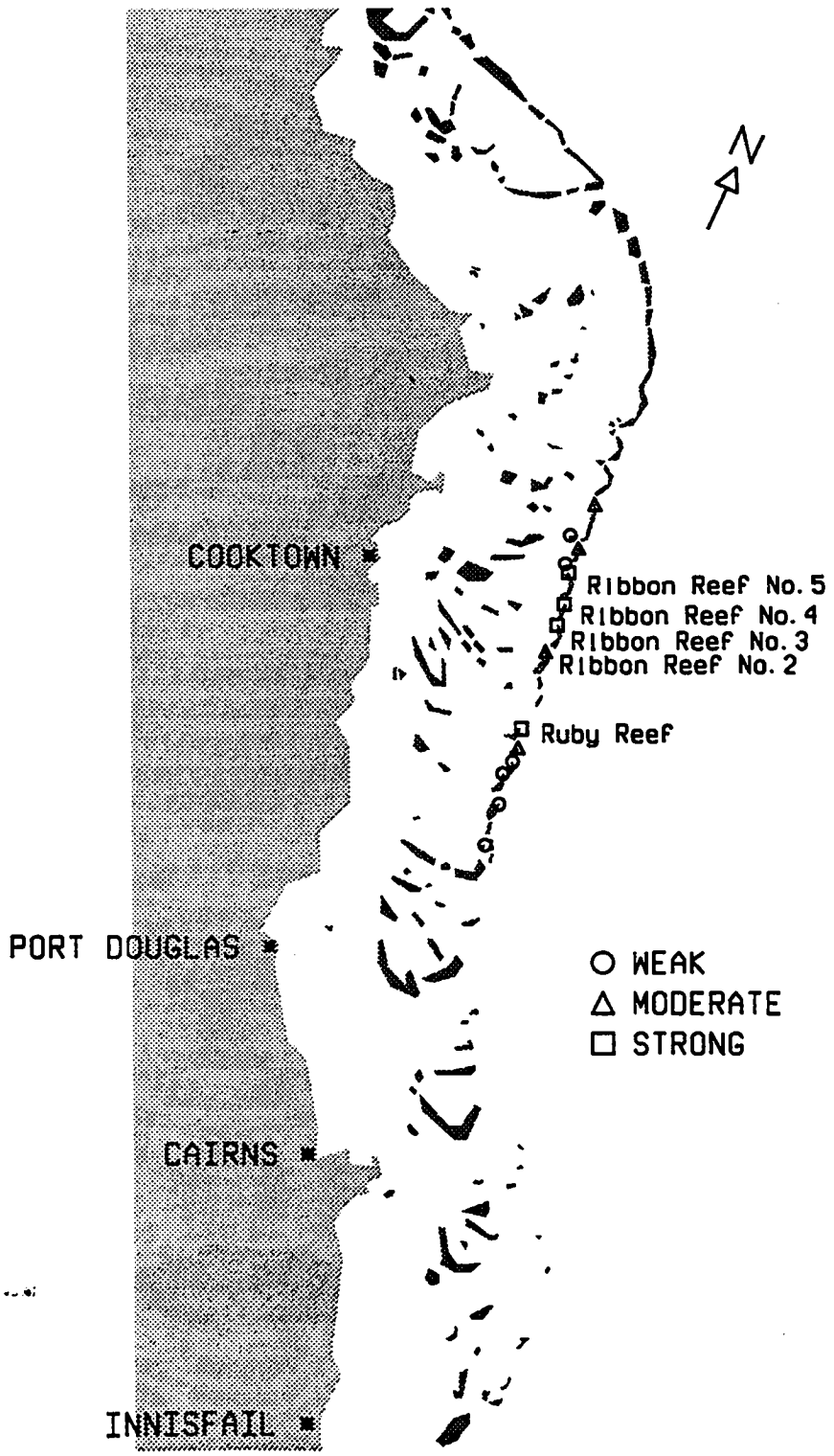


Figure 4.14a Strength of connectivity with respect to Ribbon Reef No.2. The relative strengths (weak, moderate and strong) are discrete classes separated by an order of magnitude and correspond to the base data. Scale: 1cm = 12 nautical miles.

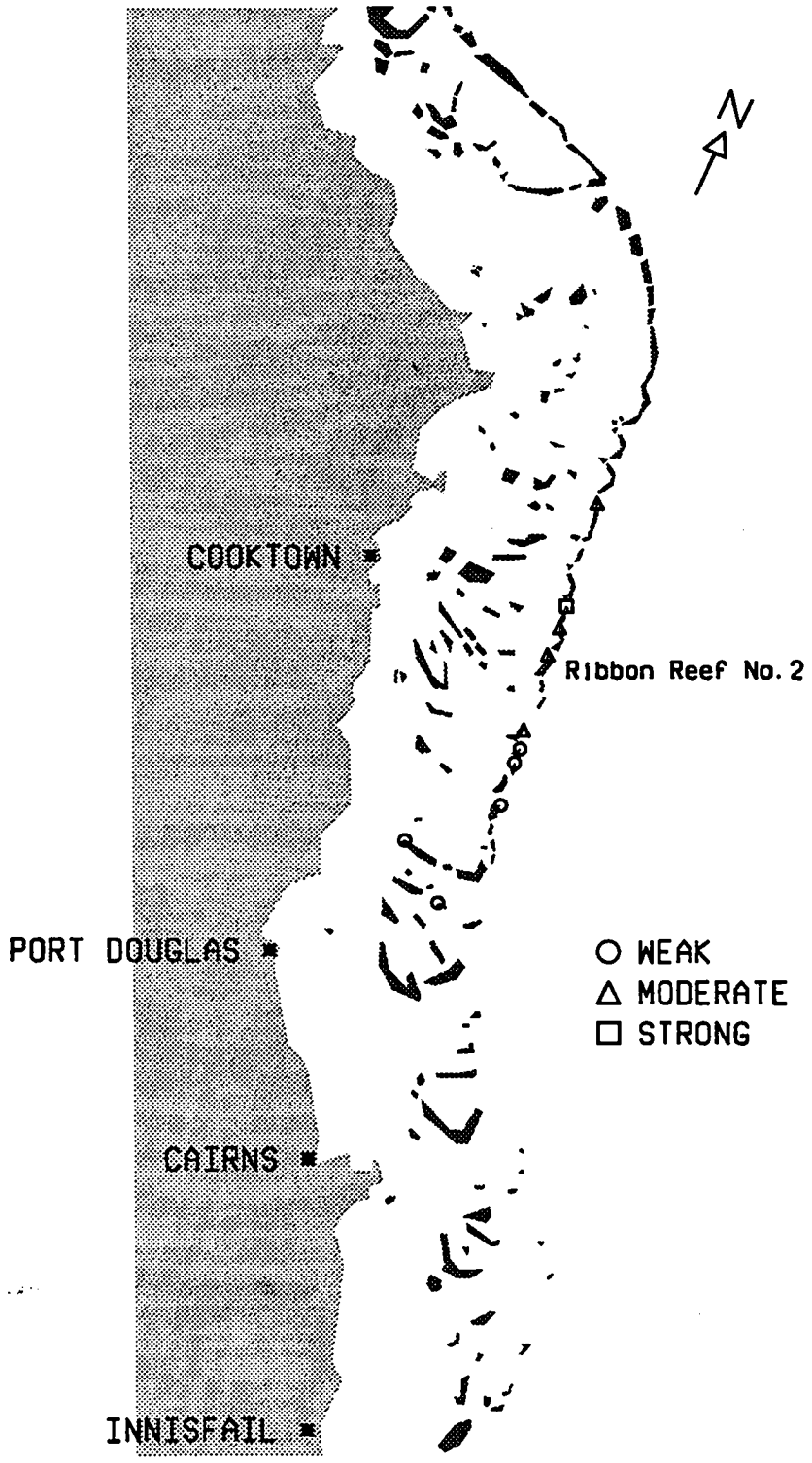


Figure 4.14b Strength of connectivity with respect to Ribbon Reef No.2. The relative strengths (weak, moderate and strong) are discrete classes separated by an order of magnitude and correspond to the **replicate** 40 dispersal events. Scale: 1cm = 12 nautical miles.

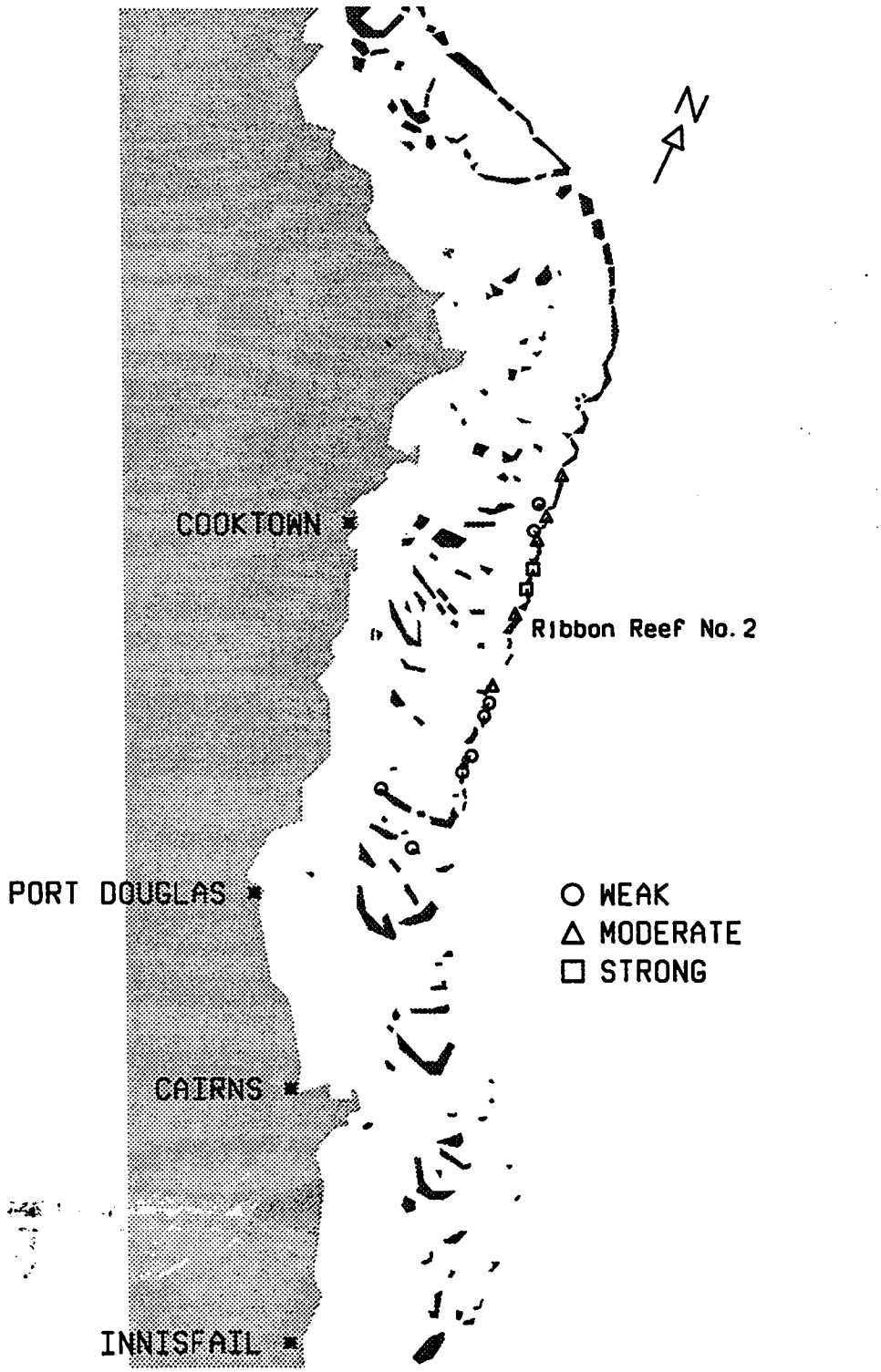


Figure 4.14c Strength of connectivity with respect to Ribbon Reef No.2. The relative strengths (weak, moderate and strong) are discrete classes separated by an order of magnitude and correspond to the combined **80 dispersal events**. Scale: 1cm = 12 nautical miles.

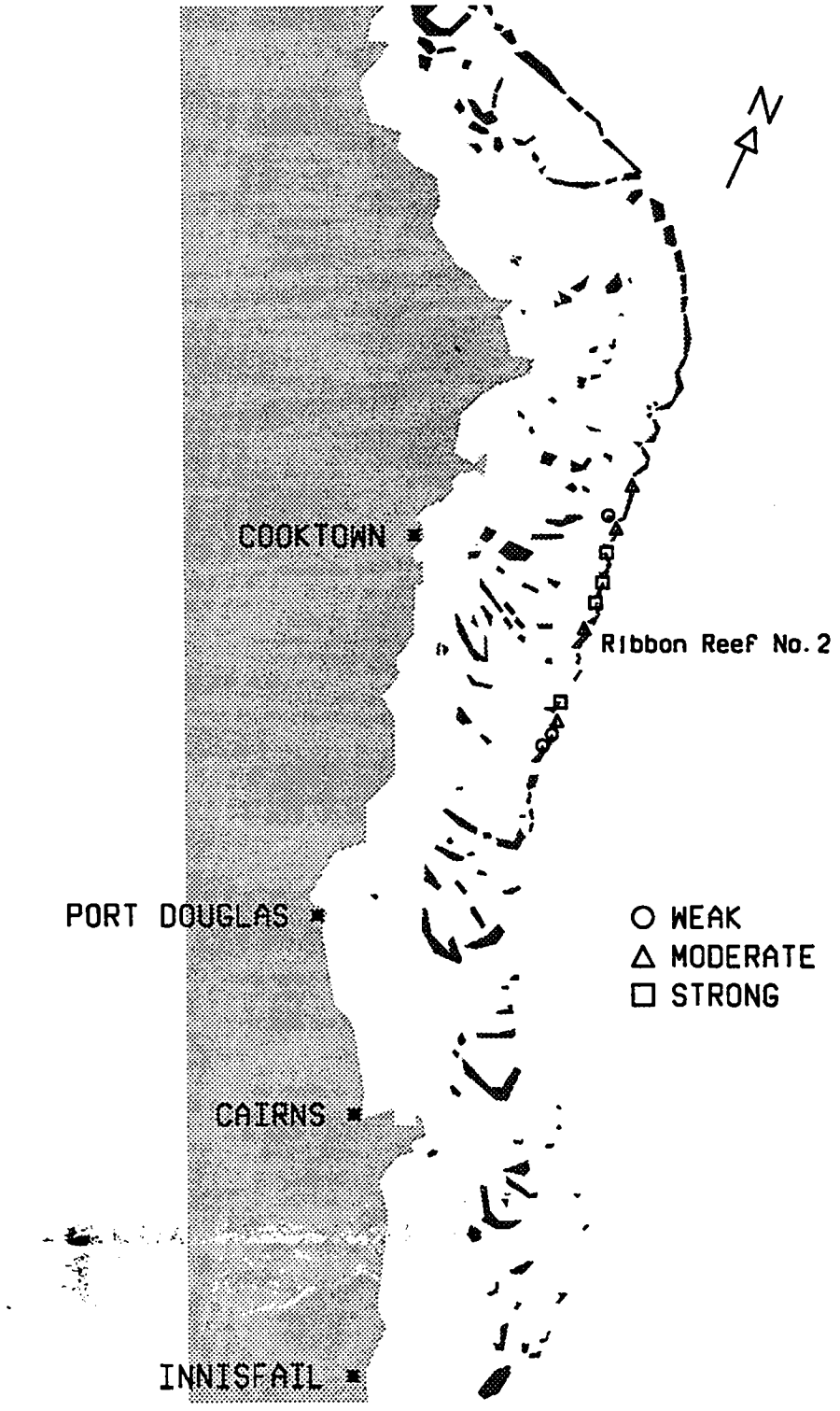


Figure 4.14d Strength of connectivity with respect to Ribbon Reef No.2. The relative strengths (weak, moderate and strong) are discrete classes separated by an order of magnitude and correspond to the **small larval cloud** analysis. Scale: 1cm = 12 nautical miles.

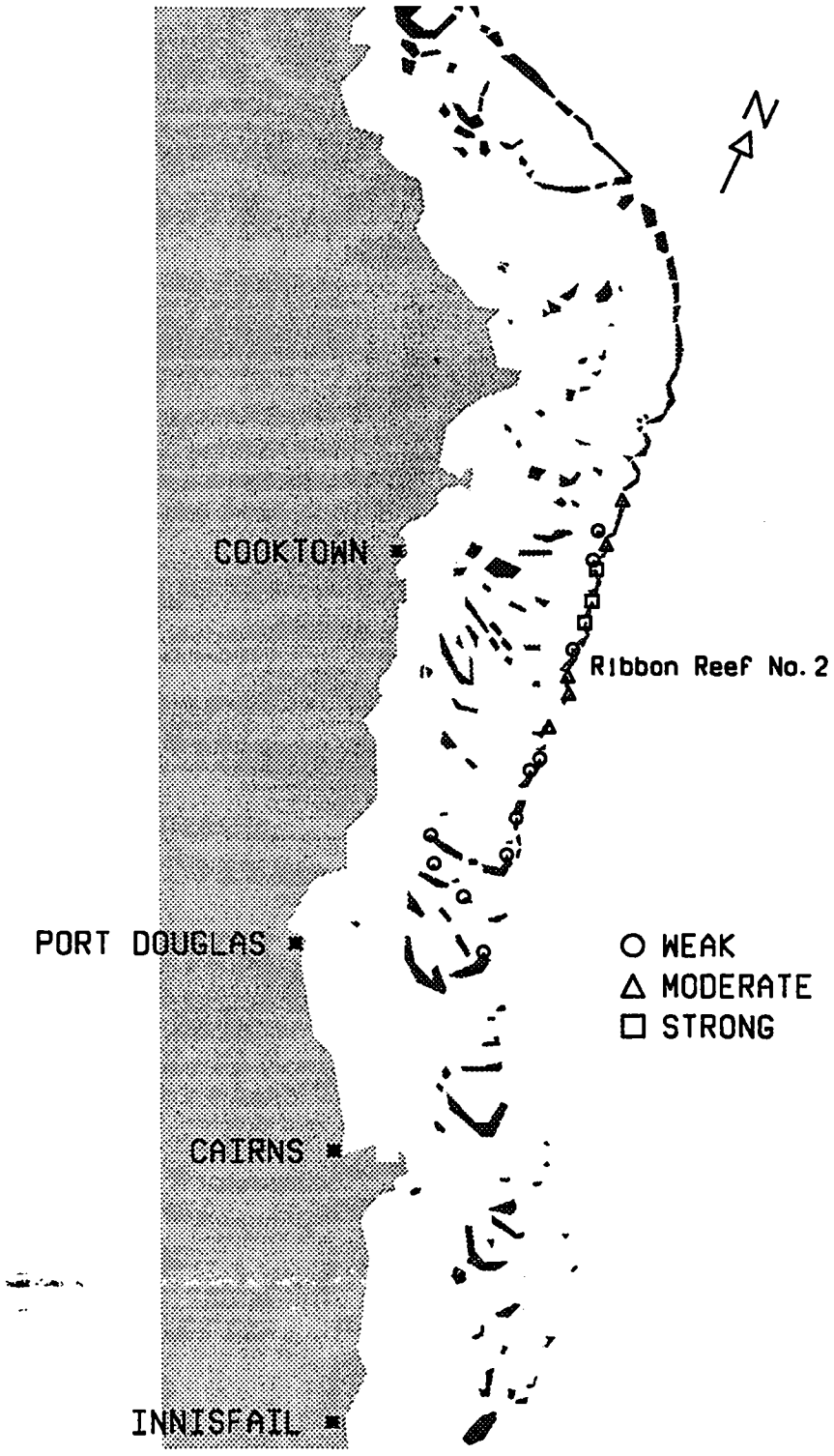


Figure 4.14e Strength of connectivity with respect to Ribbon Reef No.2. The relative strengths (weak, moderate and strong) are discrete classes separated by an order of magnitude and correspond to the **large larval cloud** analysis. Scale: 1cm = 12 nautical miles.

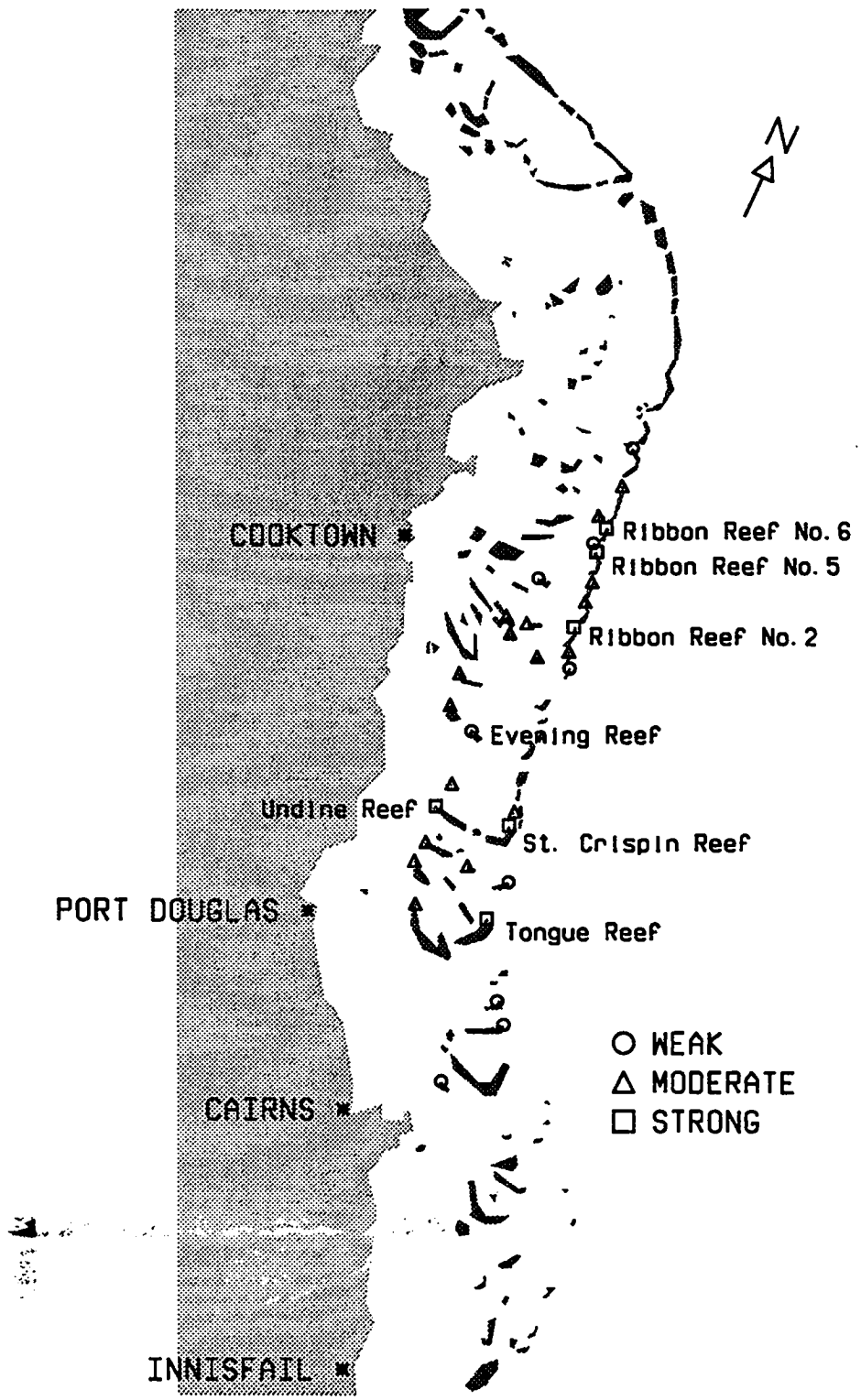


Figure 4.15a Strength of connectivity with respect to Evening Reef. The relative strengths (weak, moderate and strong) are discrete classes separated by an order of magnitude and correspond to the **base data**. Scale: 1cm = 12 nautical miles.

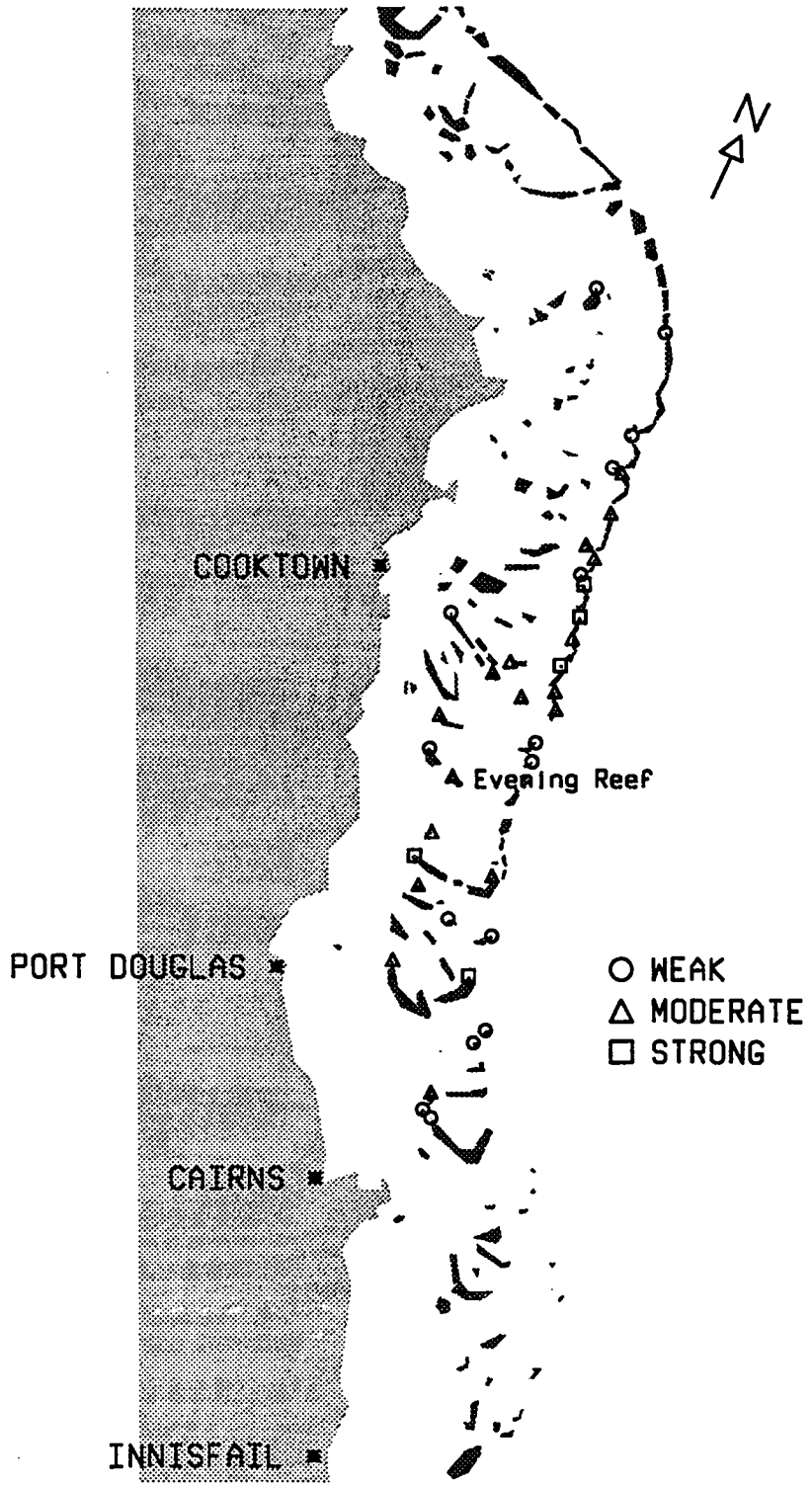


Figure 4.15b Strength of connectivity with respect to Evening Reef. The relative strengths (weak, moderate and strong) are discrete classes separated by an order of magnitude and correspond to the replicate 40 dispersal events. Scale: 1cm = 12 nautical miles.

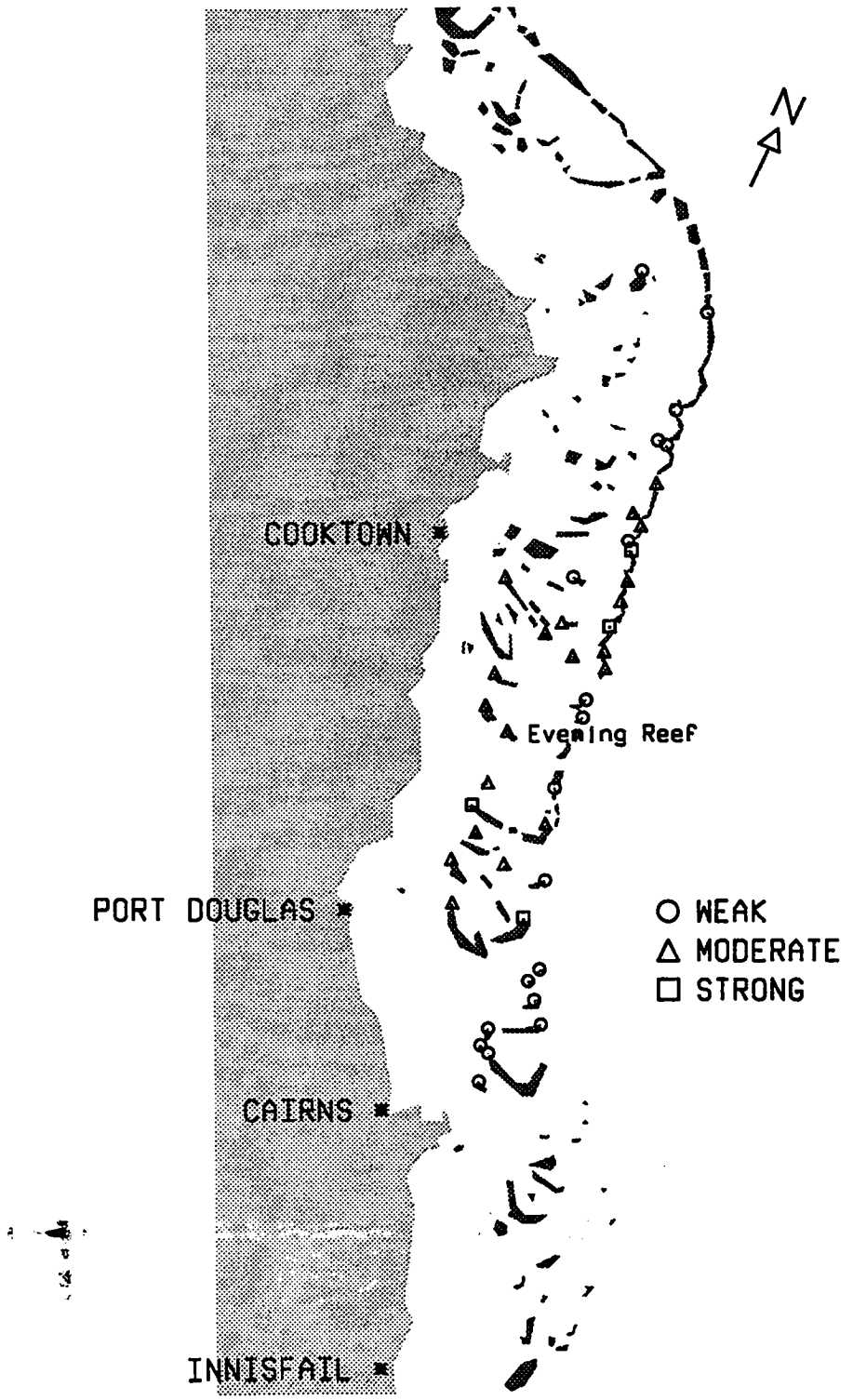


Figure 4.15c Strength of connectivity with respect to Evening Reef. The relative strengths (weak, moderate and strong) are discrete classes separated by an order of magnitude and correspond to the combined **80 dispersal events**. Scale: 1cm = 12 nautical miles.

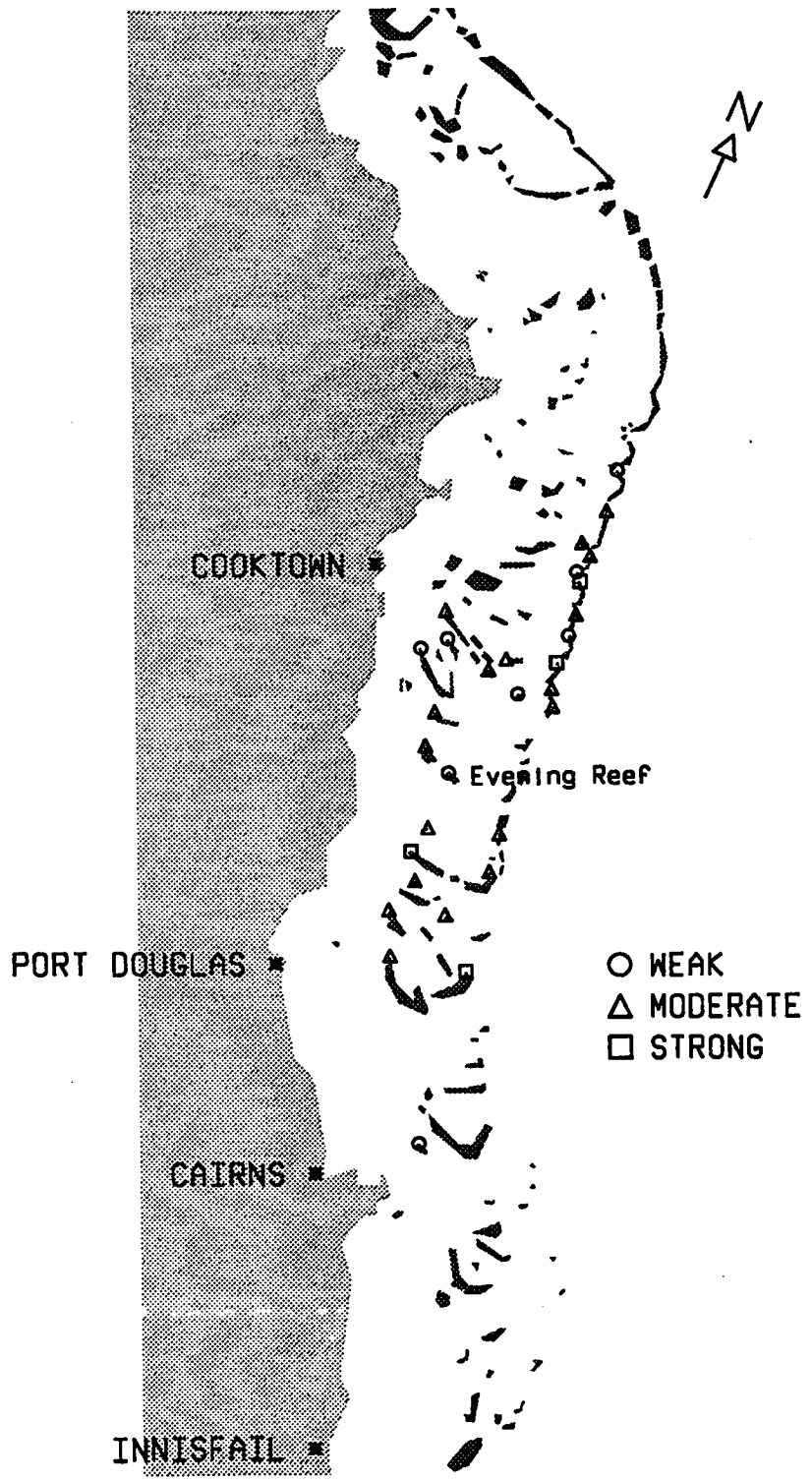


Figure 4.15d Strength of connectivity with respect to Evening Reef. The relative strengths (weak, moderate and strong) are discrete classes separated by an order of magnitude and correspond to the **interpolated wind field** analysis. Scale: 1cm = 12 nautical miles.

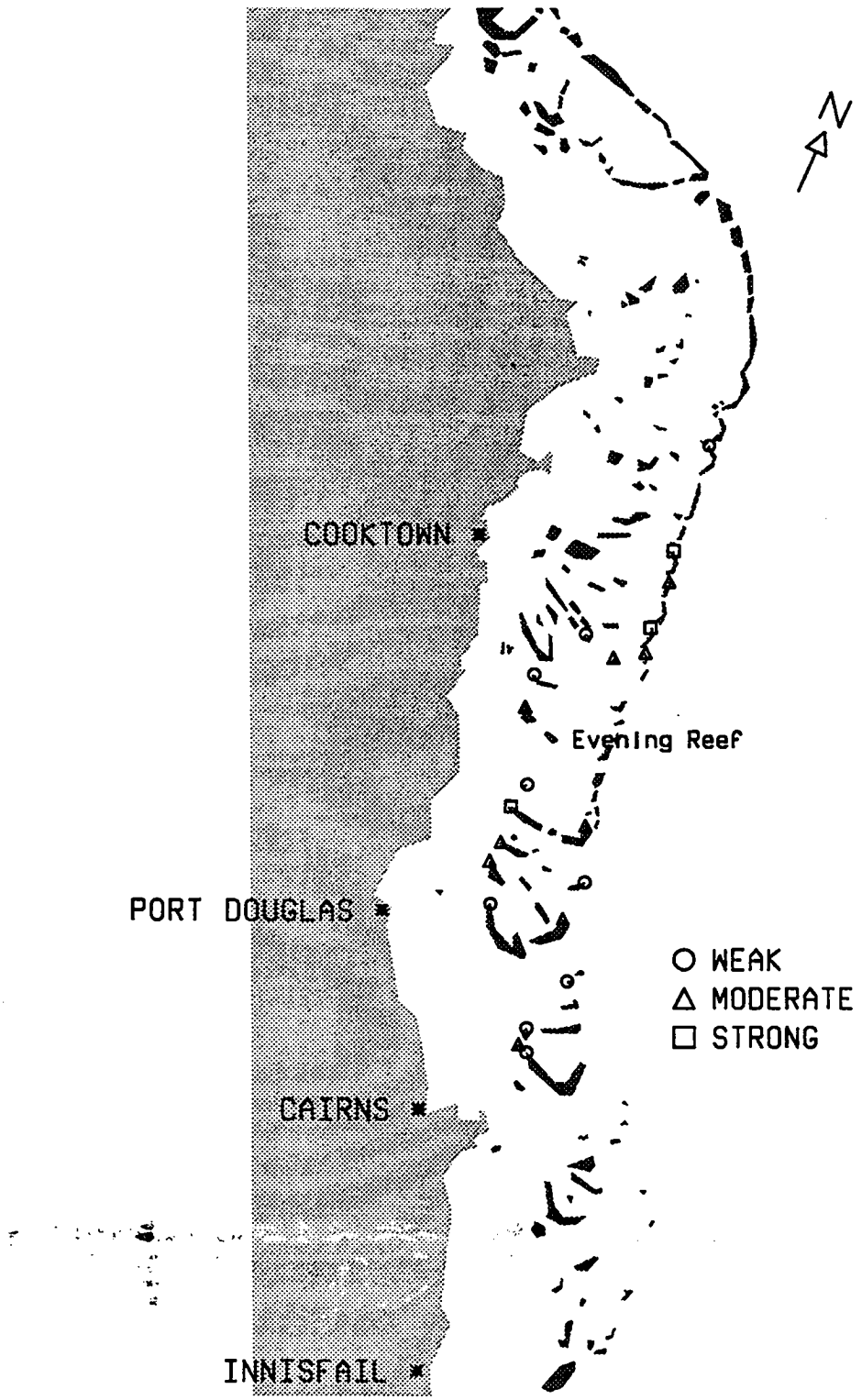


Figure 4.15e Strength of connectivity with respect to Evening Reef. The relative strengths (weak, moderate and strong) are discrete classes separated by an order of magnitude and correspond to the response time analysis. Scale: 1cm = 12 nautical miles.

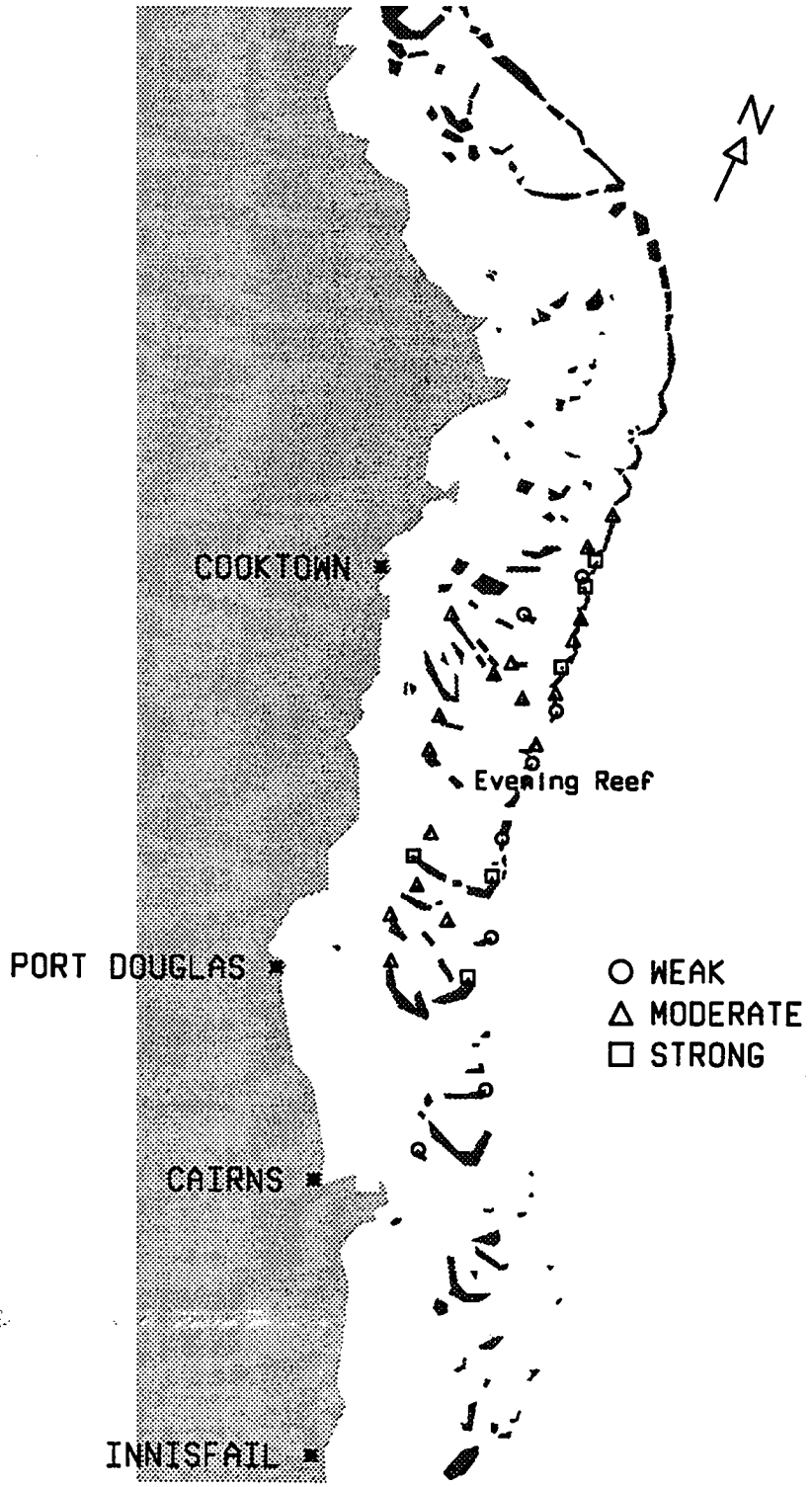


Figure 4.15f Strength of connectivity with respect to Evening Reef. The relative strengths (weak, moderate and strong) are discrete classes separated by an order of magnitude and correspond to the **small larval cloud** analysis. Scale: 1cm = 12 nautical miles.

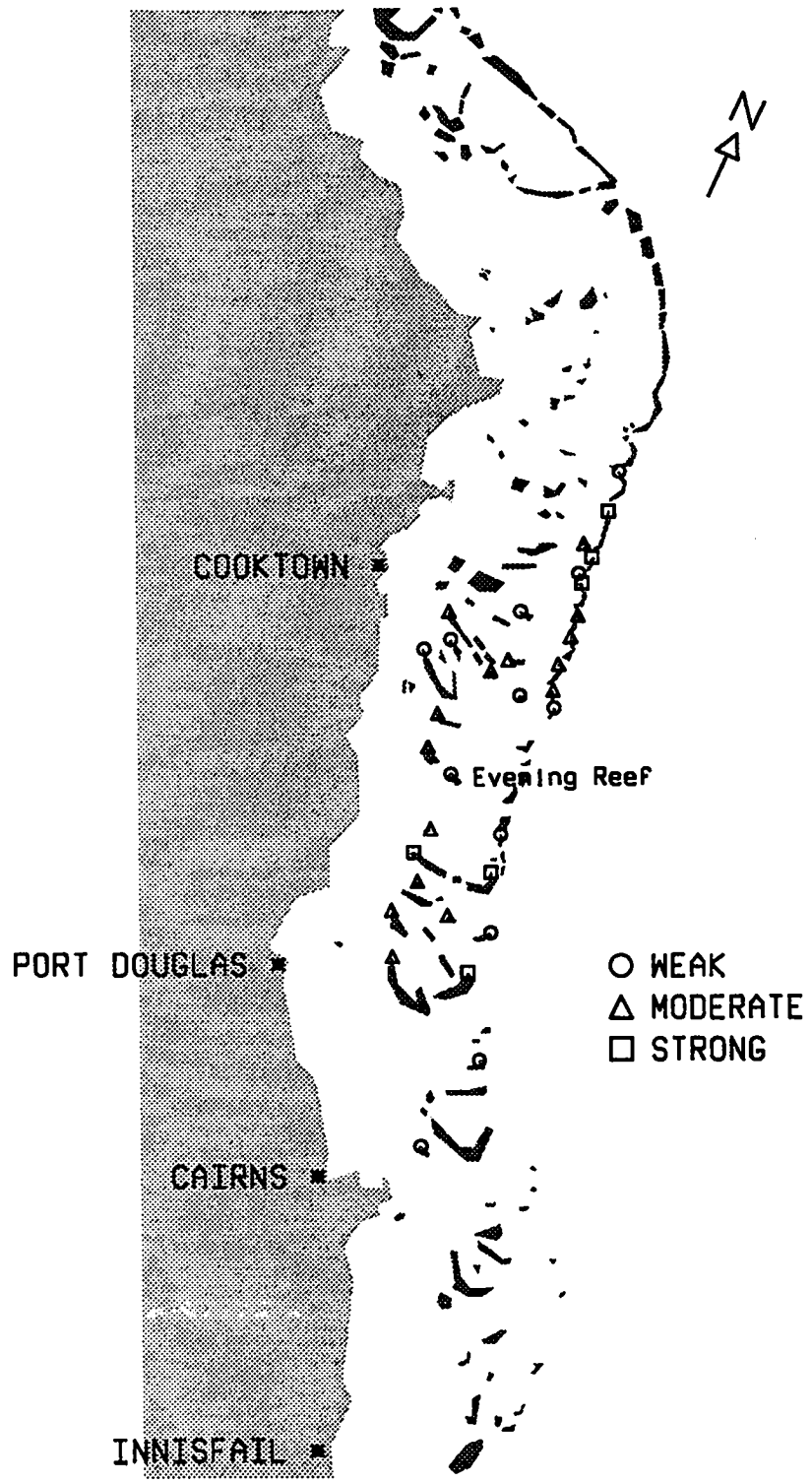


Figure 4.15g Strength of connectivity with respect to Evening Reef. The relative strengths (weak, moderate and strong) are discrete classes separated by an order of magnitude and correspond to the **large larval cloud** analysis. Scale: 1cm = 12 nautical miles.

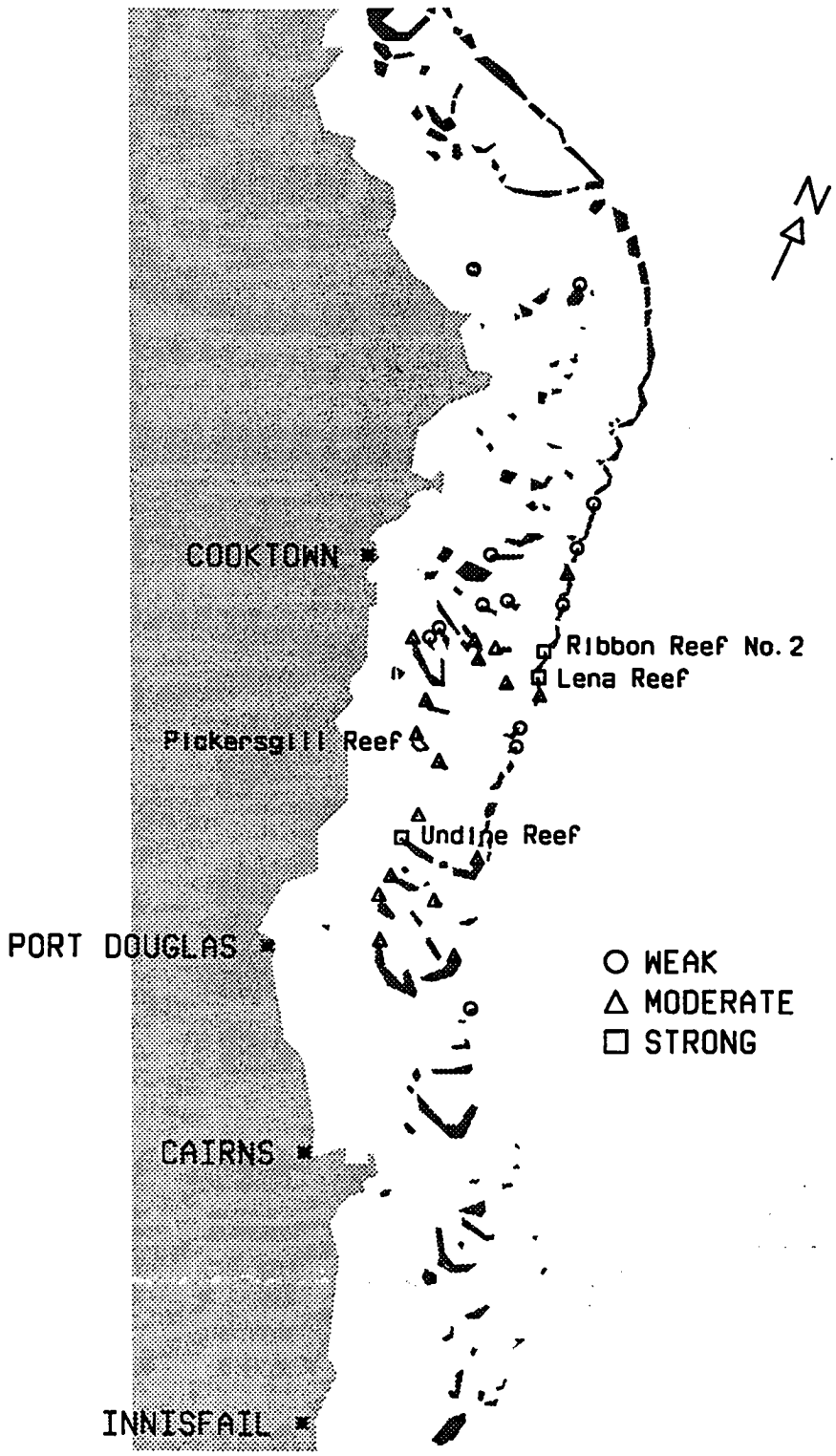


Figure 4.16a Strength of connectivity with respect to Pickersgill Reef. The relative strengths (weak, moderate and strong) are discrete classes separated by an order of magnitude and correspond to the base data. Scale: 1cm = 12 nautical miles.

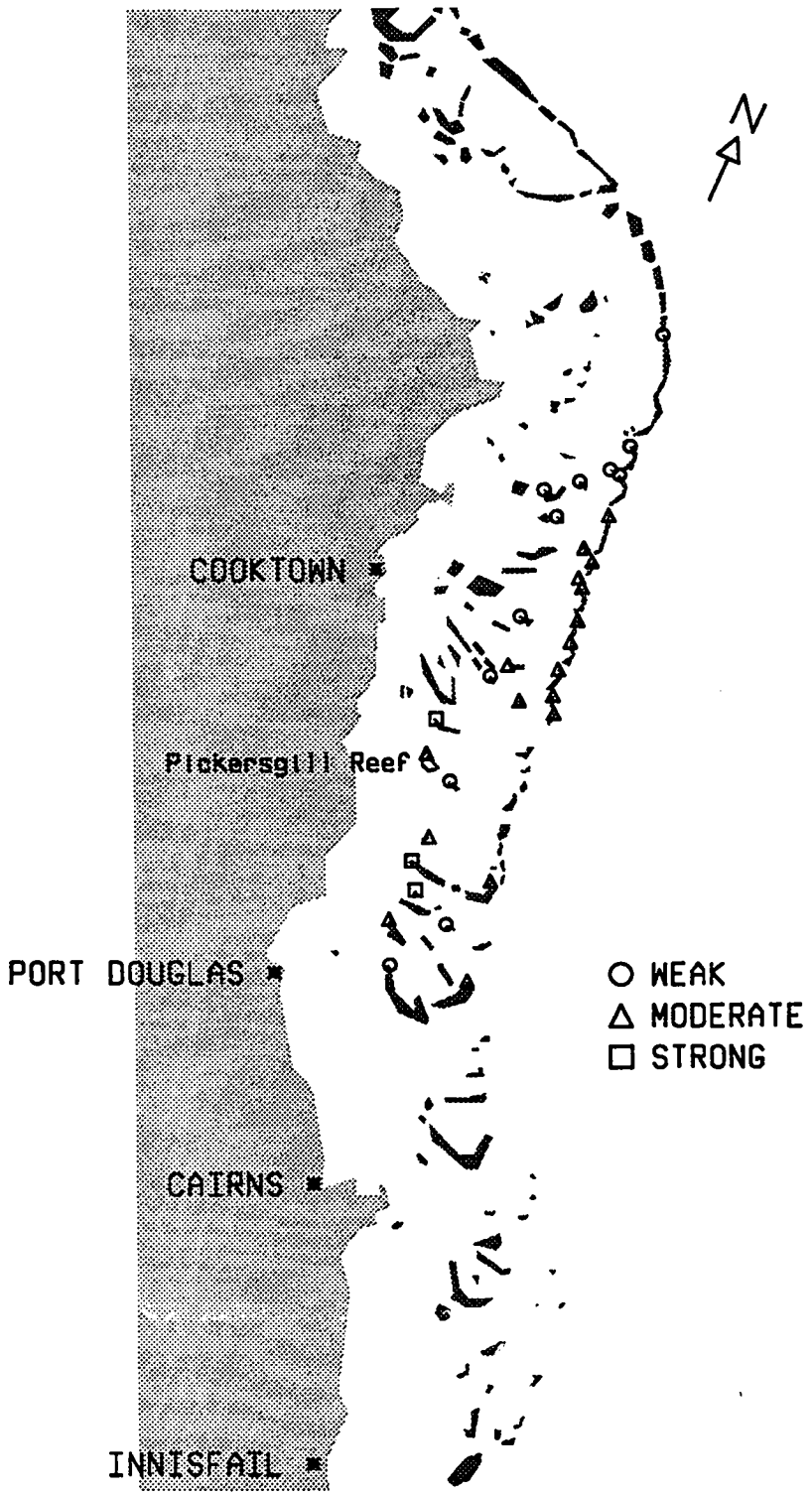


Figure 4.16b Strength of connectivity with respect to Pickersgill Reef. The relative strengths (weak, moderate and strong) are discrete classes separated by an order of magnitude and correspond to the replicate 40 dispersal events. Scale: 1cm = 12 nautical miles.

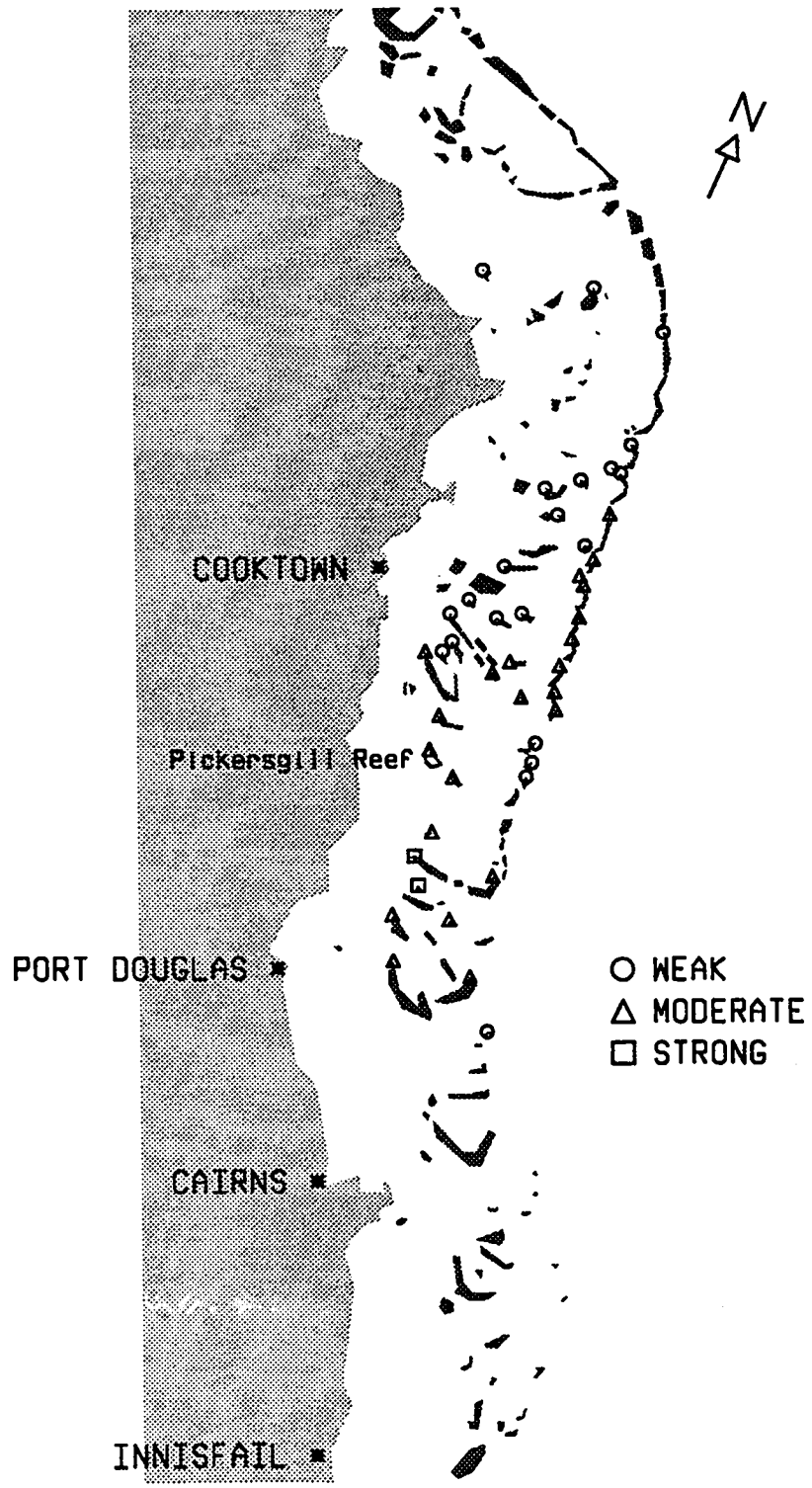


Figure 4.16c Strength of connectivity with respect to Pickersgill Reef. The relative strengths (weak, moderate and strong) are discrete classes separated by an order of magnitude and correspond to the combined 80 dispersal events. Scale: 1cm = 12 nautical miles.

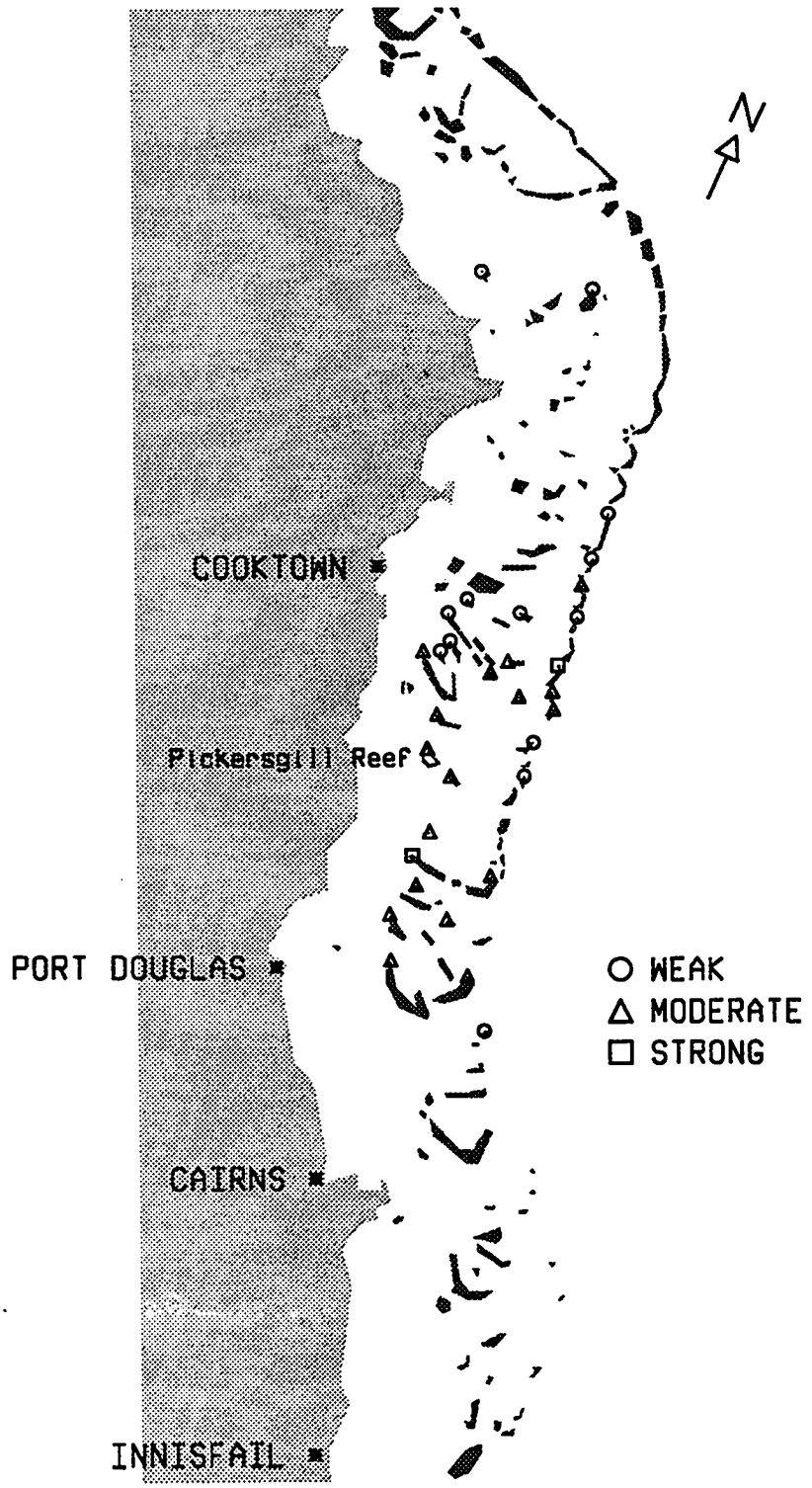


Figure 4.16d Strength of connectivity with respect to Pickersgill Reef. The relative strengths (weak, moderate and strong) are discrete classes separated by an order of magnitude and correspond to the **small larval cloud** analysis. Scale: 1cm = 12 nautical miles.

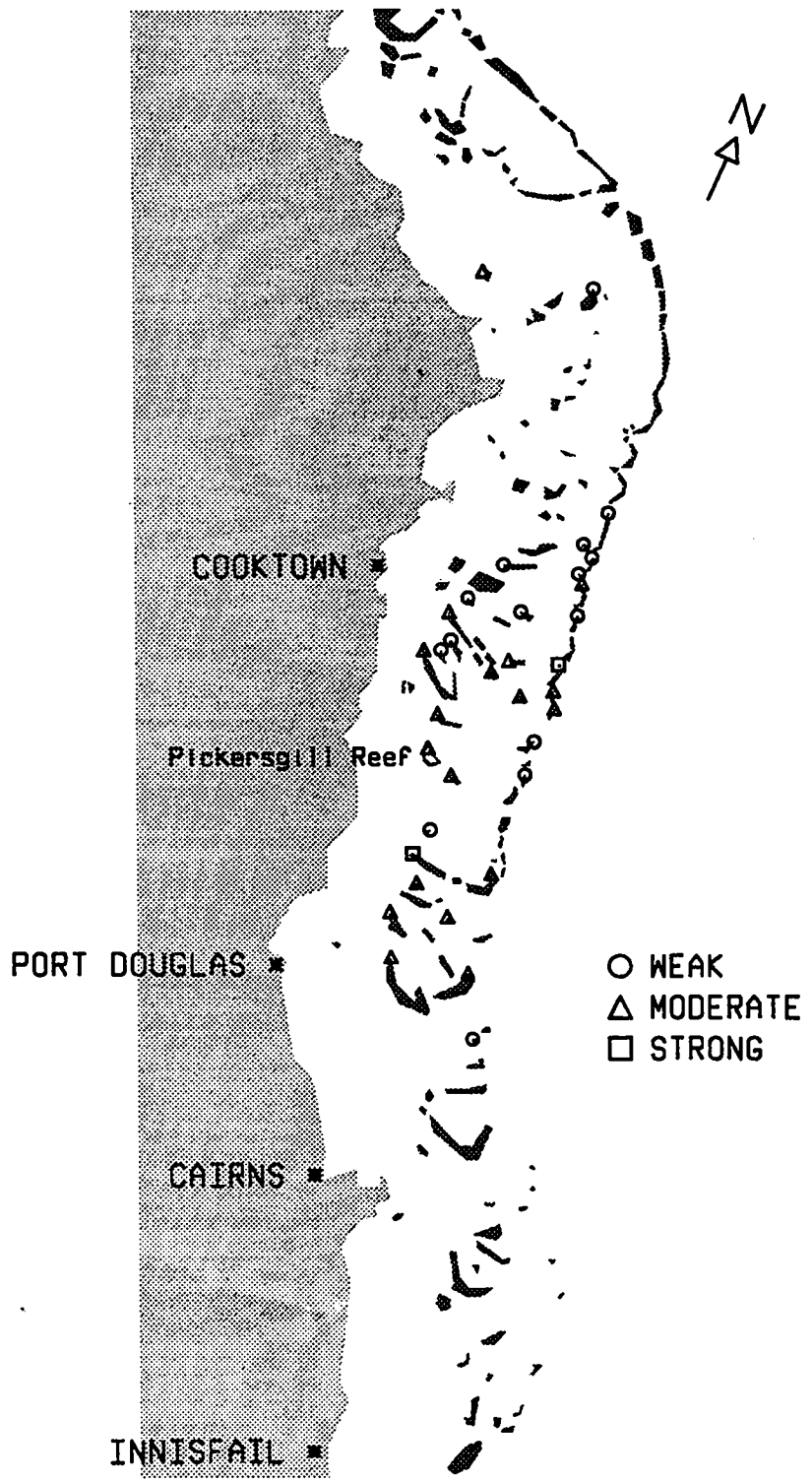


Figure 4.16e Strength of connectivity with respect to Pickersgill Reef. The relative strengths (weak, moderate and strong) are discrete classes separated by an order of magnitude and correspond to the large larval cloud analysis. Scale: 1cm = 12 nautical miles.

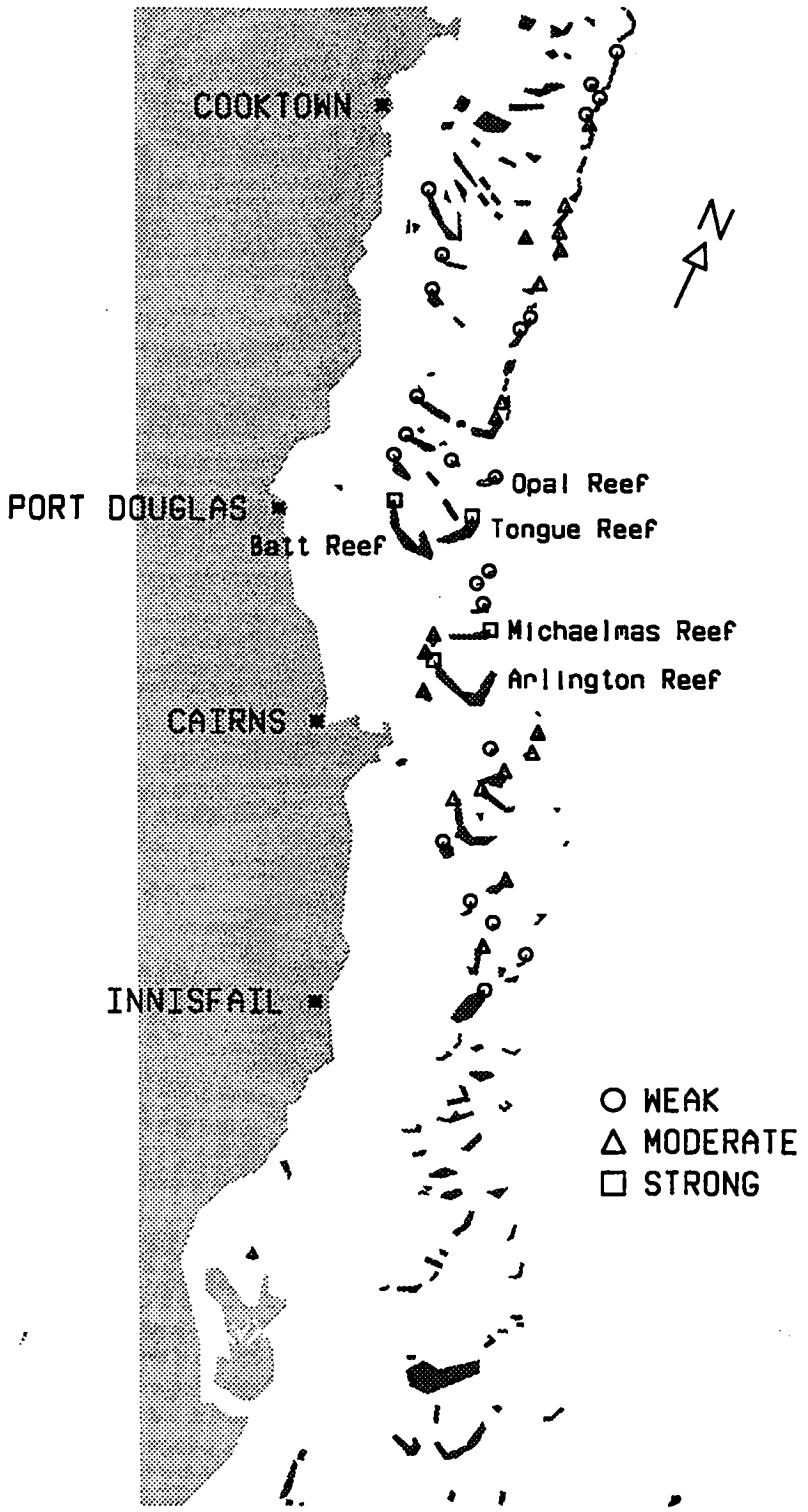


Figure 4.17a Strength of connectivity with respect to Opal Reef. The relative strengths (weak, moderate and strong) are discrete classes separated by an order of magnitude and correspond to the base data. Scale: 1cm = 12 nautical miles.

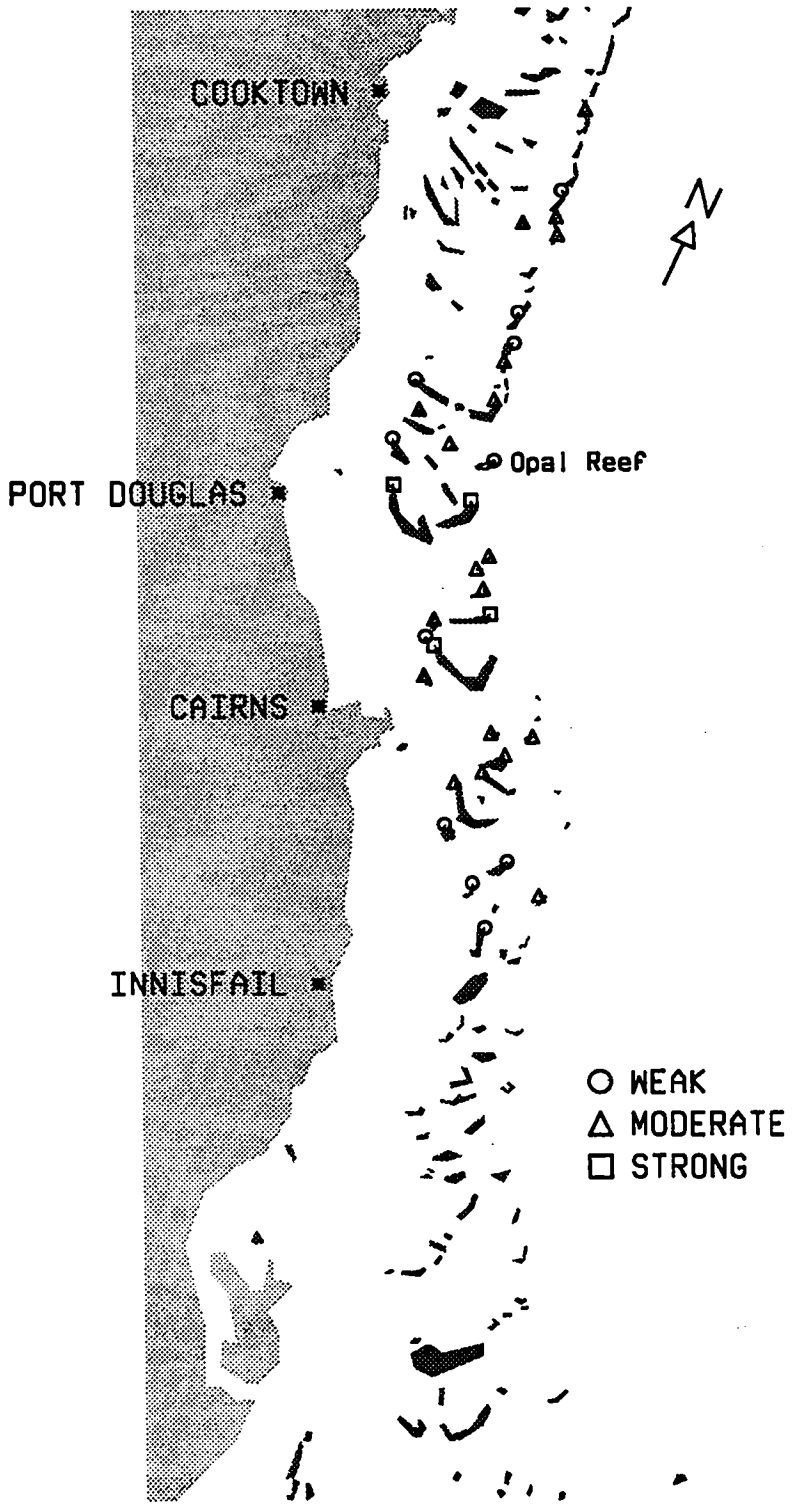


Figure 4.17b Strength of connectivity with respect to Opal Reef. The relative strengths (weak, moderate and strong) are discrete classes separated by an order of magnitude and correspond to the replicate 40 dispersal events. Scale: 1cm = 12 nautical miles.

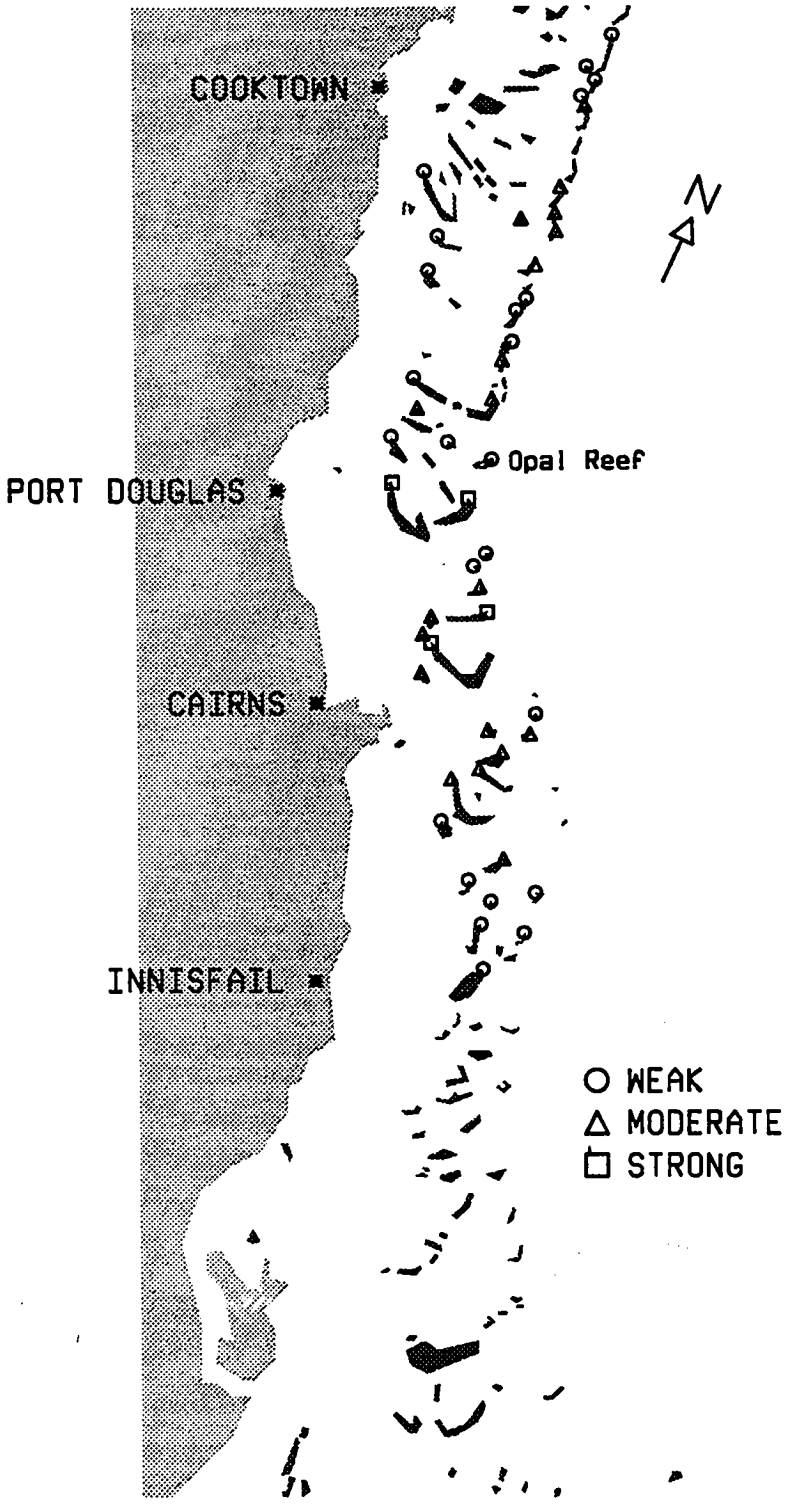


Figure 4.17c Strength of connectivity with respect to Opal Reef. The relative strengths (weak, moderate and strong) are discrete classes separated by an order of magnitude and correspond to the combined **80 dispersal events**. Scale: 1cm = 12 nautical miles.

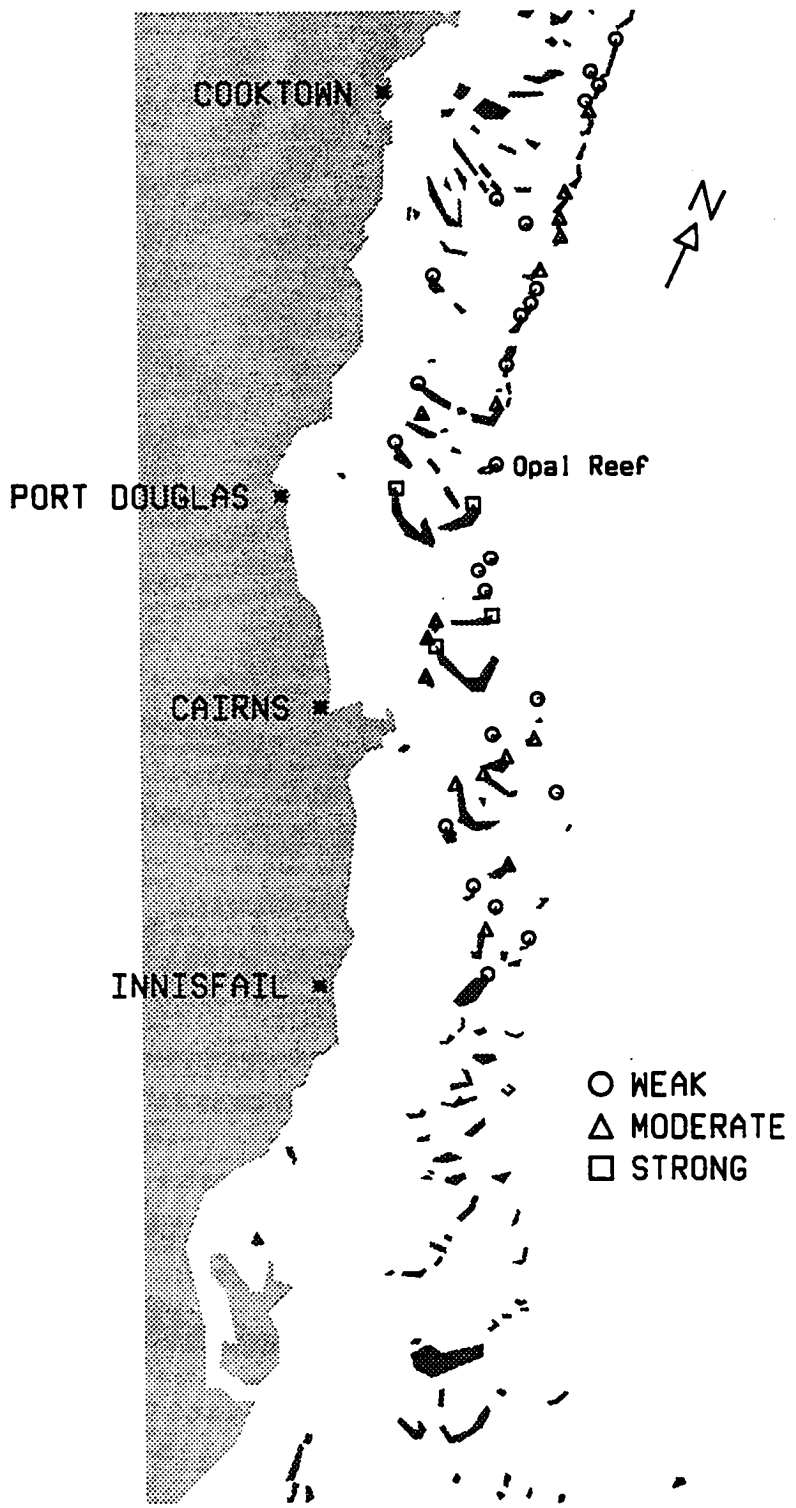


Figure 4.17d Strength of connectivity with respect to Opal Reef. The relative strengths (weak, moderate and strong) are discrete classes separated by an order of magnitude and correspond to the **interpolated wind field** analysis. Scale: 1cm = 12 nautical miles.

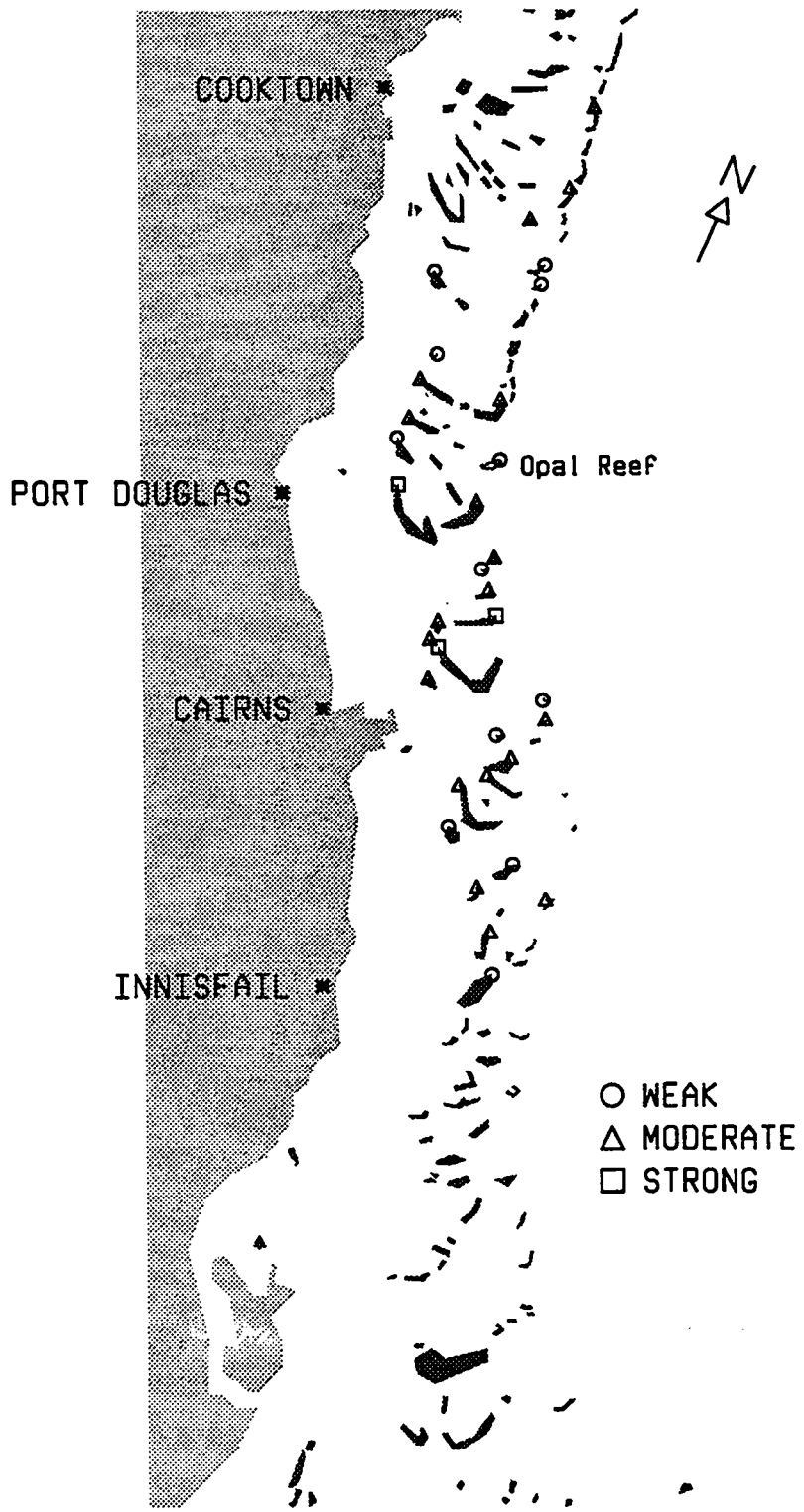


Figure 4.17e Strength of connectivity with respect to Opal Reef. The relative strengths (weak, moderate and strong) are discrete classes separated by an order of magnitude and correspond to the **response time** analysis. Scale: 1cm = 12 nautical miles.

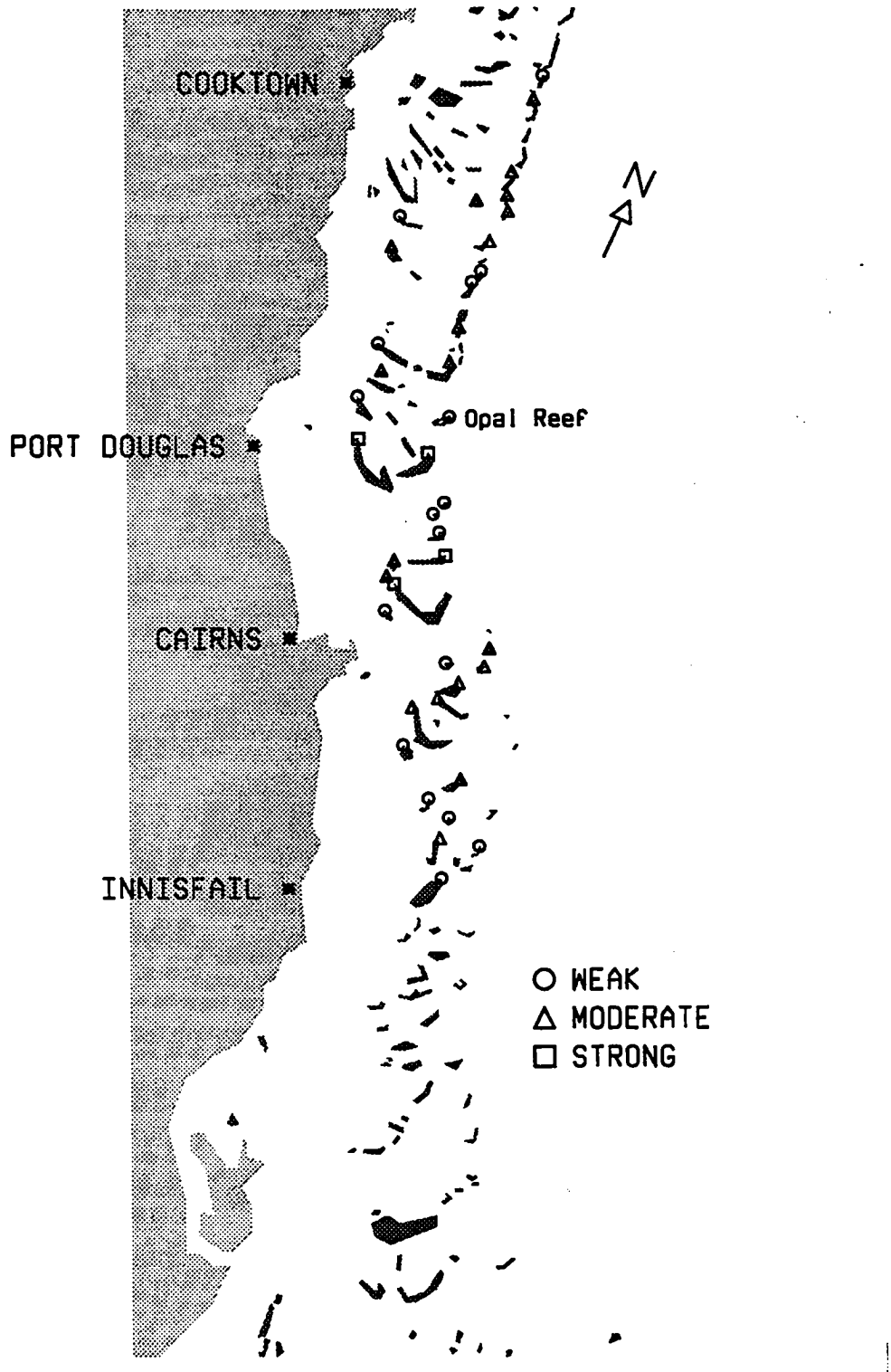


Figure 4.17f Strength of connectivity with respect to Opal Reef. The relative strengths (weak, moderate and strong) are discrete classes separated by an order of magnitude and correspond to the **small larval cloud** analysis. Scale: 1cm = 12 nautical miles.

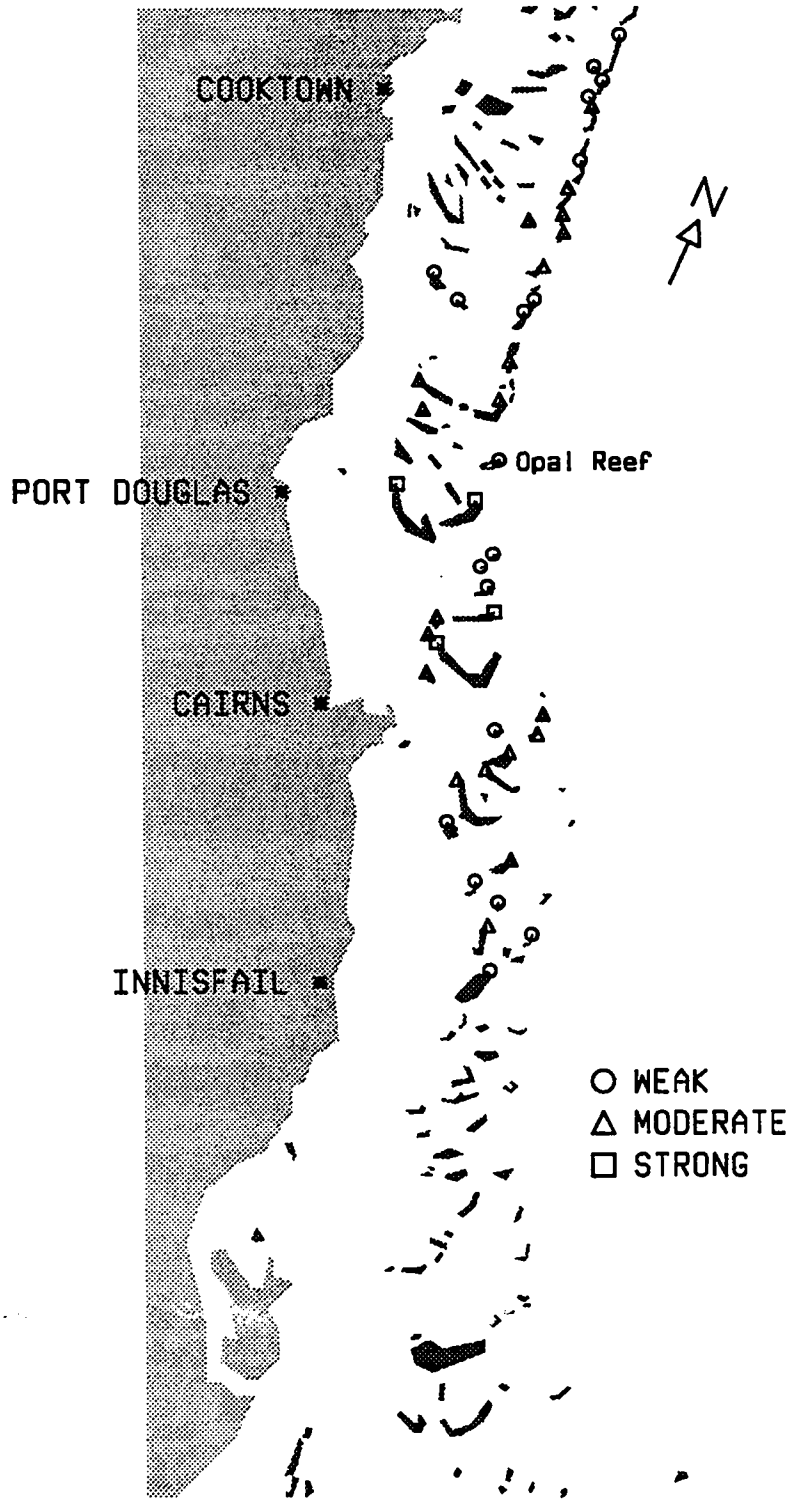


Figure 4.17g Strength of connectivity with respect to Opal Reef. The relative strengths (**weak**, moderate and strong) are discrete classes separated by an order of magnitude and correspond to the **large larval cloud** analysis. Scale: 1cm = 12 nautical miles.

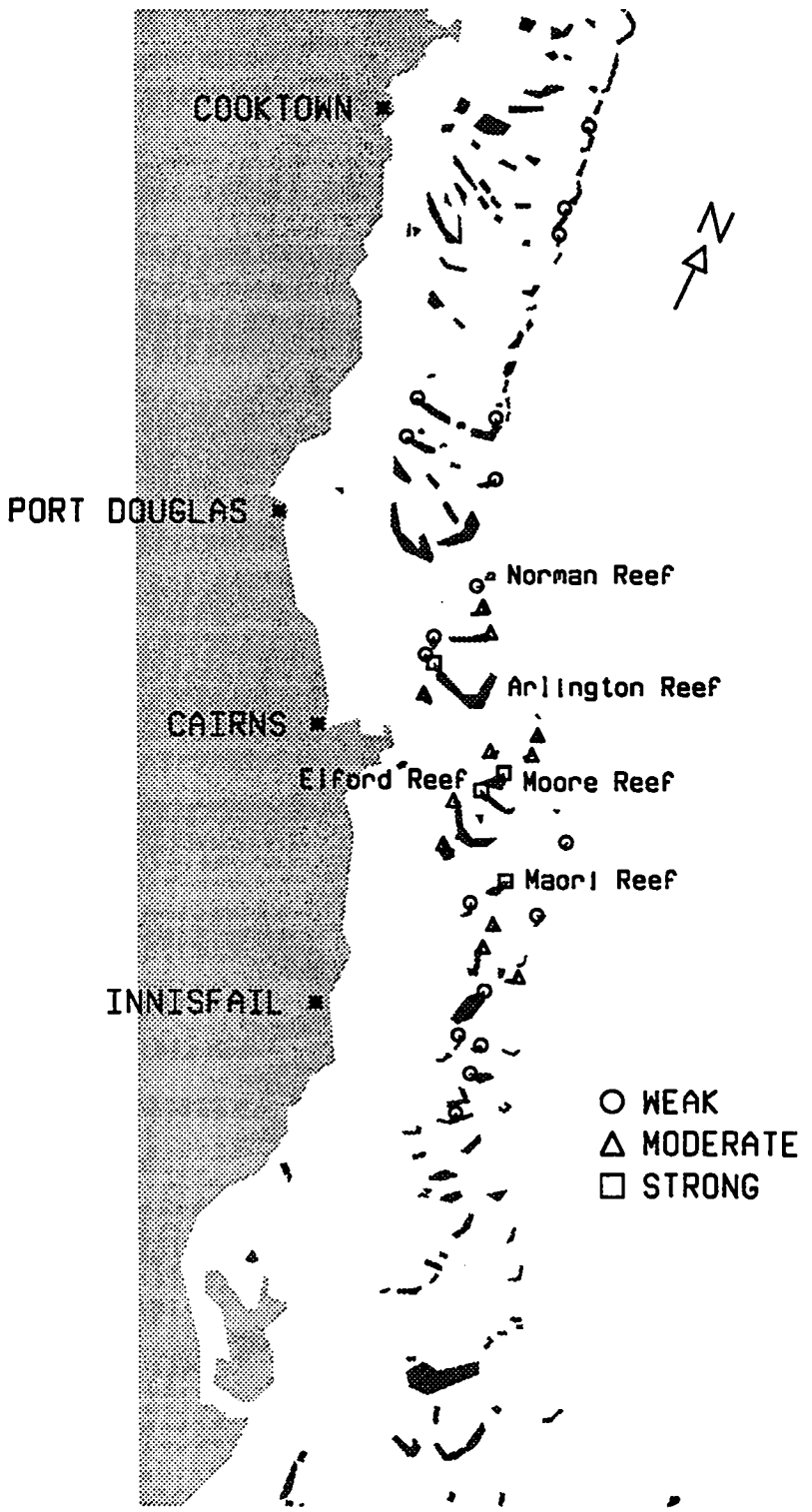


Figure 4.18a Strength of connectivity with respect to Norman Reef. The relative strengths (weak, moderate and strong) are discrete classes separated by an order of magnitude and correspond to the base data. Scale: 1cm = 12 nautical miles.

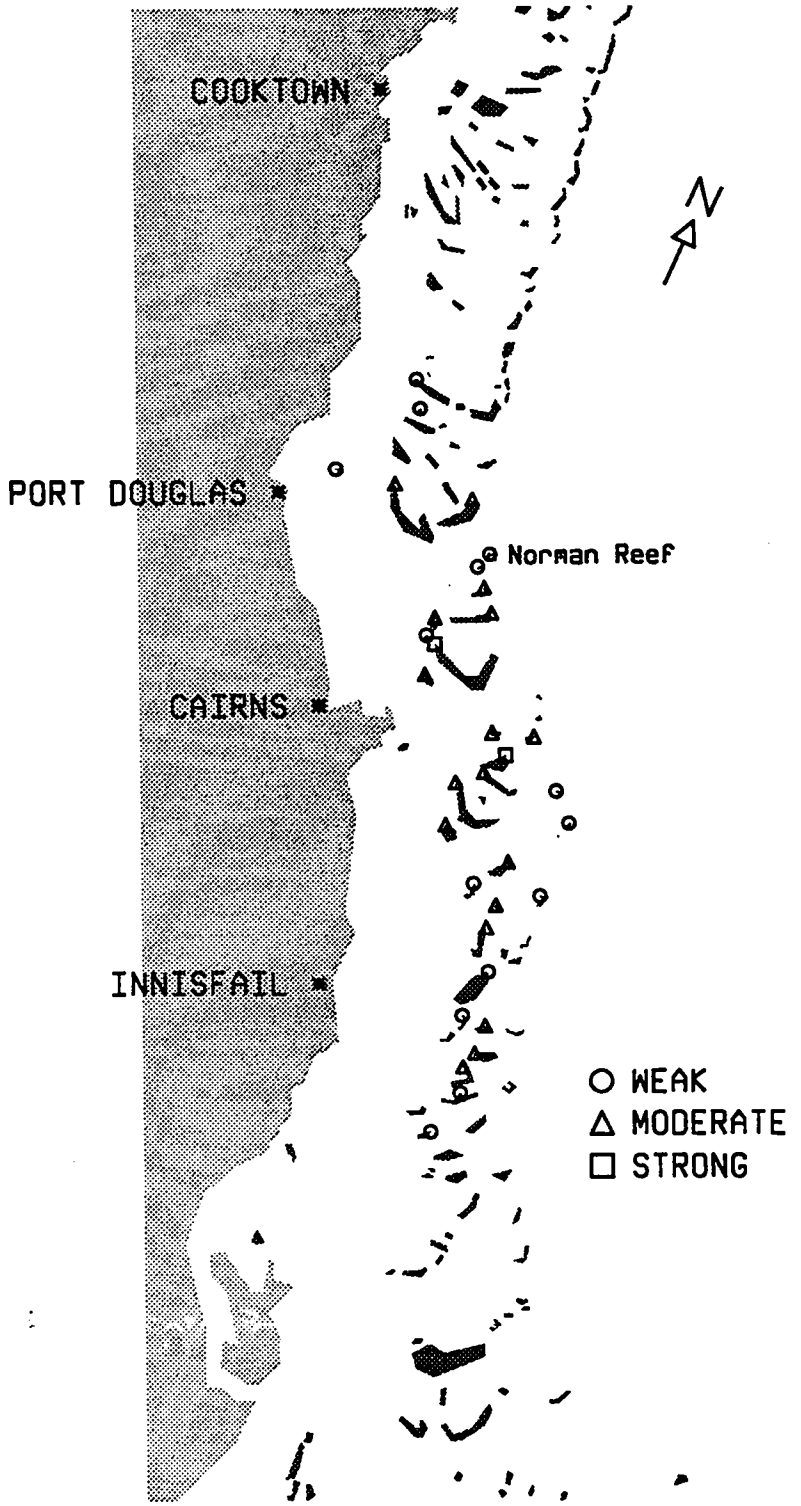


Figure 4.18b Strength of connectivity with respect to Norman Reef. The relative strengths (weak, moderate and strong) are discrete classes separated by an order of magnitude and correspond to the replicate 40 dispersal events. Scale: 1cm = 12 nautical miles.

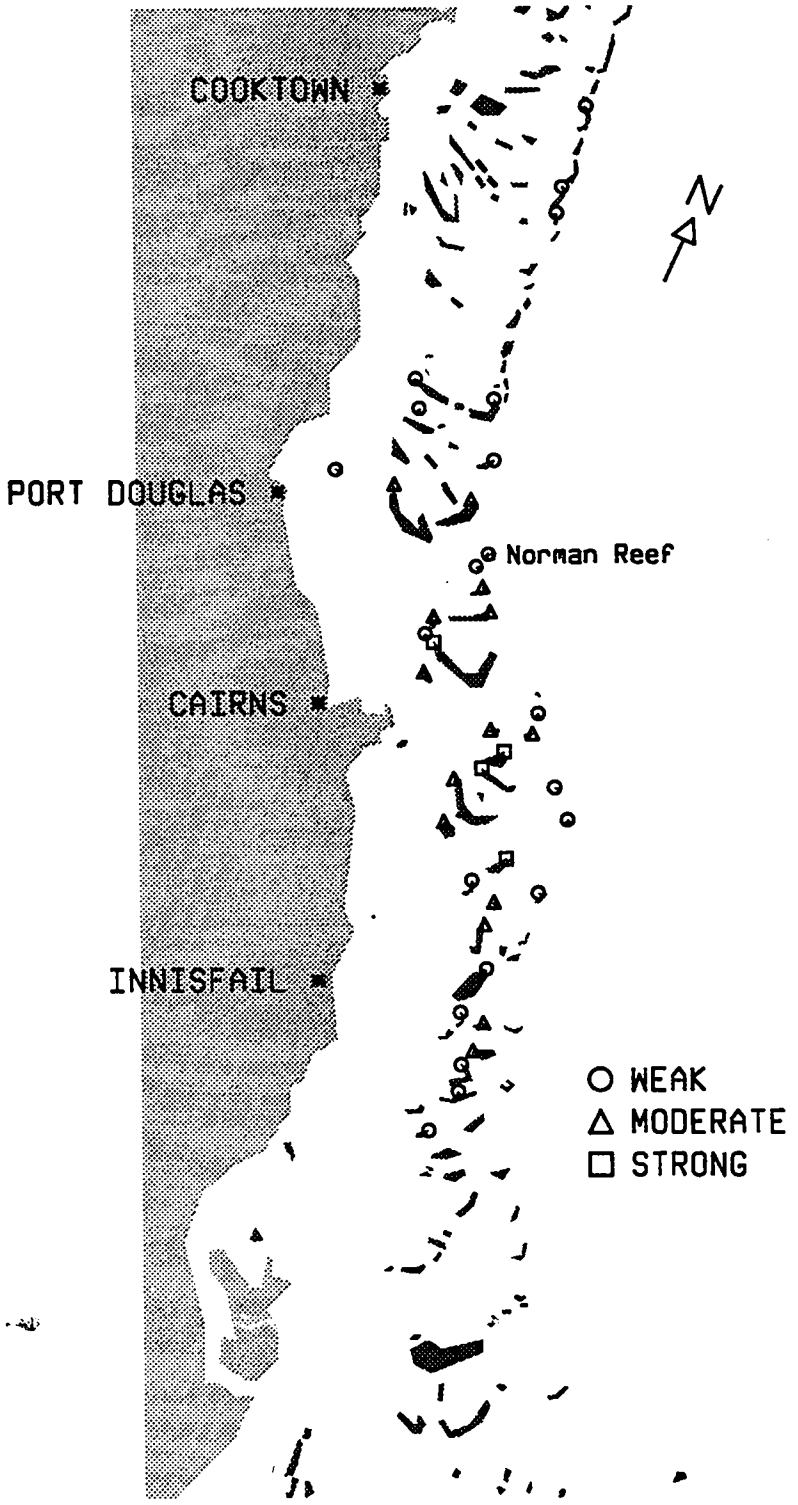


Figure 4.18c Strength of connectivity with respect to Norman Reef. The relative strengths (weak, moderate and strong) are discrete classes separated by an order of magnitude and correspond to the combined **80 dispersal events**. Scale: 1cm = 12 nautical miles.

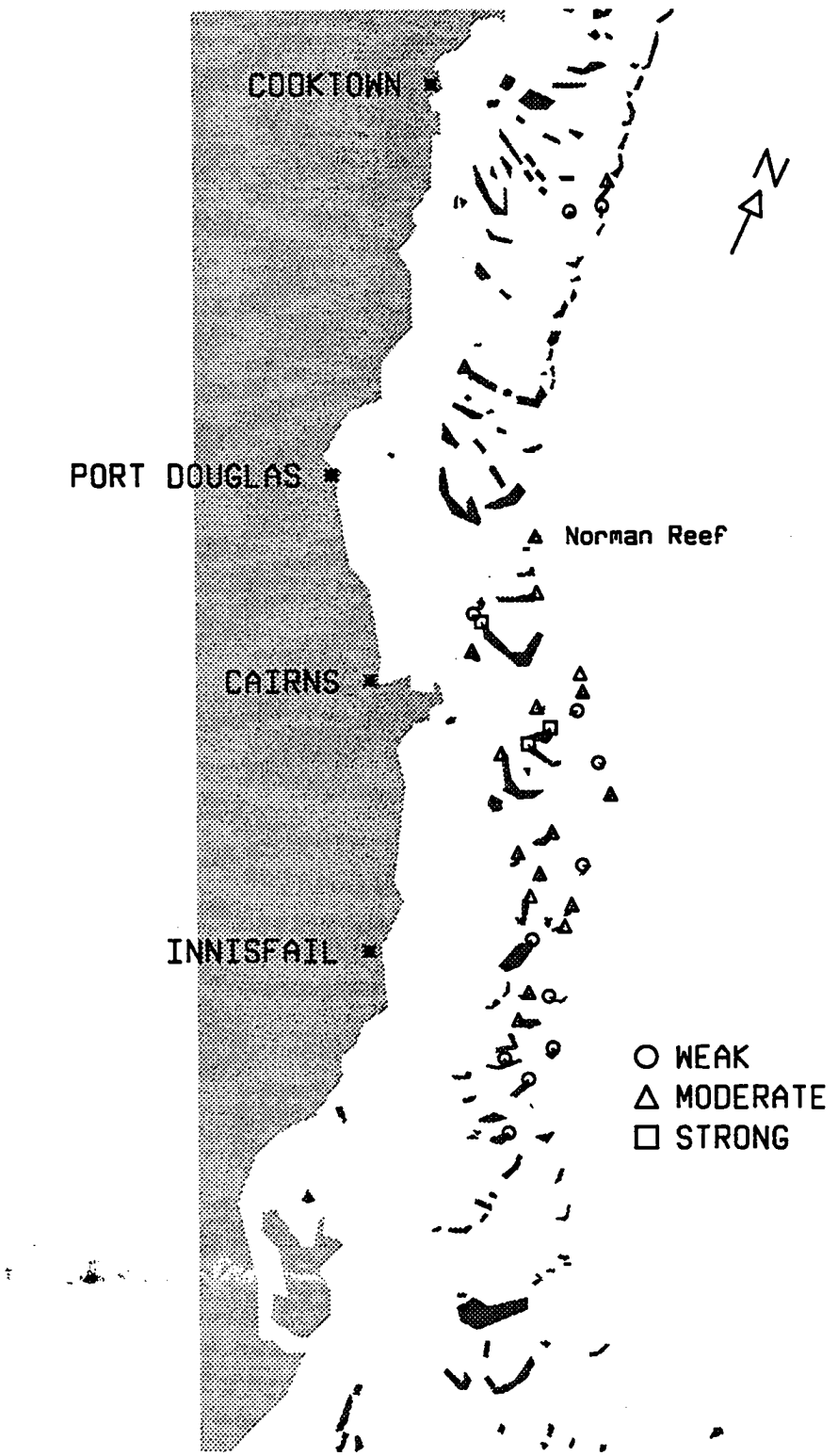


Figure 4.18d Strength of connectivity with respect to Norman Reef. The relative strengths (weak, moderate and strong) are discrete classes separated by an order of magnitude and correspond to the **response time** analysis. Scale: 1cm = 12 nautical miles.

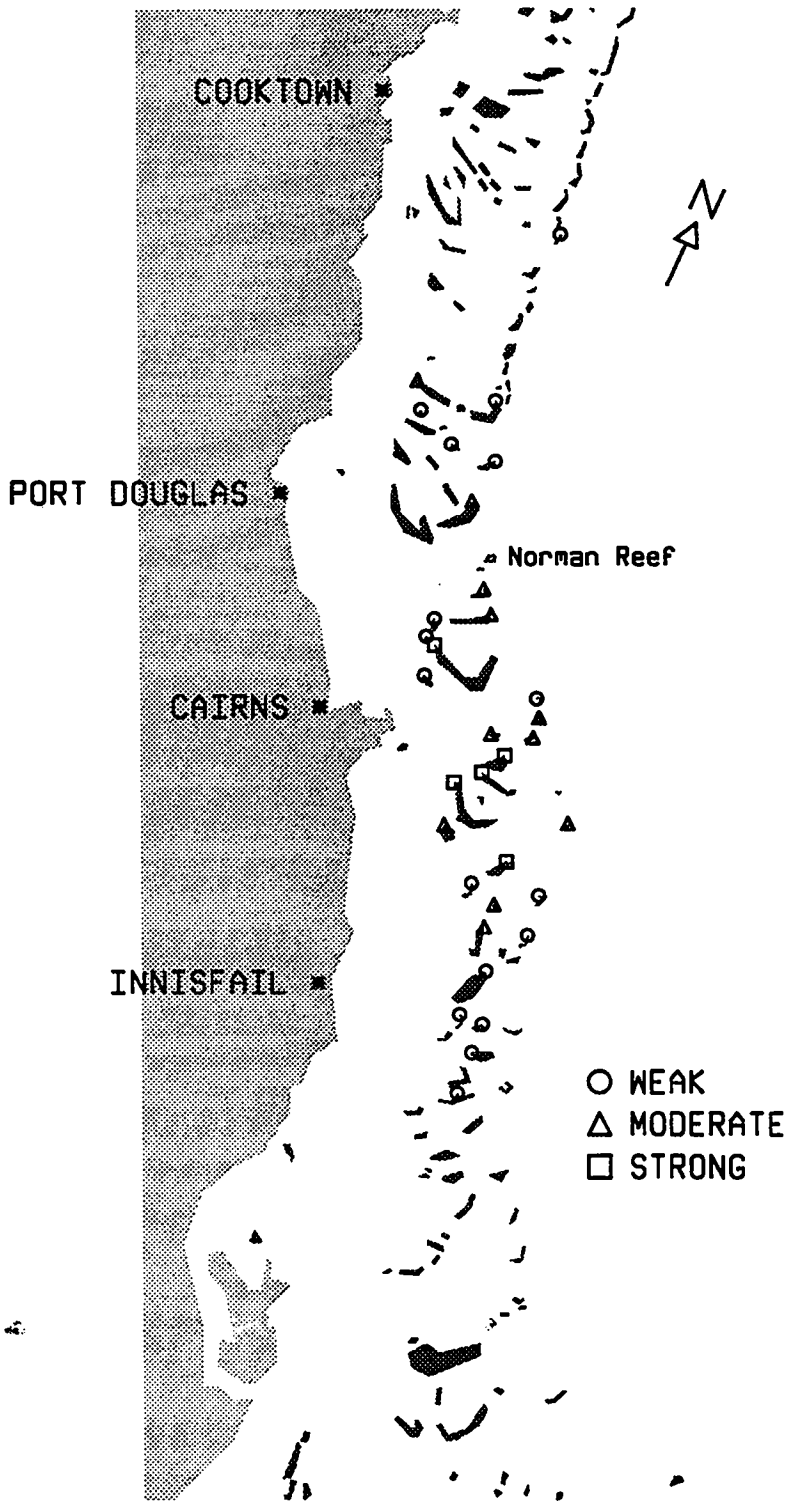


Figure 4.18e Strength of connectivity with respect to Norman Reef. The relative strengths (weak, moderate and strong) are discrete classes separated by an order of magnitude and correspond to the **small larval cloud** analysis. Scale: 1cm = 12 nautical miles.

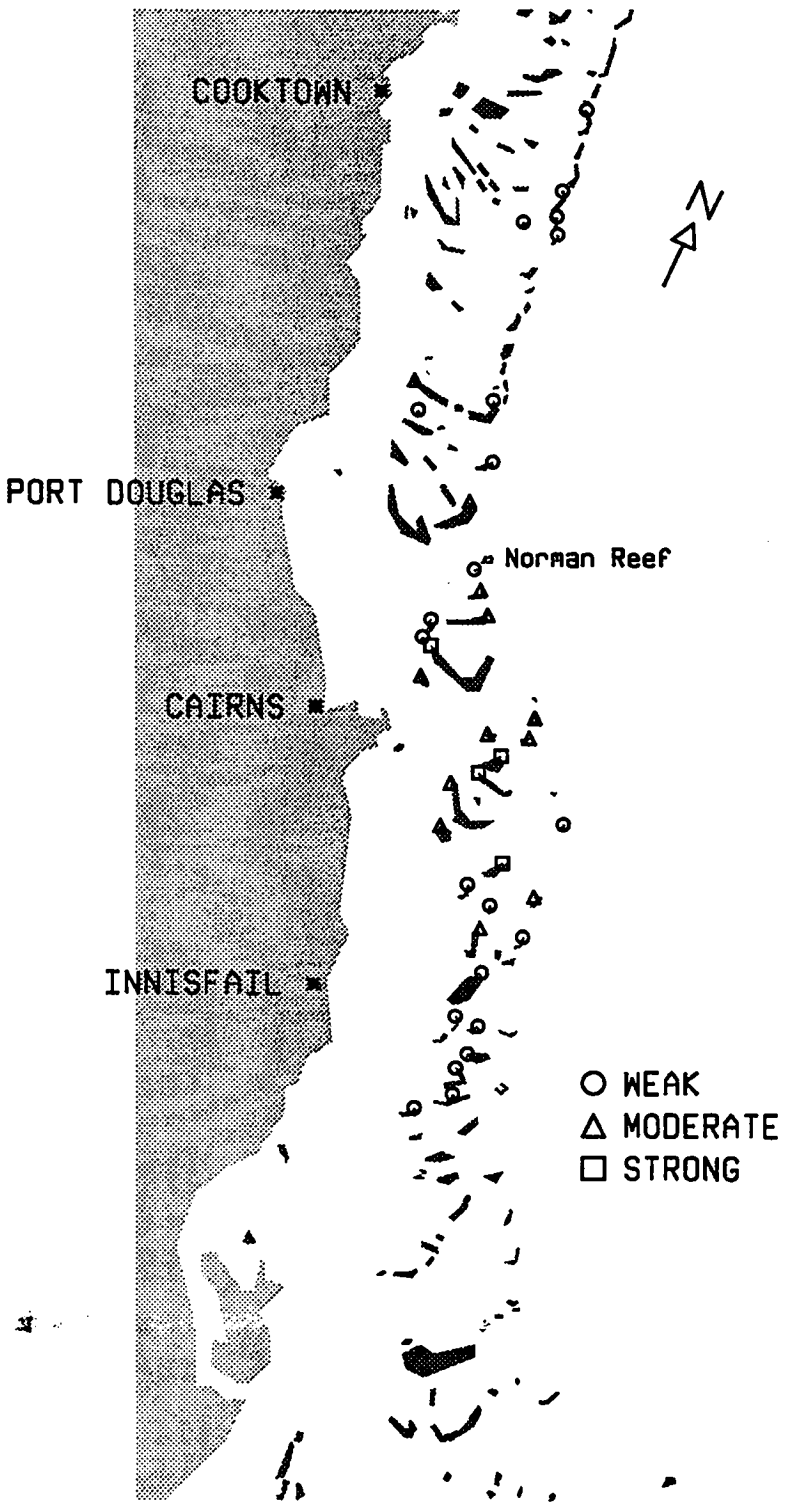


Figure 4.18f Strength of connectivity with respect to Norman Reef. The relative strengths (weak, moderate and strong) are discrete classes separated by an order of magnitude and correspond to the **large larval cloud** analysis. Scale: 1cm = 12 nautical miles.

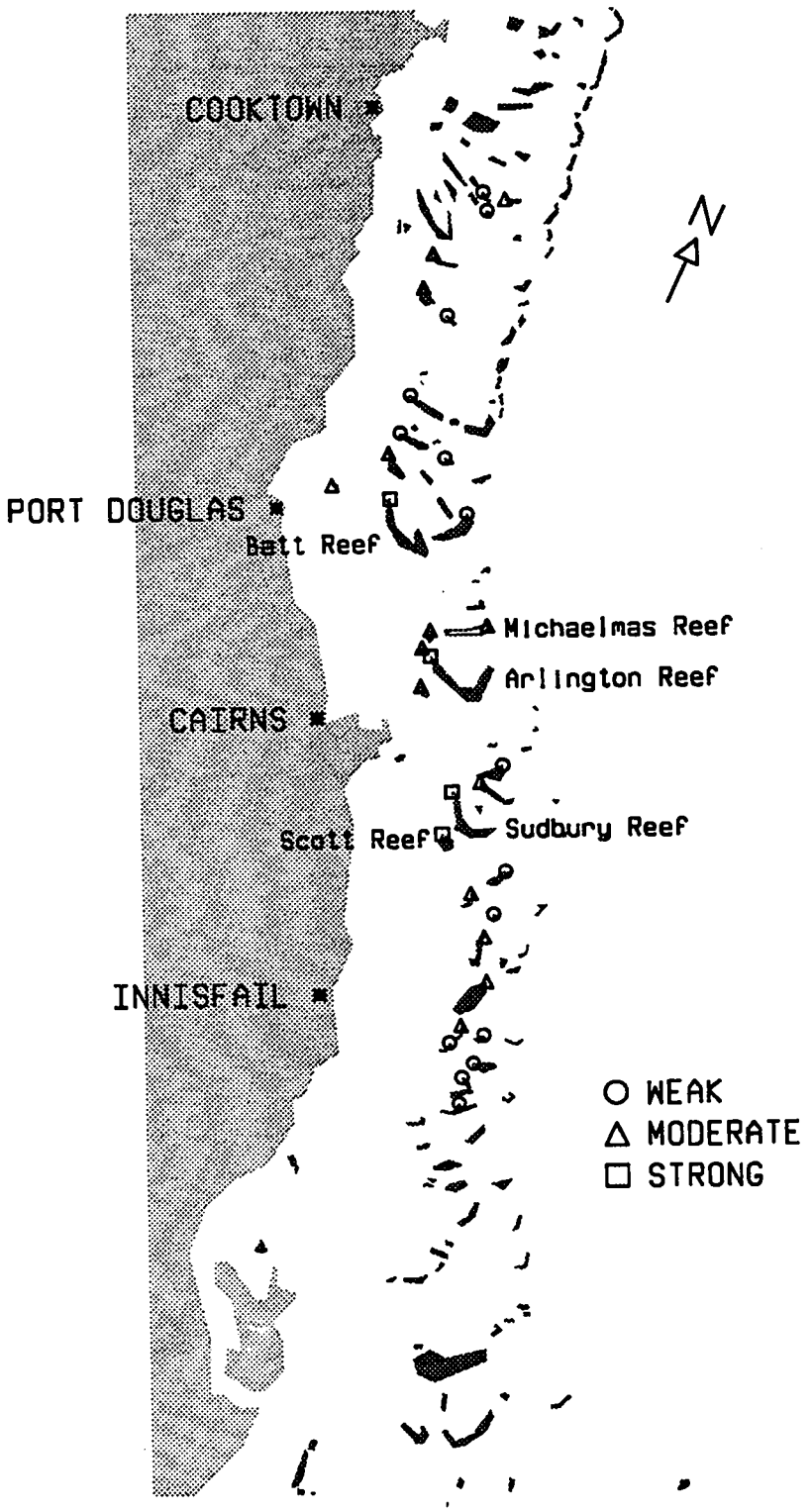


Figure 4.19a Strength of connectivity with respect to Michaelmas Reef. The relative strengths (weak, moderate and strong) are discrete classes separated by an order of magnitude and correspond to the **base data**. Scale: 1cm = 12 nautical miles.

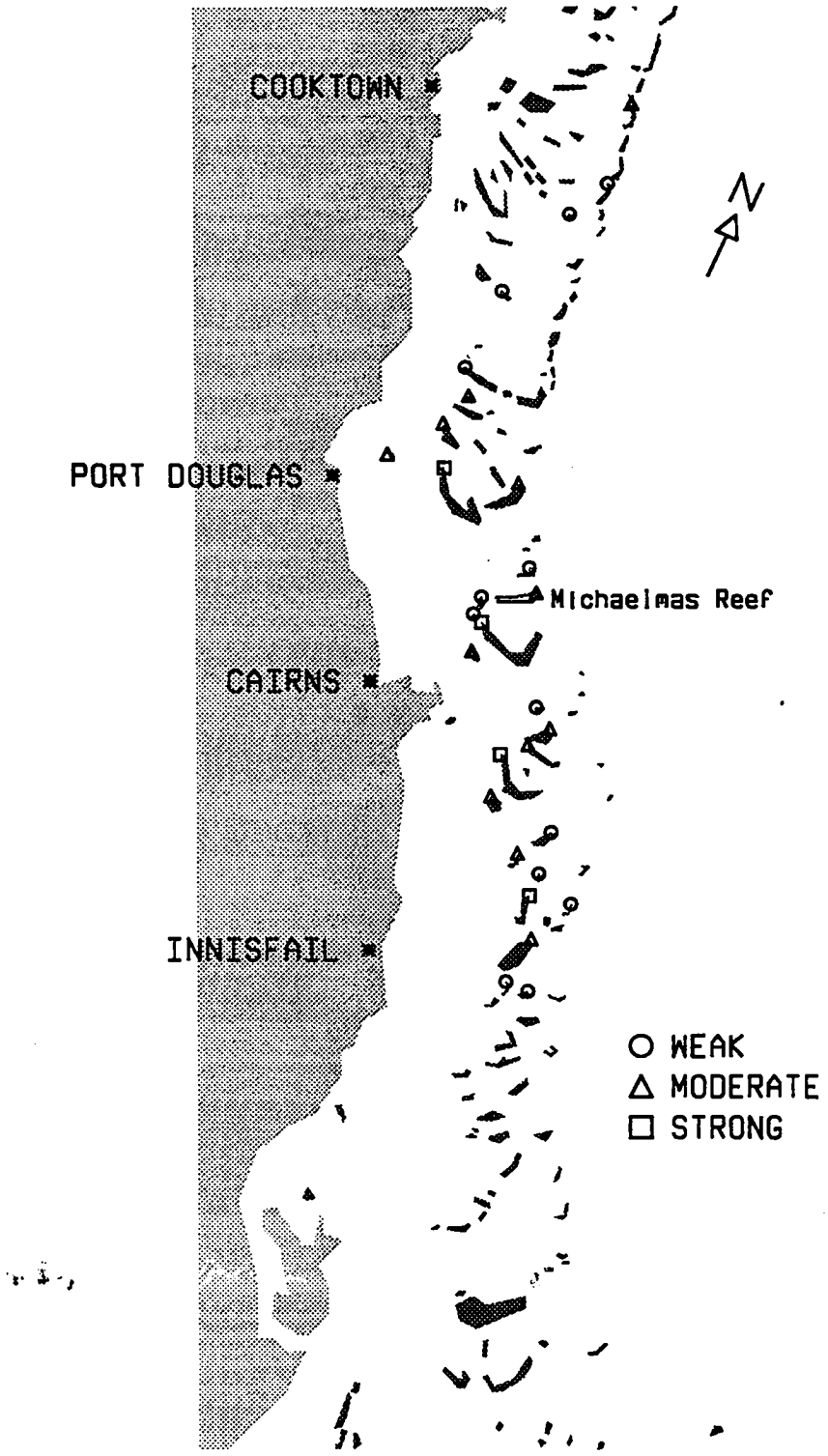


Figure 4.19b Strength of connectivity with respect to Michaelmas Reef. The relative strengths (weak, moderate and strong) are discrete classes separated by an order of magnitude and correspond to the **replicate** 40 dispersal events. Scale: 1cm = 12 nautical miles.

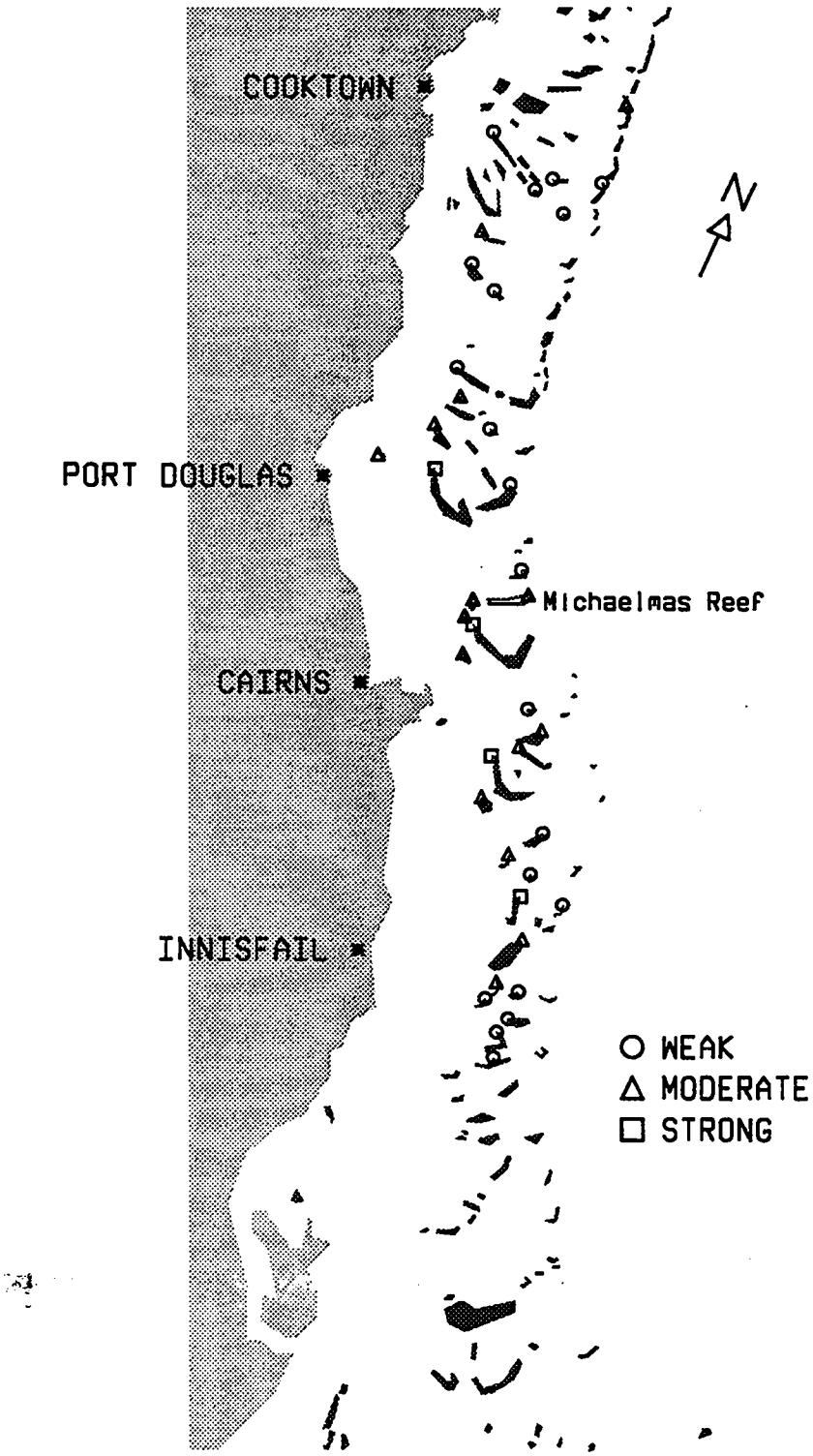


Figure 4.19c Strength of connectivity with respect to Michaelmas Reef. The relative strengths (weak, moderate and strong) are discrete classes separated by an order of magnitude and correspond to the combined 80 **dispersal events**. Scale: 1cm = 12 nautical miles.

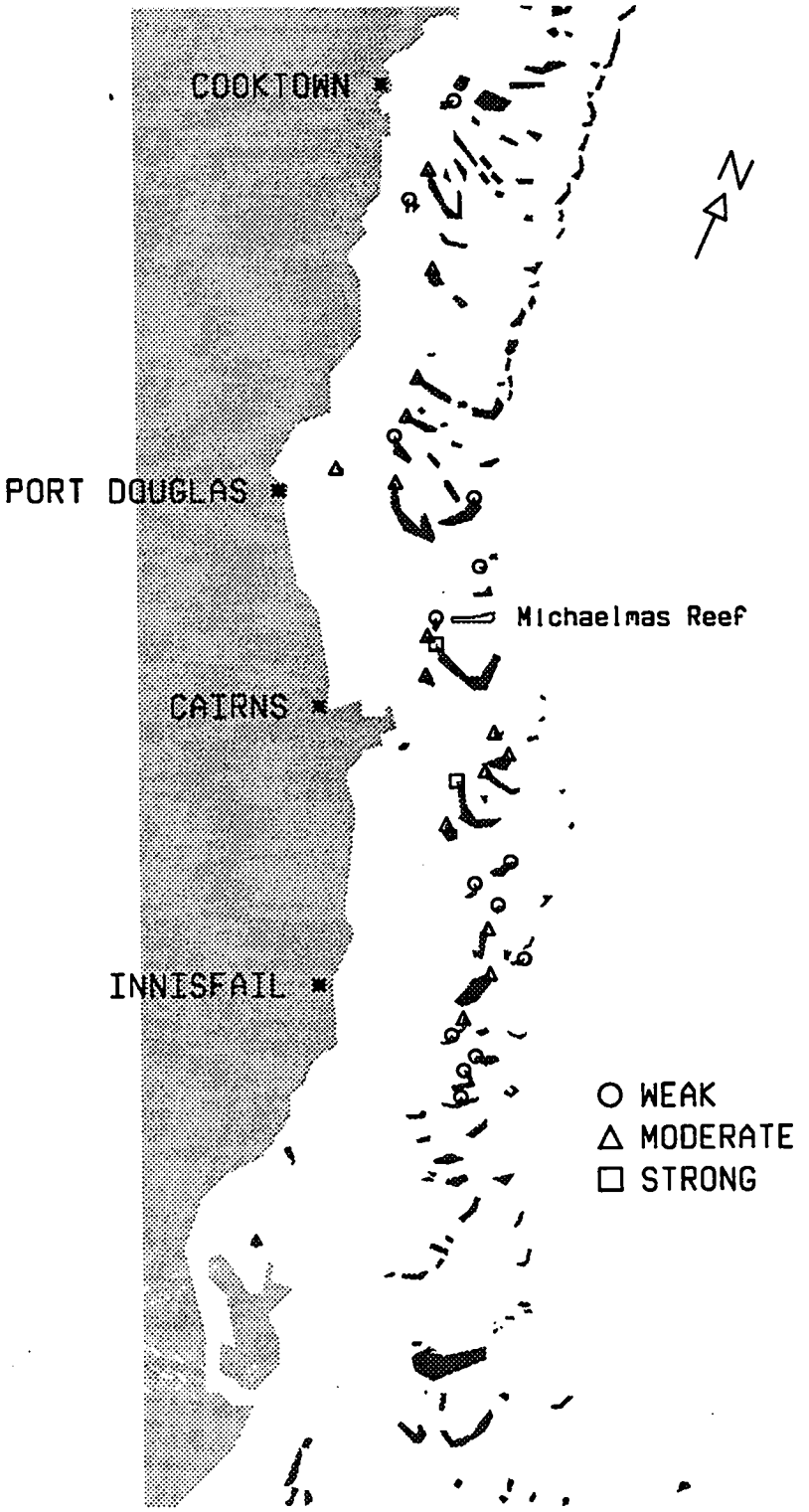


Figure 4.19d Strength of connectivity with respect to Michaelmas Reef. The relative strengths (weak, moderate and strong) are discrete classes separated by an order of magnitude and correspond to the response time analysis. Scale: 1cm = 12 nautical miles.

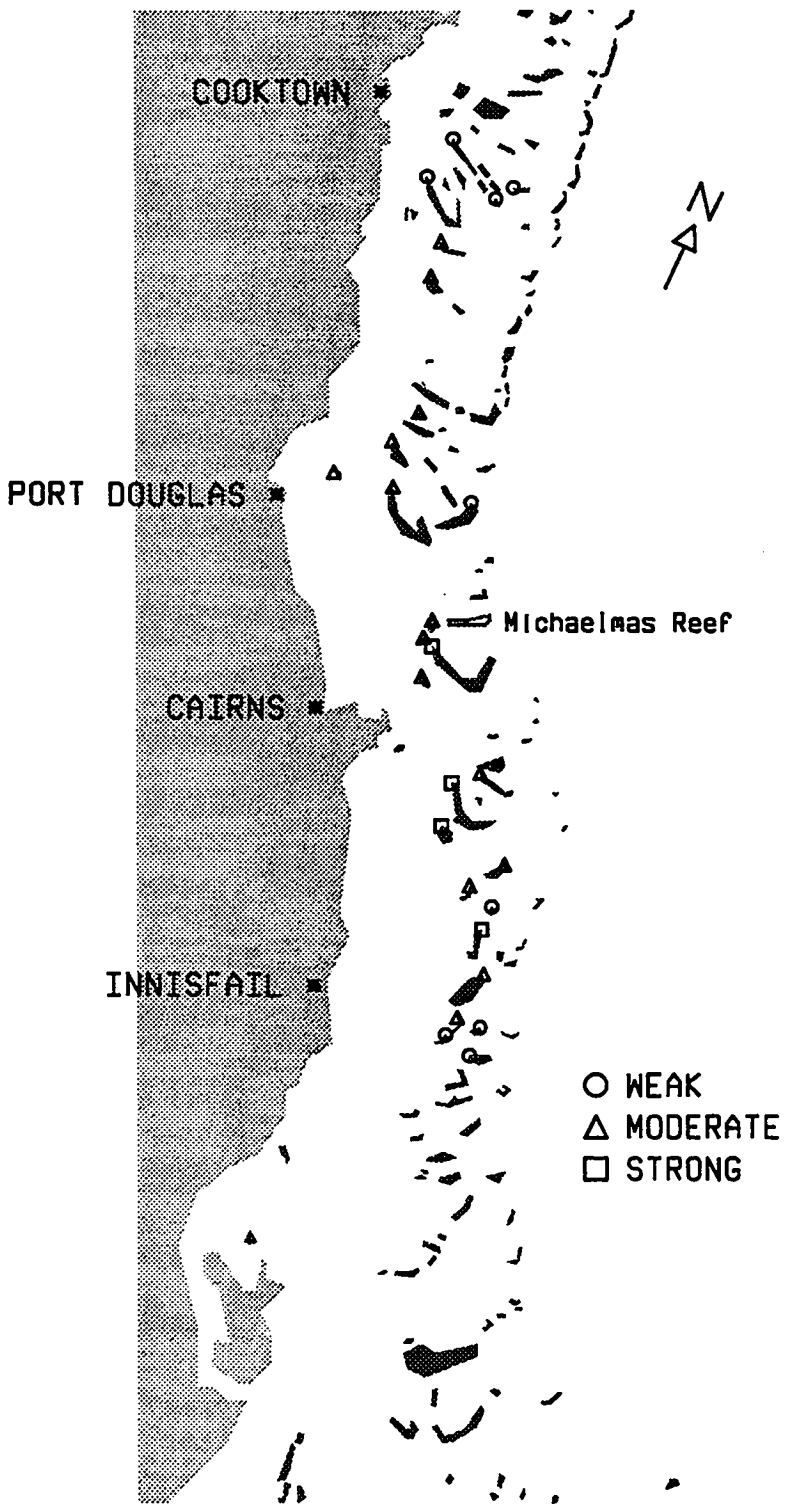


Figure 4.19e Strength of connectivity with respect to Michaelmas Reef. The relative strengths (weak, moderate and strong) are discrete classes separated by an order of magnitude and correspond to the **small larval cloud** analysis. Scale: 1cm = 12 nautical miles.

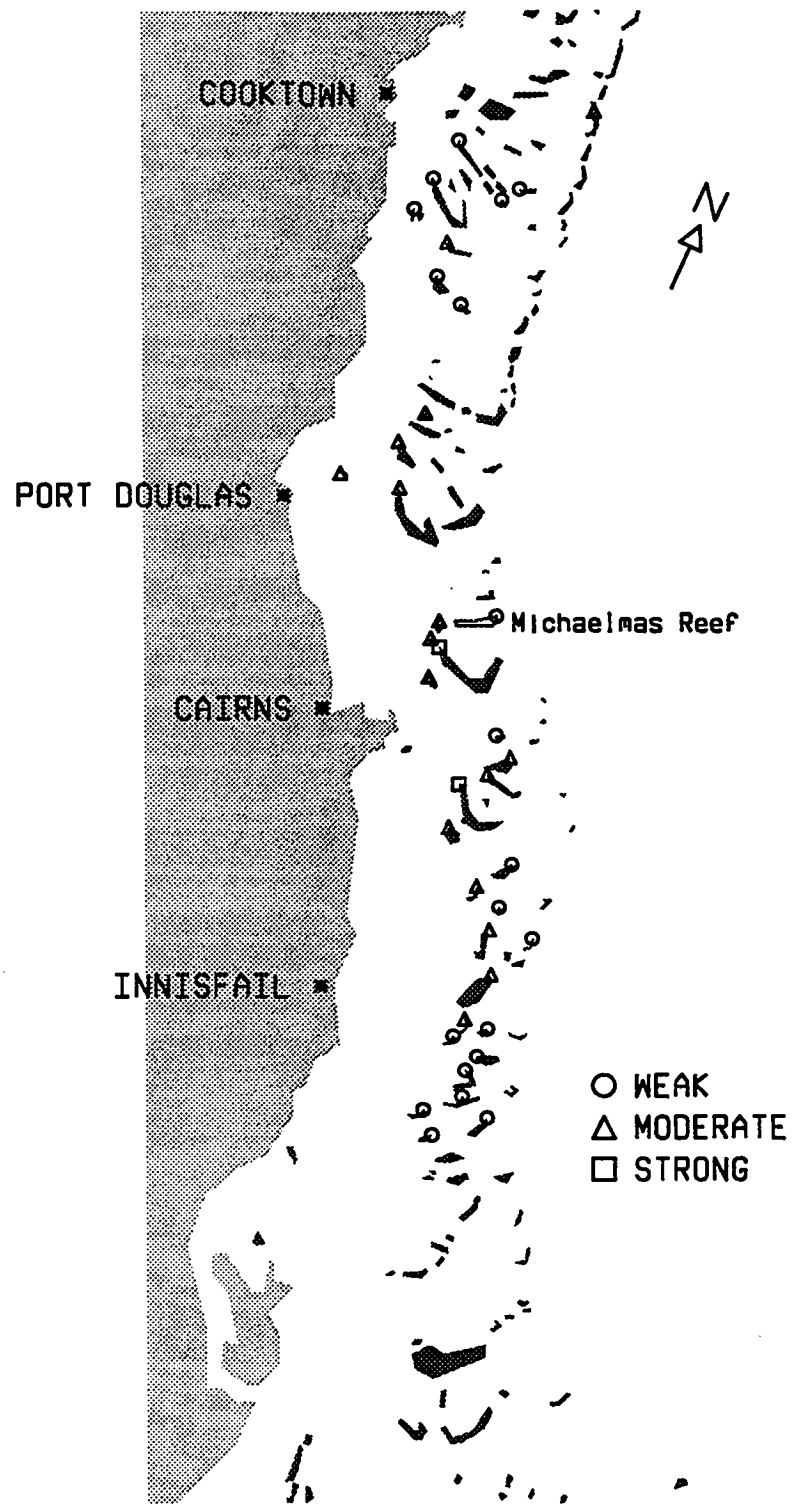


Figure 4.19f Strength of connectivity with respect to Michaelmas Reef. The relative strengths (weak, moderate and strong) are discrete classes separated by an order of magnitude and correspond to the large larval cloud analysis. Scale: 1cm = 12 nautical miles.

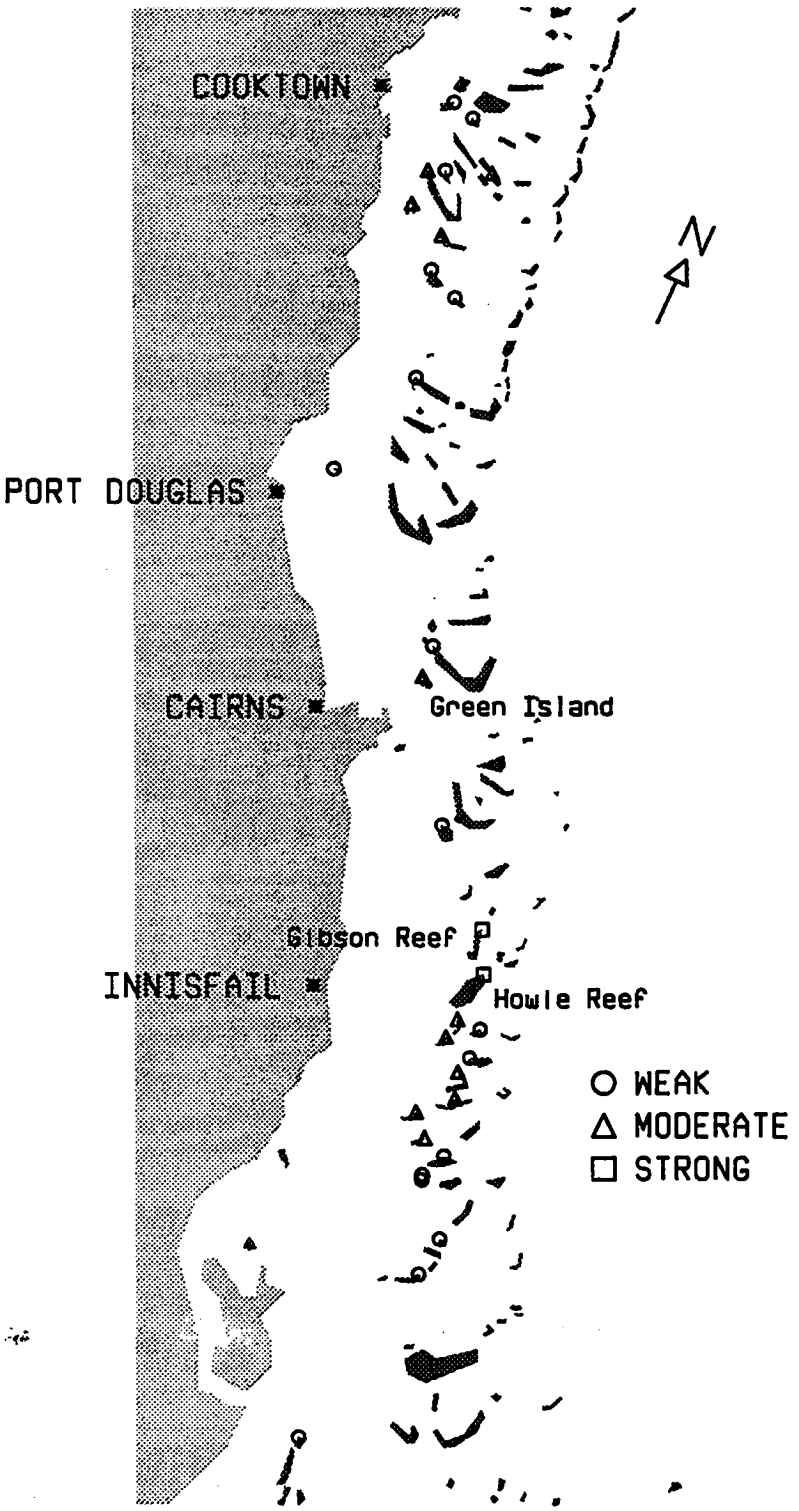


Figure 4.20a Strength of connectivity with respect to Green Island. The relative strengths (weak, moderate and strong) are discrete classes separated by an order of magnitude and correspond to the base data. Scale: 1cm = 12 nautical miles.

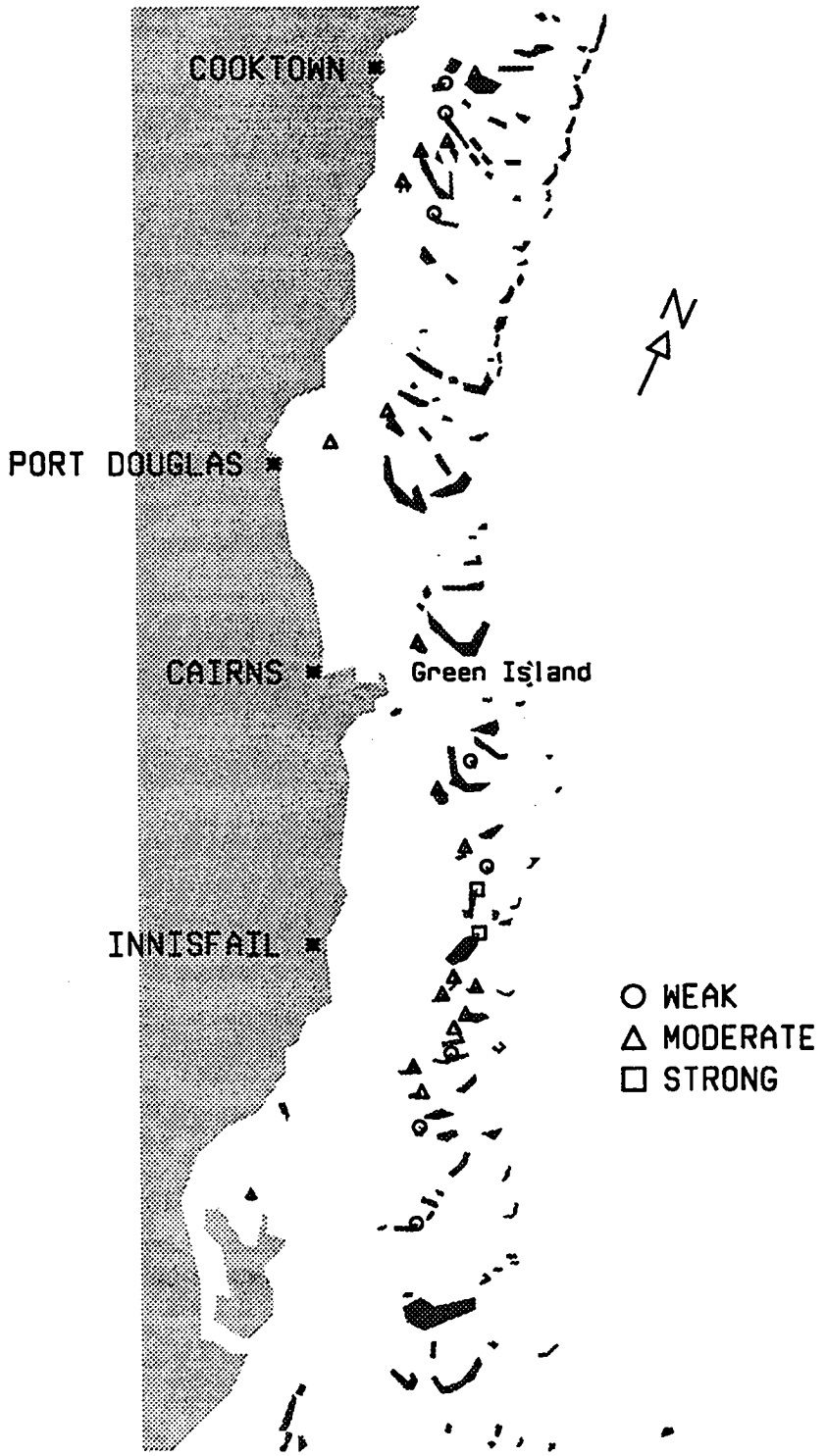


Figure 4.20b Strength of connectivity with respect to Green Island. The relative strengths (weak, moderate and strong) are discrete classes separated by an order of magnitude and correspond to the **replicate** 40 dispersal events. Scale: 1cm = 12 nautical miles.

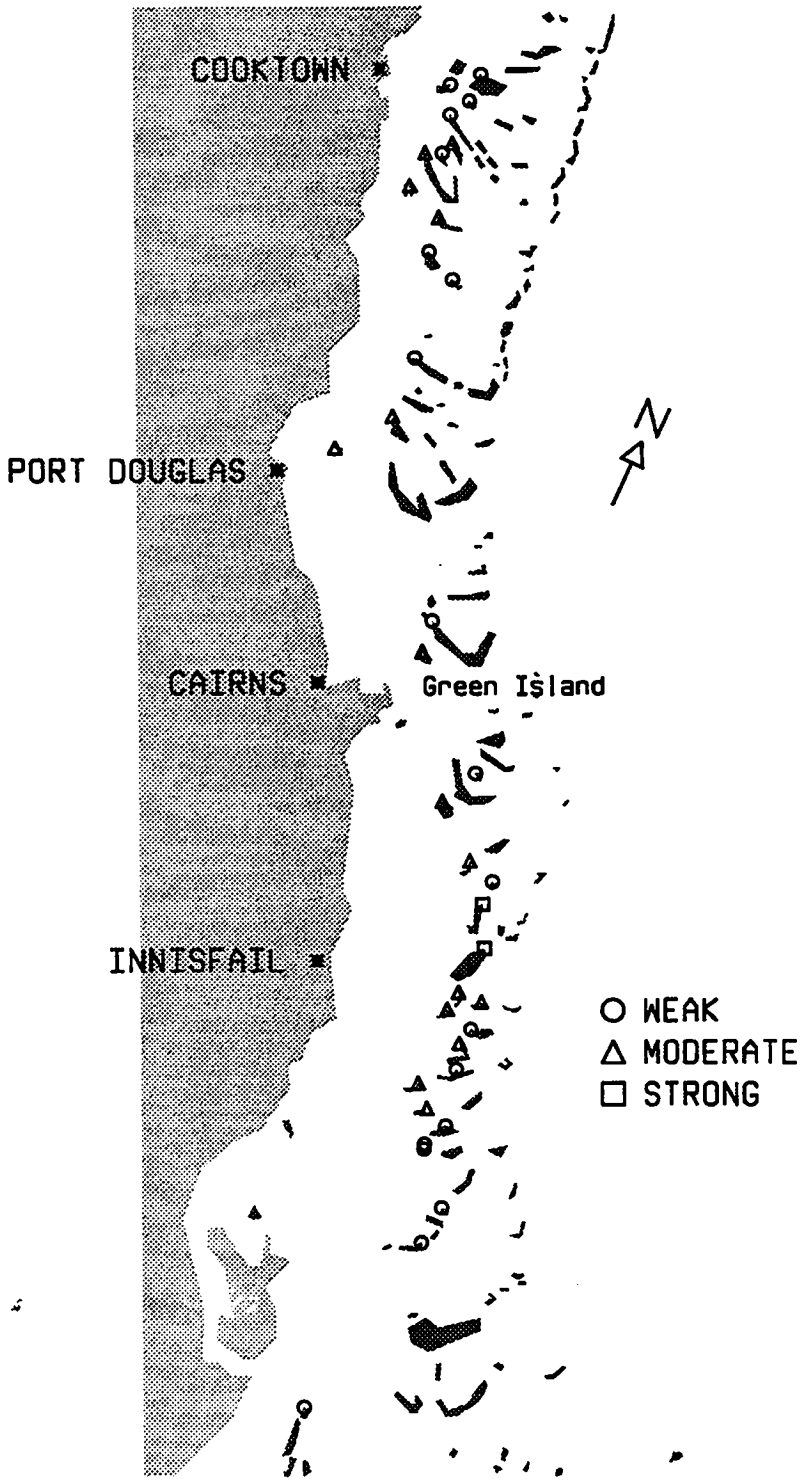


Figure 4.20c Strength of connectivity with respect to Green Island. The relative strengths (weak, moderate and strong) are discrete classes separated by an order of magnitude and correspond to the combined 80 dispersal events. Scale: 1cm = 12 nautical miles.

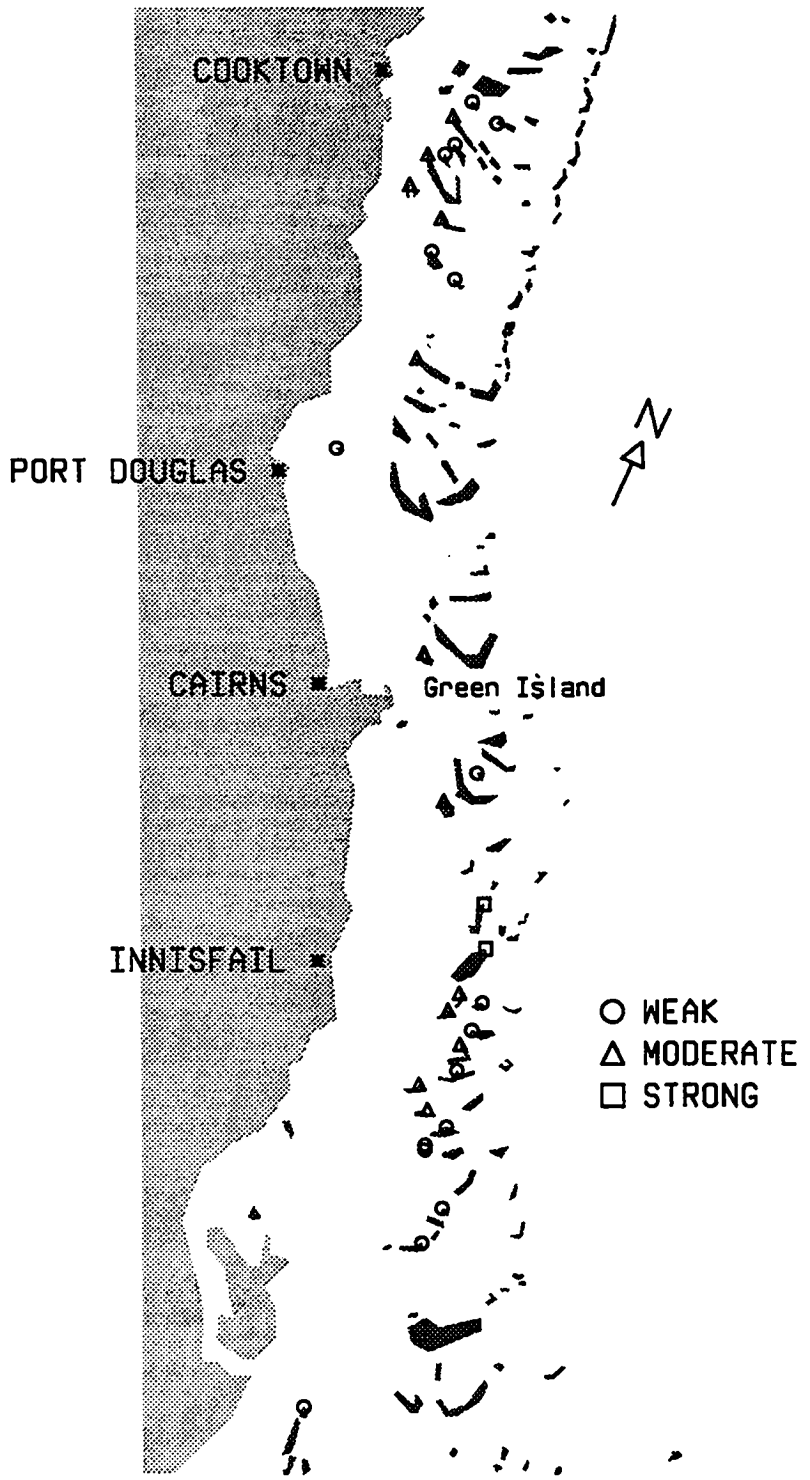


Figure 4.20d Strength of connectivity with respect to Green Island. The relative strengths (weak, moderate and strong) are discrete classes separated by an order of magnitude and correspond to the interpolated wind field analysis. Scale: 1cm = 12 nautical miles.

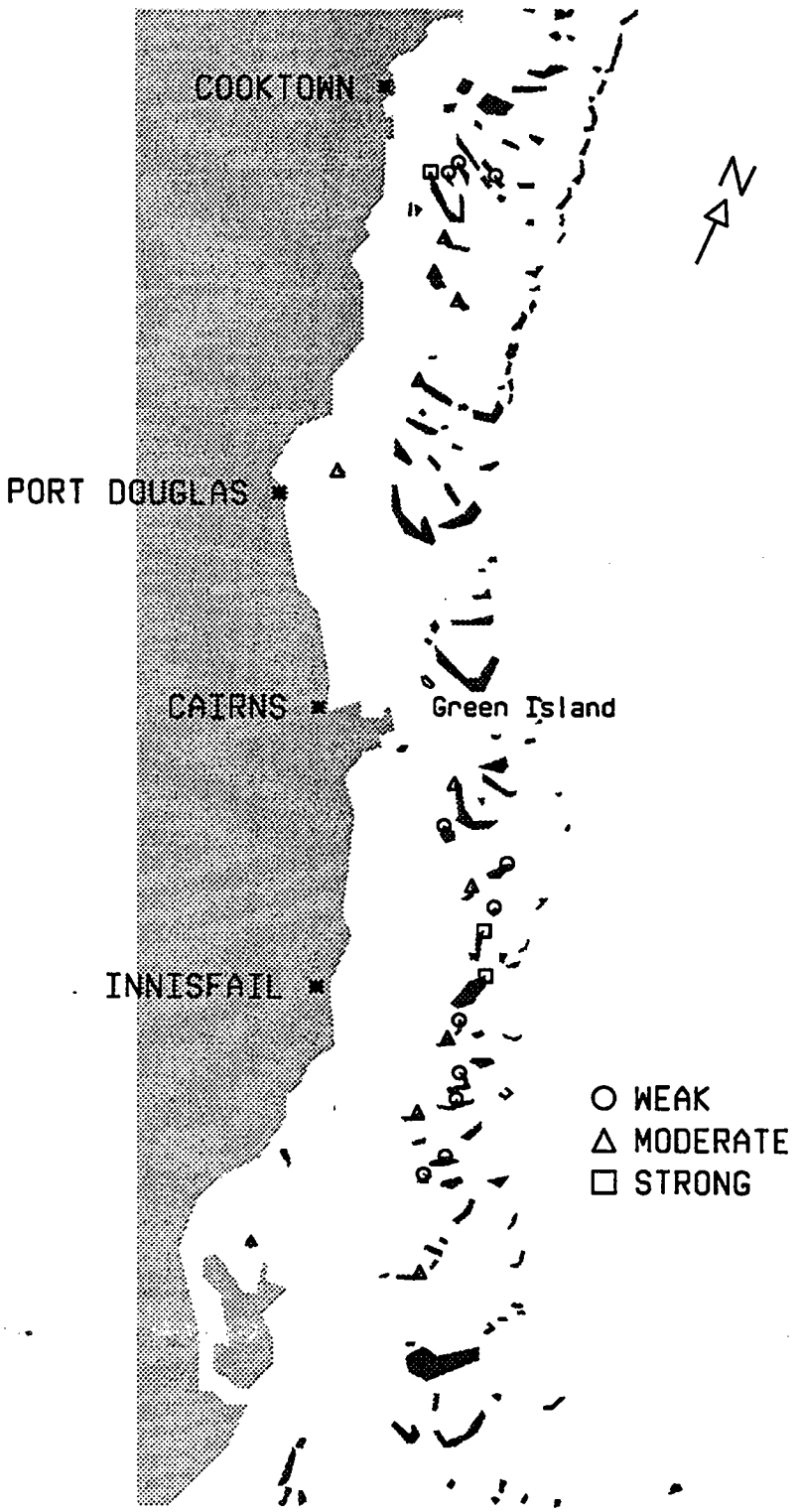


Figure 4.20e Strength of connectivity with respect to Green Island. The relative strengths (weak, moderate and strong) are discrete classes separated by an order of magnitude and correspond to the **response time** analysis. Scale: 1cm = 12 nautical miles.

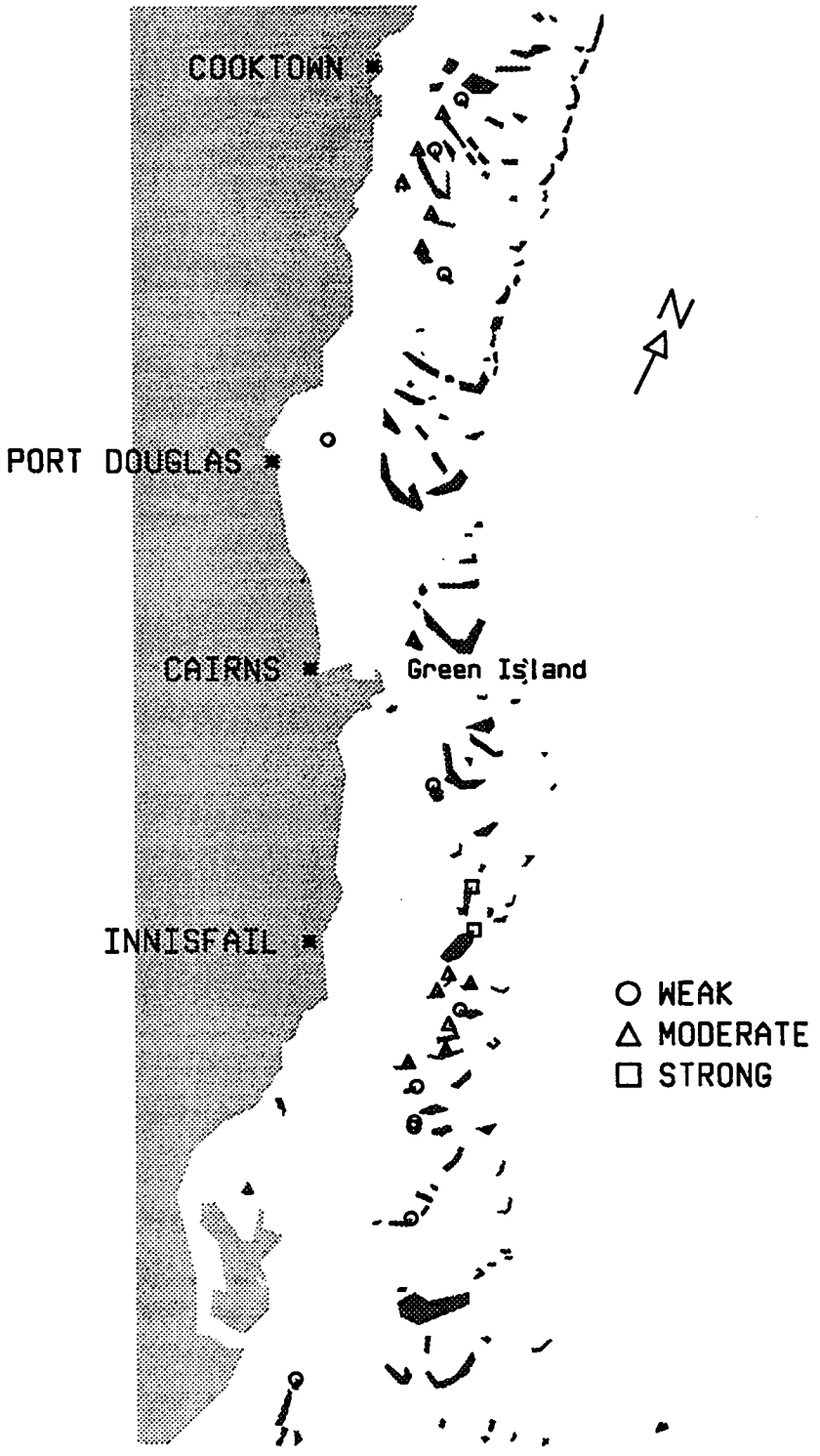


Figure 4.20f Strength of connectivity with respect to Green Island. The relative strengths (weak, moderate and strong) are discrete classes separated by an order of magnitude and correspond to the **small larval cloud** analysis. Scale: 1cm = 12 nautical miles.

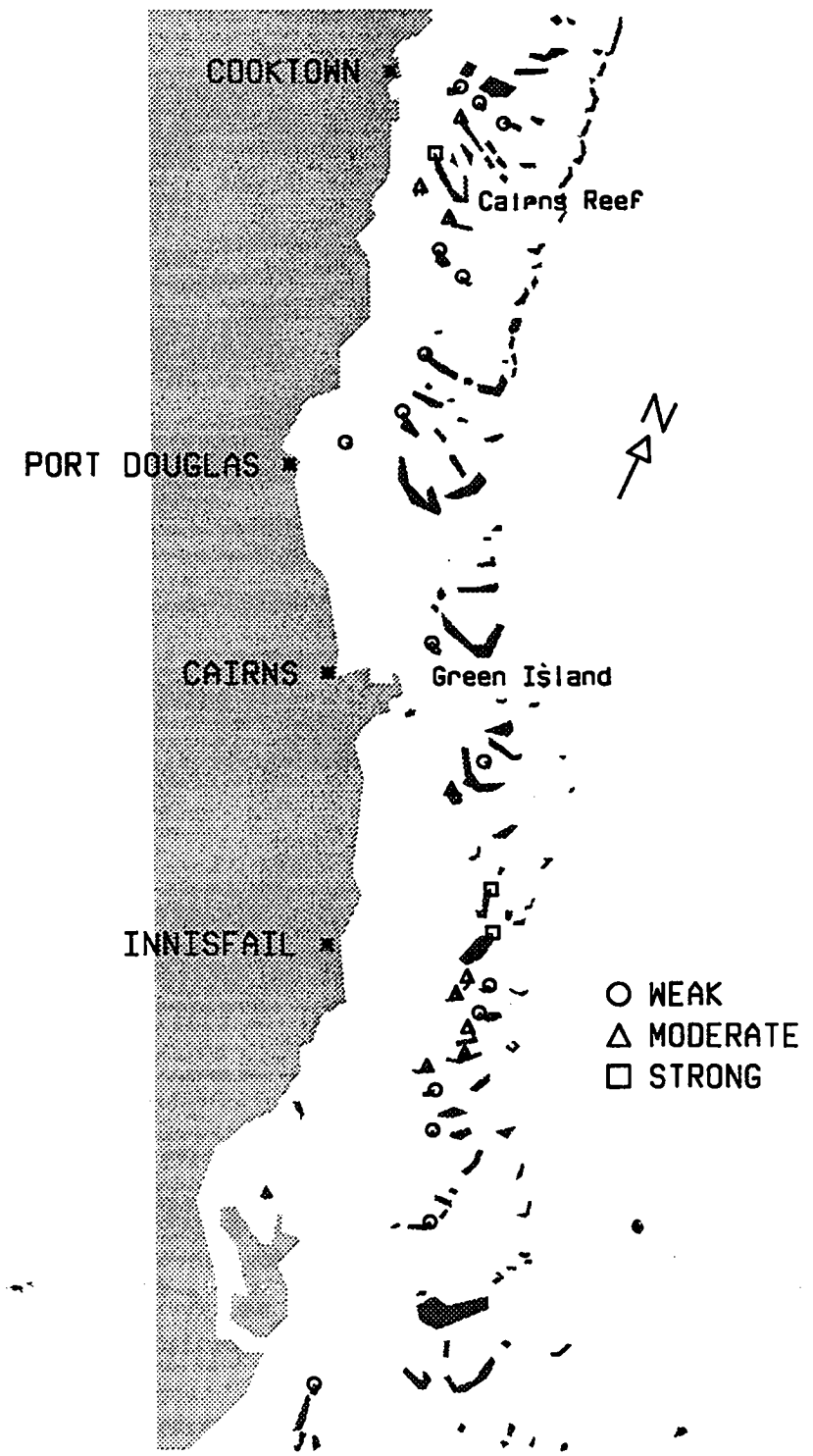


Figure 4.20g Strength of connectivity with respect to Green Island. The relative strengths (weak, moderate and strong) are discrete classes separated by an order of magnitude and correspond to the **large larval cloud** analysis. Scale: 1cm = 12 nautical miles.

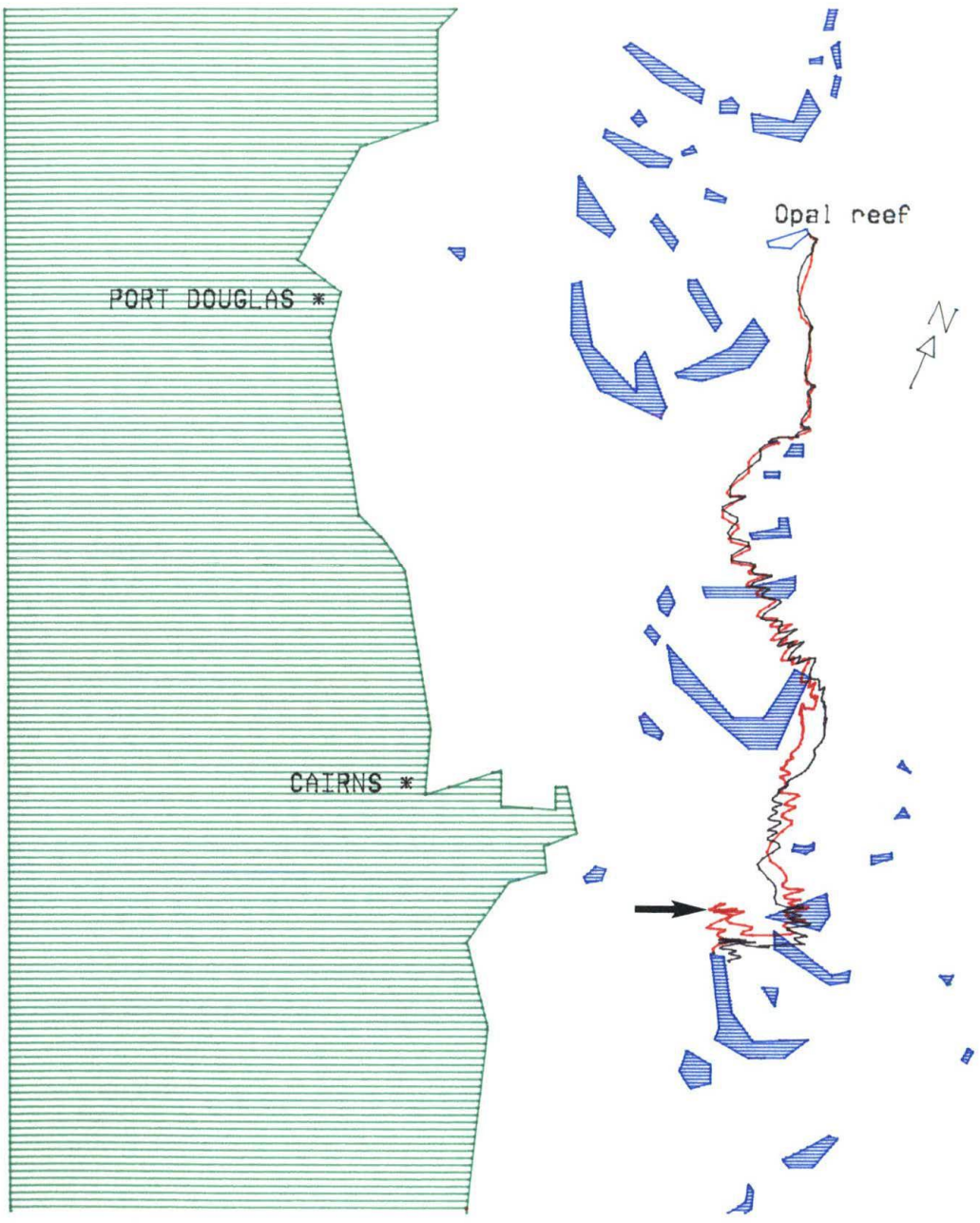


Figure 4.21 Comparison of a **base data** particle trajectory (black) with one simulated using an **interpolated wind field** (red, arrowed). Often there may be little difference between the trajectories. Scale: 1cm = 4.5 nautical miles.

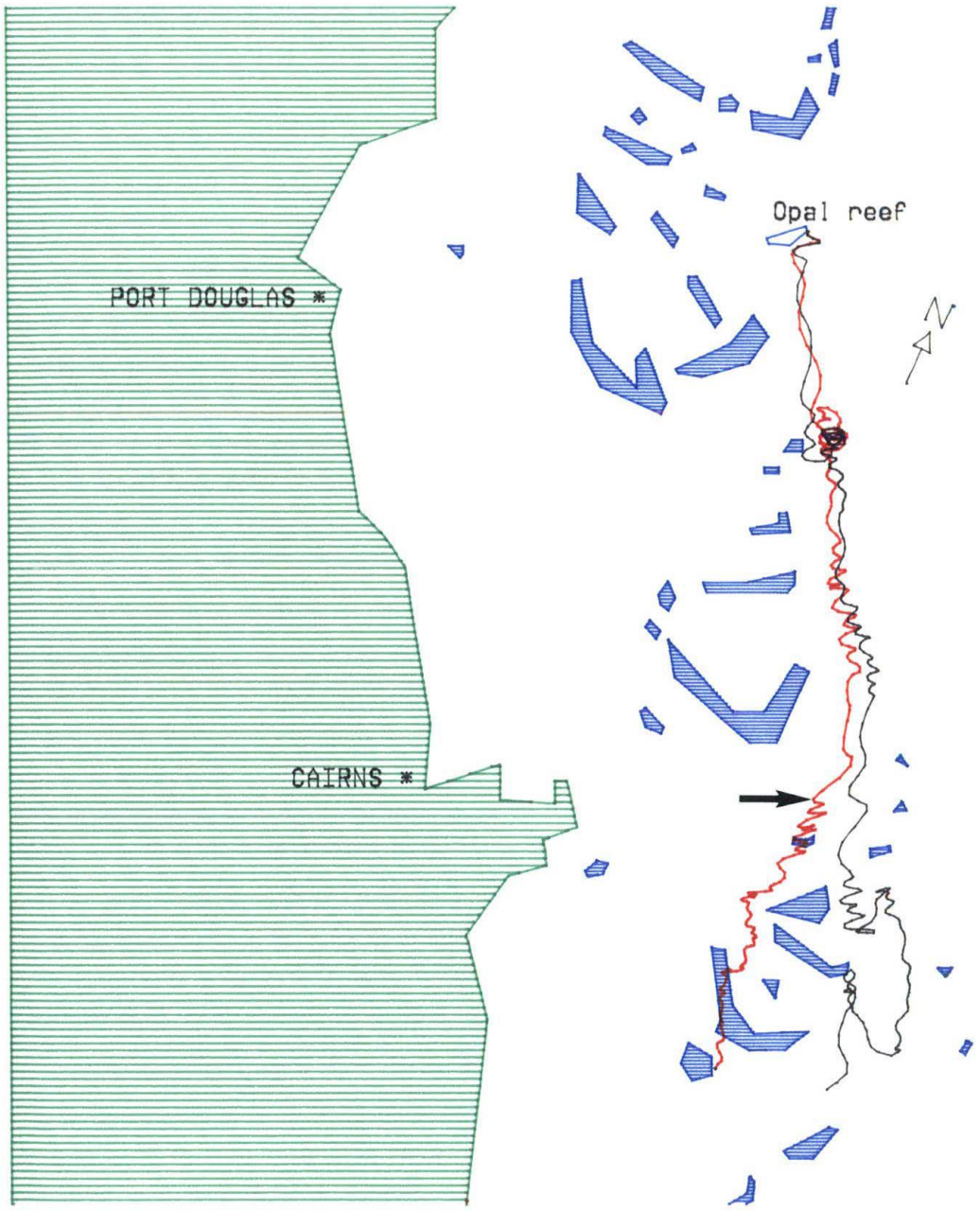


Figure 4.22 Comparison of a **base data** particle trajectory (black) with one simulated using an **interpolated wind field** (red, arrowed). In some cases there may be substantial differences between the trajectories. Scale: 1cm = 4.5 nautical miles.

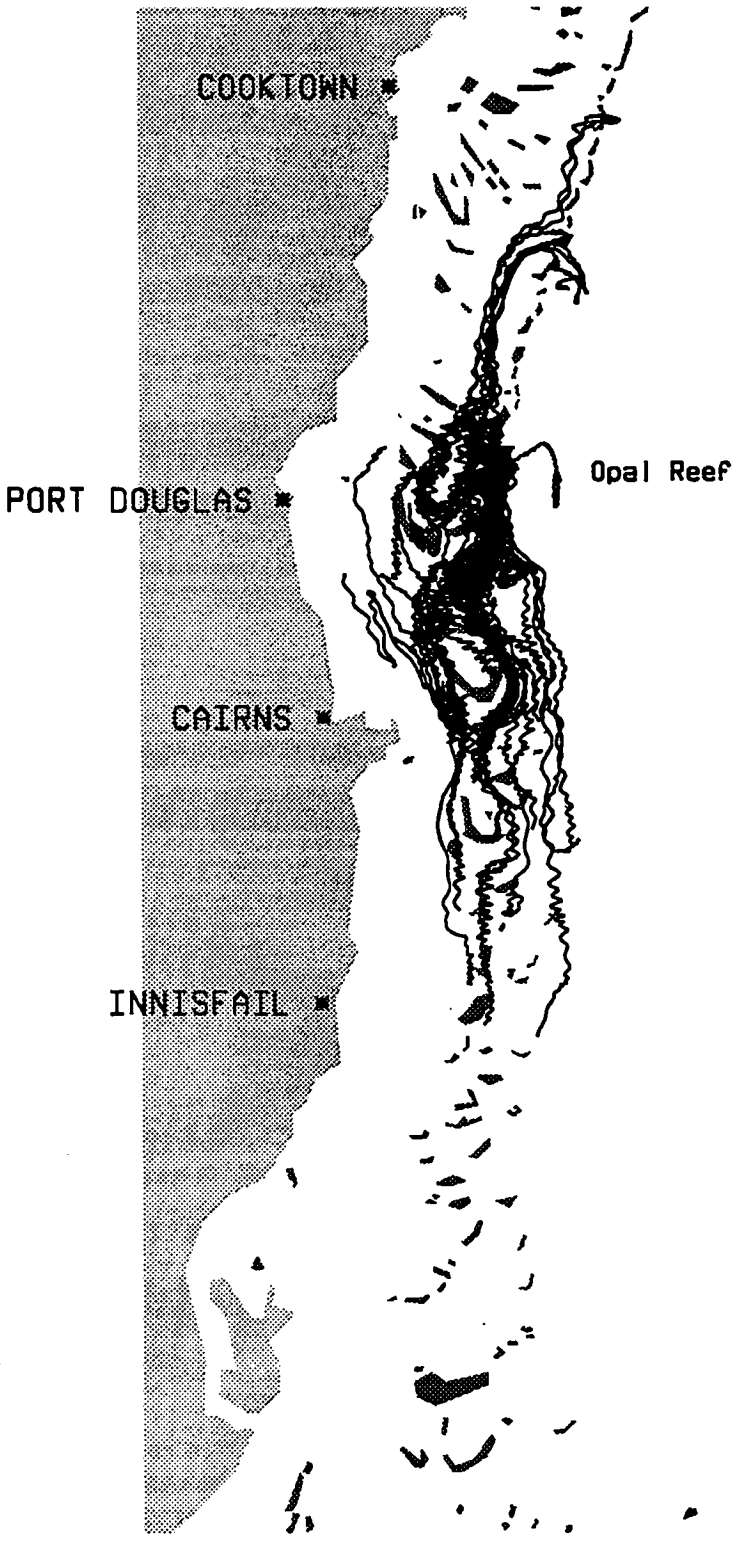


Figure 4.23 The trajectories of all 40 dispersal events representing the **base data** analysis illustrate the domain of influence of Opal Reef. Each trajectory represents the centroid of the larval cloud over the period when larvae are competent to settle. Scale: 1cm = 10.5 nautical miles.

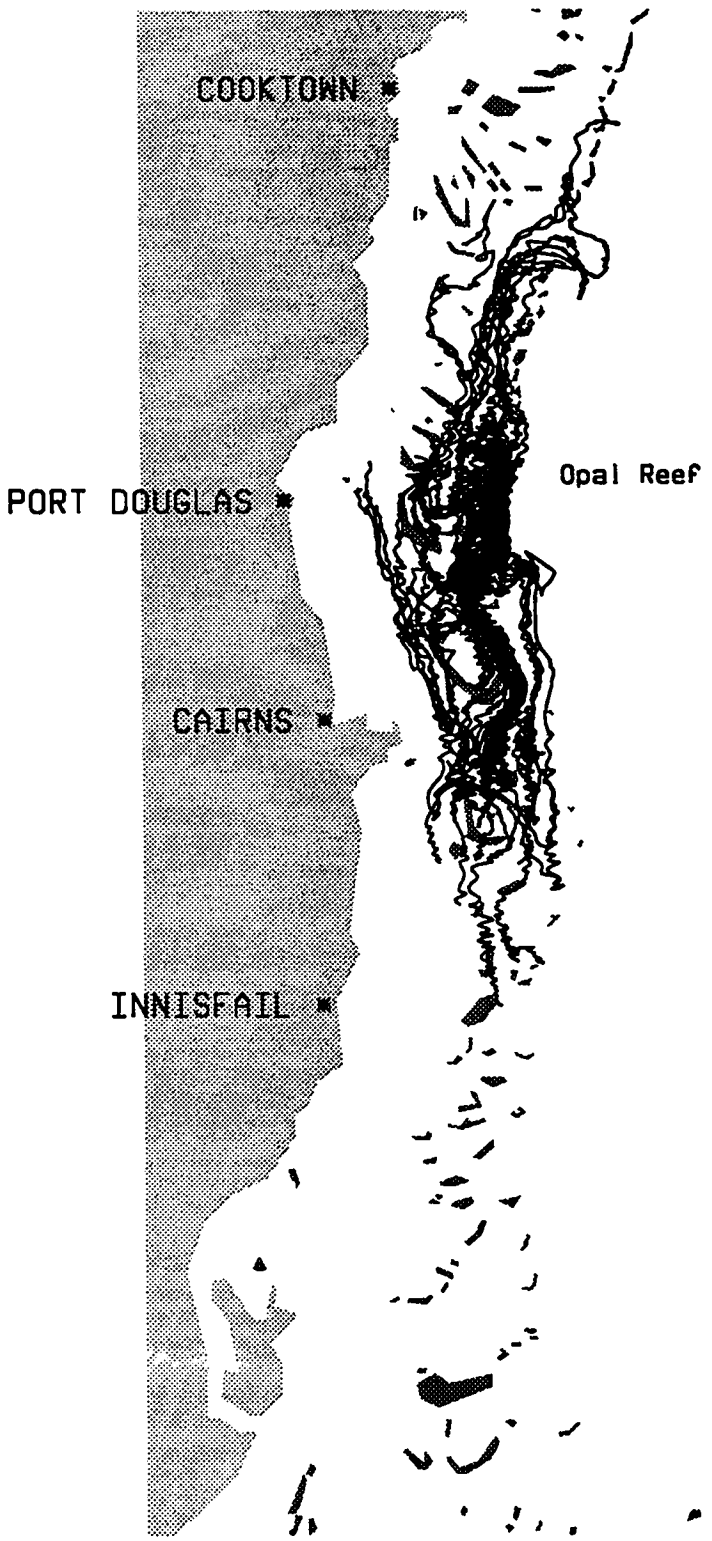
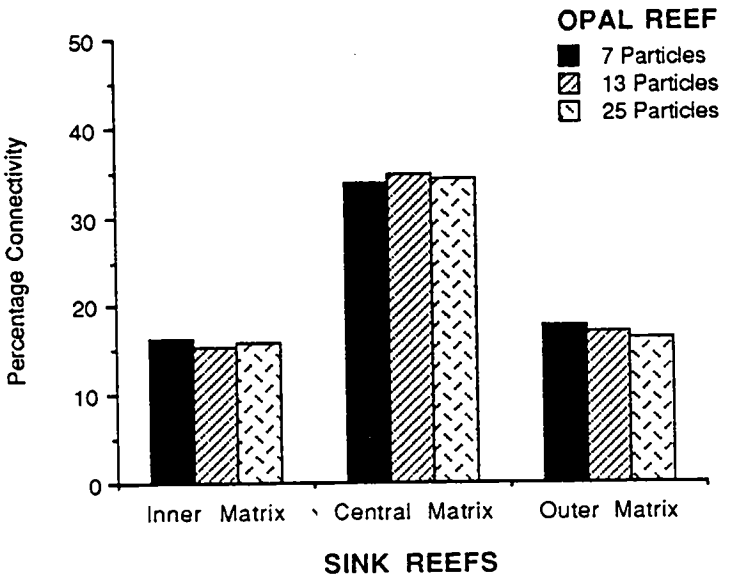
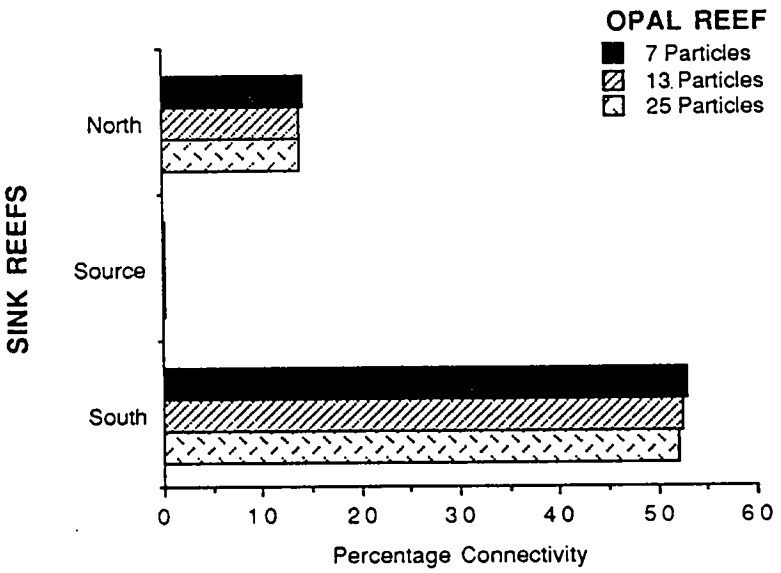


Figure 4.24 The trajectories of all 40 dispersal events representing the **response time** analysis illustrate the domain of influence of Opal Reef. Each trajectory represents the centroid of the larval cloud over the period when larvae are competent to settle. Scale: 1cm = 10.5 nautical miles.



(a) Level of reef connectivity with respect to the cross-shelf transport of larvae from Opal Reef. Sink reefs are classified as lying along the outer edge of the reef matrix and continental shelf (outer matrix), central within the reef matrix (central matrix) and along the inner edge of the reef matrix bordering the main lagoon (inner matrix).



(b) Level of reef connectivity with respect to the long-shelf transport of larvae from Opal Reef. Sink reefs are classified as lying to the north or south with respect to the source reef, or recruitment back onto the parent reef (source).

Figure 4.25 Data are presented for three analyses based on the random selection of 20 dispersal events from Opal Reef and represent the number of particles that intersect with sink reefs, expressed as a percentage of the total number of particle trajectories simulated. The three analyses correspond to: (1) a larval cloud represented by **7 particles**; (2) a larval cloud represented by **13 particles**; and (3) a larval cloud represented by **25 particles**.

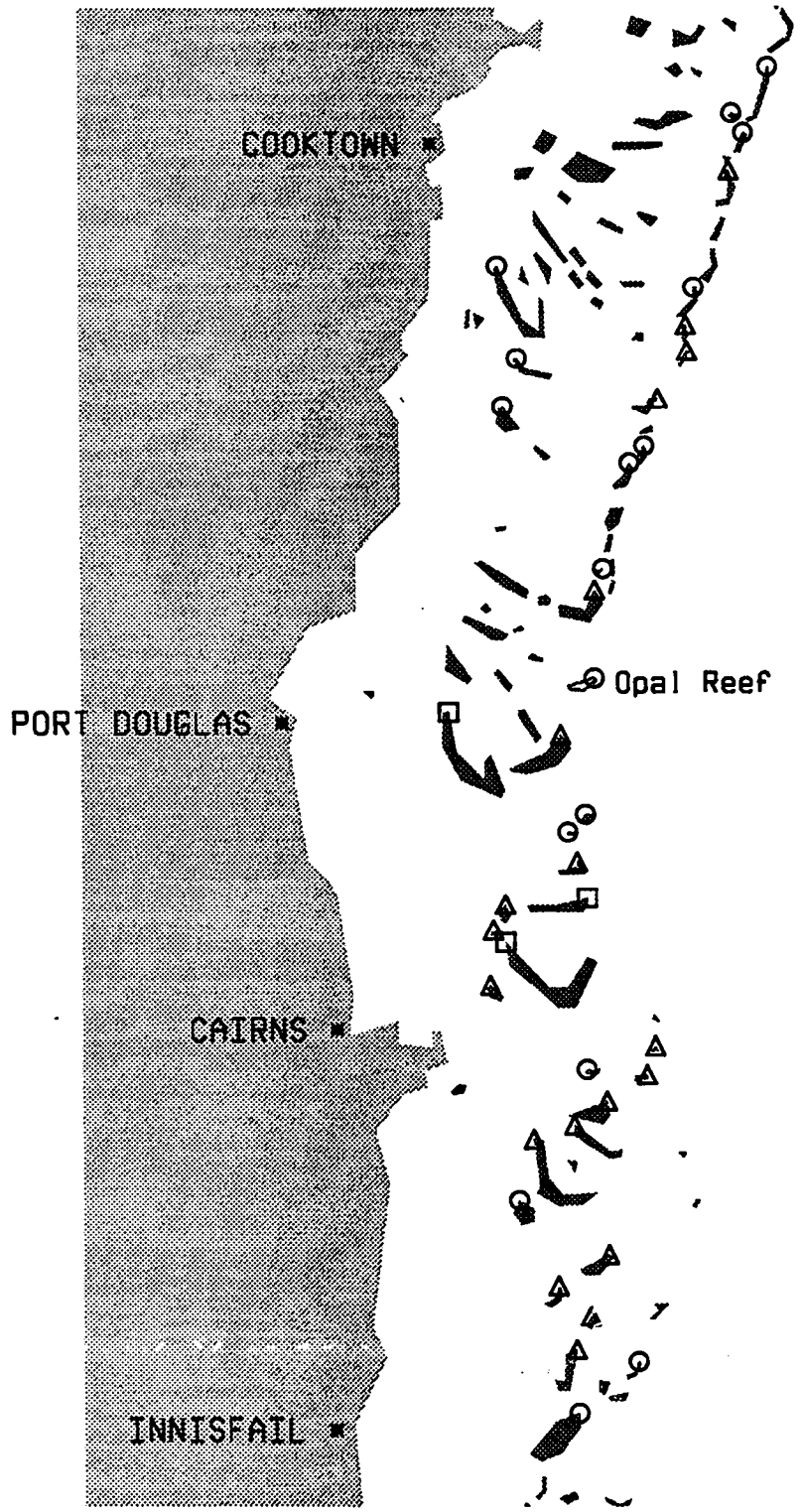


Figure 4.26a Strength of connectivity with respect to Opal Reef based on the random selection of 20 dispersal events. The larval cloud was represented by **7 particles**. Scale: 1cm = 8 nautical miles.

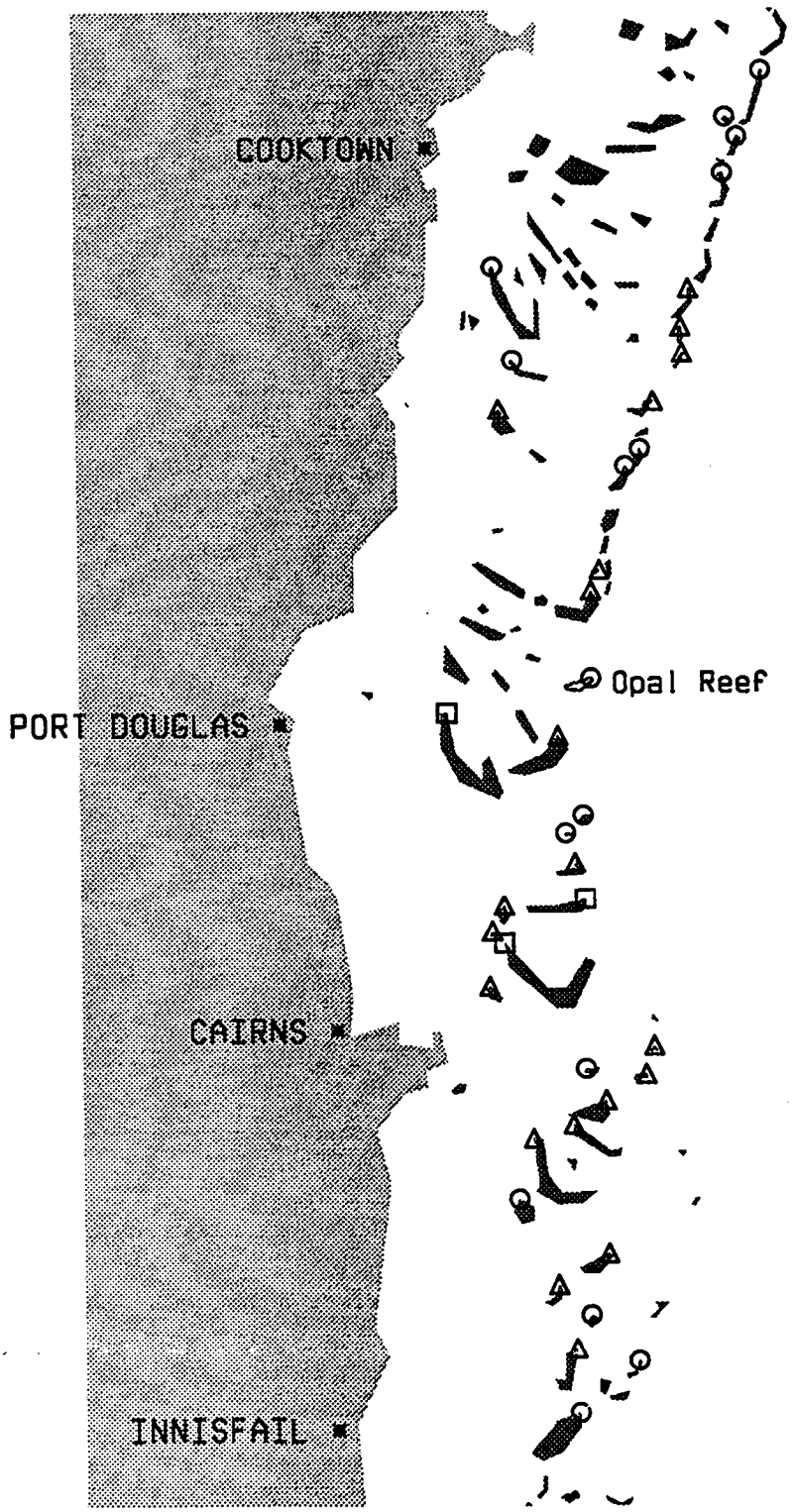


Figure 4.26b Strength of connectivity with respect to Opal Reef based on the random selection of 20 dispersal events. The larval cloud was represented by **13 particles**. Scale: 1cm = 8 nautical miles.

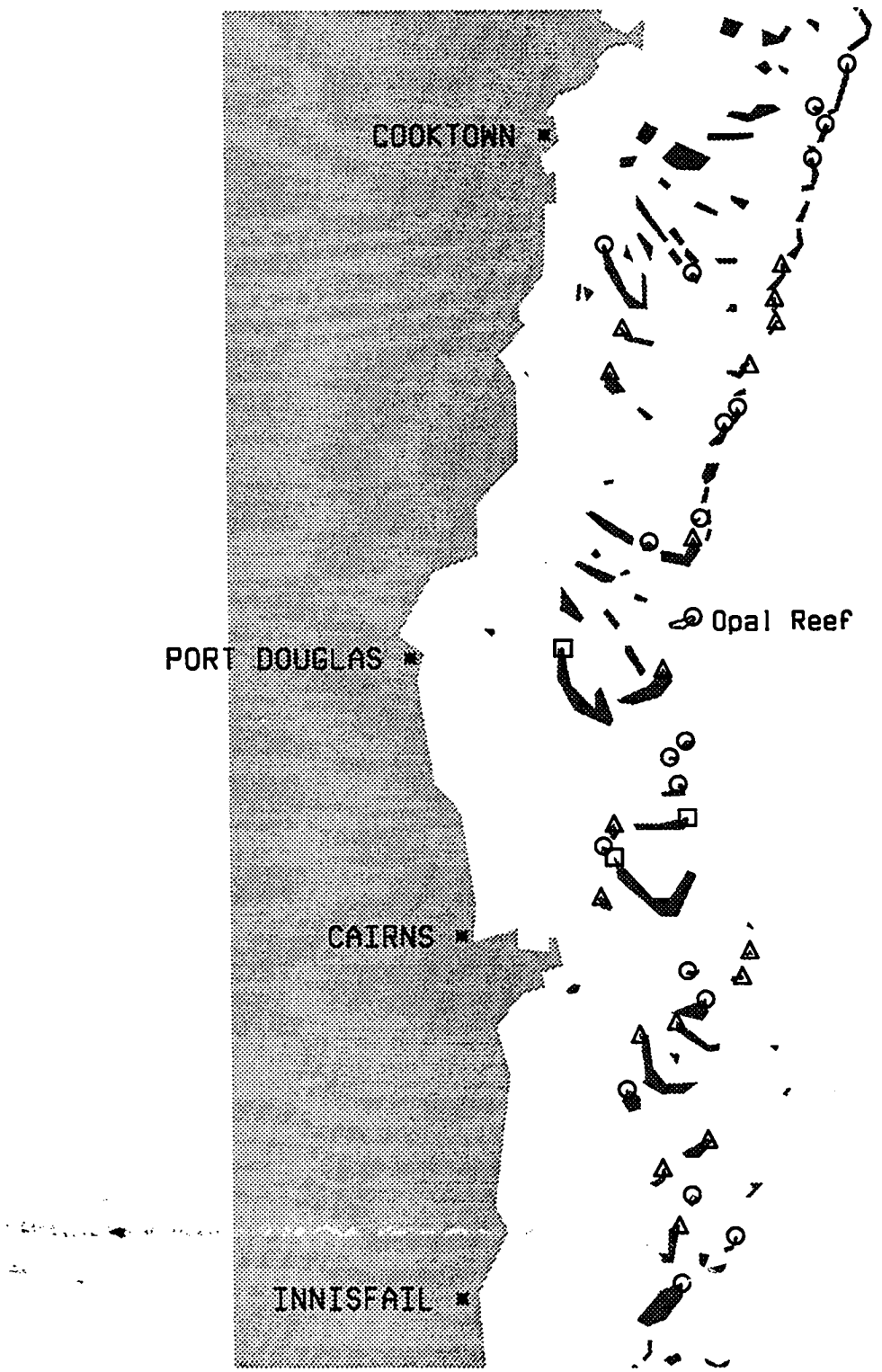


Figure 4.26c Strength of connectivity with respect to Opal Reef based on the random selection of 20 dispersal events. The larval cloud was represented by **25 particles**. Scale: 1cm = 8 nautical miles.

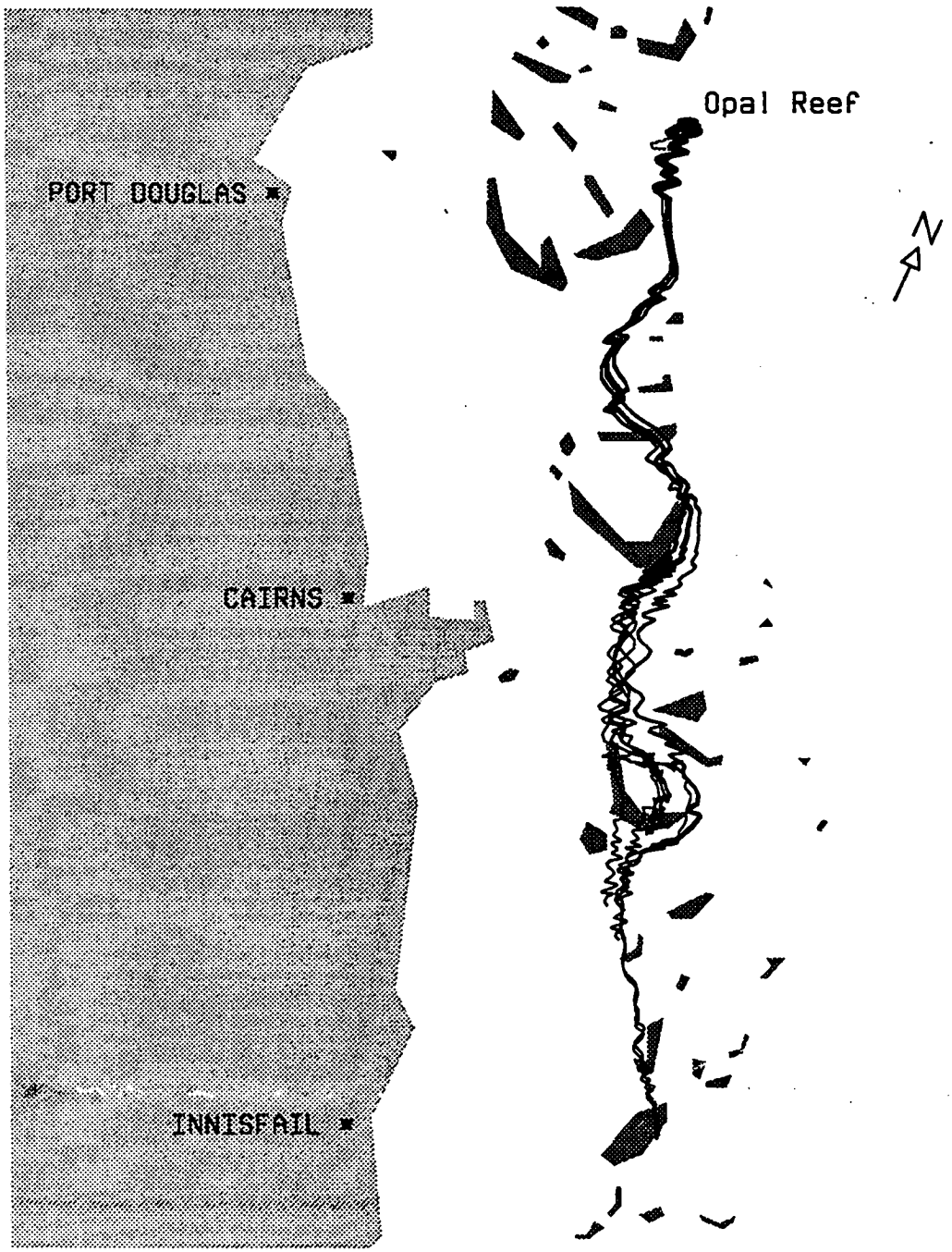


Figure 4.27 The trajectories of 7 **particles** representing a single dispersal event from Opal Reef. Scale: 1cm = 5.5 nautical miles.

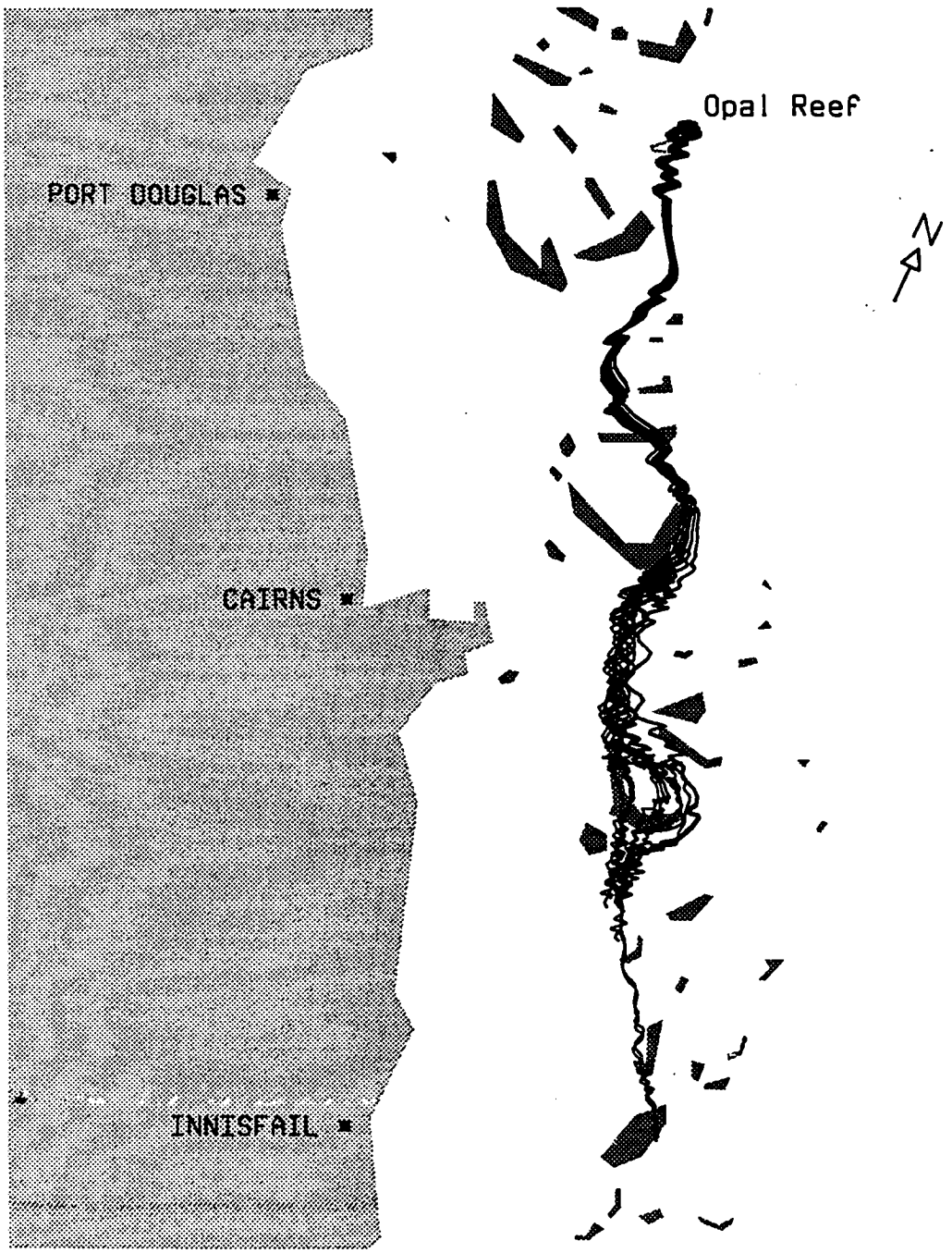


Figure 4.28 The trajectories of **13 particles** representing a single dispersal event from Opal Reef. Scale: 1cm = 5.5 nautical miles.

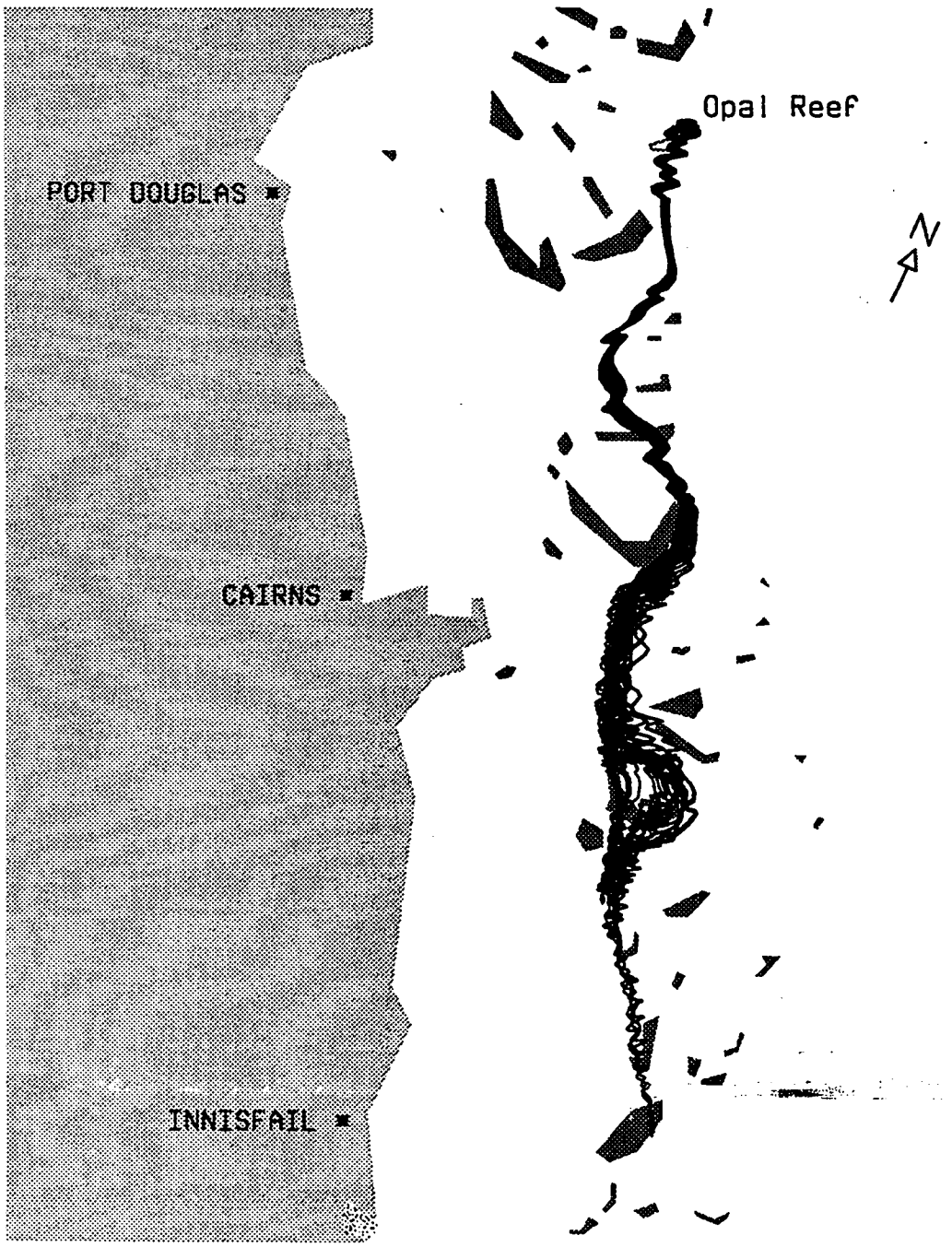
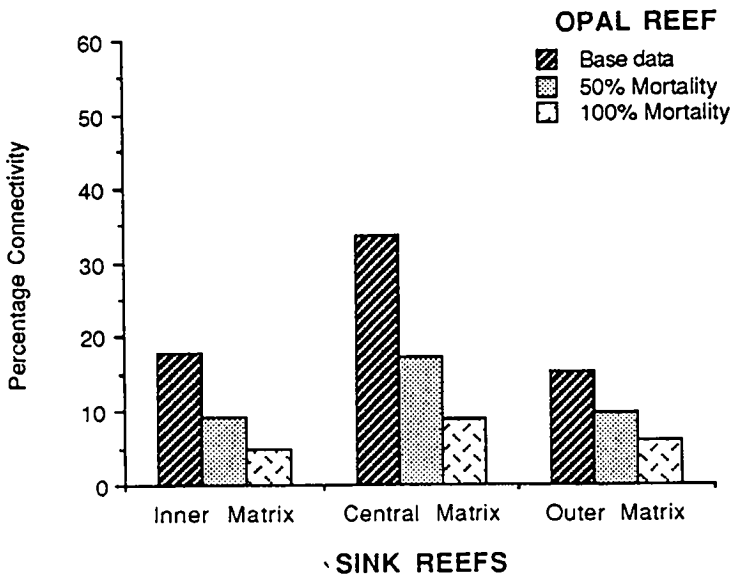
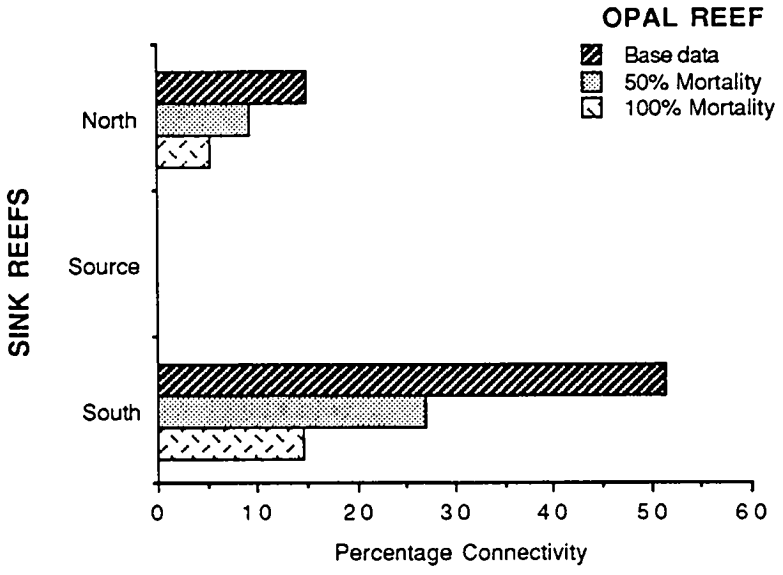


Figure 4.29 The trajectories of **25 particles** representing a single dispersal event from Opal Reef. Scale: 1cm = 5.5 nautical miles.

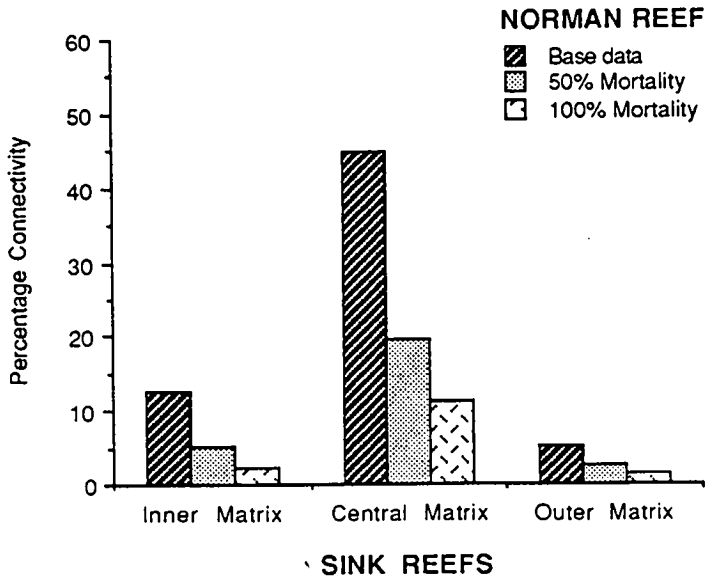


(a) Level of reef connectivity with respect to the cross-shelf transport of larvae from Opal Reef. Sink reefs are classified as lying along the outer edge of the reef matrix and continental shelf (outer matrix), central within the reef matrix (central matrix) and along the inner edge of the reef matrix bordering the main lagoon (inner matrix).

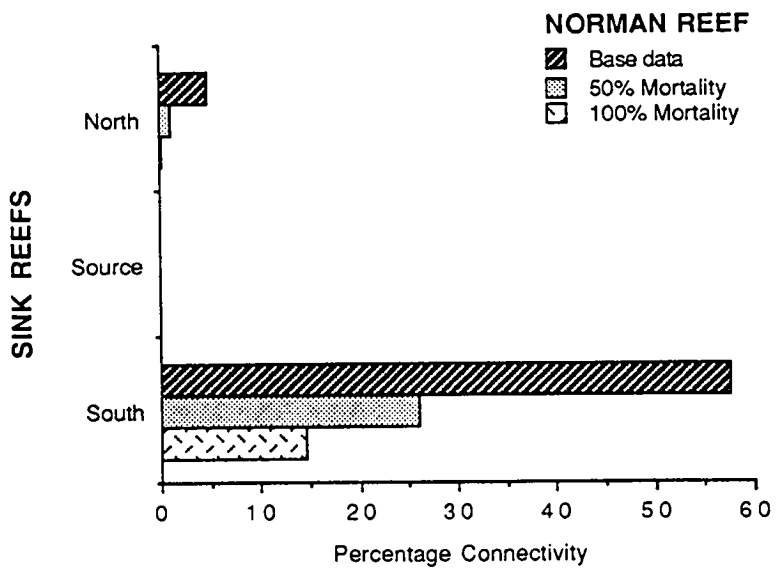


(b) Level of reef connectivity with respect to the long-shelf transport of larvae from Opal Reef. Sink reefs are classified as lying to the north or south with respect to the source reef, or recruitment back onto the parent reef (source).

Figure 4.30 Data are presented for three analyses and represent the number of particles that intersect with sink reefs, expressed as a percentage of the total number of particle trajectories simulated. The three analyses correspond to: (1) **base data** derived from 40 randomly selected dispersal events with which the other analyses are compared; (2) the application of a **50% mortality** factor; and (3) a **100% mortality** factor for larvae encountering a reef during their pre-competent period.

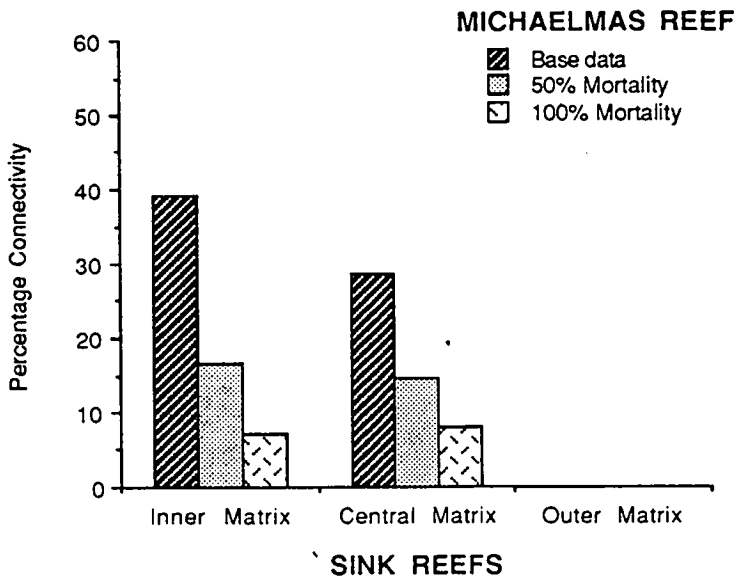


(a) Level of reef connectivity with respect to the cross-shelf transport of larvae from Norman Reef. Sink reefs are classified as lying along the outer edge of the reef matrix and continental shelf (outer matrix), central within the reef matrix (central matrix) and along the inner edge of the reef matrix bordering the main lagoon (inner matrix).

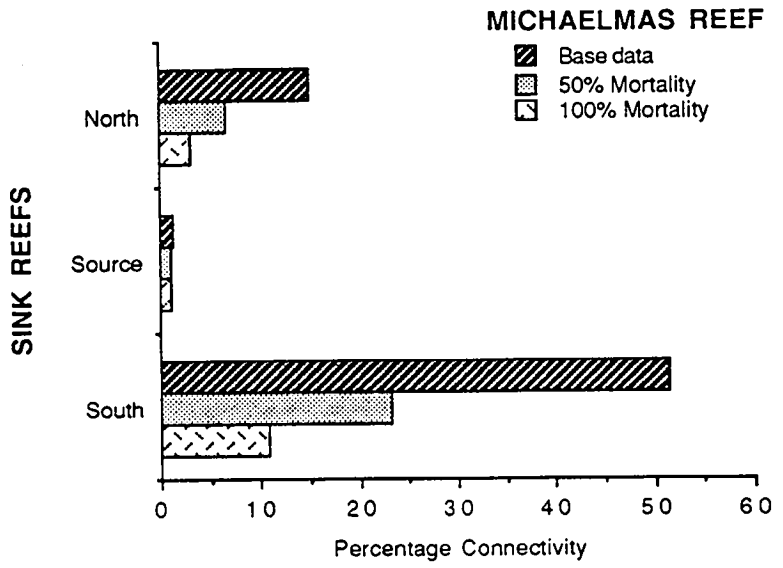


(b) Level of reef connectivity with respect to the long-shelf transport of larvae from Norman Reef. Sink reefs are classified as lying to the north or south with respect to the source reef, or recruitment back onto the parent reef (source).

Figure 4.31 Data are presented for three analyses and represent the number of particles that intersect with sink reefs, expressed as a percentage of the total number of particle trajectories simulated. The three analyses correspond to: (1) **base data** derived from 40 randomly selected dispersal events with which the other analyses are compared; (2) the application of a **50% mortality** factor; and (3) a **100% mortality** factor for larvae encountering a reef during their pre-competent period.

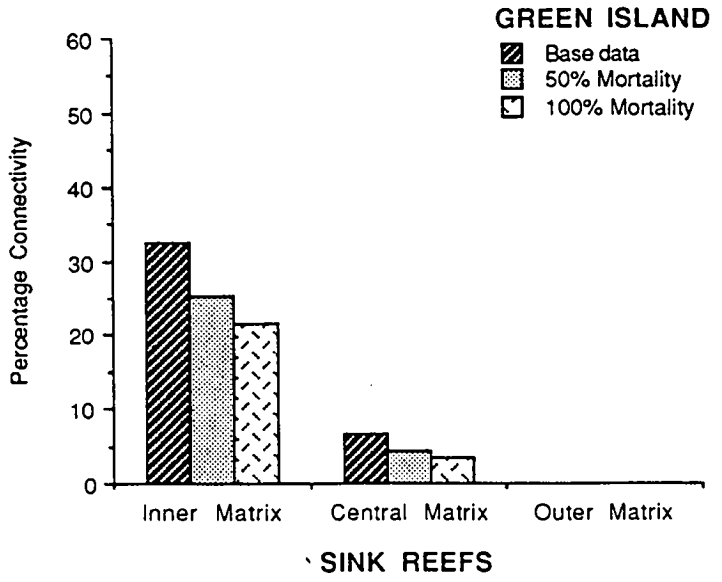


(a) Level of reef connectivity with respect to the cross-shelf transport of larvae from Michaelmas Reef. Sink reefs are classified as lying along the outer edge of the reef matrix and continental shelf (outer matrix), central within the reef matrix (central matrix) and along the inner edge of the reef matrix bordering the main lagoon (inner matrix).

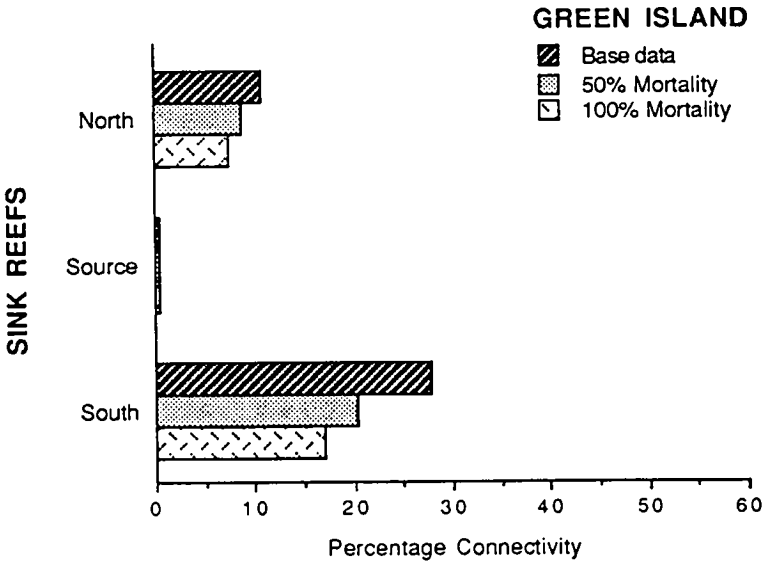


(b) Level of reef connectivity with respect to the long-shelf transport of larvae from Michaelmas Reef. Sink reefs are classified as lying to the north or south with respect to the source reef, or recruitment back onto the parent reef (source).

Figure 4.32 Data are presented for three analyses and represent the number of particles that intersect with sink reefs, expressed as a percentage of the total number of particle trajectories simulated. The three analyses correspond to: (1) **base data** derived from 40 randomly selected dispersal events with which the other analyses are compared; (2) the application of a **50% mortality** factor; and (3) a **100% mortality** factor for larvae encountering a reef during their pre-competent period.



(a) Level of reef connectivity with respect to the cross-shelf transport of larvae from Green Island. Sink reefs are classified as lying along the outer edge of the reef matrix and continental shelf (outer matrix), central within the reef matrix (central matrix) and along the inner edge of the reef matrix bordering the main lagoon (inner matrix).



(b) Level of reef connectivity with respect to the long-shelf transport of larvae from Green Island. Sink reefs are classified as lying to the north or south with respect to the source reef, or recruitment back onto the parent reef (source).

Figure 4.33 Data are presented for three analyses and represent the number of particles that intersect with sink reefs, expressed as a percentage of the total number of particle trajectories simulated. The three analyses correspond to: (1) **base data** derived from 40 randomly selected dispersal events with which the other analyses are compared; (2) the application of a **50% mortality** factor; and (3) a **100% mortality** factor for larvae encountering a reef during their pre-competent period.

CHAPTER FIVE

DISCUSSION

An understanding of the large-scale patterns of *Acanthaster* population dynamics has required, as an initial step, the development of a model capable of simulating the hydrodynamics associated with large assemblages of reefs over the time scale that larvae disperse. Larval dispersal of *A. planci*, and most corals and reef fish, may last many weeks (Yamaguchi, 1973; Sale, 1980; Brothers et al., 1983; Babcock & Heyward, 1986). The model has incorporated the major processes forcing water circulation within the GBR. Its development has required a new modelling approach which pays attention to the accurate geometric representation of reef structure and the large-scale dynamics of water motion, while incorporating the fine-scale features of water circulation over and around individual reefs. Results from an earlier version of the model, which did not include the fine-scale parameterization of reefs and recruitment, have been published (Dight et al., 1988,1990a,b; Dight & James, in press). Results of fine-scale circulation modelling and the entrainment of larvae onto reefs, and their implementation into the large-scale dispersal model have been reported by Dight and Black (1991).

The dispersal model has been designed with a limited number of quite specific objectives in mind (see Section 1.4). The modelling approach reflects these objectives, and as such, various simplifications and approximations have been incorporated into the model. The principal simplifications and approximations were addressed in Chapter 4 and shown to have no significant influence on the large scale patterns of reef connectivity. Others are discussed below. The present model has not been designed to accurately predict the fine-scale details of advection and relative dispersion of larvae within a patch. However, it is a significant advancement over previous models, particularly with respect to the incorporation of the large scale spatial and temporal variability in hydrodynamics and larval dispersal within such a physically complex region. It also represents the only attempt to integrate the fine-scale features of

water circulation over and around individual reefs, and their influence on larval dispersal and recruitment, with mainstream circulation patterns and larval transport.

The hydrodynamic model, on which the dispersal model is based, is two-dimensional and depth integrated, and does not reproduce the vertical structure of water motion. This does not, however, seem to be a significant limitation. Field observations indicate that there is little variation in current direction with depth over the continental shelf (Wolanski & Pickard, 1983; Williams et al., 1984; Frith et al., 1986). Similarly, Andrews and Bode (1988) found only minor variations in both the orientation and magnitude of tidal ellipse axes with depth for stations within the reef matrix. However, some vertical structure in the velocity field is expected for wind driven flows, where the current speed will decrease with depth. Deviations between predicted and observed current speeds will be greatest in the surface layer where, also, the water motion will be more closely aligned to the direction of wind stress. The extrapolation to surface wind-driven current direction and speed from model results should therefore be conducted with some caution.

The transport of larvae with distinct patterns of behaviour, such as those of penaeid shrimp which move diurnally from the water column into the benthic boundary layer (Rothlisberg et al., 1983) or others which may be able to maintain themselves within the surface wind-driven layer, may not be reproduced accurately by the model. However, for larvae with less pronounced positional behaviour, the variation in current speed with depth is likely to result simply in differences in the time spent within the water column and the distances over which they will be advected. Such variation should be small relative to the total time and distance over which larvae are transported. Vertical structure will be most complex close to reefs where bathymetry changes rapidly and flow is directed topographically.

Fine-scale, topographically directed flows around individual reefs result in eddies and fronts. These appear to play an important role in larval retention (Black, 1988) and in the initial aggregation of

biological material flowing off reefs (Wolanski et al., 1986,1989), particularly the positively buoyant eggs and larvae of corals (Oliver & Willis, 1987). Whether such features can concentrate neutrally buoyant objects has not yet been determined. Sammarco and Andrews (1988) have shown that circulation over and around reefs may influence patterns of coral recruitment to individual reefs. Such patterns, however, are likely to result regardless of whether larvae originate from the reef under consideration or from any other reef, and do not imply that reefs are primarily self-seeding. Fine-scale water circulation and the entrainment of larvae onto and around individual reefs have been incorporated into the dispersal model through a parameterization scheme based on schematized reefs. Despite this attempt to incorporate fine-scale particle transport around reefs into a model capable of simulating the dynamics of larval dispersal over large spatial and temporal scales, the relative dispersion of larvae within a patch is probably underestimated. This and the consequences of various approximations within the model were discussed more extensively in Section 4.3.

Mainstream circulation patterns will determine the movement of the centre of mass of the larval cloud once it is advected away from its natal reef and, therefore, the available larval pool of species such as *A. planci* with a larval life-span of several weeks. Reef connectivity will then be strongly influenced by fine-scale features of water circulation around individual reefs, which will vary with respect to oceanographic conditions and reef morphology. The behaviour of larvae and their ability to swim towards what may be perceived as habitat will also influence the proportion of the available larval pool which will become entrained within the near-reef circulation and have the potential to recruit to that reef. A more complete understanding of dispersal processes and their impact upon recruitment needs an integrated approach which recognizes that there is a spectrum of physical phenomena which affect the organism at different spatial and temporal scales.

5.1 PHYSICAL PROCESSES AND LARVAL DISPERSAL

This study identifies hydrodynamic processes which result in distinctively different patterns of larval dispersal, and hence juvenile recruitment, at three spatial scales: (1) regional scale (100s kilometres); (2) shelf scale (10s kilometres); and (3) inter-reef scale (kilometres). An understanding of the distribution and abundance of populations within coral reef systems will require consideration of physical phenomena operating at all three scales.

5.1.1 Regional Scale Phenomena

5.1.1.1 Hydrodynamics

The physical organization of the Great Barrier Reef is diverse in its structure. Bathymetry, reef density and shelf width vary markedly along the continental shelf (Pickard et al., 1977), resulting in regional variation in water circulation. Such variation can cause significant regional scale differences in the movement of larvae (Frith et al., 1986). A markedly different hydrodynamic regime is evident in the north of the Cairns Section behind the ribbon reefs (corresponding to the northern region reported here) compared with that in the southern portion of the Cairns Section (central region). In the north, the dense reef matrix extends across most of the shelf and restricts the development of appreciable wind driven circulation to narrow passages. Off the shelf edge, currents associated with the EAC are generally weak. The almost continuous chain of outer ribbon reefs in the northern region, which have a linear density of around 80%, appears to act as a semi-permeable barrier, greatly reducing the effect of the East Australian Current on the continental shelf in this area. Frith et al. (1986) were unable to detect any flow which could be directly attributed to the EAC in the passage between the ribbon reefs and Lizard Island.

In contrast, within the central and southern regions flow associated with the EAC is stronger and penetrates across the continental shelf. Here, the linear density of shelf-edge reefs is as low as 10% (Pickard et al., 1977). Within the central and southern regions, longer-period

circulation dominates within the main passages over the continental shelf and is predominantly longshore, parallel to the isobaths. The direction (poleward or equatorward) is strongly correlated with the longshore wind component (Wolanski & Pickard, 1985). The reef matrix within the northern portion of the Central Section (southern region) is less dense than further north within the Cairns Section of the GBR Marine Park.

5.1.1.2 Larval Distributions

Model results indicate that the physical organization and associated hydrodynamics of the northern region result in patterns of larval dispersal which are highly symmetric. This region is likely, therefore, to be partially closed and self-recruiting. Larval transport to reefs lying to the north, or back onto the source reef as a result of current reversals, is just as frequent as southward transportation. Frith et al. (1986) note that the variable winds during summer are likely to result in current reversals and little net longshore transport of larvae. Larval distributions, when averaged over many years, should be roughly uniform in space where species are distributed across the entire shelf. These larval dispersal patterns suggest that, in the absence of a cross-shelf gradient in selection pressure, there should be no strong consistent spatial trends in the distribution of species with planktonic larvae among the reefs of this region. This is certainly true with respect to *A. planci*. This issue is discussed in more detail in Section 5.3.

The central and southern regions are very different. Here there is very limited offshore transportation of larvae, and cross-shelf larval distributions become progressively less uniform towards the south. The southward transportation of larvae is so frequent that most dispersal events will result in the establishment of new populations on reefs lying to the south of the source. The central and southern regions must, therefore, be considered as open systems in which populations will be maintained by larval recruitment from farther to the north. Williams et al. (1984) argued, similarly, that the central and southern regions appeared not to behave as closed or self-recruiting systems on the basis of progressive vector plots derived

from current meter records at a limited number of locations.

5.1.2 Shelf-scale Phenomena

5.1.2.1 Hydrodynamics

The combination of Coriolis forces and shelf topography result in wind-driven flow being channelled essentially along-shore and into the natural passages of this coastal/reef complex. This is particularly evident in the main lagoon and in passages behind the ribbon reefs. Within the northern region, flow is seen from model results to be concentrated in two narrow passages, one adjacent to the coast and the other behind the ribbon reefs. Current meter records from within the passage behind the ribbon reefs confirm this (Frith et al., 1986). Wind driven currents are greatly reduced within the reef matrix of the northern region as a result of the blocking effect of reefs to the development of long-shelf currents.

In contrast, the water circulation of the central and southern regions is dominated by relatively large transports within the main lagoon and the larger passages connecting the lagoon and Coral Sea, including Trinity Opening (Cresswell & Greig, 1978; Wolanski & Pickard, 1985). Within the relatively less dense reef matrix of the central and southern regions, the longshore pressure gradient associated with the EAC results in westward flow penetrating across the continental shelf (Andrews, 1983; Wolanski & Pickard, 1983,1985).

5.1.2.2 Larval Distributions

In contrast to the northern region, where the patterns of larval dispersal had a high degree of symmetry, within the central and southern regions three forms of asymmetry in reef connectivity are identified. Asymmetry in the cross-shelf transport of larvae, together with the longshore currents within the main lagoon, provide a mechanism which passively concentrates larvae in the vicinity of inner matrix reefs adjacent to the main lagoon. Reefs such as Green Island, which lie adjacent to the main lagoon, are situated within the

path of larvae from many reefs (Fig. 5.1).

Furthermore, model results indicate that the low frequency longshore currents within the main lagoon of the southern region act as an effective barrier to the larval transport of many species between nearshore and mid-shelf communities. Limited cross-shelf mixing, therefore, can account for the maintenance of distinctive nearshore and mid-shelf communities. The significance of this to cross-shelf variation in the structure of benthic communities within the Central Section of the Marine Park has been reported by Dight et al. (1988) and is discussed in more detail in Section 5.3.

5.1.3 Inter-reef Scale Phenomena

5.1.3.1 Hydrodynamics

Hamner and Wolanski (1988) point out that a shelf current approaching a reef will diverge around the reef with only a fraction of the water mass coming into direct contact with the reef itself. That is, a significant proportion of an approaching larval cloud may not be provided with the opportunity to settle onto the reef but will be transported farther afield. In this way, the fine-scale features of water circulation around individual reefs, or groups of reefs, can strongly influence recruitment by determining the proportion of the available larval pool which is able to settle onto a reef under particular conditions. Research to date has concentrated primarily on larval retention by reefs and the initial aggregation and transport of coral larvae off reefs (e.g. Black, 1988; Oliver & Willis, 1987; Sammarco & Andrews, 1988; Wolanski et al., 1989), while neglecting the entrainment of larvae onto reefs from the mainstream circulation.

The research documented here is the first to investigate the influence of hydrodynamics associated with different reef shapes and sizes, and the magnitudes of long-shelf and cross-shelf tidal currents on the entrainment of larvae from the mainstream circulation into the near-field circulation around reefs. Results indicate that the entrainment of larvae into the near-field circulation is spatially and temporally variable, and that all of the factors cited above may influence the

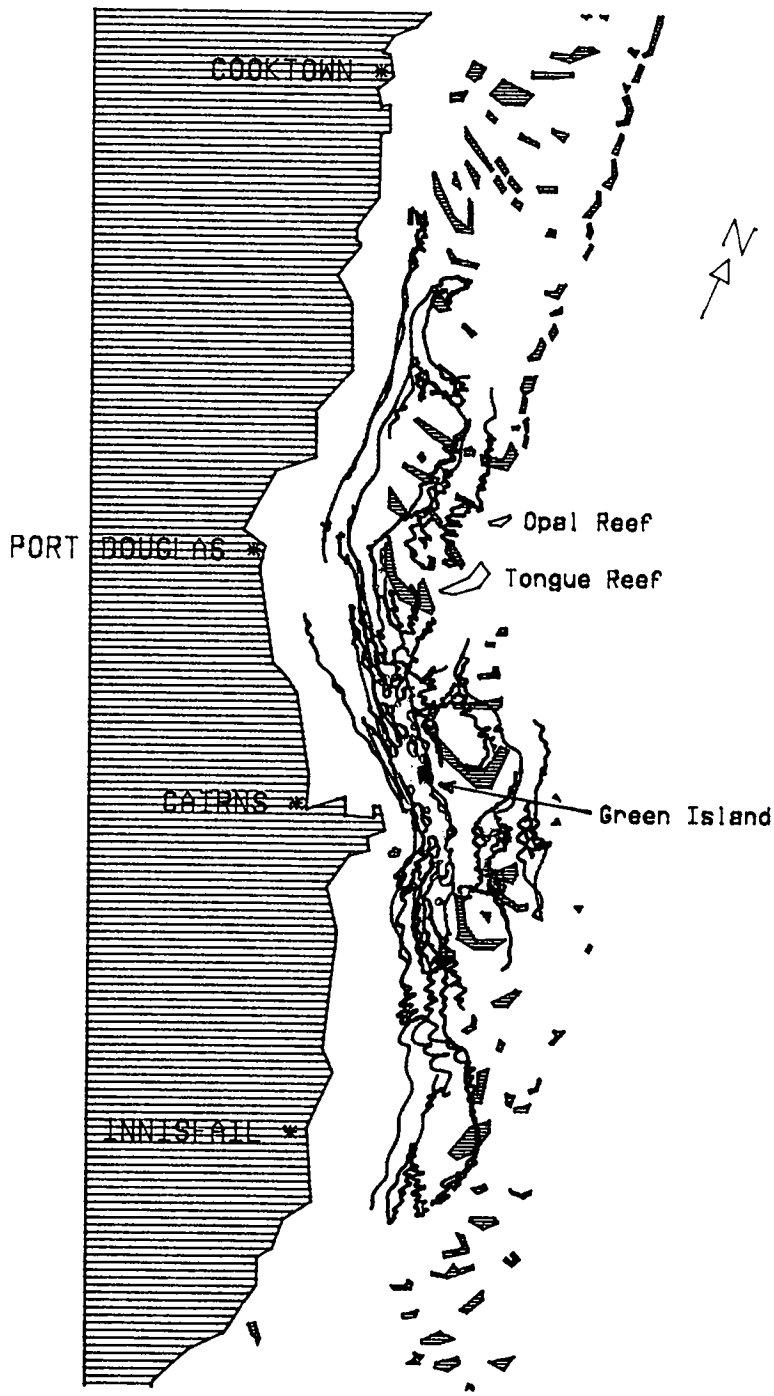


Figure 5.1 Particle trajectories representing thirty dispersal events from Opal and Tongue Reefs (source reefs indicated without fill). Each trajectory corresponds to the centroid of the larval cloud during the second two weeks of dispersal when the larvae of *A. planci* are assumed to be competent to settle. Reefs such as Green Island, which lie within or adjacent to the main lagoon off Cairns, are exposed to a concentrated pool of larvae from many reefs. Scale: 1cm = 9 nautical miles.

proportion of an approaching larval cloud which will have the potential to settle onto a reef. The hydrodynamics associated with different reef shapes and sizes also appear to influence larval retention and self-seeding (Black, 1988; Black et al., 1990).

5.1.3.2 Larval Distributions

Larvae approaching a potential sink reef may not all become entrained within its circulation, rather, many will be transported farther afield (see Figs. 3.24 to 3.27). The proportion of a larval patch which becomes entrained within the near reef circulation is predicted to vary with the state of the tide, the point of intercept with respect to the reef edge and the reef size and shape. In particular, the timing with respect to the tidal cycle and location of intercept strongly influence the entrainment of larvae and recruitment. It appears that large reefs have the potential to entrain more larvae from the mainstream into the near-field circulation than small reefs. Larvae which are transported farther afield then have the potential to recruit to other reefs they may encounter.

The entrainment of larvae within the near-reef circulation during their pre-competent period of development may result in high rates of mortality due to predation by reef-associated species. Recent research by Hamner at al. (1988) suggests that predation by diurnally active reef-associated planktivorous fish is intense. Mortality from this source may contribute significantly to stochastic variation in recruitment pulses. Thus, the interaction between a larval cloud and the reefs with which it is brought in contact may have important consequences for the population dynamics of many reef species.

5.1.4 Recruitment

There is increasing evidence that populations of many coral reef species are often recruitment limited (Doherty & Williams, 1988a; Warner & Hughes, 1988). Similarly, studies on fish and echinoderms indicate that recruitment is frequently pulsed and that successful year-classes may continue to dominate the population structure into the future (Doherty & Davidson, 1988; Doherty & Williams, 1988a).

The population density and overall age structure is expected to reflect longer-term temporal patterns in recruitment (Warner & Hughes, 1988), at least for short-lived species, in recruitment limited populations. Thus, an understanding of recruitment processes and the factors which determine variability is fundamental to the population dynamics and management of coral reef resources.

Larval connectivity presented as relative strengths for each source reef (e.g. Fig. 3.80 for Green Island) represents the integration of numerous dispersal events over many years. Results predict that reefs lying to the south of Green Island, particularly Gibson and Howie, have the highest probability of receiving recruitment from this source. However, very many reefs lying both to the north and south may receive recruitment from time to time. These results which summarize connectivity say little about individual events and their spatial and temporal variability.

There is tremendous inter-annual variation in the direction and distance over which larvae are transported. This is seen in the individual trajectories of dispersal events (e.g. see Fig. 3.62 for Green Island) which may be directed either to the north or south. Larvae associated with approximately 30% or 1 in every 3 or 4 dispersal events from Green Island remain entrained within the main lagoon and are not transported to other reefs (Fig. 5.2). While particular source reefs may frequently display connectivity with certain sinks, in some years connectivity may be entirely absent. Where there is a strong dependence between particular source and sink reefs, this could significantly reduce recruitment to the sink reef. There may be years when connectivity to many reefs within a region is dramatically reduced as a result of the influence of hydrodynamics on the trajectories of dispersing larvae.

Examination of individual dispersal events shows that a patch of larvae will frequently be spread over several reefs. This is particularly likely in the case of adjacent reefs in the long-shelf direction. There appear to be conditions under which a larval patch remains reasonably coherent and recruitment is directed primarily to one reef (Fig. 5.3), while under other circumstances the larval patch becomes

dispersed and recruitment is in variable densities over many reefs (Fig. 5.4). These reefs may be separated by many kilometres. If larvae from many source reefs become concentrated, then large multi-species and, possibly, multi-aged recruitment events could result. Pitcher (reported in Doherty, 1988) has shown that recruitment pulses, presumably from a single patch, can be synchronized over many adjacent reefs.

Larval recruitment to coral reefs is a highly variable process. There is a need to identify and quantify the sources of variation in recruitment. Doherty and Williams (1988a) detail recruitment patterns over a number of different spatial and temporal scales. They note a combination of both deterministic and stochastic factors influencing recruitment patterns. These result in some reefs having consistently higher or lower relative recruitment densities, while recruitment to other reefs varies both spatially and temporally; a coherence in pulses of recruitment to adjacent reefs in a long-shelf direction, in which not all reefs participate equally; and consistent cross-shelf and regional scale differences in the density of recruitment. These patterns of recruitment are consistent with model results and suggest that some, if not most, of the pattern and variability in recruitment that has been documented may be accounted for by the physical processes which are identified and discussed above.

5.2 THE *ACANTHASTER* PHENOMENON

The model results indicate three forms of asymmetry in reef connectivity with respect to the larval dispersal of *A. planci* populations within the southern portion of the Cairns Section (central region) and northern portion of the Central Section (southern region) of the GBR Marine Park. This contrasts with a lack of asymmetry in the larval dispersal patterns within the northern portion of the Cairns Section (northern region). These forms of asymmetry, which were discussed above in Section 5.1, relate to: (1) the long-shelf transport of larvae towards the south; (2) the cross-shelf transport of larvae onshore through the matrix towards the lagoon; and (3) source-sink

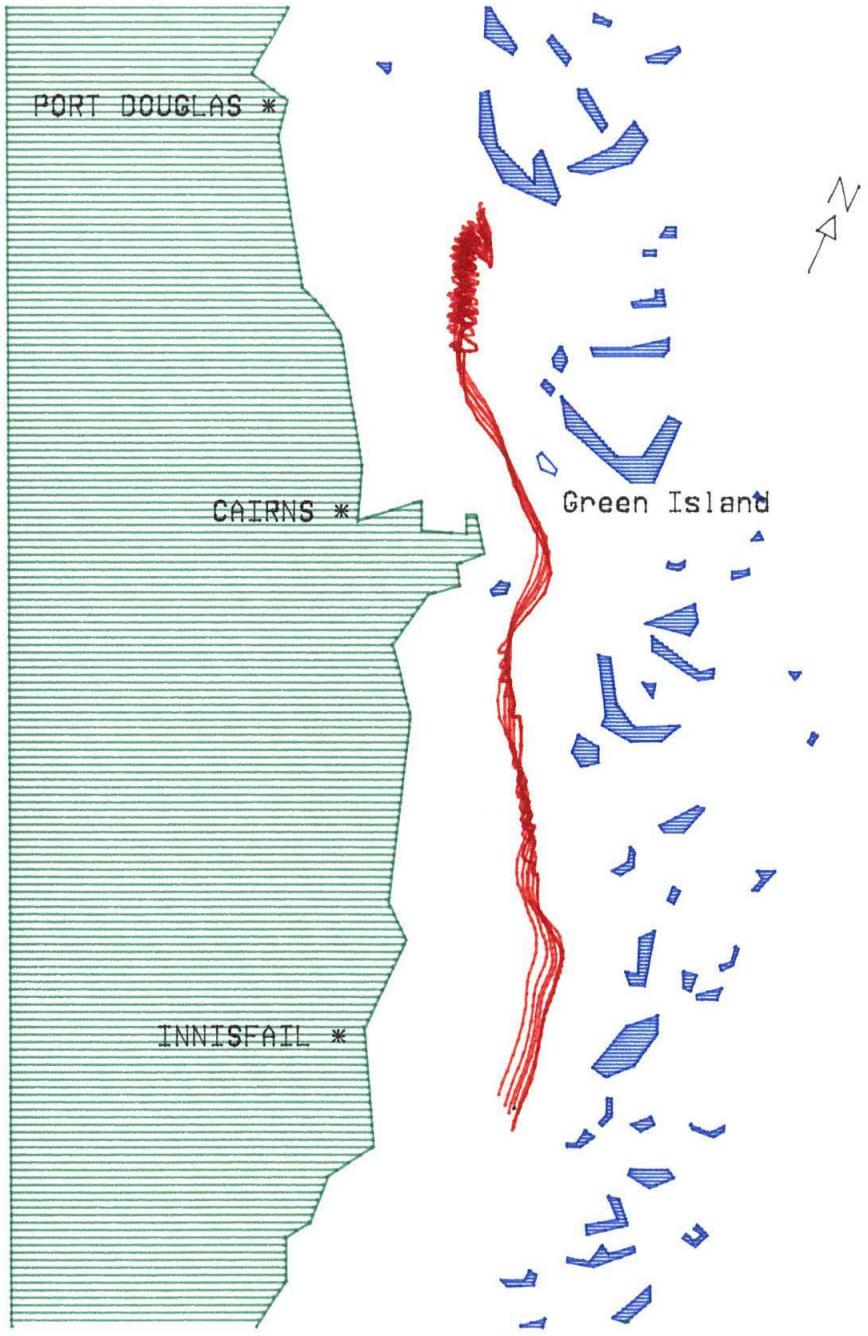


Figure 5.2 Particle trajectories, representing a single dispersal event originating from Green Island, correspond to the competent period of larval development only. Often larvae become entrained within the main lagoon and are not transported to other reefs. Scale: 1cm = 6 nautical miles.

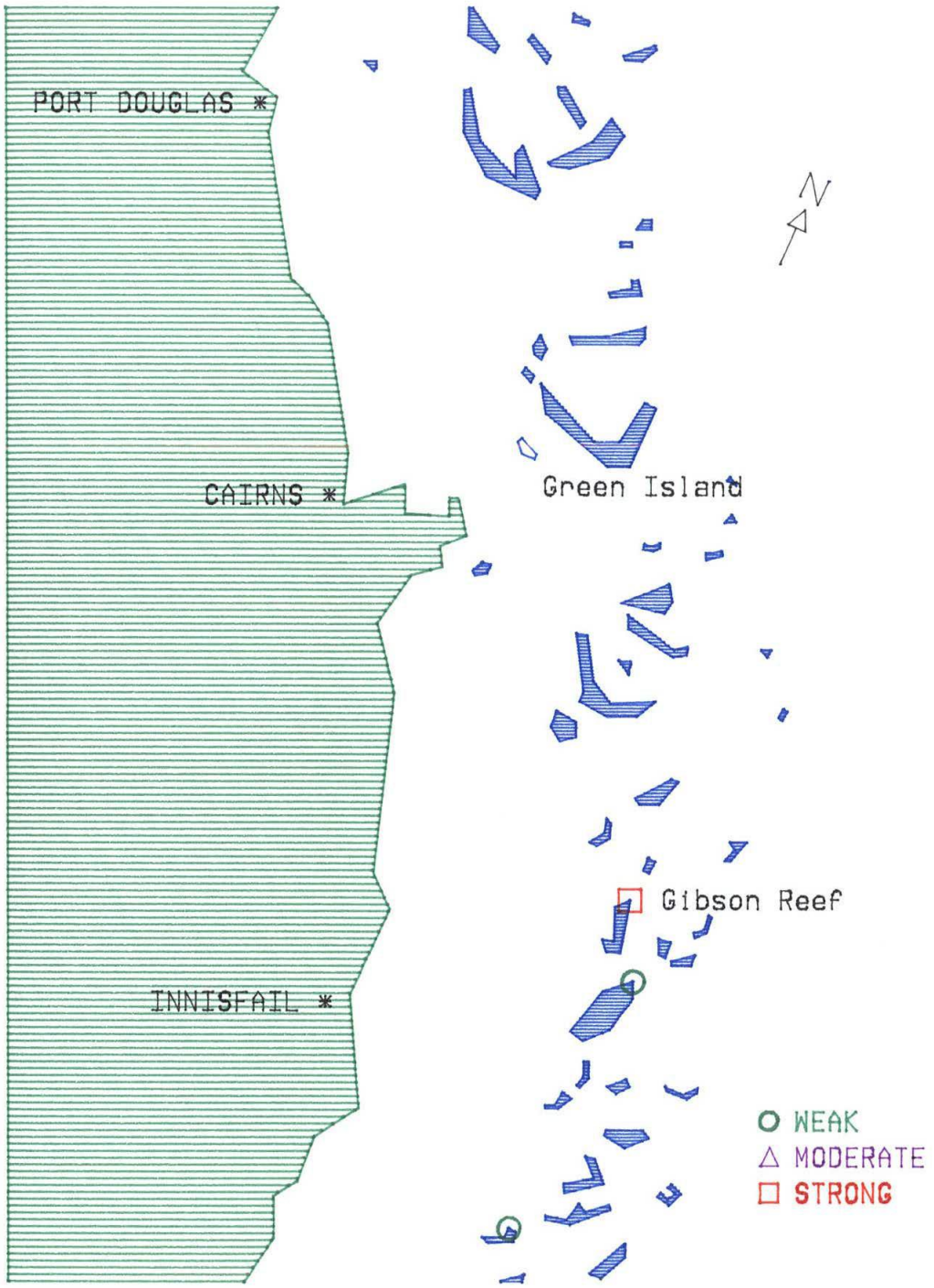


Figure 5.3 Reef connectivity representing a single dispersal event originating from Green Island. The relative strengths (S) are classified into 3 classes: weak, moderate and strong, where weak S < 0.05; moderate 0.05 <= S < 0.5; and strong S => 0.5. There are conditions under which a larval cloud remains reasonably coherent and recruitment is directed primarily to one reef. Here, greater than 50% of larvae associated with this dispersal event were transported to Gibson Reef while less than 5% were transported to each of Howie and Ellison Reefs. Scale: 1cm = 5.5 nautical miles.

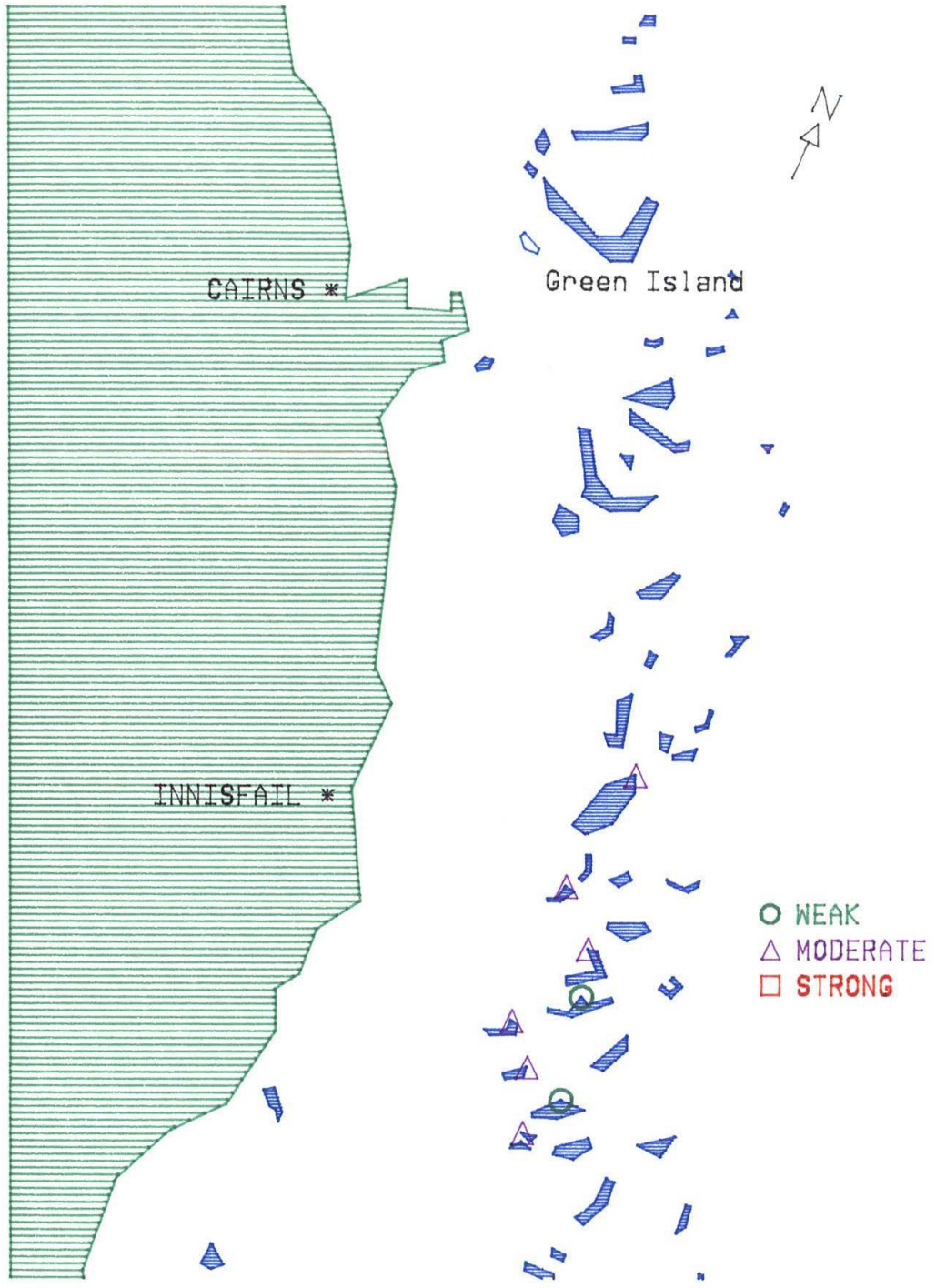


Figure 5.4 Reef connectivity representing a single dispersal event originating from Green Island. The relative strengths (S) are classified into 3 classes: weak, moderate and strong, where weak S < 0.05; moderate 0.05 <= S < 0.5; and strong S => 0.5. Under certain conditions a larval cloud can become dispersed and recruitment will be in variable densities over many reefs, frequently in a long-shelf direction. Scale: 1cm = 5.5 nautical miles.

relationships in the level and strength of connectivity. The three forms of asymmetry, and their absence within the northern region, not only aid in an understanding of the observed patterns of *Acanthaster* population spread throughout the central GBR, but also have implications for far broader management issues related to *A. planci* and other reef species.

5.2.1 Source of Outbreaks

During the two recorded episodes of *Acanthaster* activity within the GBR, large populations of *A. planci* were first recorded on Green Island (Moran, 1986). Surveys undertaken after the initial appearance of large populations of *A. planci* on Green Island in 1963 and 1979 found that populations were also present on contiguous reefs at the same time (Barnes, 1966; Nash & Zell, 1982). Pearson and Endean (1969) conducted the first systematic surveys several years after the initial appearance of *A. planci* on Green Island reef during the first episode. From their records, we know that in 1966 there were also large numbers of *A. planci* on reefs as far north as Lizard Island. The surveys by Nash and Zell (1982), in contrast to those of Pearson and Endean (1969), were conducted shortly after the initial appearance of *A. planci* at Green Island during the second episode of *Acanthaster* activity. These results indicate that not only reefs contiguous with Green Island, but many as far north as Lizard Island again carried populations of *A. planci* in 1980. Available records suggest then, that there were likely to have been large populations of *A. planci* within and possibly throughout the northern region at the same time or prior to the appearance of populations on Green Island. Green Island, therefore, would appear to be the site of primary observation rather than primary outbreak (Fisk et al., 1988).

Kenchington's (1977) hypothesis that the source of the *Acanthaster* populations, in the region of Cairns and farther south, was to the north of this region is supported by the results from the present study. In the face of such strongly southward directed transportation of larvae within the central and southern regions, it is not clear how substantial populations of *A. planci* could be maintained by means other than larval recruitment from farther to the north. Furthermore,

model results indicate that primary outbreaks within the central region would be unlikely to result in the observed distribution of *A. planci* populations to the north.

It is proposed, therefore, that the source of outbreak populations of *A. planci* in the region of Cairns, and further south into the Central Section of the GBR Marine Park, is from within this northern region. Water circulation and patterns of connectivity suggest that populations of *A. planci* may be maintained indefinitely within the northern region: populations which occasionally propagate southwards and result in the pattern of outbreaks that has been well documented.

5.2.2 Pattern of Outbreaks

In light of the strongly directed southward pattern of connectivity from all reefs within the central and southern regions, and hence larval recruitment, the present research supports the observations of an apparent southward trend in the spread of *A. planci* populations from Green Island during both episodes of activity within the GBR. The distances over which larvae are predicted to disperse are consistent with observations and Kenchington's (1977) model of the southward spread of *Acanthaster* populations. Recent analyses of starfish abundance and distribution data from 1981 to 1989 also support the hypothesis of southward movement of outbreaks during the latest episode (Reichelt et al., 1990a,b).

The absence of any apparent cross-shelf pattern in outbreaks within the northern region (Great Barrier Reef Marine Park Authority database, unpublished) is consistent with model results which indicate that there should be no strong cross-shelf gradient in adult distribution. This is in contrast to the central region where a greater proportion of inner and central matrix reefs experienced outbreaks than outer matrix reefs (Moran et al., 1988) and inner matrix reefs bordering the lagoon carried higher populations of *A. planci* than other reefs (Pearson & Endean, 1969). These patterns can be explained by the passive concentration of larvae in the vicinity of these reefs. Model results indicate that there is a general movement

of larvae onshore across the shelf towards the lagoon. This appears to result from both the predominance of onshore winds during the summer period and flow associated with the East Australian Current. Andrews (1983) observed a persistent onshore component to flow in the Central Section of the GBR off Townsville. Mid-shelf reefs, therefore, will be exposed to higher numbers of larvae. Once within the main lagoon, larvae are transported longshore by currents which are primarily wind driven.

According to the present model, most onshore movement of larvae will occur as a result of flow being channelled into the natural passages of the reef matrix. This is clearly evident in the paths of larvae crossing Trinity Opening and Grafton Passage. Larvae advected away from Opal and Tongue Reefs, which lie to the north of Trinity Opening, are moved onshore through the passages (see Fig. 5.1). Cresswell and Greig (1978) observed flow within Trinity Opening to be cross-isobath. The same pattern is also observed elsewhere, and accounts for the high connectivity of Gilbey and Cayley Reefs with others bordering the lagoon. The physical location of reefs with respect to these natural passages is likely to play an important role in determining the degree of cross-shelf/onshore movement and connectivity.

The maximum distances over which larvae were transported during the 28 day simulation period were as great as 110 nautical miles within the central region, although such distances were the exception rather than the rule. Reduced net flows within the reef matrix, and current reversals, generally resulted in smaller larval excursions. Most larvae encountered reefs much closer to their source, typical distances being 10 to 50 nautical miles. The relatively rare events which resulted in larvae being transported large distances (e.g. from Upolu Reef to Otter Reef - see Fig. 3.79) may explain some of the inconsistencies noted by Moran (1986) in the sequence of outbreaks. However, what often appear as inconsistencies may only reflect a simplistic view of larval dispersal, whereby outbreaks are 'expected' to move at a rate which is related to the average current speed and direction. In reality, larval dispersal is a highly variable phenomenon.

The infrequent events which resulted in transportation of larvae offshore cannot, alone, fully account for the widespread yet progressively lower population densities of *A. planci* on central and outer matrix reefs that were observed by Pearson and Endean (1969) and Pearson (1972). A possible explanation for the occurrence of outbreak populations on outer matrix reefs is provided below in Section 5.2.3.

The longshore transportation of larvae within the GBR lagoon, resulting from shelf topography and synoptic-scale low frequency current modulation and reversals, places reefs lying either within or bordering the lagoon in prime locations to receive recruitment from this concentrated larval pool. Reefs within the central region such as Green Island, Feather, Ellison and Otter, and within the southern region such as Bramble, John Brewer, Lodestone, Old, Bait and Credlin Reefs, which protrude into the lagoon, therefore appear *a priori* to be most susceptible to *Acanthaster* recruitment. Support for this is obtained from comparative coral recruitment studies on Green Island and adjacent reefs which indicate consistently higher recruitment on Green Island than adjacent reefs (Harriott & Fisk, 1988; Fisk & Harriott, 1990).

Similarly, reefs such as Low and Fitzroy Islands which lie within the lagoon are ideally situated to receive *Acanthaster* recruitment. All these reefs have a history of *A. planci* populations and subsequent high coral mortality. Holbourne Island, also located within the lagoon to the south of Townsville, had outbreaks years before adjacent mid-shelf reefs (Johnson et al., 1988). The source of populations on Holbourne Island could have been any of numerous reefs to the north. Holbourne Island, in turn, could well have been the source of outbreak populations that are reported from the Swain Reef complex at approximately the same time as those off Townsville, and not necessarily the result of localized primary outbreaks and dispersal (cf. Moran et al., 1988).

A further important mechanism which results in some of the same reefs being particularly susceptible to *A. planci* outbreaks is the focusing of recruitment by currents on particular reefs or groups of

reefs from multiple sources. One such group of reefs identified as a sink for many source reefs is off Innisfail and includes Gibson, Howie, Peart and Feather Reefs. This group has strong connectivity with many reefs lying to the north including Upolu, Green Island and Scott Reefs which were among the first to be identified as sources of large *Acanthaster* populations (see Figs. 3.79 to 3.81). The focusing of recruitment on this group of reefs off Innisfail places in perspective the observation that they were severely damaged by large populations of *A. planci* some two years after that of Green Island (Moran, 1986). This pattern was observed during both major outbreak periods.

Some reefs within the Central Section (southern region) also appear to receive recruitment from several different sources. Large populations of *A. planci* were observed on many reefs off Townsville during 1985/1986, including Grub, Arab and Needle Reefs (Brunckhorst & Johnson, 1985; Bass et al., 1988,1989; Great Barrier Reef Marine Park Authority database, unpublished). These three reefs, together with others, have strong connectivity with Big Broadhurst, Old, Stanley and Darley Reefs (see Figs. 3.95, 3.96, 3.98 to 3.100), all of which are reported to have been severely damaged by *Acanthaster* outbreaks during the period 1987 to 1989 (Johnson et al., 1988; Bass et al., 1989).

Considered as sources, the inner matrix reefs from where the largest populations of *A. planci* have been reported show, overall, the lowest connectivity. This is a pattern which becomes progressively more pronounced towards the south. That is, while their physical location makes them potentially strong sinks for larvae, the propagation of populations from these same reefs is relatively inefficient. Patterns of reef connectivity indicate that the establishment of successive populations of *A. planci* will be to the south and in an onshore direction across the shelf towards the main lagoon. The southward spread of populations during both episodes of *Acanthaster* activity within the GBR appeared to terminate towards the bottom of the southern region (Central Section). South of 19^{0} 30' latitude, outbreak populations of *A. planci* have, by and large, been few and reported only from reefs lying within (e.g. Holbourne Island) or bordering the main lagoon (e.g. Bait and Credlin).

Many reefs which lie towards the southern limits of *Acanthaster* activity within the Central Section, including Old and Stanley, are reported by Bikaunieks (1991) to be particularly efficient sinks for larvae. However, these two reefs, in particular, are also identified as very poor and unreliable sources of larvae as their overall level of connectivity is very low and most dispersal events fail to result in the transportation of larvae to other reefs. The apparent cessation of outbreaks within the Central Section is therefore proposed to have resulted from this strengthening cross-shelf asymmetry towards the south, together with the unreliability of the southern most reefs as sources of larvae. The cessation of outbreaks can therefore be explained by purely physical processes.

Overall, a high proportion of larvae originating from inner matrix reefs are likely to remain entrained within the lagoon and effectively lost from the system. In contrast, the larval pool available to central matrix reefs will be much smaller, yet these reefs have high levels of connectivity, with most larvae originating from central matrix reefs likely to be transported within the vicinity of another reef. The complex relationships inherent within the three forms of asymmetry will play an important role in the fundamental dynamics of the spread of *Acanthaster* populations on the scale of the GBR.

5.2.3 Path of Outbreaks

In light of the cross-shelf asymmetry that has been identified, the distribution of outbreak populations of *A. planci* within the central and southern regions suggests that their origin was not from reefs lying along the inner edge of the matrix. Larvae originating from these reefs are predicted to be strongly directed to other inner matrix reefs with larvae rarely being transported offshore. While the inner matrix reefs were reported to be more severely affected by *Acanthaster* populations, many reefs lying central within the matrix - e.g. Tongue, Michaelmas and Arlington (Pearson & Endean, 1969; Nash & Zell, 1982) - and others lying along the outer edge of the continental shelf - e.g. Opal and Flynn (Nash & Zell, 1982; Great Barrier Reef Marine Park Authority database, unpublished) - were also reported to have

carried populations.

The distribution of outbreaks that has been documented within the region of Cairns is consistent only with the transport of larvae from outer matrix ribbon reefs lying at the southern end of the northern region. Connectivity from Saint Crispin Reef was strongly directed towards Tongue, Arlington and Batt Reefs (Fig. 5.5), but was also directed towards Opal, Michaelmas, Oyster, Upolu and Green Island Reefs. Connectivity from Opal and Tongue Reefs is primarily directed towards reefs off Cairns, including Michaelmas, Arlington, Oyster, Upolu and Green Island (see Figs. 3.68 and 3.73). These reefs constitute those which were amongst the most severely affected by *Acanthaster* outbreaks in the region of Cairns during both episodes of starfish activity (Pearson & Endean, 1969; Nash & Zell, 1982). While some recruitment to reefs in the region off Cairns may have been derived from inner and central matrix reefs farther to the north, model results suggest that many of these reefs are poor sources of larvae. Undine Reef, which lies on the inner edge of the reef matrix at the southern end of the northern region, displayed connectivity with Batt Reef and the western extremity of Tongue Reef (Fig. 3.56). Both these reefs have very weak connectivity with reefs lying to the south. Most larvae are likely to become entrained within the main lagoon and to be transported along-shore without encountering another reef (Figs. 3.66 and 3.78), except possibly Green Island.

The origin of populations of *A. planci* on Green Island and contiguous reefs in 1979 is therefore predicted to have been at the southern end of the ribbon reefs by the mid 1970s. Unfortunately, there were no surveys conducted within the region during this period (Moran, 1986). Interest, by then, was focused on the Far Northern and Mackay-Capricorn Sections of the GBR Marine Park.

Records of *A. planci* within the Far Northern Section of the GBR Marine Park (Fig. 1.1) are few (Sorokin et al., 1985; Brunckhorst & Young, 1985b; Moran et al., 1988). However, populations of *A. planci* on reefs lying within or to the north of Princess Charlotte Bay could have resulted from the northward transport of larvae from south of Cape Melville. While the continental shelf is largely constricted at the

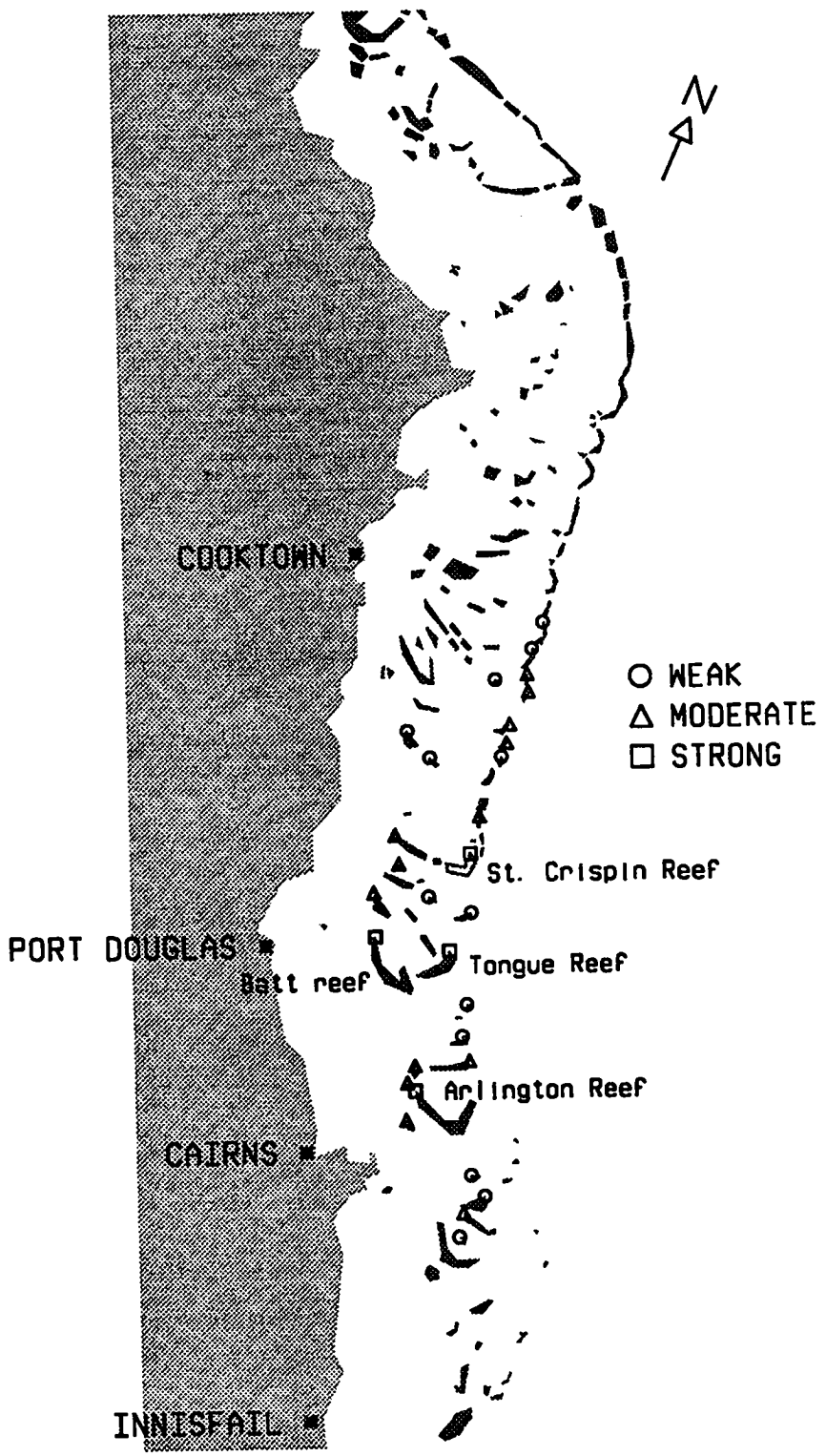


Figure 5.5 Strength of connectivity with respect to St. Crispin Reef (source reef indicated without fill). The relative strength classes (weak, moderate and strong) represent probabilities separated by an order of magnitude. Strongest connectivity is with St. Crispin (source), Tongue, Batt and Arlington Reefs. Scale: 1cm = 12 nautical miles.

southern end of this region, thus inhibiting free larval transport between adjacent areas to some extent, results from the hydrodynamic models indicate a distinct connection between the Far Northern and Cairns Sections. Furthermore, remotely sensed surface drogues have been observed to drift backwards and forwards between this northern region of the Cairns Section and Princess Charlotte Bay (H. Marsh, pers. comm.).

5.2.4 Cause of outbreaks

Moran (1986) places the various hypotheses that have been advanced to account for *Acanthaster* outbreaks into two categories, based on whether they account for the population fluctuations either as natural or unnatural phenomena. He notes that implicit within the idea that outbreaks are unnatural, novel and of unprecedented magnitude, is that they originate near centres of human population and from regions that are affected by human activities. Advocates of this position argue that, normally, population densities are stable and that individual starfish are dispersed and in low abundance. The removal of predators on both juveniles and adults is proposed to have resulted in a gradual increase in population density to beyond a threshold level, at which stage larval survivorship is enhanced through fertilization success and other reefs become colonized (Endean 1973; Endean & Stablum, 1973; Cameron & Endean, 1982; Endean & Cameron, 1990). If accessibility to centres of human population has influenced predator abundance, the remoteness of the northern region suggests that the predator removal hypothesis of Endean and Cameron is questionable. The intensity of fishing pressure within this relatively remote region in the 1950s when primary outbreaks would have first developed is not known. Yet, it is feasible that within this region populations of *A. planci* may have gradually built up to higher levels. This in itself, though, does not explain the spatial and temporal variability in *A. planci* population abundance within the region, nor the apparent large-scale episodicity within the system at this scale.

An alternative position, that outbreaks are a consequence of natural processes (possibly influenced by human activities), has been

developed based on the assumption that larval survivorship is normally nutrient limited (Birkeland, 1982; Lucas, 1982). Survivorship was proposed to be enhanced under conditions of high food availability (e.g. phytoplankton blooms) and to result in the occurrence of outbreak populations. Largely on the basis of more recent research by Olson (1987), Birkeland and Lucas (1990) now consider that spatial and temporal variation in food availability may not be a major factor influencing the larval survivorship and recruitment of *A. planci*. However, they maintain that the most acceptable hypothesis is "one in which the potential timing and location of outbreaks result largely from larval survival (strongly influenced by environmental conditions) and distribution by current patterns" (p. 202). The environmental conditions considered by Birkeland and Lucas (1990) include water salinity and temperature, increased organic matter, turbulent mixing of water layers and availability of suitable substrate for larval settlement and juvenile survivorship.

The terrestrial runoff hypothesis of Birkeland (1982) does not gain support from the present study, as the northern region from where primary outbreaks are proposed to have spread has few rivers. However, if food availability can influence larval survivorship either directly or indirectly through more rapid development and, say, reduced exposure to predation, then a potential source of nutrient rich water in the form of tidally induced upwelling has been identified along the outer edge of the continental shelf (Wolanski et al. 1986,1988). Nutrient rich water from the continental shelf slope is advected between the ribbon reefs and is maintained within the passage behind the reefs by jet-generated vortices. The physical location of the nutrient rich water is consistent with the along-shore path of larvae within the passage behind the ribbon reefs and the proposed spread of *Acanthaster* populations from the outer shelf reefs. The outer shelf ribbon reefs are also characterized by extensive areas of substrate which is suitable for larval settlement by *A. planci*.

Once substantial populations become established on the ribbon reefs, or within the reef matrix, further increases in larval survivorship as a consequence of the same mechanism or more successful fertilization

of gametes could lead to increases in population abundance and the spread of outbreaks both southward towards the central and southern regions where most activity has been documented, and throughout the northern region of the Cairns Section. The frequency of these events could result simply from the presence of larvae from low density populations being in the right place at the right time. Primary outbreaks could then develop if other conditions, such as coral abundance, facilitated juvenile survivorship.

Moran (1986) suggested that both positions have in common the assumption that *Acanthaster* populations are normally dispersed and low in abundance, but that larval survivorship hypotheses fail to explain how large numbers of larvae are successfully produced from normally dispersed populations. It appears unlikely that outbreak populations of *A. planci*, of the same magnitude that have been observed to devastate central GBR reefs, exist permanently within the northern region of the Cairns Section. These reefs appear to have undergone the same cyclic processes of high coral mortality and regeneration as has been documented elsewhere within the GBR. However, coastal areas adjacent to the northern region are sparsely populated and, consequently, relatively fewer surveys and observations of either the absence or presence of *Acanthaster* activity have been documented (Moran, 1986; Great Barrier Reef Marine Park Authority database, unpublished). Furthermore, population estimates from casual records and even surveys are unreliable (Fernandez et al., 1990).

The northern region of the Cairns Section, however, provides the physical conditions necessary for the maintenance of population densities at relatively low levels. The persistence of low-density populations has been investigated using a simple population model based on a weighted digraph (James et al., 1991). The digraph weights were based on connectivity relationships derived from the present study. The results from this modelling exercise indicate that the potential exists for long term persistence of populations within the northern region, provided a significant proportion of reefs in the region become populated. Bradbury et al. (1990) support the concept of such a discrete area as a necessary condition for the generation of

episodes of *Acanthaster* activity which spread southward throughout the GBR. However, while they consider it necessary, Bradbury et al. (1990) argue that it is not a sufficient condition and that predation is the trigger.

Larval dispersal has been shown to be a highly variable process, both spatially (between reefs) and temporally. Variation in endogenous factors, including population densities between reefs, successful fertilization, dispersal, survivorship and recruitment could result in primary outbreaks, without the need to invoke external triggers, such as predators or nutrients. This scenario is supported by the population model results of James et al. (1991) which also suggest that the potential for unstable population growth exists within the northern region purely because of the complex patterns of reef connectivity. However, external triggers could alter the frequency of primary outbreaks.

It should be possible, in the long-term, to differentiate between many of the hypotheses that have been proposed, including those postulated above, by further development of dispersal and population models, together with the implementation of a well designed survey strategy. Knowledge of what constitutes a normal, pre-outbreak situation within the northern region and details surrounding the initial appearance of outbreak populations should provide insight into the mechanism initiating primary outbreaks and their subsequent spread.

5.3 CROSS-SHELF AND REGIONAL VARIATION IN COMMUNITY STRUCTURE

Model results identify both regional and cross-shelf variation in larval transport and reef connectivity for species which are essentially passively dispersed and have larval life-spans of several weeks. Such variation is also reflected in regional and cross-shelf differences in community structure and may aid in a better understanding of the observed patterns.

5.3.1 Cross-shelf Variation

It has been argued above that the high abundance of *Acanthaster* populations on mid-shelf reefs within the Central Section of the GBR during both recorded episodes of outbreaks is the result of two characteristics of larval transport and reef connectivity. These are: (1) the onshore movement of larvae through the reef matrix towards the lagoon; and (2) the longshore transport of larvae within the main lagoon. The apparent southward movement of *A. planci* populations over time and the episodic nature of the *Acanthaster* phenomenon at both reef and shelf scales, whereby populations disappear from reefs on which they were previously present, may be peculiar to this species. It is evidently a result of not only the net southward transport of larvae by water currents during the period when populations spawn, but also the predator-prey interaction of starfish and corals. Such patterns can be expected from a species which is capable of exceeding its carrying capacity through resource depletion, but may also be evident for other species. In this way, the life-history strategy of individual species, in particular their fecundity and longevity, will influence the details of distribution and abundance.

The distributions of other reef species with pelagic larvae that are transported passively may well be similar to that which has been observed for *A. planci*: their population densities will be greatest on mid-shelf reefs within the central GBR (central and southern regions). The high abundance and diversity of many species of scleractinian coral (Done, 1982), soft coral (Dinesen, 1983), holothurians (Hammond et al, 1985) and fish (Williams, 1982; Williams & Hatcher, 1983) on mid-shelf reefs within the southern region may, at least in part, be a consequence of the two characteristics of larval transport and reef connectivity identified above. The high biomass of planktivorous fish on mid-shelf reefs (Williams & Hatcher, 1983) could, similarly, be a reflection of the abundance of mero-planktonic larvae that is predicted to be in the vicinity of mid-shelf reefs. This is not to say that other factors do not also act to limit distribution at either the larval or post-larval stages, only that they may not be the most significant factors affecting the distribution and abundance of many species across the continental shelf.

However, the apparent onshore transport of larvae across the shelf suggests that alternative explanations may be required to account for the maintenance of species distributions on outer shelf reefs. Possibilities include behavioural traits which foster the retention of larvae within the outer shelf zone, active offshore movement by larvae and short pre-competent periods of larval development. No mechanisms by which larvae might predictably be transported offshore are evident (Williams et al, 1984). The active movement of larvae offshore does not seem feasible for most invertebrate species, as they swim much more slowly than the currents by which they are transported. Offshore movements, however, may be possible for some larval fish (Leis & Goldman, 1983) whose musculature and sensory abilities are more highly developed. The third possible mechanism, that of a short pre-competent period, may be most relevant to invertebrate larvae: many species of scleractinian coral settle after as few as four days (Babcock & Heyward, 1986). Some species of reef fish may also be able to settle after only a few days (Sale, 1985). Results from the present study indicate that a pre-competent period of only four days can significantly enhance connectivity between reefs within the same cross-shelf zone, particularly the outer shelf reefs. Also, larval retention by reefs may be more important for the maintenance of populations and distributions on outer shelf reefs than further onshore. This, in turn, could have consequences for recruitment densities and population abundance.

The virtual absence of large populations of *A. planci* on nearshore reefs within the southern region (Moran et al., 1988; Great Barrier Reef Marine Park Authority database, unpublished) provides support for model results which indicate that the main lagoon acts as a virtual barrier to the cross-shelf transport of larvae between nearshore and mid-shelf communities (see Figs. 3.88 and 3.89). However, relatively rare events are predicted to result in the transport of larvae from mid-shelf reefs within the southern portion of the Cairns Section (central region) to nearshore reefs within the Central Section (southern region), in particular, the Palm Islands (see Figs. 3.77, and 3.80 to 3.82). Such events are likely to have resulted in the relatively low numbers of *A. planci* that have been observed within the

Palm Islands (Great Barrier Reef Marine Park Authority database, unpublished) and populations of reef fish which are normally associated with mid-shelf reefs (G. Russ, pers. comm.).

Williams et al. (1986) favoured either differential larval survivorship or habitat selection by larvae as an explanation for the uneven distribution of larvae that has been observed within the central GBR. They did so on the basis that physical oceanographic processes should promote the widespread dispersal of larvae across the shelf. However, model results indicate that this is not necessarily the case. The relatively infrequent events which transport larvae offshore from mid-shelf reefs or onshore to nearshore reefs show that cross-shelf larval distributions will generally mirror the distribution of adults. In light of the present results, limited cross-shelf dispersal of larvae is the most parsimonious explanation for the observed patterns of recruitment and larval distribution, which reflect the distribution of adults.

The absence of any apparent cross-shelf pattern in *A. planci* outbreaks within the northern portion of the Cairns Section (northern region) (Great Barrier Reef Marine Park Authority database, unpublished) is consistent with model results which indicate that there should be no significant cross-shelf gradient in adult distribution and abundance in the absence of a strong gradient in selection pressure. Substantial cross-shelf movement of larvae, particularly in an off-shore direction, was predicted by Frith et al. (1986) during summer on the basis of current records from near Lizard Island and progressive vector plots. Also, Leis and Goldman (1987) report inshore larval fish assemblages off Lizard Island. The results from these studies are also consistent with model predictions. Yet, there are evidently tremendous differences in the physical environment between the nearshore and outer-shelf ribbon reefs.

Anderson et al. (1981) and Williams (1983a) provide some indication that there is also substantial cross-shelf variation in species distribution and abundance at the latitude of Lizard Island, particularly between the nearshore and outer-shelf reefs. However, such variation is not as great as further south within the Central

Section of the Marine Park. Many species in the northern region appear to be widely distributed across most of the shelf. The major causes of variation in the distribution and abundance of many species with pelagic larvae in the northern region are likely to be different to those operating within the Central Section, where limited cross-shelf dispersal is predicted to be important.

5.3.2 Regional Variation

Regional variation in circulation patterns that result in different larval distributions and their passive concentration in the vicinity of particular reefs or groups of reefs could result in consistent differences in recruitment densities, population abundance and species distributions between regions. For example, mid-shelf reefs within the central and southern regions, particularly those bordering the main lagoon, might be expected to have higher levels of recruitment of species with pelagic larvae than mid-shelf reefs within the northern region. This might then be manifest in higher population densities if these same species are recruitment limited.

On the basis of latitudinal variation in *A. planci* distribution and, in particular, abundance, whereby large populations are virtually absent within the Far Northern, southern Central and Mackay-Capricorn Sections, similar variation in distribution and abundance might be expected for other species whose larvae are passively dispersed and are widely distributed. Insufficient data are presently available within the published literature to assess this hypothesis. However, there appears to be some support for such differences. Williams (1983a) notes that mid and outer shelf fish communities from the Swain and Pompey reef complexes appear to be distinct from mid and outer shelf communities further north. Also, Done (1983) reports that coral communities from the Swain and Pompey reef complexes are distinct from mid and outer shelf communities within the Central Section off Townsville. Done also reports that the Far Northern Section reef communities are quite different again. Clearly, however, there are a great many other factors which could cause such differences in community structure over such large spatial scales. Greater consideration should, though, be given to how

physical oceanographic processes might interact with basic life-history characteristics and influence species distributions and community structure.

5.4 LARVAL DISPERSAL AND LIFE-HISTORY THEORY

Life-history theory may provide a useful approach to enhance understanding of *A. planci* population dynamics, and aid resolution of the issue of whether or not outbreaks are a natural or human-influenced phenomenon. Two current, yet opposing, views of the *Acanthaster* phenomenon are, firstly, that populations are normally regulated and held at a level below the carrying capacity of the environment by predators of both juveniles and adults. Consequently, the observed population fluctuations and consequent disturbance to coral communities should rarely, if ever, occur (Endean, 1977,1982). The other view, in contrast, holds that the observed population fluctuations are normal characteristics of the dynamics of coral reef communities (Moore, 1978).

Life-history theory may be able to contribute to this debate through a comparison of the life history characteristics that are best suited to an organism adapted to such different 'life-styles'. A number of life-history characteristics of *A. planci*, including high fecundity and iteroparity in spawning behaviour, suggest that its life-style is one which is adapted to survival in a patchy and unpredictable environment. Model results indicate that larval dispersal and recruitment will be highly variable and often unreliable as a result of physical oceanographic processes.

Given this patchy and unpredictable environment, is the reproductive strategy of *A. planci* best adapted to independent spatial and temporal variation in favourability among sites? Or alternatively, is the reproductive strategy of *A. planci* better adapted to predictability in environmental favourability? Where there is no spatial or temporal order to habitat favourability, then the scale of dispersal should be reduced to a level suited to the spatial scales of patch availability. This is while there is a significant cost to increased dispersal. In

contrast, where there is spatial correlation in favourability among sites (reefs) due, for example, to outbreak populations of *A. planci* exceeding their carrying capacity, then increased spatial spread of larvae would be adaptive (Murphy, 1968; Stearns, 1976; Palmer & Strathmann, 1981).

The significance of two life-history characteristics, in particular, have been quite widely discussed in the literature. These are: the sources and intensity of mortality during the larval phase; and the length of larval life. Both are discussed below in light of model results.

5.4.1 Environmental Predictability and Sources of Mortality

Larval mortality is widely recognized to be very high (Thorson, 1950; Sale, 1980), although agreement on the principal causes of mortality is not found (see Section 1.2.1 for an overview). Results from the present study indicate that the failure of water currents to transport larvae to suitable habitat, i.e. another coral reef, will not only be a significant source of mortality for coral reef species with pelagic larvae within the GBR, but also very unpredictable. The relative importance of this cause of mortality varies between reefs with their physical location on the continental shelf and their relationship to surrounding reefs. Entire cohorts of larvae may frequently suffer mortality from this source (see also Section 5.5).

On the basis of the present study, larval mortality as a result of the failure to encounter habitat may vary between 15 and 95% for different reefs when averaged over many years. These values may be overestimates in relation to species which have the ability to identify habitat from a distance and actively swim against the prevailing current towards a reef. This may be the case for many species of reef fish, but is unlikely to be the situation for most invertebrate larvae. On the other hand, these values may be underestimates of mortality from this source for invertebrate larvae which must be passively transported to a specific substrate, and with habitat requirements which are more restricted than those of *A. planci*, such as the reef crest and flat.

An additional source of mortality may be significant during larval dispersal. This is predation by reef-associated species as larvae become entrained within the near-field circulation of reefs during their pre-competent period of development. Cohorts of larvae with relatively long pre-competent periods of development may often be exposed to mortality from this source. Predation on reefs may increase larval mortality by up to 75%. However, while estimates of mortality from predation by suspension feeding invertebrates and planktivorous fish are high (Hamner et al., 1988; Westneat & Resing, 1988), the relative importance of this source is not clear. Once again, the importance of this source of mortality is predicted to vary between source reefs in relation to their physical location on the continental shelf and their relationship to surrounding reefs. Clearly, coral reef species with extended larval lives will be susceptible to increased predation not only from within the pelagic environment, but also from reef-associated species.

5.4.2 Duration of Larval Life

In the absence of larval mortality due to predation, either in the pelagic environment or from reef-associated species, an increase in the duration of larval life does not appear from the present study to result in any advantage with respect to encountering suitable habitat within a reef system such as the GBR. In fact, there may be a slight disadvantage in an increase from 4 to 14 days minimum. That is, the spatial scale of habitat availability is well suited to a relatively short pre-competent period of only 4 days. Longer pre-competent periods of larval development appear more likely to result in inappropriate scales of dispersal. If predation within the pelagic environment or from reef-associated species is intense, then there is likely to be a decided disadvantage in increasing the scale of dispersal beyond that which is afforded by a relatively short pre-competent period of 4 days. The fact that *A. planci* has a relatively long pre-competent period therefore implies that it is adapted (or pre-adapted) to a life-style where habitat favourability on contiguous reefs is strongly correlated.

However, recruitment of many reef fish may not regularly exceed the carrying capacity of their habitat patches. Yet, most have relatively

long pre-competent periods of larval development. On this basis, there must be advantages to long pre-competent periods of larval development which lie in other factors, such as the production of more, but smaller, eggs and larvae. These results are in agreement with the more theoretical approach taken by Palmer and Strathmann (1981). Population models based on larval connectivity are required to determine how trade-offs between fecundity and duration of larval life, in light of adult longevity, mortality and trophic requirements, relate to the population dynamics of coral reefs organisms. Such a model and approach may shed light on the *Acanthaster* phenomenon.

5.5 THE APPLICATION OF HYDRODYNAMIC AND DISPERSAL MODELS TO THE MANAGEMENT OF MARINE RESOURCES

The significance of larval dispersal models to the management of tropical marine resources lies in two increasingly apparent characteristics of coral reef systems: (1) that most invertebrates and fish have a pelagic larval phase to their life cycle during which they have the potential to be dispersed quite widely; and (2) that recruitment from this pelagic larval pool is likely to structure communities and influence the population abundance of many species. Concern has been raised that, in the face of increasing population pressure on coral reefs as resources for exploitation, recreation and tourism, a stronger biological basis for the management of marine resources is required. Models which are capable of predicting reef connectivity by means of larval dispersal can provide a stronger biological basis to management, and the zoning process within the GBR Marine Park is a particularly relevant application. Hydrodynamic models, in conjunction with a field programme, also have a fundamental role to play in environmental impact assessment and the design of monitoring programmes.

5.5.1 The *Acanthaster* Phenomenon

Model results identify a region that corresponds to the northern portion of the Cairns Section which is predicted to be the source of *Acanthaster* outbreaks which, from time to time, propagate

southwards. Identification of this region and an explanatory mechanism for the maintenance of *A. planci* populations within the region provides management with a focus for future research, including monitoring, which aims to understand the cause or causes of *Acanthaster* outbreaks. It illustrates the exploratory and explanatory value of models and how they can help to provide direction to future research.

If or when future outbreaks of *A. planci* develop within this northern region, then models of larval dispersal can be used to predict the path of outbreaks. This situation would provide an excellent test of the predictive ability of dispersal models. Some modifications to the present models will be required before accurate and reliable predictions of specific dispersal events over a single season can be made. For example, rather than use random combinations of tide and wind records over many years to generate the patterns, actual combinations of tides and wind over specific spawning seasons will be required. Also, sensitivity analyses show that inertial effects would need to be incorporated into the model. Should control of *A. planci* populations be seen as necessary or desirable, then dispersal models will aid in identifying the reef or reefs on which most effort should be focussed. Control procedures may be more effective by concentrating on reefs which act as effective sources.

5.5.2 Zoning of the Great Barrier Reef Marine Park

The probabilistic interpretation of larval dispersal and reef connectivity that is provided by the model is well suited to contribute valuable, biologically relevant input to zoning of the GBR Marine Park. Reefs can be viewed as both sources of larvae to surrounding reefs and sinks for larvae from various source reefs. This is an important distinction, as the application of dispersal models to the management of reefs as sources and sinks is quite different.

The ability of a reef to act as an effective and efficient source of larvae varies from reef to reef. The relative levels of connectivity can be equated with the supply of larvae, although this will be strongly influenced by reef size and population density. Source reefs which

have high levels of connectivity overall and connectivity with many reefs serve to ensure a supply of larvae throughout the system. The reliability with which dispersal events encounter sink reefs is another feature of source reefs. Such reef characteristics should be considered as important criteria in the selection of high priority reefs which are afforded protection from extractive activities.

Where a particular reef is subjected to high levels of exploitation, then consideration should be given to the protection of source reefs which have strong connectivity with that particular reef. The choice of appropriate source reefs for protection as replenishment reefs must also consider cross-shelf differences in community structure.

The ability of a reef to act as an efficient and effective sink for larvae is determined by its shape and size, location on the shelf, and its relationship to surrounding reefs. Reefs which can be identified as effective and efficient sinks for larvae are better suited to exploitation by extractive activities as they can be expected to sustain a higher level of exploitation and to recover more quickly from over-exploitation. The efficiency of a reef as a sink is best assessed by the sum of its connectivity with all source reefs.

Identification of the northern portion of the Cairns Section as a region which is the likely source of primary outbreaks of *A. planci*, from which secondary outbreaks subsequently developed to the south, and a mechanism for the maintenance of populations within the region, has important implications for management of the GBR. This northern region may also be important to the maintenance of populations of many other reef species throughout the central GBR. Adequate protection of reefs within the northern region could be important to the long term maintenance and sustainable exploitation of populations on many reefs further to the south. Adequate protection needs to be considered for a series of connected reefs extending from north to south in order to facilitate the supply of larvae throughout the Cairns and Central Sections of the GBR Marine Park. A preliminary study has already identified gaps in the existing zoning plan for the Cairns Section (James et al., 1990), and provided input to a revised zoning plan which is presently under

consideration.

If models of larval dispersal are to be used for this purpose, then it is important that their predictions be validated and that the models continue to be developed and improved. Future applications to zoning need to consider the reproductive characteristics of key species. The behaviour and timing of spawning and dispersal of these species should be carefully incorporated into the models. Such developments must go hand in hand with the acquisition of more detailed information on distribution, population abundance and the life-history of the particular species which are subjected to exploitation.

5.5.3 Environmental Impact Assessment

The physical oceanography and hydrodynamics of the GBR are complex and dynamic. Coastal and continental shelf features, such as headlands, bays, reef density, bathymetry and shelf width, have been identified as the major determinants of circulation patterns on continental shelves and result in spatial variation in the contribution and relative importance of the different components which force water circulation. The primary forcing in one area is not necessarily important in another.

The magnitude and orientation of tidal forcings can vary substantially over relatively short distances, both across and along the continental shelf. Tidal currents in isolation show greatest variation in magnitude and direction over time scales of hours, followed by days. Recirculation and the formation of eddies as a result of tidal currents persist only over periods of hours. On the other hand, greatest variation in the magnitude and direction of wind-driven currents is over time scales of days, and can result in relatively stable recirculation patterns which persist over this period. In contrast, the EAC varies only in magnitude throughout most of the GBR, with fluctuations over time scales of weeks.

The design of water quality sampling programmes should consider the spatial and temporal occurrence of physical features such as recirculation, which have the potential to either concentrate or

disperse pollutants. Water samples taken from within such features may give consistently different measurements from others taken in close proximity, but outside the eddy circulation. The variance within samples from a particular site can be minimized by sampling consistently in relation to such features. Insufficient attention is frequently paid to physical oceanography and hydrodynamics in the impact assessment of water quality within the GBR. There is a need for greater consideration of water motion in environmental impact assessment and the design of baseline and monitoring programmes from the outset. Without prior understanding of the physical environment and the ability to predict where and when impacts are most likely to occur, then researchers can only hope to sample, and therefore detect, such impacts.

The appropriate location of sewage outfalls can ensure effective dilution and dispersion of effluent. Furthermore, assessment of the appropriateness of 'control' sites must require an understanding of the oceanography of the area and the distance and direction of pollutant transport. Because of these interactions and dynamics, it is fundamental to the interpretation of all water quality results that an understanding of the hydrodynamics is achieved and that accurate records of tidal and wind conditions be recorded and presented. Careful attention should be paid to focus on the scale which is appropriate to the forcings and questions which are being asked.

Dispersal models can also contribute to studies which aim to determine the impacts of human activities on reefs, such as the effects of fishing. Models which can account for some of the spatial and temporal variation that is observed in recruitment and abundance can assist in the assessment of human impacts on reefs, by enhancing our ability to distinguish these impacts from natural variability. The present research has identified several sources of variation, including inter-annual differences in larval transport, regional differences in levels of connectivity, large-scale features of water circulation which concentrate larvae, specific source-sink interactions and fine-scale features of water circulation which influence the entrainment of larvae onto reefs. Dispersal models may also illustrate confounding influences in the design of experiments

through source-sink interactions.

5.6 SUMMARY AND CONCLUSIONS

Latitudinal variation in shelf width, reef structure and density, and bathymetry will result in significant differences in circulation and the transport of larvae. These include: (1) regional differences in the degree of symmetry in larval dispersal, the level and pattern of recruitment and, therefore, possibly population density and age-structure; (2) passive mechanisms which both concentrate and separate larval pools at the scale of 10s of kilometres; (3) extensive inter-annual variability in larval transport; and (4) fine-scale features of water circulation and reef morphology which influence the entrainment of larvae from the mainstream circulation onto and around individual reefs. This combination of stochastic and deterministic factors may account for much of the pattern and variability in recruitment that has been documented not only for *A. planci*, but for reef species with pelagic larvae in general.

Model results provide a physical explanation for many of the observed features of *Acanthaster* population spread throughout the central Great Barrier Reef. These include: (1) identification of a source region from which *Acanthaster* populations are proposed to have spread; (2) the apparent southward spread of populations from this region; (3) the high incidence of outbreaks on mid-shelf reefs south from Green Island; (4) the susceptibility of particular reefs to repeated recruitment, notably Green Island and many others which border the main lagoon; and (5) the cessation of outbreaks causing high coral mortality throughout the mid-shelf reefs within the Central Section of the Marine Park. The susceptibility of particular reefs to repeated recruitment can arise due to their physical location bordering the lagoon, strong connectivity with other reefs which are themselves efficient sinks and the focusing of recruitment by currents on individual reefs or groups of reefs from multiple sources. The high incidence of outbreaks on inner matrix reefs south from Green Island can therefore be explained as a purely physical phenomenon, without the need to invoke human interference in the ecology of these more

accessible reefs (cf. Pearson & Endean, 1969). The application of life-history theory, through population models which consider the accurate geometric representation of reef complexes and larval connectivity, could shed light on the *Acanthaster* debate.

Asymmetries in the long-shelf and cross-shelf transport of larvae indicate that larval dispersal cannot be considered as an isotropic random process and that recruitment to reefs is not from a homogeneous larval pool. Physical processes within the GBR do not always act to disperse larvae widely. Limited cross-shelf mixing can account for the maintenance of nearshore and mid-shelf communities within the central GBR. The currents which transport larvae are directed by shelf topography and result in distributions of larvae which are not spatially uniform. Temporal variation in larval transport and differences in the level and strength of connectivity between source and sink reefs further emphasize the unsuitability of viewing the larval pool, and hence recruitment, as homogeneous.

Sale (1985) observes that while many species of reef fish breed frequently, their larvae settle infrequently, if at all. The apparent mortality during the larval dispersal phase of many species may not result primarily from predation, but rather, from the inability to encounter a suitable habitat within the time constraints of larval life.

Results indicate that larvae of species with relatively long pre-competent periods of development will be transported considerable distances from their natal reefs and will only rarely recruit back onto the source reef. There is likely to be a high net export of larvae southwards from the southern portion of the Cairns Section and northern portion of the Central Section of the GBR Marine Park. This was predicted by Williams et al. (1984) on the basis of progressive vector plots.

Larval dispersal models are also well suited to management issues and applications. In the face of increasing pressure on coral reefs as resources for exploitation, recreation and tourism, a better understanding of reef connectivity through numerical hydrodynamic models provides a stronger, and more rational, biological basis for

zoning within the GBR Marine Park. The following guide-lines are proposed for the development of future zoning plans within the GBR:

(1) Section zoning plans should identify any hydrodynamically distinctive regions which are likely to result in different patterns of dispersal and recruitment. The possibility that particular regions may be important to the maintenance of populations on reefs over a more extensive area should be considered. The degree to which areas of the GBR can be considered in isolation and the relevance of existing Section boundaries needs to be determined.

(2) Effective and reliable source reefs which are representative of the existing cross-shelf patterns of species distribution should be identified within regions. Suitably located and representative reefs should be given adequate protection to ensure the continued supply of larvae to other reefs within the region and throughout the system.

(3) The selection of reefs where extractive activities are to be permitted should consider their ability to behave as efficient and reliable sinks for larvae. The ability of reefs to recover from over exploitation will depend to a large degree on the availability of recruits to the population. Reefs which behave as efficient sinks should be better able to sustain increased population pressure and are thus more suited to exploitation.

(4) Attention should be paid to identify reefs which are poor sinks for larvae. Extractive activities on such reefs should be discouraged as these reefs are likely to be less able to sustain elevated levels of resource exploitation, while recovery from over-exploitation will be slow.

REFERENCES

Allen, J.S. (1980) Models of wind-driven currents on the continental shelf. Ann. Rev. Fluid Mech. 12: 389-433.

Anderson, G.R.V., Ehrlich, A.H., Ehrlich, P.R., Roughgarden, J.D., Russell, B.C. & Talbot, F.H. (1981) The community structure of coral reef fishes. Am. Nat. 117: 476-495.

Andrews, J.C. (1983) Water masses, nutrient levels and seasonal drift on the outer central shelf (Great Barrier Reef). Aust. J. Mar. Freshw. Res. 34: 821-834.

Andrews, J.C. & Bode, L. (1988) The tides of the central Great Barrier Reef. Cont. Shelf Res. 8: 1057-1085.

Andrews, J.C. & Furnas, M.L. (1986) Subsurface intrusions of Coral Sea water into the central Great Barrier Reef - I. Structures and shelf-scale dynamics. Cont. Shelf Res. 6: 491-514.

Andrews, J.C. & Gentien, P. (1982) Upwelling as a source of nutrients for the Great Barrier Reef ecosystems: A solution to Darwin's question? Mar. Ecol. Prog. Ser. 8: 257-269.

Babcock, R.C. (1988) Fine-scale spatial and temporal patterns in coral settlement. Proc. 6th. Int. Coral Reef Symp., Australia 2: 635-639.

Babcock, R.C. & Heyward, A.J. (1986) Larval development of certain gamete-spawning scleractinian corals. Coral Reefs 5: 111-116.

Babcock, R.C., Bull, G., Harrison, P.L., Oliver, J.K., Wallace, C.C. & Willis, B.L. (1986) Synchronous spawnings of 105 scleractinian coral species on the Great Barrier Reef. Mar. Biol. 90: 379-394.

Bak, R.P.M. (1985) Recruitment patterns and mass mortalities in the sea urchin *Diadema antillarum*. Proc. 5th. Int. Coral Reef Congress, Tahiti 5: 267-272.

Barlow, G.W. (1981) Patterns of parental investment, dispersal and size among coral-reef fishes. Env. Biol. Fish. 6(1): 65-85.

Barnes, J. & Endean, R. (1964) A dangerous starfish - *Acanthaster planci* (Linne.). Med. J. Aust. 1: 592.

Barnes, J.H. (1966) The crown of thorns starfish as a destroyer of corals. Aust. Nat. Hist. 15: 257-261.

Barnett, L., DeVantier, L., Styles, T. & West, T. (1985) An assessment of the distribution and effects of *Acanthaster planci* (L.) on the Great Barrier Reef: 7. Innisfail. Australian Institute Marine Science, Townsville. 101 pp.

Bass, D.K., Davidson, J., Johnson, D.B., Miller, I.R., Miller-Smith, B.A., Mundy, C.N., Thompson, A.A. & Baker, V.J. (1989) Broadscale surveys of crown-of-thorn starfish on the Great Barrier Reef 1988 to 1989. Australian Institute of Marine Science, Townsville. 166 pp.

Bikaunieks, P.J. (1991) Model based study of larval dispersal in the Central Section of the Great Barrier Reef Marine Park. Department of Civil and Systems Engineering, James Cook University of North Queensland. 99 pp. (unpublished report)

Birkeland, C. (1982) Terrestrial runoff as a cause of outbreaks of *Acanthaster planci* (Echinodermata: Asteroidea). Mar. Biol. 69: 175-185.

Birkeland, C. & Lucas, J.S. (1990) *Acanthaster planci*: Major management problem of coral reefs. CRC Press, Boston. 257 pp.

Birtles, A. & Arnold, P. (1983) Between the reefs: Some patterns of soft substrate epibenthos on the central Great Barrier Reef shelf. Proc. Great Barrier Reef Conf., Townsville. pp. 159-163.

Black, K.P. (1983) Sediment transport and tidal inlet hydraulics. PhD Thesis, University of Waikato, Hamilton, New Zealand, Vols. 1 & 2. 331 pp.

Black, K.P. (1988) The relationship of reef hydrodynamics to variations in numbers of planktonic larvae on and around coral reefs. Proc. 6th. Int. Coral Reef Symp., Australia 2: 125-130.

Black, K.P. & Gay, S.L. (1987a) Eddy formation in unsteady flows. J. Geophys. Res. 92: 9514-9522.

Black, K.P. & Gay, S.L. (1987b) Hydrodynamic control of the dispersal of crown-of-thorns starfish larvae. 1. Small scale hydrodynamcis on and around schematized and actual reefs. Victorian Institute of Marine Sciences, Technical Report No.8. 62 pp.

Black, K.P., Gay, S.L. & Andrews, J.C. (1990) Residence times of neutrally-buoyant matter such as larvae, sewage or nutrients on coral reefs. Coral Reefs 9(3): 105-114.

Bode, L. & Sobey, R.J. (1984) Initial transients in long wave computations. J. Hyd. Engineering, ASCE 110: 1371-1397.

Bode, L., Mason, L.B. & Middleton, J.H. (1991) The response of a shelf/sea barrier reef system to tidal oscillations: Analytical and numerical methodologies. J. Phys. Oceanogr. (in press)

Bode, L., Mason, L.B., Sobey, R.J. & Stark, K.P. (1981) Hydrodynamic studies of water movements within the Great Barrier Reef. Res. Bull. CS27, Dept. Civil & Systems Engineering, James Cook University of North Queensland.

Bradbury, R.H., Done, T.J., English, S.A., Fisk, D.A., Moran, P.J., Reichelt, R.E. & Williams, D.McB. (1985) The crown-of thorns: Coping with uncertainty. Search 16: 106-109.

Bradbury, R.H., Hammond, L.S., Moran, P.J. & Reichelt, R.E. (1985a) Coral reef communities and the crown-of-thorns starfish: Evidence for qualitatively stable cycles. J. Theor. Biol. 113: 69-80.

Bradbury, R.H., Hammond, L., Moran, P.J. & Reichelt, R.E. (1985b) The stable points, stable cycles and chaos of the *Acanthaster* phenomenon: A fugue in three voices. Proc. 5th. Int. Coral Reef Congress, Tahiti 5: 303-308.

Bradbury, R.H., Laan, J.D. van der & MacDonald, B. (1990) Modelling the effects of predation and dispersal on the generation of waves of starfish outbreaks. Mathl. Comput. Modelling 13(6): 61-67.

Brothers, E.B., Williams, D.McB. & Sale, P.F. (1983) Length of larval life in twelve families of fishes at "One Tree Lagoon", Great Barrier Reef, Australia. Mar. Biol. 76: 319-324.

Brunckhorst, D. & Johnson, D. (1985) An assessment of the distribution and effects of the starfish *Acanthaster planci* (L.) on the Great Barrier Reef: 8. Townsville sector. Australian Institute of Marine Science, Townsville. 81 pp.

Brunckhorst, D. & Young, R. (1985a) An assessment of the distribution and effects of the starfish *Acanthaster planci* (L.) on the Great Barrier Reef: 6. Cairns sector. Australian Institute of Marine Science, Townsville. 105 pp.

Brunckhorst, D. & Young, R. (1985b) An assessment of the distribution and effects of *Acanthaster planci* (L.) on the Great Barrier Reef: 4. Cape Grenville. Australian Institute Marine Science, Townsville. 119 pp.

Bull, G. (1986) Distribution and abundance of coral plankton. Coral Reefs 4: 197-200.

Butman, C.A. (1987) Larval settlement of soft-sediment invertebrates: The spatial scales of pattern explained by active habitat selection and the emerging role of hydrodynamic processes. Oceanogr. Mar. Biol. Ann. Rev. 25: 113-165.

Cameron, A.M. & Endean, R. (1982) Renewed population outbreaks of a rare and specialized carnivore (the starfish *Acanthaster planci*) in a complex high-diversity system (the Great Barrier Reef). Proc. 4th. Int. Coral Reef Symp. 2: 593-596.

Christensen, F.B. & Fenchel, T.M. (1979) Evolution of marine invertebrate reproductive patterns. Theor. Popul. Biol 16: 267.

Church, J.A. (1987) East Australian Current adjacent to the Great Barrier Reef . Aust. J. Mar. Freshw. Res. 38: 671-683.

Church, J.A. & Boland, F.M. (1983) A permanent undercurrent adjacent to the Great Barrier Reef. J. Phys. Oceanogr. 13: 1747-1749.

Cresswell, G.R. & Greig, M.A. (1978) Currents and water properties in the north-central Great Barrier Reef during the south-east trade wind season. Aust. J. Mar. Freshw. Res. 29: 345-353.

Dana, T.F., Newman, W.A. & Fager, E.W. (1972) *Acanthaster* aggregation: Interpreted as primarily responses to natural phenomena. Pacif. Sci. 26: 355-372.

Day, R. & McEdward, L. (1984) Aspects of the physiology and ecology of pelagic larvae of marine benthic invertebrates. Marine Plankton Life Cycle Strategies. Steidinger, K.A. & Walker, L.M. (eds). CRC Press, Boca Raton, Fl. pp. 93-120.

Dight, I.J. & Black, K.P. (1991) Numerical simulation of larval dispersal and recruitment to coral reefs from the mainstream water circulation. Proc. 7th Symp. on Coastal & Ocean Management, Coastal Zone 91, Long Beach 3: 1995-2009.

Dight, I.J. & James, M.K. (in press) Physical aspects of large-scale dispersal in the crown-of-thorns starfish *Acanthaster planci.* Interdisciplinary approaches to larval dispersal and recruitment processes in the marine environment. Sammarco, P.W. & Heron, M. (eds). Lecture Notes in Biomathematics. Springer-Verlag, New York.

Dight, I.J., Bode, L. & James, M.K. (1990) Modelling the larval dispersal of *Acanthaster planci*: I. Large scale hydrodynamics, Cairns Section, Great Barrier Reef Marine Park. Coral Reefs 9(3): 115-123.

Dight, I.J., James, M.K. & Bode, L. (1988) Models of larval dispersal within the central Great Barrier Reef: Patterns of connectivity and their implications for species distributions. Proc. 6th. Int. Coral Reef Symp., Australia. 3: 217-223.

Dight, I.J., James, M.K. & Bode, L. (1990) Modelling the larval dispersal of *Acanthaster planci*: II. Patterns of reef connectivity. Coral Reefs 9(3): 125-134.

Dinesen, Z.D. (1983) Patterns in the distribution of soft corals across the central Great Barrier Reef. Coral Reefs 1: 229-236.

Doherty, P.J. (1988) Large-scale variability in the recruitment of a coral reef fish. Proc. 6th. Int. Coral Reef Symp., Australia 2: 667-671.

Doherty, P.J. & Davidson, J. (1988) Monitoring the distribution and abundance of juvenile *Acanthaster planci* in the central Great Barrier Reef. Proc. 6th. Int. Coral Reef Symp., Australia 2: 131-136.

Doherty, P.J. & Williams, D. McB. (1988a) The replenishment of coral reef fish populations. Oceanogr. Mar. Biol. Ann. Rev. 26: 487-551.

Doherty, P.J. & Williams, D.McB. (1988b) Are local populations of coral reef fishes equilibrial assemblages? The empiricle database. Proc. 6th. Int. Coral Reef Symp., Australia 1: 131-139.

Doherty, P.J., Williams, D.McB. & Sale, P.F. (1985) The adaptive significance of larval dispersal in coral reef fishes. Env. Biol. Fish. 12(2): 81-90.

Done, T.J. (1982) Patterns in the distribution of coral reef communities across the central Great Barrier Reef. Coral Reefs 1: 95-107.

Done, T.J. (1983) The distribution of coral communities on the Great Barrier Reef. Proc. Great Barrier Reef Conf., Townsville. pp. 197-202.

Ebert, T.A. (1983) Recruitment in echinoderms. Echinoderm Studies 1. Jangoux, M. & Lawrence, J.M. (eds). A.A. Balkema, Rottersdam. pp. 169-203.

Emlet, R.B. (1986) Larval production, dispersal, and growth in a fjord: A case study on larvae of the sand dollar *Dendraster excentricus*. Mar. Ecol. Prog. Ser. 31: 245-254.

Endean, R. (1973) Population explosions of *Acanthaster planci* and associated destruction of hermatypic corals in the Indo-west Pacific region. In: Biology and Geology of Coral Reefs, Vol. II, Biology 1. Jones, O.A. & Endean, R. (eds). Academic Press, New York. pp. 215-254.

Endean, R. (1974) *Acanthaster planci* on the Great Barrier Reef. Proc. 2nd. Int. Coral Reef Symp. Australia 1: 563-576.

Endean, R. (1977) *Acanthaster planci* infestations of reefs of the Great Barrier Reef. Proc. 3rd. Int. Coral Reef Symp., Miami 1: 185-191.

Endean, R. (1982) Crown-of-thorns starfish on the Great Barrier Reef. Endeavour 6: 10-14.

Endean, R. & Cameron, A.M. (1990) *Acanthaster planci* population outbreaks. Ecosystems of the World 25 Coral Reefs. Dubinsky, Z. (ed.) Elsevier, Oxford. pp. 419-437.

Endean, R. & Stablum, W. (1973) A study of some aspects of the crown-of-thorns starfish (*Acanthaster planci*) infestations of reefs of Australia's Great Barrier Reef. Atoll Res. Bull. 167: 1-62.

Fernandez, L., Marsh, H., Moran, P.J. & Sinclair, D. (1990) Bias in manta tow surveys of *Acanthaster planci*. Coral Reefs 9(3): 155-160.

Fisk, D.A. & Harriott, V.J. (1990) Spatial and temporal variation in coral recruitment on the great Barrier Reef: Implications for dispersal hypotheses. Mar. Biol. 107: 485-490.

Fisk, D.A., Harriott, V.J. & Pearson, R.G. (1988) The history and status of crown-of-thorns starfish and corals at Green Island reef, Great Barrier Reef. Proc. 6th. Int. Coral Reef Symp., Australia 2: 149-155.

Fortier, L. & Leggett, W.C. (1985) A drift study of larval fish survival. Mar. Ecol. Prog. Ser. 25: 245-257.

Frith, C.A. & Mason, L.B. (1986) Modelling wind driven circulation One Tree Reef, southern Great Barrier Reef. Coral Reefs 4: 201-211.

Frith, C.A., Leis, J.M. & Goldman, B. (1986) Currents in the Lizard Island region of the Great Barrier reef lagoon and their relevance to potential movements of larvae. Coral Reefs 5: 81-92.

Glynn, P.W. (1973) Ecology of a Caribbean coral reef. The Porites reef-flat biotope: Part II. Plankton community with evidence for depletion. Mar. Biol. 22: 1-21.

Goldman, B., Stroud, G. & Talbot, F. (1983) Fish eggs and larvae over a coral reef: Abundance with habitat, time of day and moon phase. Proc. Great Barrier Reef Conf., Townsville. pp. 203-211.

Griffin, D.A., Middleton, J.H. & Bode, L. (1987) The tidal and longer-period circulation of Capricornia, southern Great Barrier Reef. Aust. J. Mar. Freshw. Res. 38: 461-474.

Hammond, L.S., Birtles, R.A. & Reichelt, R.E. (1985) Holothuroid assemblages on coral reefs across the Central Section of the Great Barrier Reef. Proc. 5th. Int. Coral Reef Congress, Tahiti. 2: 285-290.

Hamner, W.M. & Wolanski, E. (1988) Hydrodynamic forcing functions and biological processes on coral reefs: A status review. Proc. 6th. Int. Coral Reef Symp., Townsville. 1: 103-113.

Hamner, W.M., Jones, M.S., Carlton, J.H., Hauri, I.R. & Williams, D.McB. (1988) Zooplankton, planktivorous fish, and water currents on a windward reef face: Great Barrier Reef, Australia. Bull. Mar. Sci. 42(3): 459-479.

Hamon, B.V. (1984) Diurnal and semi-diurnal tides on the Great Barrier Reef. Report 163, CSIRO Marine Lab.

Harriott, V.J. (1985) Recruitment patterns of scleractinian corals at Lizard Island, Great Barrier Reef. Proc. 5th. Int. Coral Reef Congress, Tahiti. 4: 367-372.

Harriott, V.J. & Fisk, D.A. (1988) Recruitment patterns of scleractinian corals: A study of three reefs. Aust. J. Mar. Freshw. Res. 39(4): 409-416.

Hopley, D. (1982) Geomorphology of the great Barrier Reef: Quaternary development of coral reefs. John Wiley-Interscience, New York. 453 pp.

Hopley, D., Parnell, K.E. & Isdale, P.J. (1989) The Great Barrier Reef Marine Park: Dimensions and regional patterns. Aust. Geogr. Studies 27(1): 47-66.

Jablonski, D. & Lutz, R.A. (1983) Larval ecology of marine benthic invertebrates: Paleobiological implications. Biol. Rev. 58: 21-89.

James, M.K., Dight, I.J. & Day, J.C. (1990) Application of larval dispersal models to zoning of the Great Barrier Reef Marine Park. Proc. 4th. Pacific Congress Mar. Sci. Technol. 2: 140-145.

James, M.K., Dight, I.J. & Bode, L. (1990) Great Barrier Reef hydrodynamics, reef connectivity and *Acanthaster* population dynamics. *Acanthaster* and the coral reef: A theoretical perspective. Bradbury, R.H. (ed). Lecture Notes in Biomathematics. Springer-Verlag, New York. pp. 17-44.

Johannes, R.E. (1978) Reproductive strategies of coastal marine fishes in the tropics. Env. Biol. Fish 3(1): 65-84.

Johnson, D.B., Bass, D.K., Miller-Smith, B.A., Moran, P.J., Mundy, C.N. & Speare, P.J. (1988) Outbreaks of the crown-of-thorns starfish (*Acanthaster planci*) on the Great Barrier Reef: Results of surveys 1986-1988. Proc. 6th. Int. Coral Reef Symp., Australia. 2: 165-169.

Jones, R. & Hall, W.B. (1974) Some observations on the population dynamics of the larval stage in the common gadoids. The Early Life History of Fish. Blaxter, J.S. (ed). Springer-Verlag, New York. pp. 87-102.

Kenchington, R.A. (1977) Growth and recruitment of *Acanthaster planci* (L.) on the Great Barrier Reef. Biol. Conserv. 11: 103-118.

Kenchington, R.A. & Pearson, R. (1982) Crown of thorns starfish on the Great Barrier Reef: A situation report. Proc. 4th. Int. Coral Reef Symp., Manila 2: 597-600.

Kenchington, R.A. & Morton, B. (1976) Two surveys of the crown of thorns starfish over a section of the Great Barrier Reef: Report to the Steering Committee for the crown of thorns survey. Australian Government Publishing Service, Canberra. 186 pp.

Keough, M.J. (1988) Benthic populations: Is recruitment limiting or just fashionable? Proc. 6th. Int. Coral Reef Symp., Australia. 1: 141-148.

Kettle, B.T. & Lucas, J.S. (1987) Biometric relationships between organ indices, fecundity, oxygen consumption and body size in *Acanthaster planci* (L.) (Echinodermata: Asteroidea). Bull. Mar. Sci. 41(2): 541-551.

Leiby, M.M. (1984) Life history and ecology of pelagic fish eggs and larvae. Marine Plankton Life Cycle Strategies. Steidinger, K.A. & Walker, L.M. (eds). CRC Press, Boca Raton, Fl. pp. 121-140.

Leis, J.M. (1986) Vertical and horizontal distribution of fish larvae near coral reefs at Lizard Island, Great Barrier Reef. Mar. Biol. 90: 505-516.

Leis, J.M. & Goldman, B. (1983) Studies on the biology of larval fishes in the Lizard Island area, northern Great Barrier Reef. Proc. Great Barrier Reef Conf., Townsville. pp. 221-225.

Leis, J.M. & Goldman, B. (1987) Composition and distribution of larval fish assemblages in the Great Barrier Reef lagoon, near Lizard Island, Australia. Aust. J. Mar. Freshw. Res. 38: 211-223.

Leis, J.M., Goldman, B. & Uehanagi, S. (1987) Distribution and abundance of billfish larvae (Pisces: Istiophoridae) in the Great Barrier Reef lagoon and Coral Sea near Lizard Island, Australia. Fish. Bull. 85(4): 757-765.

Lucas, J. (1986) The crown of thorns starfish. Oceanus 29(2): 55-64.

Lucas, J.S. (1973) Reproductive and larval biology of *Acanthaster planci* (L.) in Great Barrier Reef waters. Micronesica 9: 197-293.

Lucas, J.S. (1982) Quantitative studies of feeding and nutrition during larval development of a coral reef asteroid *Acanthaster planci* (L.). J. Exp. Mar. Biol. Ecol. 65: 173-194.

Lucas, J.S. (1984) Growth and maturation of *Acanthaster planci* (L.) (Asteroidea) and hybrids in the laboratory, including observations on the effects of diets. J. Exp. Mar. Biol. Ecol. 79: 129-147.

McCallum, H.I. (1987) Predator regulation of *Acanthaster planci*. J. Theor. Biol. 127: 207-220.

Middleton, J.H. (1987) Steady coastal circulation due to alongshore pressure gradients. J. Phys. Oceanogr. 17: 604-612.

Middleton, J.H. & Bode, L. (unpublished manuscript) Modelling Great Barrier Reef tides: Northern Section. J. Phys. Oceanogr.

Moore, R.J. (1978) Is *Acanthaster planci* an r-strategist? Nature 271: 56-57.

Moran, P.J. (1986) The *Acanthaster* phenomenon. Oceanogr. Mar. Biol. Ann. Rev. 24: 379-480.

Moran, P.J. & Johnson, D.B. (1990) Final report on the results of COTSAC ecological research: December 1985 - June 1989. Australian Institute Marine Science, Townsville. 40 pp.

Moran, P.J., Bradbury, R.H. & Reichelt, R.E. (1985) Mesoscale studies of the crown-of-thorns/coral interaction: A case history from the Great Barrier Reef. Proc. 5th. Int. Coral Reef Congress, Tahiti 5: 321-326.

Moran, P.J., Bradbury, R.H. & Reichelt, R.E. (1988) Distribution of recent outbreaks of the crown-of-thorns starfish (*Acanthaster planci*) along the Great Barrier Reef: 1985-1986. Coral Reefs 7: 125-137.

Murphy, G.I. (1968) Pattern in life history and the environment. Am. Nat. 102: 391-403.

Nash, W. & Zell, L.D. (1982) *Acanthaster* on the Great Barrier Reef: Distribution on 5 transects between 14oS and 18oS. Proc. 4th. Int. Coral Reef Symp., Manila 2: 601-605.

Oliver, J.K. & Willis, B.L. (1987) Coral-spawn slicks in the Great Barrier Reef: Preliminary observations. Mar. Biol. 94: 521-529.

Olson, R.R. (1985) In situ culturing of larvae of the crown-of-thorns starfish *Acanthaster planci*. Mar. Ecol. Prog. Ser. 25: 207-210.

Olson, R.R. (1987) In situ culturing as a test of the larval starvation hypothesis for the crown-of-thorns starfish, *Acanthaster planci*. Limnol. Oceanogr. 32(4): 895-904.

Olson, R.R. & Olson, M.H. (1989) Food limitation of planktrotrophic marine invertebrate larvae: Does it control recruitment success? Annu. Rev. Ecol. Syst. 20: 225-247.

Palmer, A.R. & Strathmann, R.R. (1981) Scale of dispersal in varying environments and its implications for life histories of marine invertebrates. Oecologia 48: 308-318.

Parslow, J.S. & Gabric, A.J. (1989) Advection, dispersal and plankton patchiness on the Great Barrier Reef. Aust. J. Mar. Freshw. Res. 40: 403-419.

Pearson, R.G. (1972) Changes in distribution of *Acanthaster planci* populations on the Great Barrier Reef. Nature 237: 175-176.

Pearson, R.G. & Endean, R. (1969) A preliminary study of the coral predator *Acanthaster planci* (L.) (Asteroidea) on the Great Barrier Reef. Qld. Dept. Harbours & Marine, Fisheries Notes 3: 27-55.

Pennington, J.T. (1985) The ecology of fertilization of echinoid eggs: The consequences of sperm dilution, adult aggregation, and synchronous spawning. Biol. Bull. 169: 417-430.

Phillips, B.F. (1981) The circulation of the southeastern Indian Ocean and the planktonic life of the western rock lobster. Oceanogr. Mar. Biol. Ann. Rev. 19: 11-39.

Pickard, G.L., Donguy, J.R., Henin, C. & Rougerie, F. (1977) A review of the physical oceanography of the Great Barrier Reef and western Coral Sea. Aust. Inst. Mar. Sci., Monograph Series, Vol.2. 134 pp.

Potts, D.C. (1981) Crown-of-thorns starfish - man-induced pest or natural phenomenon. The Ecology of Pests. Kitching, R.L. & Jones, R.E. (eds). CSIRO, Melbourne. pp. 55-86.

Prandle, D. (1978) Residual flows and elevations in the North Sea. Proc. R. Soc. Lond. A. 359: 189-228.

Reichelt, R.E., Bradbury, R.H. & Moran, P.J. (1990a) Distribution of *Acanthaster planci* outbreaks on the Great Barrier Reef between 1966 and 1989. Coral Reefs 9(3): 97-103.

Reichelt, R.E., Bradbury, R.H. & Moran, P.J. (1990b) The crown-of-thorns starfish, *Acanthaster planci*, on the Great Barrier Reef. Mathl. Comput. Modelling 13(6): 45-60.

Reichelt, R.E., Greve, W., Bradbury, R.H. & Moran, P.J. (1990) *Acanthaster planci* outbreak initiation: A starfish-coral site model. Ecological Modelling 49: 153-177.

Rothlisberg, P.C., Church, J.A. & Forbes, A.G.M. (1983) Modelling the advection of vertically migrating shrimp larvae. J. Mar. Res. 41: 511-538.

Sale, P.F. (1980) The ecology of fishes on coral reefs. Oceanogr. Mar. Biol. Ann. Rev. 18: 367-431.

Sale, P.F. (1985) Patterns in recruitment in coral reef fishes. Proc. 5th. Int. Coral Reef Congress, Tahiti 5: 391-396.

Sale, P.F., Douglas, W.A. & Doherty, P.J. (1984) Choice of microhabitats by coral reef fishes at settlement. Coral Reefs 3: 91-99.

Sammarco, P.W. (1983) Coral recruitment across the central Great Barrier Reef: A preliminary report. Proc. Great Barrier Reef Conf., Townsville. pp. 245-250.

Sammarco, P.W. & Andrews, J.C. (1988) Localized dispersal and recruitment in Great Barrier Reef corals: The Helix Experiment. Science 239: 1422-1424.

Sammarco, P.W. & Crenshaw, H. (1984) Plankton community dynamics of the central Great Barrier Reef lagoon: Analysis of data from Ikeda et al. Mar. Biol. 82: 167-180.

Scheltema, R.S. & Williams, I.P. (1983) Long-distance dispersal of planktonic larvae and the biogeography and evolution of some Polynesian and western Pacific molluscs. Bull. Mar. Sci. 33(3): 545-565.

Serate, E.B. (1988) Coastal wind field data analysis. Master of Eng. Sci. Thesis, James Cook Univ. Nth. Qld. 155 pp.

Sobey, R.J., Harper, B.A. & Stark, K.P. (1977) Numerical simulation of tropical cyclone storm surge. Res. Bull. CS14, Dept. Civil & Systems Eng., James Cook Univ. Nth. Qld.

Sobey, R.J., Harper, B.A. & Mitchell, G.M. (1980) Numerical modelling of tropical cyclone storm surge. Proc. 17th. Int. Conf. Coastal Eng., Sydney, March 23-28.

Sorokin, S., Weaver, K. & Lyall, I. (1985) An assessment of the distribution and effects of *Acanthaster planci* (L.) on the Great Barrier Reef: 3. Princess Charlotte Bay. Australian Institute Marine Science, Townsville. 86 pp.

Stearns, S.C. (1976) Life-history tactics: A review of the ideas. Quart. Rev. Biol. 51(1): 3-47.

Strathmann, R. (1974) The spread of sibling larvae of sedentary marine invertebrates. Am. Nat. 108: 29-44.

Thorson, G. (1950) Reproductive and larval ecology of marine bottom invertebrates. Biol Rev. 25: 1-45.

Vance, R.R. (1973) On reproductive strategies in marine benthic invertebrates. Am. Nat. 107: 339-361.

Victor, B.C. (1986) Larval settlement and juvenile mortality in a recruitment-limited coral reef fish population. Ecol. Monogr. 56(2): 145-160.

Wallace, C.C. (1985a) Four years of juvenile coral recruitment to five reef front sites. Proc. 5th. Int. Coral Reef Congress, Tahiti 4: 385-390.

Wallace, C.C. (1985b) Seasonal peaks and annual fluctuations in recruitment of juvenile scleractinian corals. Mar. Ecol. Prog. Ser. 21: 389-398.

Warner, R.R. & Hughes, T.P. (1988) The population dynamics of reef fishes. Proc. 6th. Int. Coral Reef Symp., Australia 1: 149-155.

Watson, W. & Leis, J.M. (1984) Ichthyoplankton of Kaneohe Bay, Hawaii: A one-year study of the fish eggs and larvae. Tech. Rep. No.75, Univ. of Hawaii Sea Grant Program, Honolulu. 178 pp.

Westneat, M.W. & Resing, J.M. (1988) Predation on coral spawn by planktivorous fish. Coral Reefs 7: 89-92.

Wilkinson, C.R. (1986) The nutritional spectrum of coral reef benthos. Oceanus 29(2): 68-75.

Wilkinson, C.R. & Cheshire, A.C. (1988) Cross-shelf variations in coral reef structure and function: Influences of land and ocean. Proc. 6th. Int. Coral Reef Symp., Australia 1: 227-233.

Williams, D.McB. (1982) Patterns in the distribution of fish communities across the central Great Barrier Reef. Coral Reefs 1: 35-43.

Williams, D.McB. (1983a) Longitudinal and latitudinal variation in the structure of reef fish communities. Proc. Great Barrier Reef Conf., Townsville. pp. 265-270.

Williams, D. McB. (1983b) Daily, monthly and yearly variability in recruitment of a guild of coral reef fishes. Mar. Ecol. Prog. Ser. 10: 231-237.

Williams, D.McB. & Hatcher, A.I. (1983) Structure of fish communities on outer slopes of inshore, mid-shelf and outer shelf reefs of the Great Barrier Reef. Mar. Ecol. Prog. Ser. 10: 239-250.

Williams, D.McB., Russ, G. & Doherty, P.J. (1986) Reef fish: Large-scale distribution and recruitment. Oceanus 29(2): 76-82.

Williams, D.McB., Wolanski, E. & Andrews, J.C. (1984) Transport mechanisms and the potential movement of planktonic larvae in the central region of the Great Barrier Reef. Coral Reefs 3: 229-236.

Willis, B.L. & Oliver, J.K. (1988) Inter-reef dispersal of coral larvae following the annual mass spawning on the Great Barrier Reef. Proc. 6th. Int. Coral Reef Symp., Australia 2: 853-859.

Wolanski, E. & Bennett, A.F. (1983) Continental shelf waves and their influence on the circulation around the Great Barrier Reef. Aust. J. Mar. Freshw. Res. 34: 23-47.

Wolanski, E. & Pickard, G.L. (1983) Upwelling by internal tides and Kelvin waves at the continental shelf break on the Great Barrier Reef. Aust. J. Mar. Freshw. Res. 34: 65-80.

Wolanski, E. & Pickard, G.L. (1985) Long term observations of currents on the central Great Barrier Reef continental shelf. Coral Reefs 4: 47-57.

Wolanski, E., Burrage, D. & King, B. (1989) Trapping and dispersion of coral eggs around Bowden Reef, Great Barrier Reef, following mass coral spawning. Cont. Shelf Res. 9(5): 479-496.

Wolanski, E., Drew, E. & Abel, K.M. (1988) Tidal jets, nutrient upwelling and their influence on the productivity of the alga *Halimeda* in the ribbon reefs, Great Barrier Reef. Estuarine, Coastal and Shelf Sci. 26: 169-201.

Wolanski, E., Jupp, D.L.B. & Pickard, G.L. (1986) Currents and coral reefs. Oceanus 29(2): 83-89.

Wu, J. (1980) Wind-stress coefficients over sea surface near neutral conditions a revisit. J. Phys. Oceanogr. 10: 727-740.

Yamaguchi, M. (1973) Early life histories of coral reef asteroids, with special reference to *Acanthaster planci* (L.). Biology and Geology of Coral Reefs. VII, Biology I. Jones, O.A. & Endean, R. (eds). Academic Press, New York. pp. 369-387.

Yamaguchi, M. (1986) *Acanthaster planci* infestations of reefs and coral assemblages in Japan: A retrospective analysis of control efforts. Coral Reefs 5: 23-30.

Zann, L., Brodie, J., Berryman, C. & Naqasima, M. (1987) Recruitment, ecology, growth and behavior of juvenile *Acanthaster planci* (L.) (Echinodermata: Asteroidea). Bull. Mar. Sci. 41(2): 561-575.

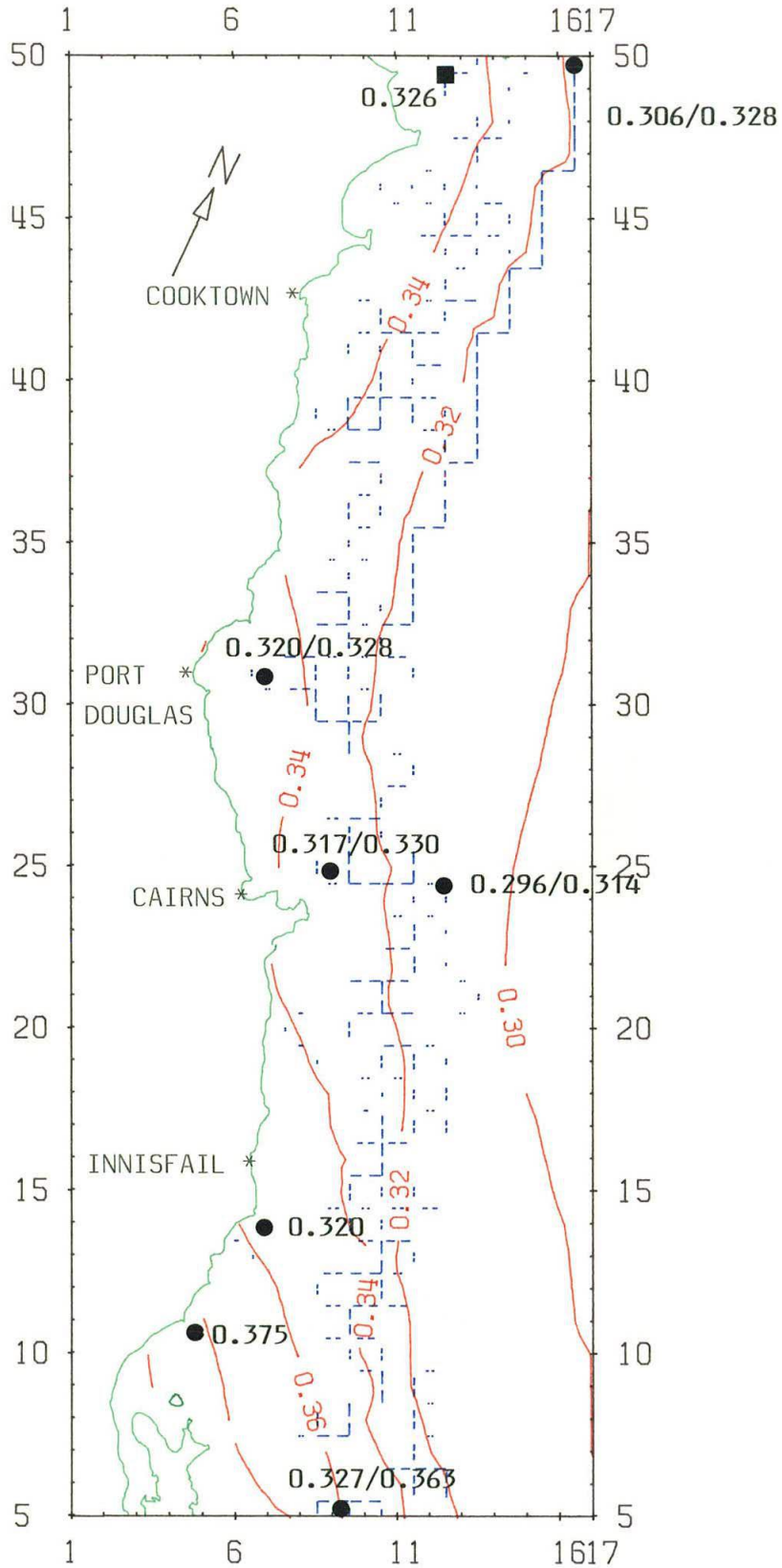


Figure A1a Comparison of observed and predicted values of tidal elevation amplitude for the S2 semi-diurnal constituent within the Cairns Section of the GBR Marine Park. Published data are from Hamon (1984) (denoted ●) and from J.H. Middleton (pers. comm.) (denoted ■). Where two values are noted, these represent the range of published observations. Tidal amplitudes are in metres.

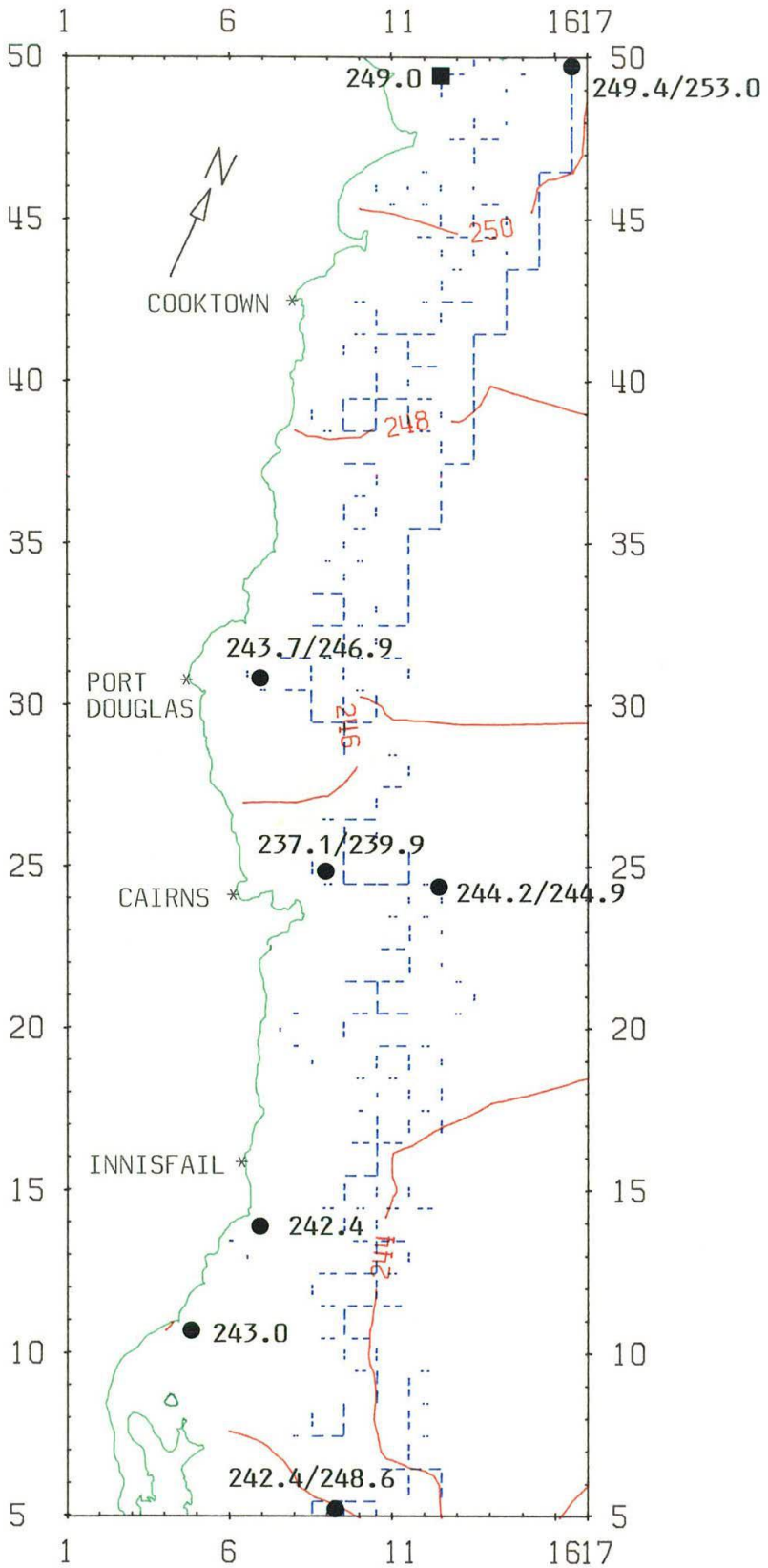


Figure A1b Comparison of observed and predicted values of tidal elevation phase for the S2 semi-diurnal constituent within the Cairns Section of the GBR Marine Park. Published data are from Hamon (1984) (denoted ●) and from JH Middleton (pers. comm.) (denoted ■). Where two values are noted, these represent the range of published observations. Greenwich phase lags are for GMT-10.

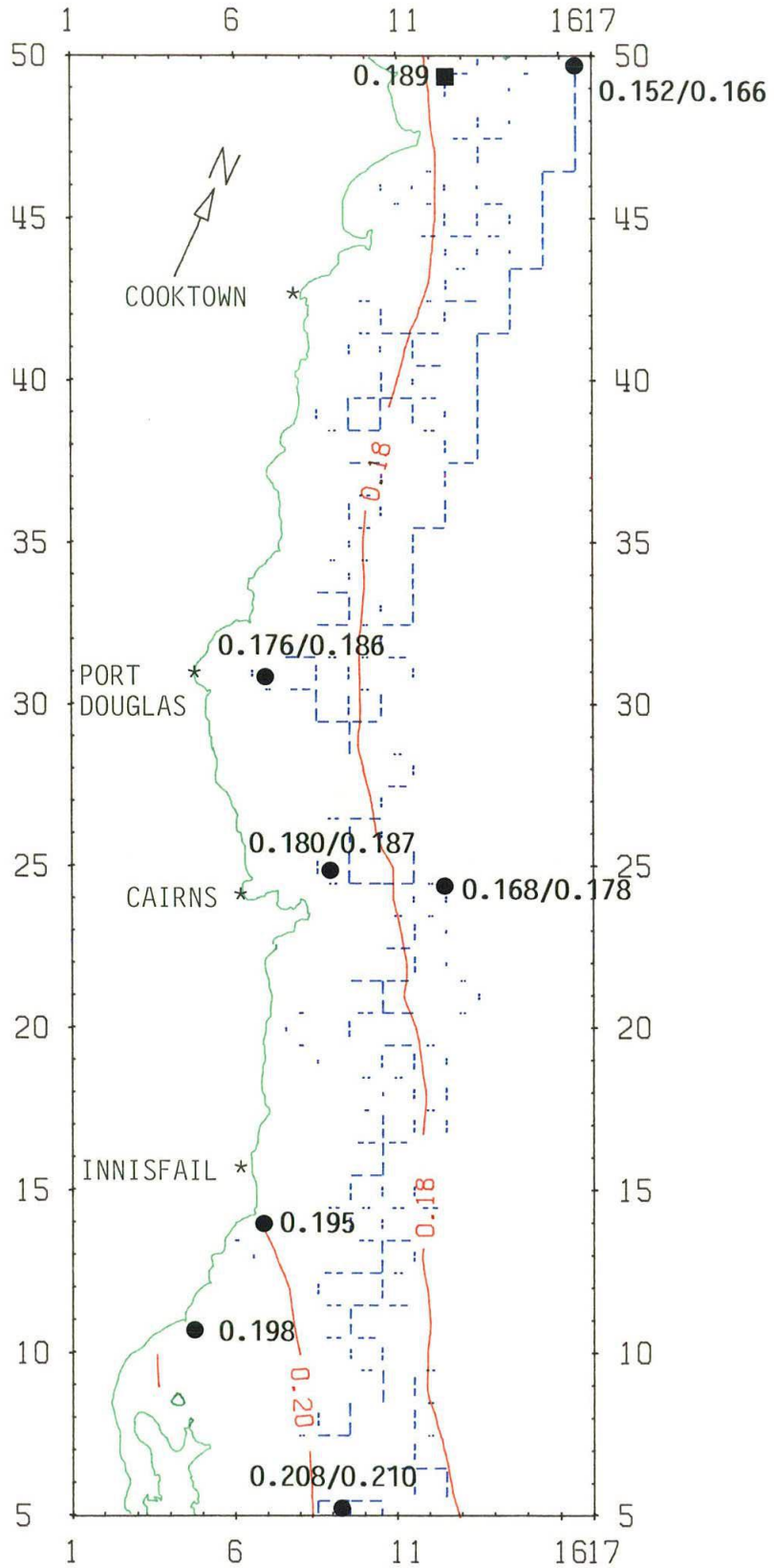


Figure A2a Comparison of observed and predicted values of tidal elevation amplitude for the N2 semi-diurnal constituent within the Cairns Section of the GBR Marine Park. See caption, Figure A1a, for further details.

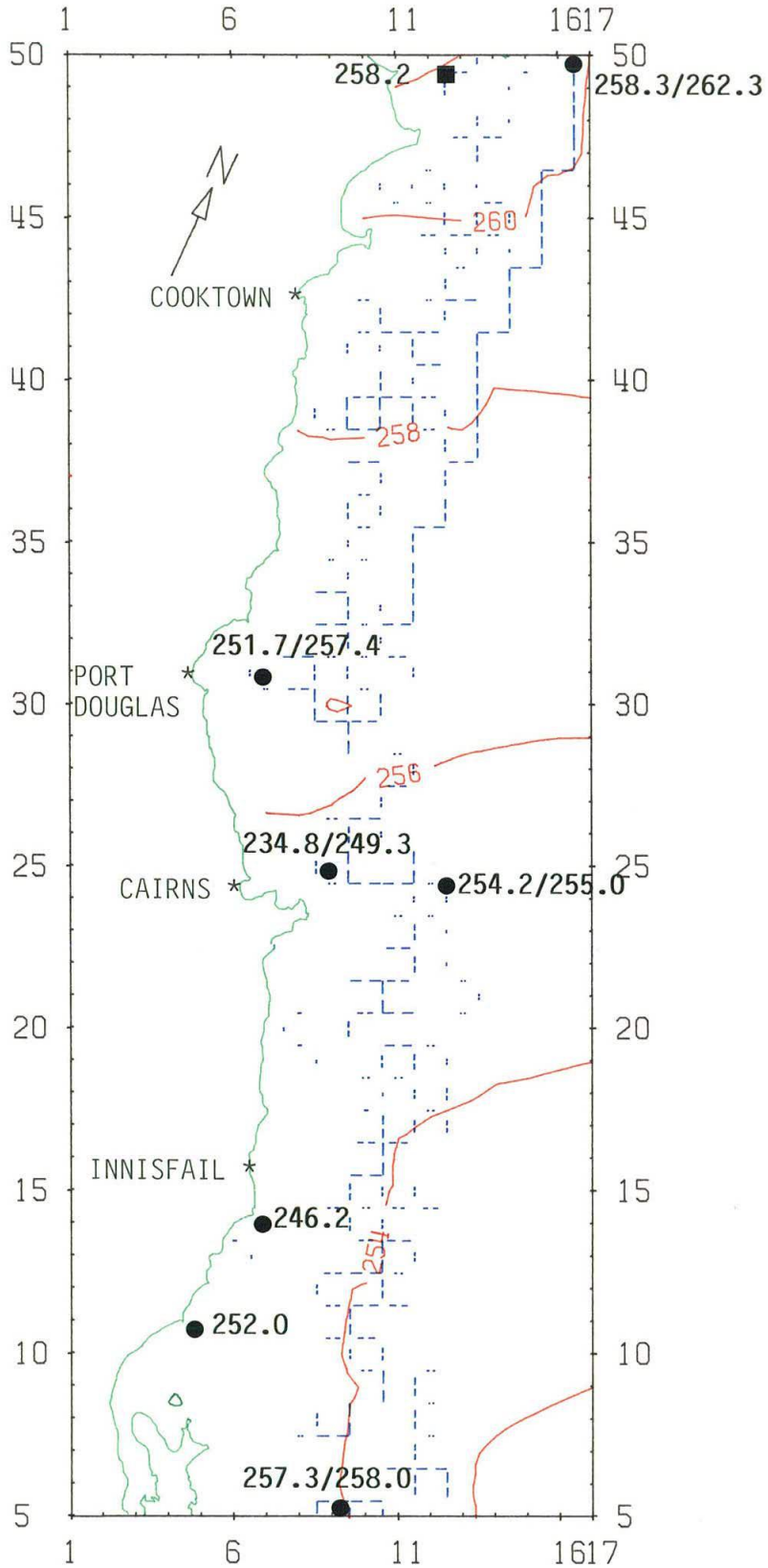


Figure A2b Comparison of observed and predicted values of tidal elevation phase for the N2 semi-diurnal constituent within the Cairns Section of the GBR Marine Park. See caption, Figure A1b, for further details.

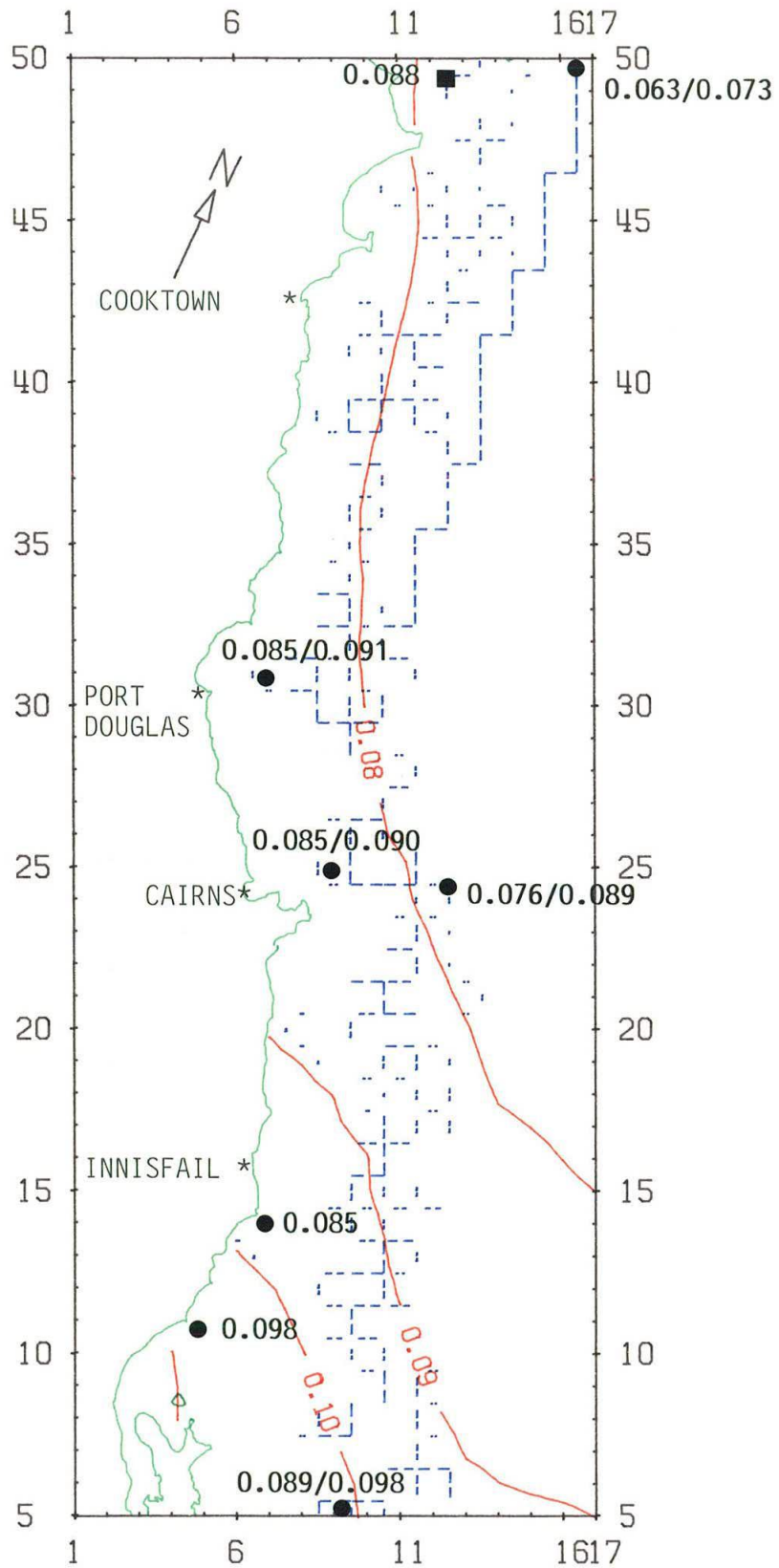


Figure A3a Comparison of observed and predicted values of tidal elevation amplitude for the K2 semi-diurnal constituent within the Cairns Section of the GBR Marine Park. See caption, Figure A1a, for further details.

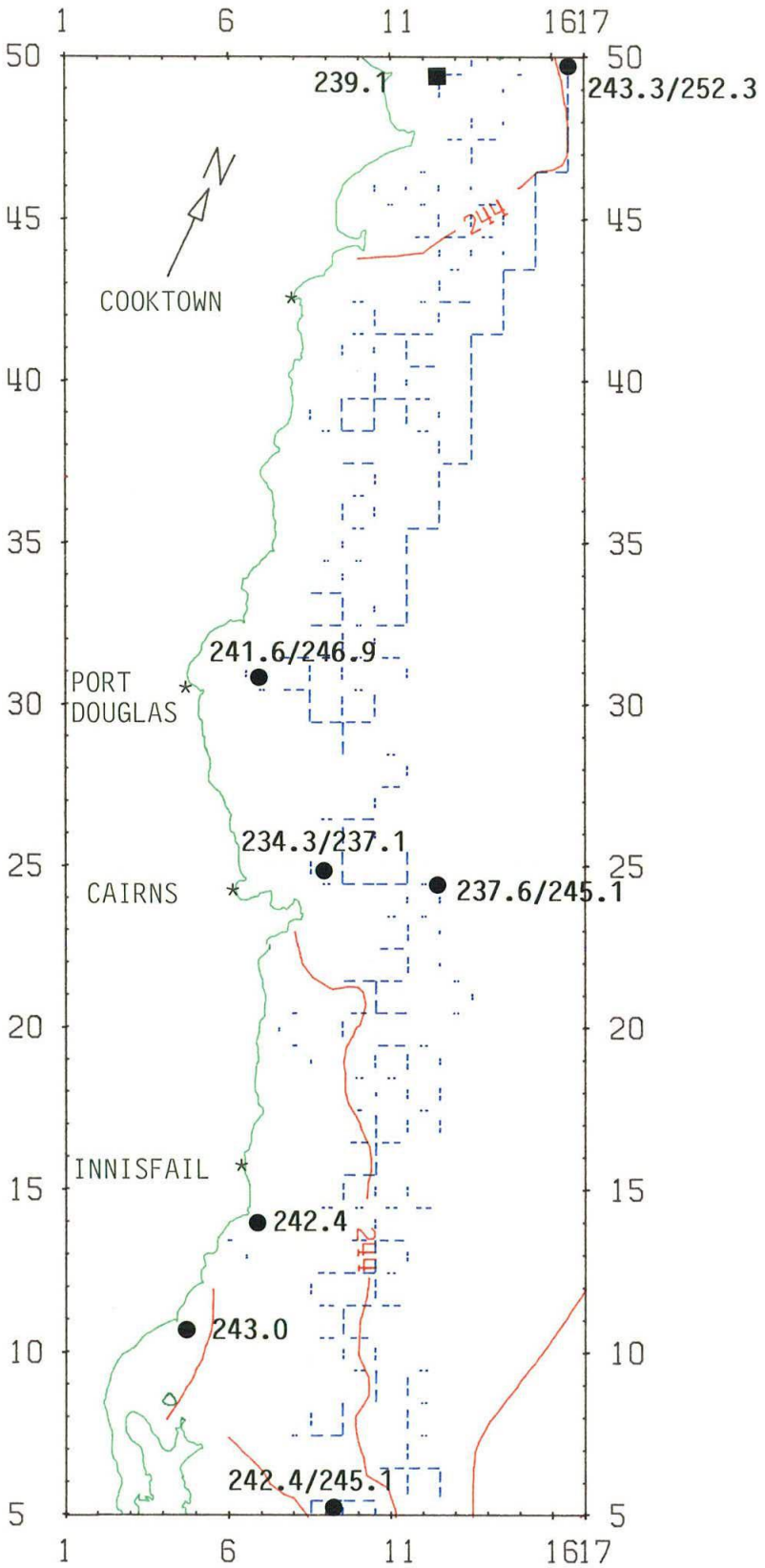


Figure A3b Comparison of observed and predicted values of tidal elevation phase for the K2 semi-diurnal constituent within the Cairns Section of the GBR Marine Park. See caption, Figure A1b, for further details.

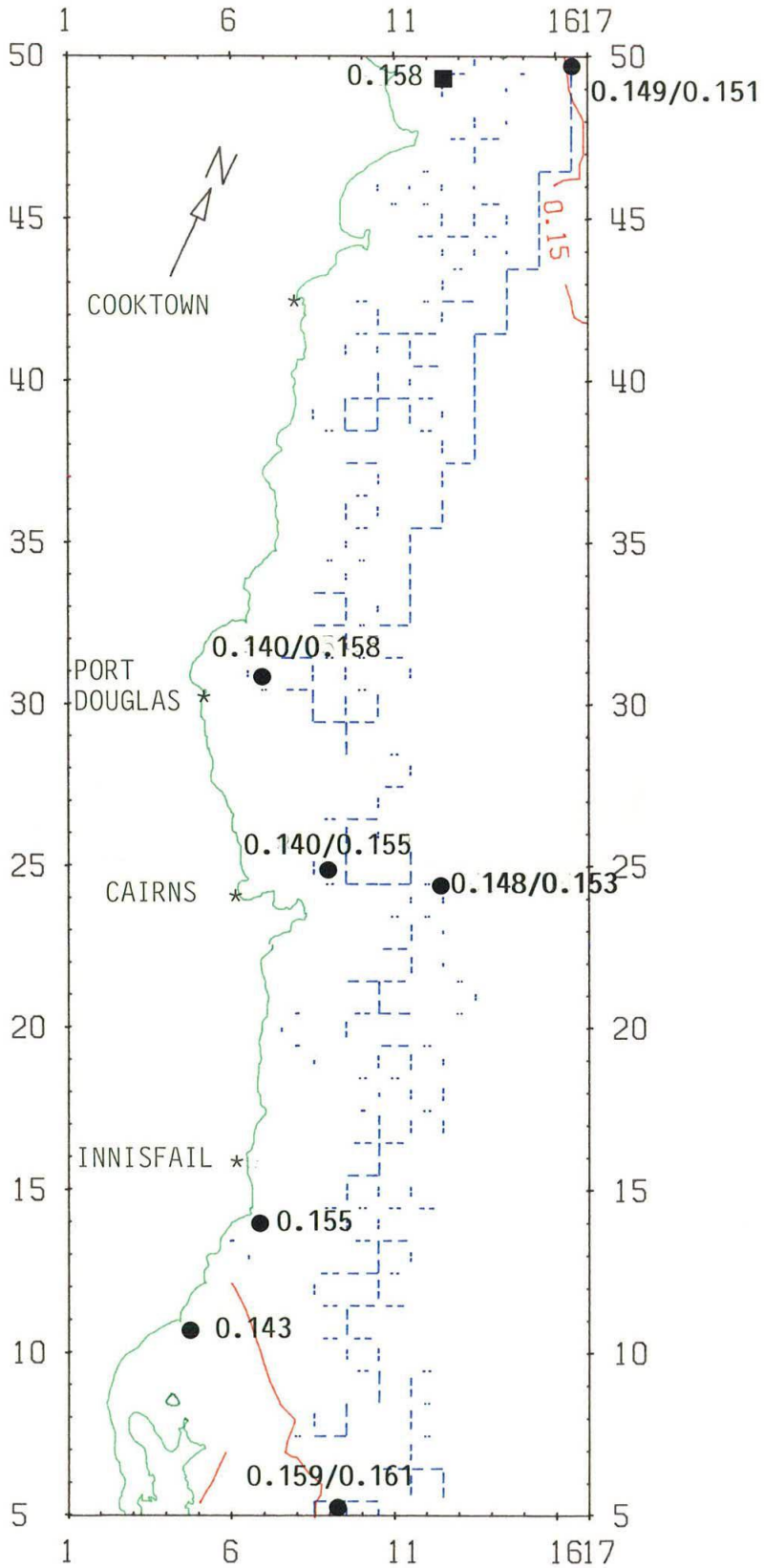


Figure A4a Comparison of observed and predicted values of tidal elevation amplitude for the O1 diurnal constituent within the Cairns Section of the GBR Marine Park. See caption, Figure A1a, for further details.

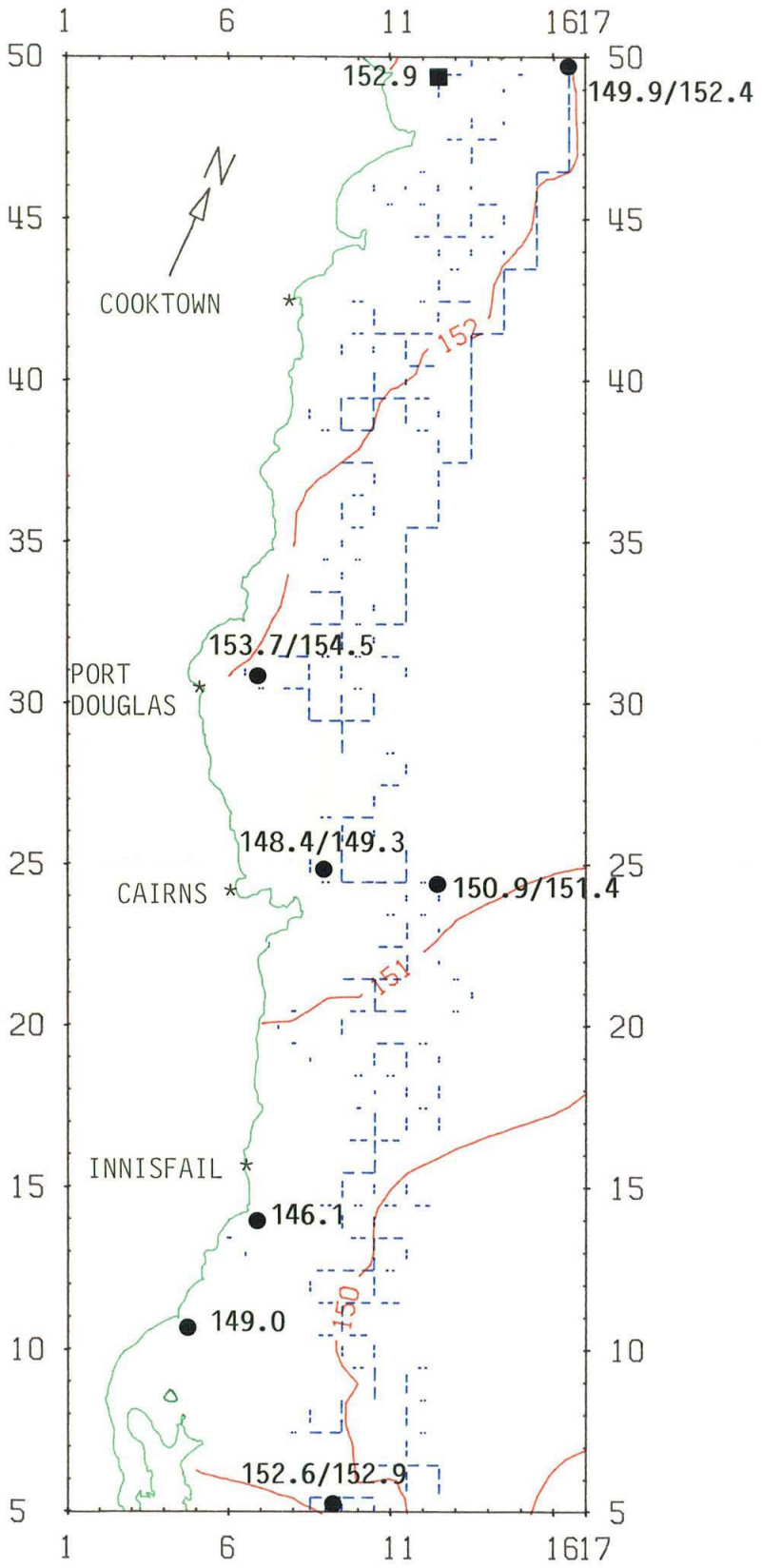


Figure A4b Comparison of observed and predicted values of tidal elevation phase for the O1 diurnal constituent within the Cairns Section of the GBR Marine Park. See caption, Figure A1b, for further details.

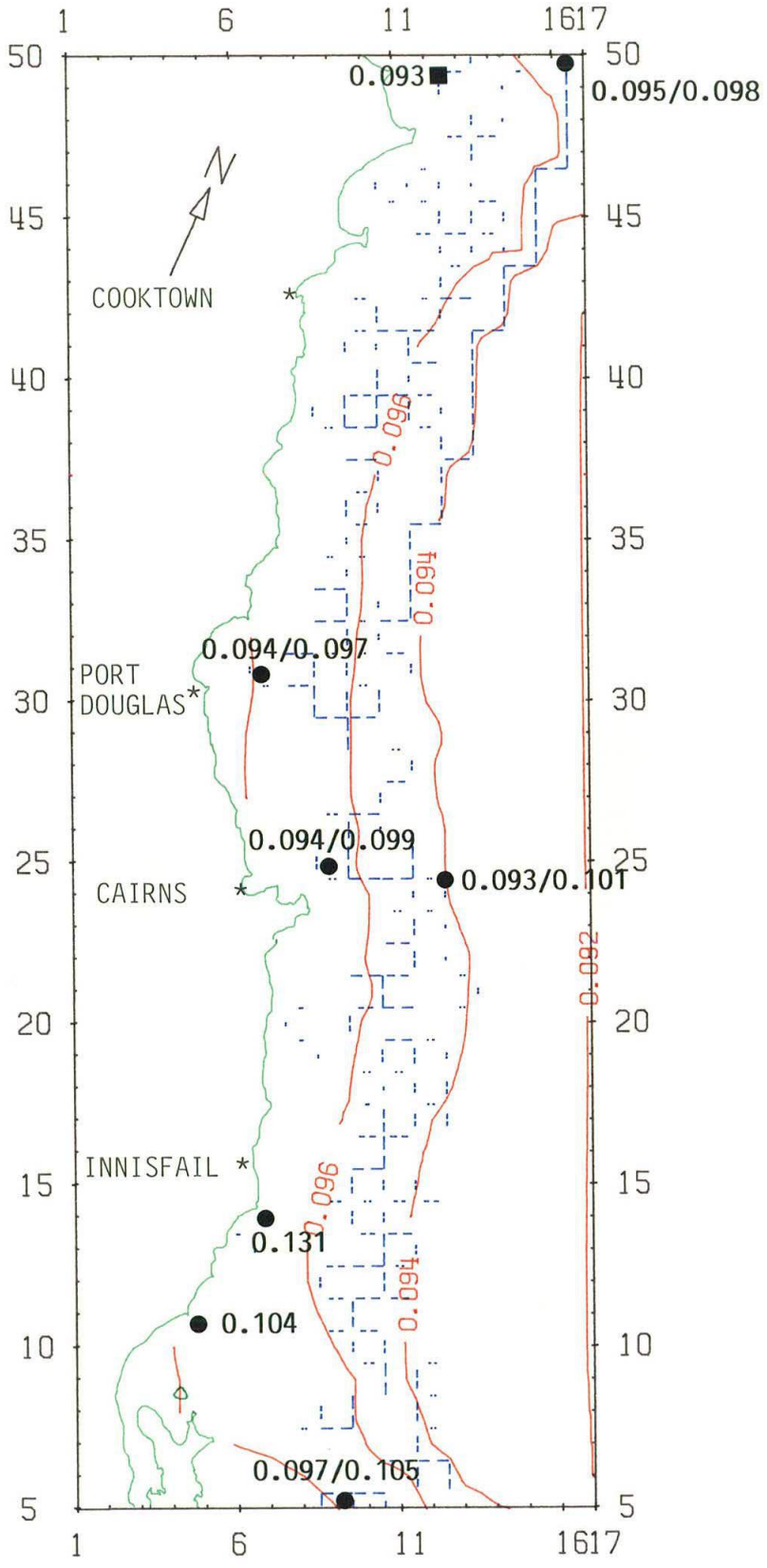


Figure A5a Comparison of observed and predicted values of tidal elevation amplitude for the P1 diurnal constituent within the Cairns Section of the GBR Marine Park. See caption, Figure A1a, for further details.

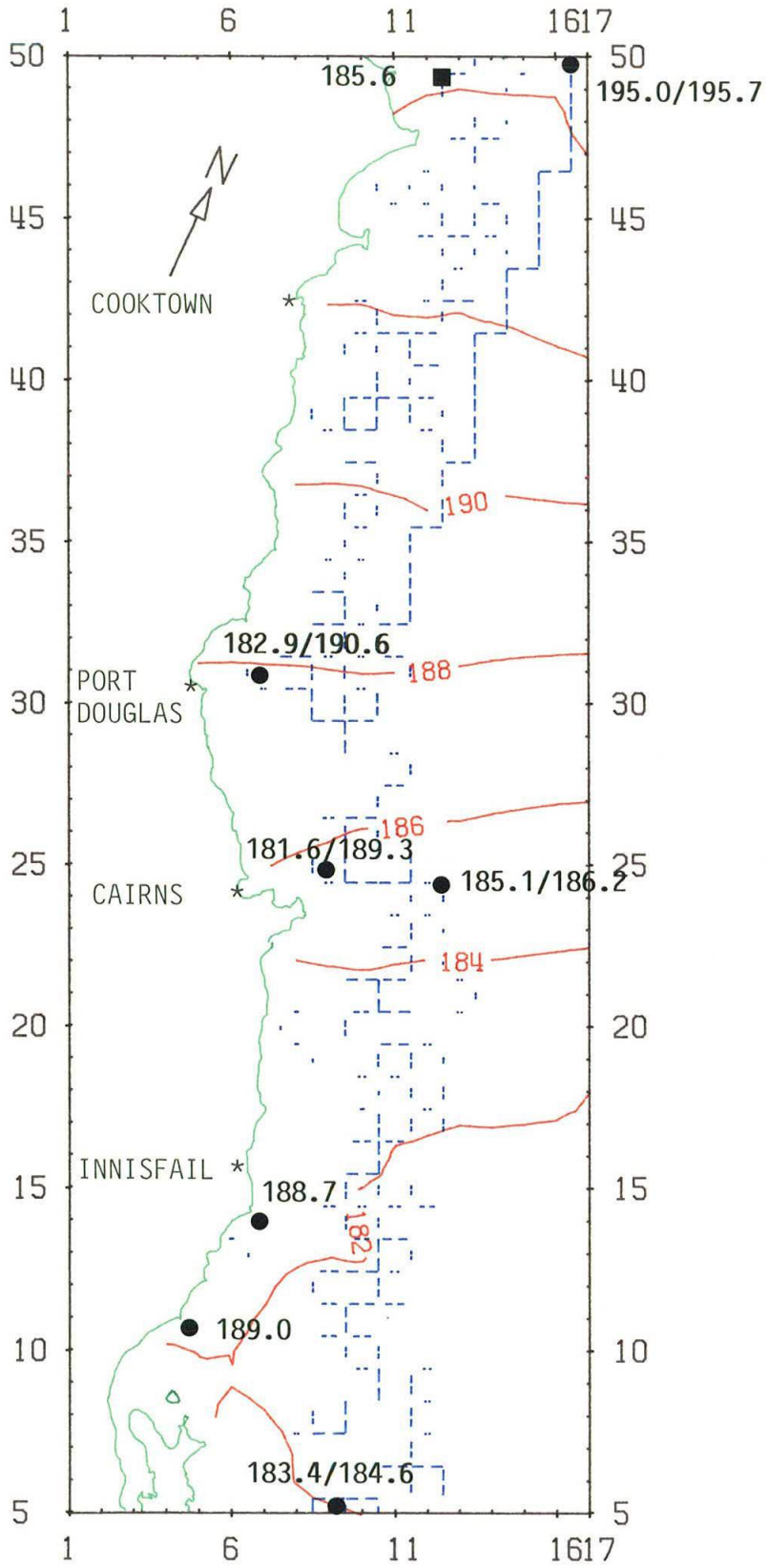


Figure A5b Comparison of observed and predicted values of tidal elevation phase for the P1 diurnal constituent within the Cairns Section of the GBR Marine Park. See caption, Figure A1b, for further details.

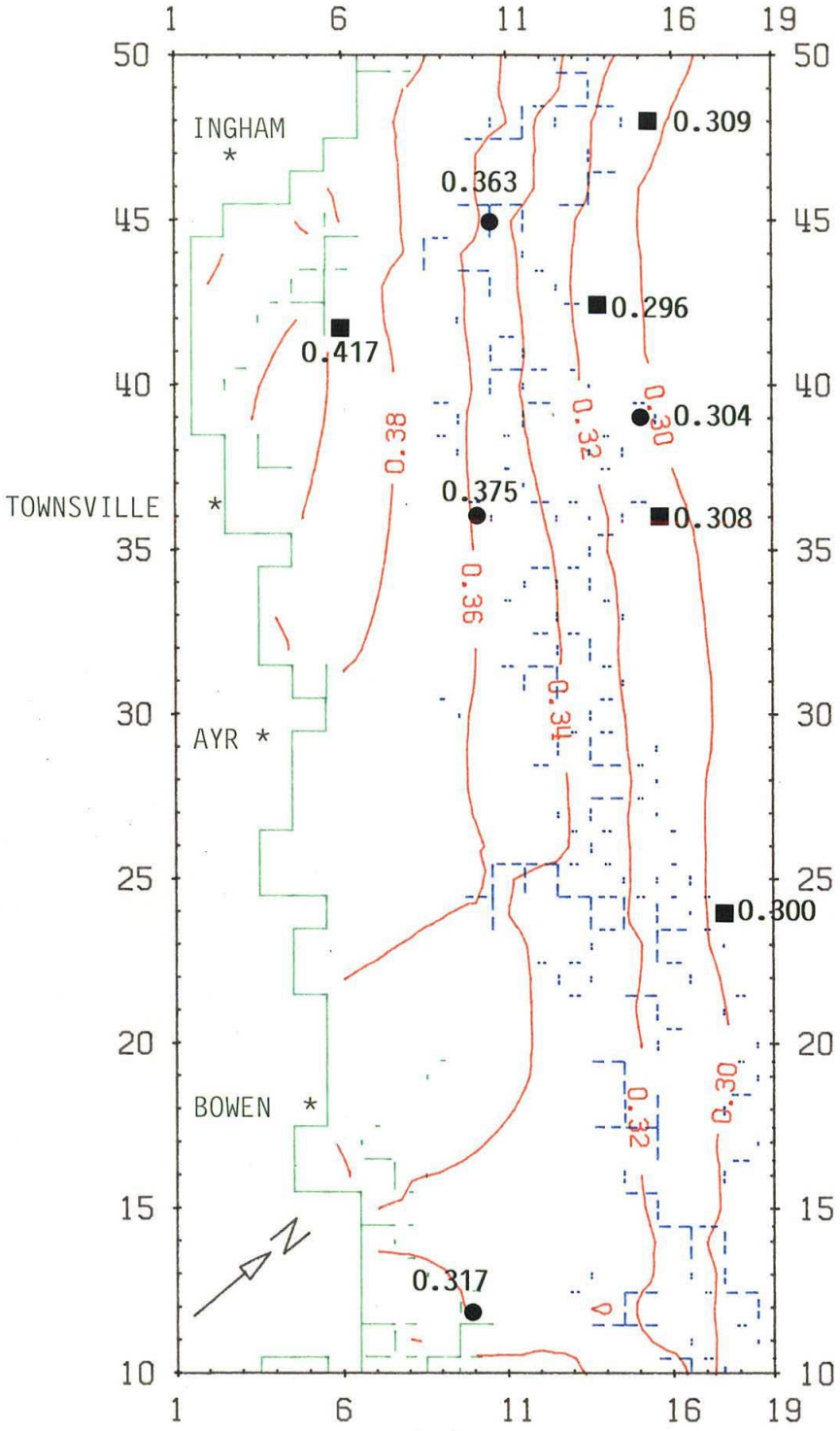


Figure A6a Comparison of observed and predicted values of tidal elevation amplitude for the S2 semi-diurnal constituent within the Central Section of the GBR Marine Park. Published data are from Hamon (1984) (denoted ●) and Andrews and Bode (1988) (denoted ■). Tidal amplitudes are in metres.

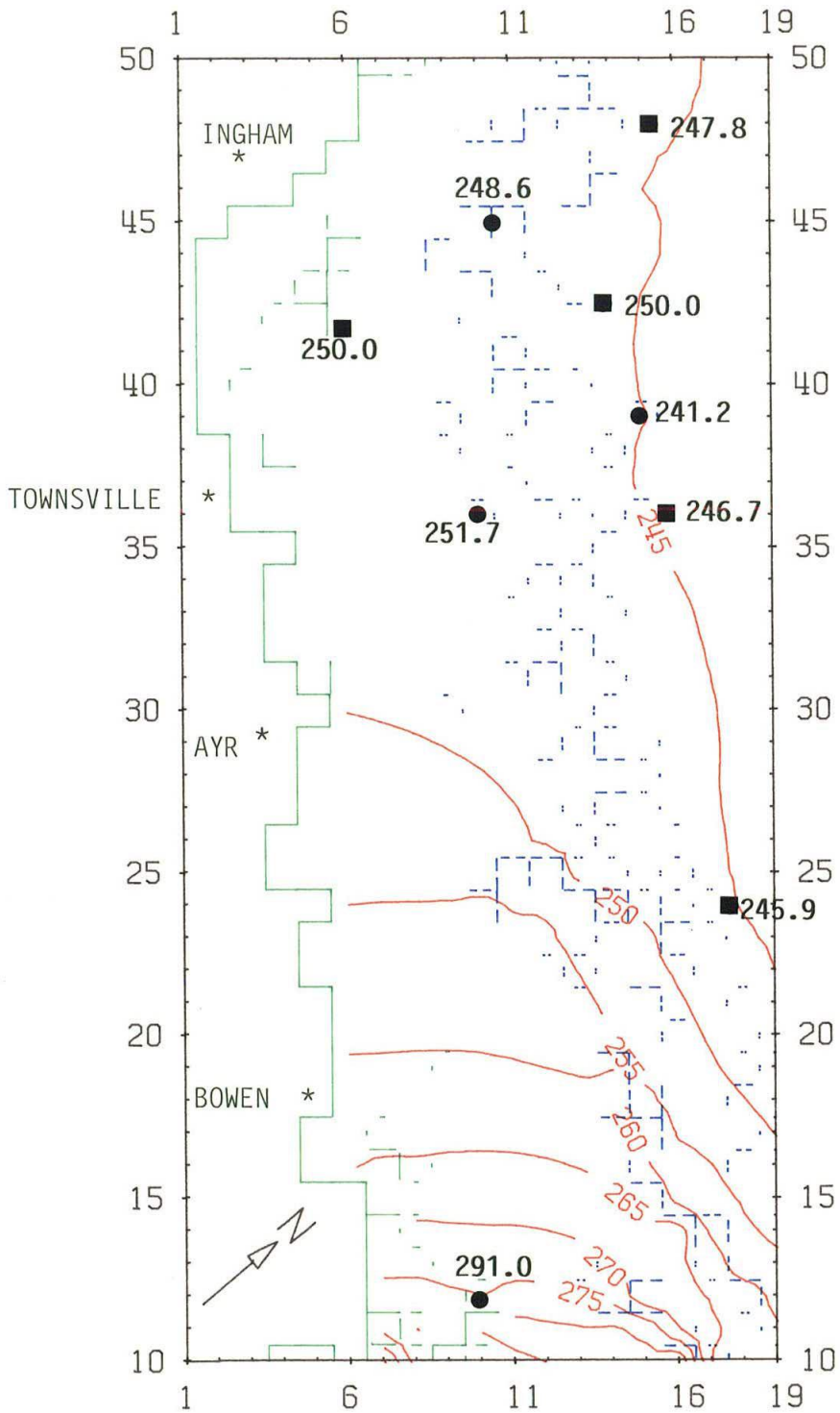


Figure A6b Comparison of observed and predicted values of tidal elevation phase for the M2 semi-diurnal constituent within the Central Section of the GBR Marine Park. Published data are from Hamon (1984) (denoted ●) and Andrews and Bode (1988) (denoted ■). Greenwich phase lags are for GMT-10.

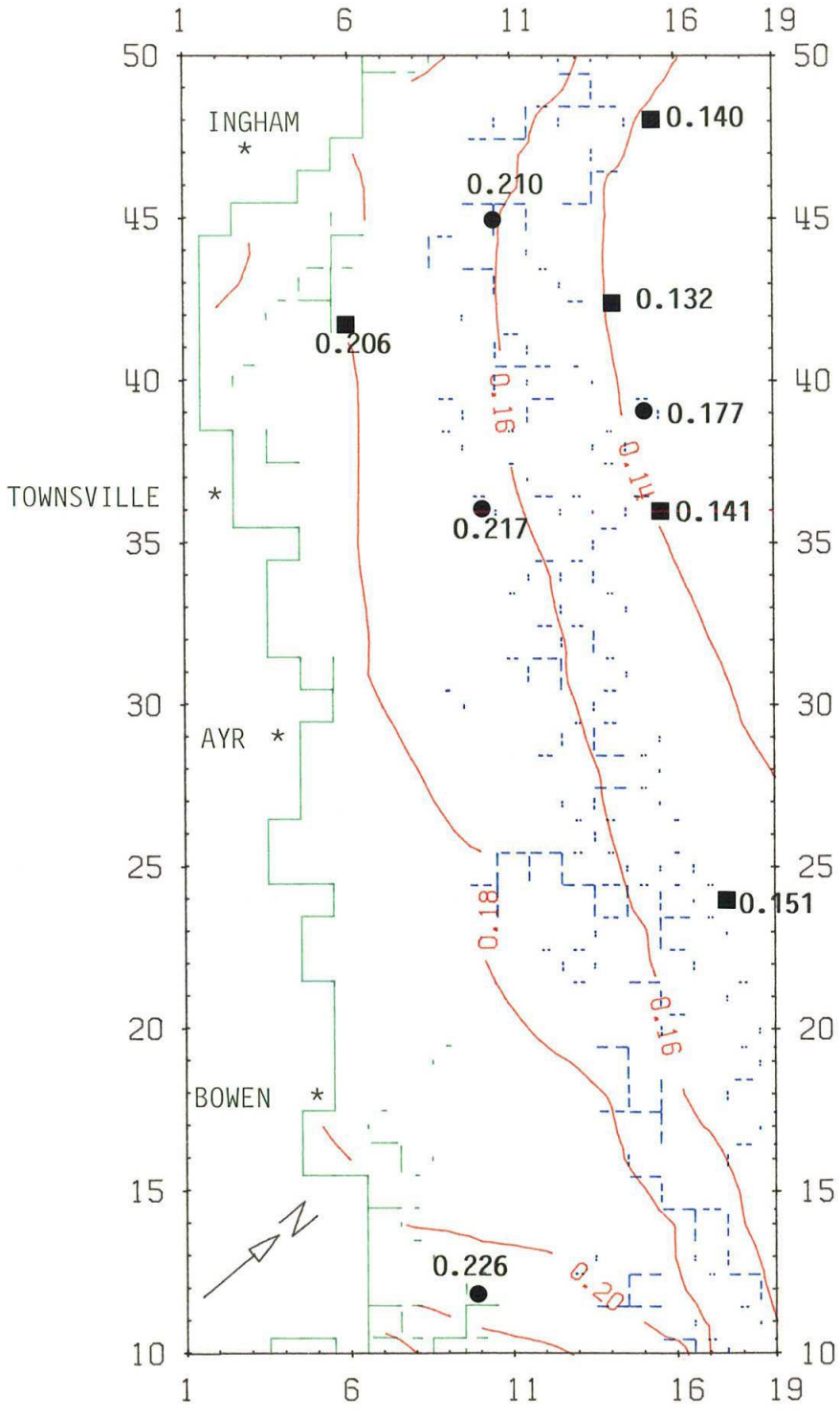


Figure A7a Comparison of observed and predicted values of tidal elevation amplitude for the N2 semi-diurnal constituent within the Central Section of the GBR Marine Park. See caption, Figure A6a, for further details.

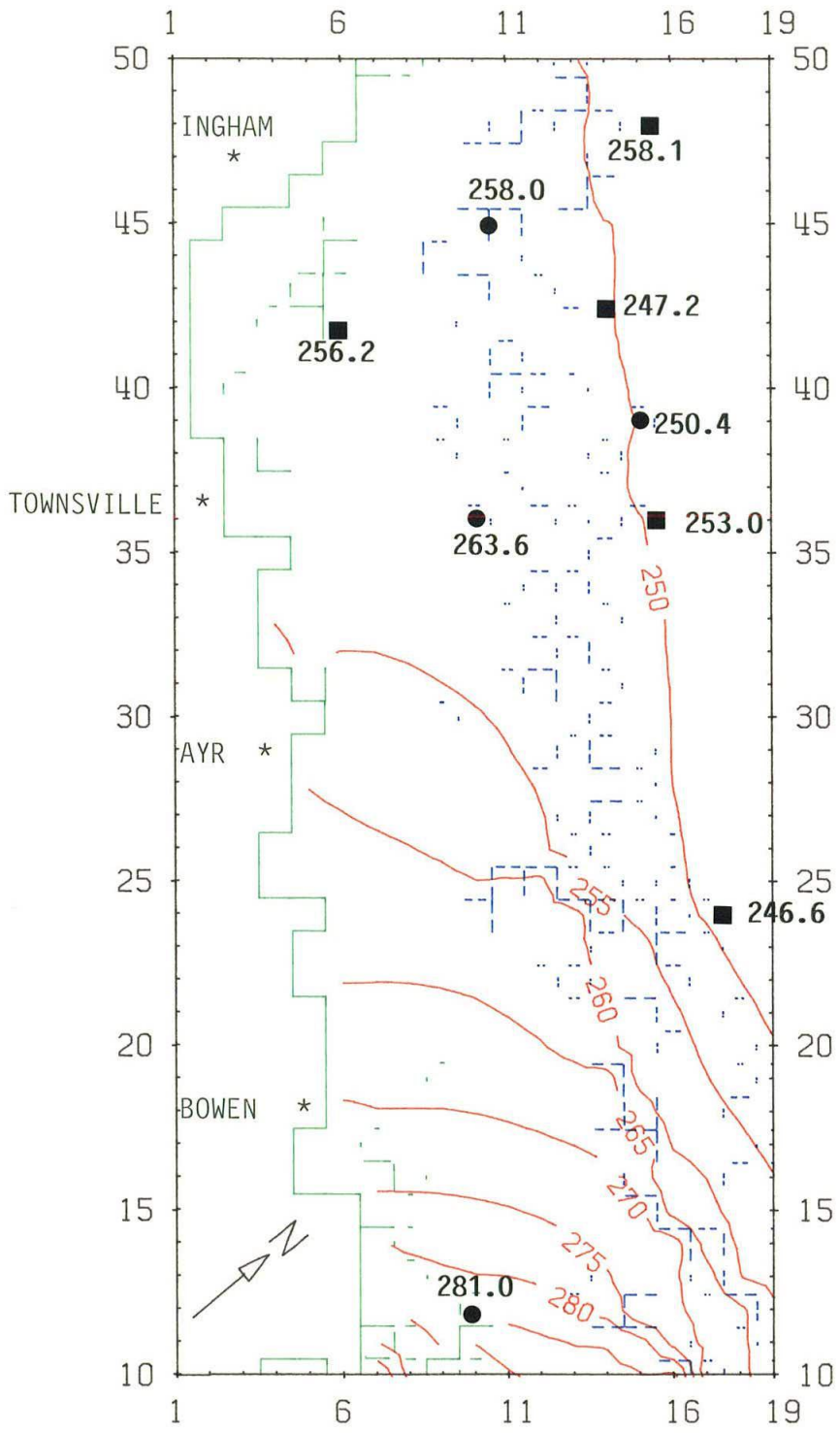


Figure A7b Comparison of observed and predicted values of tidal elevation phase for the N2 semi-diurnal constituent within the Central Section of the GBR Marine Park. See caption, Figure A6b, for further details.

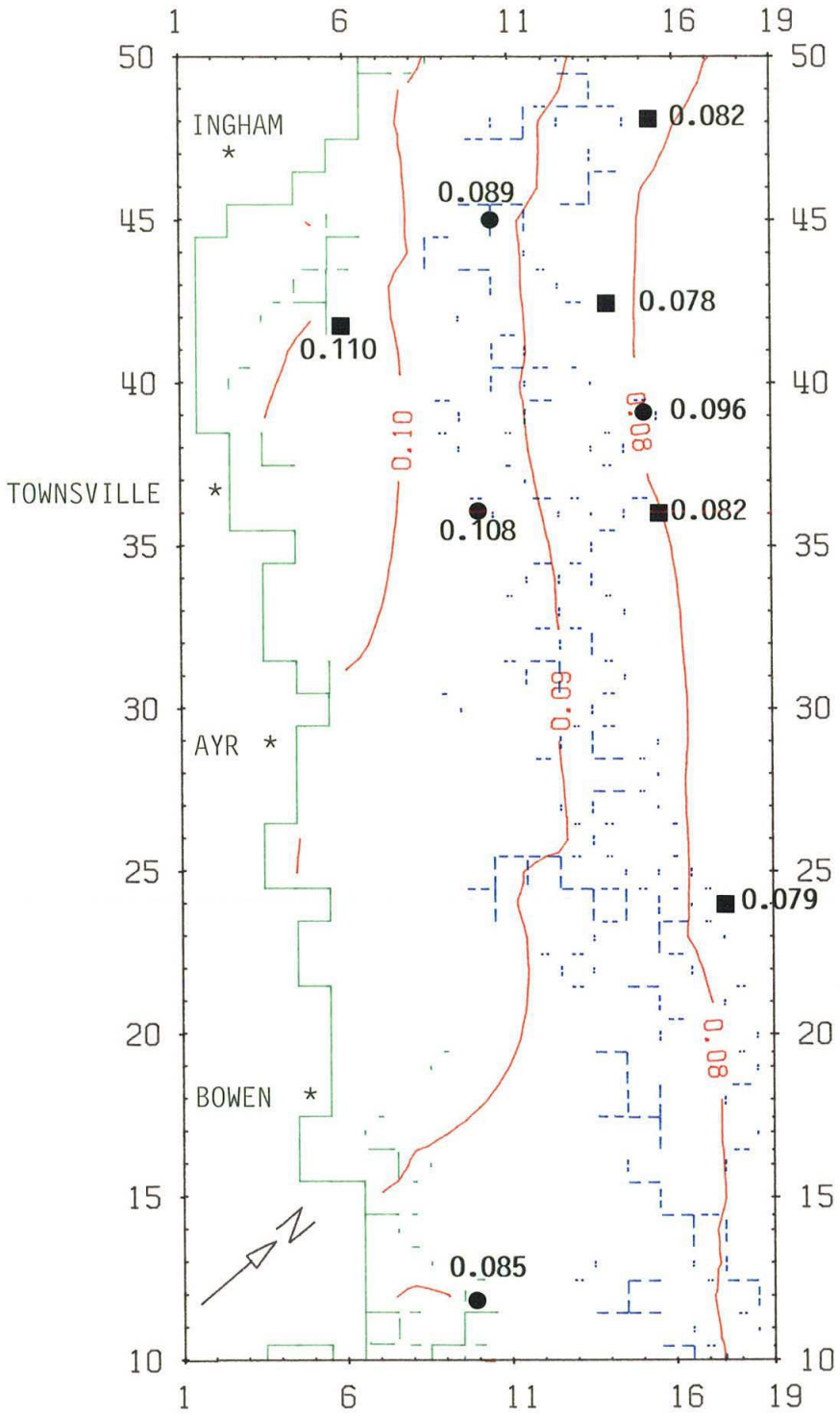


Figure A8a Comparison of observed and predicted values of tidal elevation amplitude for the K2 semi-diurnal constituent within the Central Section of the GBR Marine Park. See caption, Figure A6a, for further details.

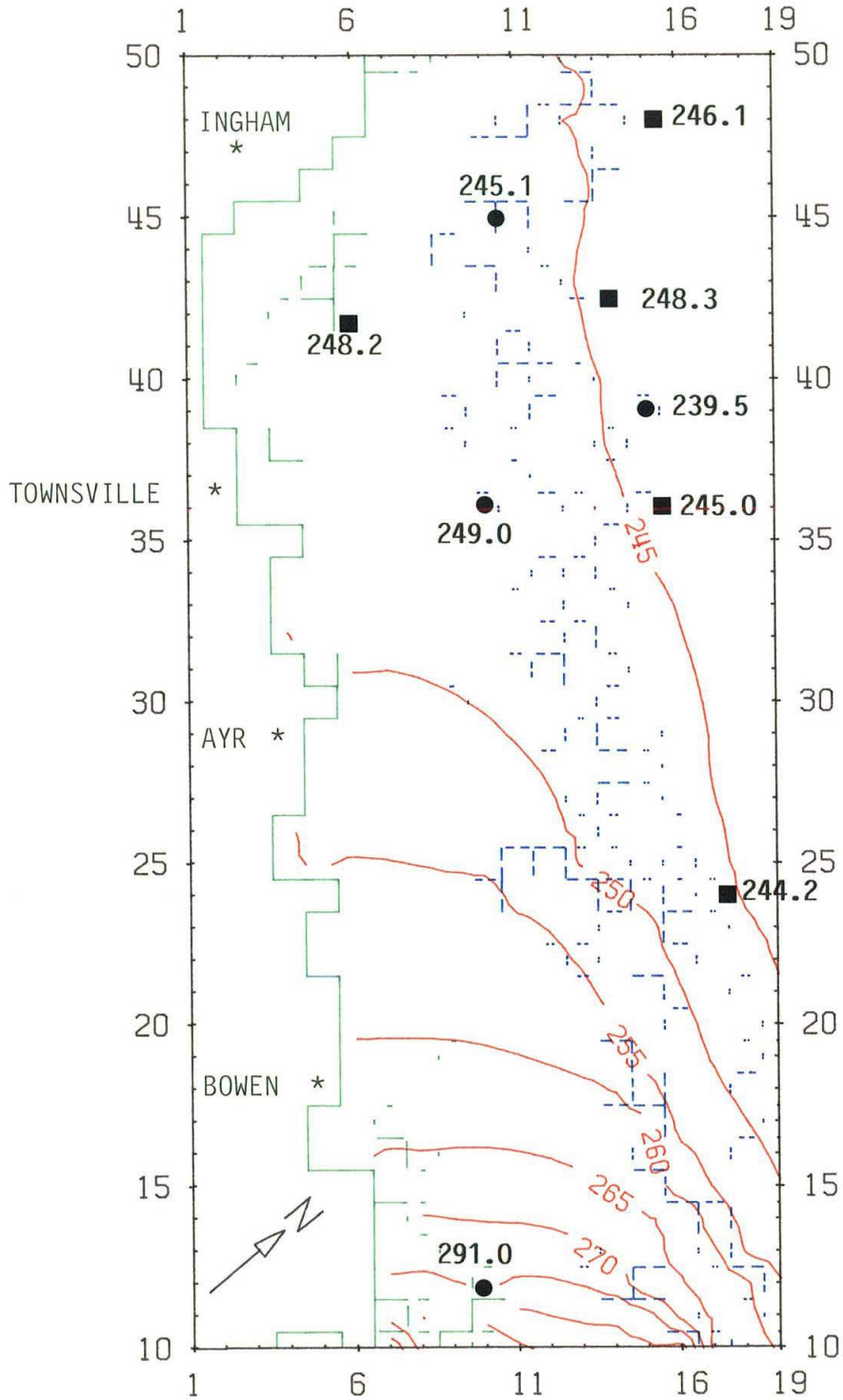


Figure A8b Comparison of observed and predicted values of tidal elevation phase for the K2 semi-diurnal constituent within the Central Section of the GBR Marine Park. See caption, Figure A6b, for further details.

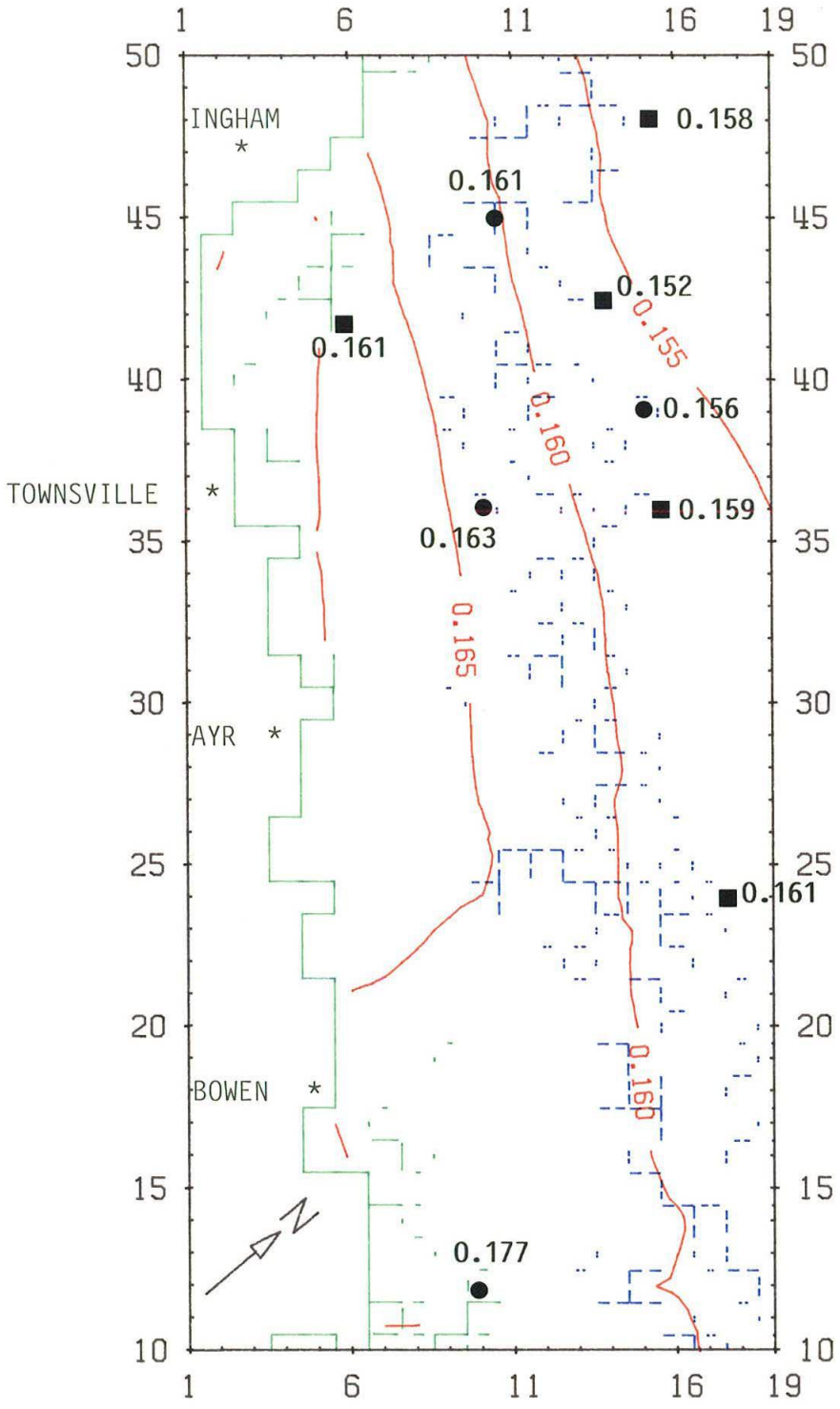


Figure A9a Comparison of observed and predicted values of tidal elevation amplitude for the O1 diurnal constituent within the Central Section of the GBR Marine Park. See caption, Figure A6a, for further details.

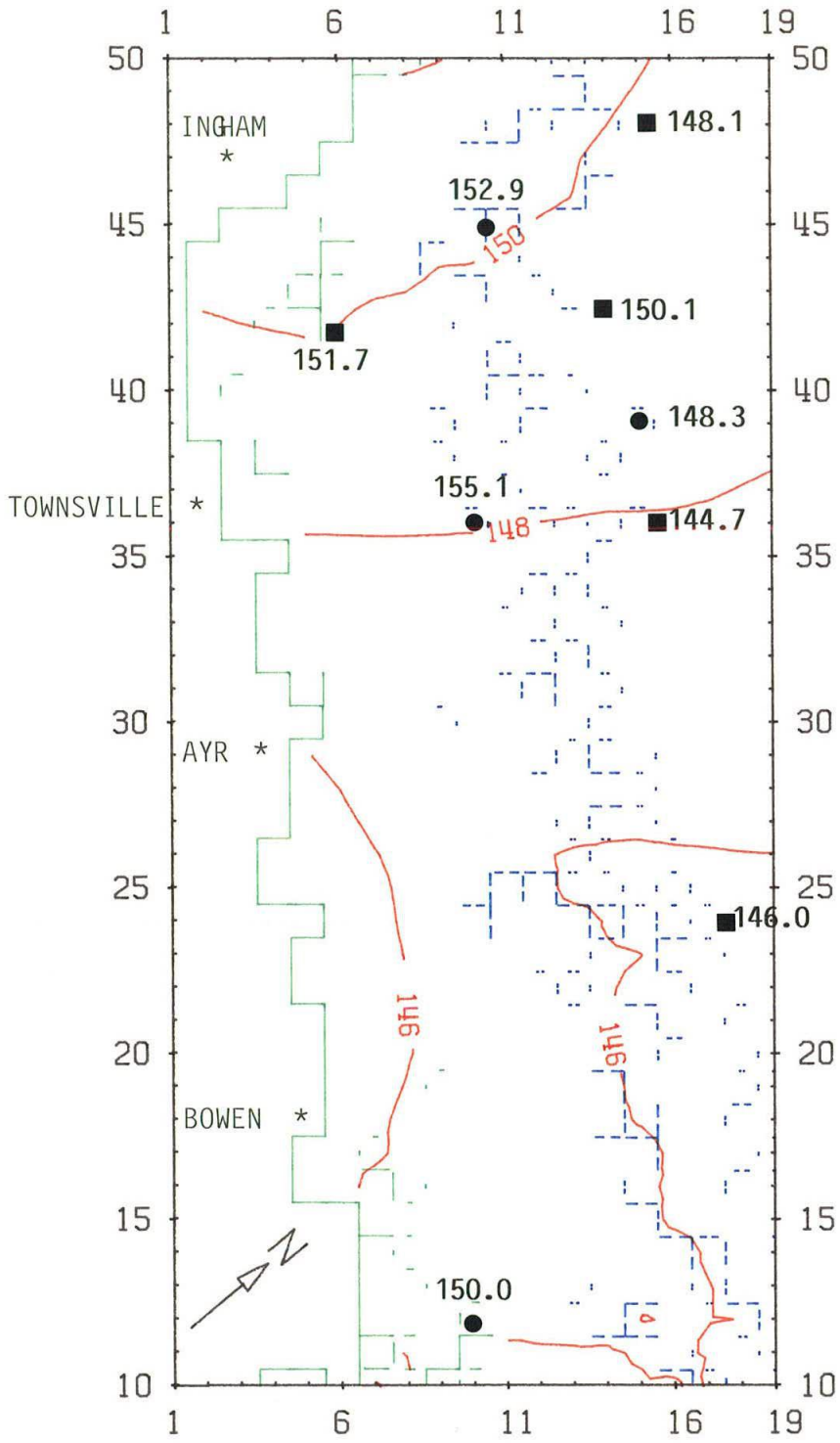


Figure A9b Comparison of observed and predicted values of tidal elevation phase for the O1 diurnal constituent within the Central Section of the GBR Marine Park. See caption, Figure A6b, for further details.

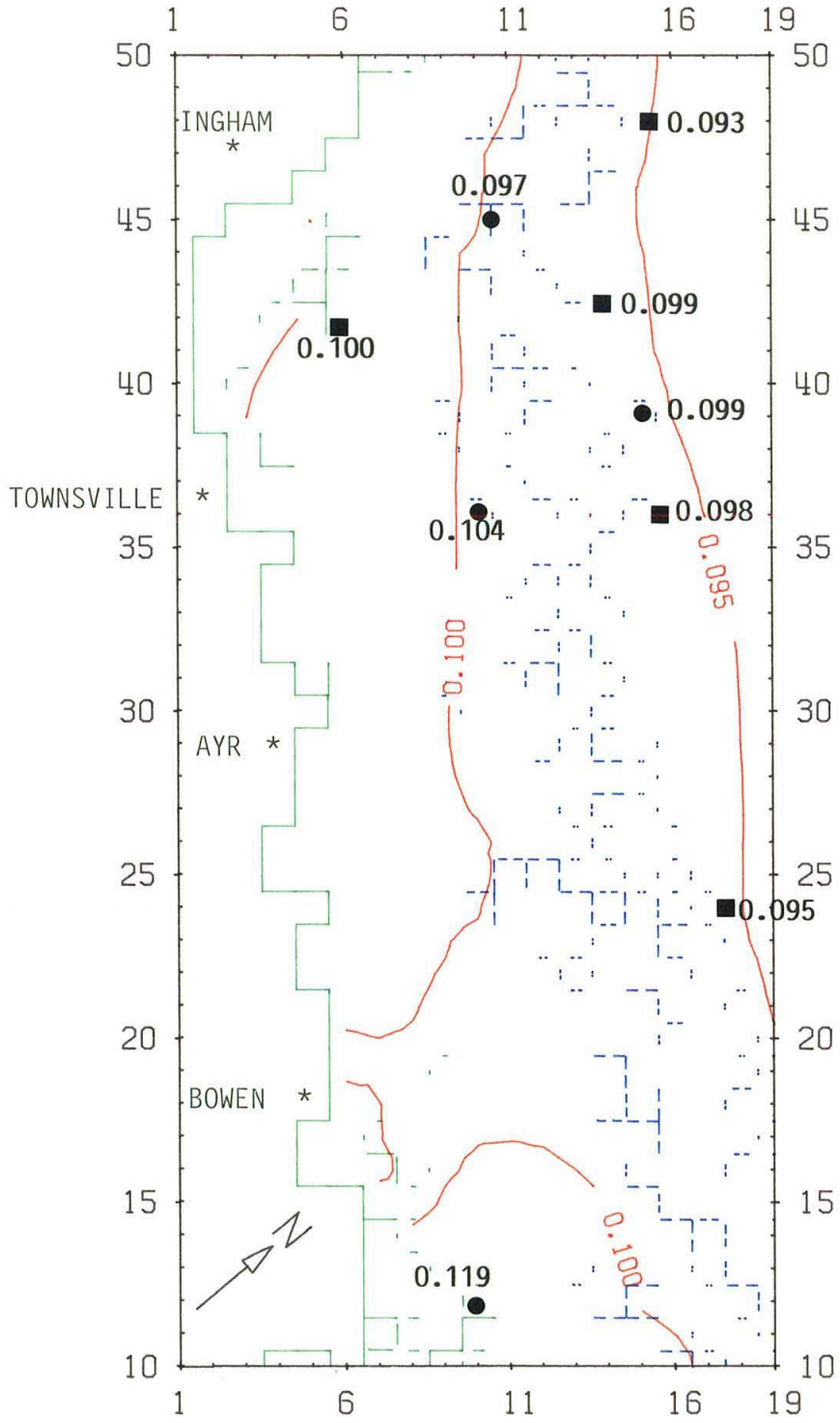


Figure A10a Comparison of observed and predicted values of tidal elevation amplitude for the P1 diurnal constituent within the Central Section of the GBR Marine Park. See caption, Figure A6a, for further details.

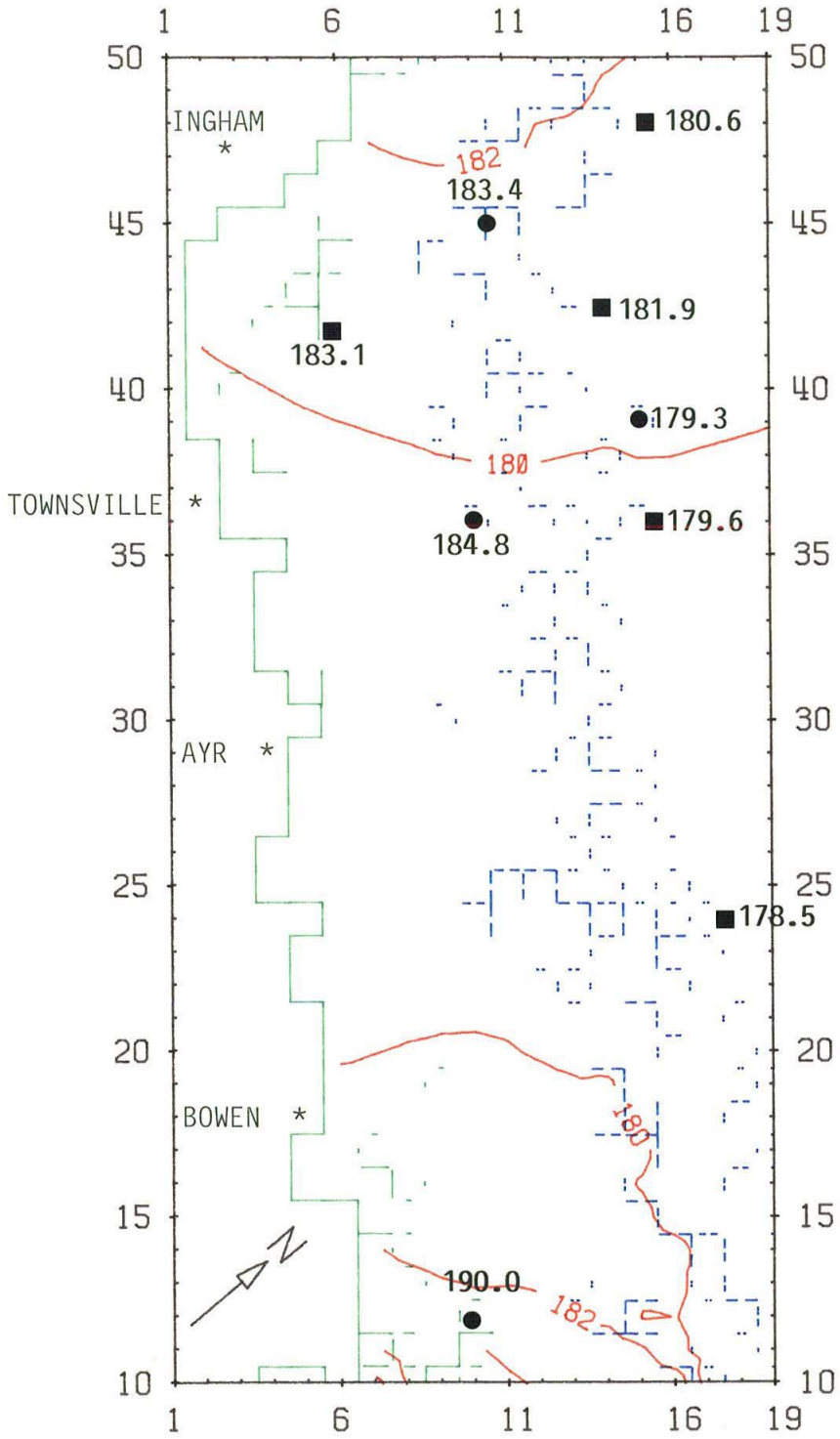


Figure A10b Comparison of observed and predicted values of tidal elevation phase for the P1 diurnal constituent within the Central Section of the GBR Marine Park. See caption, Figure A6b, for further details.

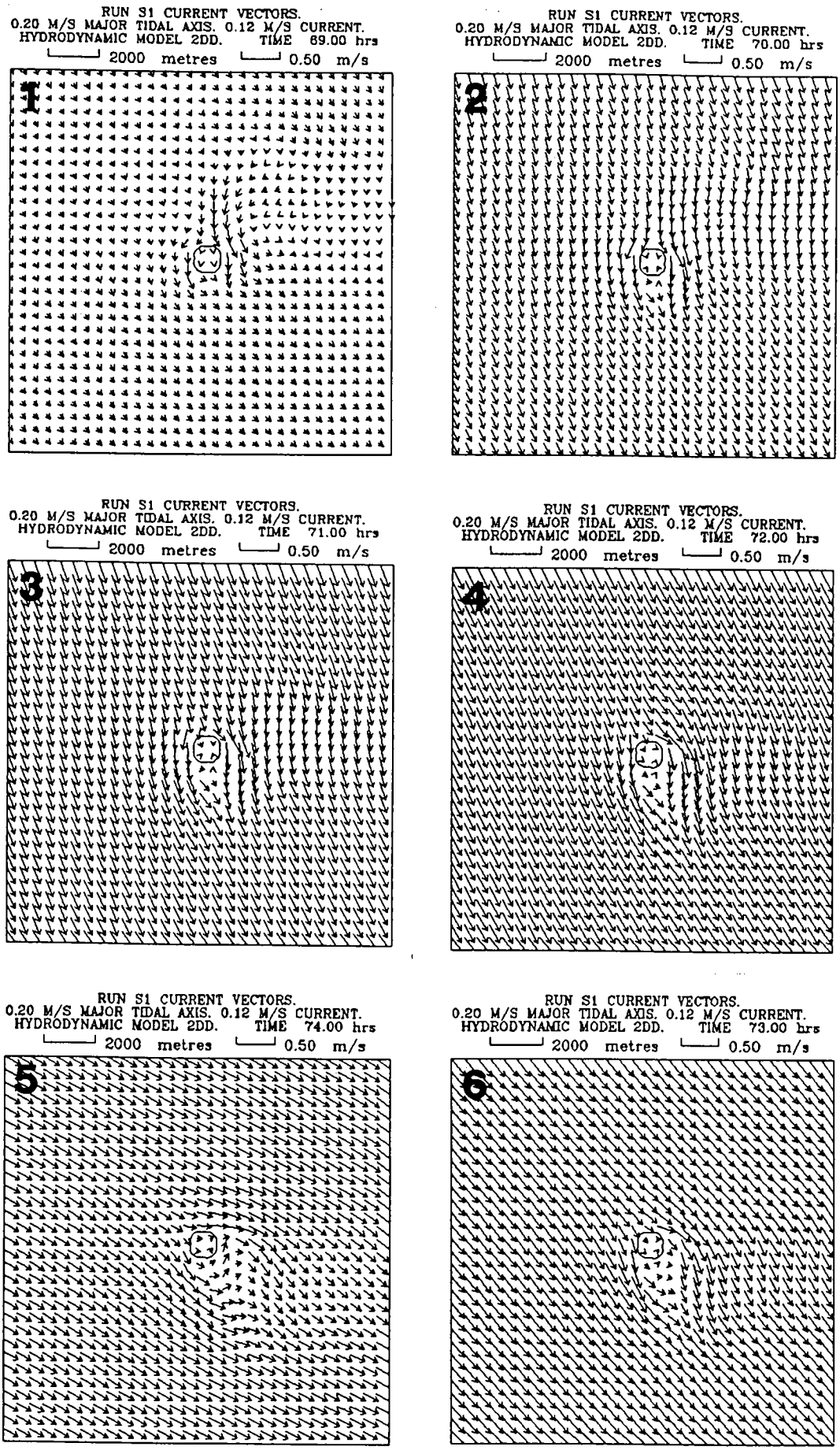


Figure B1a Representative plots of current vectors over a tidal cycle for reef type P1. Plots (labelled 1 to 6) represent currents at one hour intervals from when the tide begins to flood.

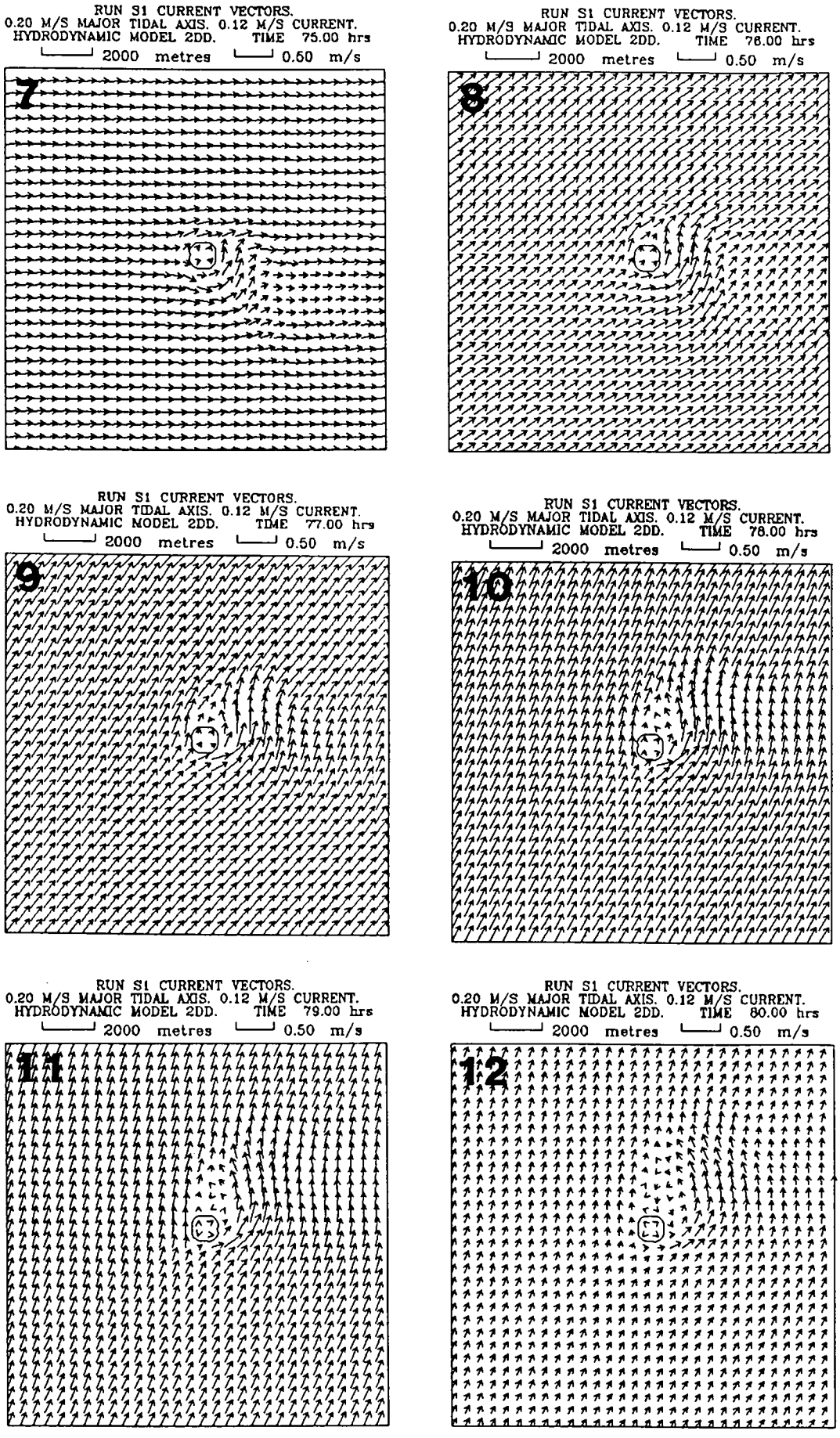


Figure B1b Representative plots of current vectors over a tidal cycle for reef type P1. Plots (labelled 7 to 12) represent currents at one hour intervals from when the tide begins to ebb.

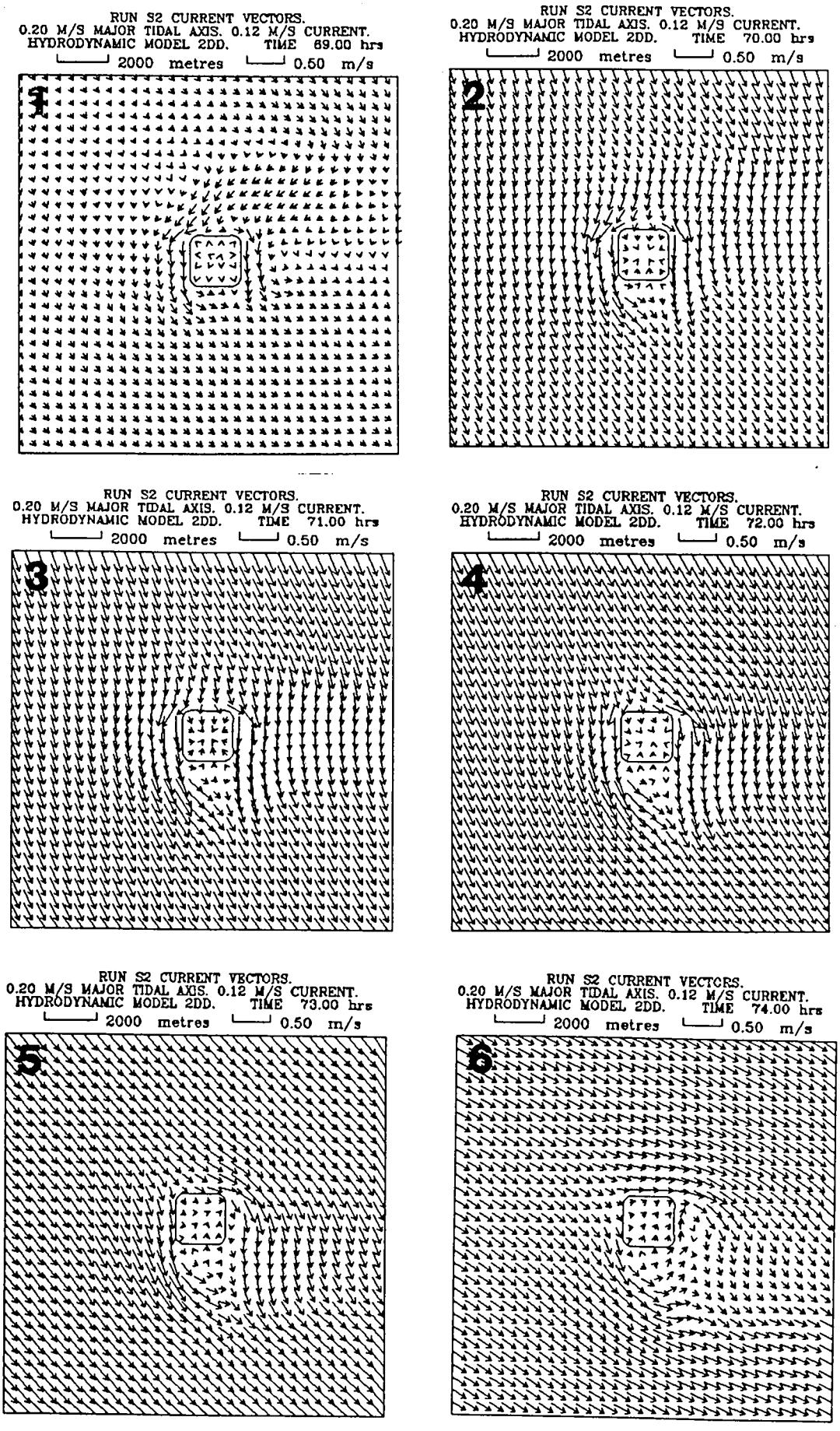


Figure B2a Representative plots of current vectors over a tidal cycle for reef type P2. Plots (labelled 1 to 6) represent currents at one hour intervals from when the tide begins to flood.

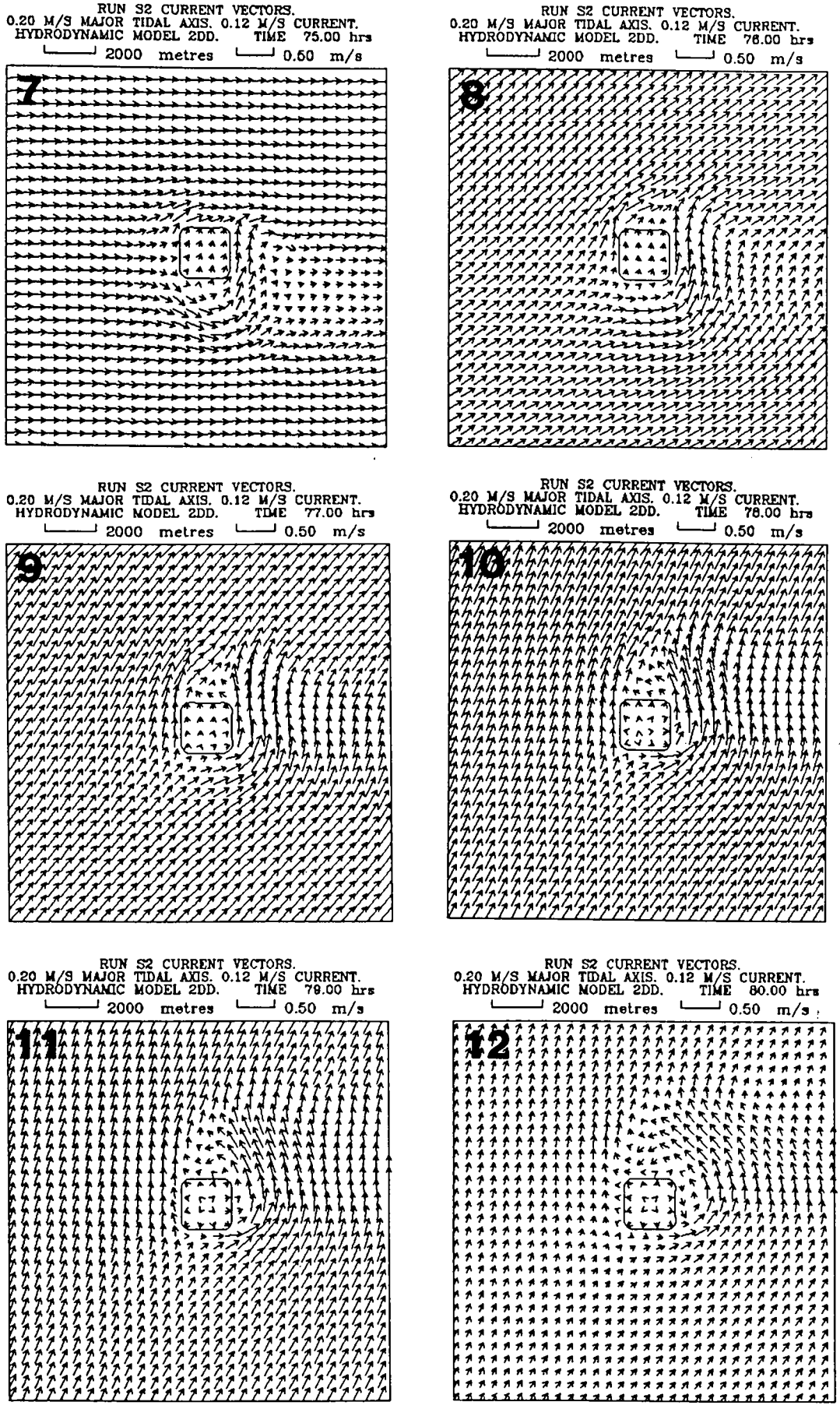


Figure B2b Representative plots of current vectors over a tidal cycle for reef type P2. Plots (labelled 7 to 12) represent currents at one hour intervals from when the tide begins to ebb.

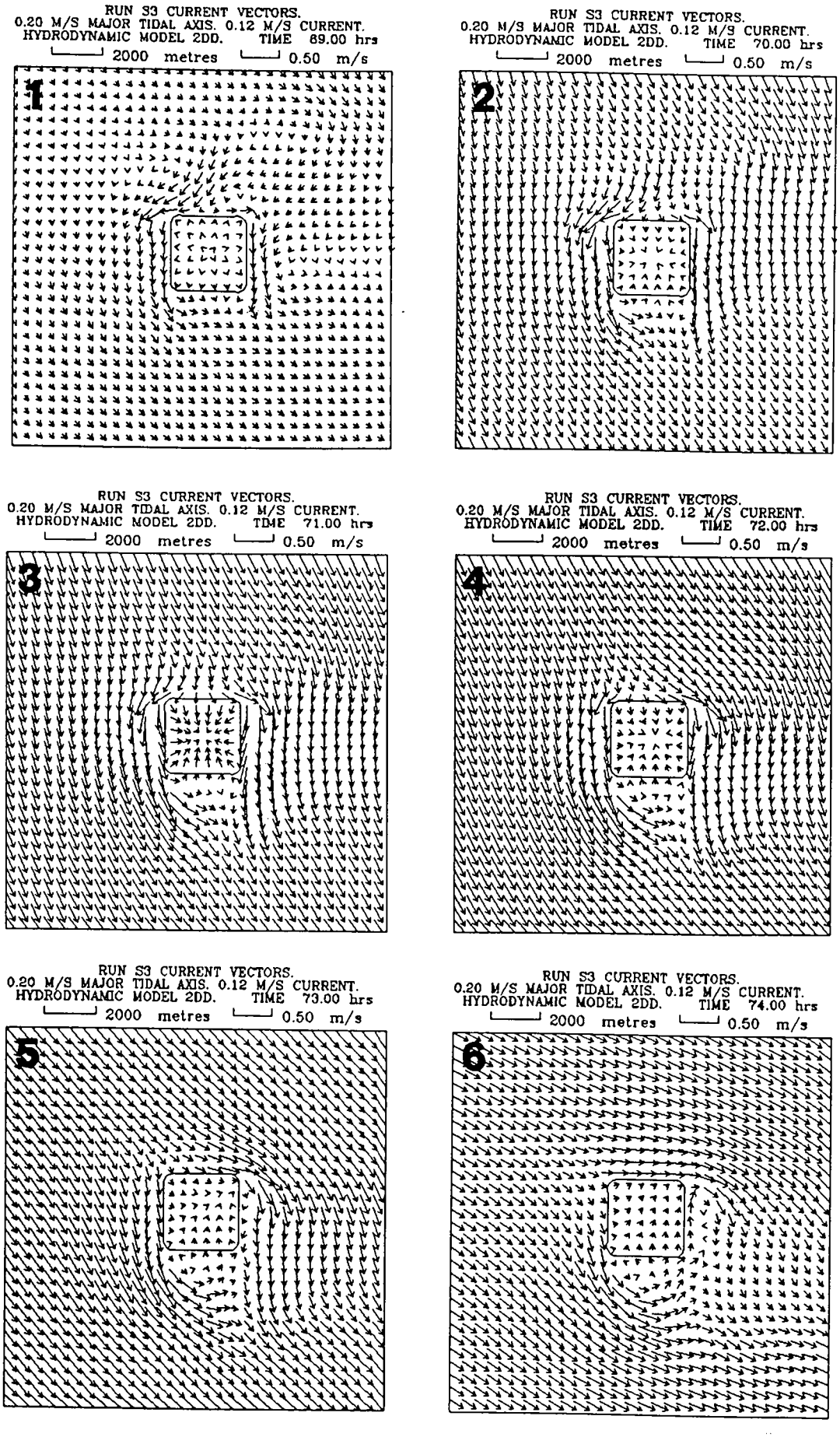


Figure B3a Representative plots of current vectors over a tidal cycle for reef type P3. Plots (labelled 1 to 6) represent currents at one hour intervals from when the tide begins to flood.

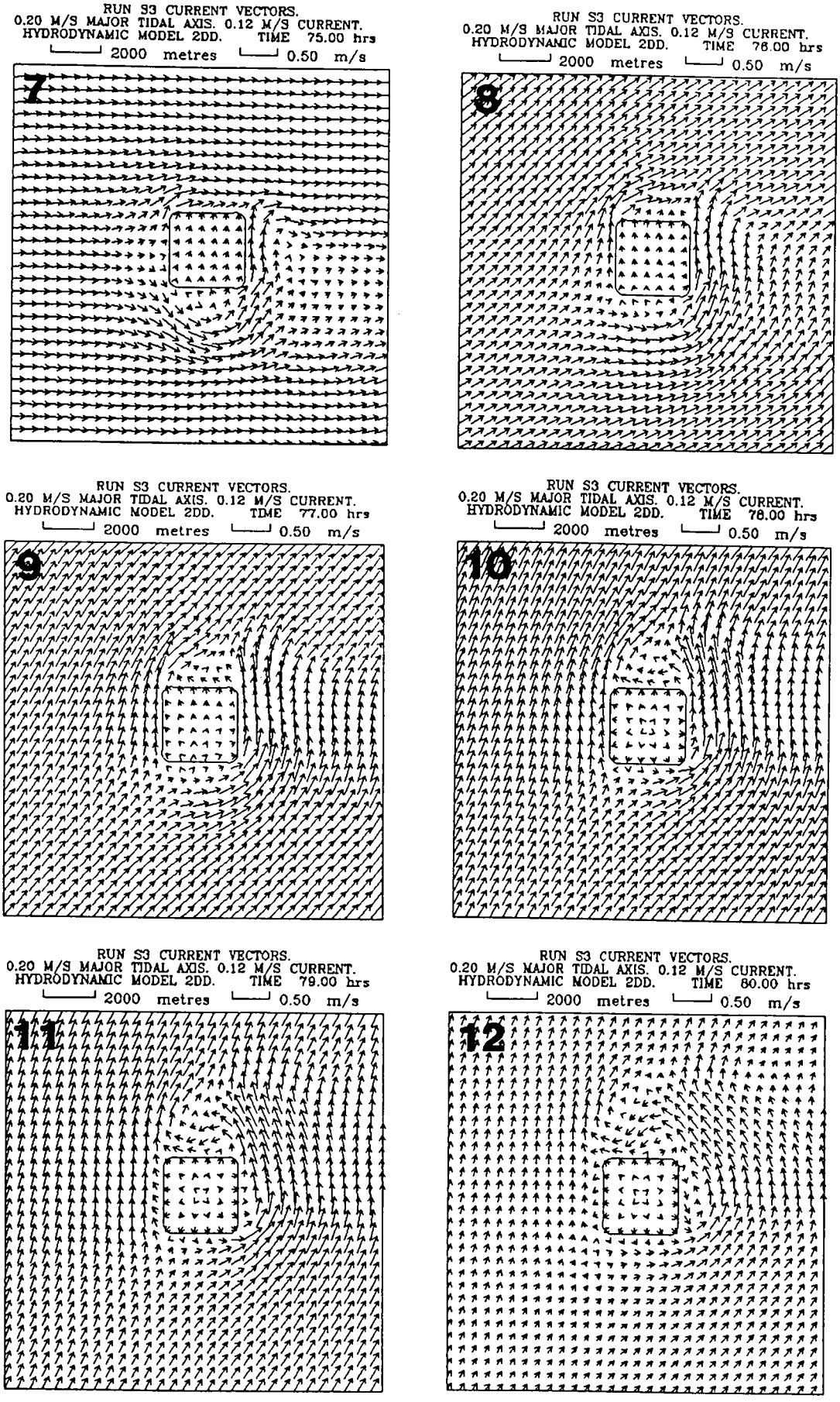


Figure B3b Representative plots of current vectors over a tidal cycle for reef type P3. Plots (labelled 7 to 12) represent currents at one hour intervals from when the tide begins to ebb.

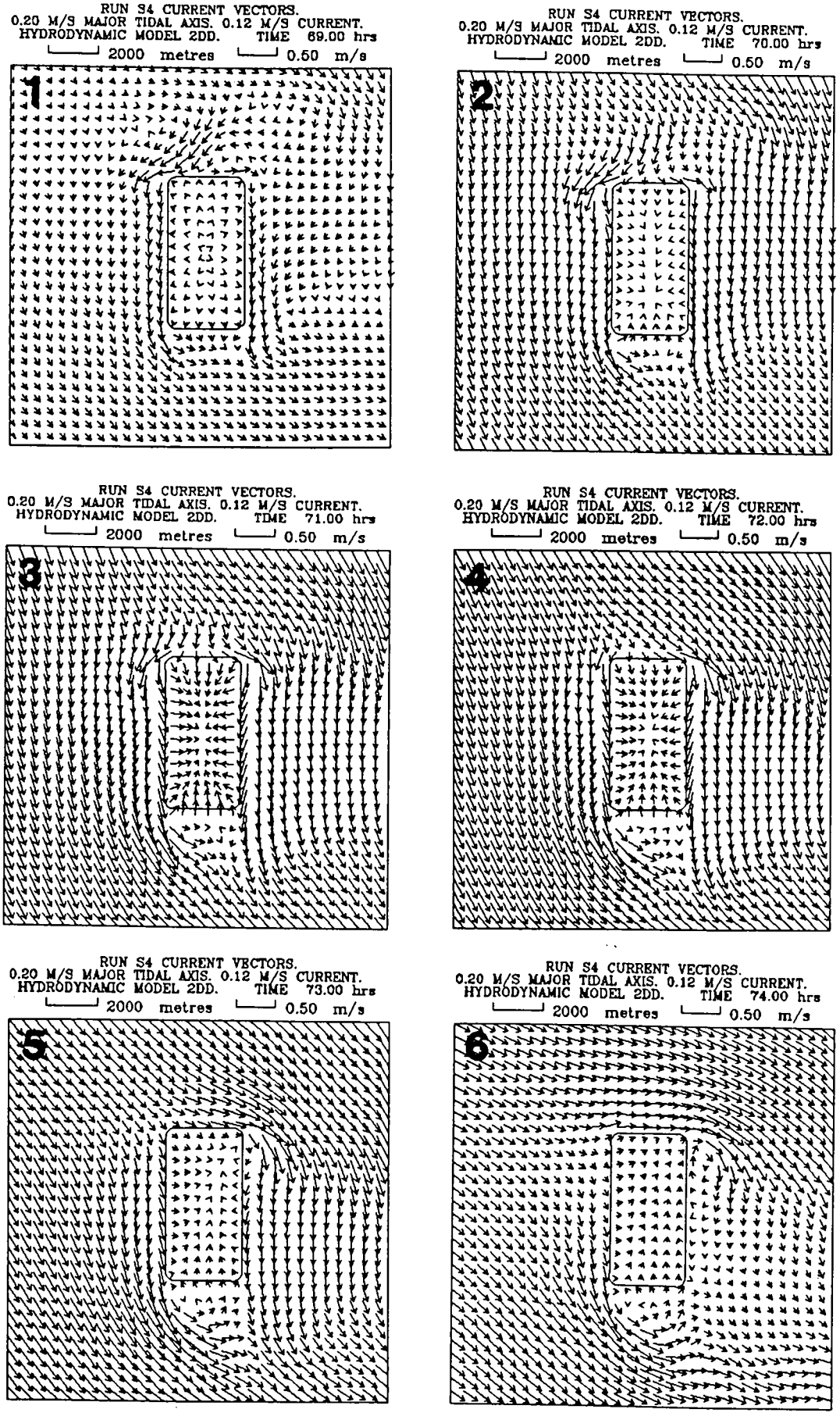


Figure B4a Representative plots of current vectors over a tidal cycle for reef type P4. Plots (labelled 1 to 6) represent currents at one hour intervals from when the tide begins to flood.

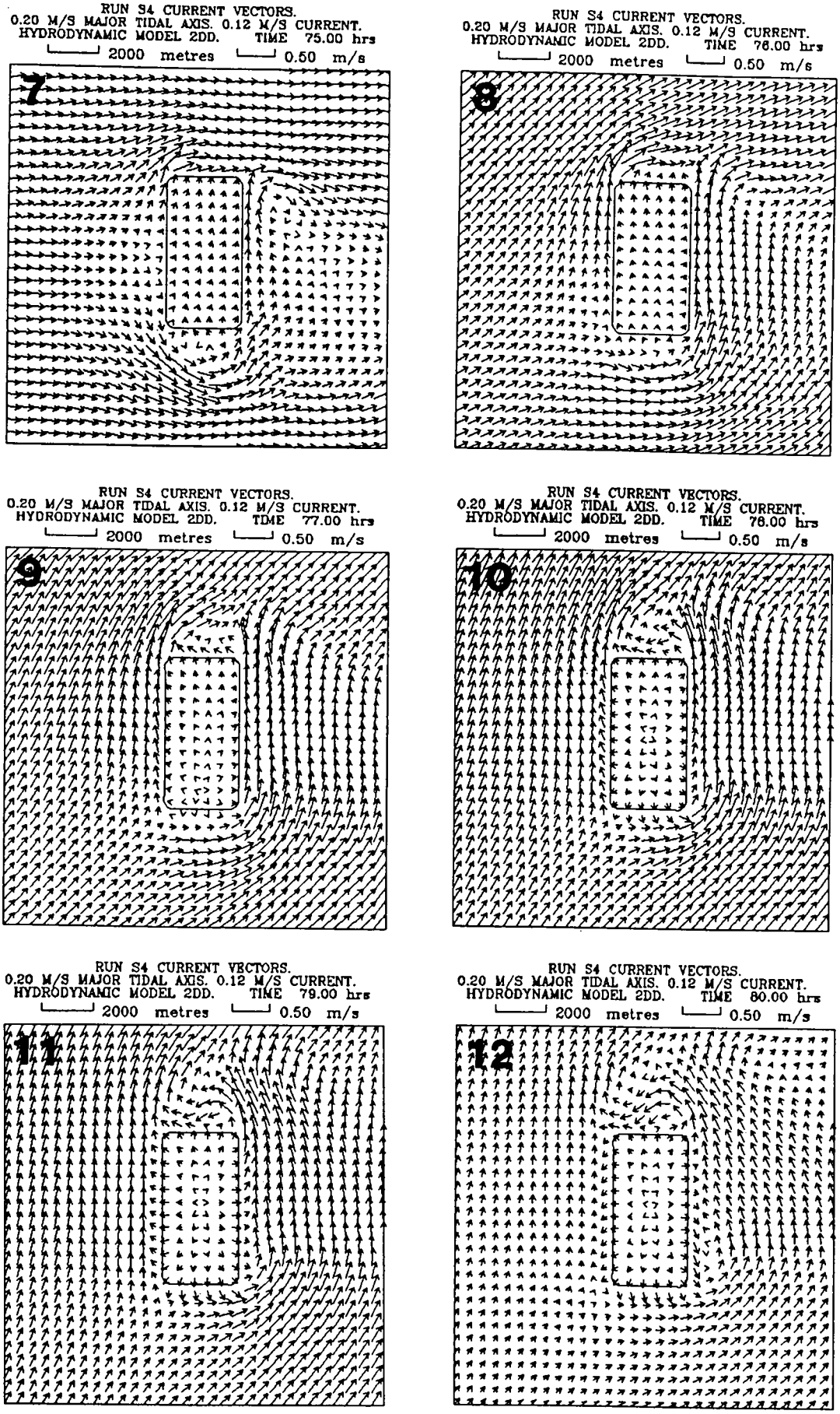


Figure B4b Representative plots of current vectors over a tidal cycle for reef type P4. Plots (labelled 7 to 12) represent currents at one hour intervals from when the tide begins to ebb.

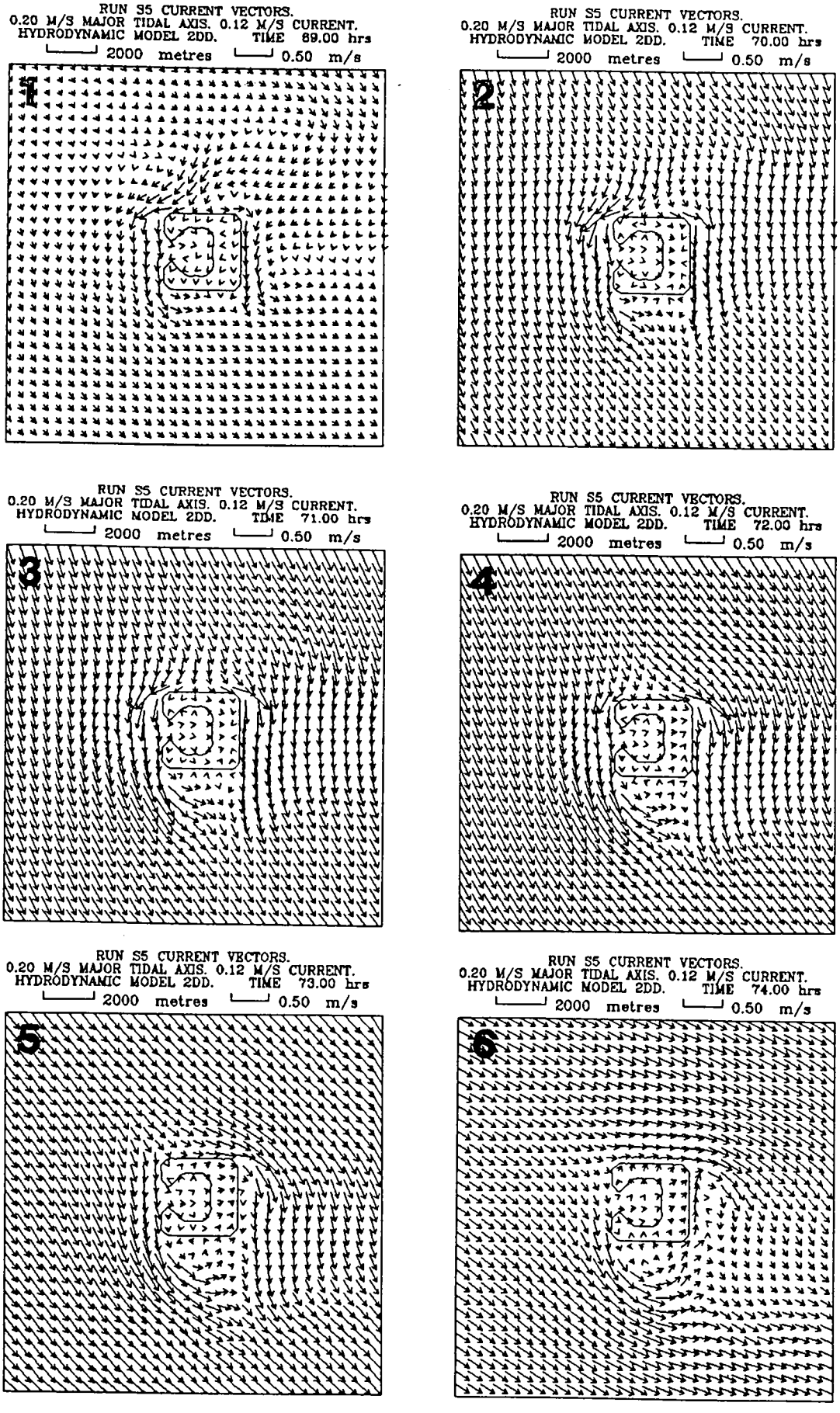


Figure B5a Representative plots of current vectors over a tidal cycle for reef type L1. Plots (labelled 1 to 6) represent currents at one hour intervals from when the tide begins to flood.

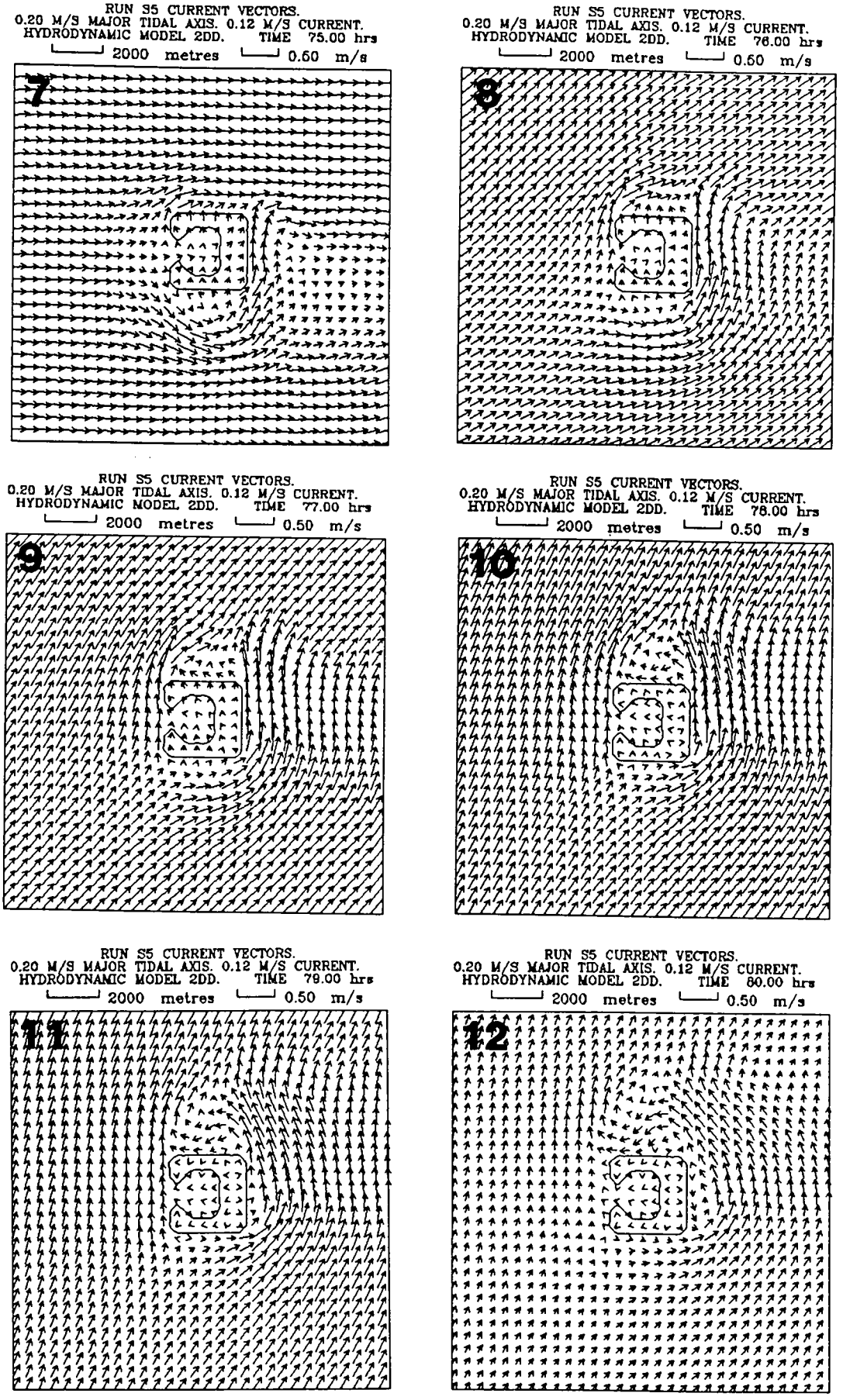


Figure B5b Representative plots of current vectors over a tidal cycle for reef type L1. Plots (labelled 7 to 12) represent currents at one hour intervals from when the tide begins to ebb.

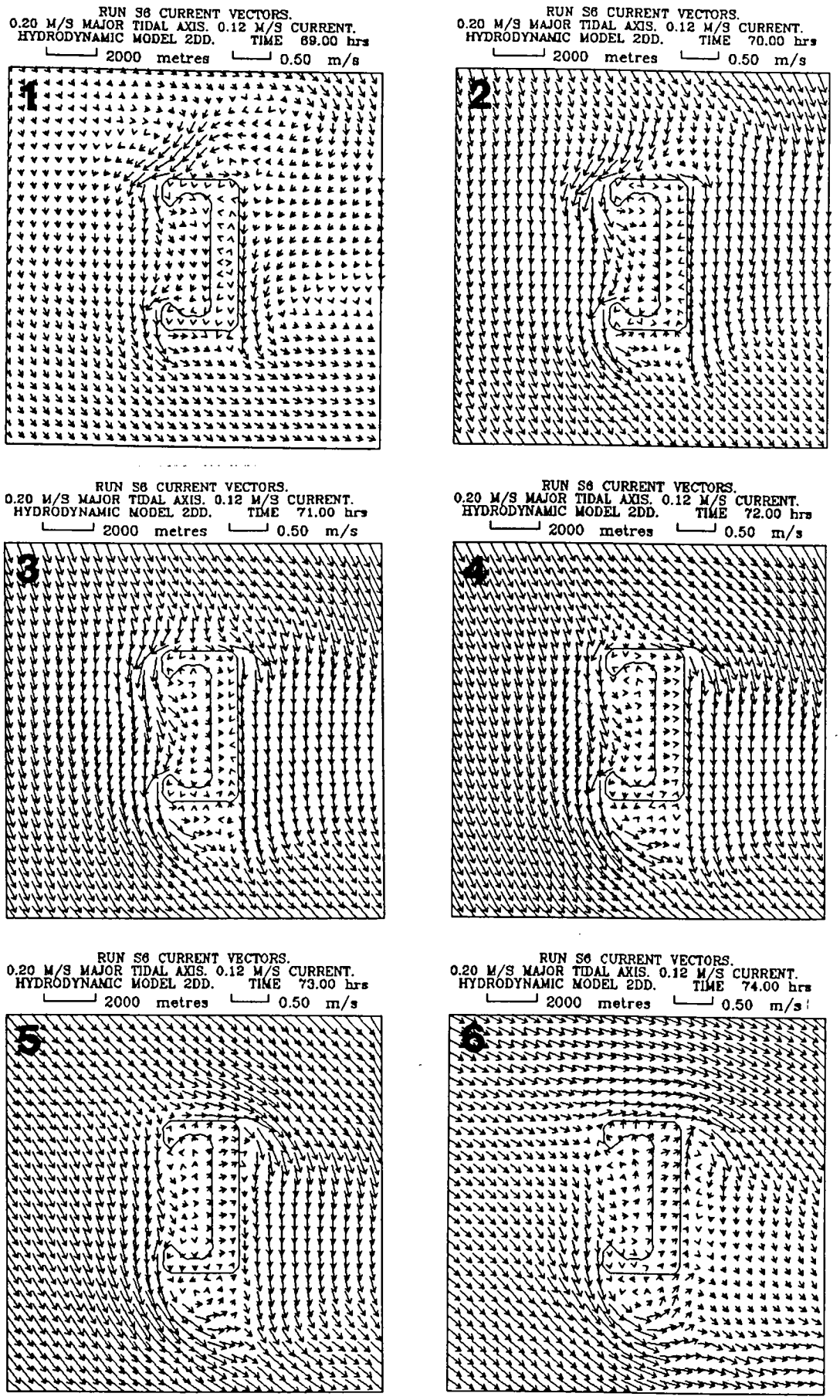


Figure B6a Representative plots of current vectors over a tidal cycle for reef type L2. Plots (labelled 1 to 6) represent currents at one hour intervals from when the tide begins to flood.

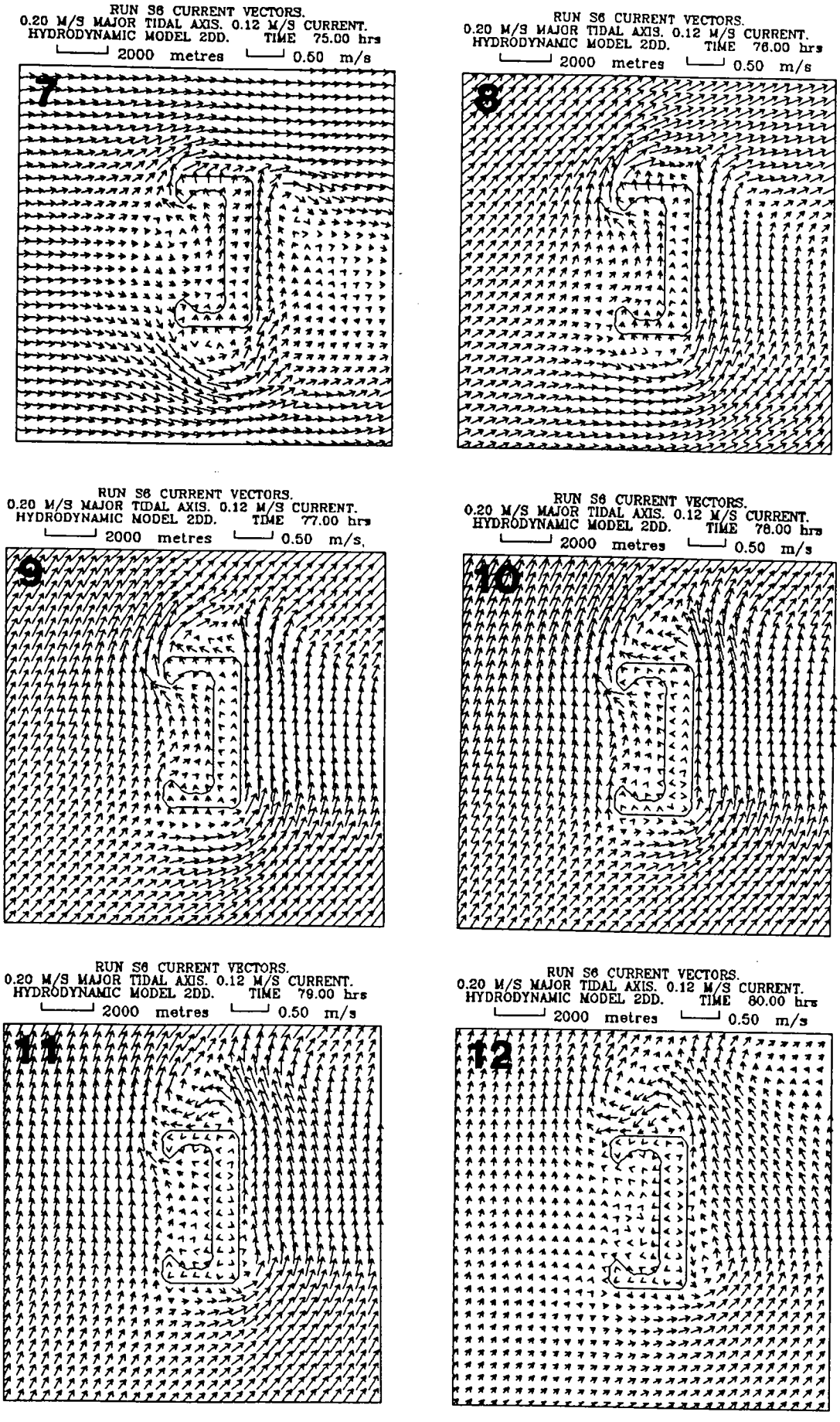


Figure B6b Representative plots of current vectors over a tidal cycle for reef type L2. Plots (labelled 7 to 12) represent currents at one hour intervals from when the tide begins to ebb.

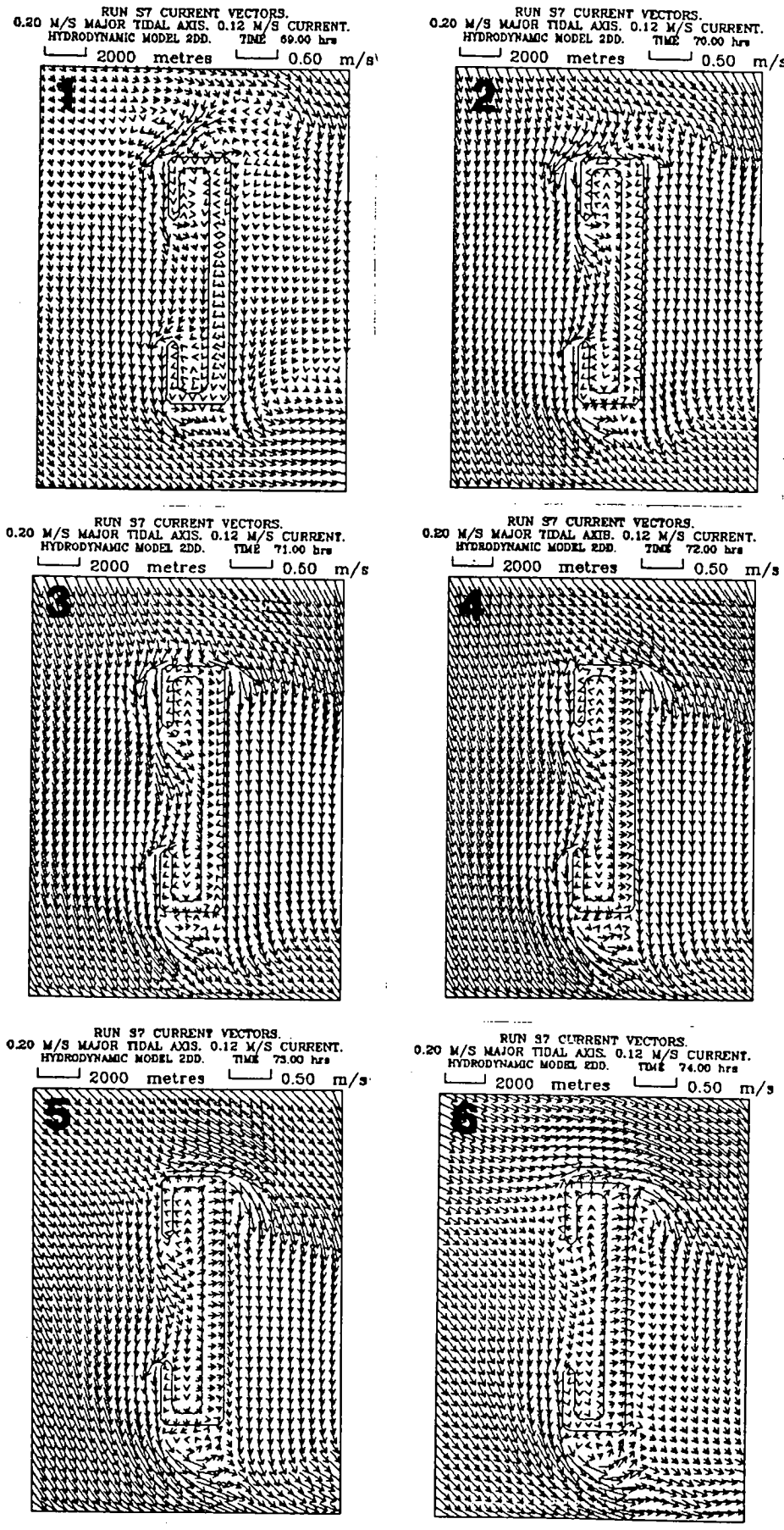


Figure B7a Representative plots of current vectors over a tidal cycle for reef type L3. Plots (labelled 1 to 6) represent currents at one hour intervals from when the tide begins to flood.

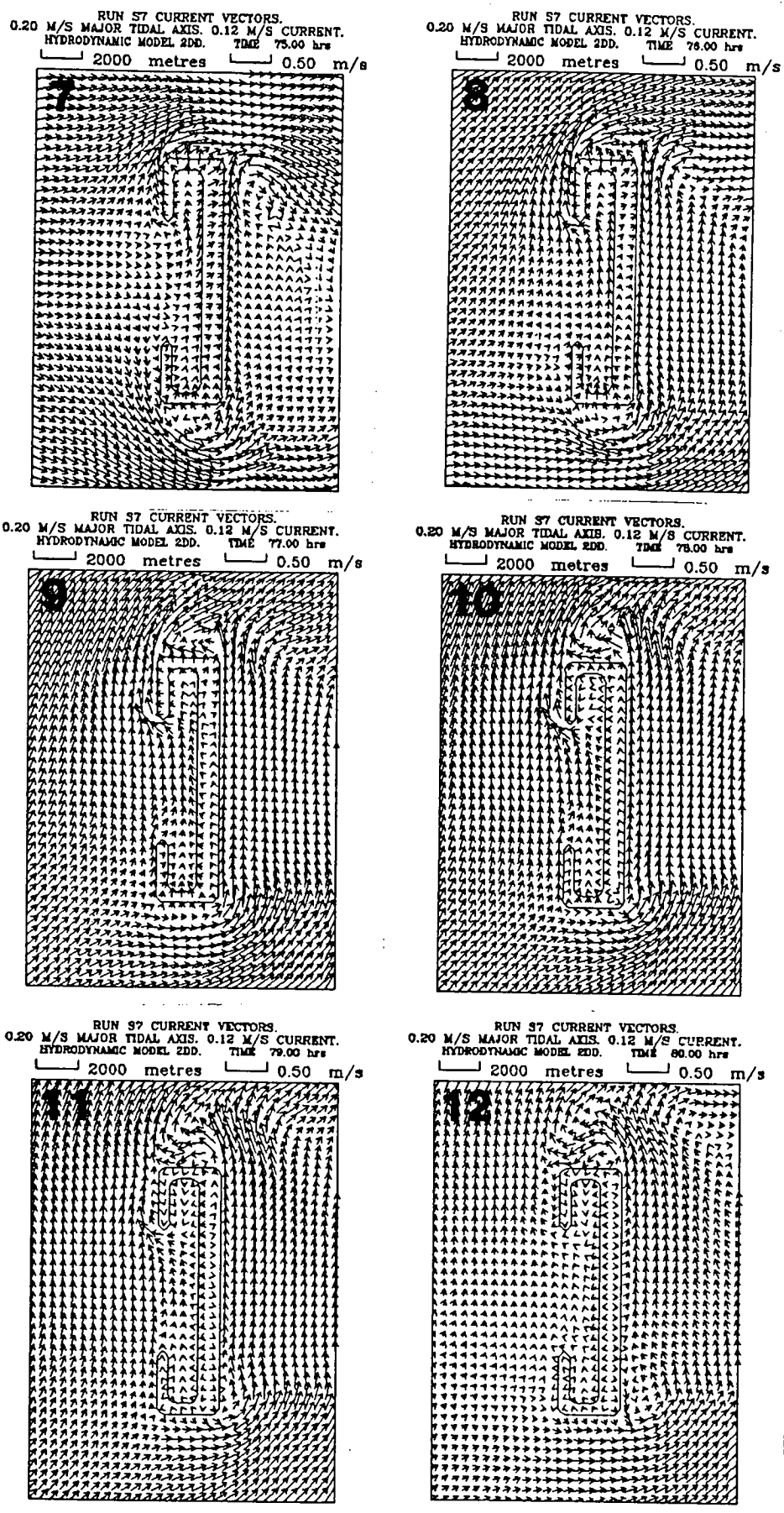


Figure B7b Representative plots of current vectors over a tidal cycle for reef type L3. Plots (labelled 7 to 12) represent currents at one hour intervals from when the tide begins to ebb.

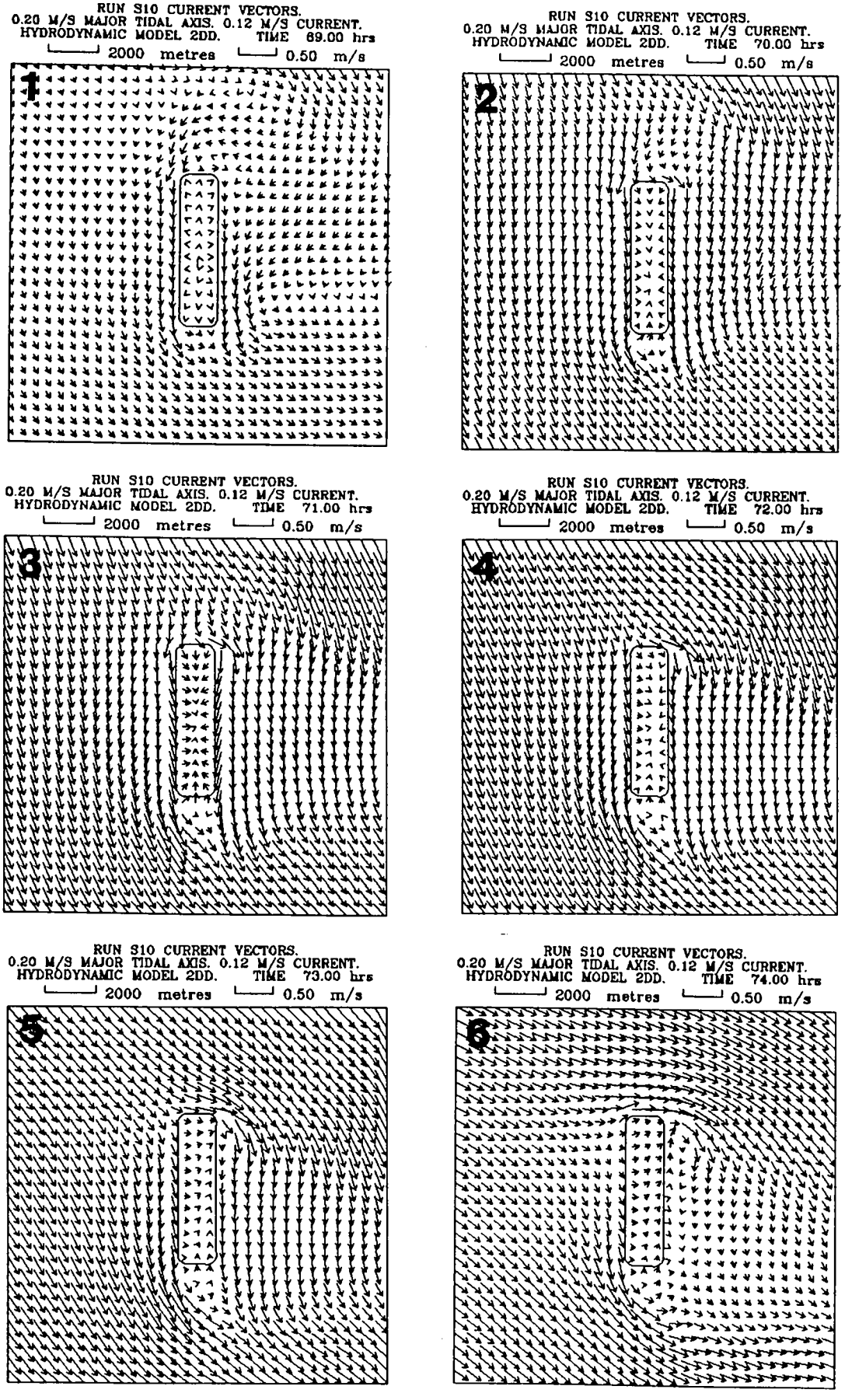


Figure B8a Representative plots of current vectors over a tidal cycle for reef type NP. Plots (labelled 1 to 6) represent currents at one hour intervals from when the tide begins to flood.

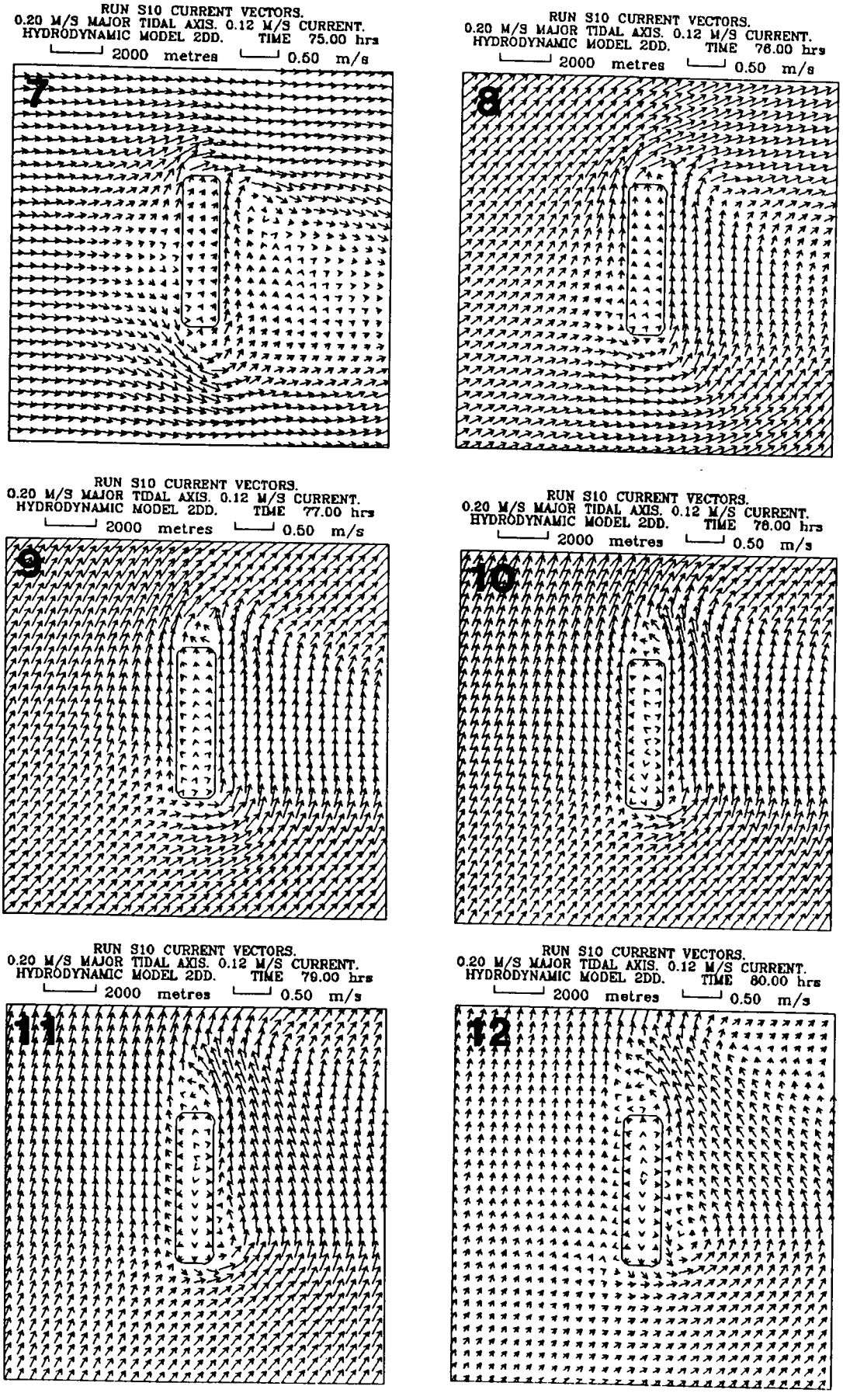


Figure B8b Representative plots of current vectors over a tidal cycle for reef type NP. Plots (labelled 7 to 12) represent currents at one hour intervals from when the tide begins to ebb.

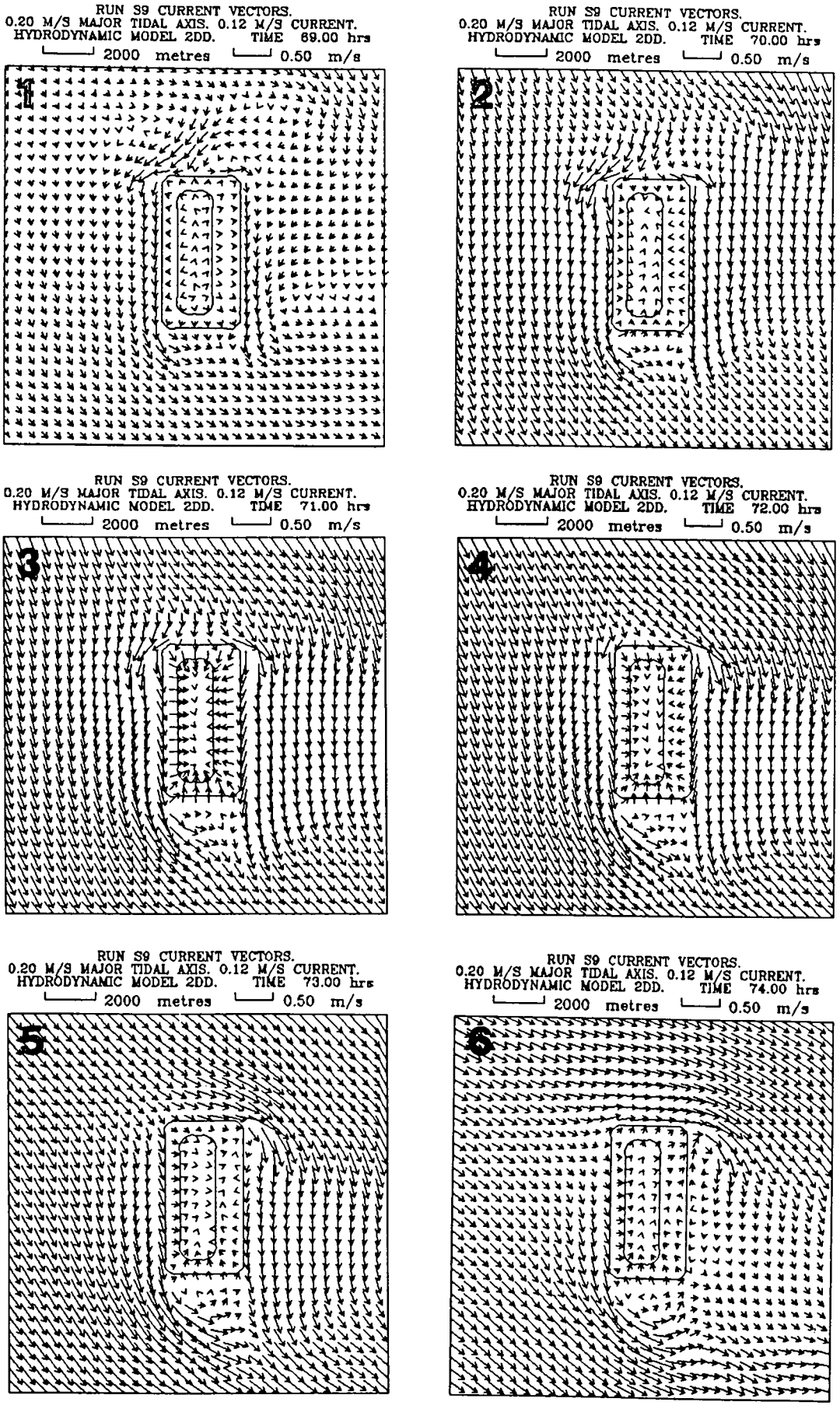


Figure B9a Representative plots of current vectors over a tidal cycle for reef type EL. Plots (labelled 1 to 6) represent currents at one hour intervals from when the tide begins to flood.

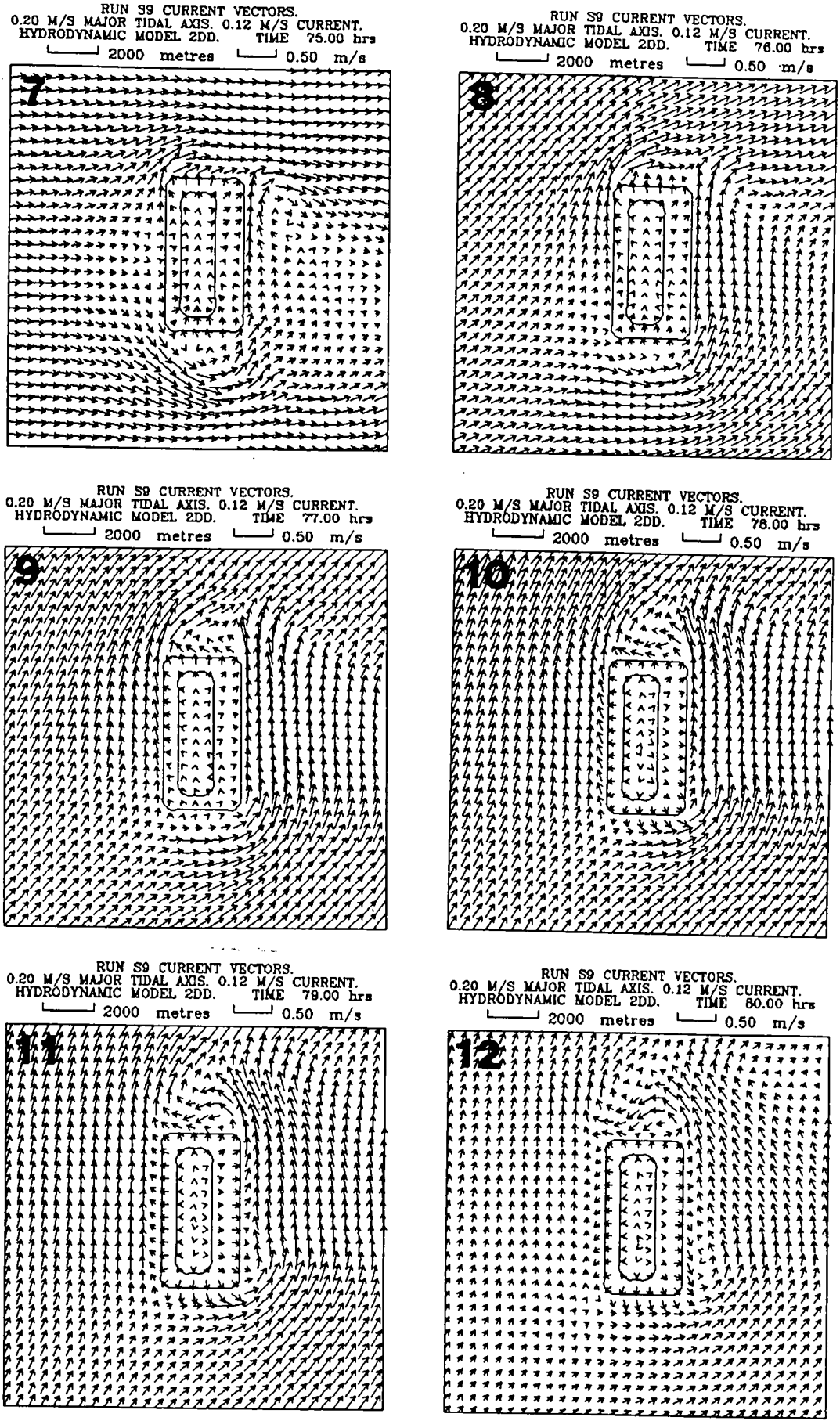


Figure B9b Representative plots of current vectors over a tidal cycle for reef type EL. Plots (labelled 7 to 12) represent currents at one hour intervals from when the tide begins to ebb.

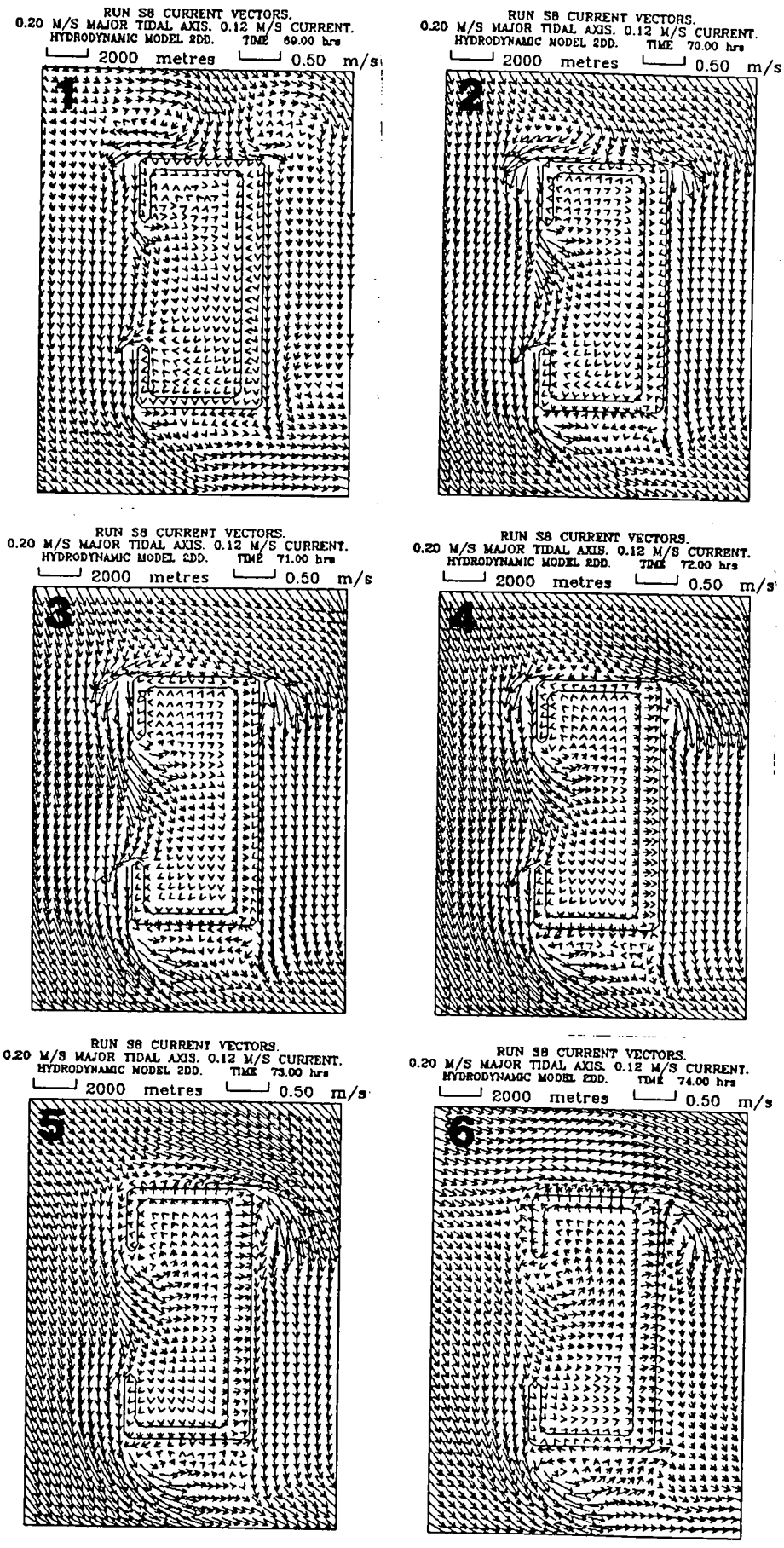


Figure B10a Representative plots of current vectors over a tidal cycle for reef type ML. Plots (labelled 1 to 6) represent currents at one hour intervals from when the tide begins to flood.

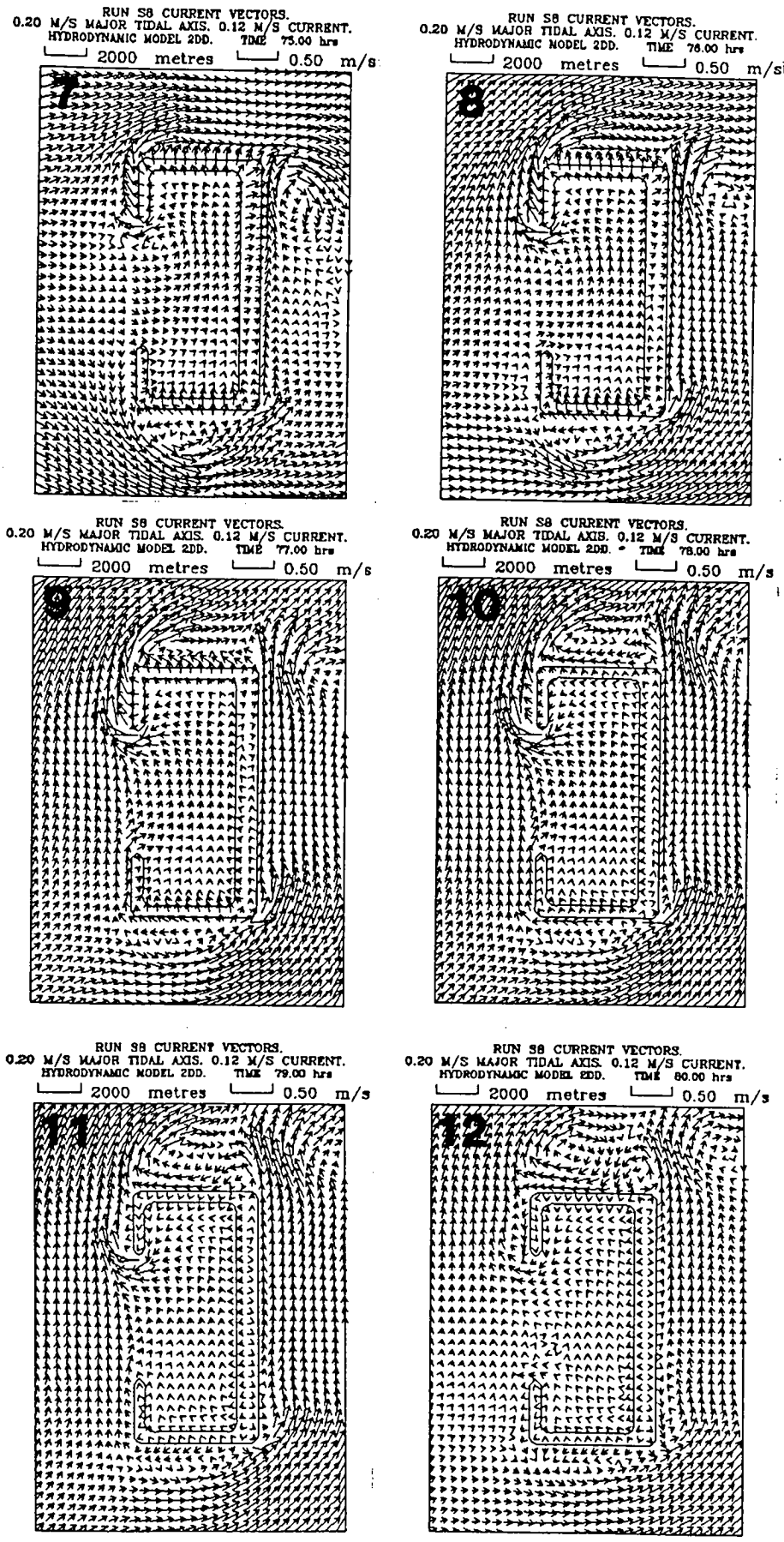


Figure B10b Representative plots of current vectors over a tidal cycle for reef type ML. Plots (labelled 7 to 12) represent currents at one hour intervals from when the tide begins to ebb.

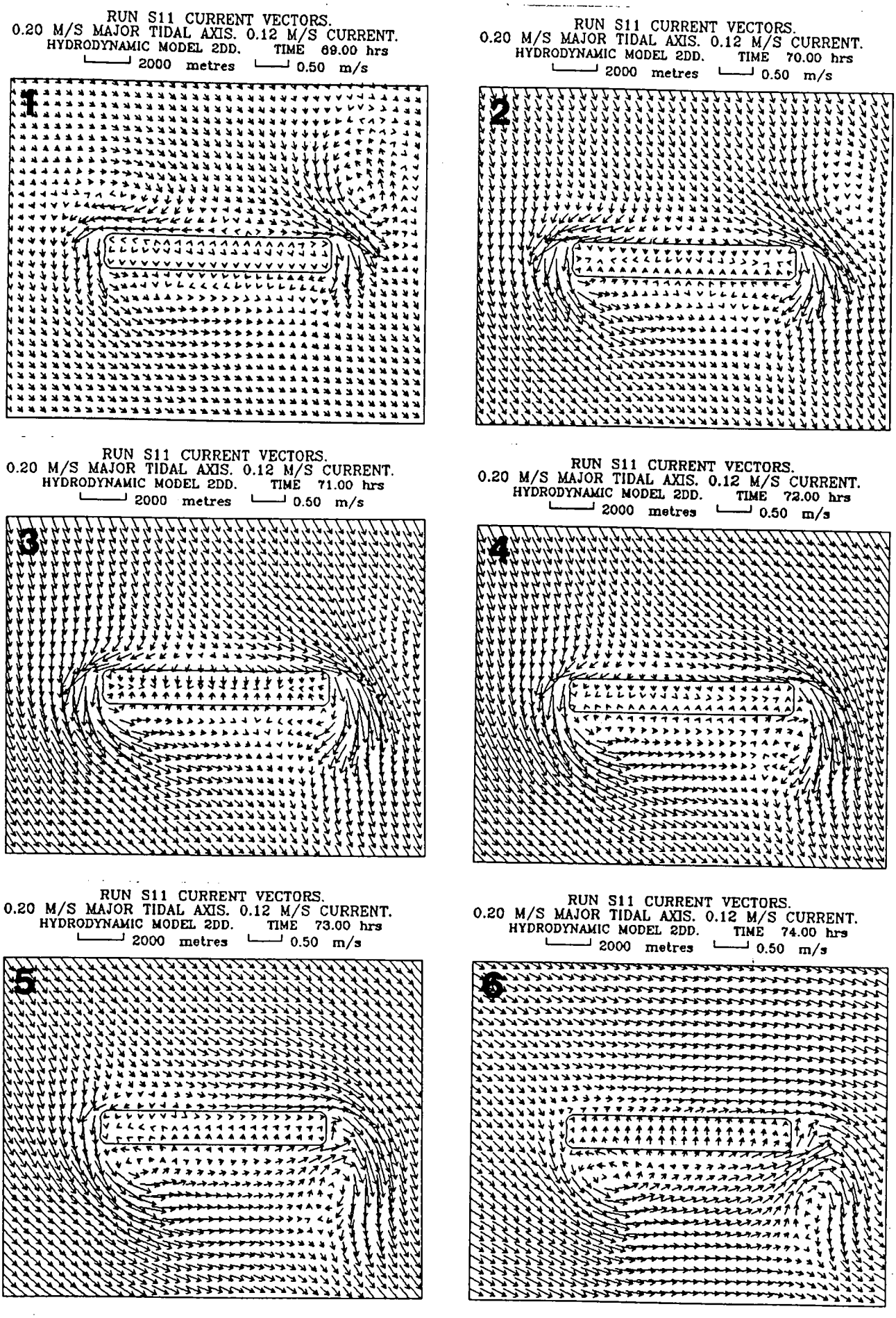


Figure B11a Representative plots of current vectors over a tidal cycle for reef type R1. Plots (labelled 1 to 6) represent currents at one hour intervals from when the tide begins to flood.

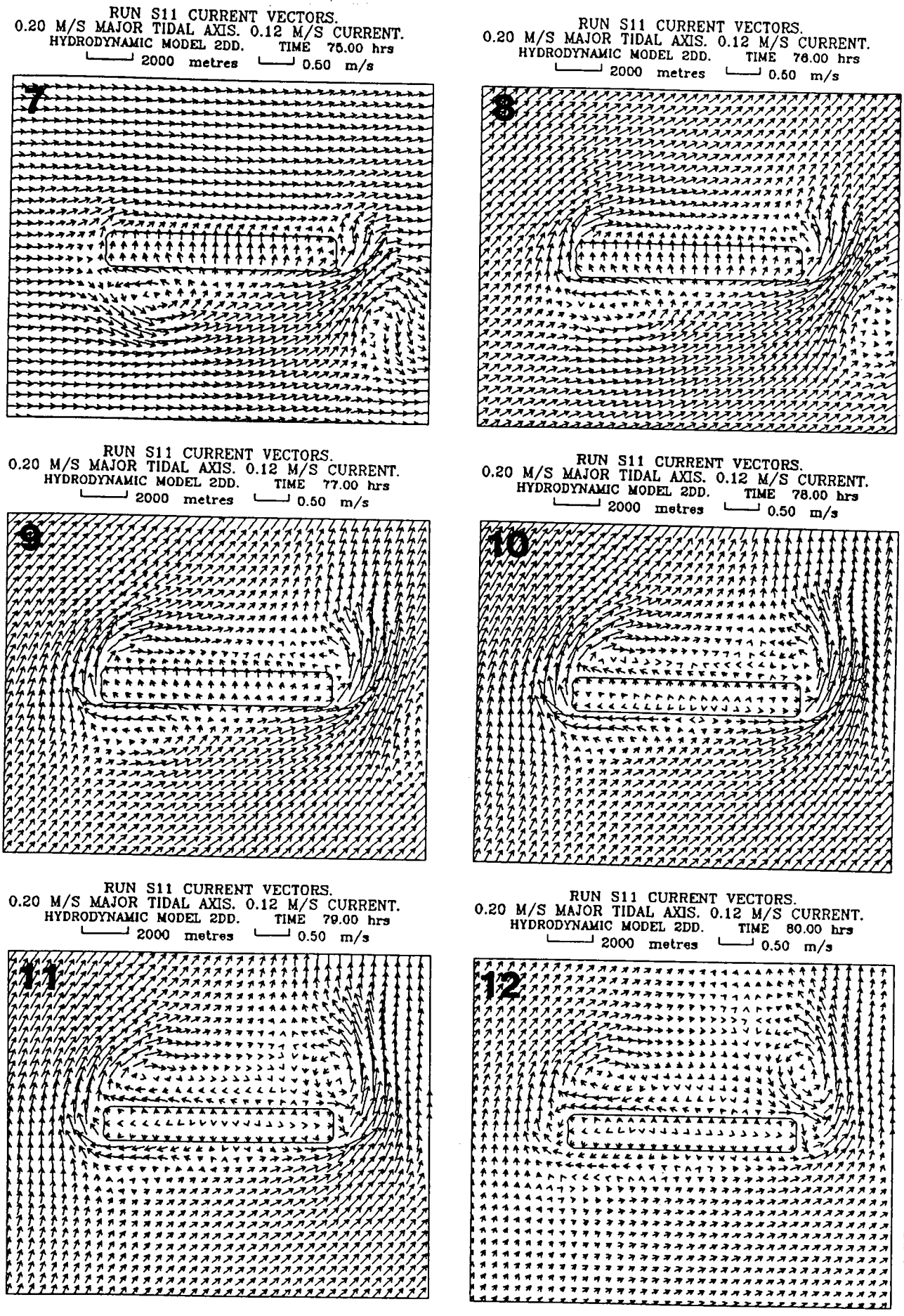


Figure B11b Representative plots of current vectors over a tidal cycle for reef type R1. Plots (labelled 7 to 12) represent currents at one hour intervals from when the tide begins to ebb.

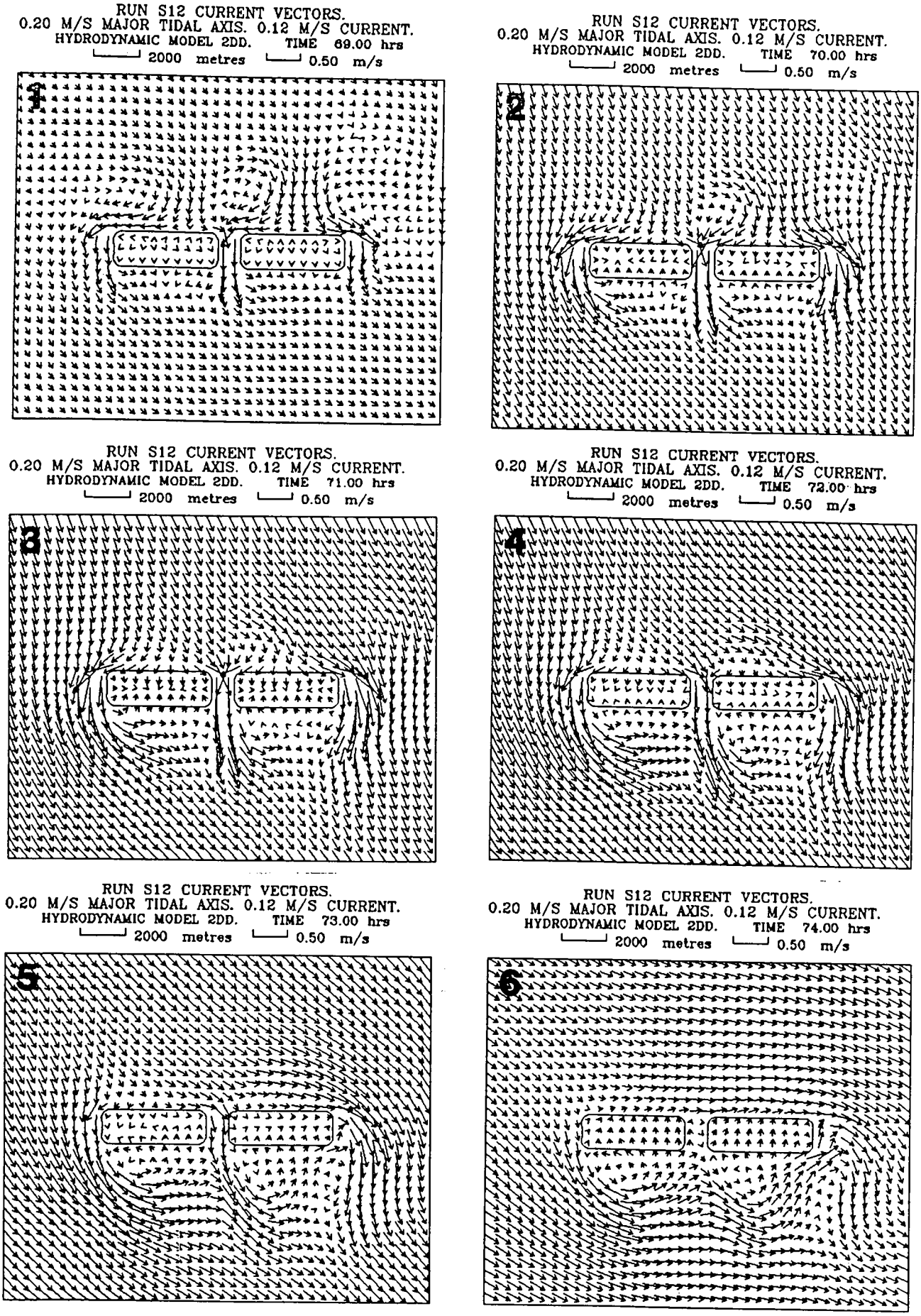
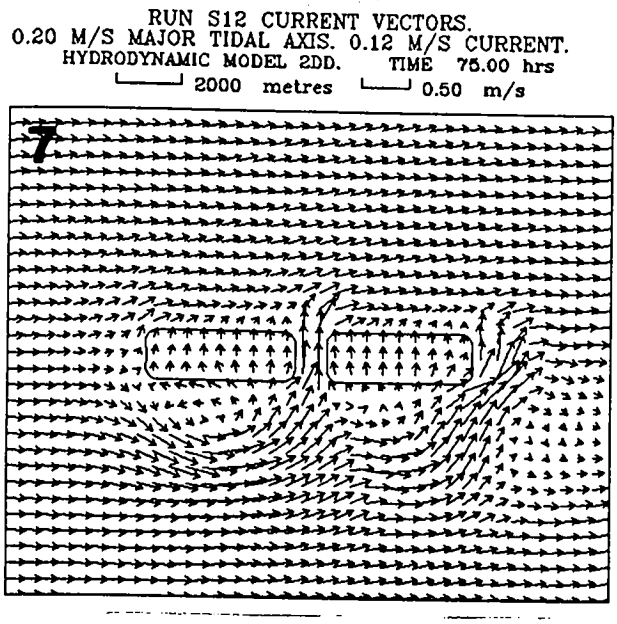
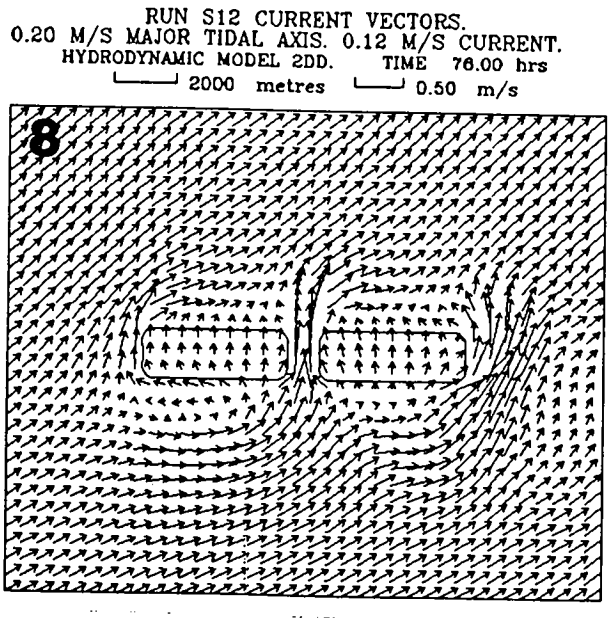
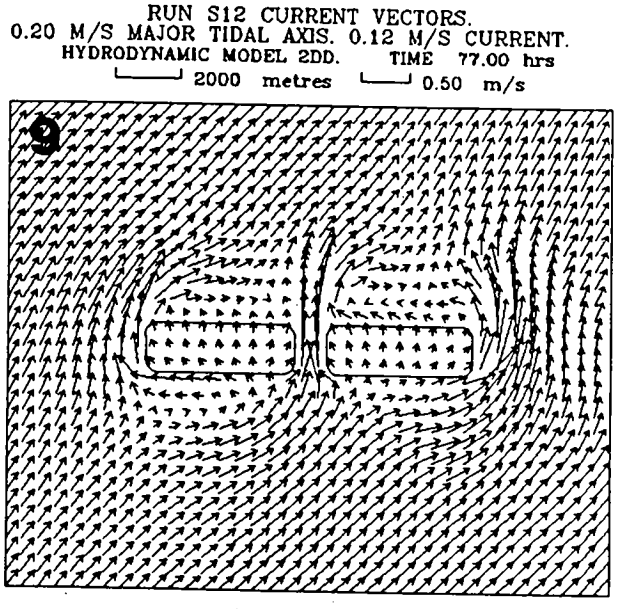
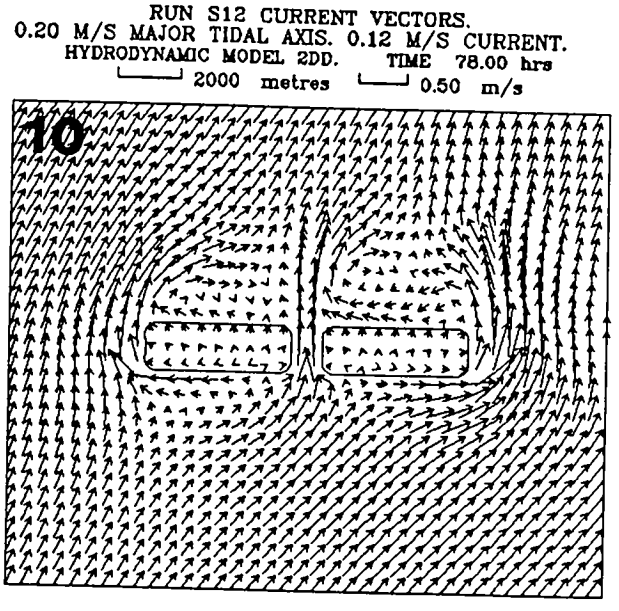


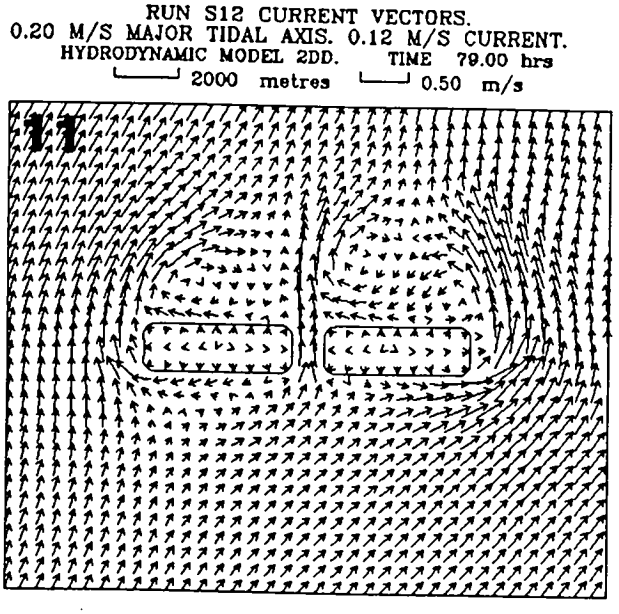
Figure B12a Representative plots of current vectors over a tidal cycle for reef type R2. Plots (labelled 1 to 6) represent currents at one hour intervals from when the tide begins to flood.











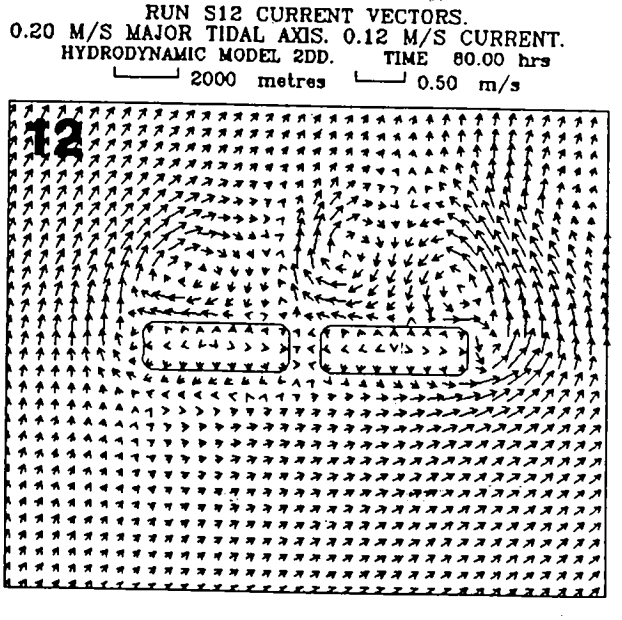


Figure B12b Representative plots of current vectors over a tidal cycle for reef type R2. Plots (labelled 7 to 12) represent currents at one hour intervals from when the tide begins to ebb.

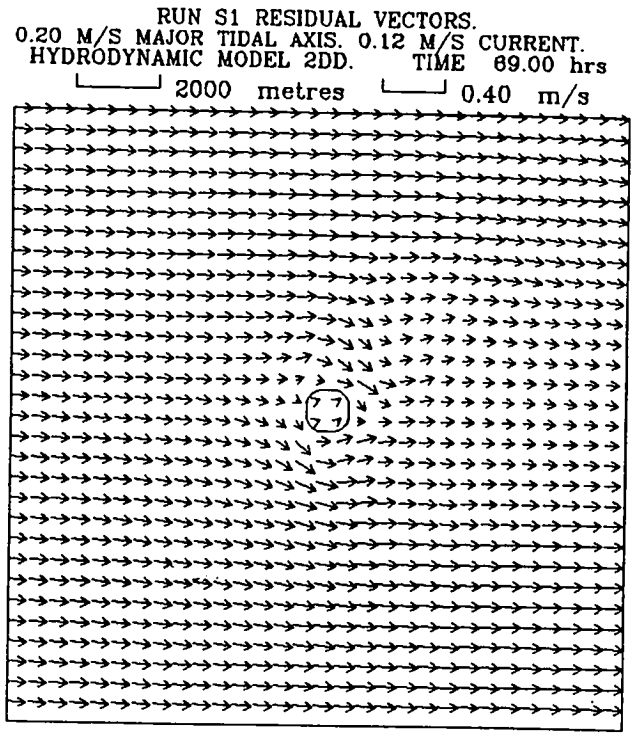


Figure B13 Current vectors representing the residual circulation around reef type P1.

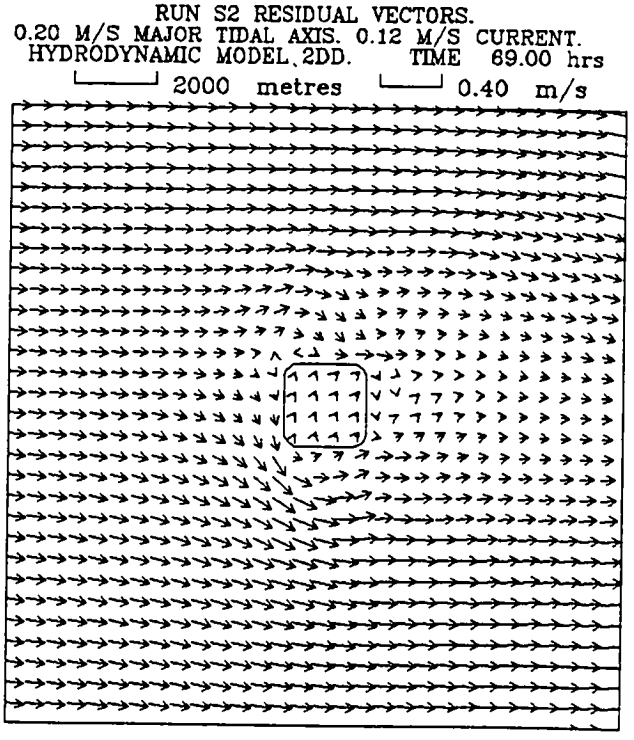


Figure B14 Current vectors representing the residual circulation around reef type P2.

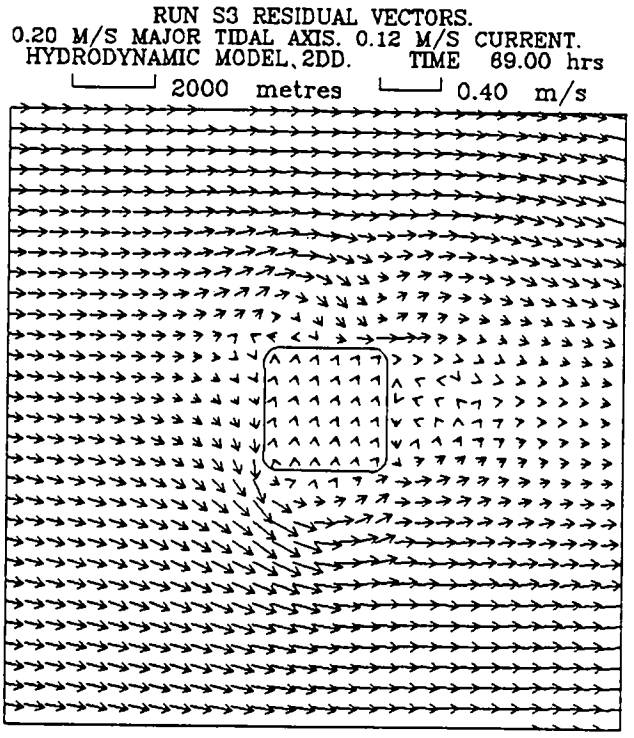


Figure B15 Current vectors representing the residual circulation around reef type P3.

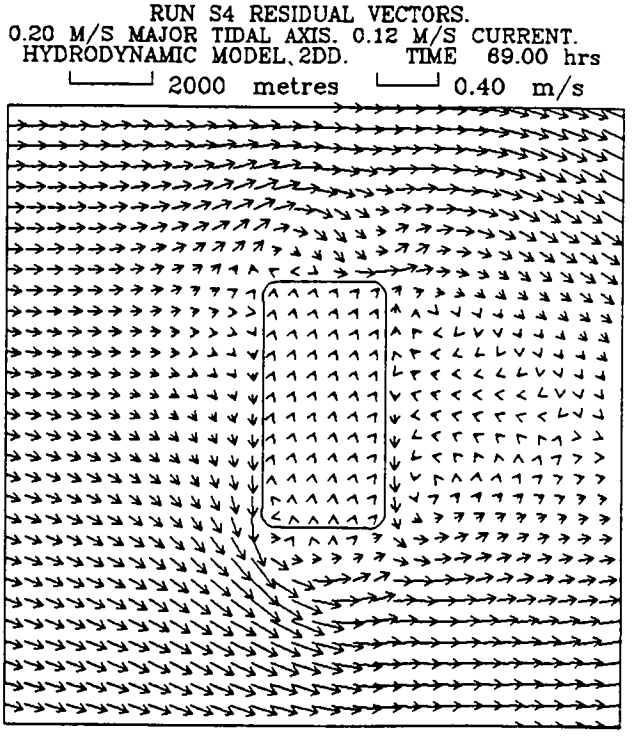


Figure B16 Current vectors representing the residual circulation around reef type P4.

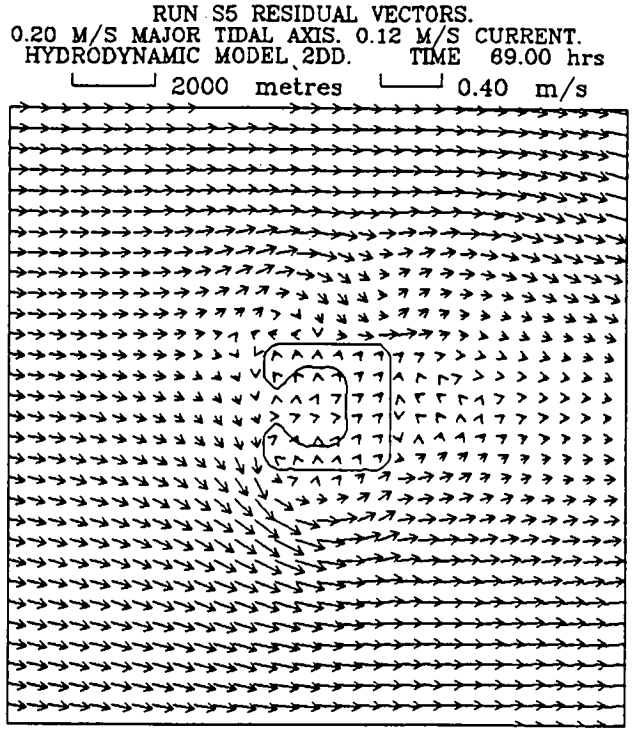


Figure B17 Current vectors representing the residual circulation around reef type L1.

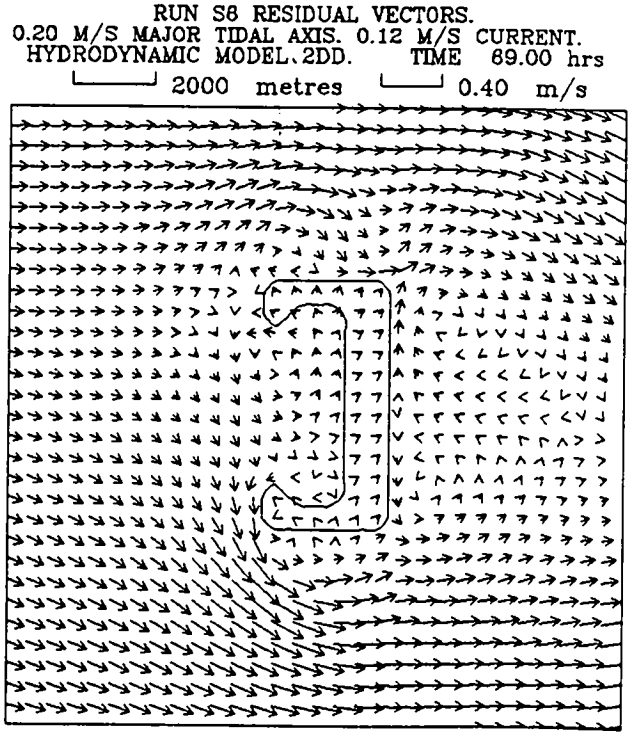


Figure B18 Current vectors representing the residual circulation around reef type L2.

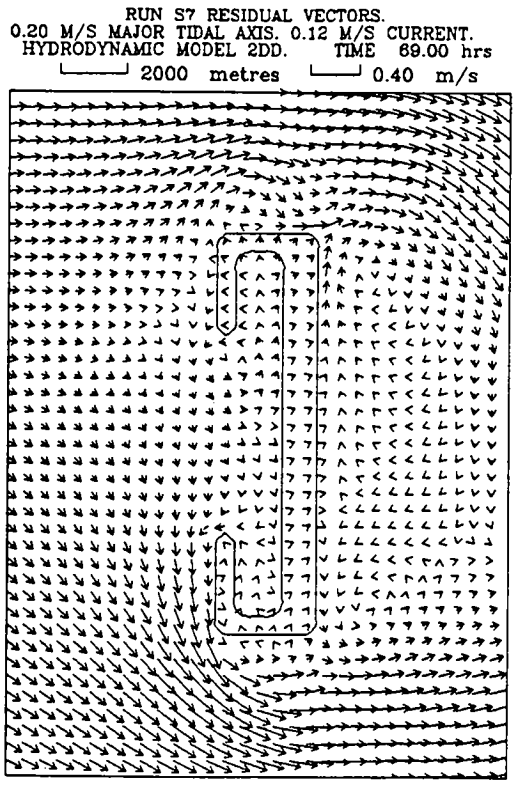


Figure B19 Current vectors representing the residual circulation around reef type L3.

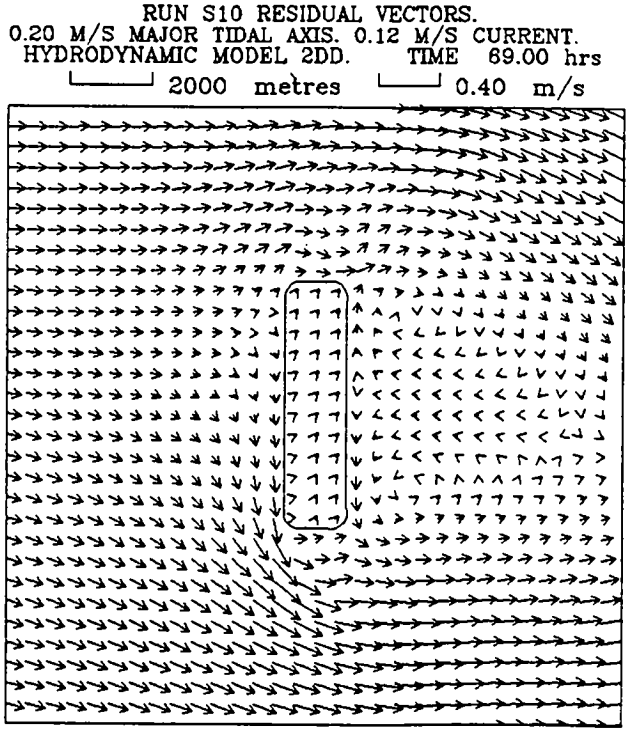


Figure B20 Current vectors representing the residual circulation around reef type NP.

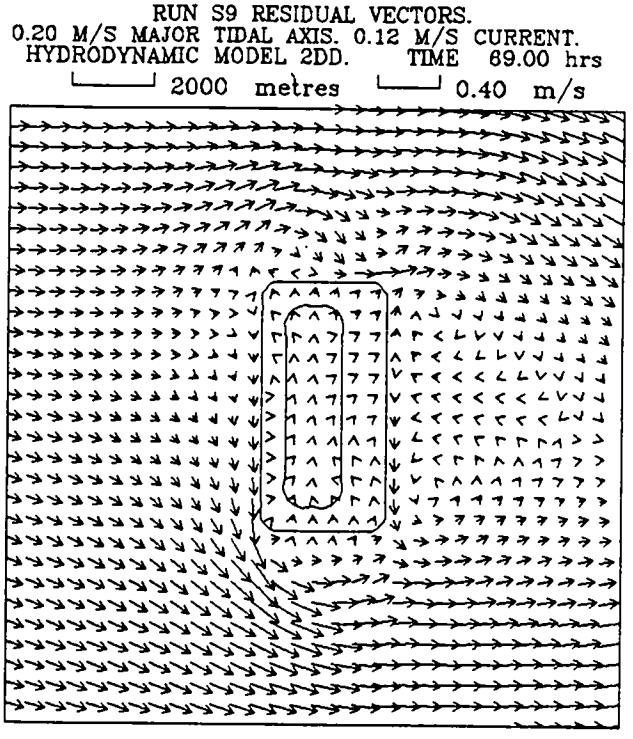


Figure B21 Current vectors representing the residual circulation around reef type EL.

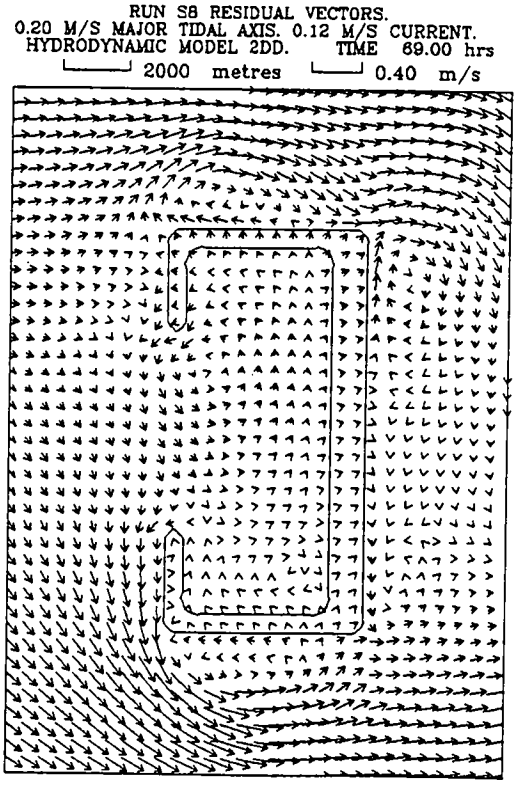


Figure B22 Current vectors representing the residual circulation around reef type ML.

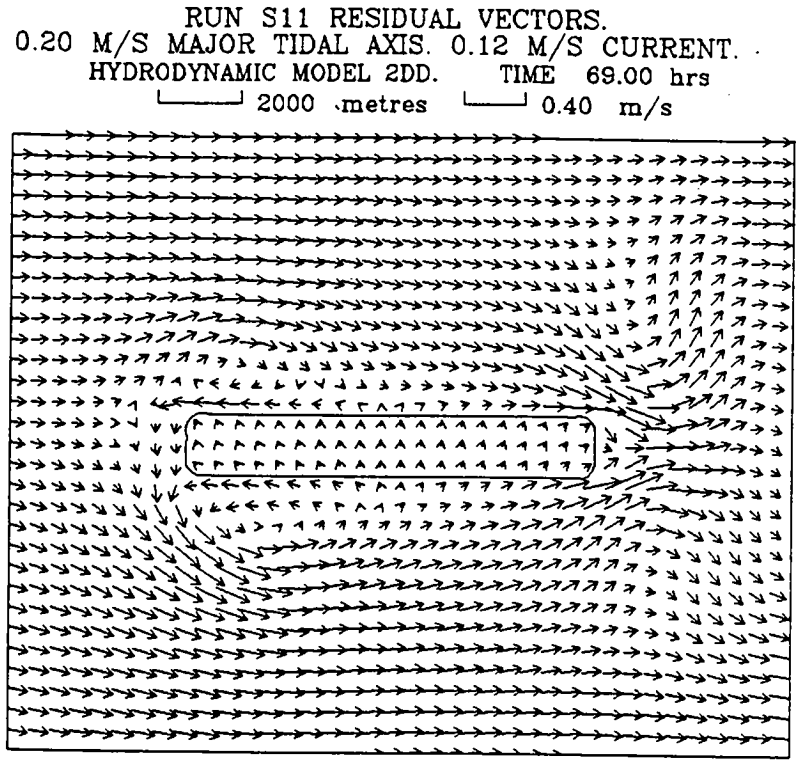


Figure B23 Current vectors representing the residual circulation around reef type R1.

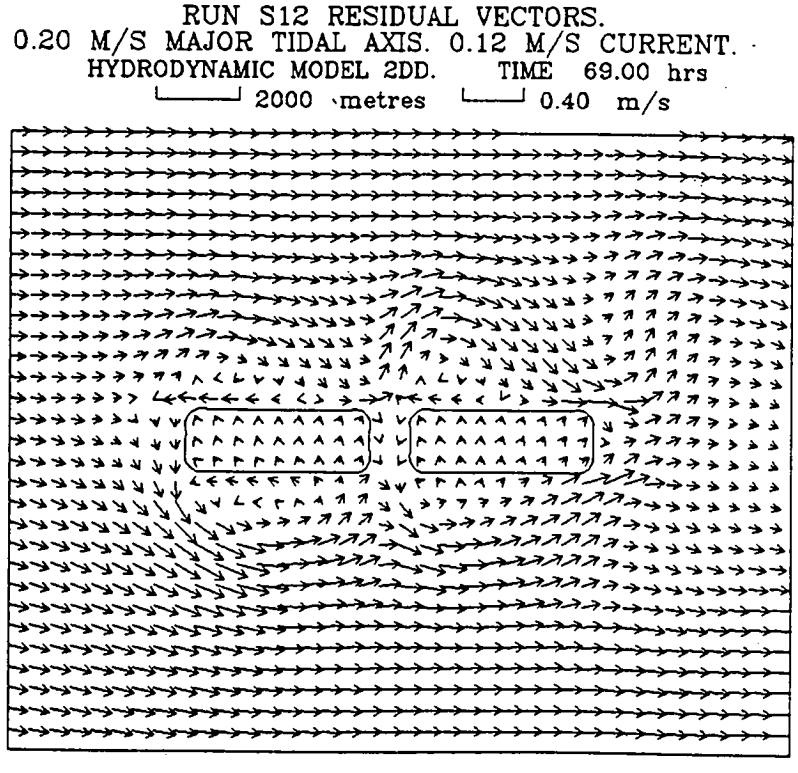


Figure B24 Current vectors representing the residual circulation around reef type R2.

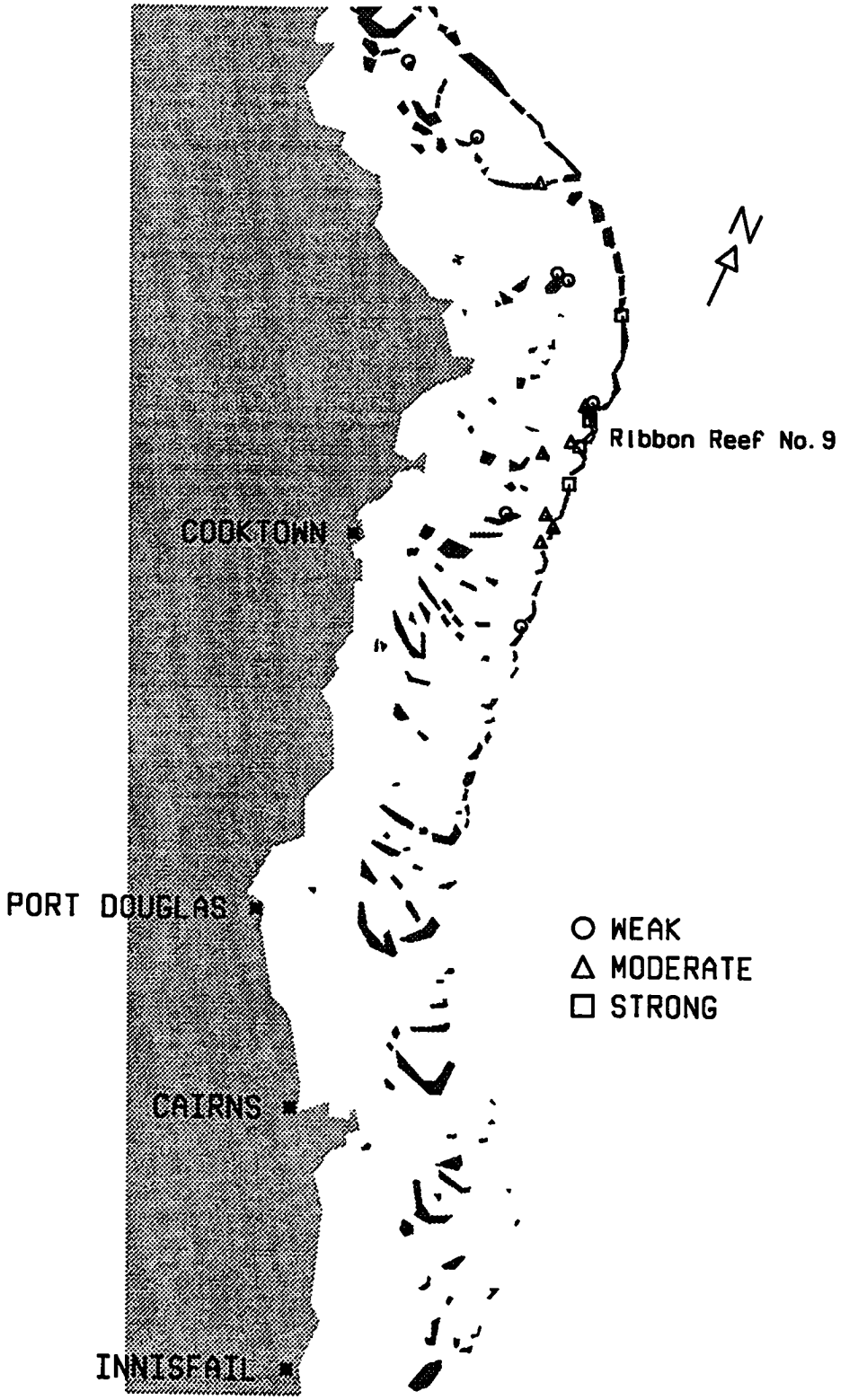


Figure C1 Strength of connectivity with respect to Ribbon Reef No.9 (source reef indicated without fill) for short pre-competent period larvae. The relative strength classes (weak, moderate and strong) represent probabilities separated by an order of magnitude. Scale: 1cm = 12 nautical miles.

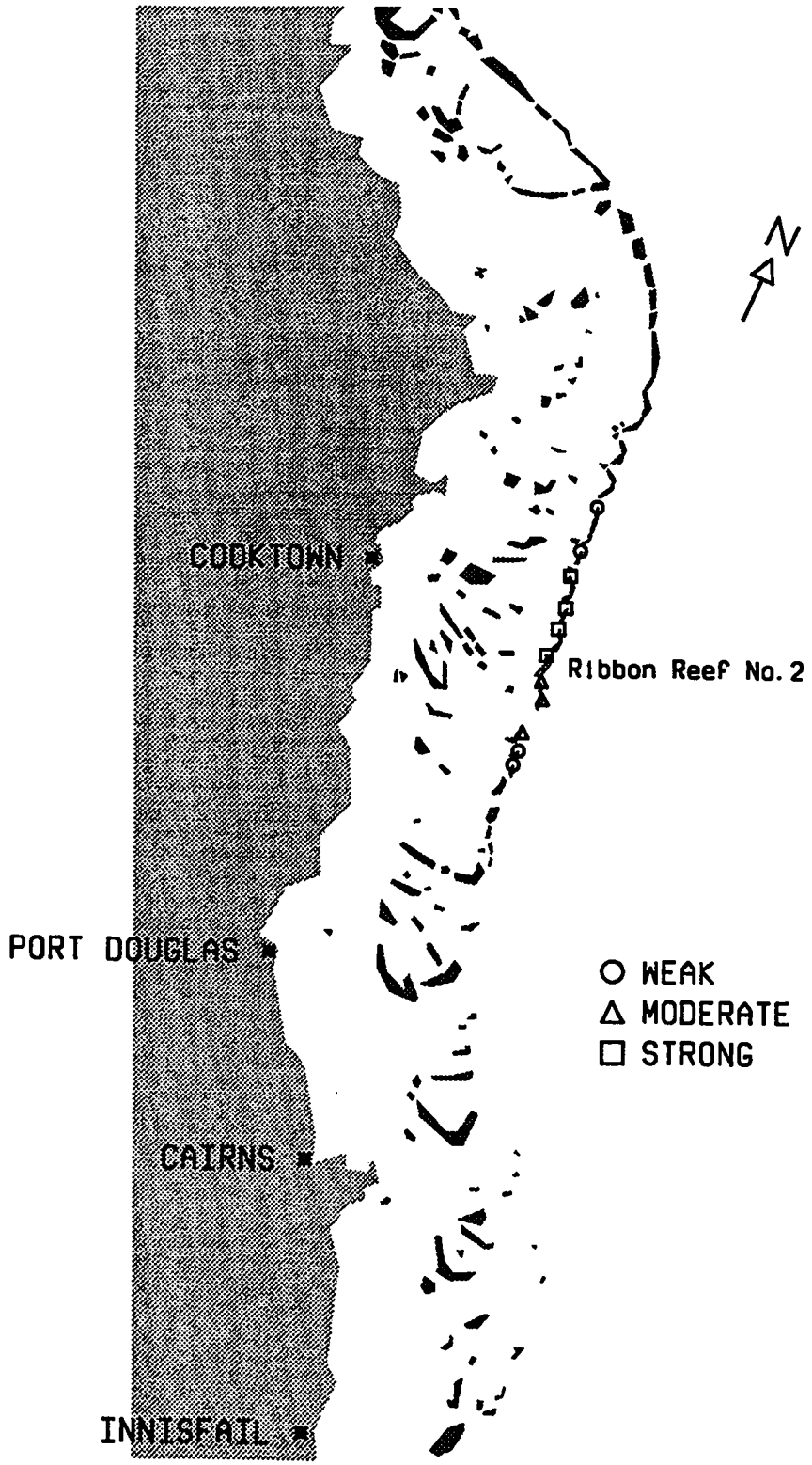


Figure C4 Strength of connectivity with respect to Ribbon Reef No.2 (source reef indicated without fill) for short pre-competent period larvae. The relative strength classes (weak, moderate and strong) represent probabilities separated by an order of magnitude. Scale: 1cm = 12 nautical miles.

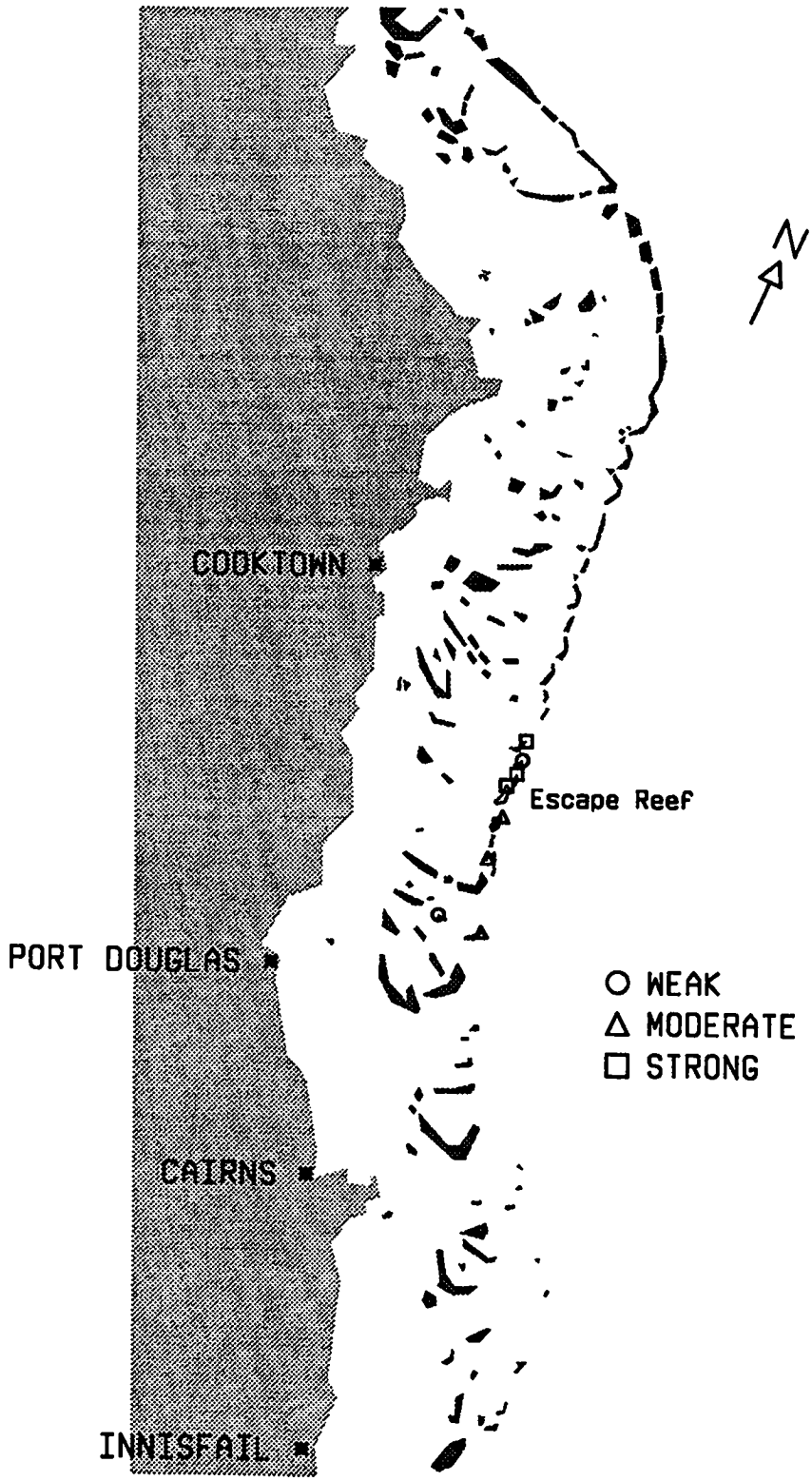


Figure C5 Strength of connectivity with respect to Escape Reef (source reef indicated without fill) for short pre-competent period larvae. The relative strength classes (weak, moderate and strong) represent probabilities separated by an order of magnitude. Scale: 1cm = 12 nautical miles.

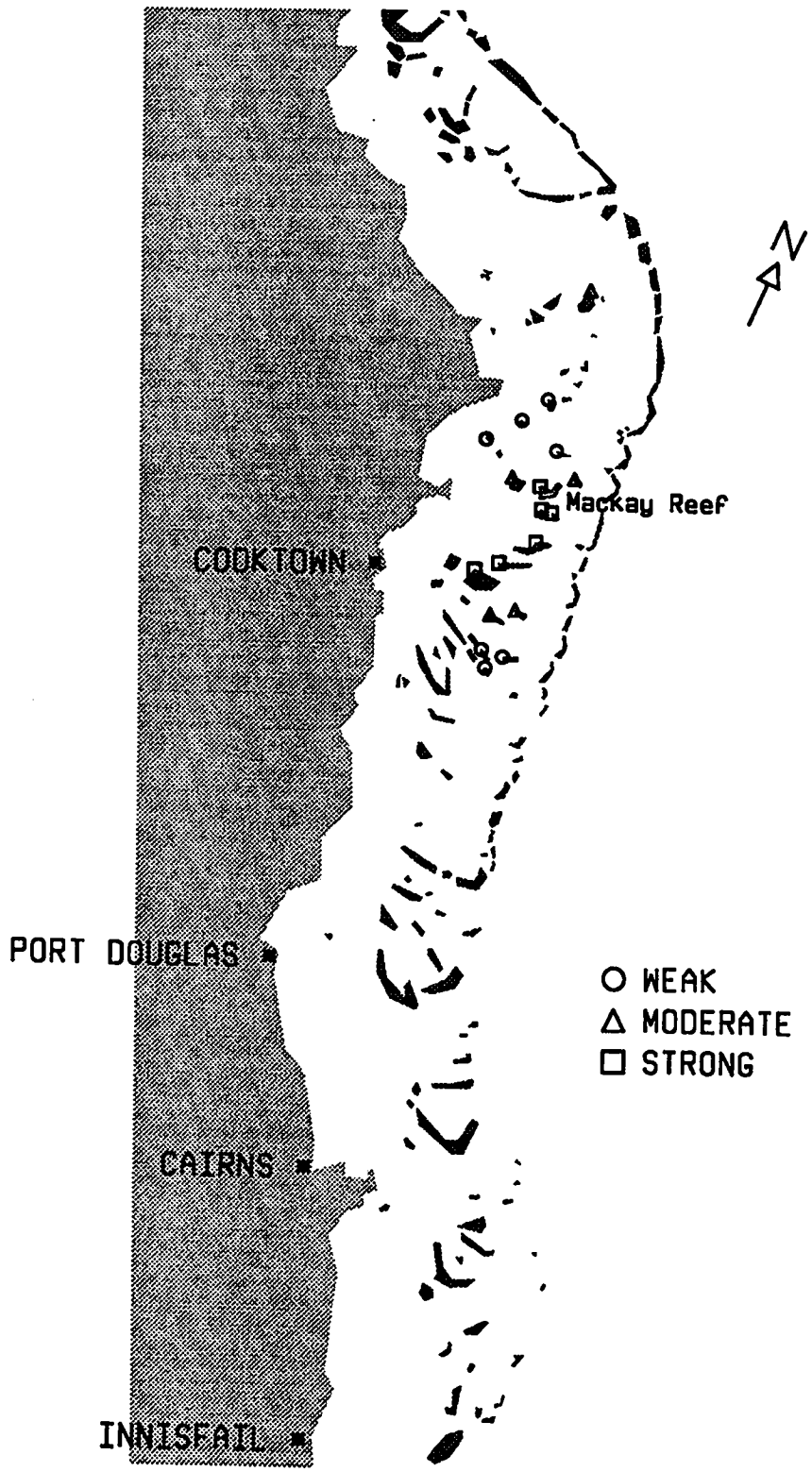


Figure C6 Strength of connectivity with respect to Mackay Reef (source reef indicated without fill) for short pre-competent period larvae. The relative strength classes (weak, moderate and strong) represent probabilities separated by an order of magnitude. Scale: 1cm = 12 nautical miles.

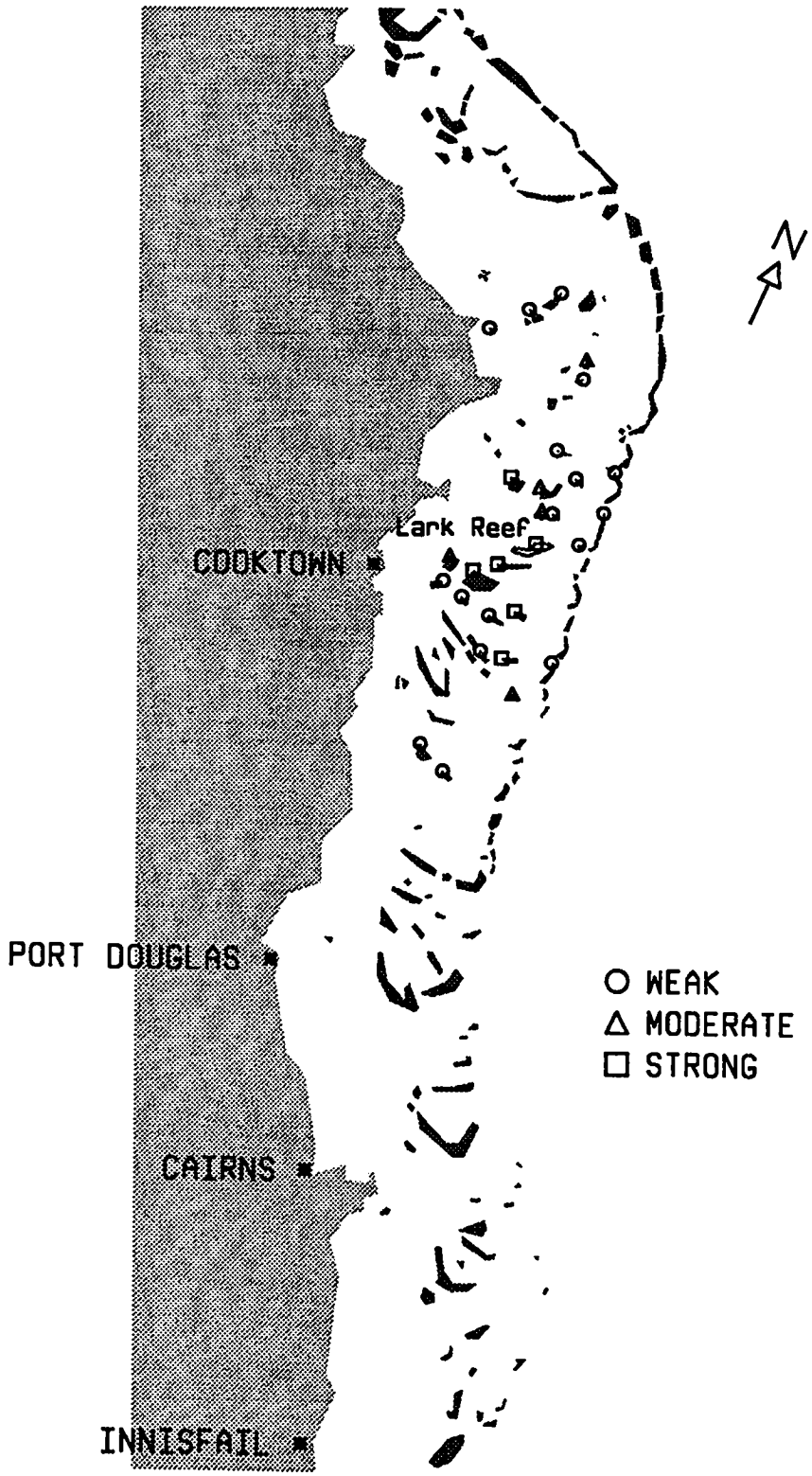


Figure C7 Strength of connectivity with respect to Lark Reef (source reef indicated without fill) for short pre-competent period larvae. The relative strength classes (weak, moderate and strong) represent probabilities separated by an order of magnitude. Scale: 1cm = 12 nautical miles.

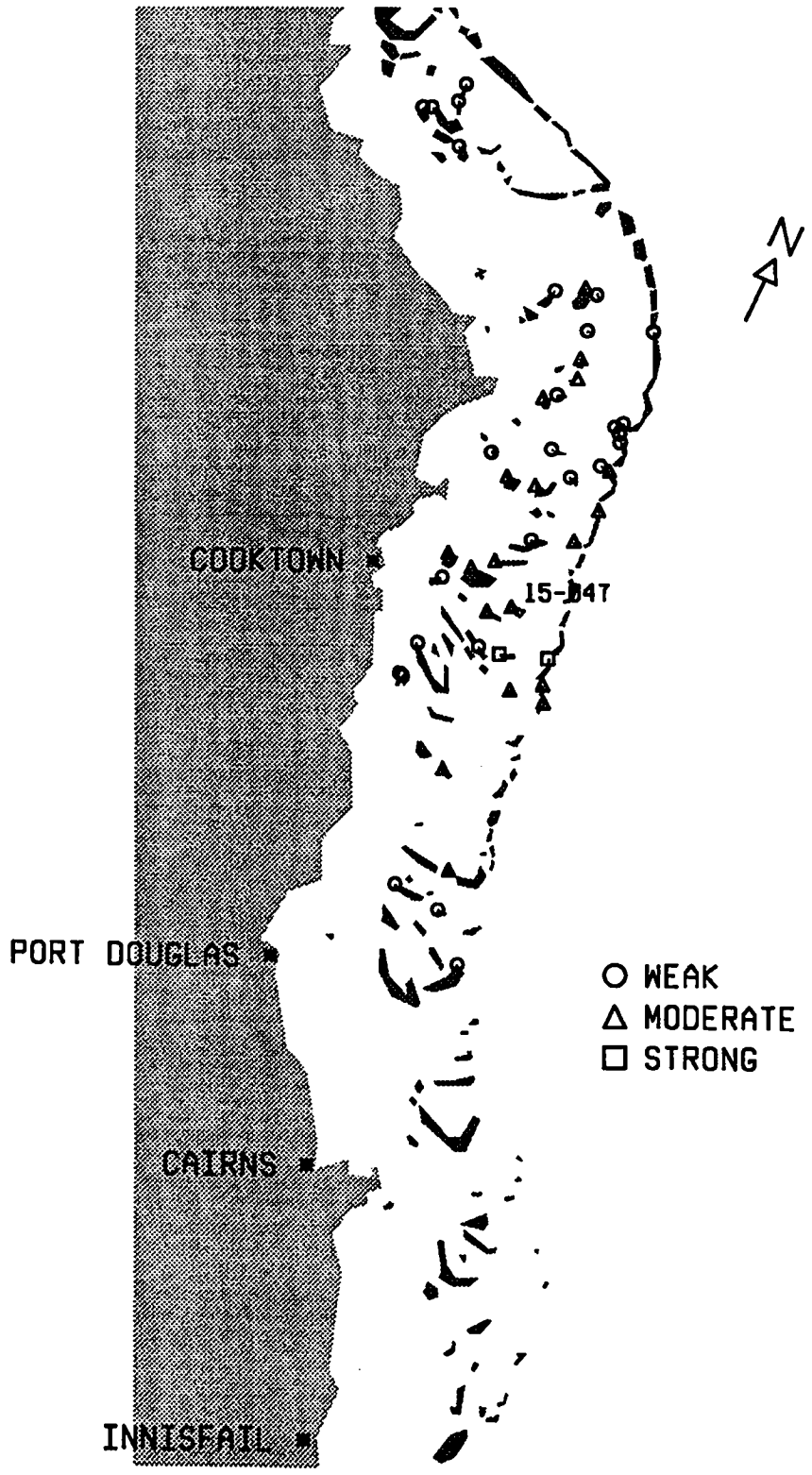


Figure C8 Strength of connectivity with respect to reef No.15-047 (source reef indicated without fill) for short pre-competent period larvae. The relative strength classes (weak, moderate and strong) represent probabilities separated by an order of magnitude. Scale: 1cm = 12 nautical miles.

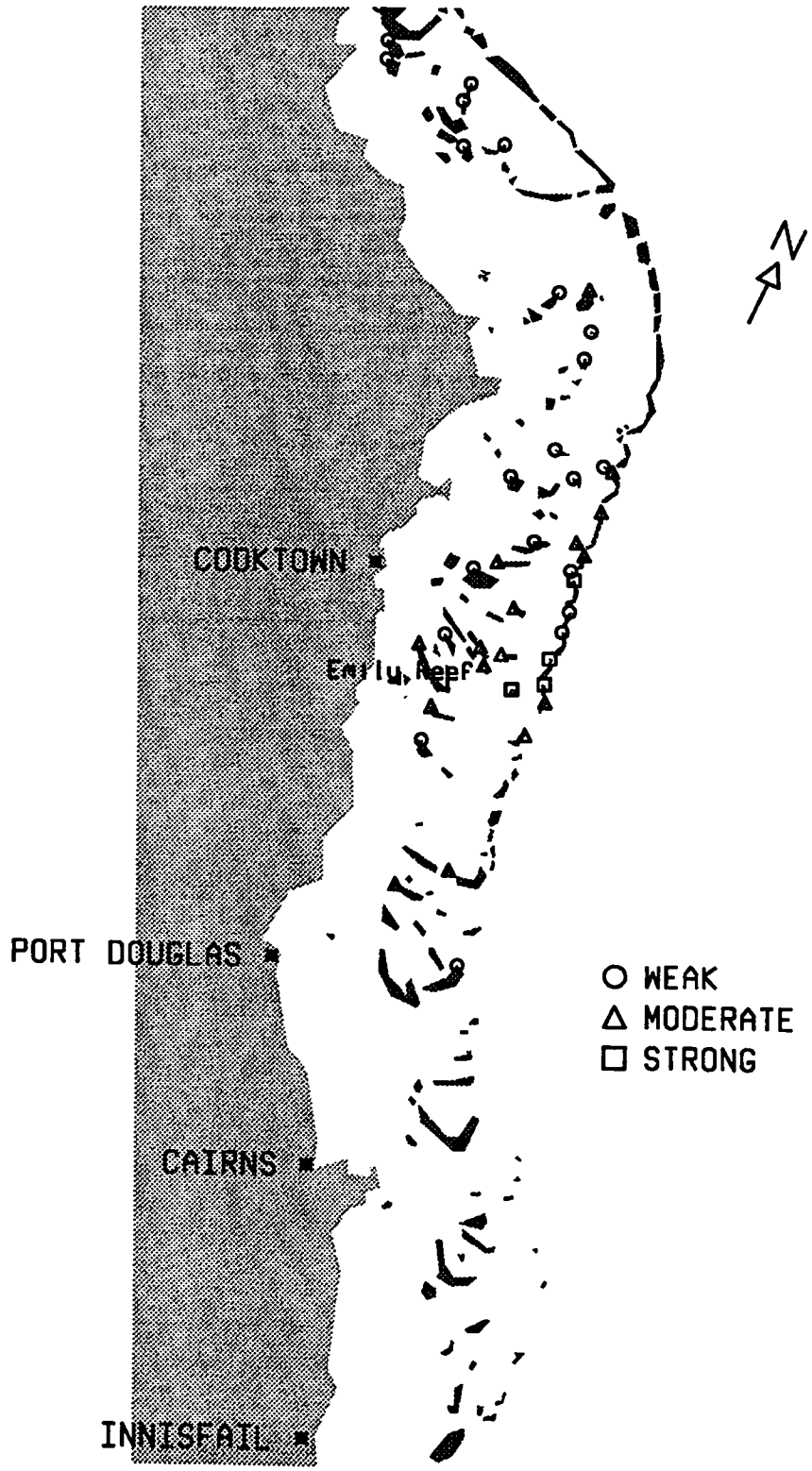


Figure C9 Strength of connectivity with respect to Emily Reef for short pre-competent period larvae. The relative strength classes (weak, moderate and strong) represent probabilities separated by an order of magnitude. Scale: 1cm = 12 nautical miles.

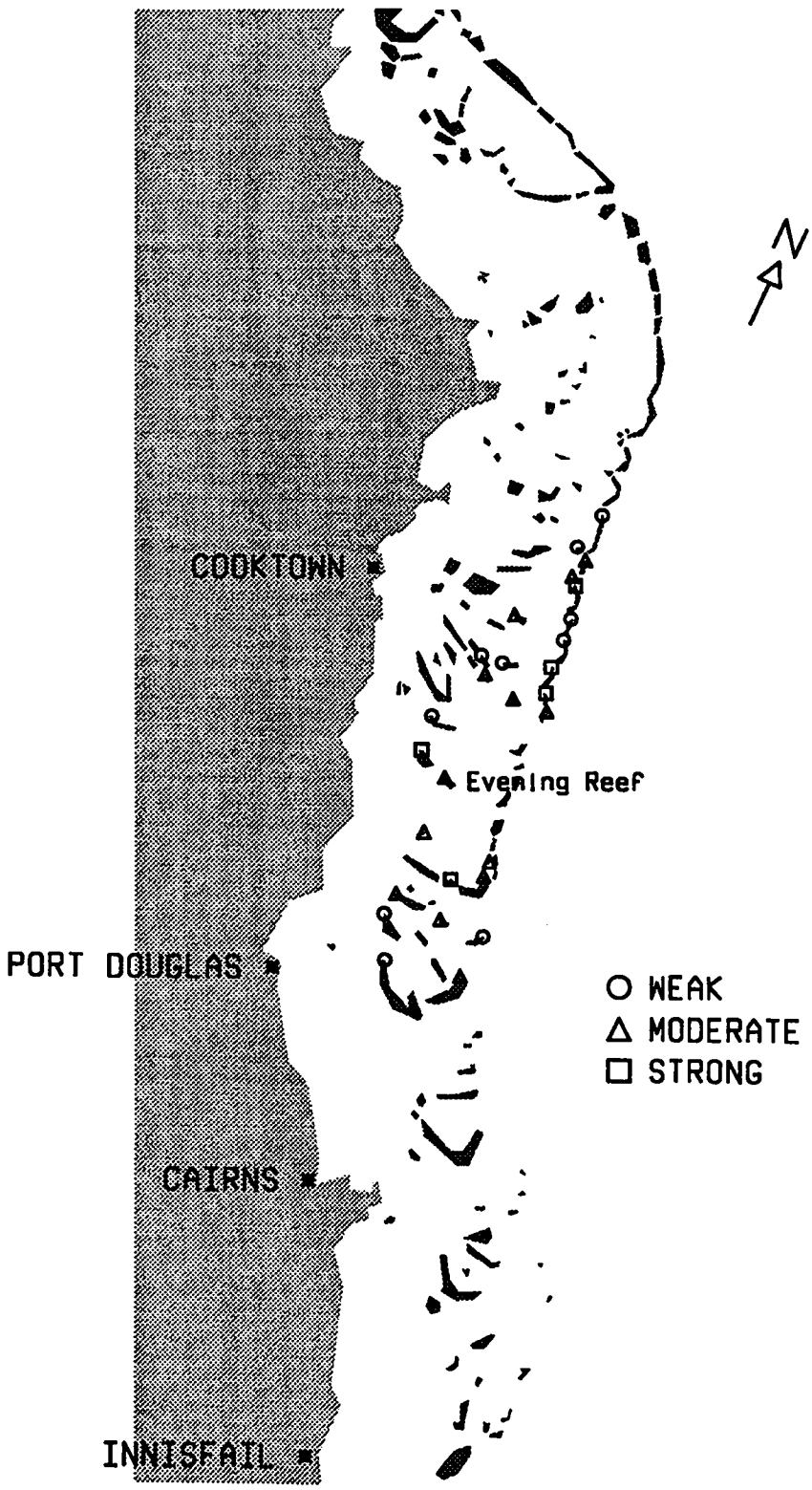


Figure C10 Strength of connectivity with respect to Evening Reef for short pre-competent period larvae. The relative strength classes (weak, moderate and strong) represent probabilities separated by an order of magnitude. Scale: 1cm = 12 nautical miles.

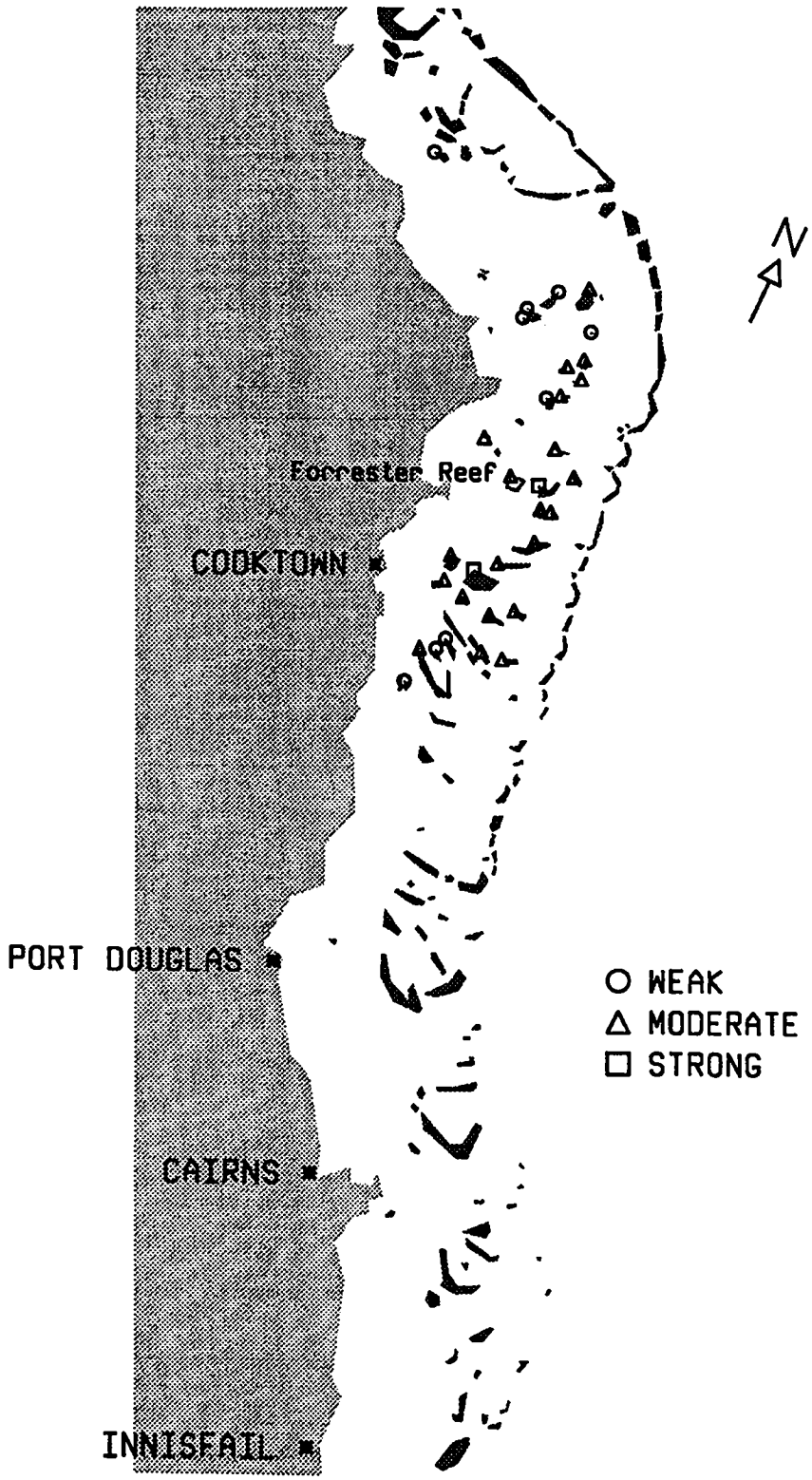


Figure C11 Strength of connectivity with respect to Forrester Reef (source reef indicated without fill) for short pre-competent period larvae. The relative strength classes (weak, moderate and strong) represent probabilities separated by an order of magnitude. Scale: 1cm = 12 nautical miles.

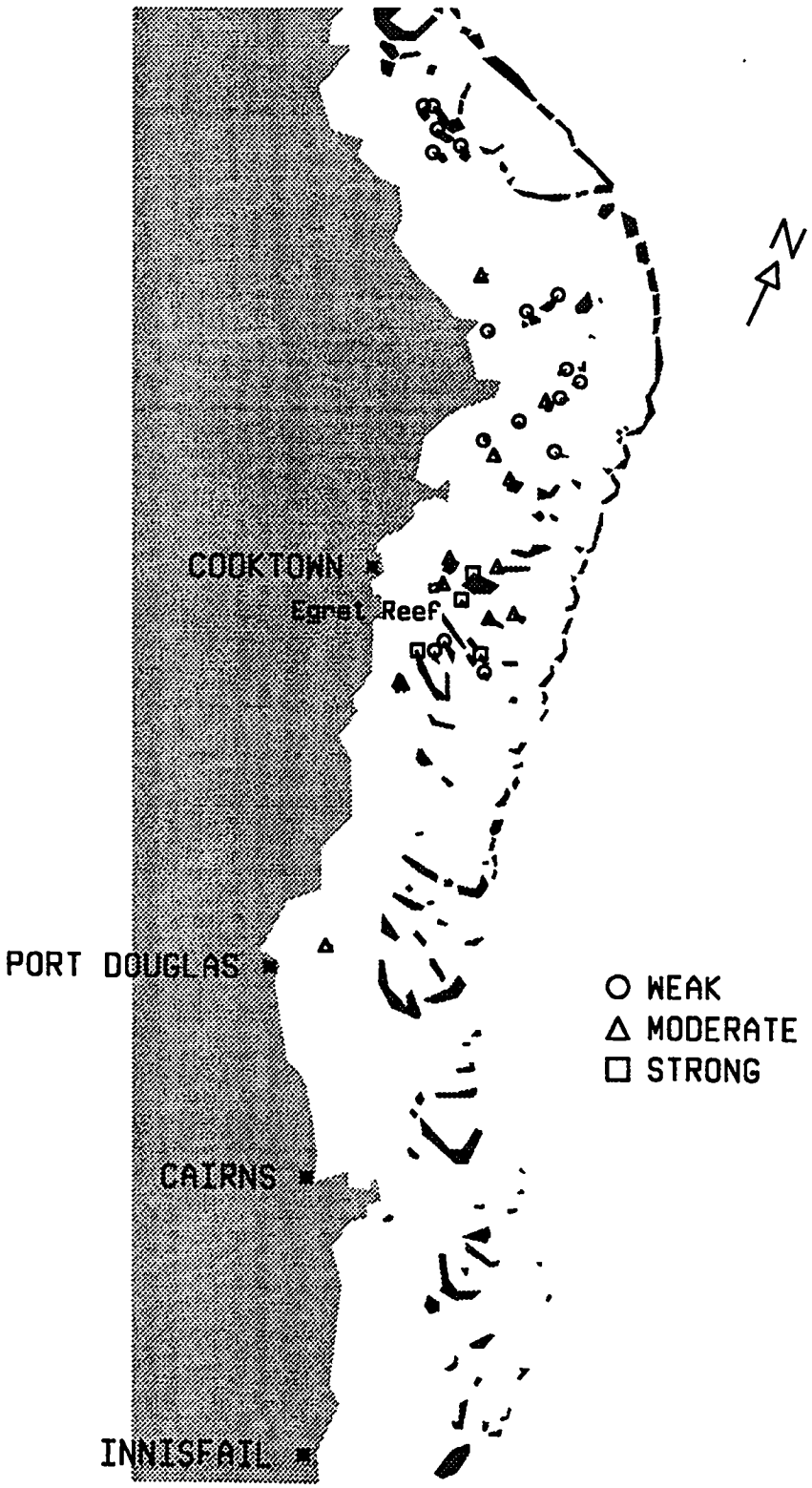


Figure C12 Strength of connectivity with respect to Egret Reef (source reef indicated without fill) for short pre-competent period larvae. The relative strength classes (weak, moderate and strong) represent probabilities separated by an order of magnitude. Scale: 1cm = 12 nautical miles.

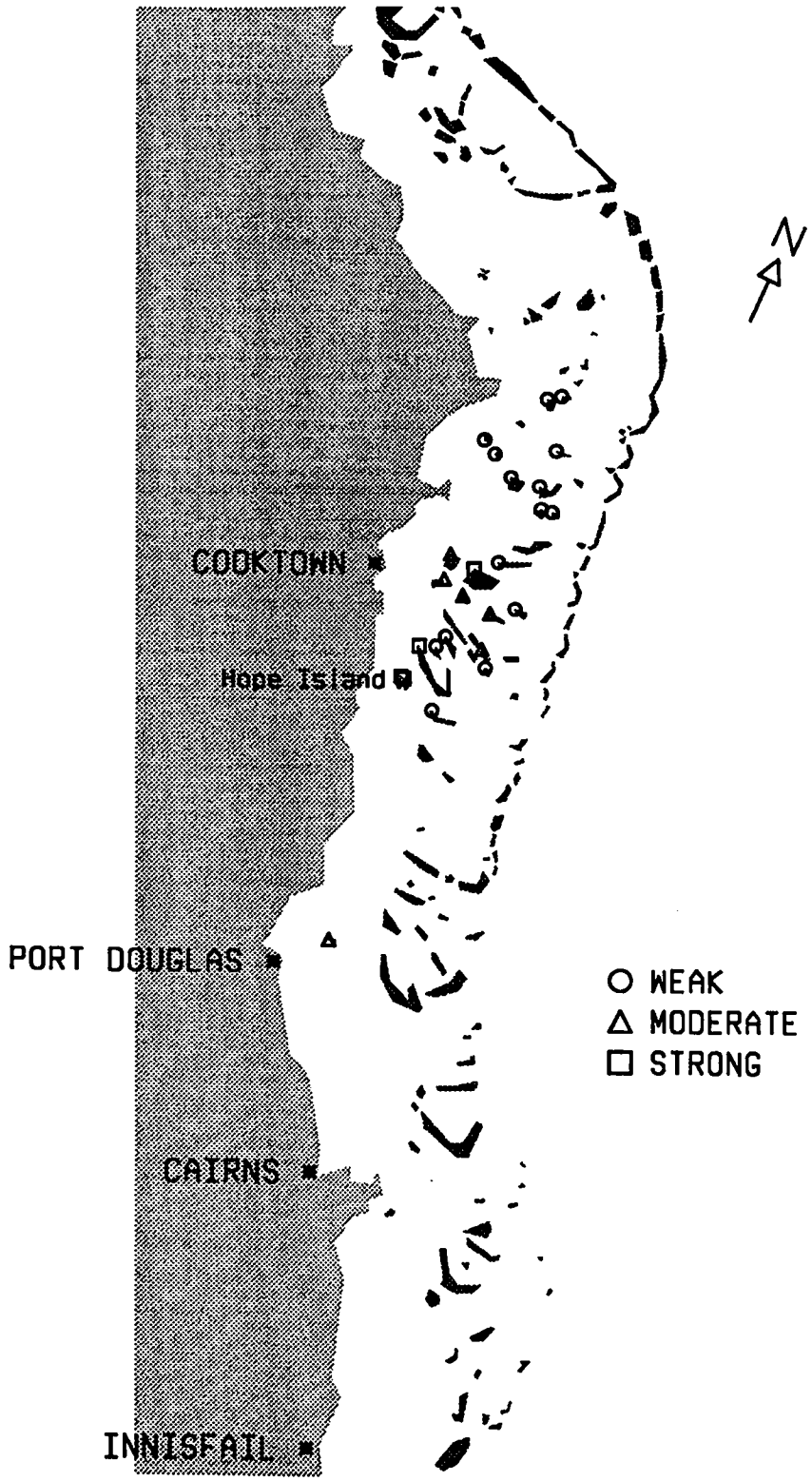


Figure C13 Strength of connectivity with respect to Hope Island for short pre-competent period larvae. The relative strength classes (weak, moderate and strong) represent probabilities separated by an order of magnitude. Scale: 1cm = 12 nautical miles.

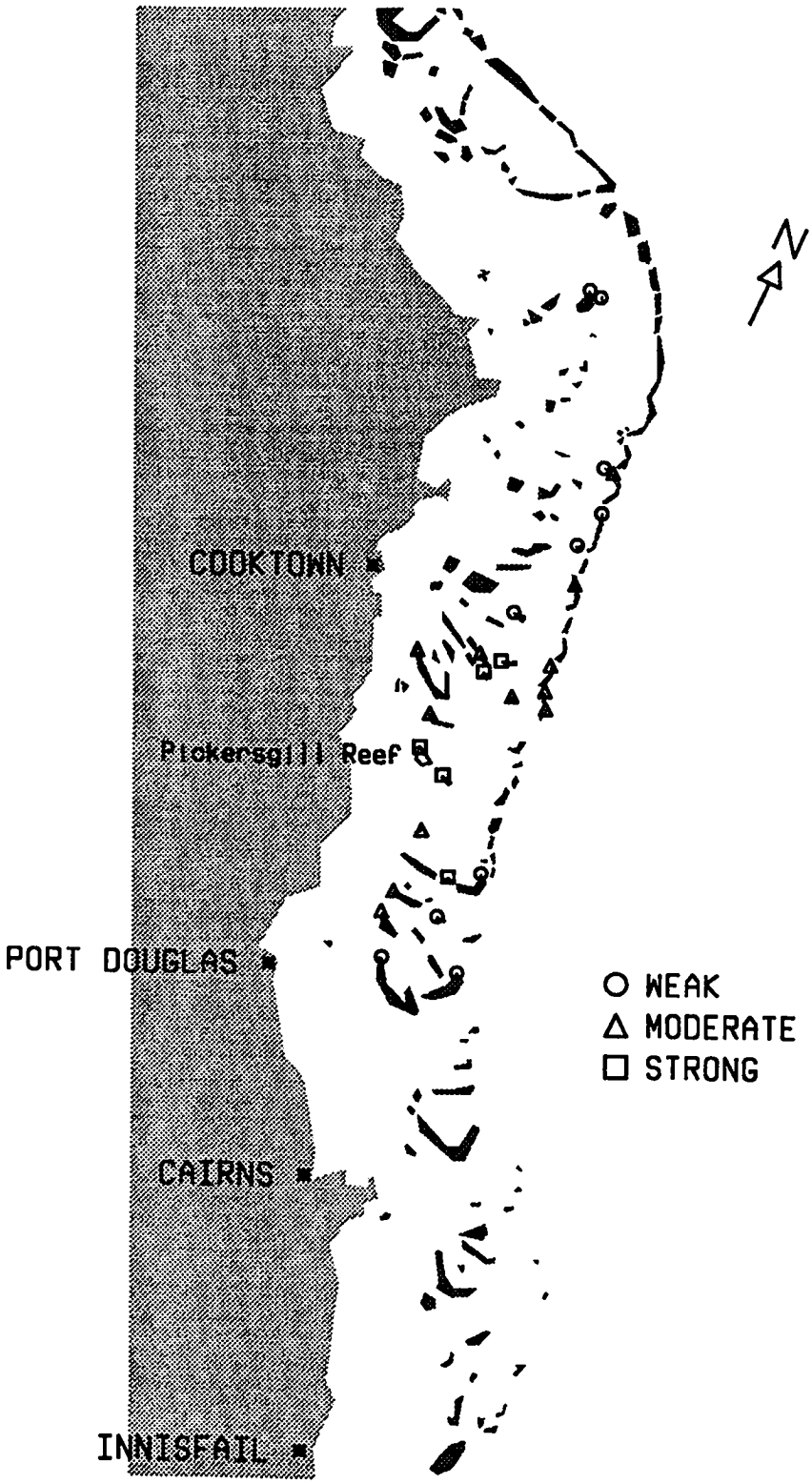


Figure C14 Strength of connectivity with respect to Pickersgill Reef (source reef indicated without fill) for short pre-competent period larvae. The relative strength classes (weak, moderate and strong) represent probabilities separated by an order of magnitude. Scale: 1cm = 12 nautical miles.

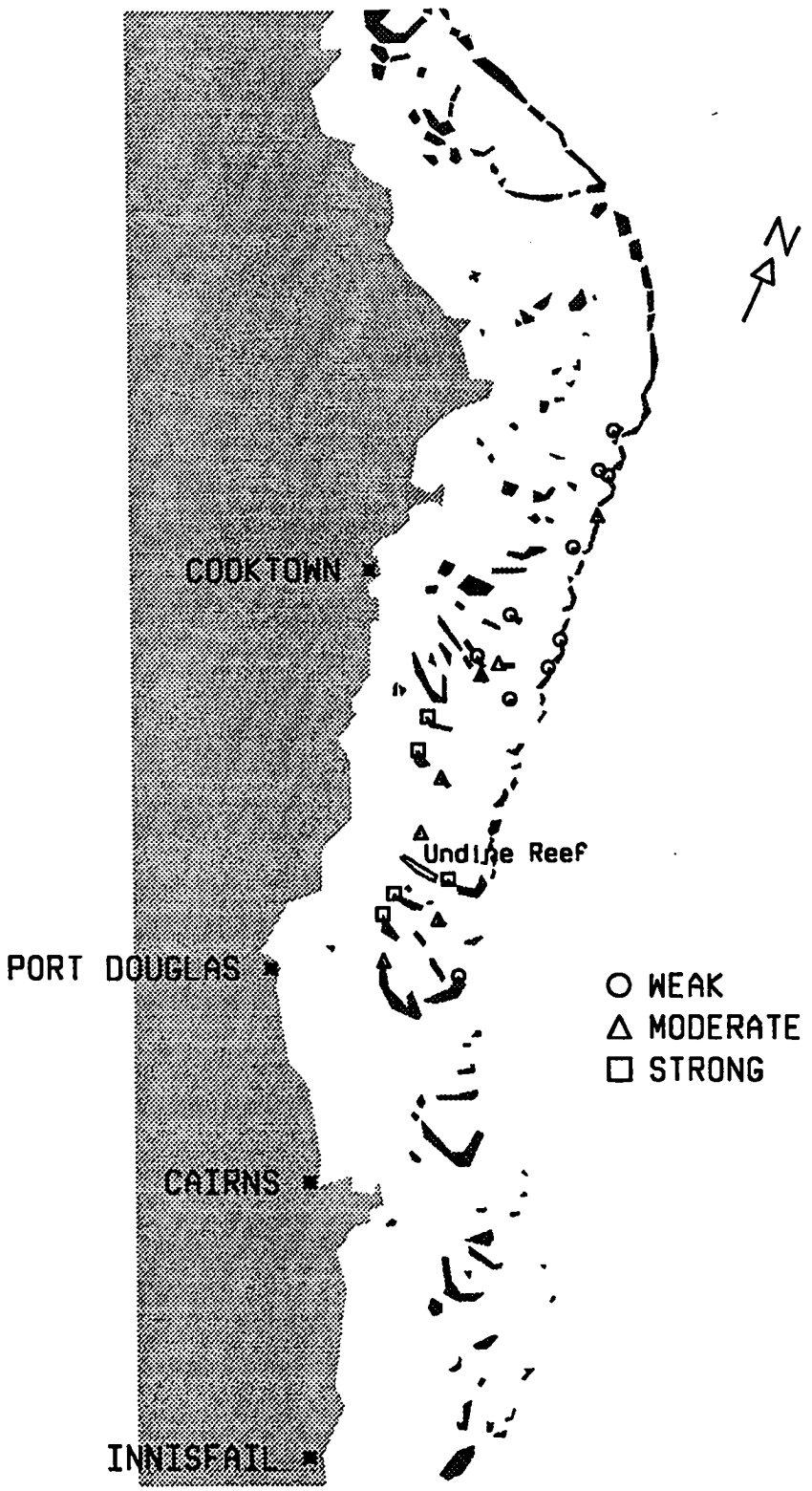


Figure C15 Strength of connectivity with respect to Undine Reef (source reef indicated without fill) for short pre-competent period larvae. The relative strength classes (weak, moderate and strong) represent probabilities separated by an order of magnitude. Scale: 1cm = 12 nautical miles.

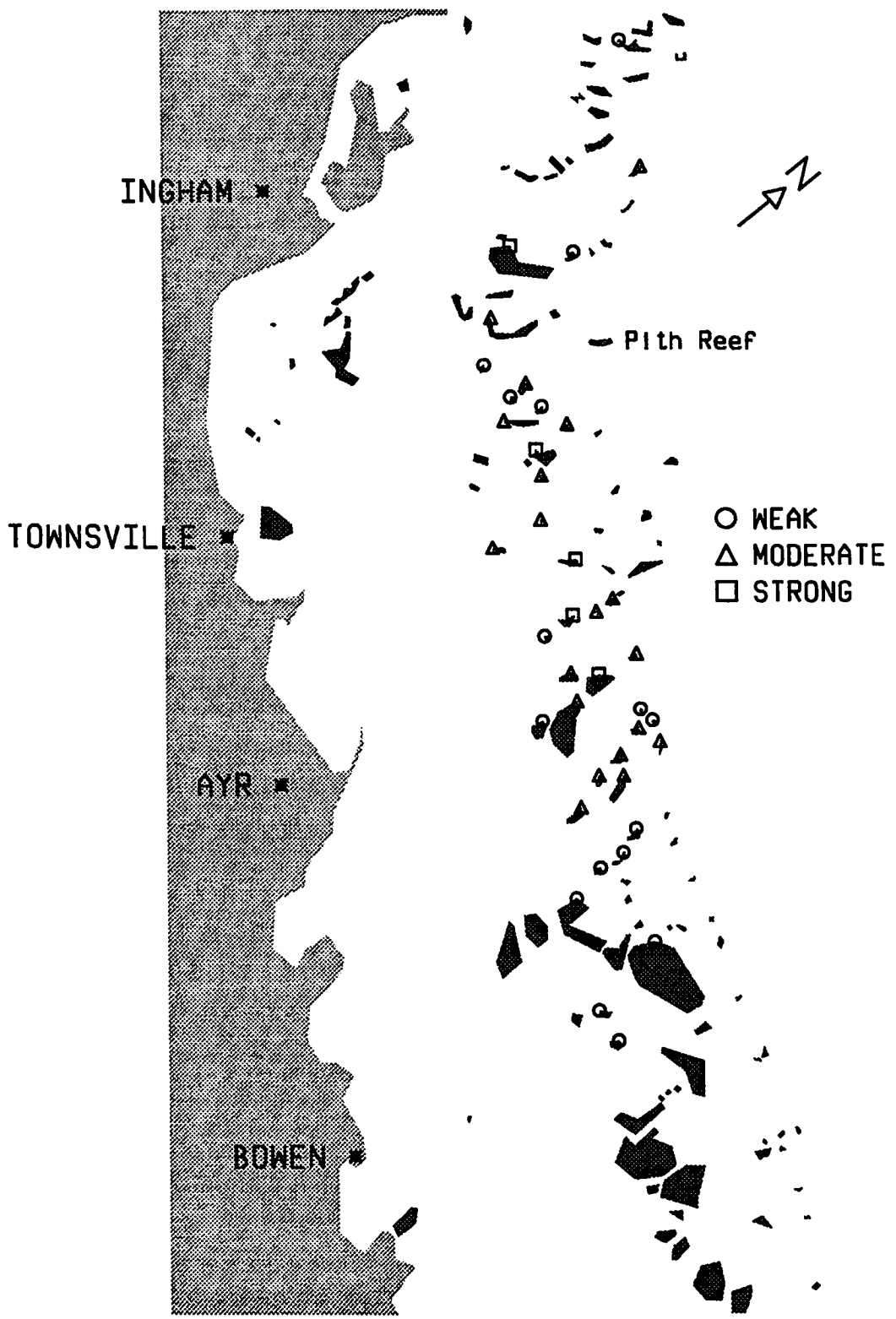


Figure C16 Strength of connectivity with respect to Pith Reef (source reef indicated without fill) for short pre-competent period larvae. The relative strength classes (weak, moderate and strong) represent probabilities separated by an order of magnitude. Scale: 1cm = 10 nautical miles.

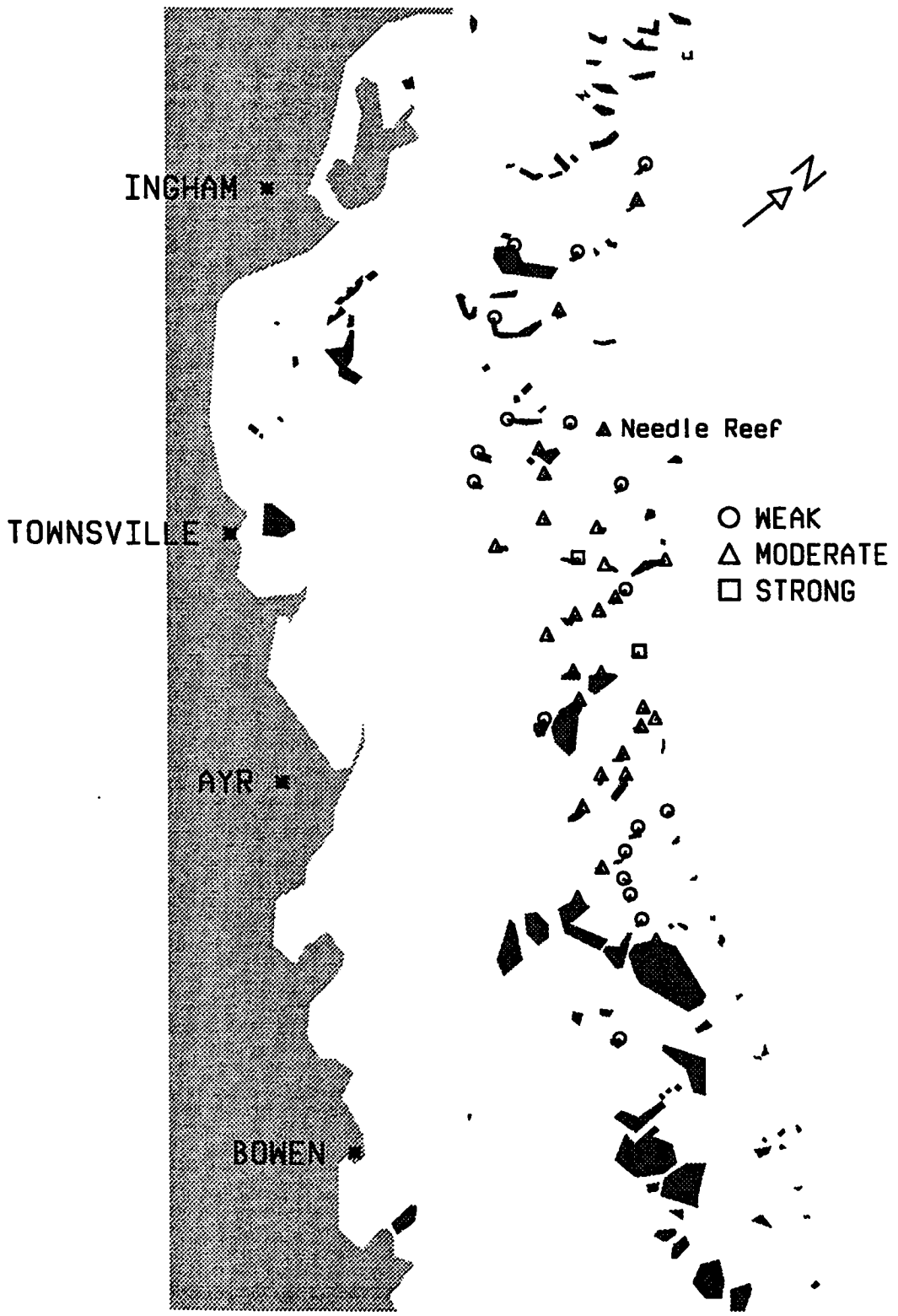


Figure C17 Strength of connectivity with respect to Needle Reef for short pre-competent period larvae. The relative strength classes (weak, moderate and strong) represent probabilities separated by an order of magnitude. Scale: 1cm = 10 nautical miles.

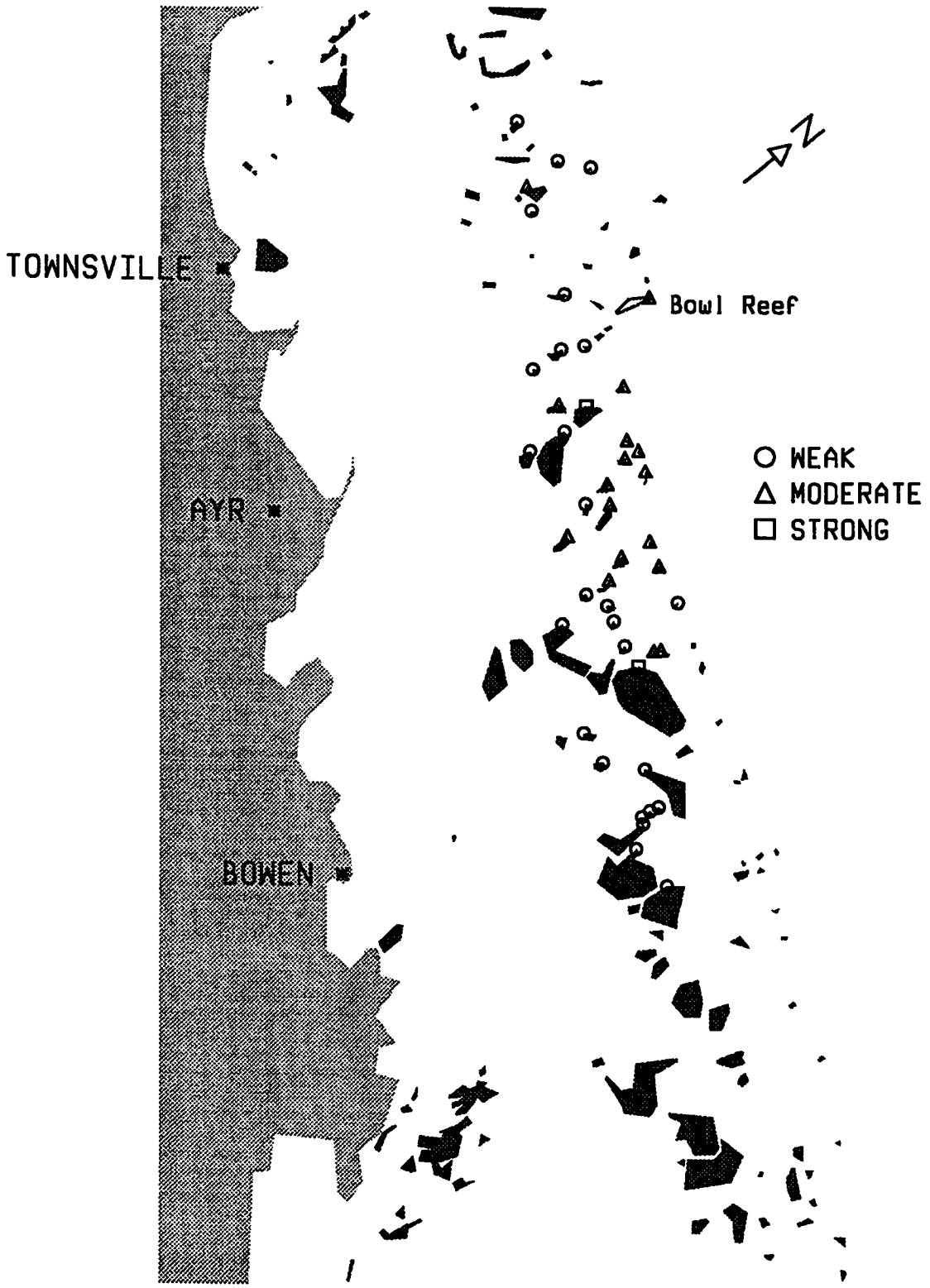


Figure C18 Strength of connectivity with respect to Bowl Reef (source reef indicated without fill) for short pre-competent period larvae. The relative strength classes (weak, moderate and strong) represent probabilities separated by an order of magnitude. Scale: 1cm = 10 nautical miles.

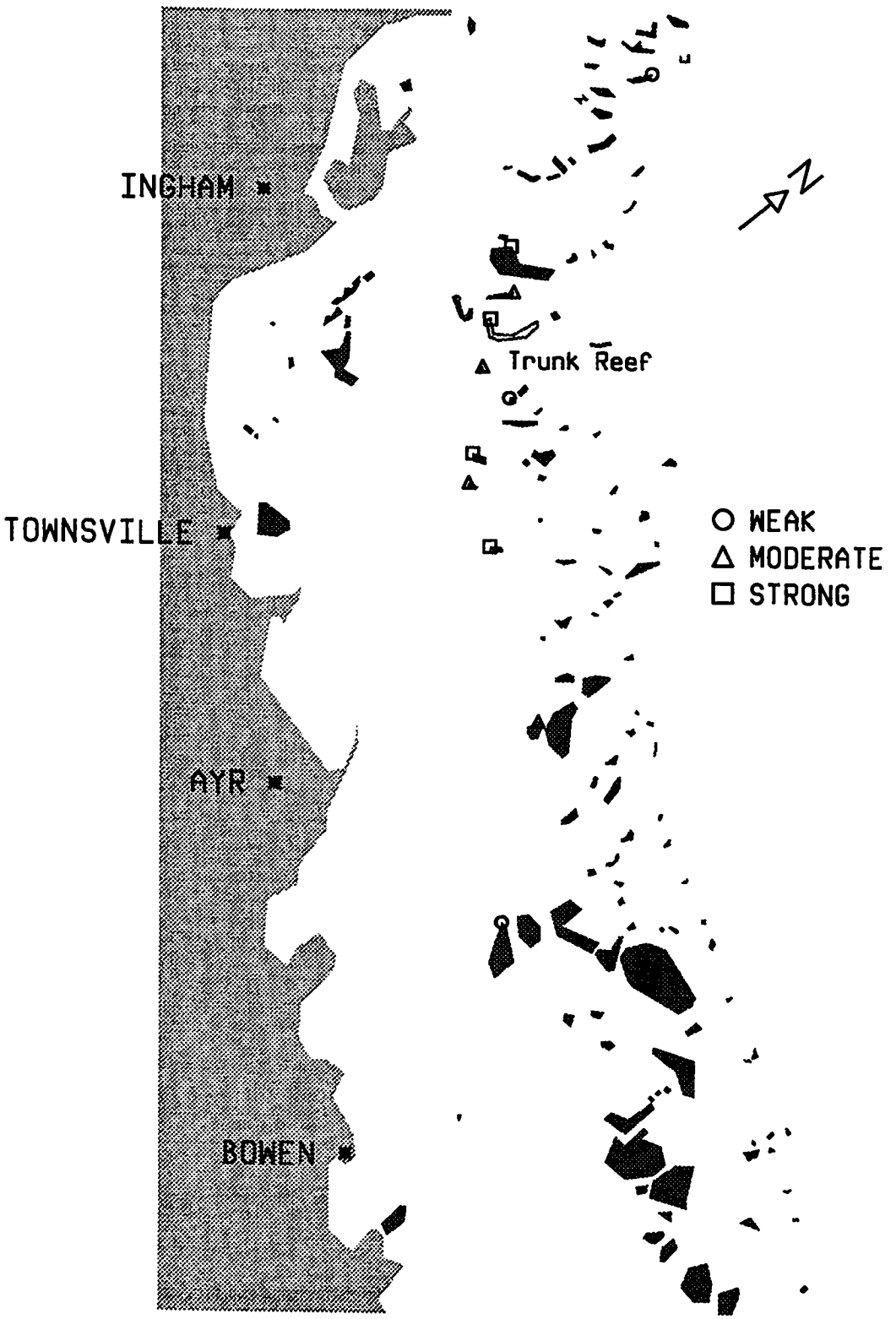


Figure C19 Strength of connectivity with respect to Trunk Reef (source reef indicated without fill) for short pre-competent period larvae. The relative strength classes (weak, moderate and strong) represent probabilities separated by an order of magnitude. Scale: 1cm = 10 nautical miles.

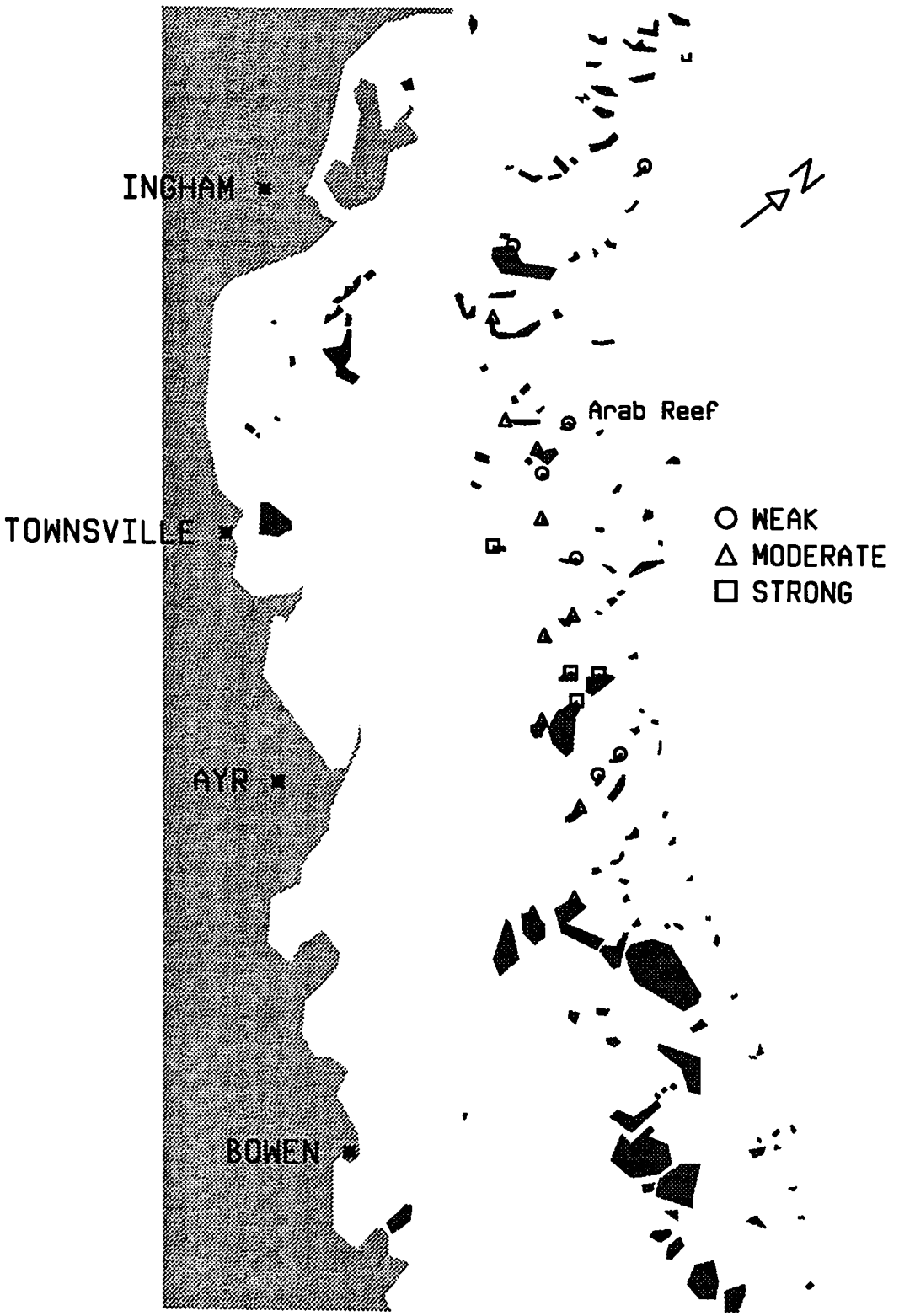


Figure C20 Strength of connectivity with respect to Arab Reef (source reef indicated without fill) for short pre-competent period larvae. The relative strength classes (weak, moderate and strong) represent probabilities separated by an order of magnitude. Scale: 1cm = 10 nautical miles.

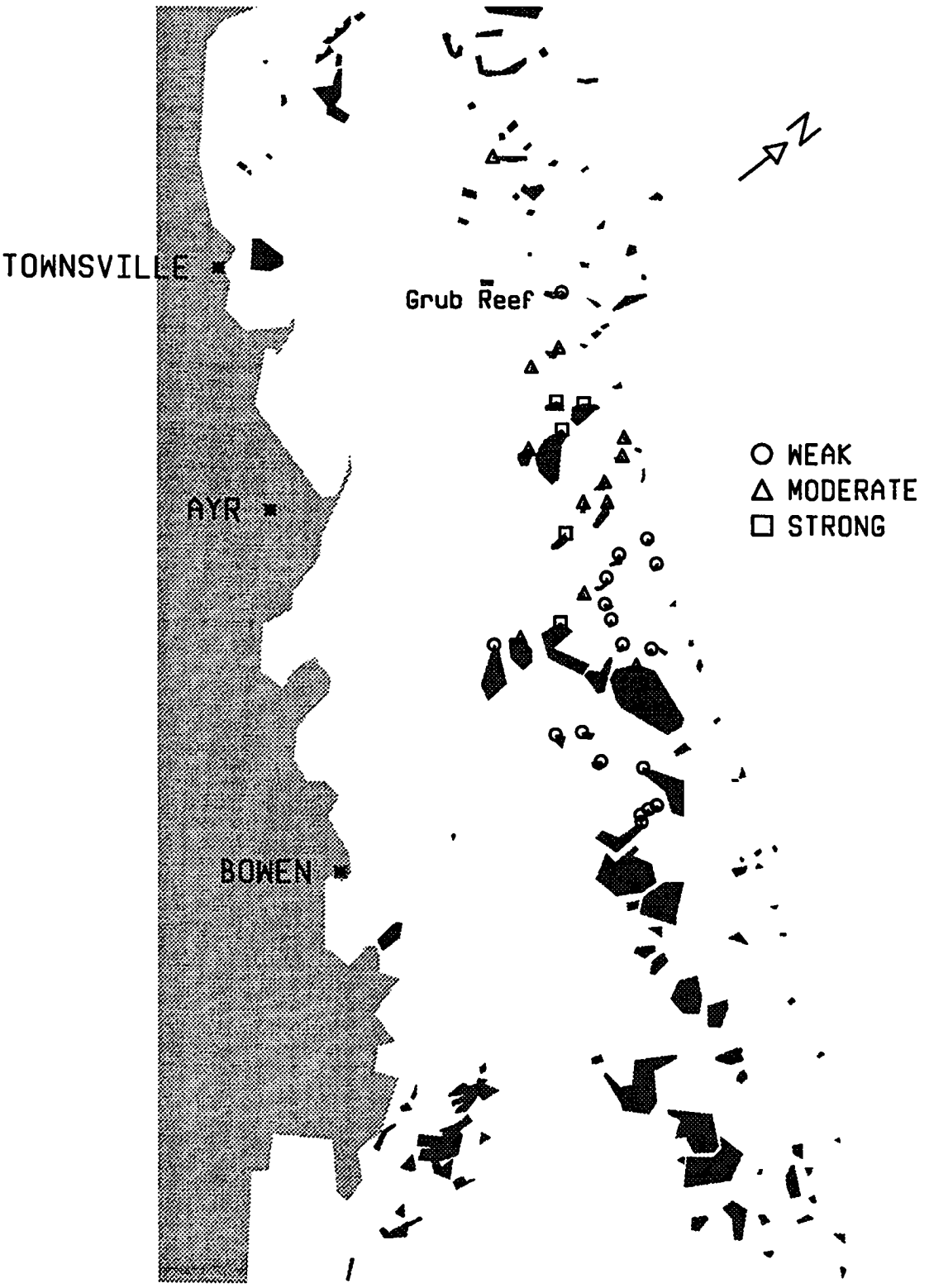


Figure C21 Strength of connectivity with respect to Grub Reef (source reef indicated without fill) for short pre-competent period larvae. The relative strength classes (weak, moderate and strong) represent probabilities separated by an order of magnitude. Scale: 1cm = 10 nautical miles.

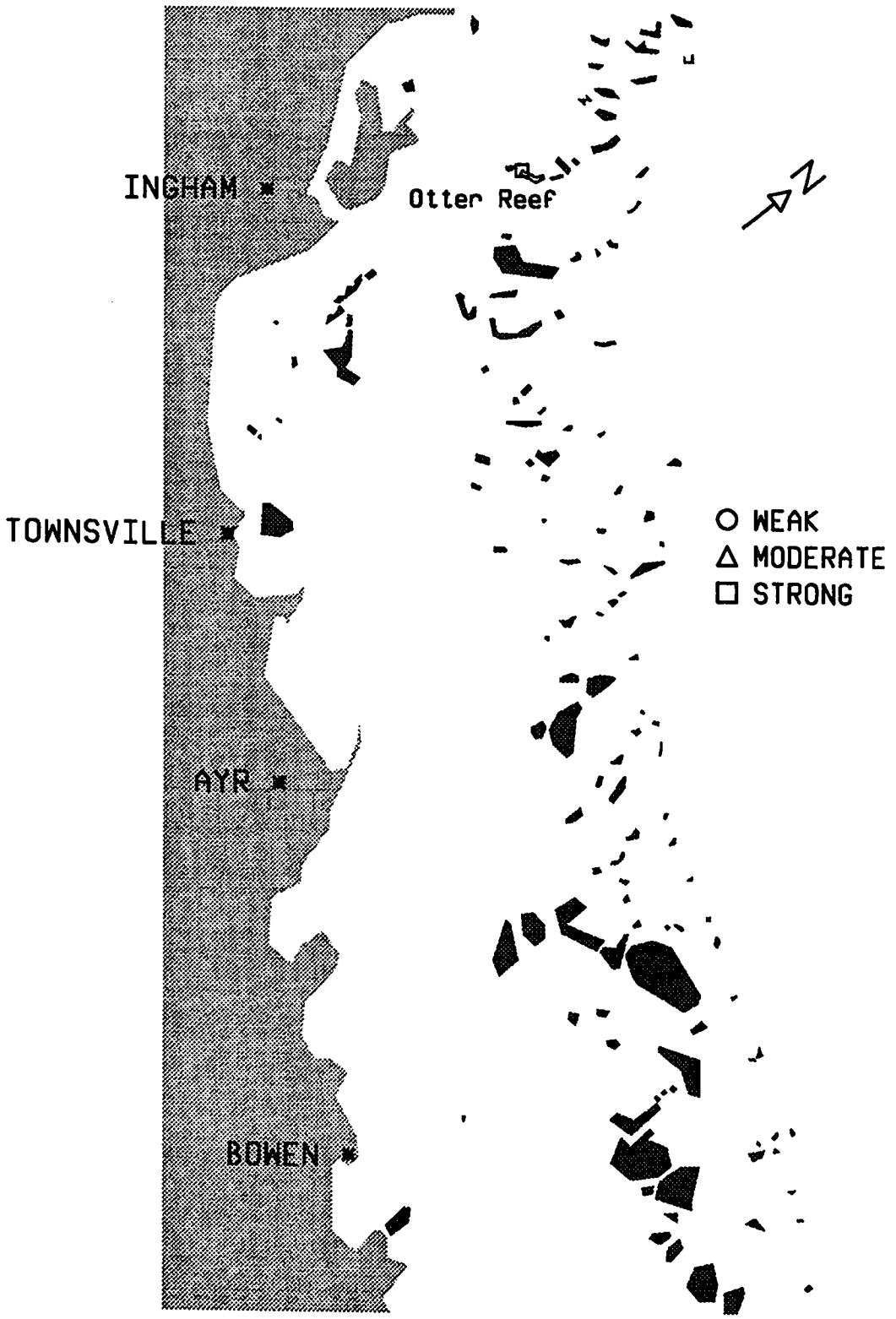


Figure C22 Strength of connectivity with respect to Otter Reef (source reef indicated without fill) for short pre-competent period larvae. The relative strength classes (weak, moderate and strong) represent probabilities separated by an order of magnitude. Scale: 1cm = 10 nautical miles.

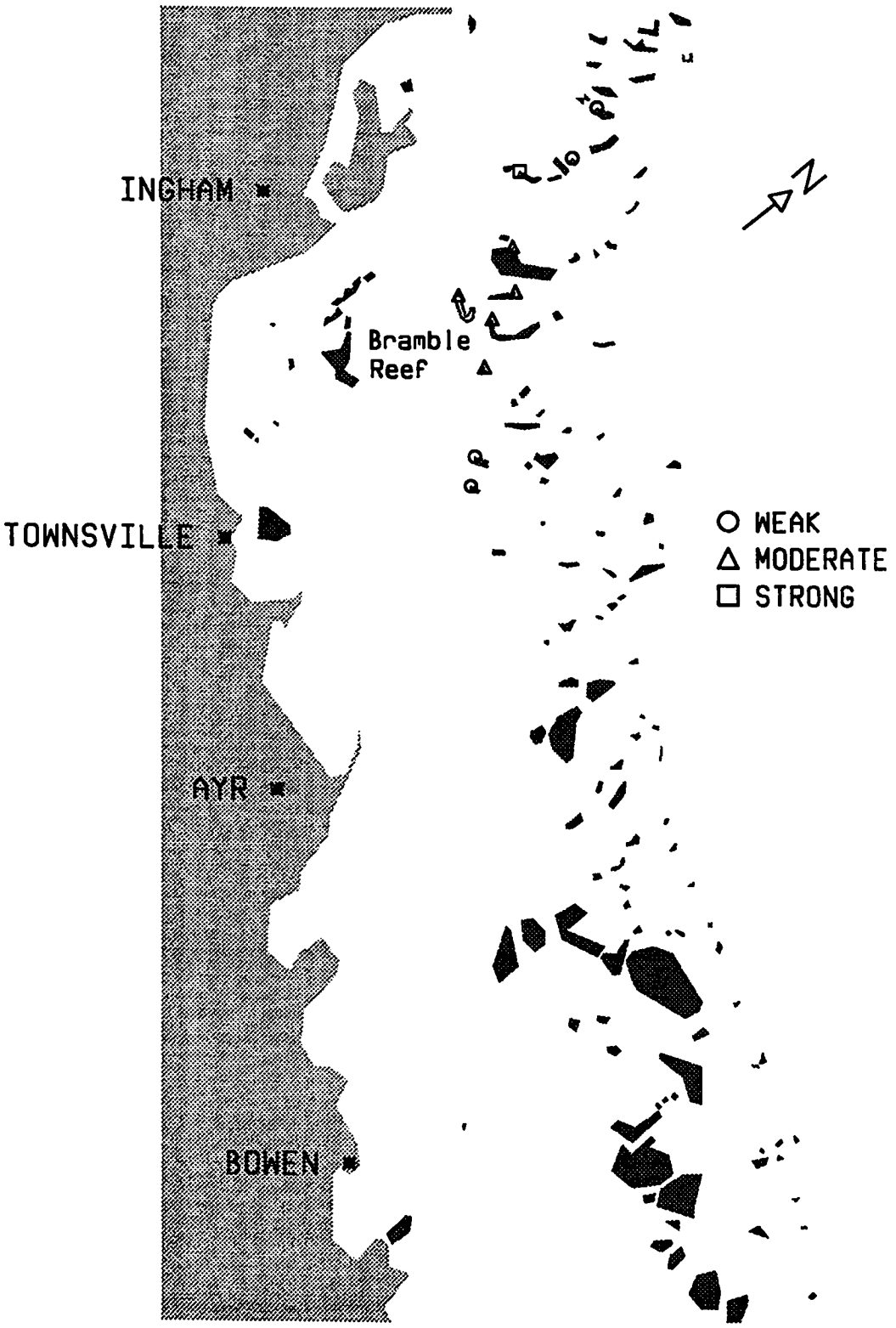


Figure C23 Strength of connectivity with respect to Bramble Reef (source reef indicated without fill) for short pre-competent period larvae. The relative strength classes (weak, moderate and strong) represent probabilities separated by an order of magnitude. Scale: 1cm = 10 nautical miles.

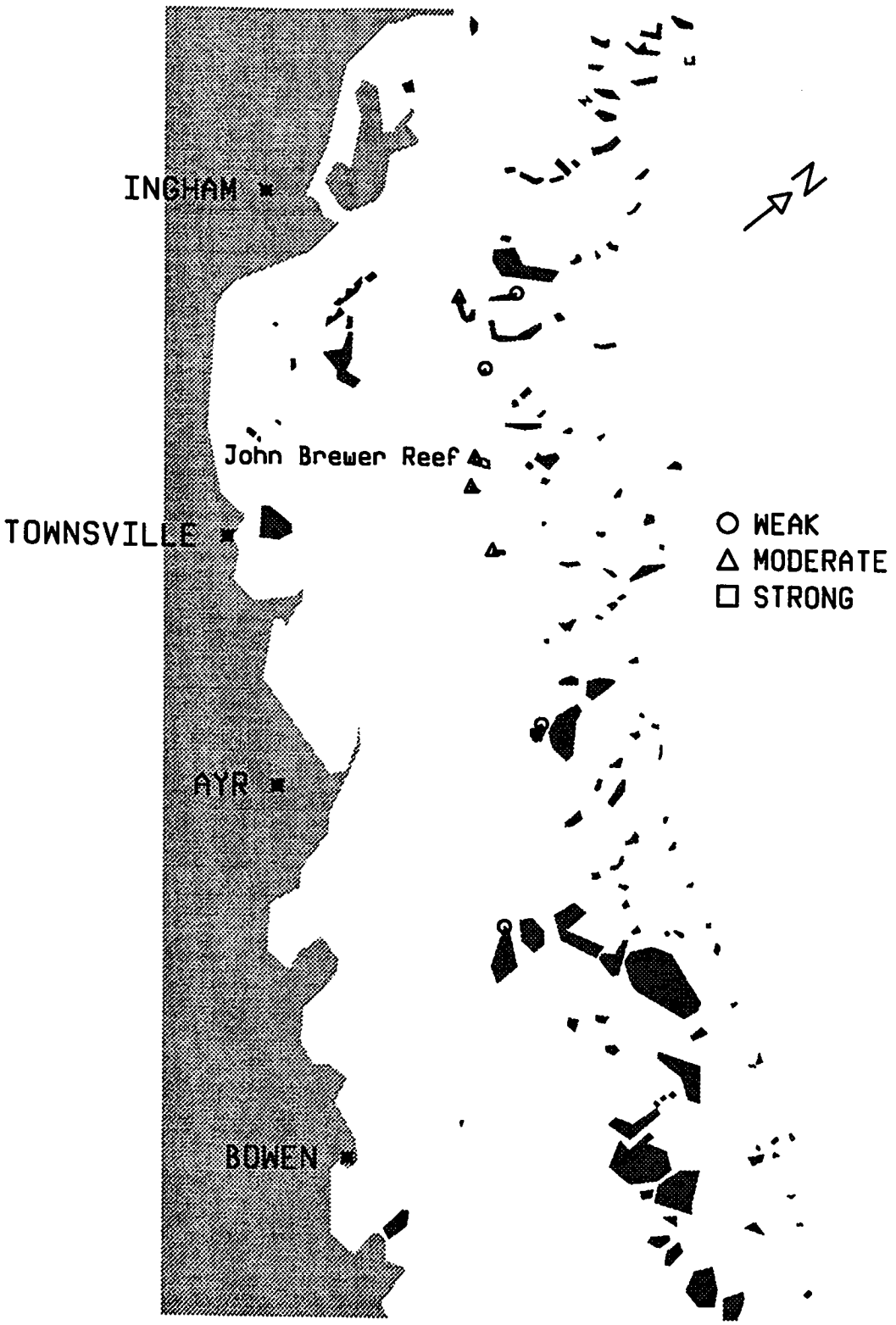


Figure C24 Strength of connectivity with respect to John Brewer Reef (source reef indicated without fill) for short pre-competent period larvae. The relative strength classes (weak, moderate and strong) represent probabilities separated by an order of magnitude. Scale: 1cm = 10 nautical miles.

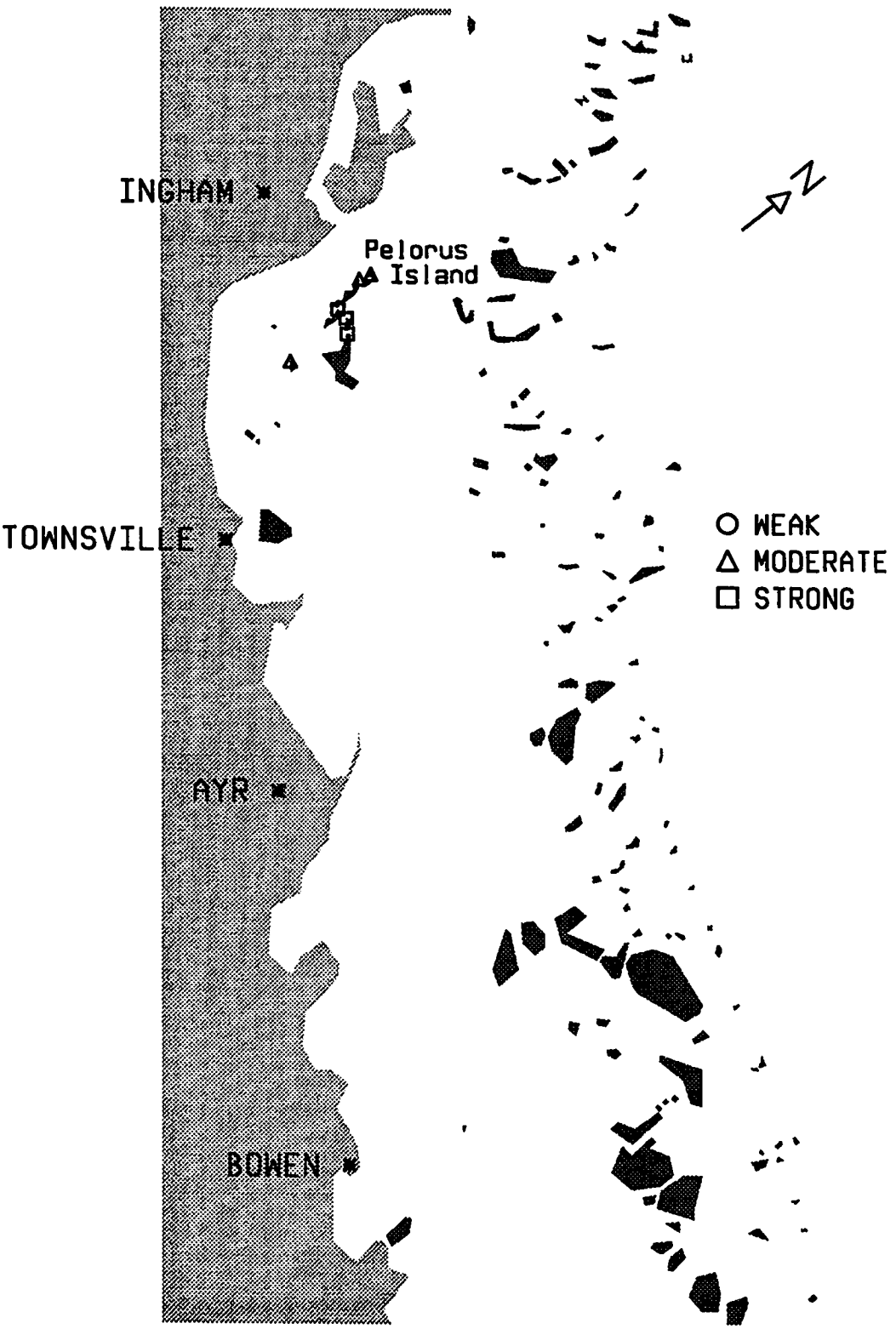


Figure C25 Strength of connectivity with respect to Pelorus Island for short pre-competent period larvae. The relative strength classes (weak, moderate and strong) represent probabilities separated by an order of magnitude. Scale: 1cm = 10 nautical miles.

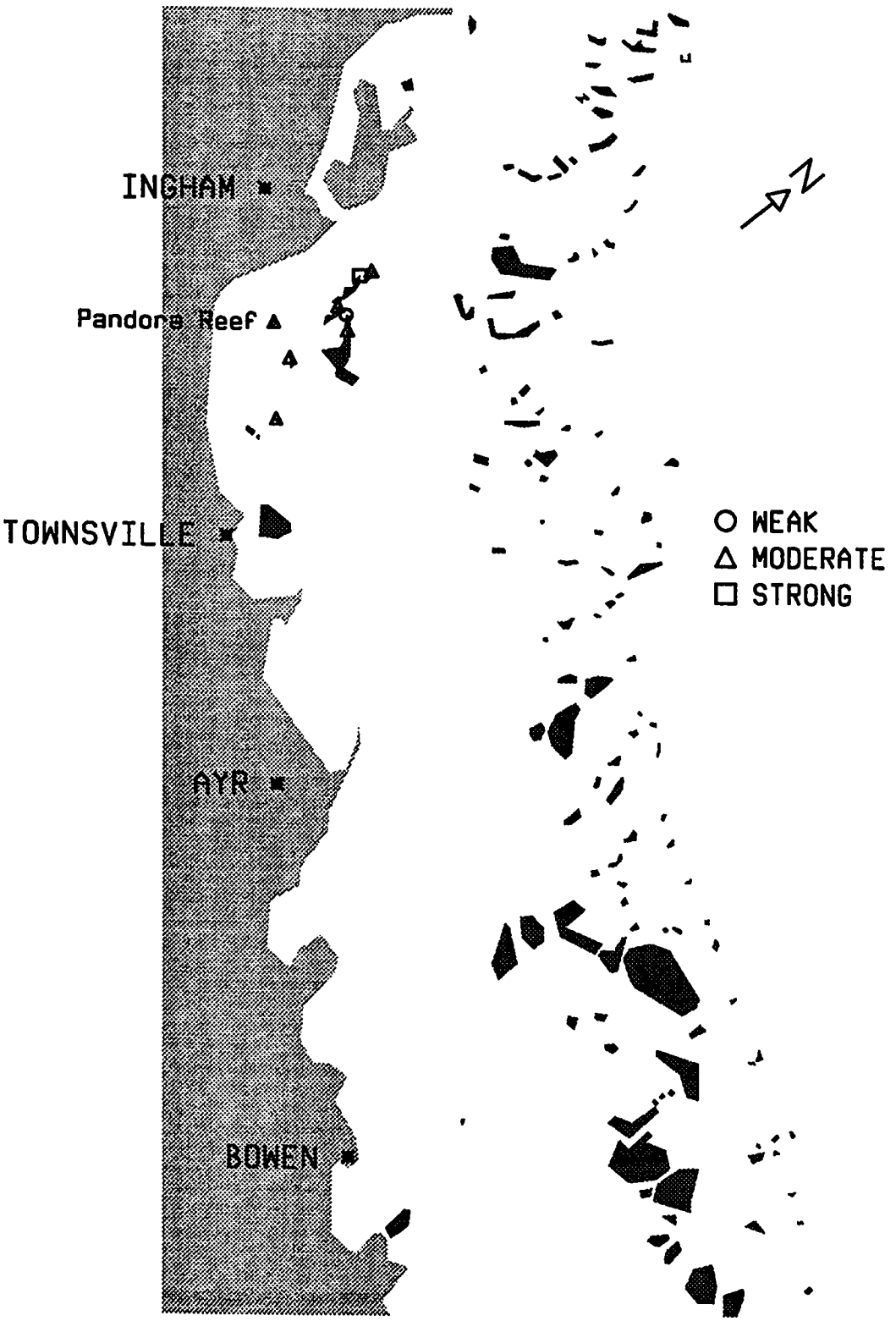


Figure C26 Strength of connectivity with respect to Pandora Reef for short pre-competent period larvae. The relative strength classes (weak, moderate and strong) represent probabilities separated by an order of magnitude. Scale: 1cm = 10 nautical miles.

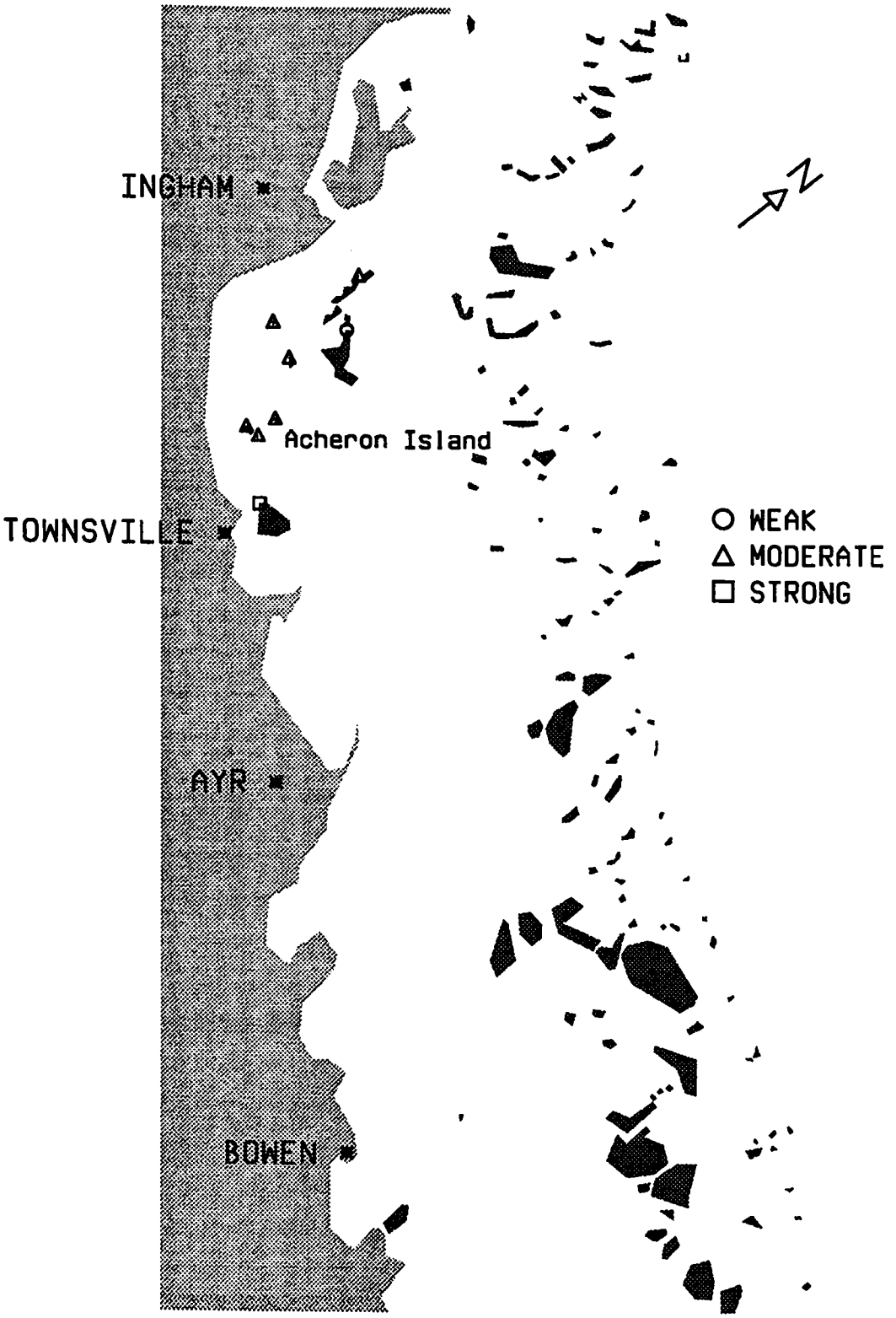


Figure C27 Strength of connectivity with respect to Acheron Island for short pre-competent period larvae. The relative strength classes (weak, moderate and strong) represent probabilities separated by an order of magnitude. Scale: 1cm = 10 nautical miles.

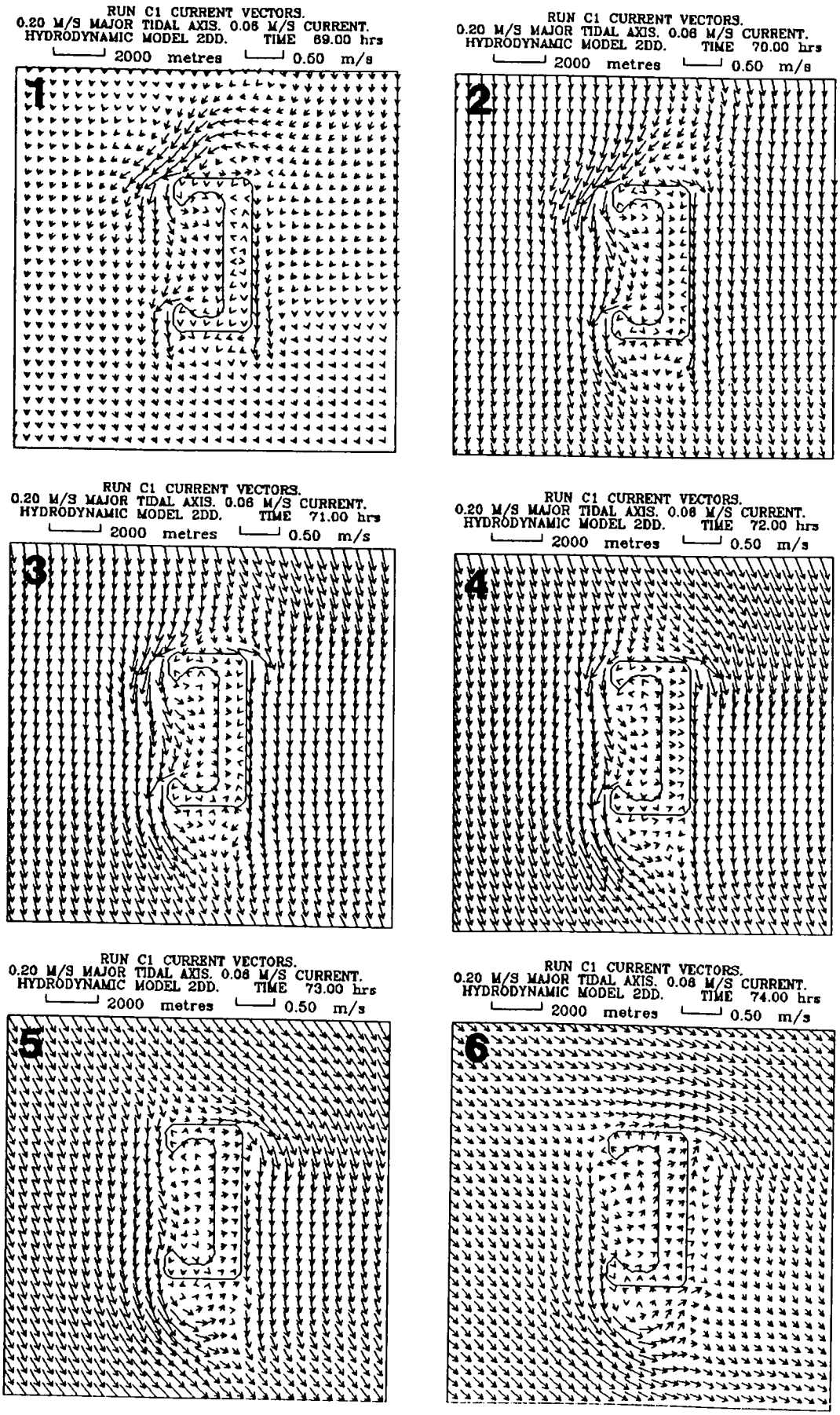


Figure D1a Representative plots of current vectors over a tidal cycle for reef type L2. The long-shelf current speed is set to 6 cm s^{-1}. Plots (labelled 1 to 6) represent currents at one hour intervals from when the tide begins to flood.

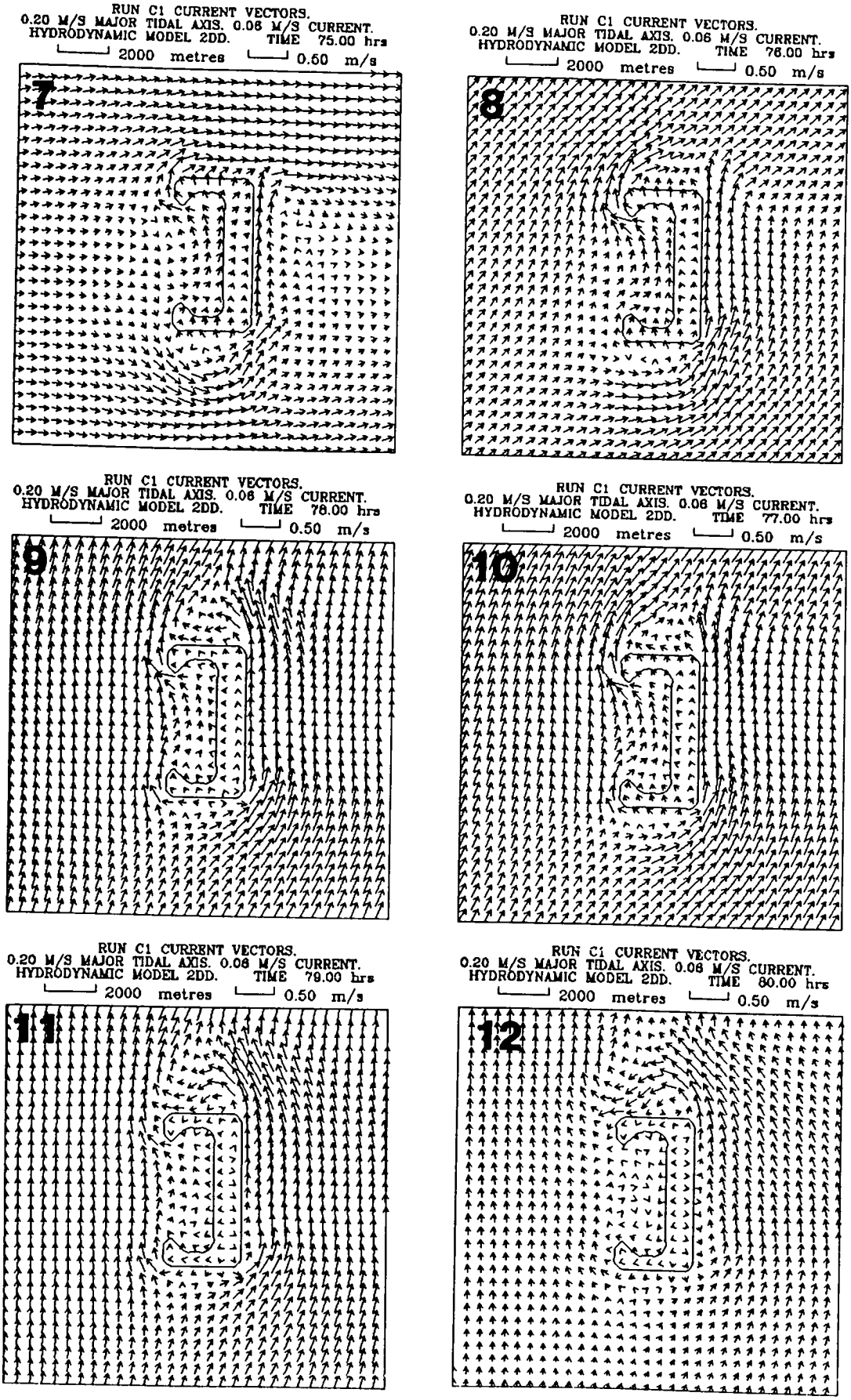


Figure D1b Representative plots of current vectors over a tidal cycle for reef type L2. The long-shelf current speed is set to 6 cm s^{-1}. Plots (labelled 7 to 12) represent currents at one hour intervals from when the tide begins to ebb.

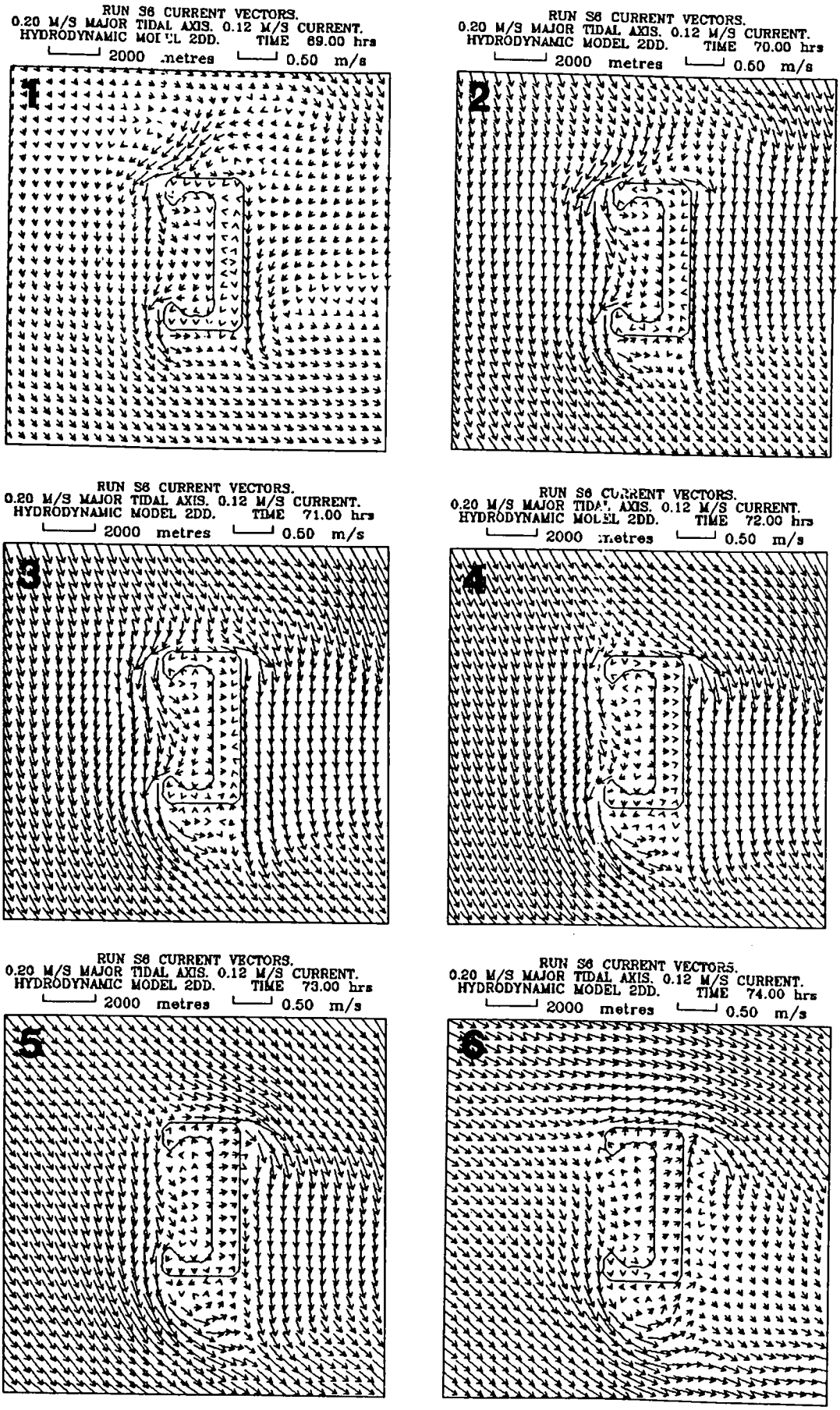


Figure D2a Representative plots of current vectors over a tidal cycle for reef type L2. The long-shelf current speed is set to 12 cm s^{-1}. Plots (labelled 1 to 6) represent currents at one hour intervals from when the tide begins to flood.

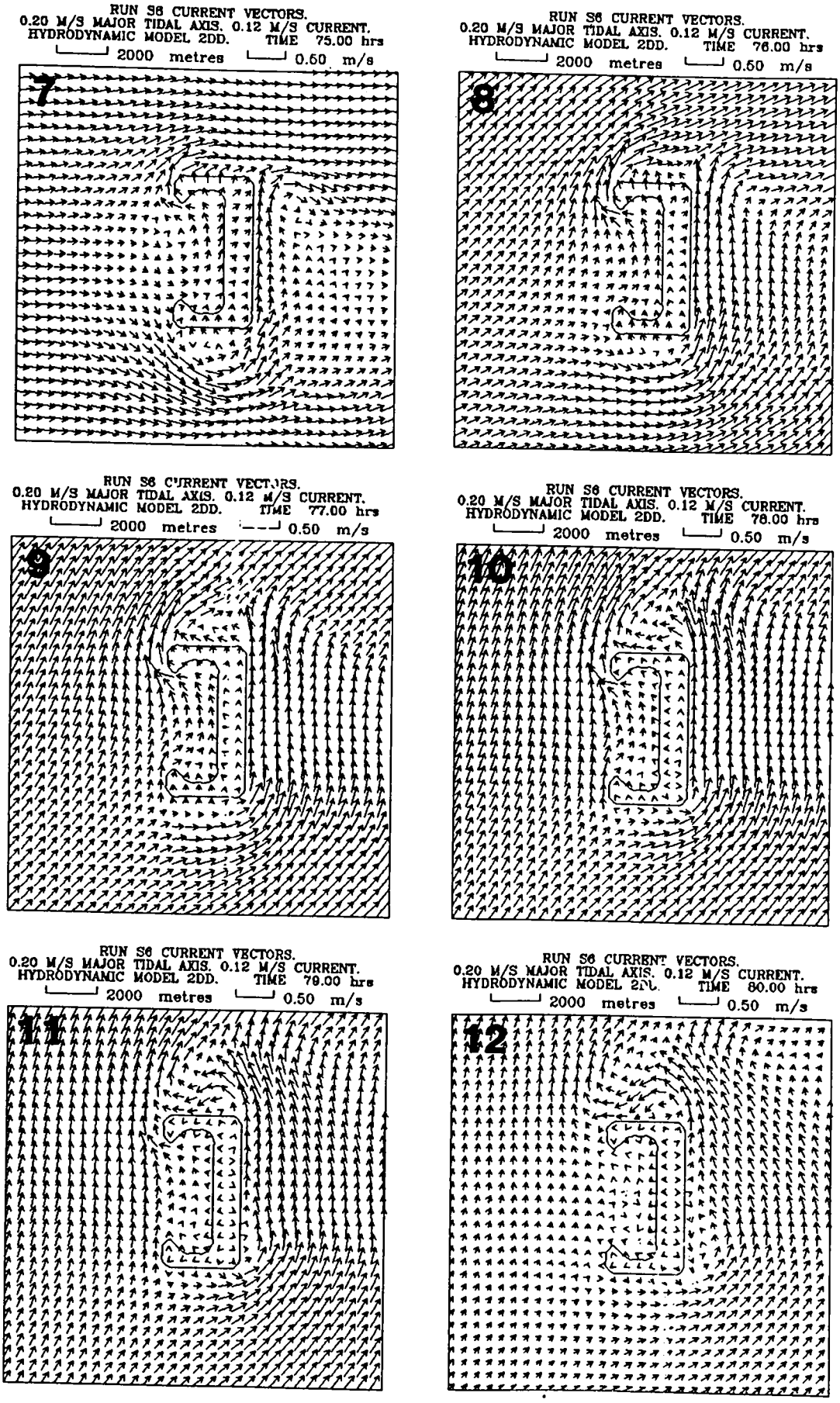


Figure D2b Representative plots of current vectors over a tidal cycle for reef type L2. The long-shelf current speed is set to 12 cm s^{-1}. Plots (labelled 7 to 12) represent currents at one hour intervals from when the tide begins to ebb.

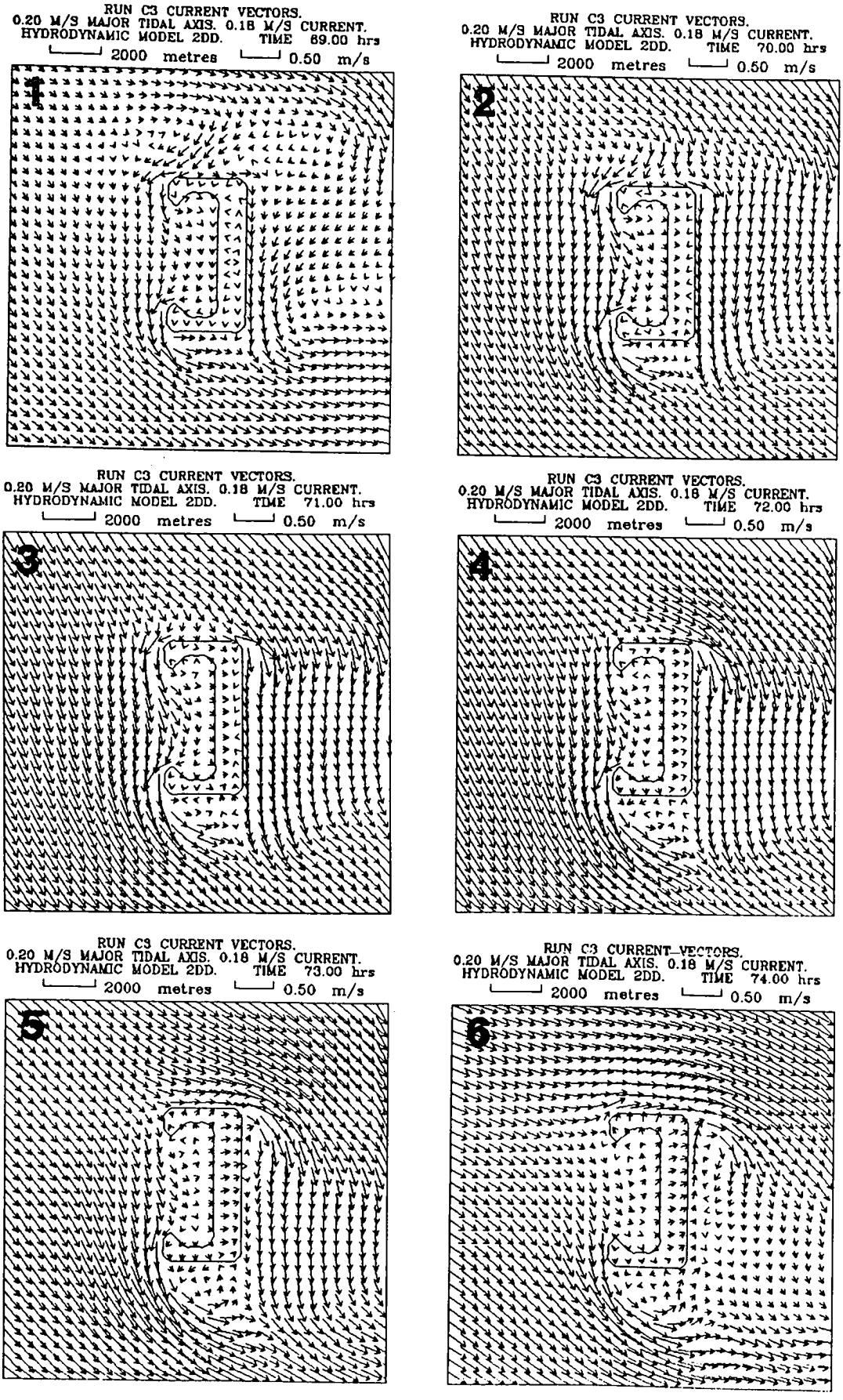


Figure D3a Representative plots of current vectors over a tidal cycle for reef type L2. The long-shelf current speed is set to 18 cm s^{-1}. Plots (labelled 1 to 6) represent currents at one hour intervals from when the tide begins to flood.

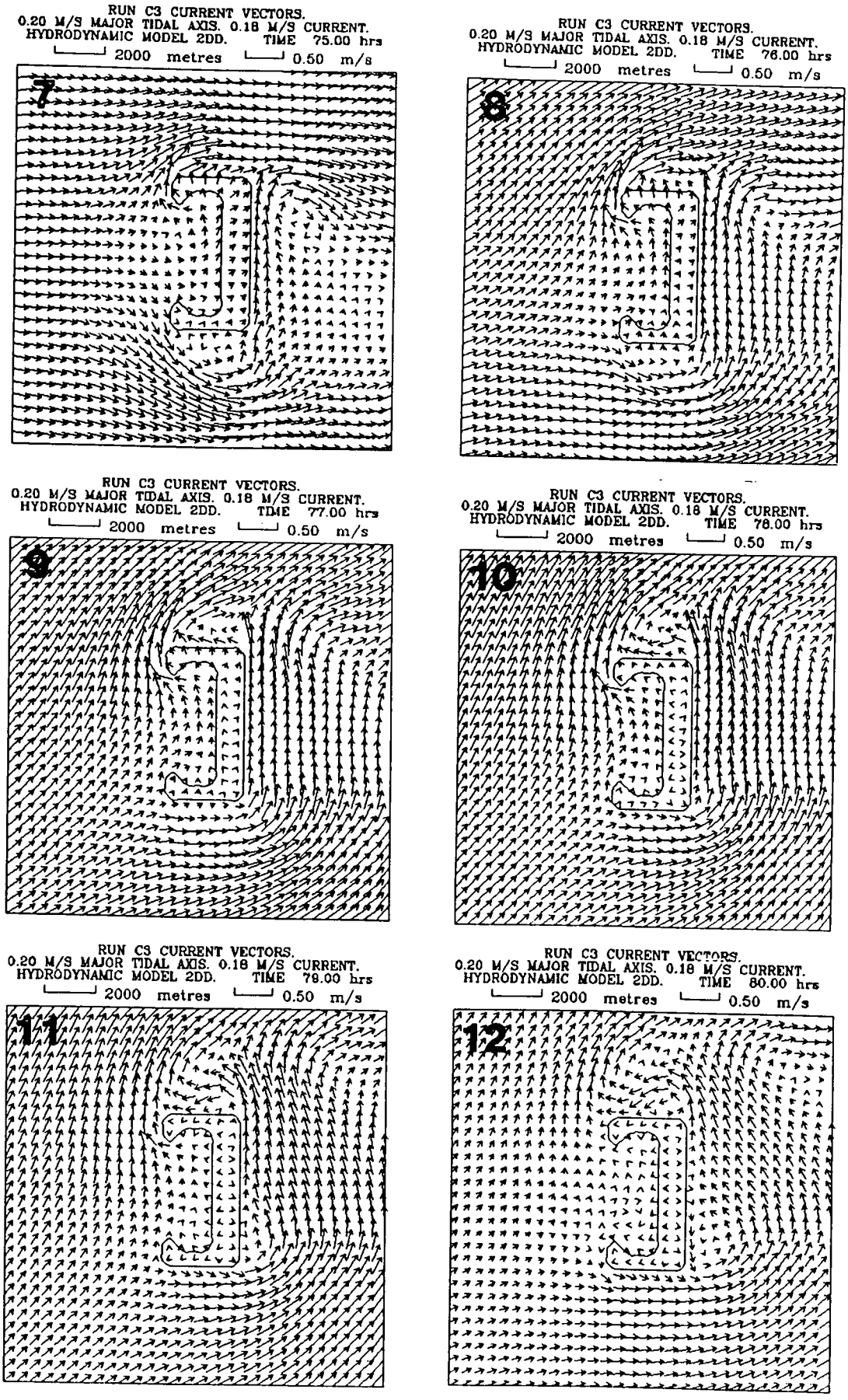


Figure B3b Representative plots of current vectors over a tidal cycle for reef type L2. The long-shelf current speed is set to 18 cm s^{-1}. Plots (labelled 7 to 12) represent currents at one hour intervals from when the tide begins to ebb.

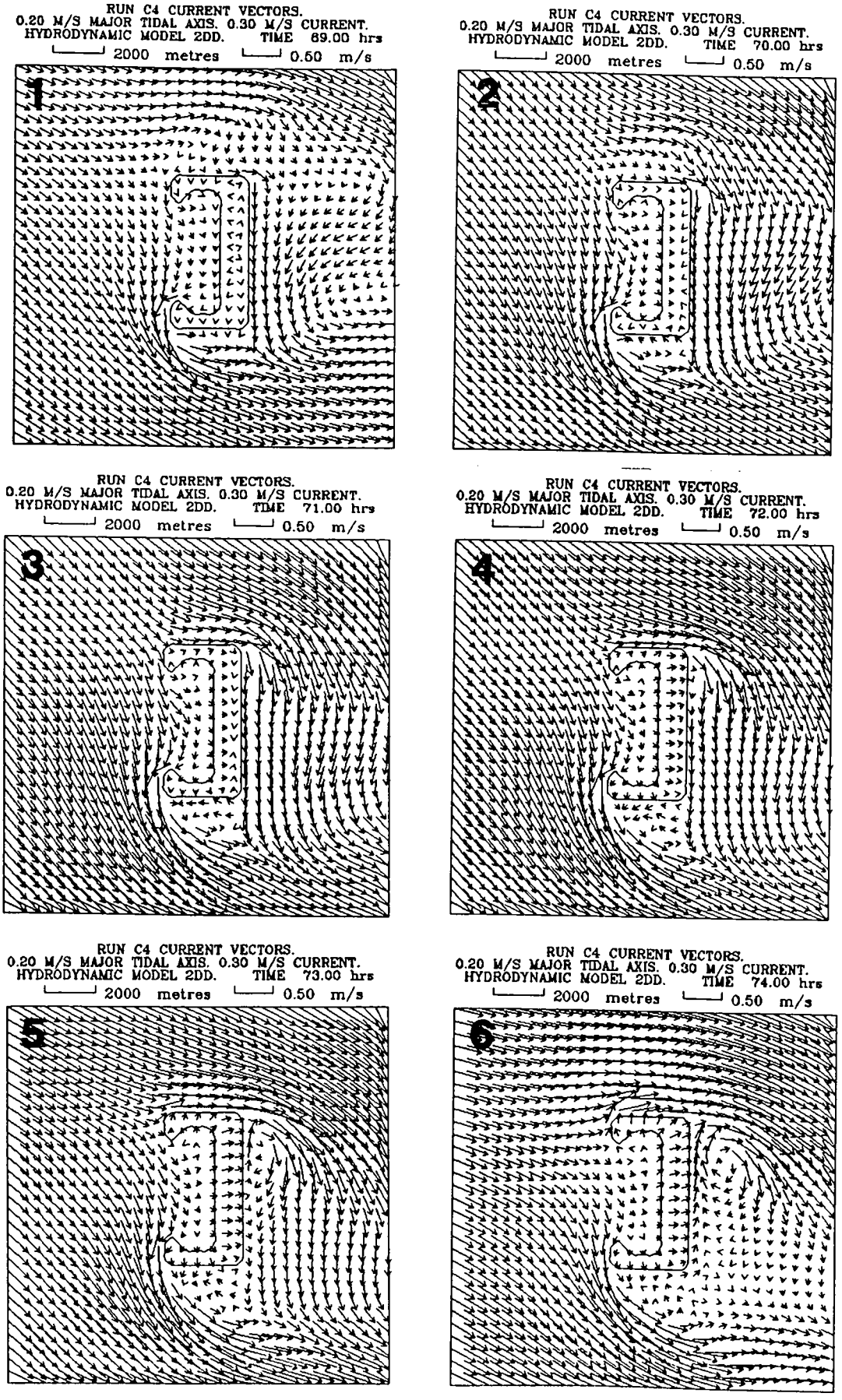


Figure D4a Representative plots of current vectors over a tidal cycle for reef type L2. The long-shelf current speed is set to 30 cm s^{-1}. Plots (labelled 1 to 6) represent currents at one hour intervals from when the tide begins to flood.

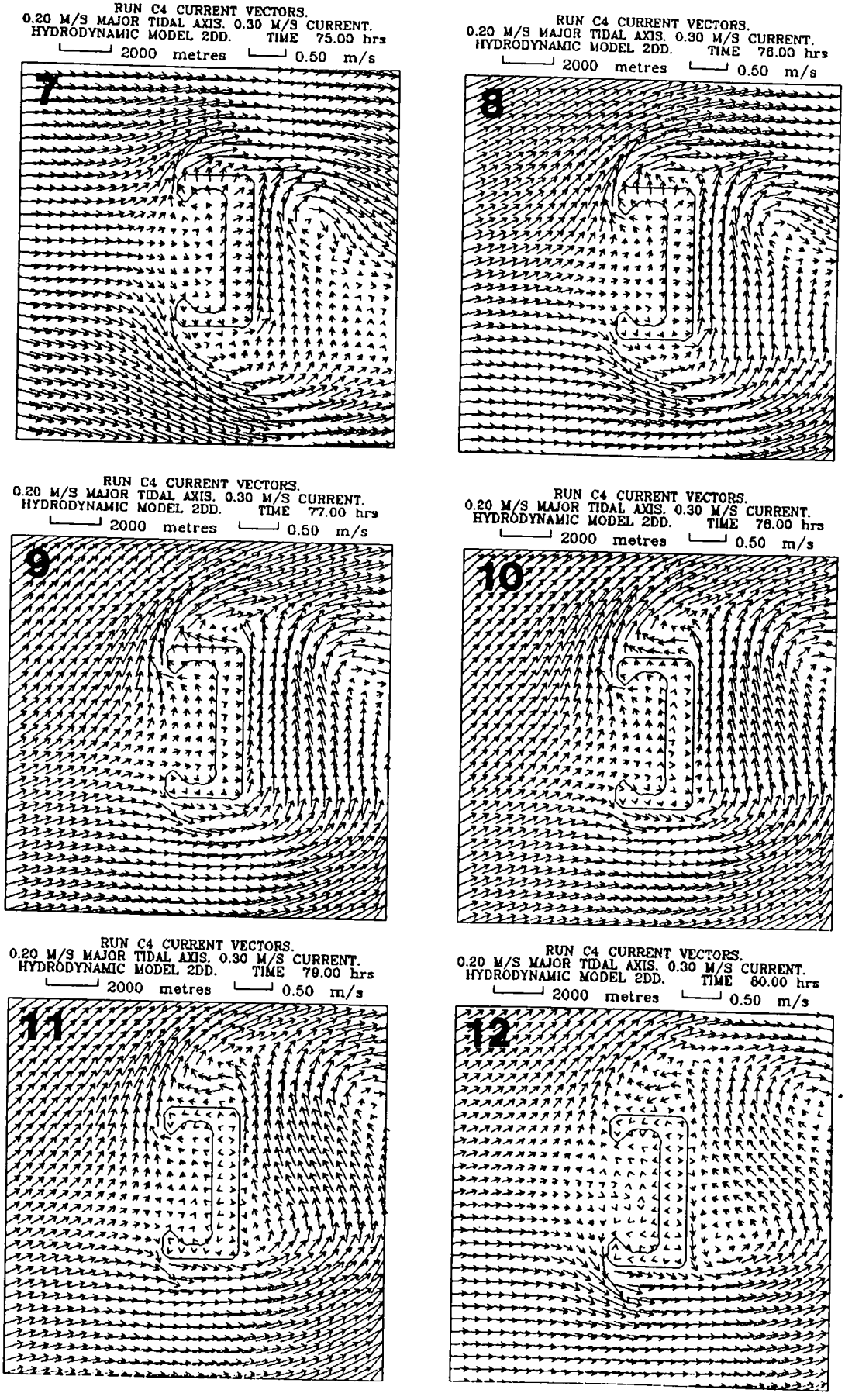


Figure D4b Representative plots of current vectors over a tidal cycle for reef type L2. The long-shelf current speed is set to 30 cm s^{-1}. Plots (labelled 7 to 12) represent currents at one hour intervals from when the tide begins to ebb.

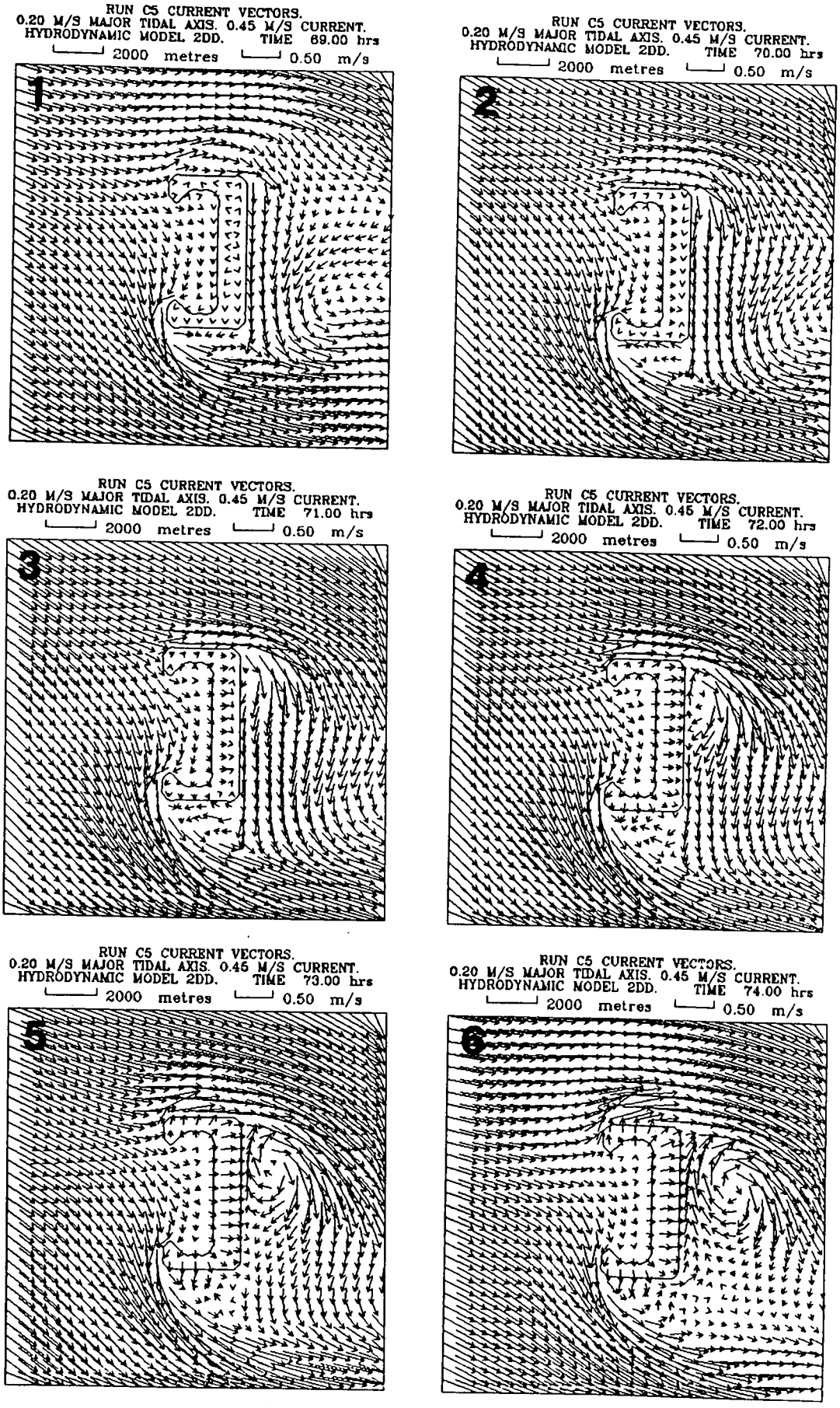


Figure D5a Representative plots of current vectors over a tidal cycle for reef type L2. The long-shelf current speed is set to 45 cm s^{-1}. Plots (labelled 1 to 6) represent currents at one hour intervals from when the tide begins to flood.

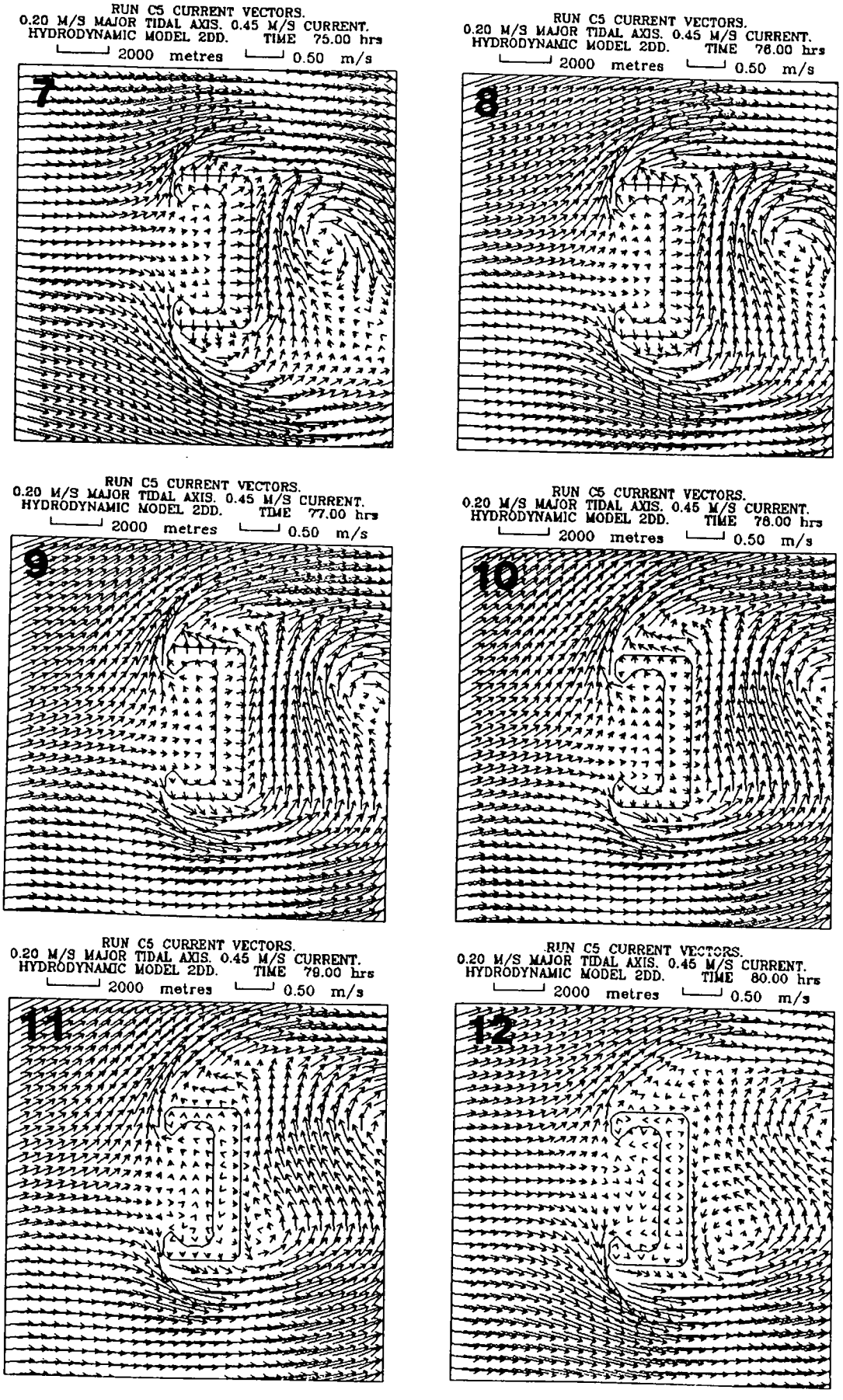


Figure D5b Representative plots of current vectors over a tidal cycle for reef type L2. The long-shelf current speed is set to 45 cm s^{-1}. Plots (labelled 7 to 12) represent currents at one hour intervals from when the tide begins to ebb.

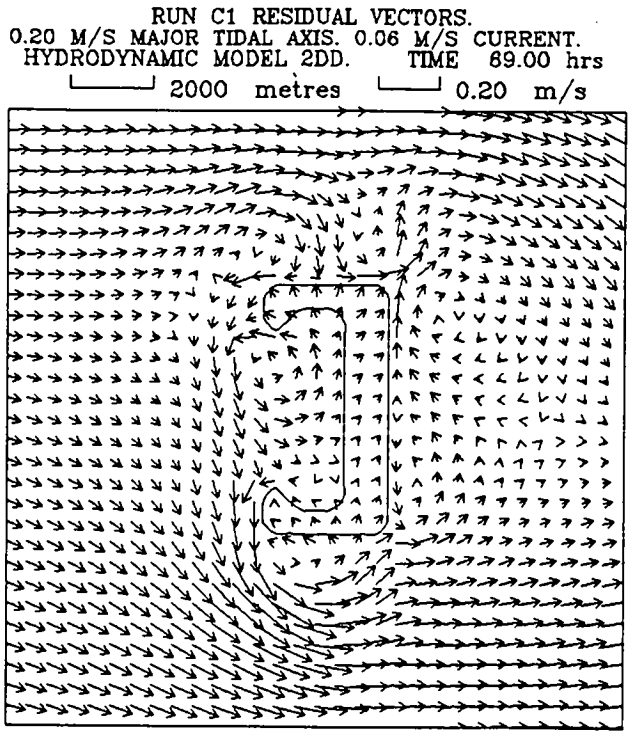


Figure D6 Current vectors representing the residual circulation around reef type L2. The long-shelf current speed is set to 6 cm s^{-1}.

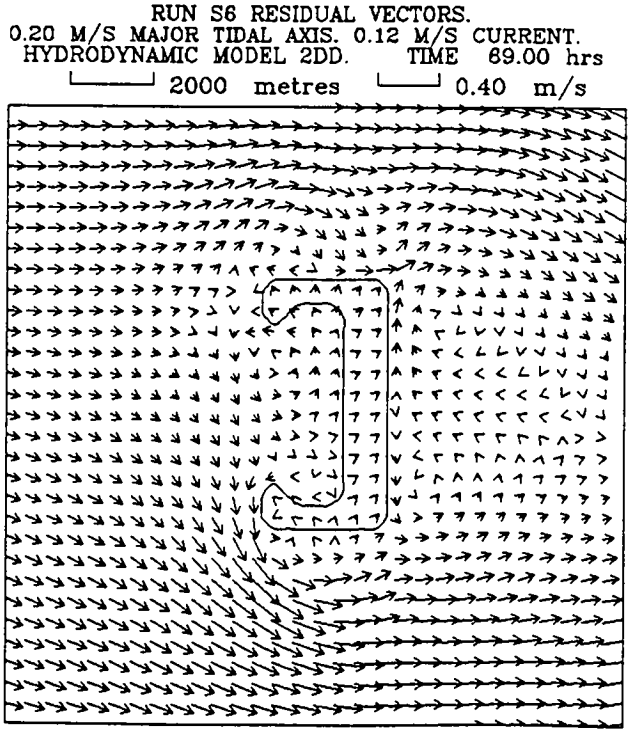


Figure D7 Current vectors representing the residual circulation around reef type L2. The long-shelf current speed is set to 12 cm s^{-1}.

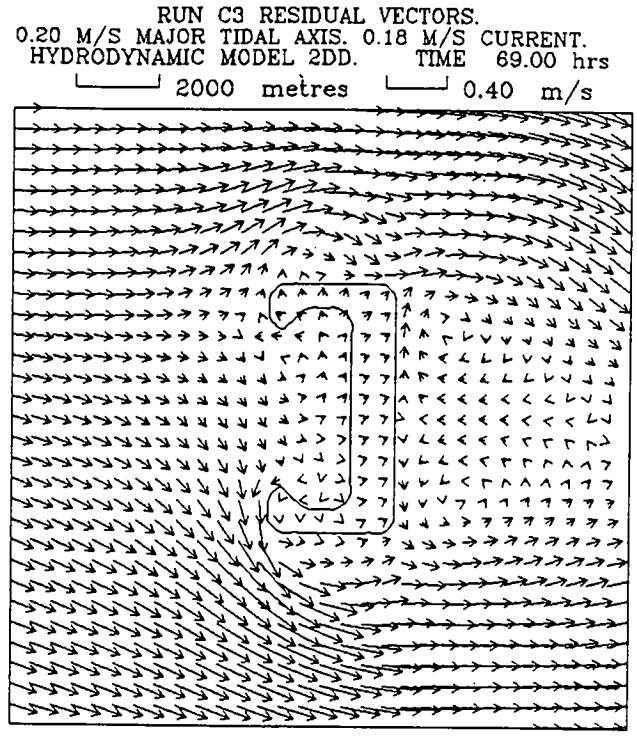


Figure D8 Current vectors representing the residual circulation around reef type L2. The long-shelf current speed is set to 18 cm s^{-1}.

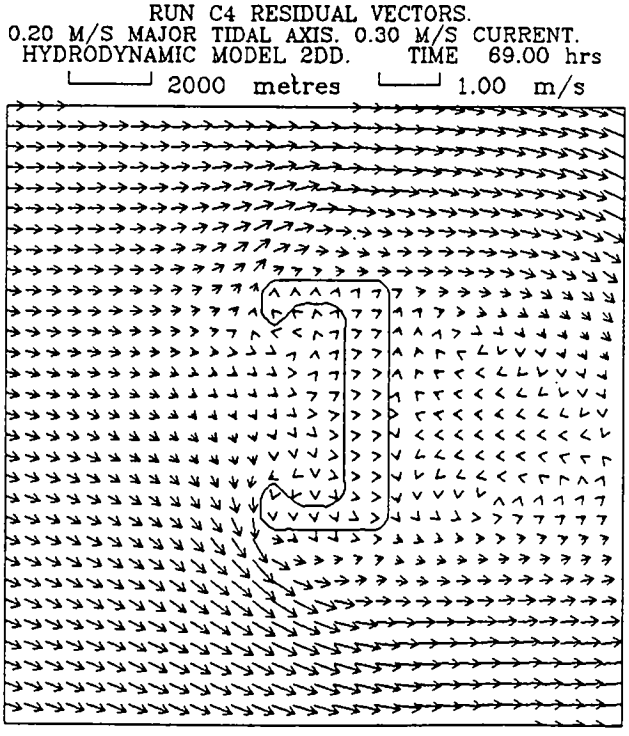


Figure D9 Current vectors representing the residual circulation around reef type L2. The long-shelf current speed is set to 30 cm s^{-1}.

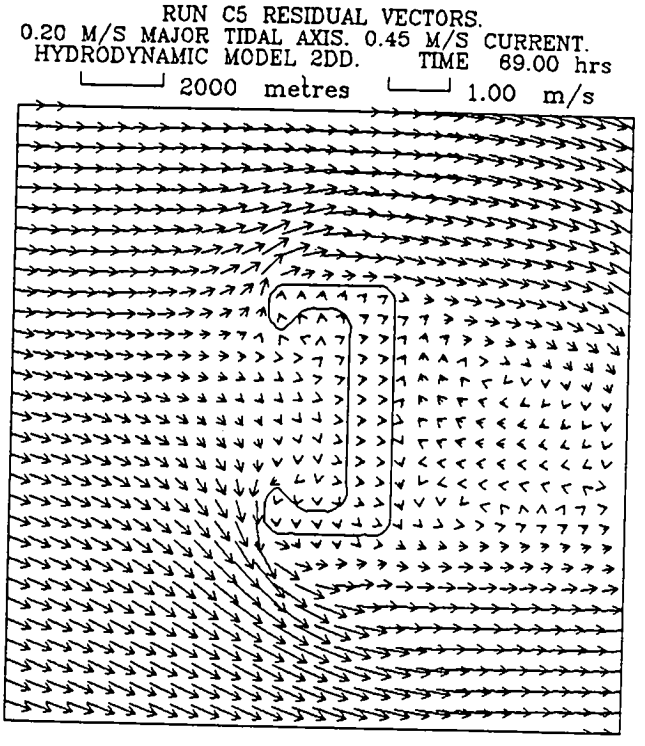


Figure D10 Current vectors representing the residual circulation around reef type L2. The long-shelf current speed is set to 45 cm s^{-1}.

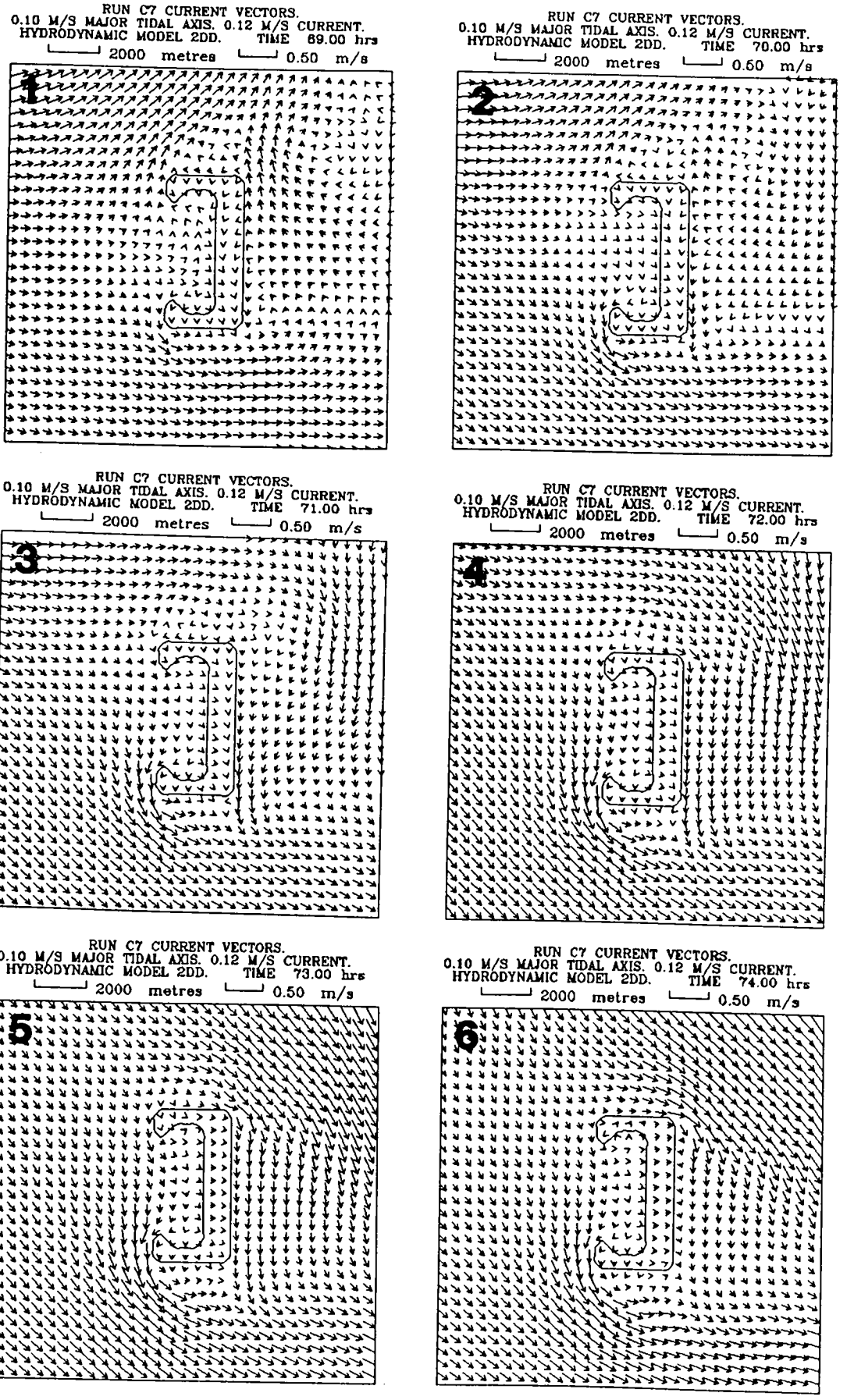


Figure D11a Representative plots of current vectors over a tidal cycle for reef type L2. The maximum cross-shelf tidal current speed is set to 10 cm s^{-1}. Plots (labelled 1 to 6) represent currents at one hour intervals from when the tide begins to flood.

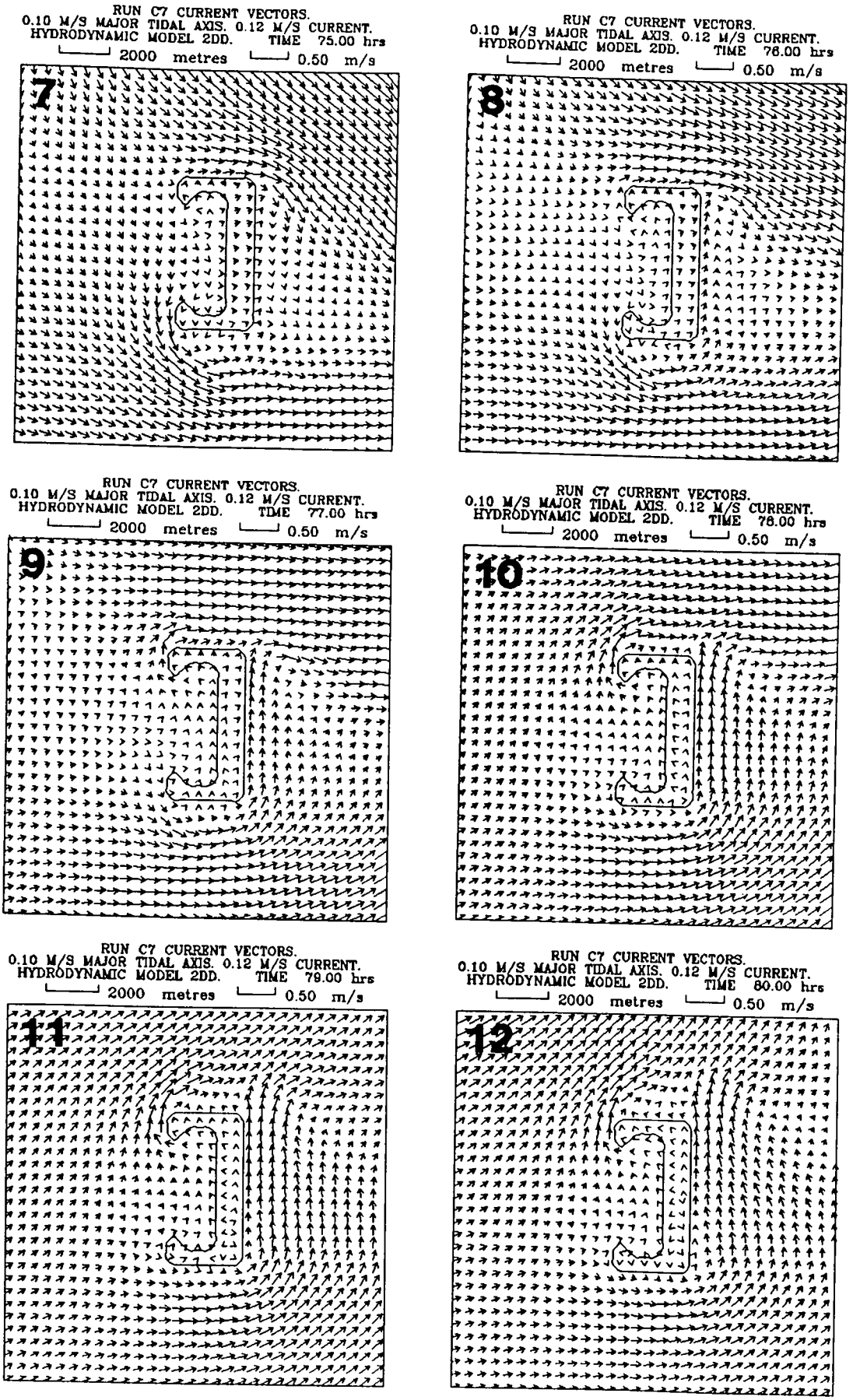


Figure D11b Representative plots of current vectors over a tidal cycle for reef type L2. The maximum cross-shelf tidal current speed is set to 10 cm s^{-1}. Plots (labelled 7 to 12) represent currents at one hour intervals from when the tide begins to ebb.

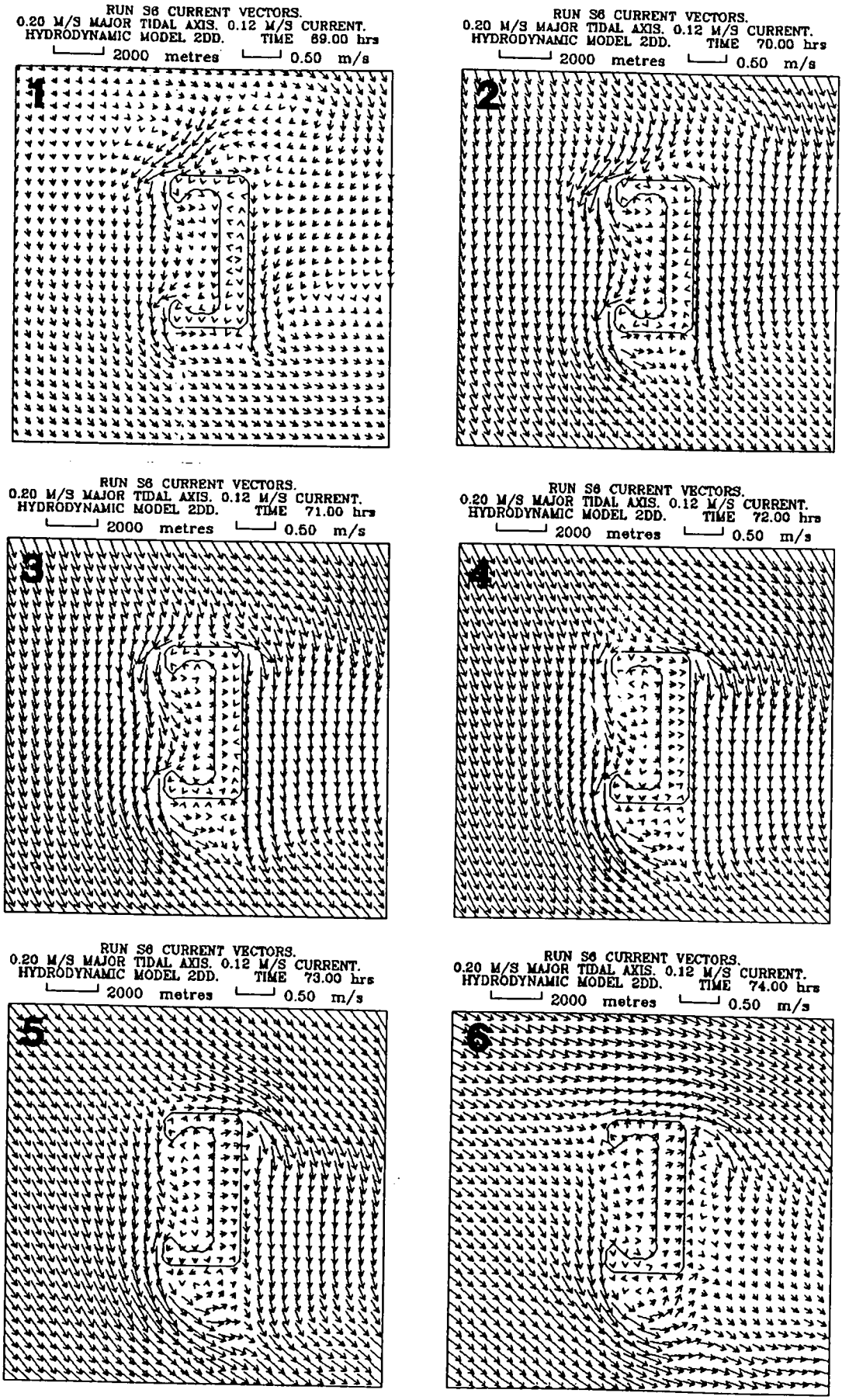


Figure D12a Representative plots of current vectors over a tidal cycle for reef type L2. The maximum cross-shelf tidal current speed is set to 20 cm s^{-1}. Plots (labelled 1 to 6) represent currents at one hour intervals from when the tide begins to flood.

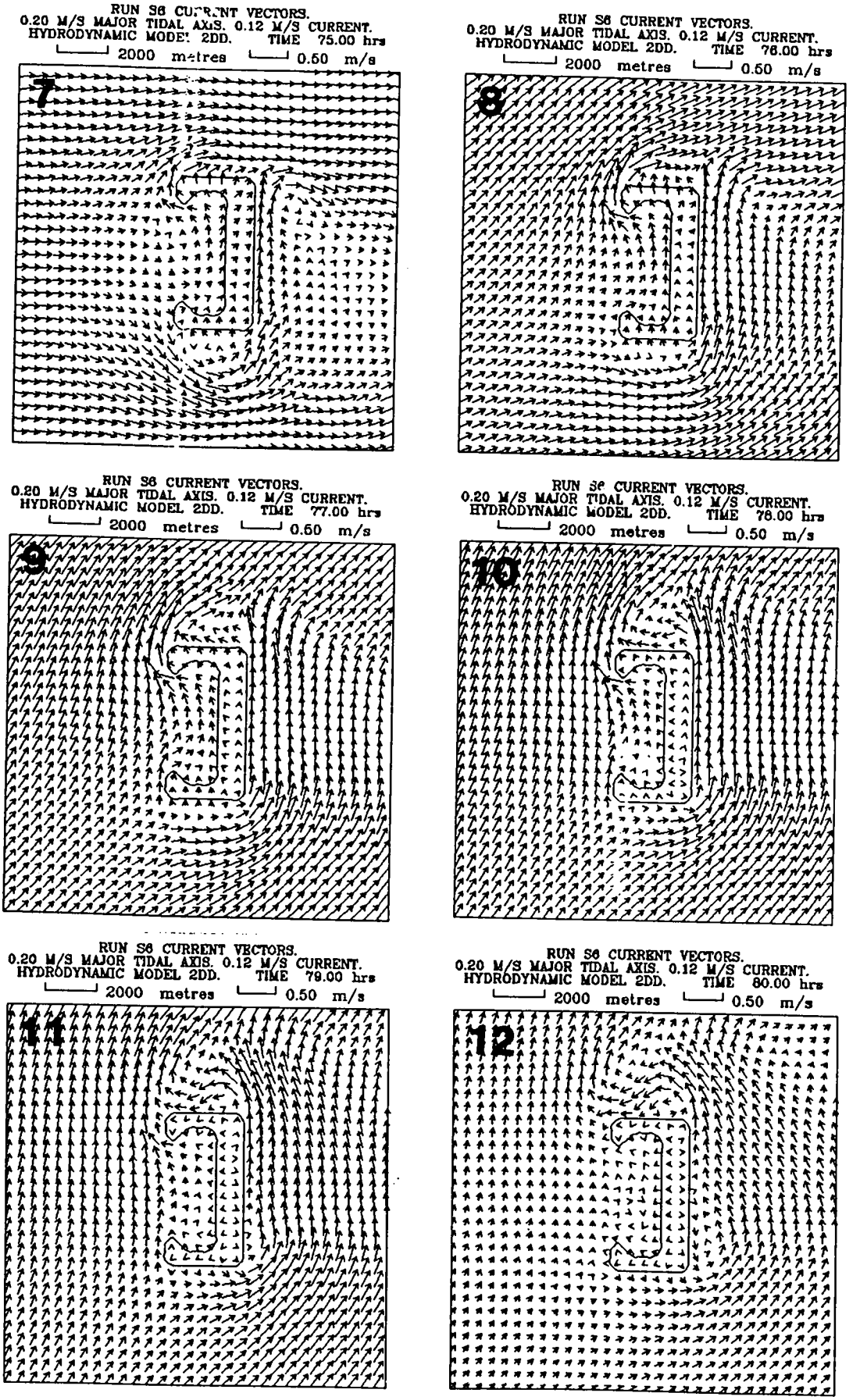


Figure D12b Representative plots of current vectors over a tidal cycle for reef type L2. The maximum cross-shelf tidal current speed is set to 20 cm s^{-1}. Plots (labelled 7 to 12) represent currents at one hour intervals from when the tide begins to ebb.

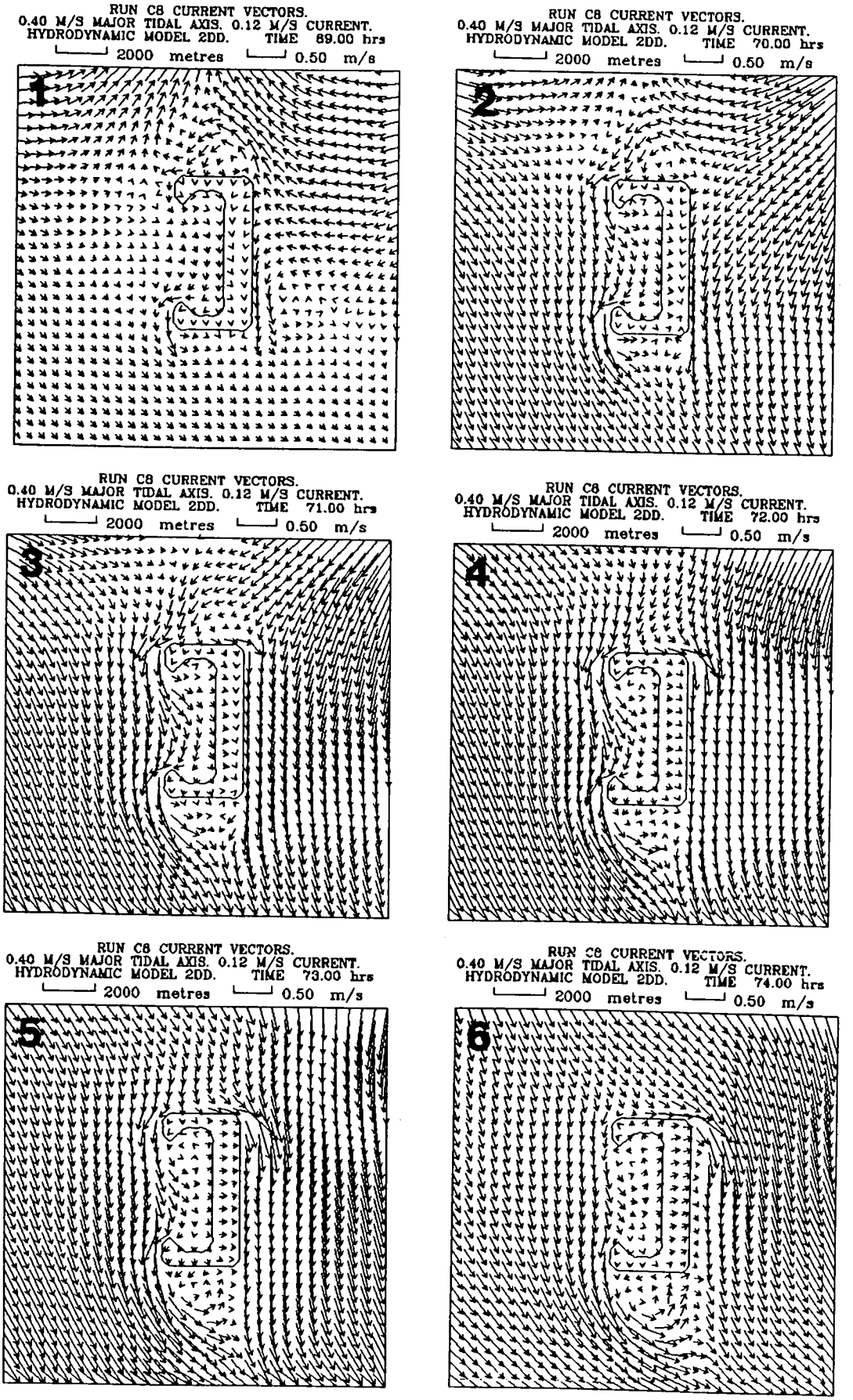


Figure D13a Representative plots of current vectors over a tidal cycle for reef type L2. The maximum cross-shelf tidal current speed is set to 40 cm s^{-1}. Plots (labelled 1 to 6) represent currents at one hour intervals from when the tide begins to flood.

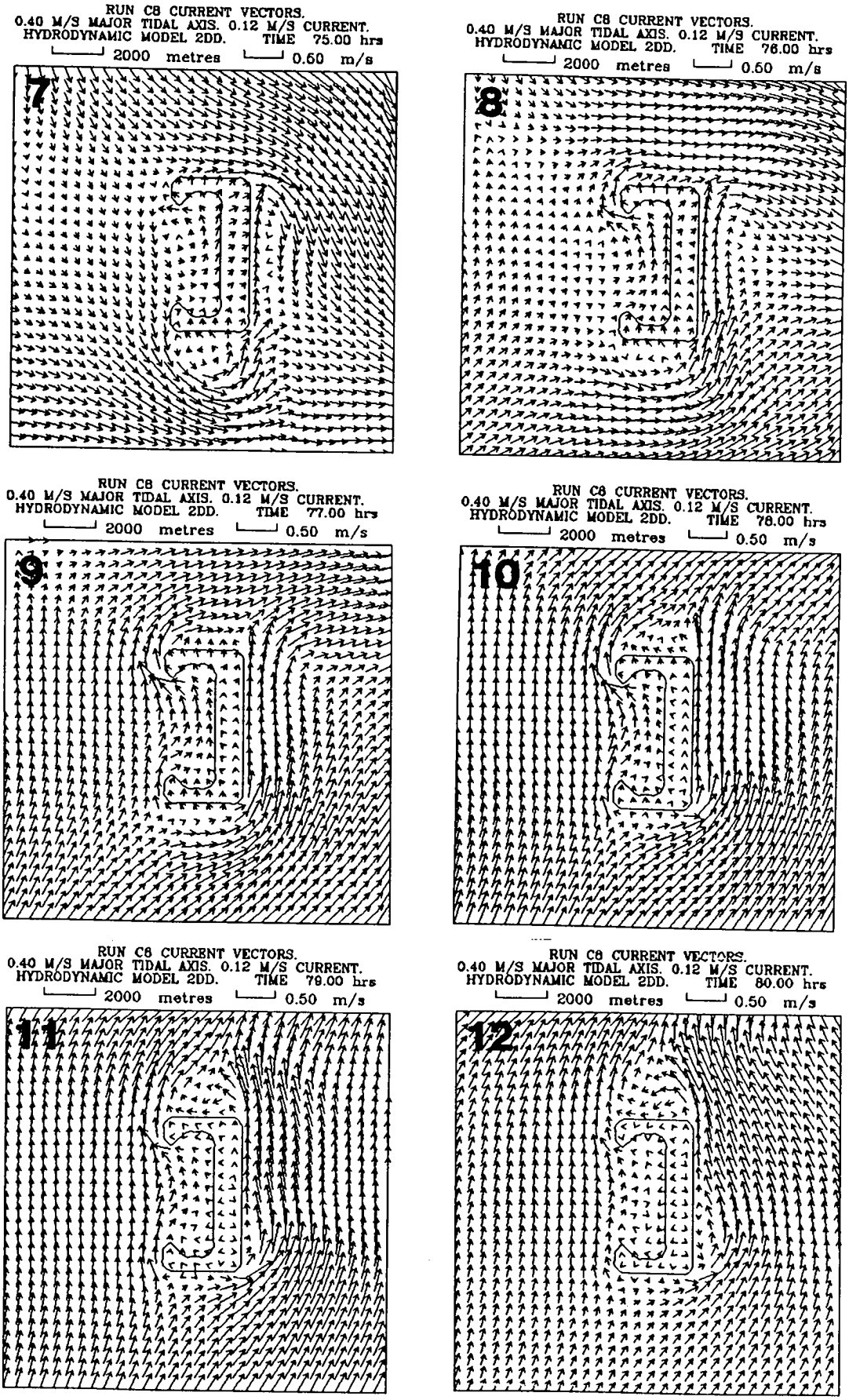


Figure D13b Representative plots of current vectors over a tidal cycle for reef type L2. The maximum cross-shelf tidal current speed is set to 40 cm s^{-1}. Plots (labelled 7 to 12) represent currents at one hour intervals from when the tide begins to ebb.

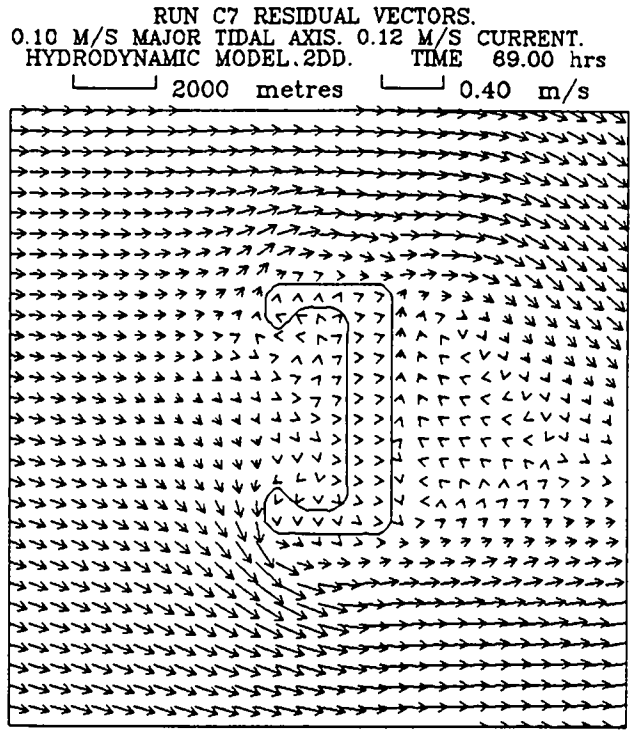


Figure D14 Current vectors representing the residual circulation around reef type L2. The maximum cross-shelf tidal current speed is set to 10 cm s^{-1}.

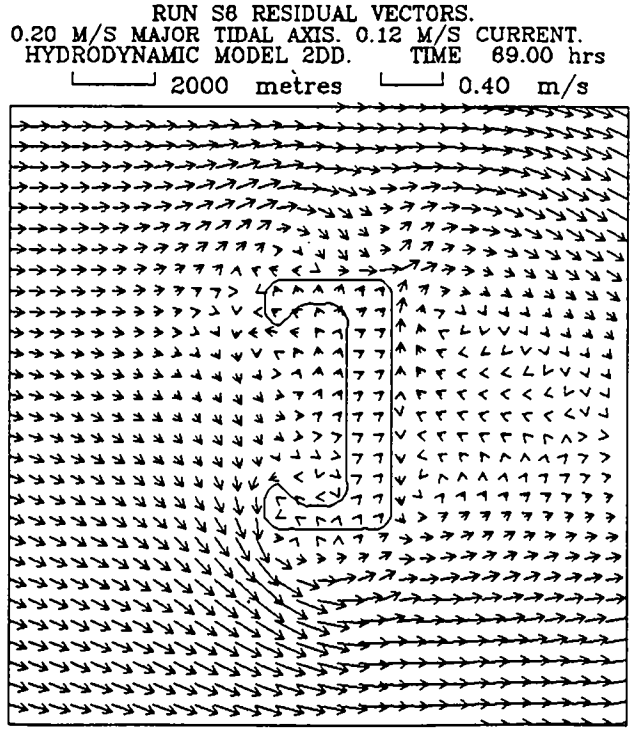


Figure D15 Current vectors representing the residual circulation around reef type L2. The maximum cross-shelf tidal current speed is set to 20 cm s^{-1}.

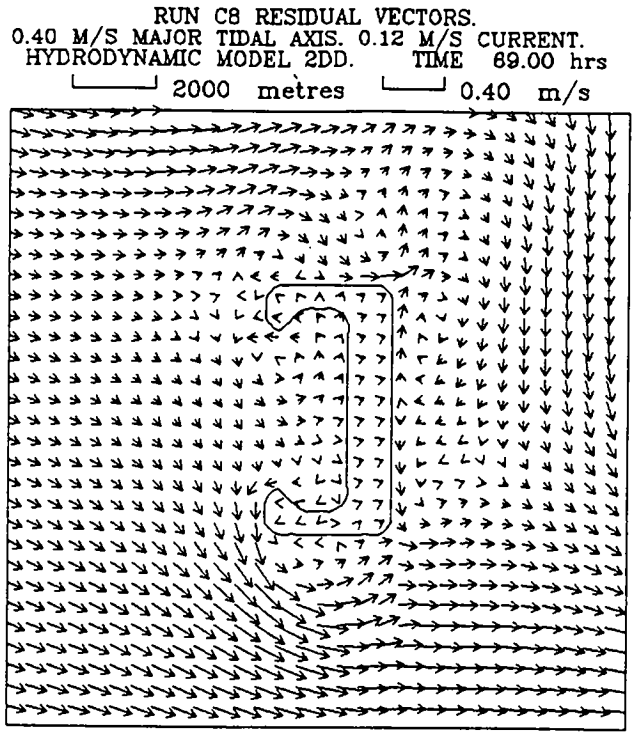


Figure D16 Current vectors representing the residual circulation around reef type L2. The maximum cross-shelf tidal current speed is set to 40 cm s^{-1}.

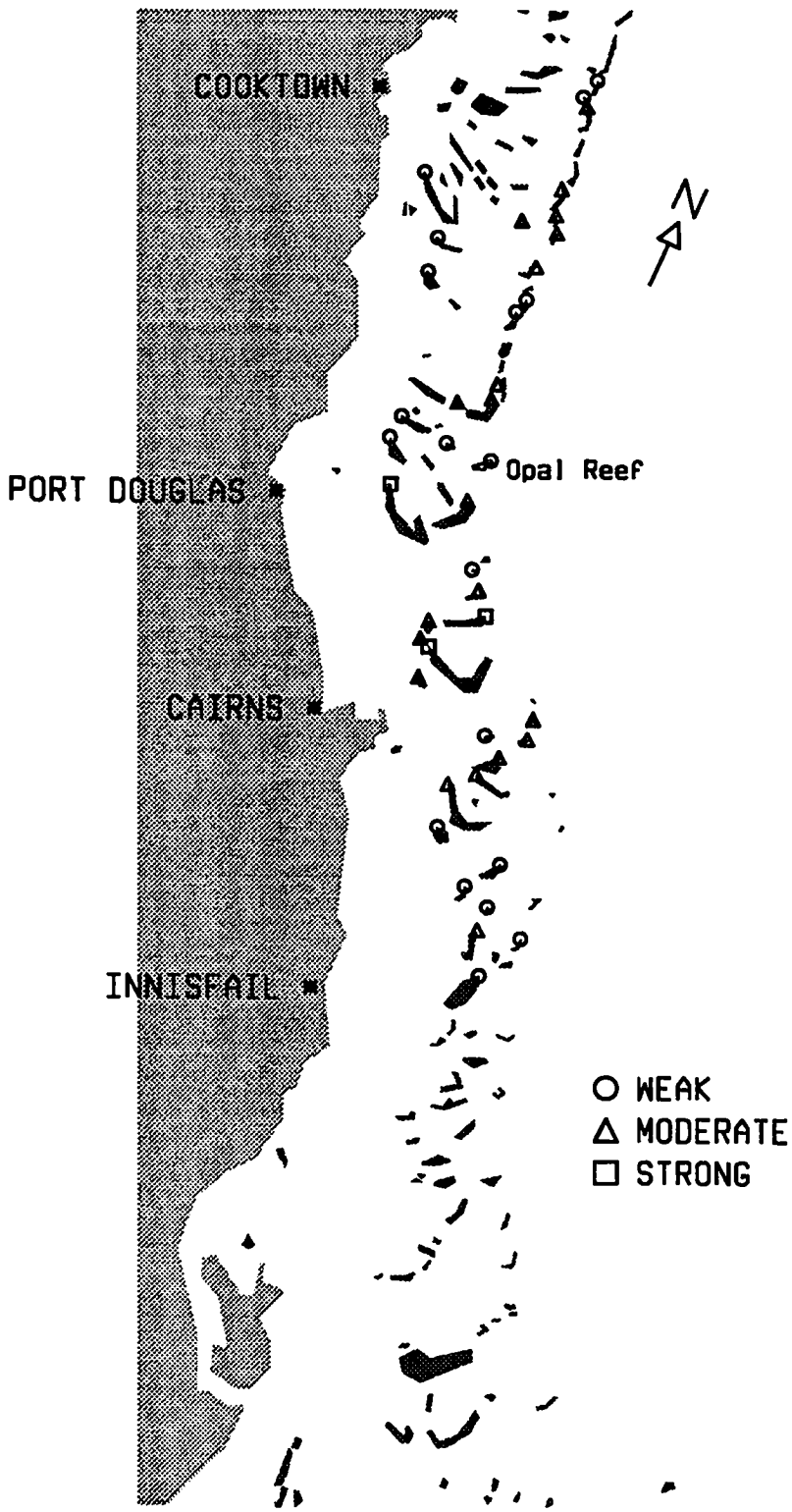


Figure E1a Strength of connectivity with respect to Opal Reef (source reef indicated without fill) where larvae encountering another reef during their pre-competent period suffer 50% mortality. The relative strength classes (weak, moderate and strong) represent probabilities separated by an order of magnitude. Scale: 1cm = 12 nautical miles.

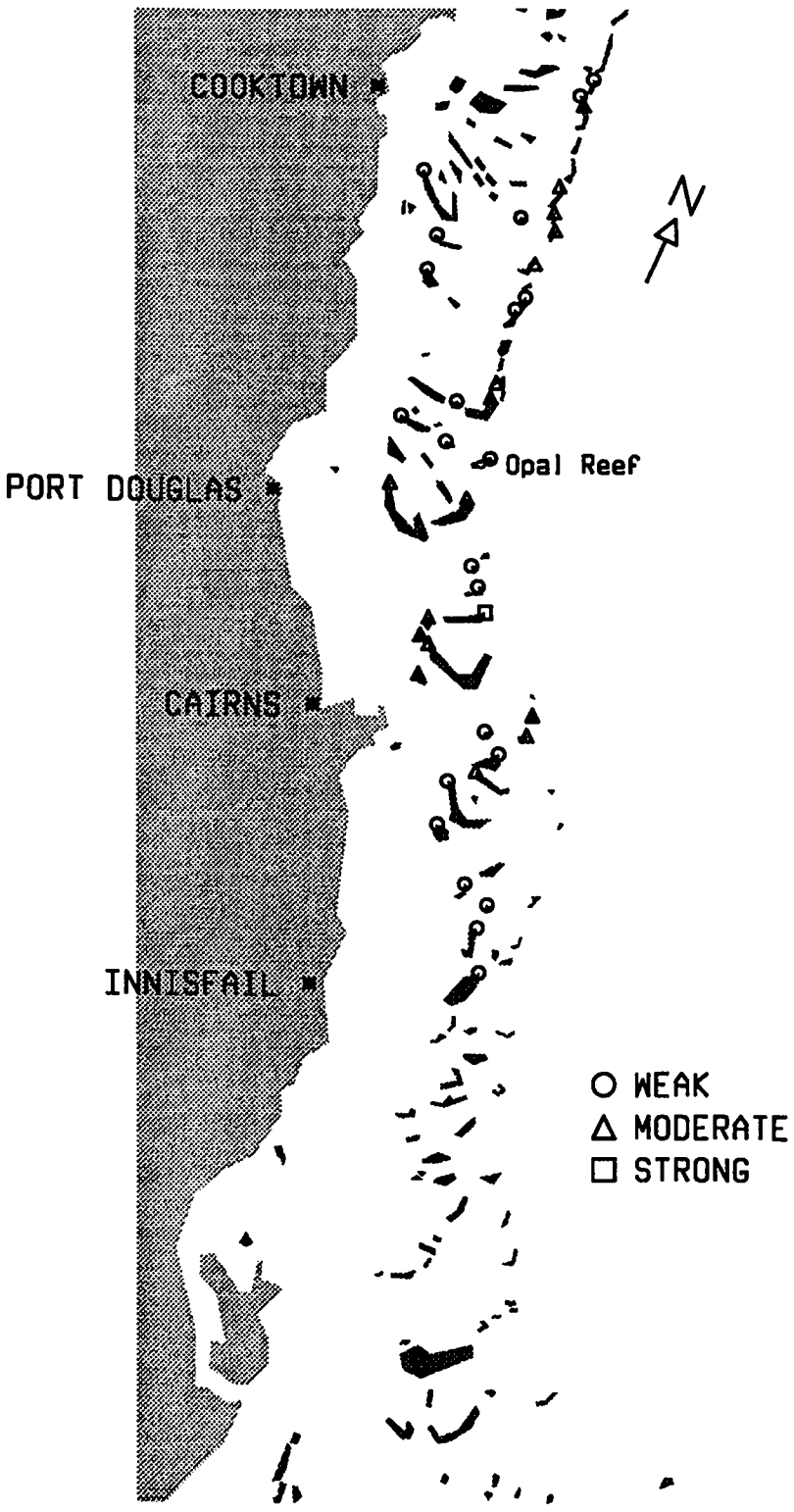


Figure E1b Strength of connectivity with respect to Opal Reef (source reef indicated without fill) where larvae encountering another reef during their pre-competent period suffer 100% mortality. The relative strength classes (weak, moderate and strong) represent probabilities separated by an order of magnitude. Scale: 1cm = 12 nautical miles.

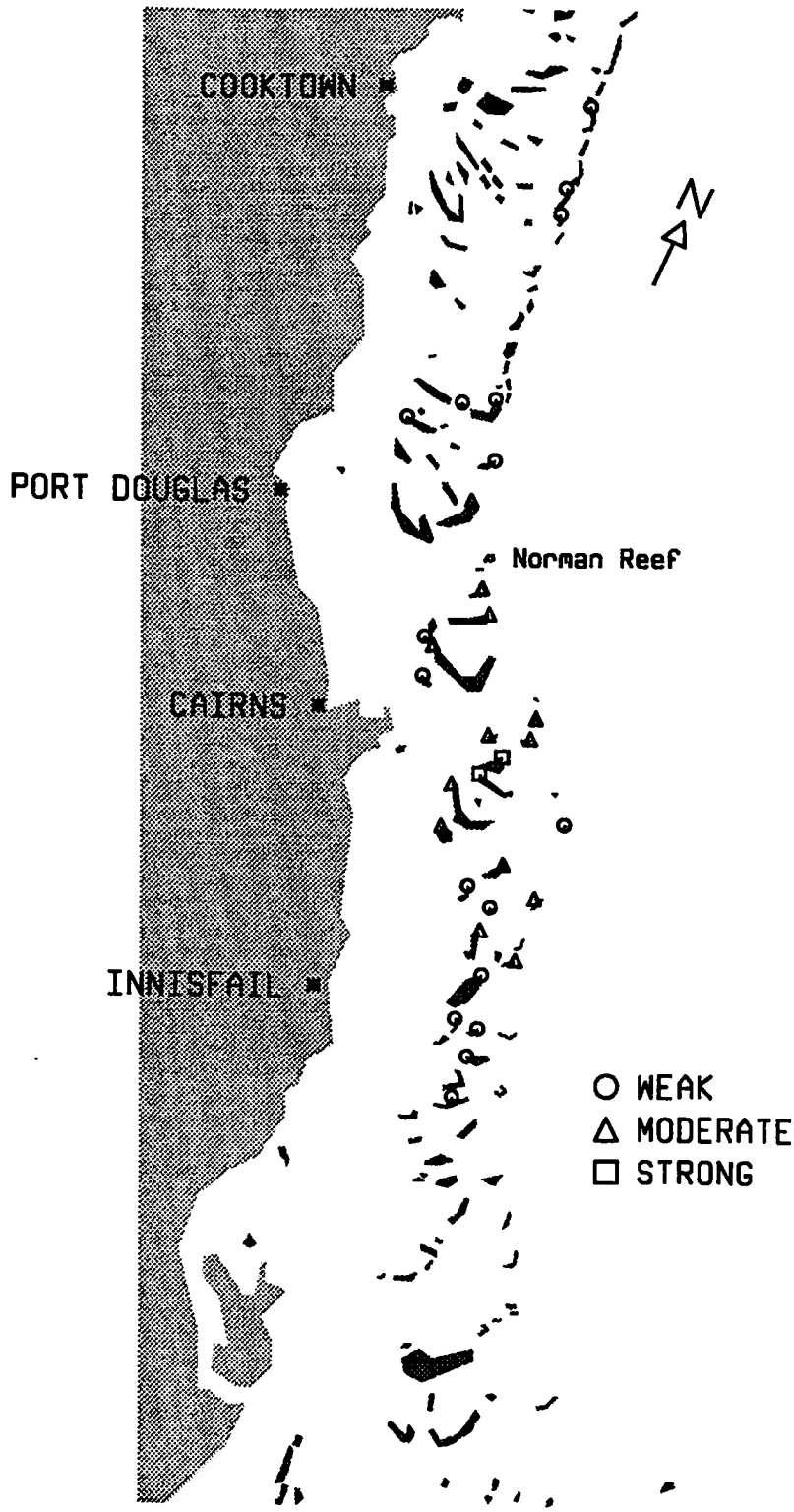


Figure E2a Strength of connectivity with respect to Norman Reef (source reef indicated without fill) where larvae encountering another reef during their pre-competent period suffer 50% mortality. The relative strength classes (weak, moderate and strong) represent probabilities separated by an order of magnitude. Scale: 1cm = 12 nautical miles.

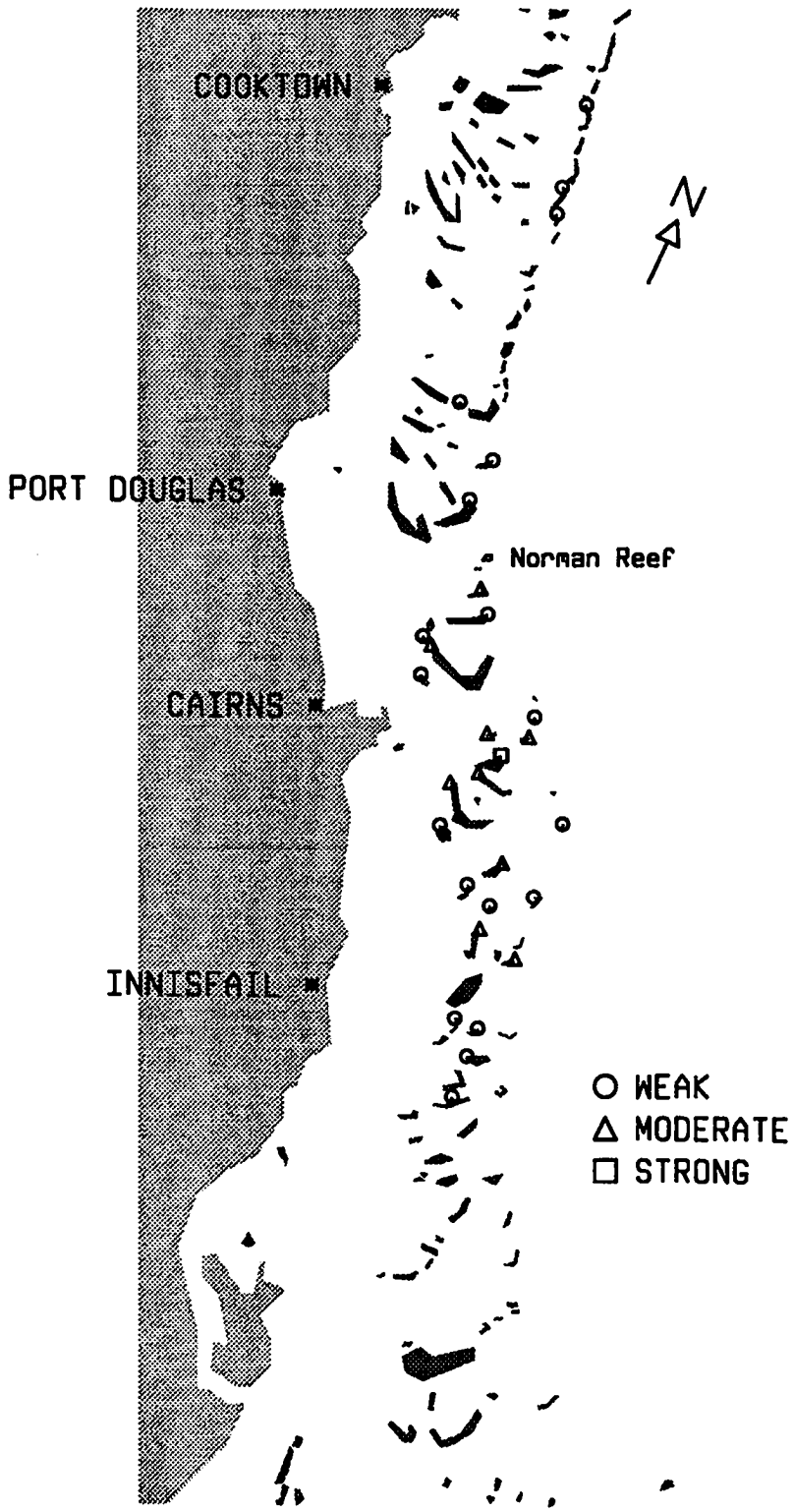


Figure E2b Strength of connectivity with respect to Norman Reef (source reef indicated without fill) where larvae encountering another reef during their pre-competent period suffer 100% mortality. The relative strength classes (weak, moderate and strong) represent probabilities separated by an order of magnitude. Scale: 1cm = 12 nautical miles.

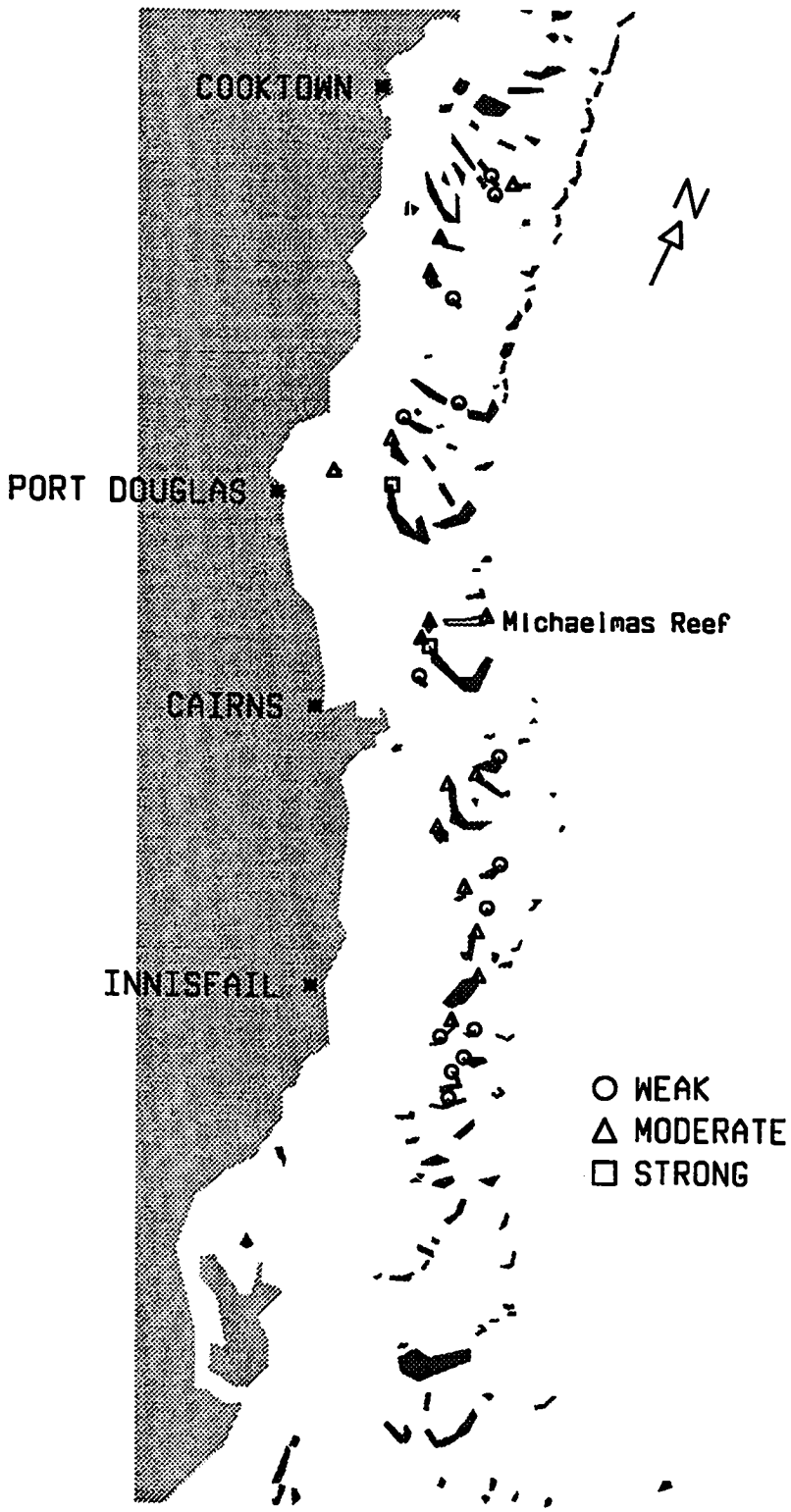


Figure E3a Strength of connectivity with respect to Michaelmas Reef (source reef indicated without fill) where larvae encountering another reef during their pre-competent period suffer 50% mortality. The relative strength classes (weak, moderate and strong) represent probabilities separated by an order of magnitude. Scale: 1cm = 12 nautical miles.

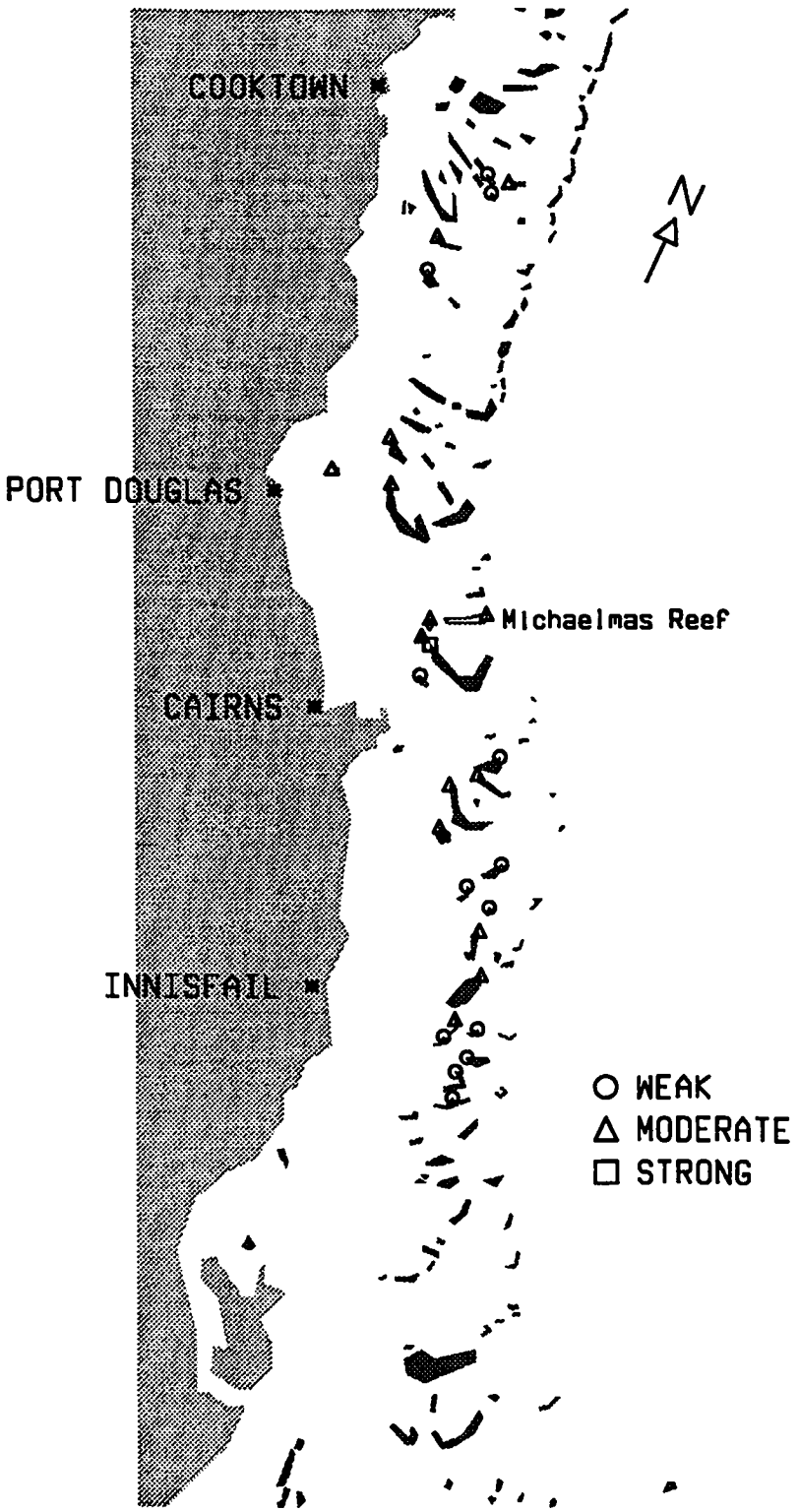


Figure E3b Strength of connectivity with respect to Michaelmas Reef (source reef indicated without fill) where larvae encountering another reef during their pre-competent period suffer 100% mortality. The relative strength classes (weak, moderate and strong) represent probabilities separated by an order of magnitude. Scale: 1cm = 12 nautical miles.

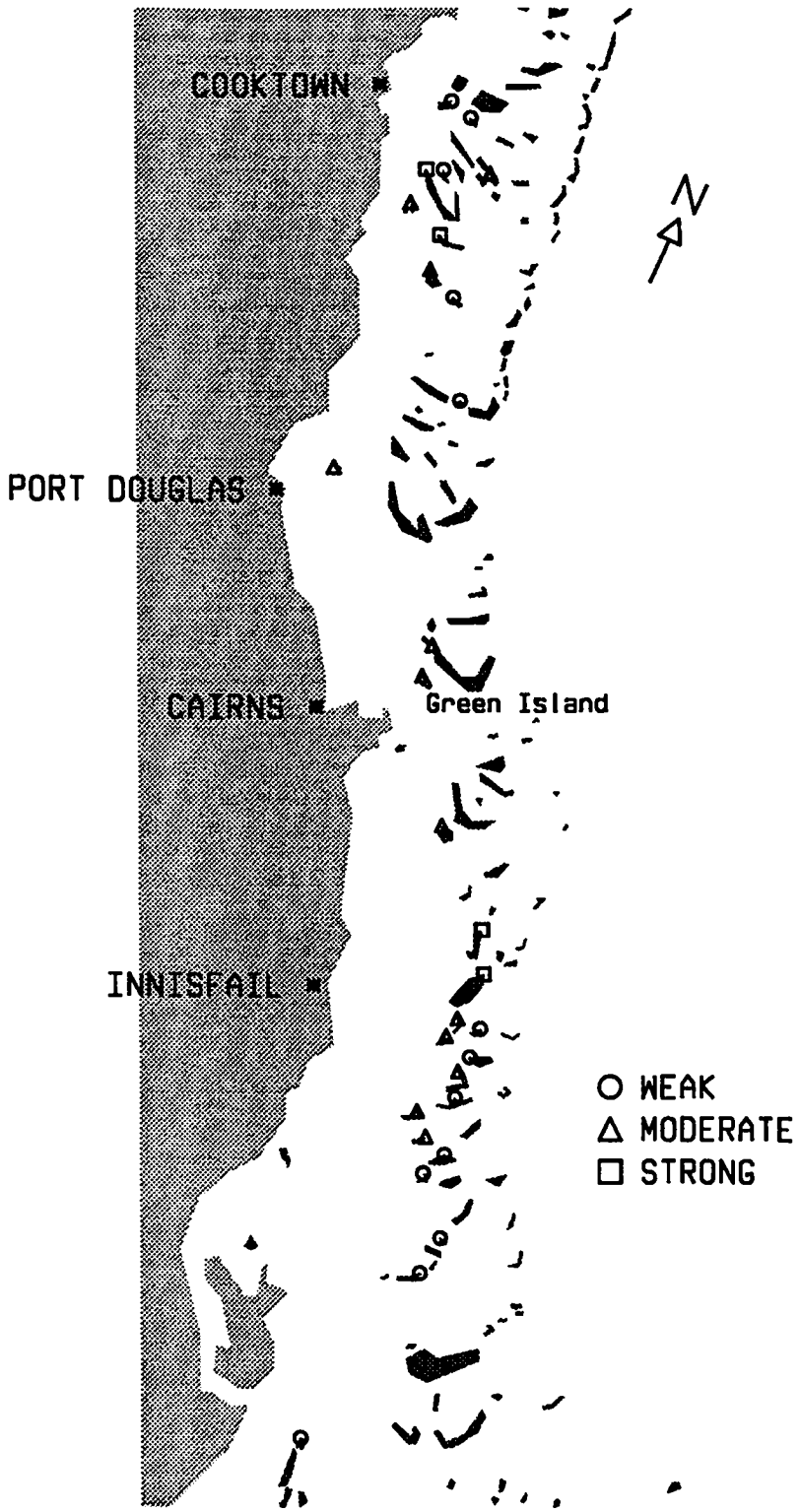


Figure E4a Strength of connectivity with respect to Green Island (source reef indicated without fill) where larvae encountering another reef during their pre-competent period suffer 50% mortality. The relative strength classes (weak, moderate and strong) represent probabilities separated by an order of magnitude. Scale: 1cm = 12 nautical miles.

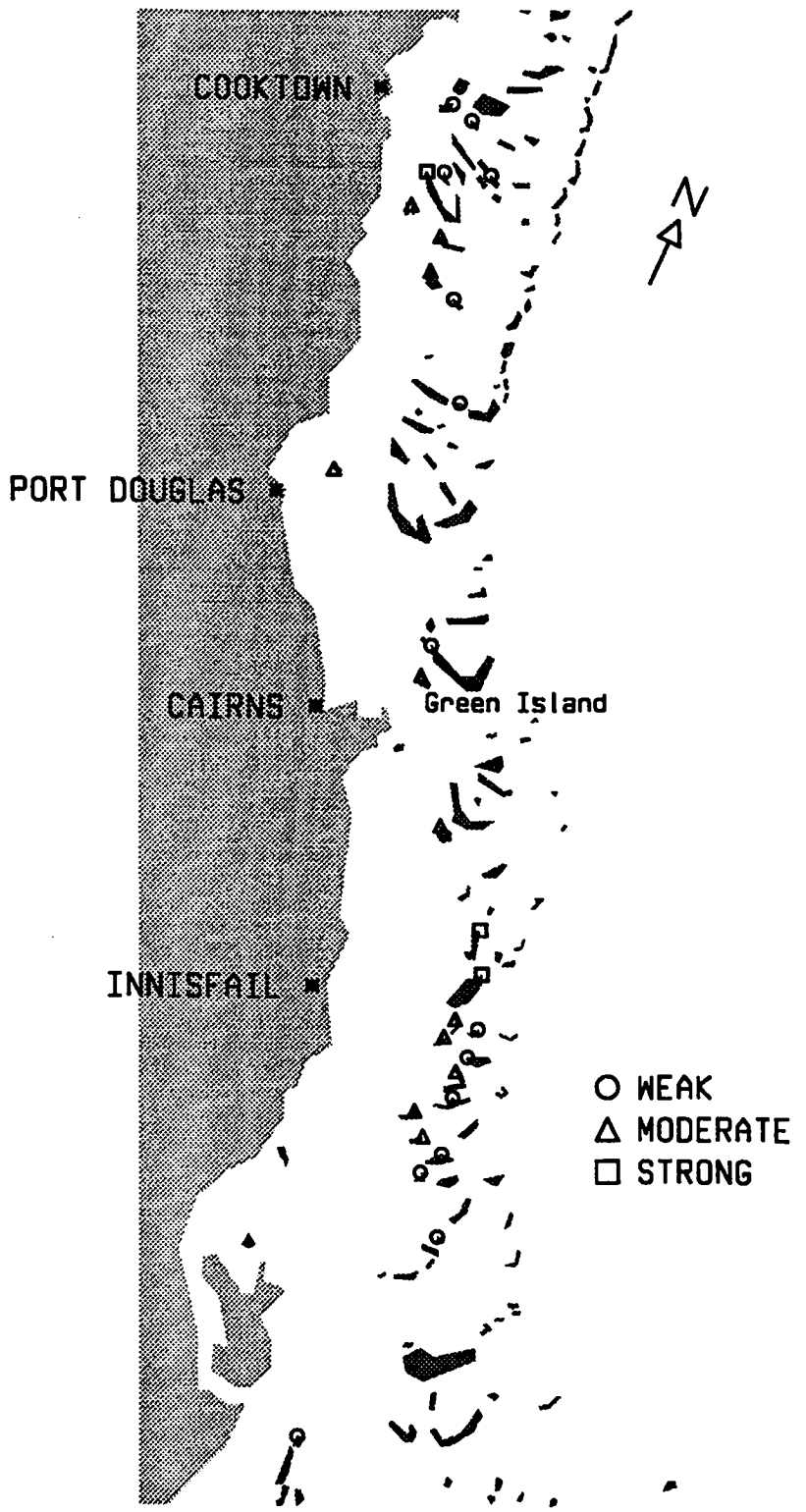


Figure E4b Strength of connectivity with respect to Green Island (source reef indicated without fill) where larvae encountering another reef during their pre-competent period suffer 100% mortality. The relative strength classes (weak, moderate and strong) represent probabilities separated by an order of magnitude. Scale: 1cm = 12 nautical miles.